Palacký University Olomouc
Faculty of Science
Department of Organic Chemistry

Diversity-Oriented Synthesis Using Immobilized 2/4-Nitrobenzensulfonamides As The Key Intermediates

Ph.D. Thesis

Author:	Mgr. Petra Králová
Study Programme:	Chemistry
Field of Study:	Organic Chemistry
Supervisor:	doc. RNDr. Miroslav Soural, Ph.D.
Opponents:	doc. RNDr. Jan Veselý, Ph.D.
	Ing. Petr Beier, Ph.D.

Olomouc 2020

Bibliographic details

Author	Mgr. Petra Králová
University	Faculty of Science, Palacký University Olomouc
Department	Department of Organic Chemistry
Title in English	Diversity-Oriented Synthesis Using Immobilized 2/4-Nitrobenzensulfonamides As The Key Intermediates
Type	Ph.D. Thesis
Supervisor	doc. RNDr. Miroslav Soural, Ph.D.
Opponents	doc. RNDr. Jan Veselý, Ph.D. (Department of Organic Chemistry, Faculty of Science, Charles University Prague) Ing. Petr Beier, Ph.D. (Institute of Organic Chemistry and Biochemistry of the Czech Academy of Sciences (IOCB) Prague)
Study Programme and Field of Study	P1417 Chemistry – Organic Chemistry
Language	English
Year	2020
Number of pages	143 + 64 pages of Appendices
Available at	http://portal.upol.cz/
Keywords	solid-phase synthesis, nitrobenzensulfonamide, α-amino ketone, amino acid, α-bromoketone, cinnamyl alcohol, alkynol, oxazine, morpholine, imidazole, oxazepane

Bibliografický záznam

Autor	Mgr. Petra Králová
Univerzita	Přírodovědecká fakulta Univerzita Palackého v Olomouci
Katedra	Katedra organické chemie
Nadpis česky	Divergentně orientovaná syntéza pomocí imobilizovaných 2/4-nitrobenzensulfonamidů jako klíčových intermediátů
Typ závěrečné práce	Ph.D. práce
Vedoucí práce	doc. RNDr. Miroslav Soural, Ph.D.
Oponenti	doc. RNDr. Jan Veselý, Ph.D. (Katedra organické chemie, Přírodovědecká fakulta, Karlova univerzita Praha) Ing. Petr Beier, Ph.D. (Institut organické chemie a biochemie Akademie věd České republiky, Praha)
Studijní program a obor	P1417 Chemie – Organická chemie
Jazyk práce	angličtina
Rok obhajoby	2020
Počet stran	143 + 64 stran příloh
Dostupné na	http://portal.upol.cz/
Klíčová slova	syntéza na pevné fázi, nitrobenzensulfonamid, *α*-amino keton, aminokyselina, *α*-bromketon, cinnamyl alkohol, alkynol, oxazin, morfolin, imidazol, oxazepan

Declaration of originality

I declare hereby with my signature, that this Ph.D. thesis represents my original work made with the best of my knowledge and that I have used no other sources except for referred citations. Neither the thesis nor any of its substantial parts were previously used for awarding of any other academic degree.

In Olomouc, 29th May 2020

.....

Mgr. Petra Králová

Acknowledgement

First and foremost, I would like to gratefully thank to my amazing supervisor, assoc. prof. Miroslav Soural, Ph.D. for the opportunity to participate in the scientific work in his research group, then for his professional guidance and valuable advices in solving several chemical problems, for helpfulness and optimism that he never lost. Further, I am very grateful for his help with the choosing my internship at Jagellonian University in Krakow (Poland) under the direction of Dr. hab Paweł Zajdel and Dr. Katarzyna Grychowska. These thirteen weeks were great time and beneficial for me. During this internship, I got acquainted closer with solution-phase chemistry as I was interested in synthesis of new potential anti-cancer agents. Therefore, I would like to express my gratitude for the opportunity to work in Paweł´s research group and to participate in this interesting project. Last but not least, I would like to sincerely thank to all co-authors of my publications, especially Dr. Michal Maloň for his willingness and valuable advices in solving complex 2D NMR spectra.

Finally, my deep thanks also belong to my family and those few close friends for their patience, help, love and support even in the most difficult times. Thank you all for everything!

Nevertheless, this research would not have been done without financial support, so I thank the following financial supports coming from European Social Fund (CZ.1.07/2.3.00/20.0009), the European Regional Development Fund – Project ENOCH (No. CZ.02.1.01/0.0/0.0/16_019/0000868), the internal grants of Palacký University (IGA_PrF_2016_020, IGA_PrF_2017_009, IGA_LF_2017_028, IGA_PrF_2018_29, IGA_LF_2018_032, IGA_LF_2019_019 and IGA_PřF_2020_012), and projects of Institute of Molecular and Translational Medicine (LO1304) and the Ministry of Health of the Czech Republic (17-31834A).

ABSTRACT

My Ph.D. thesis is focused on the diversity-oriented synthesis using immobilized 2/4-nitrobenzensulfonamides as the key intermediates to prepare single and fused nitrogenous heterocycles. The preparation of these derivatives was performed using solid-phase synthesis (SPS) that yielded the common intermediate, i.e. *α*-amino ketone which was further modified to final products. The general concept of SPS and its (dis)advantages are briefly discussed in *Introduction* of this thesis. The following subchapter introduces the previous research in the field of *N*-sulfonyl and *N*-acyl morpholine-3-carboxylic acid derivatives[1,2] which has become a major inspiration for all of our projects described in this thesis. The following chapter *Aims of the work* provides the specific goals in more details.

After that, the thesis continues as the *State of the art* to display shortly the general application of immobilized 2/4-nitrobenzensulfonamides and *α*-amino ketones to prepare diverse heterocycles. This subchapter is supplemented by our review article summarizing the polymer-supported syntheses of heterocycles bearing oxazine and thiazine scaffolds which is attached in Appendix B at the end of this thesis. Then the part of *Results and discussion* follows which is divided into eight subchapters according to the individual synthetic projects.

The first two subchapters of *Results and discussion* are dealing with the synthesis of fused [7+6] morpholine derivatives, namely benzoxazino[4,3-*b*][1,2,5]thiadiazepinone 6,6-dioxides **I** and benzo[*e*][1,4]oxazino[4,3-*a*][1,4]diazepine-6,12-diones **II**. These derivatives were prepared from immobilized *α*-amino ketones which were reacted with 2-nitrobenzensulfonyl chlorides or 2-nitrobenzoic acid derivatives. In the first case, the immobilized 2-nitrobenzensulfonamides were reduced on the resin with sodium dithionite followed by the cleavage of the resulting amino derivatives from the polymer-support and subsequent cyclization to morpholino-benzothiadiazepines **I**. The applicability of triethylsilane (TES) for the stereoselective reduction of the double bond and the role of solvents in the cyclization step were studied. The configuration of all stereocenters was determined using a combination of chiral supercritical fluid chromatography (SFC) and advanced nuclear magnetic resonance (NMR) experiments. After that, the attention was paid to acylation of immobilized *α*-amino ketones with 2-nitrobenzoic acids. According to previously reported results,[3] the reduction of nitro group of the polymer-supported *N*-acyl intermediates and their cyclization yielded benzodiazepin-5-ones. In our case, the immobilized *N*-acyl intermediates were cleaved from the polymer support and then subjected to TES reduction, hydrogenation and acid-mediated cyclization to provide the corresponding benzoxazino-diazepinediones **II**.

To further extend this methodology, the immobilized *α*-amino ketones were reacted with natural *α*-amino acids or *α*-halocarboxylic acid derivatives. The corresponding intermediates were used to prepare fused [6+6] pyrazino-oxazines **III** and fused diketomorpholines **IV** depending on the types of used reaction conditions.

In the next two stages, the immobilized *α*-amino ketones were reacted with Fmoc/*N*-substituted-isothiocyanates to obtain thioureas as potential intermediates of fused [6+5] heterocycles bearing the thiohydantoin scaffold **V**. The reaction sequence was tested on two types of resins, such as Wang resin and Wang-piperazine resin; however, the expected fused morpholines were not observed. In contrast, imidazole derivatives were obtained. In the first project, we performed the synthesis on Wang resin that yielded thiohydantoins, imidazole-2-thiones and imidazo[2,1-*b*]thiazol-4-iums **VI** while the formation of 2-alkylsulfonyl-imidazoles **VII** was observed when the Wang-piperazine resin was used. The formation of imidazole scaffolds **VI-VII** was dependent on the type of resin used and also the reaction conditions.

Furthermore, alkynols were used as the alkylating agents and these intermediates were subjected to acid-mediated cleavage from the polymer-support and reacted with trimethylsilyl trifluoromethane-sulfonate (TMSOTf). In contrast to the previously reported 1,4-oxazepanes,[4] this reaction afforded pyrrolidin-3-ones **VIII** *via* pinacol-like rearrangement.

For this reason, our last project is devoted to the alternative synthesis of fused 1,4-oxazepanes **IX**. These derivatives were synthetized from the polymer-supported *N*-alkynyl, *N*-alkenyl or *N*-alkylsulfonamides prepared from commercially available Fmoc-amino acids (e.g. L-serine, L-threonine and L-homoserine), sulfonyl chlorides, alkynols, cinnamyl alcohols and *α*-bromoketones, respectively.

The developed application of immobilized *α*-amino ketones in SPS of heterocycles

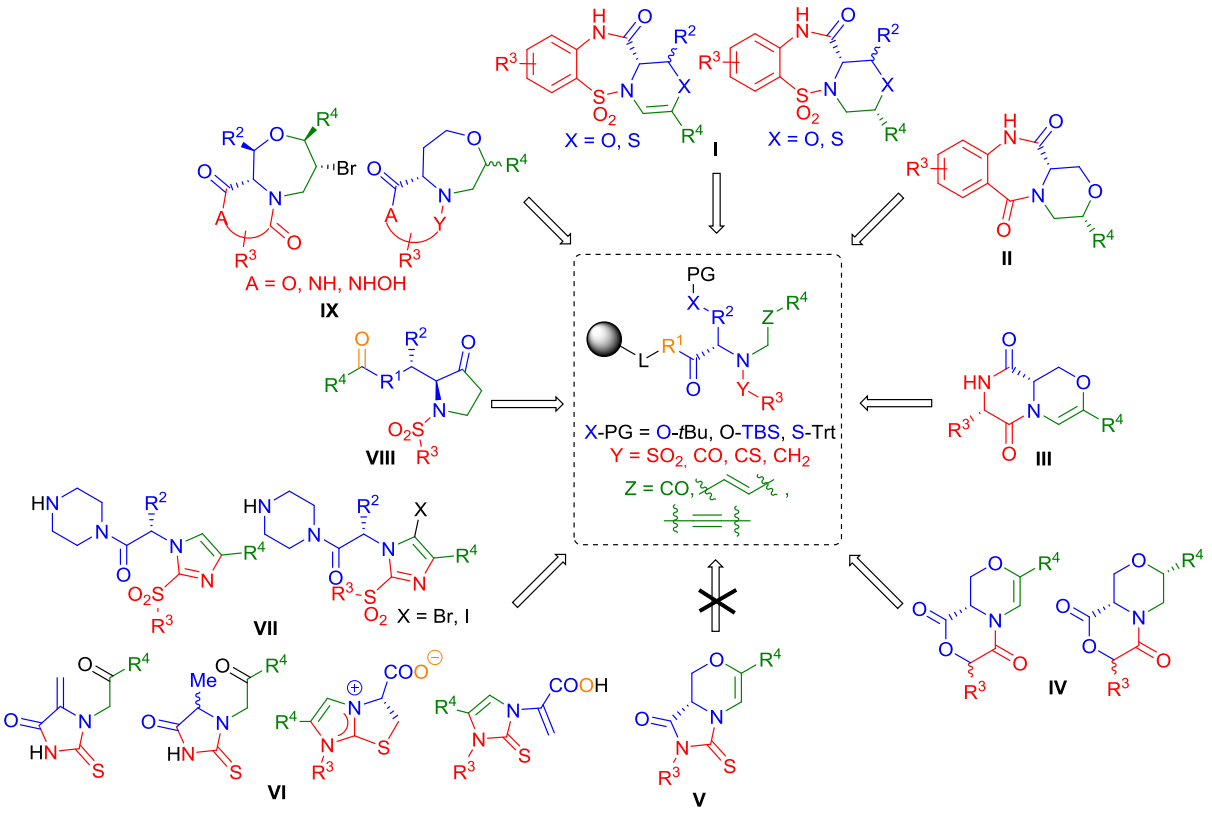

SOUHRN

Moje disertační práce je zaměřena na divergentně orientovanou syntézu pomocí imobilizovaných 2/4-nitrobenzensulfonamidů jako klíčových intermediátů za účelem přípravy jednoduchých a fúzovaných dusíkatých heterocyklů. Tyto deriváty byly připraveny pomocí syntézy na pevné fázi (SPS) vedoucí ke společnému intermediátu, tzn. *α*-amino ketonu, který byl dále modifikován na finální deriváty. V *Úvodu* této práce je stručně diskutován obecný koncept SPS a její výhody a nevýhody. Následující podkapitola uvádí čtenáře do problematiky našeho předchozího výzkumu v oblasti *N*-sulfonyl and *N*-acyl derivátů morfolin-3-karboxylových kyselin,[1,2] který byl naší hlavní inspirací pro všechny následující projekty popsané v této práci. Dále navazují *Cíle práce*, které jsou blíže specifikovány v další podkapitole této práce.

Poté tato práce pokračuje *Teoretickou části*, která stručně nastiňuje obecnou aplikaci imobilizovaných 2/4-nitrobenzensulfonamidů a *α*-amino ketonů pro přípravu rozmanitých heterocyklů. Tato kapitola je doplněna o náš přehledový článek shrnující využití syntézy na pevné fázi pro přípravu heterocyklických sloučenin obsahujících oxazinový a thiazinový skelet, který je přiložen v příloze B na konci této práce. Na tuto podkapitolu pak dále navazuje část *Výsledky a diskuse*, která je členěna do 8 samostatných podkapitol dle jednotlivých syntetických projektů.

První dvě podkapitoly části *Výsledky a diskuse* se zabývají syntézou fúzovaných [7+6] morfolinových derivátů, tedy benzoxazino[4,3-*b*][1,2,5]thiadiazepinon 6,6-dioxidů **I** a benzo[*e*][1,4]oxazino[4,3-*a*][1,4]diazepin-6,12-dionů **II**. Tyto deriváty byly připraveny z imobilizovaných *α*-amino ketonů reagujících dále s 2-nitrobenzensulfonyl chloridy a deriváty 2-nitrobenzoových kyselin. V prvním případě byly imobilizované 2-nitrobenzensulfonamidy redukovány na pryskyřici pomocí dithioničitanu sodného za následného odštěpení výsledného amino derivátu z polymerního nosiče a cyklizace na morfolino-benzothiadiazepiny **I**. Dále byla studována aplikace triethylsilanu (TES) pro stereoselektivní redukci dvojné vazby a také role rozpouštědel ovlivňující cyklizační krok. Určení přesné konfigurace na všech chirálních centrech bylo dosaženo pomocí kombinace chirální superkritické fluidní chromatografie (SFC) a pokročilých experimentů nukleární magnetické rezonance (NMR). Dále byla naše pozornost věnována acylacím imobilizovaných *α*-amino ketonů pomocí derivátů 2-nitrobenzoových kyselin. V souladu s dříve publikovanými výsledky,[3] redukce nitro skupiny na polymerně vázaných *N*-acyl intermediátech a jejich následná cyklizace vedly k benzodiazepin-5-onům. V našem případě byly imobilizované *N*-acyl intermediáty odštěpeny z polymerního nosiče a poté podrobeny redukci s TES, hydrogenaci a kysele zprostředkované cyklizaci vedoucí k odpovídajícím benzoxazino-diazepindionům **II**.

K dalšímu rozšíření metodologie byly imobilizované *α*-amino ketony reagovány s přírodními *α*-amino kyselinami a deriváty *α*-halokarboxylových kyselin. Příslušné intermediáty byly použity k přípravě fúzovaných [6+6] pyrazino-oxazinů **III** a fúzovaných diketomorfolinů **IV** vznikajících v závislosti na typů použitých reakčních podmínek.

Poté byly imobilizované *α*-amino ketony ponechány reagovat s Fmoc-/*N*-substituovanými isothiokyanáty k získání thiomočovin jako potenciálních intermediátů fúzovaných [6+5] heterocyklů nesoucích thiohydantoinový skelet **V**. Tato reakční sekvence byla testována na dvou typech pryskyřic, a to Wangově a Wang-piperazinové pryskyřici, avšak očekávané fúzované morfoliny nebyly pozorovány, neboť docházelo k tvorbě imidazolových derivátů. V prvním projektu jsme uskutečnili syntézu na Wangově pryskyřici vedoucí k thiohydantoinům, imidazol-2-thionům a imidazo[2,1-*b*]thiazol-4-iovým solem **VI**, zatímco 2-alkylsulfonyl-imidazoly **VII** byly pozorovány při použití Wang-piperazinovy pryskyřice. Tvorba imidazolového skeletu **VI-VII** byla závislá na typu použité pryskyřice a reakčních podmínkách.

Jako další alkylační činidla byly testovány alkynoly, odpovídající intermediáty byly podrobeny kyselému štěpení z polymerního nosiče a reakci s trimethylsilylmethansulfonátem (TMSOTf). V porovnání s předchozím publikovaným výzkumem 1,4-oxazepanů,[4] tato reakce poskytla pyrrolidin-3-ony **VIII** formující se pomocí pinakolinového přesmyku.

Z toho důvodu se náš poslední projekt věnuje syntéze výše zmíněných fúzovaných 1,4-oxazepanů **IX**. Tyto deriváty byly připraveny z polymerně vázaných *N*-alkynyl, *N*-alkenyl nebo *N*-alkylsulfonamidů, které byly syntetizovány z komerčně dostupných Fmoc-amino kyselin (například L-serinu, L-threoninu a L-homoserinu), sulfonyl chloridů, alkynolů, skořicových alkoholů a *α*-bromketonů.

TABLE OF CONTENTS

LIST OF ABBREVIATIONS

Ala	alanine	Het	heterocycle
Aib	2-aminoisobutyric acid, 2-methylalanine	HF	hydrofluoric acid
AM	aminomethyl resin	HOAt	1-hydroxy-7-azabenzotriazole
AmAc	ammonium acetate	HOBt	1-hydroxybenzotriazole
aq	aqueous solution	HPLC	High Performance Liquid Chromatography
BAL	backbone amide linker	HMBC	Heteronuclear Multiple Bond Correlation
Boc	*tert*-butyloxycarbonyl	HRMS	High-Revolution Mass Spectrometry
$(Boc)_2O$	di-*tert*-butyldicarbonate	HSe	homoserine
BB test	test with bromophenol blue	HSQC	Heteronuclear Single Quantum Coherence
BTPP	*tert*-butylimino-tri(pyrrolidino) phosphorane	IC_{50}	half maximal inhibitory concentration
		i.e.	*id est* (from Latin), means
Bn	benzyl	*in situ*	in the situation/position (from Latin)
Bz	benzoyl	IPA	2-isopropanol
C18	octadecyl reverse phase	LC	Liquid Chromatography
CSA	(1*S*)-(+)-camphorsulfonic acid	LiHDMS	lithium bis(trimethylsilyl)amide
CDI	1,1´-carbonyldiimidazole	M	molarity of solution
DAST	diethylaminosulfur trifluoride	MBHA	*p*-methylbenzhydrylamine resin
DBU	1,8-diazabicyclo[5.4.0]undec-7-ene	MCE	2-mercaptoethanol
DCC	*N*,*N´*-dicyclohexylcarbodiimide	*m*CPBA	*m*-chloroperoxybenzoic acid
DCE	1,2-dichloroethane	MeCN	acetonitrile
DCM	dichlormethane	MS	Mass Chromatography
DIAD	diisopropyl azodicarboxylate	Ms	mesyl, methanesulfonyl
DIEA	*N*,*N*-diisopropylethylamine	N	normality of solution
DIC	*N,N´*-diisopropylcarbodiimide	NBS	*N*-bromosuccinimide
DMAP	4-(*N*,*N*-dimethylamino)pyridine	NMP	1-methyl-2-pyrrolidinone
DME	1,2-dimethoxyethane	NMR	Nuclear Magnetic Resonance
DMF	*N*,*N*-dimethylformamide	NOESY	Nuclear Overhauser Effect Spectroscopy
DMSO	dimethyl sulfoxide	Nos-amide	nitrobenzensulfonamide
dr.r.	diastereomeric ratio	p.a.	chemically pure substance
DVB	divinylbenzene	PAM resin	*p*-(hydroxymethyl)phenylacetamidomethyl-polystyrene
EDC	1-ethyl-3-(3-dimethylaminopropyl) carbodiimide	PG	protecting group
		Phth	phthalic protecting group
EA	ethyl acetate	PIP	piperidine
e.g.	*exempli gratia* (from Latin), for example	PTSA	*p*-toluenesulfonic acid
et al.	*et alli* (from Latin), and collective	Py	pyridine
Fmoc-OSu	*N*-(9*H*-fluoren-9-ylmethoxycarbonyloxy) succinimide	PyBroP	bromotripyrrolidinophosphonium hexafluorophosphate
HBr	hydrobromic acid		

ROESY	Rotating-Frame Overhauser Effect Spectroscopy
RVO	rotavator evaporator
Ser	serine
SPS	solid-phase synthesis
TBAF	tetrabutylammonium fluoride
TBAHS	tetrabutylammonium hydrogensulfate
TBS	*tert*-butyldimethylsilane
*t*Bu	*tert*-butyl
TBP	tributylphosphine
TFA	trifluoroacetic acid
THF	tetrahydrofuran
Thr	threonine
TEA	triethylamine
TES	triethylsilane
TfOH	trifluoromethanesulfonic acid
Tf_2O	trifluoromethanesulfonic acid anhydride
TI_{50}	therapeutic index
TMS	trimethylsilylether
$TMSO^-$	trimethylsilanolate
TMSOTf	trimethylsilyl trifluoromethanesulfonate
Ts	tosyl, *p*-methylbenzensulfonyl
TPP	triphenylphosphine
UHPLC	Ultra High Performance Liquid Chromatography
UV	Ultraviolet Light
WTA	Wang trichloroacetimidate resin
XPhos Pd G2	2nd Generation XPhos Precatalyst, chloro(2-dicyclohexylphosphino-2′,4′,6′-triisopropyl-1,1′-biphenyl)[2-(2′-amino-1,1′-biphenyl)]palladium(II)

FOREWORD

The thesis is written as a compilation of my projects which have been investigated and published in less than four years of my PhD studies. Moreover, the thesis is complemented with unpublished results, e.g. unsuccessful experiments or incomplete projects.

Introduction acquaints a reader with the general concept of SPS and our previous research in the field of *N*-sulfonyl and *N*-acyl morpholine-3-carboxylic acid derivatives. The next part of the thesis, *Aims of the work*, defines individual synthetic goals. The general application of immobilized 2/4-nitrobenzensulfonamides (2/4-Nos-amides) and especially α-amino ketones to prepare diverse heterocycles is defined in the following chapter *State of the art*. This section is classified to individual subchapters according to the type and size of heterocyclic rings. One of the subchapters is supplemented with our review article summarizing the general preparation of morpholine and thiomorpholine derivatives using 2/4-Nos-amides and α-amino ketones. The manuscript is attached in Appendix B at the end of the thesis.

Fourthly, the section *Results and discussion* follows, and it is divided into eight subchapters according to the individual synthetic projects. These subchapters give a brief introduction to attached publications and provide also unpublished results and unsuccessful experiments. All discussed publications are summarized as Appendices C-I at the end of this thesis.

The results of the thesis are concisely recapped in *Conclusion*, including the overall figure showing the application of immobilized α-amino ketones in SPS and the conversion of these intermediates to diverse heterocycles.

Finally, the list of *References* and *Appendices* used are attached. The *Experimental part* contains synthetic procedures to prepare all target derivatives followed by the *Analytical data* (i.e. the extracted data from NMR analyses of the individual substances, including data of unpublished compounds) are attached as an electronic file on CD, in conjugation with *Supporting information* containing all relevant experimental and NMR data to all published articles. It is worth mentioning that Supporting information are available on the web pages of the corresponding publishers and they also are individually listed at the beginning of each subchapter in the part of *Results and discussion*.

1. INTRODUCTION

1.1 Diversity-oriented synthesis (DOS)

Diversity-oriented synthesis (DOS) is a synthetic strategy to quickly produce diverse chemical libraries taking into account four principal factors (i.e. structural, skeletal, functional and stereochemical). The main significance of DOS is a biological screening of synthesized molecules against a broad range of biological targets to find a hit, i.e. compounds exhibiting the specific type of activity.[5] Usually in no more than five synthetic steps, DOS is often applied to synthesize a collection of structurally diverse small organic molecules which are derived from natural products, commercially available derivatives and/or both above mentioned sources. Although DOS libraries are usually smaller in sizes in comparison with commercially available libraries, the target derivatives are structurally more complex, have more varied core scaffolds and more extensive stereochemical diversification.[5] In this context, the skeletal diversity in DOS is guided by two basic principles: (i) the reagent-based approach and (ii) the substrate-based approach. The reagent-based approach is a branching synthetic strategy which involves the use of one common intermediate (i.e. starting material) and different reagents, whereas the substrate-based approach is based on a folding-type reaction involving the use of different starting materials and common reaction conditions. Both synthetic principles are depicted in Figure 1 that demonstrates both DOS strategy for scaffold diversity.[5]

Figure 1. Both reagent-based approach and substrate-based approach of DOS[5]

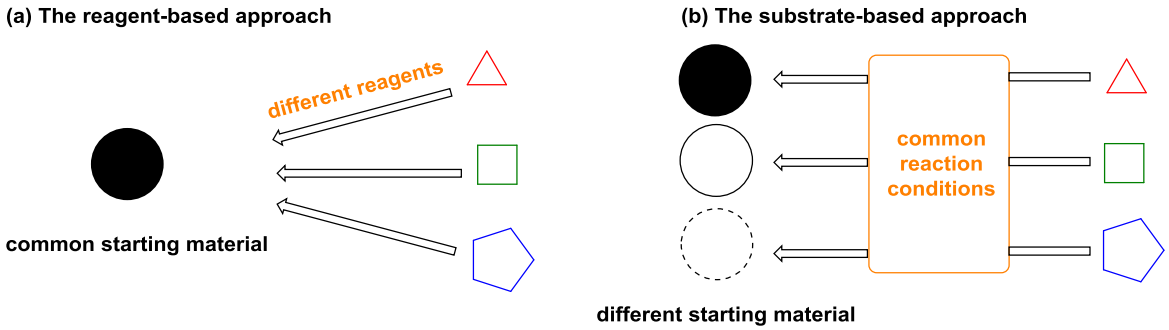

1.2 General concept and aspects of solid-phase synthesis (SPS)

The solid-phase synthesis (SPS) has undergone major development over the last three decades when a number of scholarly articles were reported to prepare peptides,[6] oligonucleotides,[7] oligosacharides (carbohydrates)[8,9] and small organic molecules.[10–12] SPS is based on a simple principle which consists in binding of the first component *via* attached linker to an insoluble solid support. The linker forms an arm among the starting material and the polymer support. It enables a product release from the resin upon appropriate cleavage conditions. To successfully apply SPS, a careful choice of a resin, a linker, an immobilization strategy of the first component (i.e. immobilization *via* carboxylic

acid, *via* ether group or *via* amino group) with respect to a suggested synthetic protocol should be taken into account.

Solid-phase synthesis is easy to do as it can be performed in a common plastic syringe with a porous disk. Typically, a significant excess of solution-phase reagents is used to achieve the complete on-resin conversion. The synthetic protocol consists of an eight simple steps (Figure 2). First, the resin is pre-washed with required solvents enabling resin swelling followed by an immobilization of the starting material on the polymer support. The reaction is shaken for individual reaction time at required temperature and then the reagent excess and soluble by-products are filtered of the resulting resin which is subsequently washed with fresh solvents. After that, the same scenario is repeated to synthesize desired product using required synthons. Finally, the product is released from the polymer support using suitable cleavage conditions depending on the type of linker used, e.g. an acid, a base, a fluoride or UV radiation. To control the reaction progress during the synthetic sequence, HPLC analysis of crude evaporator can be realized immediately after the product cleavage from the resin. Conclusively, the crude evaporator can be subjected to HPLC purification or silica gel chromatography. According to above described protocol, one does not need to purify each intermediate in comparison with solution-phase chemistry; however, only the final products are purified and fully characterized using HRMS and NMR analyses.

Figure 2. General concept of SPS

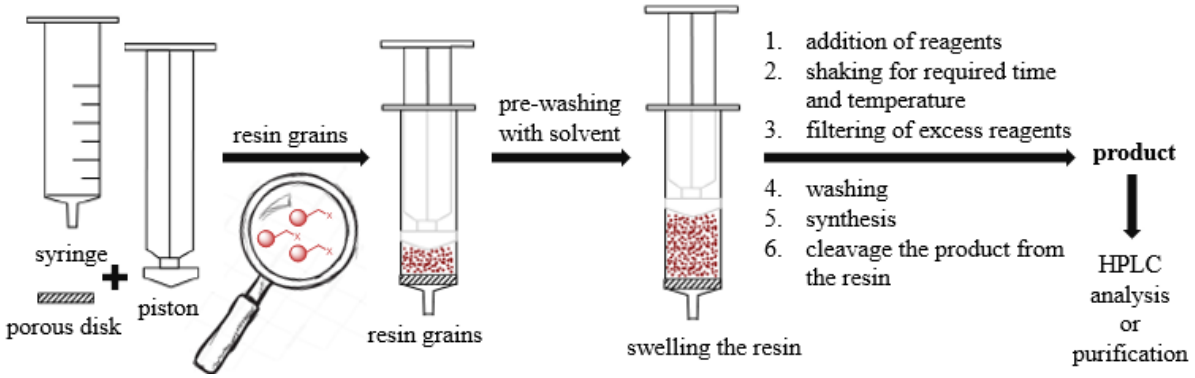

The polystyrene resins used in SPS have universally a gel-type structure allowing better penetration of reagents and solvents. The most frequently used type of the solid support is polystyrene resin cross-linked with divinylbenzene (DVB). The percentages of DVD affect the stability of the polymer during the synthetic process and its swelling capacity. The higher percentages of DVB are used, the lower swelling capacity the polymer has. For this reason, the cross-linked polystyrene resins with 1-2% DVB represent the most common type of polymers having sufficient swelling capacity and stability (Figure 3).[13]

Figure 3. The most common types of resins in SPS and their percentages of cross-linked DVB

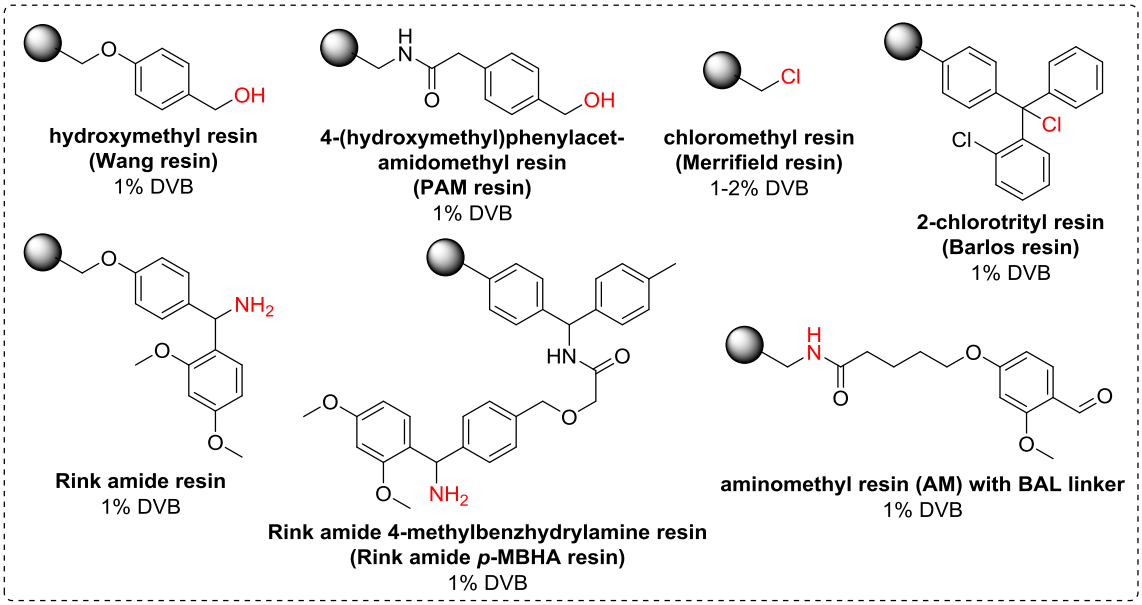

Further, use of suitable linkers represent another critical parameter in SPS. They should be stable throughout the synthesis, but they should allow to cleave product from the polymer support under specific conditions. Although the synthesis is theoretically feasible without the inserted linker between the polymer support and the first attached compound, the linker prevents synthesized product from undesired decomposition during the cleavage process. Linkers consist of two functional groups. One of them enables the covalent binding to the polymer support and it forms non-cleavable bond while the second functional group is used to immobilize the starting material to the solid support. This bond is covalent again; however, it is cleavable according to specific conditions depending on the type of linkers used (Figure 4).[14]

Figure 4. The role of linker on the solid support[14]

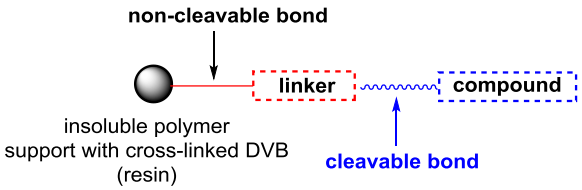

The first large class of linkers are acid-labile linkers (e.g. Wang linker, Rink amide linker, BAL linker, PAM linker etc.). They belong to the most used linkers in SPS[14] and they are generally cleavable using 50% trifluoroacetic acid (TFA) in dichloromethane (DCM).[15] The general principle of product cleavage from the resin is shown on an example of immobilized esters or amides (Scheme 1). It is based on a proton attack of a carbonyl group. After the shift of electrons, the resulting product is released from the polymer support and then the residual resin reacts with trifluoroacetyl anion providing the immobilized trifluoroacetyl ester.[14] Nevertheless, to release the product from the Merrifield resin and Rink amide *p*-MBHA resin, the use of stronger acids, e.g. 10% or neat hydrofluoric acid (HF),

hydrobromic acid (HBr) or triflic acid (TfOH), is required. These alternatives are not too popular due to their considerable danger to the surroundings;[16] however, we can often meet them.

Scheme 1. The general principle of product release from the solid support

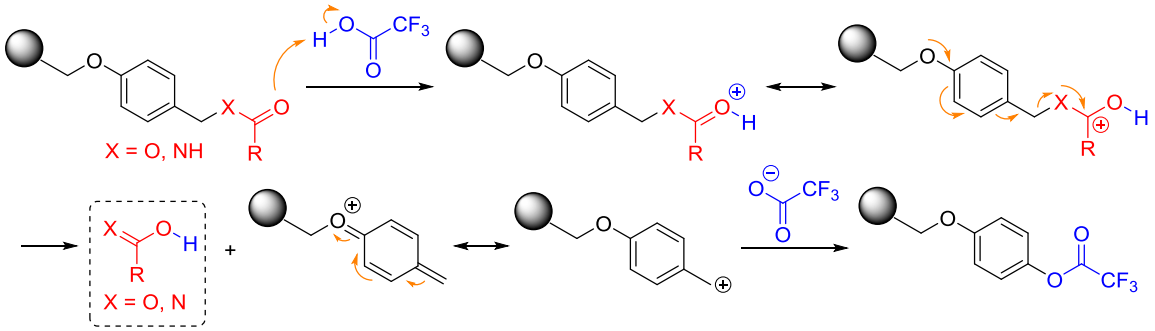

Moreover, some acid-labile linkers can eventually undergo the alkaline hydrolysis (saponification). In 1963, the hydrolysis of benzylesters yielding peptides was reported by Robert Bruce Merrifield who is called the father of solid-phase synthesis.[17] Besides the saponification, Rolland et al. reported the cleavage of polymer-supported methyl ester using alkali metal trimethylsilanolates (TMSOK, TMSONa).[18] Silyl linkers with C-Si[19,20] and O-Si[21] bonds are sensitive to acids or fluorides, e.g. tetrabutylammonium fluoride (TBAF). Additionally, some linkers are cleavable under neutral and mild conditions by photolysis;[22,23] however, the photolytic cleavage can cleave other bonds in the molecule thus the experiment requires extremely exact performance and conditions.

SPS is known for some advantages and disadvantages in comparison to solution-phase synthesis. Solid-phase chemistry represents one of basic and simple methods of organic synthesis to prepare many compounds using high-throughput synthetic concept. The method could be plainly converted to parallel semi-automated or fully automated protocols. For this reason, SPS has been a choice of pharmaceutical companies to prepare chemical libraries of various sizes. At the beginning of each synthetic strategy, the scientists should assess the suitability and usability of SPS according to type and number of optimization steps and the number of prepared compounds. In comparison to solution-phase chemistry, the general concept of SPS differs by the addition of two reaction steps into the sequence which were mentioned above in the text. All SPS reactions are done using significant reagents excess for the quantitative conversion of starting material to the product which can affect substantially the price of the synthesis. In addition, many reactions need lengthy and time-consuming optimizations of conditions which are typically more complex in comparison to solution-phase chemistry. Further, it is necessary to release the product from the solid support before each LC-MS analysis which somewhat prolongs the analysis time. Although it may appear that these negative limitations outweigh the advantages of the methodology, SPS received considerable attention due to easy and fast isolation of all reaction intermediates consisting of only filtering and washing off soluble by-products. In comparison to solution-phase chemistry, the polymer-supported intermediates do not allow full analytical characterization (HRMS, NMR etc.) after each reaction step but only at the end

of the reaction sequence. The application of SPS minimizes some losses during the synthetic process and allows the usage of high-boiling solvents, such as DMF, DMSO and NMP. It should be noted that in many cases, the cleaved intermediates are subjected to further (post-cleavage) modification thus the final compounds are achieved combining both solid-phase and solution-phase methodologies. Such post-cleavage modification has been frequently used also in several projects summarized in this thesis. In this regard, it has to be reminded that the post-cleavage modification steps should be performed using simple work-up procedures to avoid the loss of product (only small quantities of final compounds are typically synthesized) and/or to keep the high through-put synthetic concepts (to potentially apply the parallel synthesis).

1.3 Our previous research

The following brief introduction to previous morpholine and thiomorpholine chemistry is based on the results of my Diploma thesis[1] which were published in: Králová, P.; Fülöpová, V.; Maloň, M.; Volná, T.; Popa, I.; Soural, M. *ACS Comb. Sci.* **2017**, 19 (3), 173–180.[2] This article is attached in Appendix A (p. 144 – 151).

Our interest in the field of morpholines and thiomorpholines was inspired by the fact that these derivatives are widely studied compounds[24–29] with a broad application in agricultural,[30,31] pharmaceutical[32–34] and medicinal fields.[35] More specifically, we focused to morpholines, thiomorpholines and related unsaturated analogous (e.g. oxazines and thiazines) bearing the carbonyl group at the C3 position. My Diploma thesis was devoted to development of general synthetic route using solid-phase synthesis as there were only two reported articles devoted to the solid-phase synthesis of 3,4-dihydro-2*H*-1,4-oxazino-3-carboxylic acid derivatives which have been observed as synthetic by-products.[36,37]

My Diploma thesis[1] and the corresponding publication[2] reported the synthetic approach in which *N*-sulfonyl and *N*-acyl morpholine-3-carboxylic acid derivatives were synthesized from polymer-supported 2/4-nitrobenzensulfonamides (2/4-Nos-amides) which were converted to corresponding *α*-amino ketones. Generally, 2/4-Nos-amides and *α*-amino ketones were easily synthesized from readily available starting materials: (i) Fmoc-amino acids containing hydroxy or sulfanyl groups in the side chain, e.g. L-serine, L-threonine, L-cysteine; (ii) aryl/alkyl sulfonyl chlorides or carboxylic acid derivatives and (iii) *α*-bromoketones. The resulting *N*-alkyl-Nos-amides were treated with trifluoroacetic acid (TFA) which mediated the product release from the polymer-support and yielded expected unsaturated products, i.g. 1,4-oxazines and 1,4-thiazines. The saturated thio(morpholine) analogs were prepared using triethylsilane (TES) added into the cleavage cocktail. Further, we performed the stereochemical studies to reveal the configuration of the newly formed stereocenter C6 (Scheme 2, see the resulting products in rectangles on the right).

Moreover, detailed studies on rotational stability of *N*-acylmorpholines were performed. These derivatives were obtained as a mixture of inseparable rotational isomers (rotamers) around C-N amidic bond with the characteristic doubled signals in ^{1}H NMR spectra. These rotamers were obtained in different ratios depending on R^3 substitution and both isomers were investigated in detail using 2D NMR analysis.

Finally, my Diploma thesis showed the reduction test on the *N*-(2-nitrobenzoyl)-oxazines using sodium dithionite under acidic or basic conditions which afforded prospective amino derivatives theoretically applicable for further modification. Additionally, the reaction under acidic conditions (pH 1-2) triggered spontaneous cyclization of amino compound to fused [7+6] benzoxazino-diazepine-6,12-diones observed in 38% crude purity (Scheme 2). Stimulated by this preliminary result, we decided to explore this field during my Ph.D. studies to possibly apply 2/4-Nos-amides for preparation of diverse fused heterocycles.

Scheme 2. The shortened synthesis of *α*-amino ketones and their use to prepare morpholine derivatives

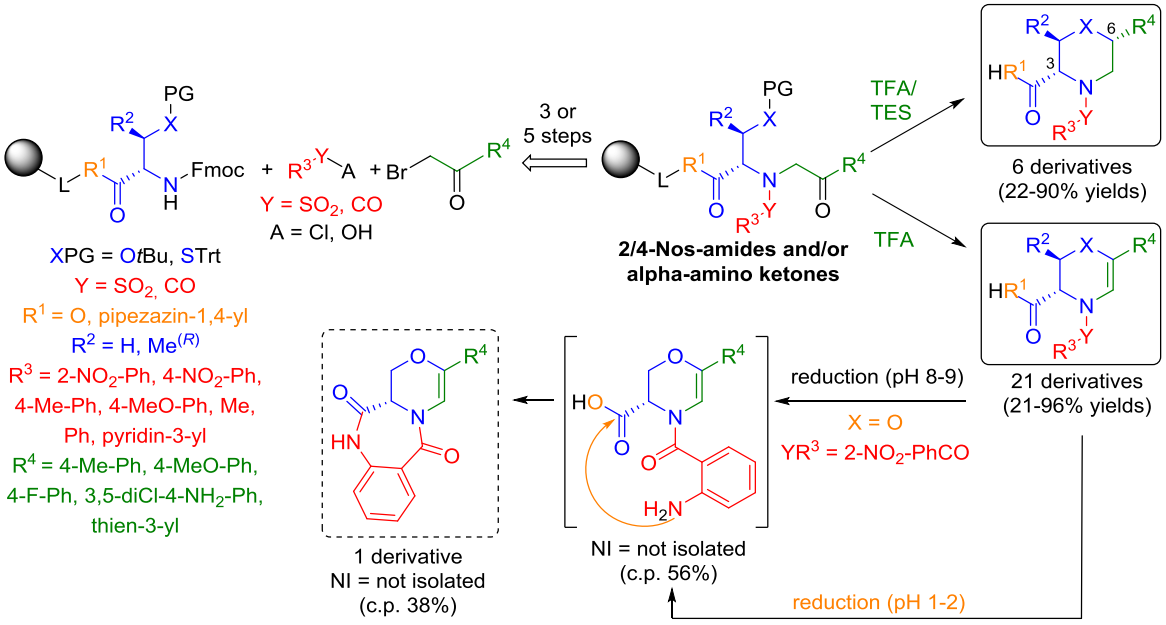

2. AIMS OF THE WORK

As stated above, the main goal of the thesis was to explore an applicability of the polymer-supported 2/4-Nos-amides as the key intermediates to prepare fused morpholine derivatives using solid-phase synthetic strategy (Figure 5-6). Consequently, it was suggested that polymer-supported 2/4-Nos-amides could be denosylated and further modified with various acylating or alkylating agents to obtain the suitable intermediates which could, after post-cleavage modification, yield the corresponding fused heterocycles. In all projects, we intended to determine the limitations and scope by using building blocks with different substitution and particularly to test TES applicability for stereoselective reduction of the double bond. In this regard, we wanted to study the configuration of all newly formed stereocenters using SFC and/or advanced NMR experiments.

First, the potential synthesis of fused [7+6] morpholine derivatives **I-II** was investigated in detail (Figure 5, **Products I-II**).[38,39] After that, the attention was paid to the preparation of fused [6+6] morpholines **III**[40] and diketomorpholines **IV**[41] (Figure 5, **Products III-IV**). We also suggested a methodology to prepare fused [6+5] heterocycles bearing the thiohydantoin scaffold **V** (Figure 5, **Product V**).[42,43] The last part of the thesis was oriented to the synthesis of functionalized 1,4-oxazepanes amenable for further diversification. In this case, the synthesis of oxazepane scaffold was suggested using four different possible scenarios **A-D** (Figure 6) which were inspired by the previously reported results from the field of 1,4-oxazepane derivatives.[4,44,45]

The research was carried out at the Institute of Molecular and Translational Medicine (IMTM) under the auspice of Department of Organic Chemistry, Palacký University Olomouc. Since the in-house screening of cytotoxic and antimicrobial activity was available, we intended to screen the target compounds against selected cancer cell lines and bacterial strains to possibly identify hit compounds for further development.

Figure 5. Overview of designed fused morpholine and thiomorpholine derivatives

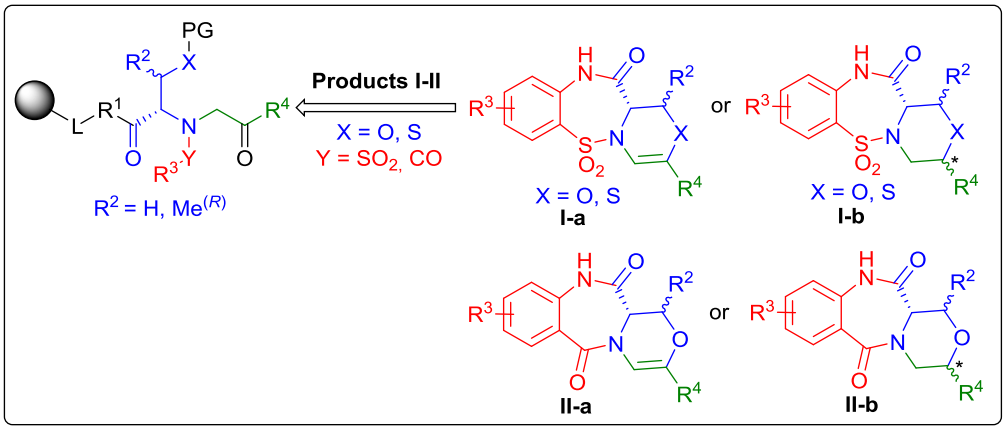

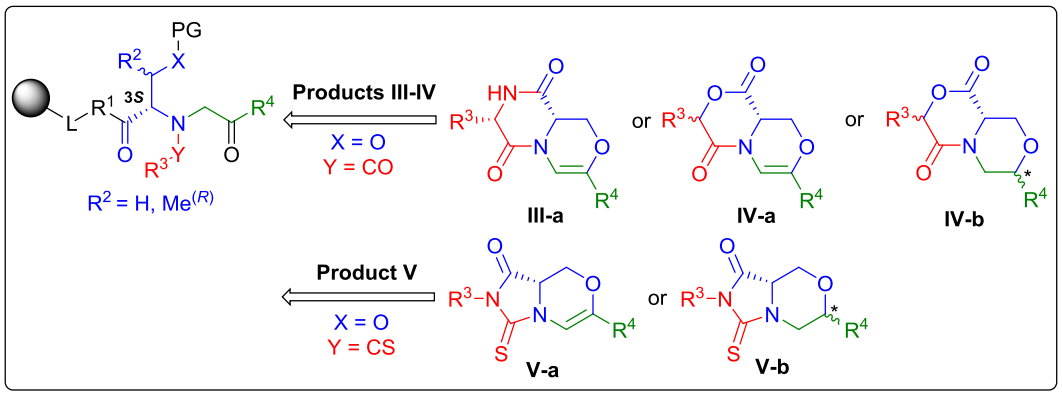

Figure 6. The possible approaches to functionalized 1,4-oxazepane derivatives

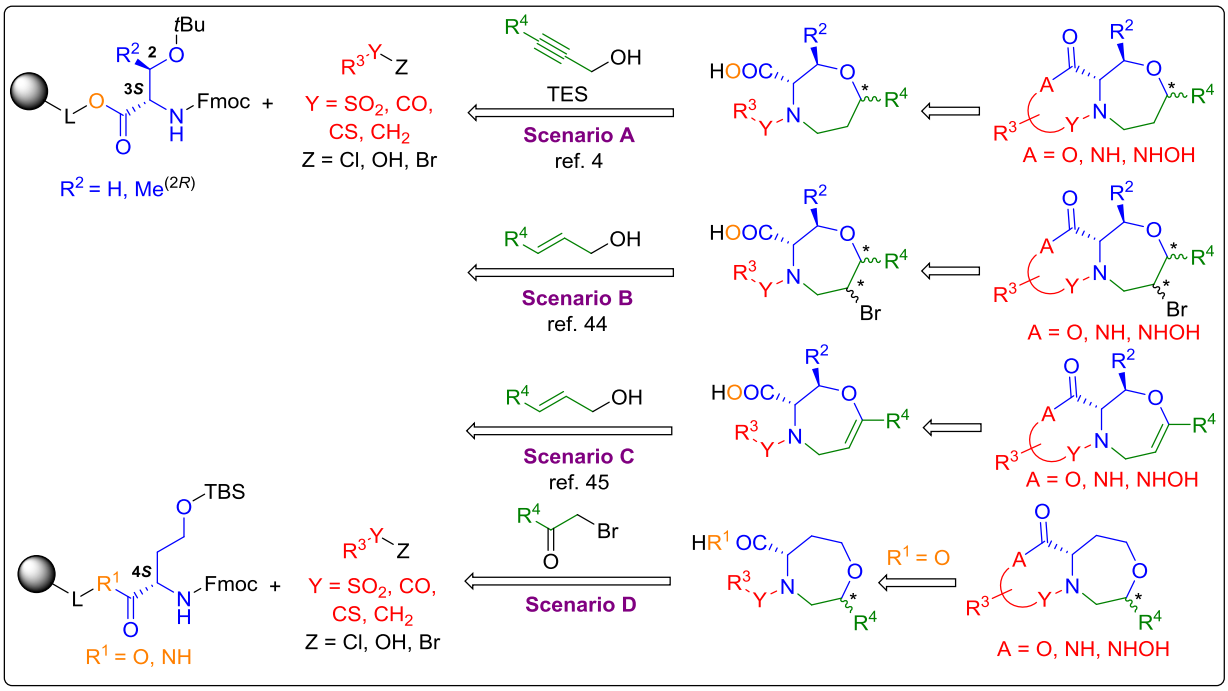

3. STATE OF THE ART

3.1 The application of immobilized 2/4-nitrobenzensulfonamides and *α*-aminoketones in heterocyclic chemistry

As the use of 2/4-nitrobenzensulfonamides (2/4-Nos-amides) was previously summarized in a well-arranged review,[10] *State of the art* of the thesis is primarily targeted to general application of immobilized *α*-amino ketones to synthesize diverse heterocyclic compounds. The individual subchapters are classified according to the size and type of the heterocyclic ring.

Generally, *α*-amino ketones have been applied to prepare diverse nitrogenous heterocycles using traditional solution-phase synthesis[46–51] or solid-phase synthesis.[3,36,52–55] The number of reported articles in the field of heterocyclic chemistry is obviously caused by simple synthetic availability and high reactivity of these intermediates. For this reason, the first part of this chapter shows only a brief overview of selected synthetic approaches yielding *α*-amino ketones using SPS or using combination of SPS and solution-phase chemistry.

Resin-bound *α*-amino ketones are readily available from primary amines or amino acids and from *α*-haloketones[56–58] or organometallic reagents, e.g. organolithium and organomagnesium compounds.[59,60] *α*-Amino ketones can be further modified using various electrophiles, e.g. sulfonyl chlorides,[56,58] carboxylic acid derivatives[53,59,61] or urea/thiourea derivatives[62,63] to yield corresponding products. The synthesis of *α*-amino ketones can be performed using three alternative ways (Scheme 3, Methods A-C). The method A displays the synthesis of immobilized *α*-amino ketones **3** from *α*-amino acids **1** and *α*-haloketones **2a** followed by *N*-acylation which yields the final derivatives **5**.[57] The opposite order of reaction steps results in Method B.[56,58] Both synthetic approaches provide resin-bound *α*-amino ketones which can be subjected to further on-resin modification; however, the reaction of *N*-acyl amino acids **7** with organomagnesium bromides **2b** leads to release from the resin (Method C). Except for shown ester, amide and thioester bonds, the starting amines can be anchored to the resin *via* carbamate, ether or alkylamine linkers.

Scheme 3. The general methods to synthesize *N*-acyl *α*-amino ketones using SPS concept

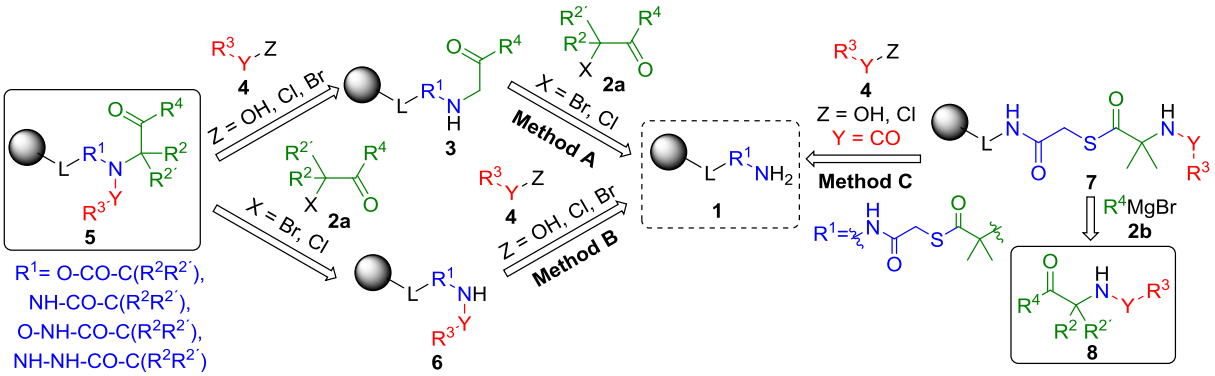

Besides the above-mentioned approaches, the synthesis *via* Weinreb amide can be applied.[64–66] Weinreb amides can be prepared from Weinreb amide resin **9**[60] or hydroxylamine Wang resin **13**,[59] Fmoc-amino acids and carboxylic acids. Generally, *α*-amino ketones **12** were obtained after a liberation of the polymer-supported Weinreb amide from the Weinreb amide resin **11**[60] or hydroxylamine Wang resin **14**[59] mediated by Grignard reagents (Scheme 4). Nevertheless, this methodology has significant limitations for disubstituted amino acids because of the steric influence of *α*-alkyl substituents.[67]

Scheme 4. The use of Weinreb amide resin **9**, **13** for solid-phase synthesis of *α*-amino ketones **12**[a]

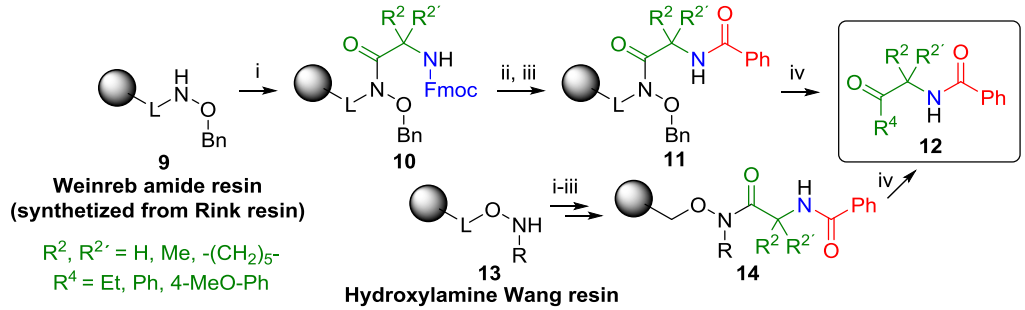

[a]Reagents and conditions: (i) Fmoc-amino acid, DIC, DMF/DCM (3:7), 3 days, rt; (ii) PIP/DMF (1:4), 20 min, rt; (iii) PhCOOH, DIC, HOAt, 5 h, rt; (iv) R^4MgBr, anhydrous THF, 18 h, rt; 2 derivatives (31-51% yields).

Tice et al. reported synthesis *via* Weinreb amide **17** immobilized on Wang resin converted to *p*-nitrophenyl chloroformate **18**. In this case, the authors combined both synthetic approaches, traditional solution-phase chemistry to prepare desired amide from Boc-*α*-methylalanine (Boc-Aib-OH) **15** and *N*,*O*-dimethylhydroxylamine hydrochloride **16**, and solid-phase synthesis which yielded the immobilized Weinreb amide **19**. The final product **22** was obtained after a three-step reaction sequence consisting of the reaction of intermediate **19** with the corresponding Grignard reagent and then product cleavage from the resin followed by *N*-acylation with activated carboxylic acid anchored to hydroxybenzotriazole resin (Scheme 5).[68]

Scheme 5. The synthesis of *α*,*α*-disubstituted-*N*-acyl *α*-amino ketones **22** *via* Weinreb amide in combination with solution-phase chemistry and SPS[a]

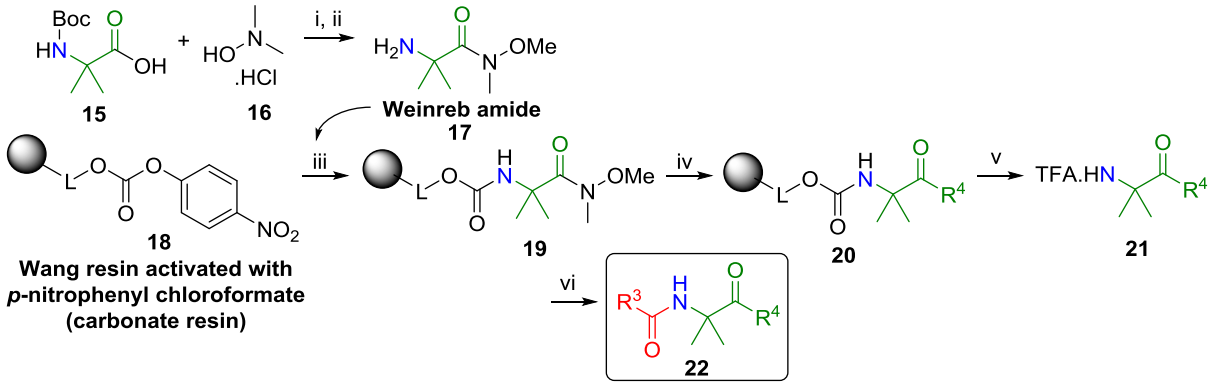

[a]Reagents and conditions: (i) DMAP, DIEA, DCC, DCM, 5 days, 25 °C; (ii) 50% TFA/DCM, 20 min, 25 °C; (iii) DIEA, NMP, 16 h, 60 °C; (iv) R^4MgBr, anhydrous THF, 4 h, 25 °C and then AcOH/DCM (9:1); (v) TFA/H_2O (95:5); (vi) hydroxybenzotriazole resin, R^3COOH, DIC, DMAP, DMF, DCM, 5 h 25 °C, then filtration and addition of a solution of DIEA, DCM and **21**, 16 h, 25 °C; 25 derivatives (61-92% yields).

Furthermore, the synthesis of *α*-amino ketones was performed *via* thioester linker which is resistant to conventional cleavage conditions.[69] Thioesters are generally more reactive toward Grignard reagents than methoxyamides and potentially less sterically demanding.[59] First, the starting thiol resin **18** was prepared using a three-step reaction sequence consisting of an acylation of Rink amide *para*-methylbenzhydrylamine (*p*-MBHA) resin **15** with bromoacetic acid and nucleophilic substitution of terminal bromide with thioacetic acid followed by 2-mercaptoethanol (MCE)-mediated removal of acetyl protecting group.[69,70] After that, Boc-Aib-OH was coupled with the thiol resin **18** followed by Boc-deprotection and acylation of the liberated amine **20** with benzoic acid. Finally, the *N*-acyl intermediate **21** was reacted with excess (3 equiv) of organomagnesium compounds, e.g. EtMgBr or PhMgBr, providing a mixture of the resulting *α*-amino ketones **12** and tertiary alcohols **22** in a ratio of 1:1 (Scheme 6). Although this approach afforded expected product, the applicability of the methodology was limited because of poor product purity.[59]

Scheme 6. The synthesis of the polymer-supported *α*-amino ketones **21** *via* thioesters[a]

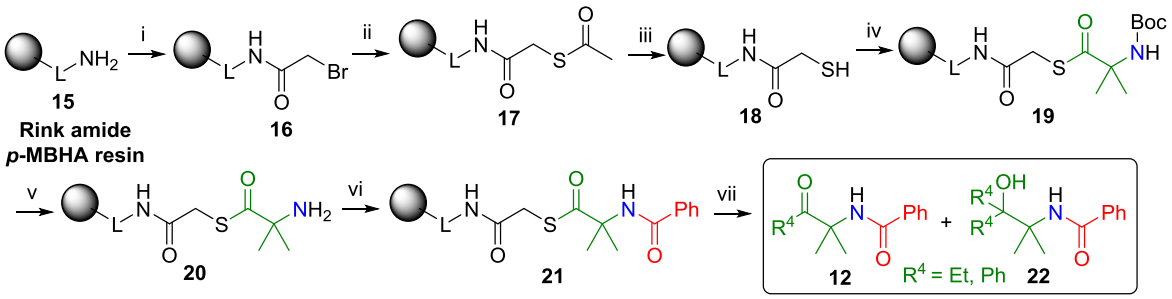

[a]Reagents and conditions: (i) $BrCH_2COOH$, DCC, DCM, 2 h, rt; (ii) 10% AcSH/DMF, DIEA, 2×20 min, rt; (iii) 10% MCE/DMF, DIEA, 2×20 min, rt; (iv) Boc-Aib-OH, HATU, DIEA, DMF, 2 h, rt; (v) 40% TFA/DCM, 20 min, rt; (vi) PhCOOH, DIC, HOBt, DCM, DMF, 2 h, rt; (vii) R^4MgBr, anhydrous THF, 30 min, 0 °C; 2 derivatives (50-60% yields).

3.1.1 The synthesis of five-membered heterocycles

This subchapter focuses on the most common five-membered heterocycles synthesized *via* *α*-amino ketones, i.e. imidazoles,[36,56,57] pyrrazoles,[36] pyrroles,[36] oxazoles,[61,63] thiazoles,[62,63] pyrrolinones[55] and their benzene-fused analogues.[35,55]

In 2009, Krchňák et al. reported the syntheses of indazole oxides **28**[56] and 1,2,4-trisubstituted-1*H*-imidazoles **36**[58] from immobilized 2/4-Nos-amides. In the first case, the starting 2-Nos-amides **24 (2-NO_2)** have undergone Fukuyama monoalkylation with various *α*-bromoketones providing polymer-supported *N*-alkyl 2-Nos-amides **25 (2-NO_2)**. Their DBU-mediated cyclization triggered the formation of indazole oxides **26** which were further cyclized to fused [6+5] pyrrazino-indazole oxides **28** in 16-96% yields (17 derivatives). In addition, fused [6+5] pyrazolo-pyrazines **30** and **32** were prepared *via* 2*H*-indazoles **29** from immobilized indazole oxides **26** in 7-99% yields (17 derivatives; Scheme 7, Pathway A and later in subchapter 3.1.4).[56]

The replacement of 2-Nos-amides to 4-Nos-amides pointed out a striking difference in the reaction outcome between both sulfonamides. Key 4-Nos-amides **25 (4-NO_2)** were prepared according

to the previously reported protocol[56] differed by the type of Nos-Cl used as sulfonylating agents.[58] The following cleavage of the 4-Nos protecting group using MCE/DBU yielded immobilized *α*-amino ketones **33** which were acylated with carboxylic acid derivatives to *N*-acyl derivatives **34**. These derivatives could be converted to imidazoles **36** using acid-catalyzed cyclization on the resin followed by TFA treatment to release the desired products; optionally these two steps could be reversed in solution. While the cyclization on the resin (**35**) required longer cyclization time, acyclic products **37** cyclized faster in solution. The purities and yields of both methods were comparable; however, the authors preferred cyclization on the resin to yield 48 representative derivatives in 6-81% yields (Scheme 7, Pathway B).[58]

Scheme 7. The reaction outcome of 2/4-nitrobenzensulfonamides[a]

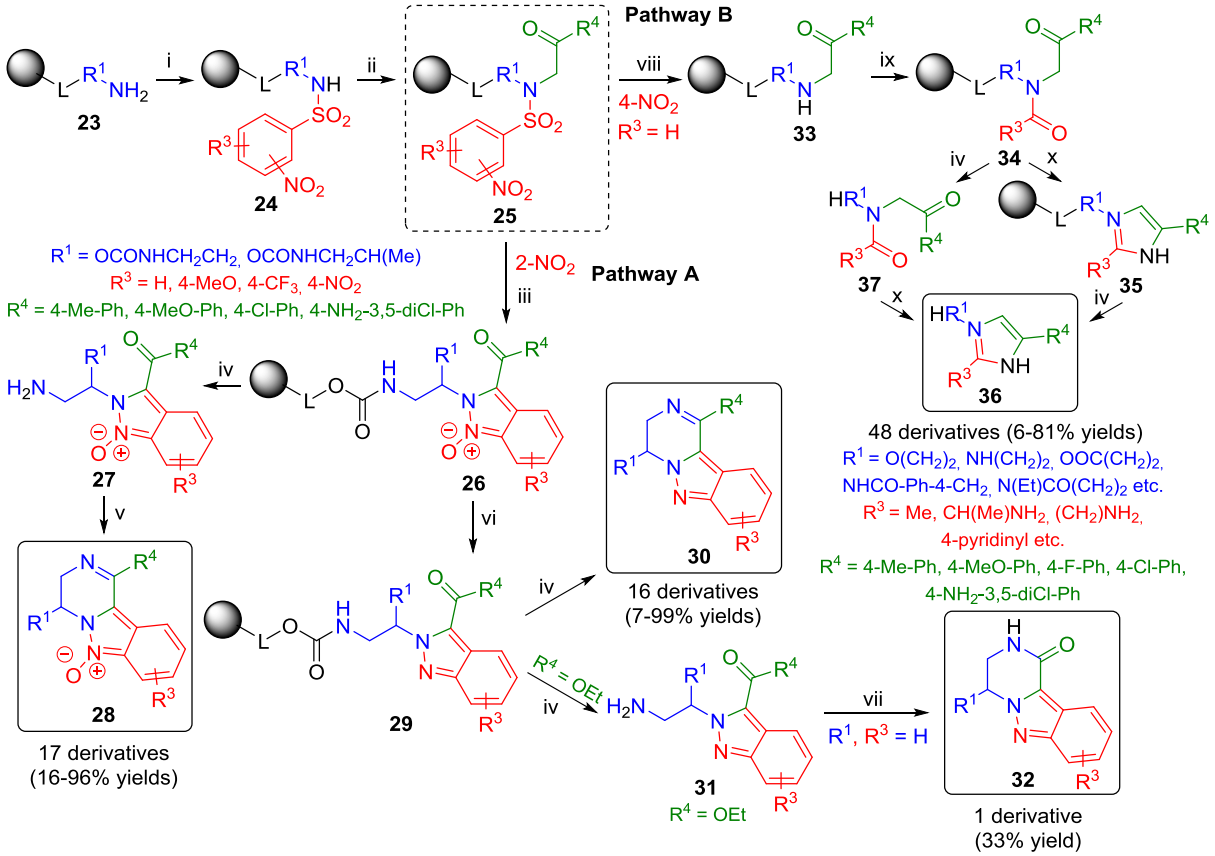

[a]Reagents and conditions: (i) R^3-substituted 2-Nos-Cl or 4-Nos-Cl, 2,6-lutidine, DCM, 16 h, rt; (ii) R^4COCH_2Br, DIEA, DMF, 16 h, rt; (iii) DBU, DMF, 30 min, rt; (iv) 50% TFA/DCM, 1 h, rt; (v) AcOH, 2 h, rt; (vi) MsCl, TEA, DCM, on, rt; (vii) TEA, MeOH, on, rt; (viii) MCE, DBU, DMF, 5 min, rt; (ix) R^3COZ (Z = OH, Cl, R^3COO), DCM, 16 h, rt; (x) AmAc, AcOH, 16 h, 100 °C; (xi) AmAc, AcOH, 6-10 h, 100 °C; 48 derivatives (6-81% yields).

To extend Krchňák´s research, Mjalli et al. had developed the similar methodology providing imidazoles **36** using immobilized *α*-amino ketones **38** anchored *via* ester or amide linkers. The synthesis of **36** was performed using a simple three-step procedure consisting of acid-mediated cyclization of *N*-acyl intermediate **34** according to above described conditions and the product cleavage from the polymer support (Scheme 8).[57]

Scheme 8. The alternative pathway for preparation of 1,2,4-trisubstituted-1*H*-imidazoles **36**[a]

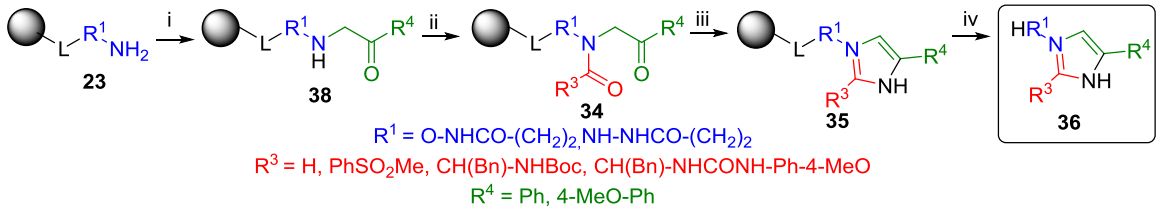

[a]Reagents and conditions: (i) DIEA, anhydrous THF, then R^4COCH_2Br, anhydrous DCM, 3-12 h, rt; (ii) R^3COOH, DIC, DMF, 12 h, rt; (iii) AmAc, AcOH, 10-20 h, 100 °C; (iv) 25% TFA/DCM, 0.5-1 h, rt.

In addition, the synthesis of indoles **45** (4 compounds, 3-37% yields) and indazole **46** (1 compound, 19%) derivatives containing at least one strong electron withdrawing CF_3 group as R^3 or R^4 substitutions were described. In this case, the Fukuyama monoalkylation of immobilized 2-Nos-amides **40** gave a mixture of two products, i.e. C-aryl products **41** and indazole oxides **42**. The subsequent reduction of nitro group using sodium dithionite and TFA-mediated release from the solid support provided the resulting separable compounds **45-46** in lower yields (Scheme 9).[36]

Scheme 9. The solid-phase synthesis of indoles **45** and indazole **46**[a]

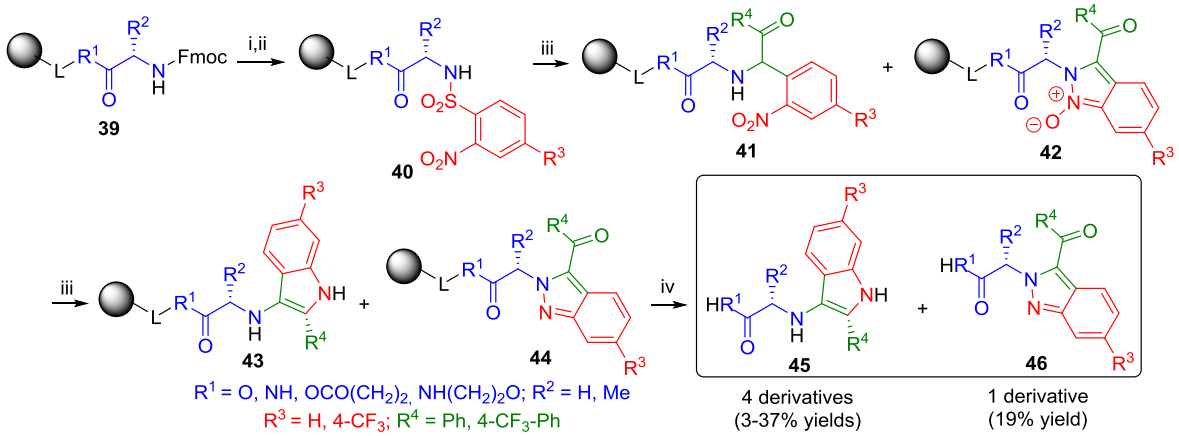

[a]Reagents and conditions: (i) 50% PIP/DMF, 30 min, rt; (ii) R^3-substituted 2-Nos-Cl, 2,6-lutidine, DCM, 16 h, rt; (iii) R^4COCH_2Br, DIEA, DMF, on, rt; (iv) $Na_2S_2O_4.2H_2O$, K_2CO_3, TBAHS, 50% DCM/H_2O, on, rt; (v) 50% TFA/DCM, 1 h, rt; 5 derivatives (3-37% yields).

Finally, the synthesis of oxazole and thiazole derivatives was reported. Oxazole/thiazole moieties occur in many natural products which exhibited a wide range of biological effects by interaction with nucleic acids and proteins.[62,63] The solid-phase synthesis of oxazoles **50**, **52** *via* Robinson-Gabriel reaction was explored in detail by Felder et al.[61] The authors investigated several different approaches, resins, cyclocondensation conditions and solvents for final cyclization (e.g. toluene, DCM, MeCN, DME, THF, 1,4-dioxane etc.); however, the synthesis was accomplished only using Rink amide resin. In the first protocol (Scheme 10, Pathway A), the immobilized *α*-amino ketones **49** were prepared using reductive amination of glyoxals and Rink amide resin **47**. Their *N*-acylation with acyl chlorides and the treatment of product **49** with trifluoroacetic anhydride (TFAA) provided disubstituted 1,3-oxazoles **50** in 71-72% yields (2 derivatives); however, the synthesis was applicable only for aromatic substituents in R^3 = Ph, 4-Br-Ph and R^4 = Ph.[61] Additionally, Ugi-four multicomponent

reaction consisting of Rink amide resin **47**, glyoxals, carboxylic acids and isocyanides was designed for a one-step synthesis of immobilized *α*-amino ketones **51**. Their TFAA cleavage from the resin afforded expected trisubstituted oxazoles **52** in 39-40% yields (2 derivatives, Scheme 10, Pathway B).[61]

Scheme 10. The solid-phase synthesis of substituted oxazoles **50**, **52** *via* amide linker[a,b]

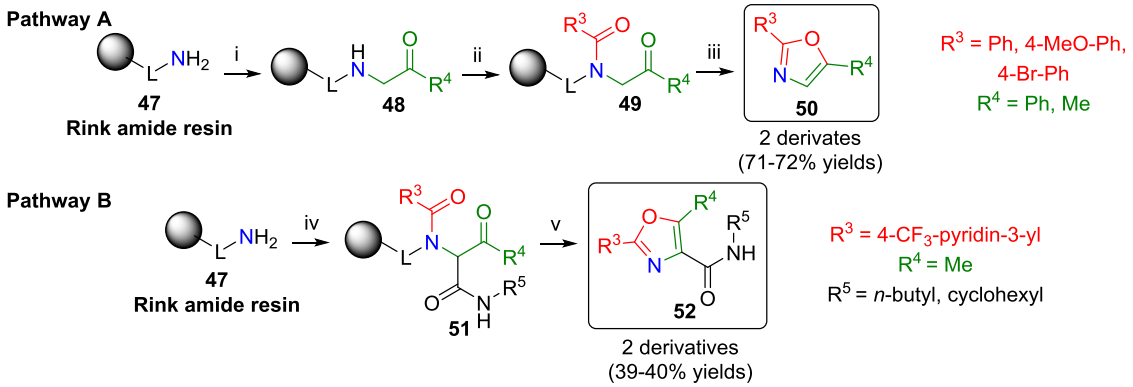

[a]Reagents and conditions: (i) R^4COCHO, AcOH, DCM, 7 h, rt, then add Cl_3SiH, on, rt; (ii) R^3COCl, DIEA, DCM, 5 h, rt; (iii) TFAA/DME (1:3), on, rt; (iv) R^3COOH, R^4COCHO, R^5NC, DCM/MeOH (2:1), 24 h, rt; (v) 25% TFAA/DME, 6 h, rt.

2-Aminothiazoles and oligoaminothiazoles are useful agents in different fields, e.g. in medicine as dopamine agonists used as anti-Parkinsonian agents,[62] or in electrochemistry as compounds with great thermal stability.[71] Scheme 11 depicts the parallel synthesis of diversified oligoaminothiazoles **58**, **60** prepared from Rink amide MBHA resin-supported oligopeptides **52** and **59**. Oligopeptides **52** were reduced to alkanes **54** using a solution of borane in THF followed by the reaction with Fmoc-isothiocyanate (Fmoc-NCS) to thiourea derivatives **55**. Their modification to thiazole derivatives **58** was done by a three-step sequence consisting of Fmoc-deprotection using a mixture of PIP/DMF, heating with *α*-haloketones in DMF and HF-mediated product cleavage from the solid-support. The final products **58** were obtained in excellent yields (84-94%, 23 derivatives). Moreover, the developed methodology was utilized to synthesize tetraaminothiazoles **60** in great yields again (82-87%, 7 derivatives), prepared from the corresponding tripeptides **59**.[62]

Scheme 11. The parallel synthesis of oligoaminothiazoles **58** and **60**[a]

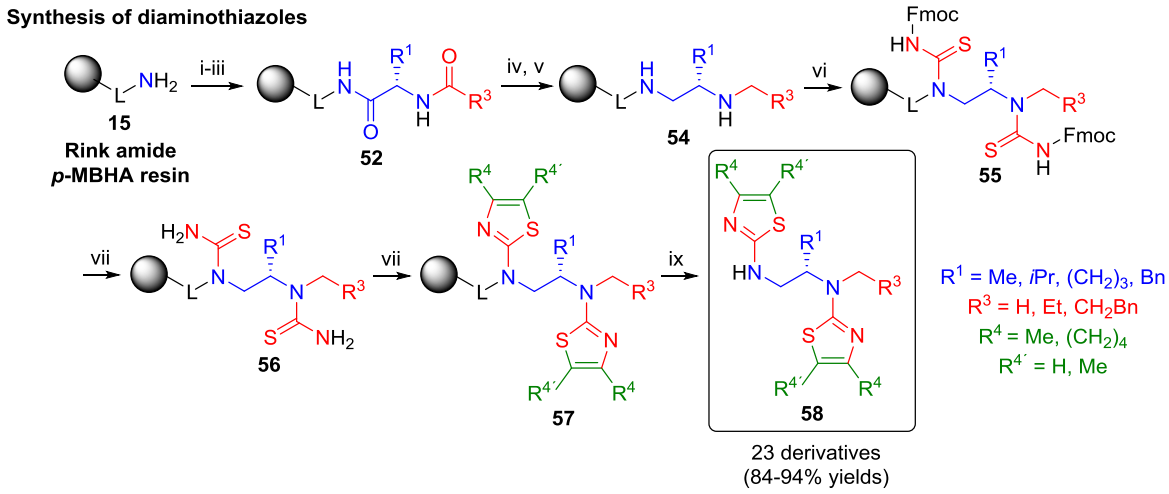

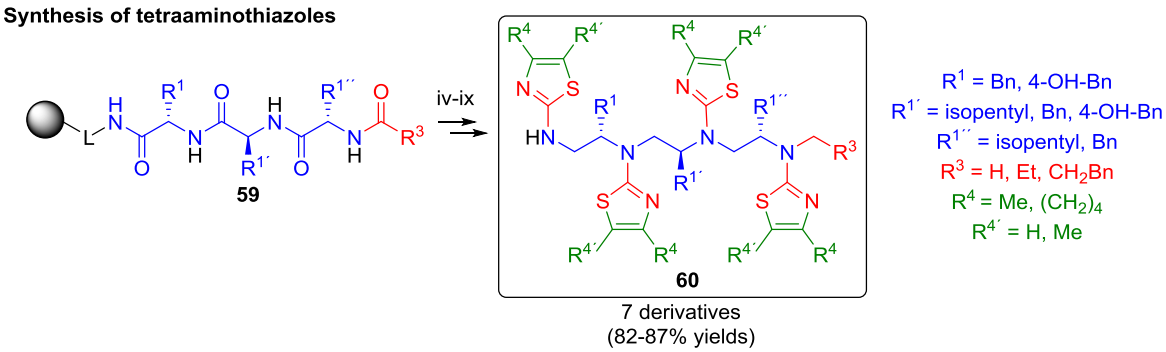

[a]Reagents and conditions: (i) Boc-amino acid, HOBt, DIC, DMF, 2 h, rt; (ii) 55% TFA/DCM, 30 min, rt; (iii) R^3COOH, DIC, DMF, on, rt; (iv) BH_3.THF, 72 h, 65 °C; (v) PIP, on, 65 °C; (vi) Fmoc-NCS, DMF, on, rt; (vii) 20% PIP/DMF, 2×10 min, rt; (viii) $R^4COCHR^{4'}X$, DMF, on, 70 °C; (ix) anhydrous HF, 1.5 h, 0 °C.

At the beginning of the second millennium, the combination of SPS and traditional solution-phase synthesis have received much attention. Whereas a parallel synthesis of both components (oxazole and thiazole scaffolds) has been reported rarely, the synthesis of oxazol-thiazole bis-heterocycles was published by Nefzi et al. in 2014.[63] First, oxazole amino acids **64** were prepared in solution from serine methyl ester and various amino acids **61** *via* HOBt coupling. This was followed by cyclodehydratation with diethylaminosulfur trifluoride (DAST) and oxidation mediated by bromotrichloromethane ($BrCCl_3$) which furnished oxazole esters **63**. The following hydrolysis using NaOH yielded oxazole-3-carboxylic acids **64** which were hung on Rink amide *p*-MBHA resin **15** and subjected to Boc-deprotection using TFA. The resulting intermediates **65** were converted to products **68**[63] using a three-step sequence which was somewhat similar to the previously reported protocol (20 derivatives in 56-89% yields; Scheme 12).[62]

Scheme 12. The parallel synthesis of oxazol-thiazole bis-heterocycles **68**[a]

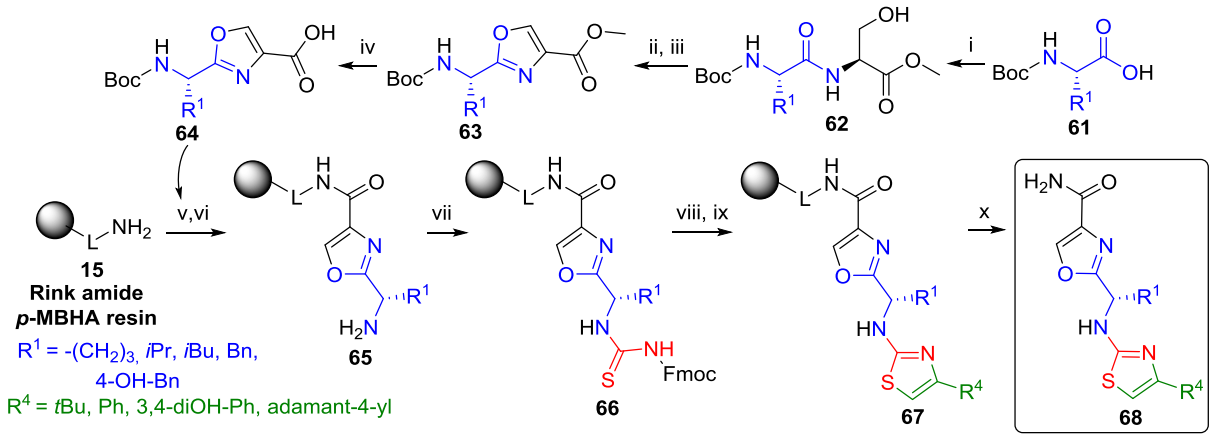

[a]Reagents and conditions: (i) HOBt, DIC, DIEA, DCM, 1 h, 0 °C, then Fmoc-L-Ser-OMe.HCl, 8 h, rt; (ii) DAST, DCM, -78 °C; (iii) $BrCCl_3$, DBU, DCM, 0 °C; (iv) 1N NaOH (aq), dioxane/H_2O, 10% $KHSO_4$ (aq), 0 °C; (v) HOBt, DIC, DMF, on, rt; (vi) 55% TFA/DCM, 30 min, rt; (vii) Fmoc-NCS, 10 h, rt; (viii) 20% PIP/DMF, 10 min, rt; (ix) R^4COCH_2X, DMF, on, 80 °C; (x) HF-cleavage; 20 derivatives (56-89% yields).

Finally, Jones et al. reported a simple procedure to synthesize 3-carboxypyrrolinones **77**. First, alkyl amino alcohols **72** were prepared in solution using reductive amination and then coupled to the

polymer-supported malonic acid **73**.[55] The obtained secondary alcohols **74** were oxidized to ketones **75** using *in situ* generated di-*tert*-butyl chromate ($CrO_2(OtBu)_2$)[72] and then exposed to the on-resin mediated cyclization to yield 7 representative compounds **77** in 64-96% yields (Scheme 13). The developed methodology was applied to prepare analogous compounds started from alkenes to obtain 4 derivatives in 73-99% yields.[55]

Scheme 13. The combination of SPS and solution-phase chemistry to prepare 3-carboxypyrrolinones **77**[a]

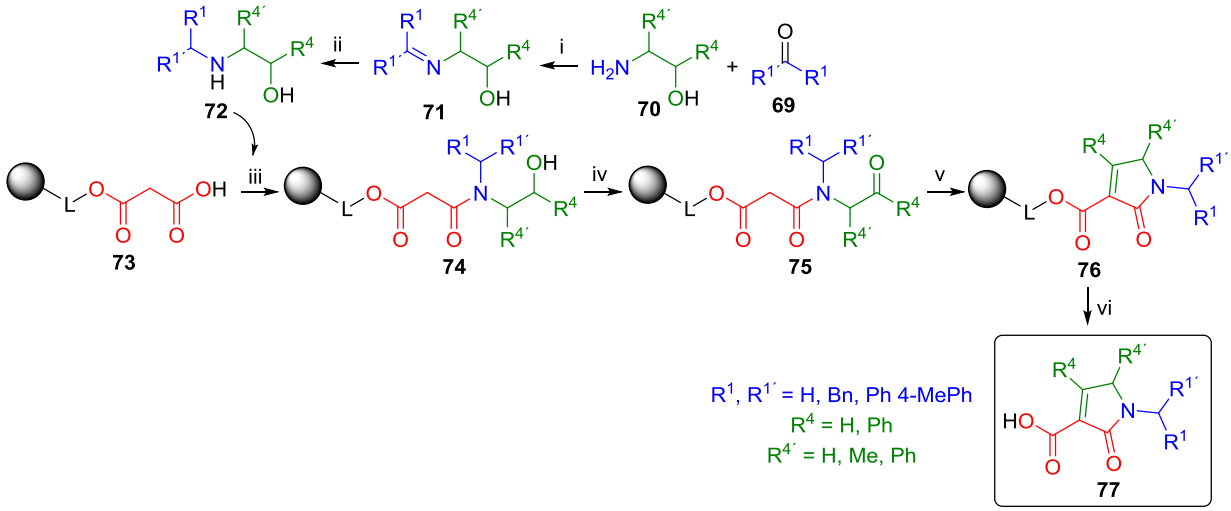

[a]Reagents and conditions: (i) $MgSO_4$, DCM, 8-18 h, rt; (ii) $NaBH_4$, MeOH, 8-18 h, 0 °C to rt; (iii) HOBt, DIC, DMF, 12-120 h, rt; (iv) a solution of *t*BuOH, Py, DCM cool in a CO_2/acetone bath, then add CrO_2Cl_2, 5 min ($CrO_2(OtBu)_2$ generated *in situ*), then add to the resin, 28 h, rt; (v) LiHDMS, $ZnCl_2$, anhydrous THF, -78 °C to 0 °C, then 1.5-2 h; (vi) 50% TFA/$CDCl_3$, rt; 7 derivatives (64-96%).

3.1.2 The synthesis of six-membered heterocycles

This subchapter is dealing with a preparation of six-membered heterocycles from 2/4-Nos-amides and *α*-amino ketones using SPS, e.g. quinazoline,[54] pyrazine,[57,73] oxazine[2,36,37,74–76] and thiazine derivatives.[77–79]

A well-known group of six-membered heterocycles are quinazolines which have been extensively studied. In 2015, Krchňák et al. reported the preparation of 4-benzoylquinazolines **84** synthesized from polymer-supported *N*-alkyl sulfonamides **80**. The reaction with DBU triggered the base-catalyzed tandem C−C bond formation followed by cyclization to indazole oxides **81** *via* N−N bond formation[80] and subsequent conversion of the indazole oxides **81** to quinazolines **82**.[54,81] The releasement of resin-bound benzoquinazolines generated carboxylates **83** as it was confirmed by LC-MS analysis; however, relatively fast decarboxylation to products **84** (1-5 h) was triggered by AmAc/MeCN during semipreparative reverse-phase HPLC purification (Scheme 14). The rate of decarboxylation was dependent on the character of R^4 substituent and it was slowed in the case of electron withdrawing substituents.[54]

Scheme 14. The synthesis of polymer-supported quinazolines **84** *via* nosylamides[a]

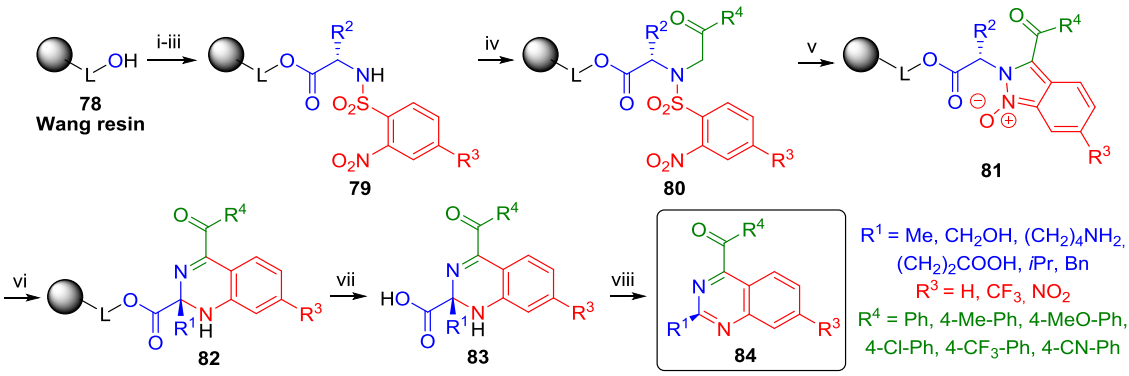

[a]Reagents and conditions: (i) Fmoc-amino acid, HOBt, DMAP, DIC, DCM, DMF, on, rt (ii) 50% PIP/DMF, 15min, rt; (iii) R^3-substituted 2-Nos-Cl, 2,6-lutidine, DCM, on, rt; (iv) R^4COCH_2Br, DIEA, DMF, on, rt; (v) DBU, DMF, 30 min, rt; (vi) DBU, DMF, on, rt; (vii) 50% TFA/DCM, 1 h, rt; (viii) AmAc/MeCN, 1-5 h, rt or semipreparetive reverse-phase HPLC purification with AmAc/0.1% TFA/MeCN and then lyophylization; 13 derivatives (8-56% yields).

Also, pyrazine derivatives were synthesized from polymer supported Nos-amides. In the first stage, 2-oxopyrazoles **86** were prepared from immobilized *N*-acyl *α*-amino ketones **39** anchored *via* ester or amide linkers.[57] The treatment of **39** with various amines and the final product cleavage from the solid-support yielded the appropriate pyrazines **86** (3 derivatives; Scheme 15).[57]

Scheme 15. The solid-phase synthesis of 2-oxopyrazole derivatives **86**[a]

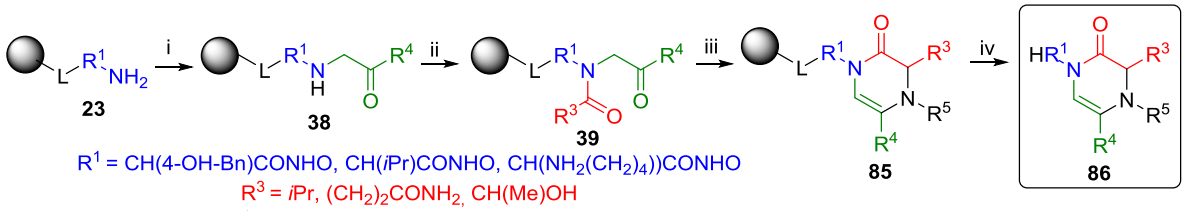

[a]Reagents and conditions: (i) DIEA, anhydrous THF, then R^4COCH_2Br, anhydrous DCM, 3-12 h, rt; (ii) Fmoc-amino acid, anhydrous NMP, HOBt, EDC, DMF, 12-18 h, rt; (iii) 25% PIP/DMF, 5 min, rt and R^5NH_2, then 30 min, rt; (iv) 25% TFA/DCM, 0.5-1 h, rt; 3 derivatives.

Later, Nadzan et al. developed an alternative approach to obtain 2-oxopyrazole derivatives **97**. The strategy was based on a one-step Ugi four-component reaction of carboxylic acid **87**, ketone **88**, aminoketone/aminoaldehyde protected with ketal/acetal groups **89** and isocyanide **90** providing the immobilized *α*-amino ketones **91**, which were treated with TFA to cleave from the solid support (Scheme 16, Pathway A). Four different strategies were reported depended on the anchoring of individual component to the solid support (Scheme 16, Pathway A-D).[73]

Scheme 16. A one-step Ugi multicomponent reaction yielding 2-oxopyrazole derivatives **92**[a]

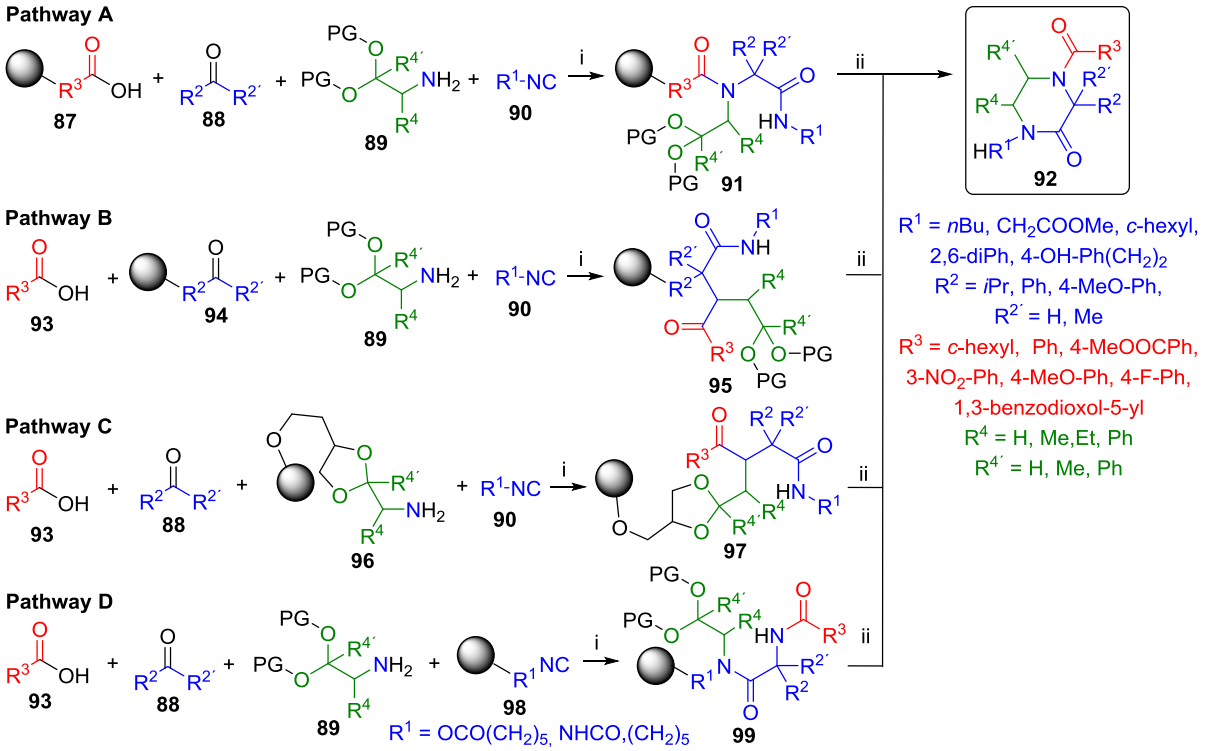

[a]Reagents and conditions: (i) 50% CH_3Cl/MeOH, on, rt; (ii) 20% TFA/DCM, 1 h, rt; 15 derivatives.

In addition, pyrazino[4,3-*a*]indole-1-one **102** (Scheme 17, Pathway A) and pyrazino[2,1-*a*]isoquinolin-1-one derivatives **104** (Scheme 17, Pathway B) were synthesized from the corresponding α-amino ketones by the reaction with 6-hydroxy-1,2,3,4-tetrahydro-isoquinoline-1-carboxylic acid and Fmoc-1*H*-indole-2-carboxylic acid.[57]

Scheme 17. The solid-phase synthesis of pyrazine derivatives **102** and **104**[a]

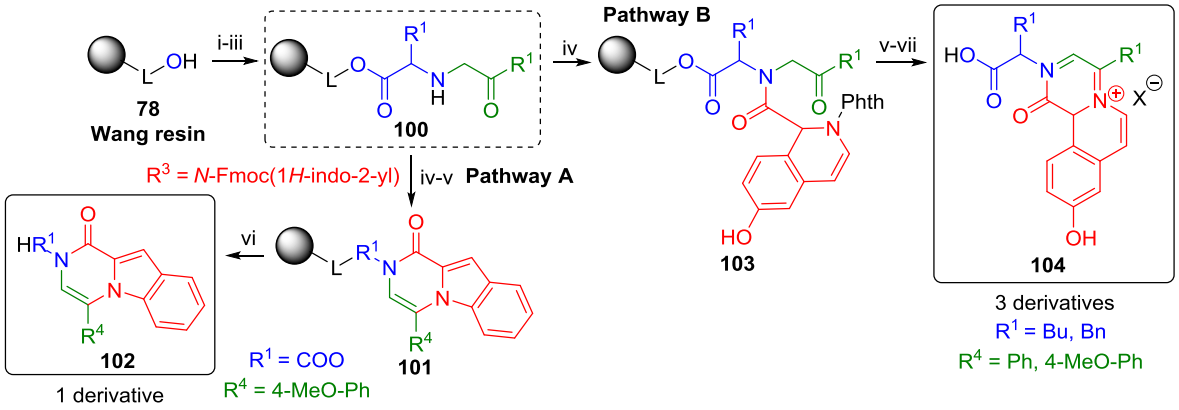

[a]Reagents and conditions: (i) Fmoc-amino acid, anhydrous NMP, HOBt, EDC, DMF, 12 h, rt; (ii) 25% PIP/DMF, 5 min, rt and then 30 min, rt; (iii) DIEA, anhydrous THF, then R^4COCH_2Br, anhydrous DCM, 3-12 h, rt; (iv) 6-hydroxy-1,2,3,4-tetrahydro-isoquinoline-1-carboxylic acid or Fmoc-1*H*-indole-2-carboxylic acid, anhydrous NMP, HOBt, EDC, DMF, 12-18 h, rt; (v) deprotection; (vi) 25% TFA/DCM, 0.5-1 h, rt; (vii) $MeCN/H_2O$, rt.

The further attention has been paid also to oxazine and thiazine derivatives. For example, immobilized 2/4-Nos-amides and *α*-amino ketones were used to synthesize oxazines/thiazines **115**

and morpholines/thiomorpholines **116** (Scheme 20, Pathway B) which were obtained during the solid-phase synthesis of 1,4-benzodiazepin-5-ones **114** (Scheme 20, Pathway A) started from L-serine, L-threonine and L-cysteine.[2,82] Further, immobilized 2-Nos-amines (Scheme 21) were used to prepare benzothiazine 1,1-dioxides **122** *via* unexpected rearrangement of benzothiadiazepine 1,1-dioxides **121**. Both methodologies are discussed later in the paragraph 3.1.3.

Recently, the known solid-phase synthetic approaches to prepare heterocycles bearing oxazine and thiazine scaffolds were summarized in a review article.[11] The manuscript: Králová, P.; Ručilová, V.; Soural, M. *ACS Comb. Sci.* **2018**, *20* (9), 529–543 is attached in Appendix B at the end of the thesis (p. 153 – 167 and shows the applicability of *α*-amino ketones[2,36,37,74–79] to synthesize the target heterocycles (Scheme 18).

Scheme 18. List of oxazines and thiazines (without showing further substitution of the scaffold) accessible from immobilized *α*-amino ketones[11]

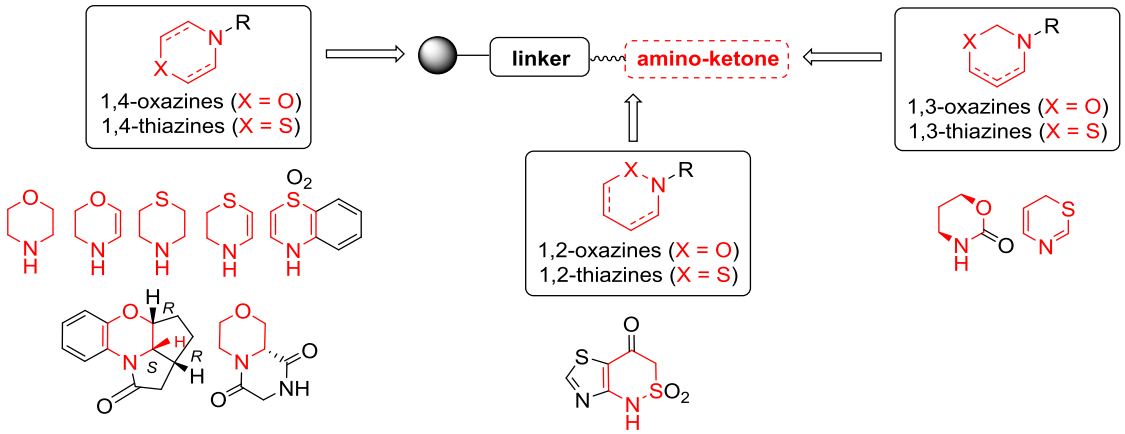

3.1.3 The synthesis of seven-membered heterocycles

This subchapter is devoted to the preparation of seven-membered heterocycles, especially to diazepine derivatives synthesized from 2/4-Nos-amides and *α*-amino ketones. In the literature, the syntheses of 1,4-benzodiazepin-5-ones[3,57,82] and benzothiadiazepine 1,1-dioxides[36,78] are reported.

1,4-benzodiazepin-5-ones were obtained using two different synthetic approaches *via* immobilized 4-Nos-amides and *α*-amino ketones (Schemes 19-21). In the first case, 4-Nos-amides **25** anchored *via* ether (aminoethanol linker), ester (*β*-amino acids) or amide functionalities (Rink amide resin and aminomethyl resin with BAL linker) were subjected to MCE/DBU-mediated deprotection to remove the 4-Nos protecting group (**33**) followed by *N*-acylation with 2-nitrobenzoic acid and reduction of the nitro group on the resin. The resulting amino derivatives **106** were cleaved from the solid-support which yielded 1,4-benzodiazepin-5-ones **107** in 14-33% yields (12 derivatives, Scheme 19).[3]

Scheme 19. The solid-phase synthesis of 1,4-benzodiazepin-5-one **107** derivatives *via* 4-Nos-amides[a]

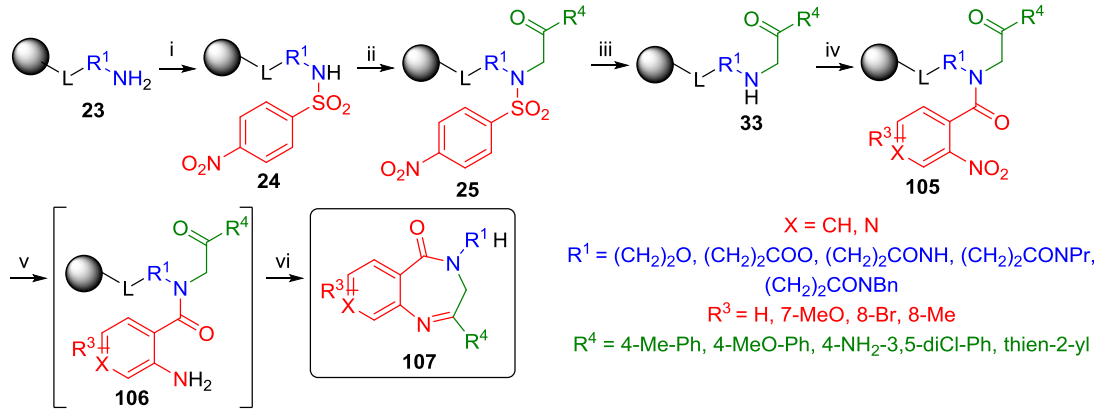

[a]Reagents and conditions: (i) 4-Nos-Cl, 2,6-lutidine, DCM, 16 h, rt; (ii) R^4COCH_2X, DIEA, DMF, 16 h, rt; (iii) MCE, DBU, DMF, 10 min, rt; (iv) R^3-substituted 2-NO_2PhCOOH, DIC, DMF, 16 h, rt; (v) SnCl.2H_2O, DIEA, degassed DMF, 16 h, rt (repeated); (vi) 50% TFA/DCM, 30 min, rt; 12 derivatives (14-33% yields).

To investigate the possible synthesis of 1,4-benzodiazepin-5-ones **114** derived from α-amino acids (Scheme 20, Pathway A, 3 derivatives in 12-29% yields), the same approach was applied using immobilized amino acids **109** (Scheme 20, Pathway B, 3 derivatives in 13-79% yields).[82] Nevertheless, the use of hydroxy/sulfanyl group containing amino acids,[1,2] such as L-serine, L-threonine and L-cysteine led to the formation of 1,4-oxazine (X = O) and 1,4-thiazine (X = S) derivatives **115** after the cleavage of *N*-alkyl-*N*-sulfonyl **110** and *N*-acyl intermediates **112** from the solid-support (3 derivatives, 13-77% yields). This reaction was later extensively studied to determine limitations and

Scheme 20. The solid-phase approaches leading to 1,4-benzodiazepin-5-ones **114** and oxazines/thiazines **115-116** depending on R^2 substituent[a]

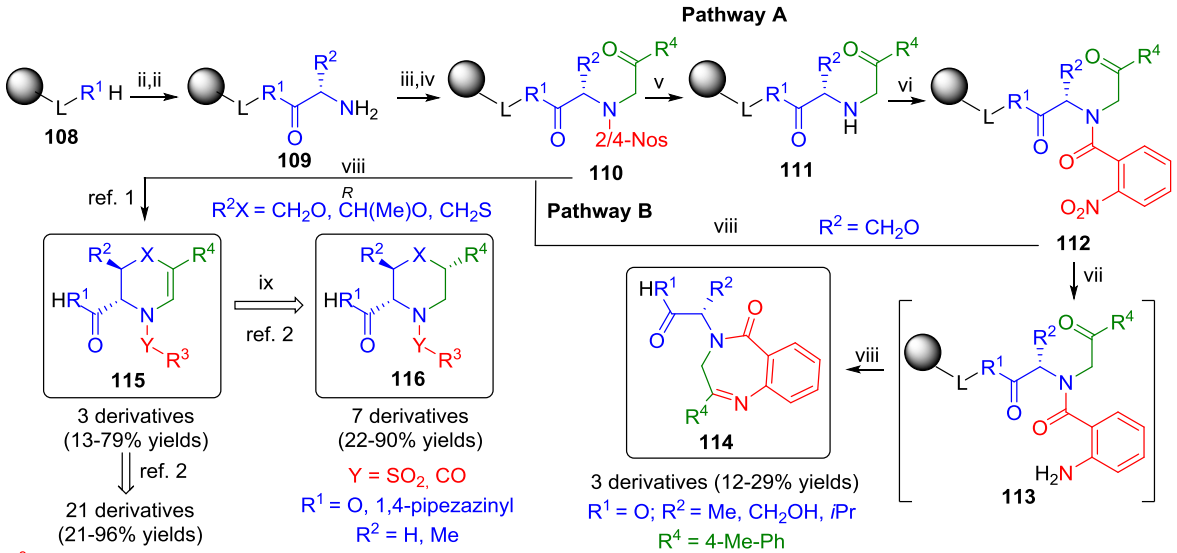

[a]Reagents and conditions: (i) Fmoc-amino acid, HOBt, DMAP, DIC, DCM, DMF, 24 h, rt; (ii) 50% PIP/DMF, 30 min, rt; (iii) 2/4-Nos-Cl, 2,6-lutidine, DCM, 24 h, rt; (iv) R^4COCH_2Br, DIEA, DMF, 24 h, rt; (vi) MCE, DBU, DMF, 30 min, rt; (iv) 2-NO_2PhCOOH, DIC, DMF, 2 d, rt; (vi) SnCl.2H_2O, DIEA, degassed DMF, 24 h, rt (repeated) or $Na_2S_2O_4$.2H_2O, K_2CO_3, TBAHS, 50% DCM/H_2O, on, rt; (viii) 50% TFA/DCM, 24 h, rt (X = O), or neat TFA, 6-9 h, rt (X = S); (ix) TFA/TES/DCM (10:1:9), 5-8 h, rt or 50% TFA/DCM, 24 h, rt, then TES, 1 h, rt.

scope for R^1-R^4 substitutions and the TES applicability for stereoselective reduction to receive morpholine (X = O) and thiomorpholine (X = S) derivatives **116** (28 derivatives, 21-96% yields).[2]

Mjalli et al. reported the solid-phase synthesis of 1,4-benzodiazepin-5-ones **114** using a slightly different building blocks, thus starting from polymer-supported α-amino ketones **117** followed by the coupling with anthranilic acid under bromotripyrrolidinophosphonium hexafluorophosphate (PyBroP)-catalysis. The final products **118** were cleaved by TFA from the resin to yield 3 derivatives (Scheme 21).[57]

Scheme 21. The alternative synthesis of 1,4-benzodiazepin-5-ones **114** *via* immobilized *α*-amino ketones[a]

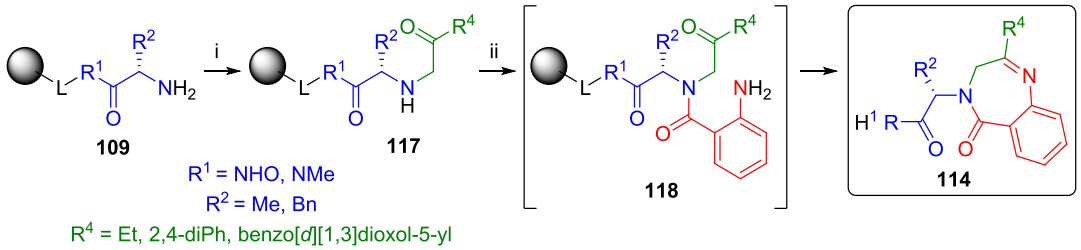

[a]Reagents and conditions: (i) DIEA, anhydrous THF, then R^4COCH_2Br, anhydrous DCM, 3-12 h, rt; (ii) anthranilic acid, THF, DIEA, DCE, then add PyBroP, DCE, 18 h, rt; (iii) 25% TFA/DCM, 30 min, rt; 3 derivatives.

Finally, Krchňák et al. developed the simple synthetic protocol to prepare benzothiadiazepine 1,1-dioxides **121**. The synthesis was performed according to above described procedure;[2] however, 2-nitrobenzoic acid derivatives were replaced with substituted 2-Nos-Cls. The TFA cleavage of amine derivatives **119** from the resin triggered the slow cyclization of acyclic intermediate **120** to corresponding benzothiadiazepinone 1,1-dioxides **121**; however, the final cyclization was furnished in DMSO-d_6 for 1.3-6.3 days providing 12 derivatives in 13-77% yields (Scheme 22, Pathway A).[36]

Scheme 22. The synthesis of benzodiazepinone analogues **121** started from immobilized 2-Nos-amides[a]

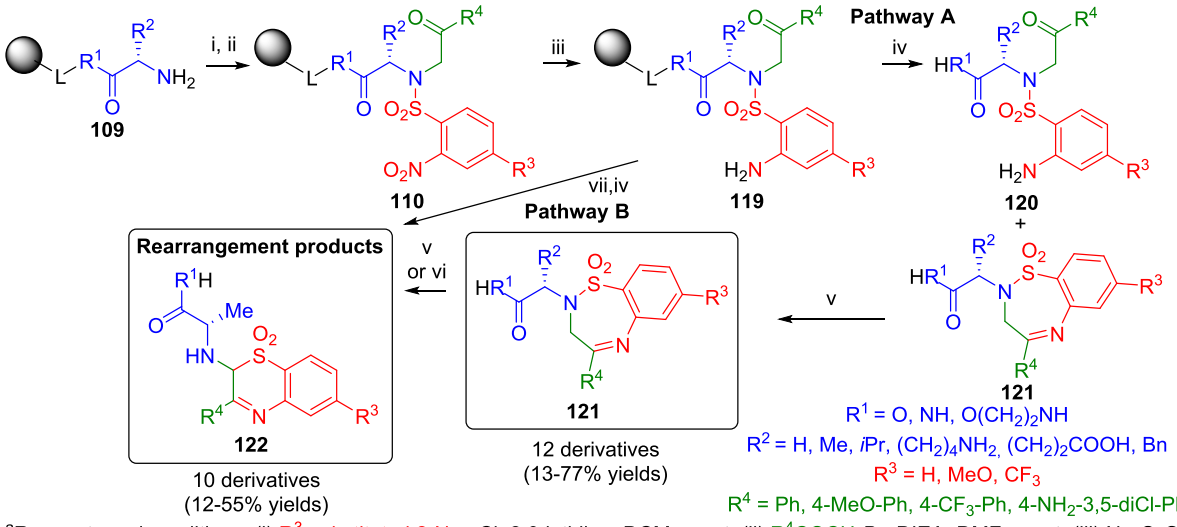

[a]Reagents and conditions: (i) R^3-substituted 2-Nos-Cl, 2,6-lutidine, DCM, on, rt; (ii) R^4COCH_2Br, DIEA, DMF, on, rt; (iii) $Na_2S_2O_4 .2H_2O$, K_2CO_3, TBAHS, 50% DCM/H_2O, on, rt; (iv) 50% TFA/DCM, 1 h, rt; (v) DMSO-d_6, 1.3-6.3 days, rt; 12 derivatives (13-77% yields); (vi) DMSO, 3-18.5 h, 70 °C. **Rearrangement conditions to benzothiazine 1,1-dioxides:** (vi) 5% AcOH, DMSO, on, 80 °C; 10 derivatives (12-55% yields).

When derivatives **121** were heated in DMSO, the authors observed set of other signals in ^{1}H NMR spectra which did not correspond with the structure **121**. For this reason, the reaction was surveyed assiduously and finally, the notable comparison of in ^{1}H NMR spectra of **121** and **122** confirmed the ring contraction *via* unprecedented rearrangement (Scheme 22, Pathway B). Because the reaction conversion to **122** was not quantitative under any tested conditions and the best results were obtained in DMSO (31-88% conversion calculated from HPLC-UV-MS traces), the authors proposed the alternative synthetic route. In this Pathway B, the rearrangement of immobilized amino intermediates **119** was performed on the resin followed by TFA treatment of the resin providing benzothiazine 1,1-dioxides **122** in 12-55% yields (10 derivatives). An electron donating group (MeO) in R^3 position accelerated the reaction whereas a strongly electron withdrawing group (CF_3) gave no product.[78] In addition, the authors reported two plausible reaction mechanism of the rearrangement based on ring opening followed by ring closure or direct ring contraction.[78]

3.1.4 The synthesis of fused [6+5] heterocycles

The immobilized 2-Nos-amides were applied not only to prepare fused indazole derivatives as well as indazole oxides **28** and their analogues **30** and **32**[56] (Scheme 6, discussed before in the subchapter 3.1.1.), but also the syntheses of oxazolo-pyrazino-indazoles was reported. Starting from immobilized 2-Nos-amide **124**, the transformation to immobilized *N*-alkyl-2-Nos-amide **127** was performed using

Scheme 23. The synthesis of oxazolo-pyrazino-indazole **131**[a]

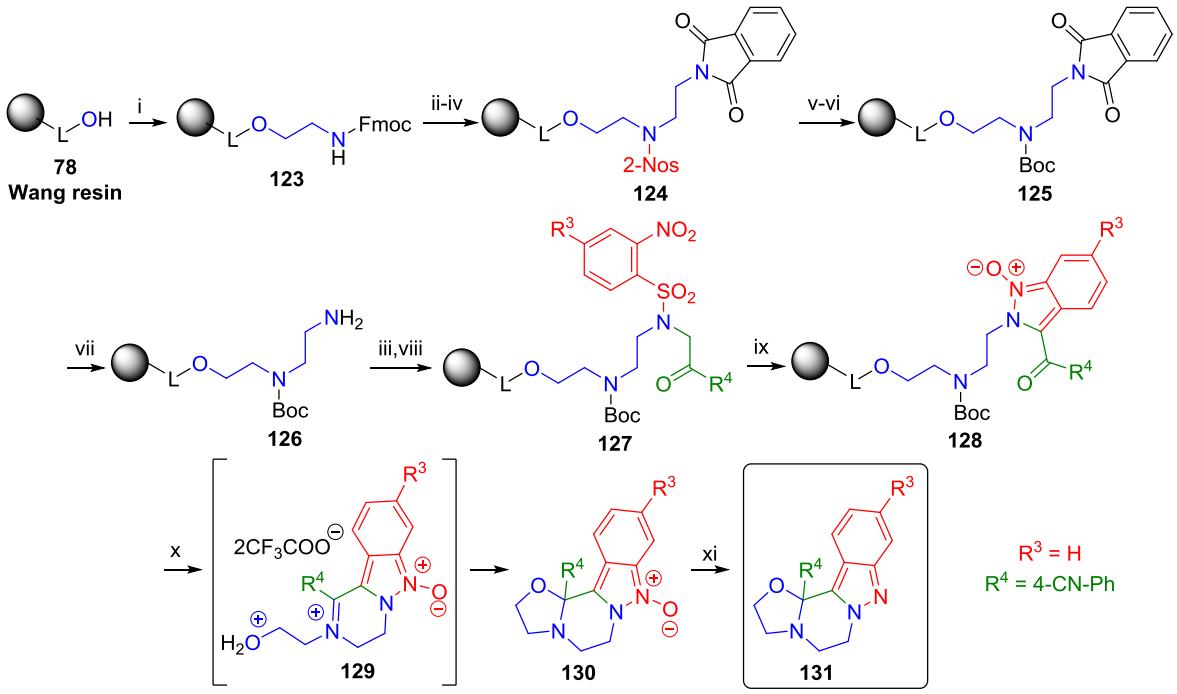

[a]Reagents and conditions: (i) trichloroacetonitrile, DBU, DCM, 2 h, 0 °C to rt, DCM wash, then Fmoc-ethanolamine, $BF_3.Et_2O$, anhydrous THF, 30 min, rt; (ii) 50% PIP/DMF,20 min, rt; (iii) R^3-substituted 2-Nos-Cl, 2,6-lutidine, DCM, 16 h, rt; (iv) *N*-(2-hydroxyethyl)phthalimide, DIAD, anhydrous THF, 5 h, rt; (v) MCE, DBU, DMF, 30 min, rt; (vi) Boc_2O, Py, DCM, 2 h, rt; (vii) $N_2H_2.H_2O$, MeOH/THF (1:1), 4 h, rt, 4 h; (viii) R^4COCH_2Br, DIEA, DMF, 16 h, rt; (ix) DBU, DMF, 30 min, rt; (x) 50% TFA/DCM, 1 h, rt; (xi) MsCl, TEA, DCM, 30 min at 0°C, then 16 h, rt; 1 derivative (63% yield).

a five-step sequence (Scheme 23). The following C-C rearrangement to indazole oxide **128** was accomplished using the previously reported protocol[56] and TFA-mediated cleavage from the resin triggered the spontaneous cyclization to oxazolo-pyrazino-indazole oxide **130**. Finally, the obtained *N*-oxide **130** was reduced by MsCl to the final product **131** in 63% yield (1 derivative).[83]

Scheme 24 points to the syntheses of 6,8-dioxa-3-azabicyclo[3.2.1]octan-2-ones **135**, **139**, **143** prepared from amines, α-bromoketones and sugar moieties. The review article summarizes three alternative synthetic strategies classified according to the type of component anchored to Wang trichloroacetimidate resin (WTA resin) **132** *via* ether bond. In the first case, *p*-hydroxy-2-bromo acetophenone was attached to WTA resin (**133**) followed by nucleophile attack by amine providing the desired secondary amines **134**. These substrates were reacted with ketal of tartaric acid 1-methyl ester and subsequent treatment with TFA yielded bicycles **135** (Scheme 24, Pathway A). The second strategy (Scheme 24, Pathway B) in which sugar derivatives were linked to the polymer-support (WTA resin) **136**, demonstrates a higher degree of diversity. Successively, both hydroxy groups of 2,3-isopropy-lidene-threitol were converted to the desired polymer-supported *O*-protected triflic-sugar **137**. The

Scheme 24. The synthesis of bicyclic compounds **135**, **139** and **143** *via* immobilized α-amino ketones[a]

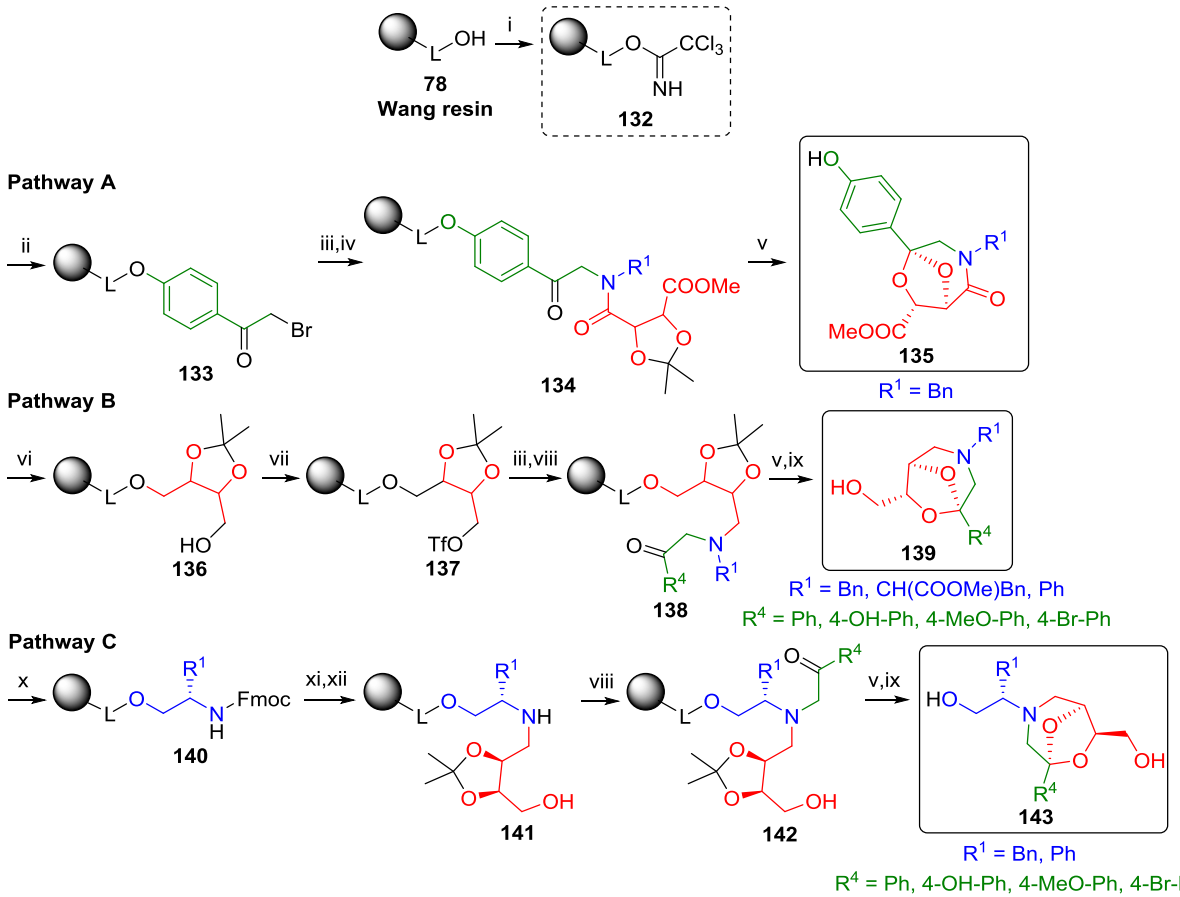

[a]Reagents and conditions: (i) CCl_3CN, anhydrous DCM, 0 °C, then DBU, 40 min, 0 °C; (ii) $BF_3.Et_2O$, *p*-OH-PhCOCH$_2$Br, 40 min, rt; (iii) R^1NH_2, DMF, on, rt; (iv) ketal of tartaric acid 1-methyl ester, DIEA, HOBt, DIC, on, rt; (v) 50% TFA/DCM, 1 h, rt; (vi) $BF_3.Et_2O$, isopropylidene-D-threitol, 40 min, rt; (vii) Tf_2O, 2,6-lutidine, DCM, 6 h, 0 °C; (viii) R^4COCH_2Br, DIEA, 50% DMF/aceton, on, rt; (ix) $NaHCO_3$ (aq); (x) Fmoc-Phe-ol, $BF_3.Et_2O$, anhydrous THF, 1 h, rt; (xi) 20% PIP/DMF; 30 min, rt (xii) L-isopropylidene-L-erythrose, $NaBH(OAc)_3$, AcOH, DCE, 24 h, rt.

protection of sugar allowed a better leaving of the triflic group during the nucleophilic substitution with various amines followed by *N*-alkylation with *α*-bromoketones (**138**). The product cleavage from the resin caused the final cyclization to bicycles **139**. The third synthetic approach involving amine units linked to the solid support **140** is displayed in Scheme 24, Pathway C. The Fmoc-amines attached to WTA resin **140** were subjected to Fmoc-deprotection and then to reductive alkylation with L-isopropylidene-L-erythrose using $NaBH(OAc)_3$ in 1,2-dichloroethane (DCE; **141**). Finally, disubstituted bicycles **143** were obtained using a two-step sequence according to the previously reported conditions in Pathway B (viii, v, ix).[84,85]

3.1.5 The synthesis of fused [6+6] heterocycles

The immobilized 2/4-Nos-amides and *α*-amino ketones were used by Soural et al. for the preparation of piperazino-oxazines. The polymer-supported 4-Nos-amides **147** were obtained from L-serine-immobilized to Wang resin **144** and converted to *α*-amino ketones **149**. The following reaction with piperidine triggered the Fmoc deprotection (**150**) and the formation of piperazine-2,4-dione derivatives **151** *via* cyclative cleavage of *N*-acylated *α*-amino ketones **150**. The liberated intermediates **151** were converted to fused intermediates **153** using a two-step sequence consisted of TFA-mediated deprotection and the final cyclization. The reduction of pyrazino-oxazines **153** with TES yielded 13 derivatives of hexahydro-pyrazino[2,1-*c*][1,4]oxazine-6,9-dione **154** in 30-81% yields (Scheme 25).[75]

Scheme 25. The solid-phase synthesis of hexahydropyrazino[2,1-*c*][1,4]oxazine-6,9-diones **154**[a]

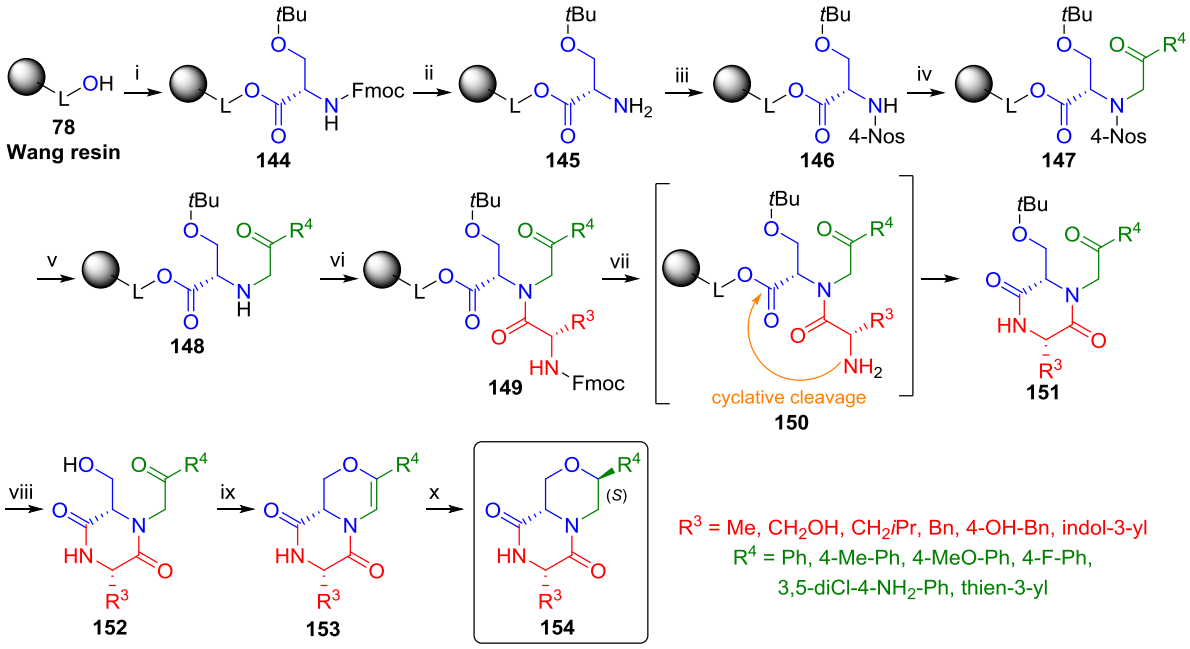

[a]Reagents and conditions: (i) Fmoc-Ser(*t*Bu)-OH, HOBt, DIC, DCM, DMF, 24 h, rt; (ii) 50% PIP/DMF, 30 min, rt; (iii) 4-NosCl, 2,6-lutidine, DCM, 24 h, rt; (iv) R^4COCH_2Br, DIEA, DMF, 24 h, rt; (v) MCE, DBU, DMF, 1 h, rt; (vi) Fmoc-amino acids, HOBt, DIC, DCM, DMF, 24 h, rt, then repeat; (vii) 50% PIP/DMF, 30 min, rt, then lyophilization for 16 h; (viii) 50% TFA/DCM, 30 min, rt, then evaporation under stream of N_2; (ix) MeCN, 1-8 h, 80-90 °C, then evaporation under stream of N_2; (x) TFA/TES/DCM (10:1:9), 16 h, rt; 13 derivatives (30-81% yields).

3.1.6 The synthesis of fused [7+5] heterocycles

Because the starting synthons, e.g. 2/4-Nos-amides and *α*-amino ketones, have been handled rarely to prepare fused [7+5] derivatives, this subchapter illustrates only one synthetic approach. Scheme 26 shows the simple preparation of imidazole-benzodiazepinones **161** starting from immobilized Fmoc-*β*-alanine on Wang resin **155** converted to the corresponding *α*-acylamino ketones **158** using a simple three-step sequence. The acid-mediated reaction in AmAc/AcOH led to formation of imidazole ring **159** followed by Phth-deprotection and final cyclization to imidazole-benzodiazepinones **161** (3 derivatives). Last three steps were performed in solution (post-cleavage modification).[57]

Scheme 26. The solid-phase synthesis of imidazole-benzodiazepinones **161**[a]

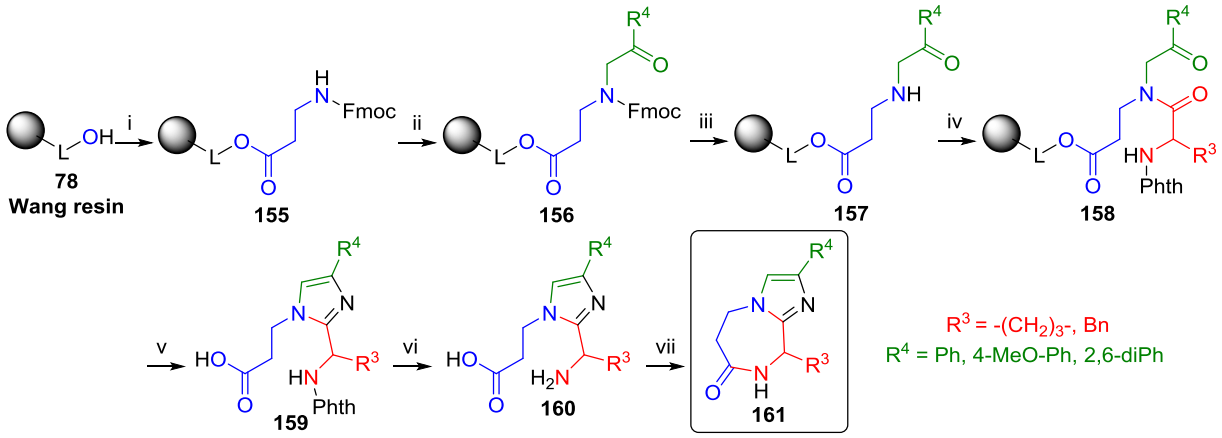

[a]Reagents and conditions: (i) Fmoc-ß-Ala-OH, anhydrous NMP, HOBt, EDC, DMF, 12 h, rt; (ii) DIEA, anhydrous THF, then R^4COCH_2Br, anhydrous DCM, 3-12 h, rt; (iii) 5% PIP/DMF, 5 min, rt; (iv) Fmoc-amino acid, DIC, DMF, 12 h, rt; (v) AmAc, AcOH, 10-20 h, 100 °C; (vi) 48% $MeNH_2$ (aq)/THF, 24 h, rt; (vii) 5% TEA/$PhCH_3$, 12 h, 100 °C; 3 derivatives.

4. RESULTS AND DISCUSSION

Numbering of the final derivatives, linkers and building blocks used in the individual sections of the thesis is served using Chemset Numbering System and it is adopted from author´s articles, unless otherwise stated.

Chemset Numbering System is a specific product numbering approach which is commonly used in a combinatorial chemistry. The system is based on a collection of at least two or more similar members in one category (e.g. Wang resin or Wang-piperazine resin for R^1 modification in Figure 7) and mutual combination of synthons R^2-R^x (e.g. Fmoc-amino acids for R^2 substituent, sulfonyl chlorides for R^3 substituent or α-bromoketones for R^4 substituent in Figure 7) to give the numbering of the corresponding products with various R^1-R^x substituents. To demonstrate the system, Figure 7 displays oxazine derivative **115**{R^1,R^2,R^3,R^4}, depicted above in Scheme 20, and the list of all tested building blocks for R^1-R^4 substituents. For example, in the case of product **115**{*1,1,1,1*}, the compound was synthesized from Wang resin, Fmoc-Ser(*t*Bu)-OH, 4-Nos-Cl and α-bromo-1-(*p*-tolyl)ethan-1-one. Designation of derivatives **115**{*1,1,1-4,1*} indicates that such compounds were synthesized from Wang resin, Fmoc-Ser(*t*Bu)-OH, various sulfonyl chlorides and α-bromo-1-(*p*-tolyl)ethan-1-one.

Figure 7. The structure of compound **115**{R^1,R^2,R^3,R^4} and the list of synthons for R^1-R^4 substitution

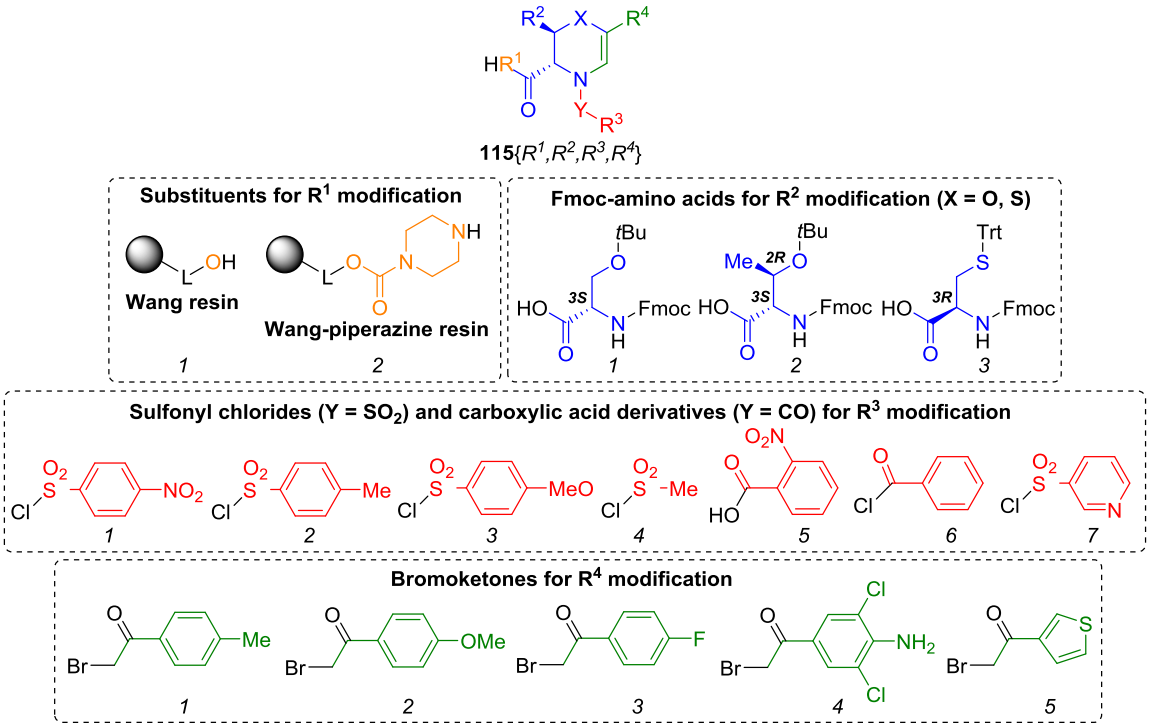

4.1 Polymer-Supported Stereoselective Synthesis of Benzoxazino[4,3-*b*][1,2,5]thiadiazepinone 6,6-Dioxides

The results of this project were published in: Králová, P.; Maloň, M; Ručilová, V.; Volná, T.; M.; Soural, M. *ACS Comb. Sci.* 2017, *19* (10), 670–674.[38] The manuscript is attached in Appendix C (p. 167 – 171). The Supporting information is available at: https://pubs.acs.org/doi/abs/10.1021/acscombsci.7b00115 and is attached as an electronic file on CD.

4.1.1 Brief introduction

The research builds on our previous results in the field of morpholine and thiomorpholine-3-carboxylic acid derivatives.[1,2] In this subchapter, the stereoselective synthesis of benzoxazino [4,3-*b*][1,2,5]thiadiazepinone 6,6-dioxides starting from immobilized *N*-phenacyl-2-Nos-amides is briefly outlined. These key intermediates were prepared according to the previously reported protocol[1,2] and then subjected to an on-resin reduction of nitro group using sodium dithionite or tin(II) chloride which yielded the immobilized amino derivatives. After the acid-mediated cleavage, the crude product should be modified using two post-cleavage reactions (i.e. acid-mediated cyclization or TES reduction) performed in solution to yield the final benzoxazino-thiadiazepinone 6,6-dioxides (Figure 8). Since the target compounds contain two stereocenters, we particularly focused on the stereochemical studies to reveal the impact of both the TES reduction and the final cyclization step on the resulting configuration. Also, limitations and scope of the method was tested using variously substituted synthons.

Figure 8. The proposed synthesis of benzoxazino[4,3-*b*][1,2,5]thiadiazepinone 6,6-dioxides

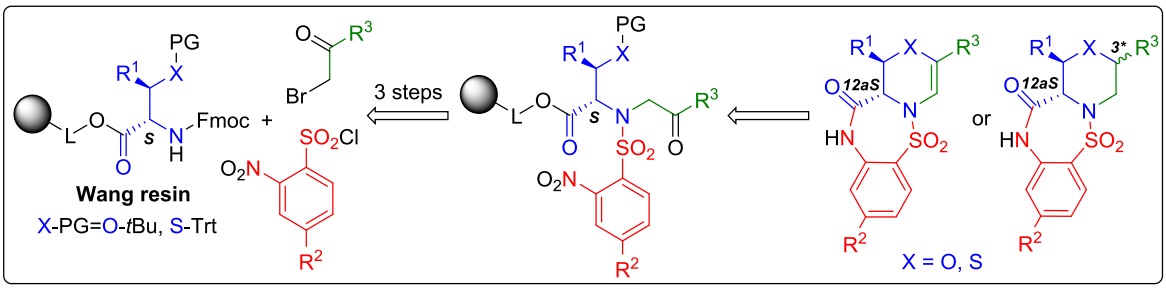

4.1.2 Synthesis

First, the Wang resin **I-1** was acylated with Fmoc-Ser(*t*Bu)-OH **I-2**{*1*} and the loading of the resulting resin was determined with the use of an external standard (Fmoc-Ala-OH) to 0.48 mmol/g. After that, the immobilized Fmoc-Ser(*t*Bu)-OH **I-2**{*1*} was subjected to the removal of the Fmoc protecting group and subsequent protection/activation with 2-Nos-Cl followed by Fukuyama monoalkylation with *α*-bromoacetophenone that yielded the resulting *N*-phenacyl sulfonamide **I-5**{*1,1,1*}. The nitro group was reduced by sodium dithionite,[86] followed by acid-mediated cleavage of intermediate **I-6**{*1,1,1*} from the solid support. Although TFA cleavage of analogous compounds previously yielded benzodiazepines **I-11**{*1,1,1*} *via* the attack of the ketone by an amino group,[3,36] we

observed the preferable formation of the morpholine scaffold (Scheme 27). The desired intermediate **I-7**{*1,1,1*} was obtained in high crude purity (92%, calculated from HPLC-UV traces at 205–400 nm).

Scheme 27. Synthesis of benzoxazino-thiadiazepinone 6,6-dioxides **I-9-10**{R^1,R^2,R^3}[a]

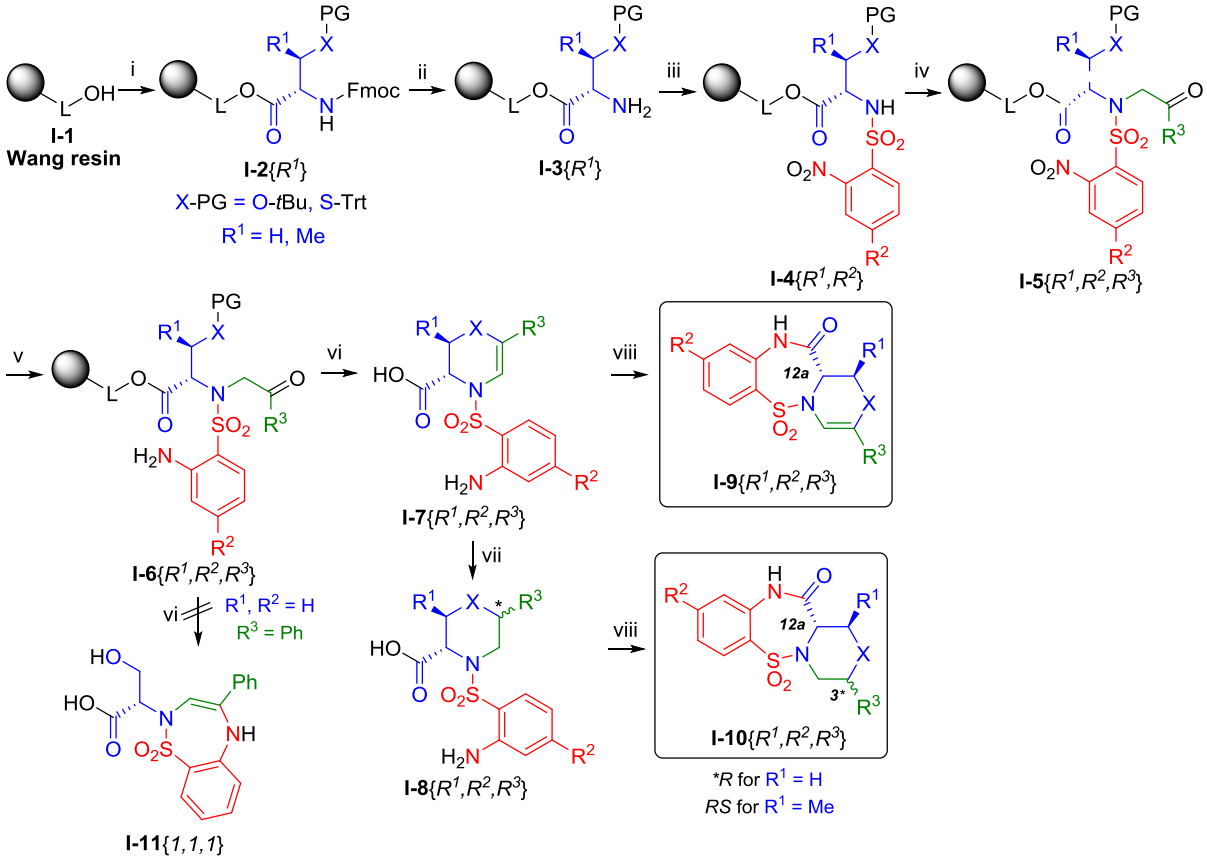

[a]Reagents and conditions: (i) Fmoc-amino acid, HOBt, DMAP, DIC, DMF, DCM, 24 h, rt; (ii) 50% PIP/DMF, 30 min, rt; (iii) 4-substituted 2-Nos-Cl, 2,6-lutidine, DCM, 24 h or 44 h for derivative **I-7**{*1,2*}, rt; (iv) R^3COCH_2Br, DIEA, DMF, 24 h or 43 h for derivative **I-7**{*1,2,1*} or 72 h for derivative **I-7**{*2,1,1*}, rt; (v) **(a)** $Na_2S_2O_4.2H_2O$, K_2CO_3, TBAHS, 50% DCM/H_2O, 2-5 h, rt (for derivatives **I-6**{*1-2*,R^2,R^3}) or **(b)** $SnCl_2.2H_2O$, DIEA, degassed DMF, 30 min, rt (for derivatives **I-6**{*3*,R^2,R^3}); (vi) 50-75% TFA/DCM, 2.5-24 h, rt; (vii) TES, 1-3 h, rt; (viii) PTSA, anhydrous $PhCH_3$, 1-12 h, 110 °C or PTSA, anhydrous DCE, 1-144 h, 90 °C.

After that, we focused on a cyclization to the benzoxazino-thiadiazepinone derivative **I-9**{*1,1,1*} (Scheme 28). As TFA was used to cleave the final intermediate from the resin, we attempted to use this acid to possibly combine the cleavage procedure with the cyclization step. After many tested attempts (Table 1), the complete conversion to the expected product **I-9**{*1,1,1*} was not achieved even using different time, temperatures, microwave irradiation and different solvents. For this reason, we turned attention to post-cleavage cyclization of oxazine **I-7**{*1,1,1*} to the benzoxazino-thiadiazepinone 6,6-dioxide **I-9**{*1,1,1*}.

Scheme 28. The TFA-mediated cleavage/cyclization of aniline **I-6**{*1,1,1*}[a]

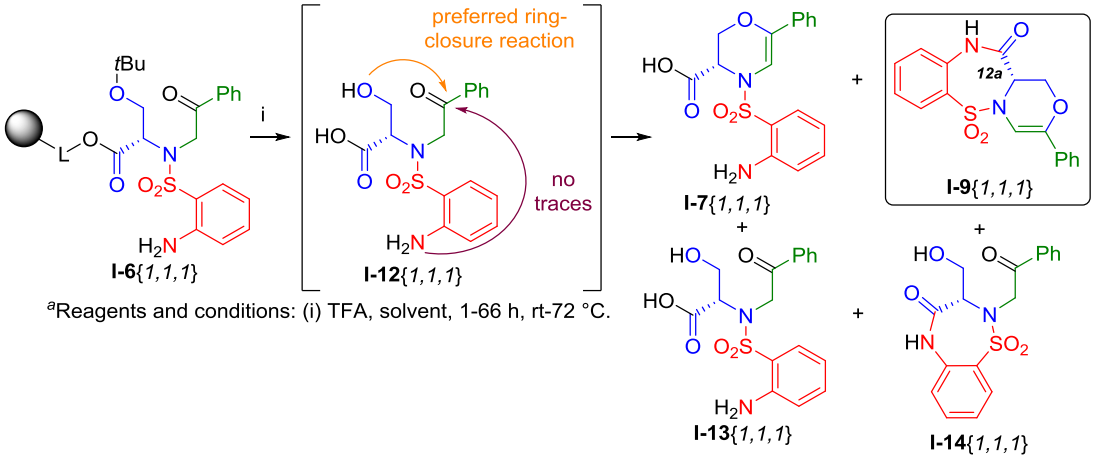

[a]Reagents and conditions: (i) TFA, solvent, 1-66 h, rt-72 °C.

Table 1. The tested conditions for a direct acid-mediated cyclization of oxazine **I-7**{*1,1,1*}[a-b]

TFA [%]	solvent	time [h]	temp [°C]	MW [W]	crude purity of I-7 [%][a]	crude purity of I-9 [%][a]	crude purity of I-13 [%][a]	crude purity of I-14 [%][a]	ratio of I-7:9:13:14 [%][a]
50	**DCM**	1	23	-	44	0	38	0	54:0:46:0
		2	23	-	73	1	14	0	83:1:16:0
		3	23	-	92	3	0	0	97:3:0:0
		24	23	-	90	5	0	0	96:4:0:0
		1	50	200	57	26	4	0	66:30:4:0
		6	**50**	**200**	**45**	**33**	**0**	**0**	**58:42:0:0**
		12	50	200	16	13	0	0	55:45:0:0
50	**$PhCH_3$**	2	23	-	63	9	6	10	72:10:7:11
		24	**23**	**-**	**41**	**22**	**4**	**17**	**49:26:5:20**
75	DCM	2	23	-	55	0	16	0	77:0:23:0
		24	23	-	31	6	27	0	48:8:44:0
100	-	2	23	-	56	0	19	0	75:0:25:0
		24	23	-	30	6	28	0	47:9:44:0
		66	23	-	34	22	29	0	40:26:34:0
		1	72	-	28	18	30	0	37:24:39:0
		24	72	-	0[b]	0	0	0	0:0:0:0

[a]Calculated from HPLC-UV traces at 205–400 nm; [b]Complete decomposition.

Subsequently, we tested diverse cyclization conditions (Scheme 29, Table 2). Since the TFA-mediated cyclization failed, we decided to test the reaction *via* carboxylic acid derivatives (e.g. ester, chloride and anhydride). In the first case, we tried the *p*-toluenesulfonic acid (PTSA)-catalyzed cyclization of ester or chloride **I-15**{*1,1,1*} (Y = OMe, Cl, Scheme 29, Methods **a-b**).[87] Both ester and chloride were synthesized from the carboxylic acid **I-7**{*1,1,1*} using the reaction with diazomethane or DMF-catalyzed reaction with oxalyl chloride. Further, we focused on an activation with DIC or HOBt/DIC (Scheme 29, Methods **c-d**).[88] In the case of methods **a-b**, the corresponding carboxylic acid derivatives were not detected due to the persistent instability of oxazine ring **I-7**{*1,1,1*} under the used conditions. Similarly, the DIC and HOBt-catalyzed reaction of oxazine **I-7**{*1,1,1*} (Method **c**)

caused the oxazine ring-opening, but also the cyclization of the benzodiazepinone scaffold to derivative **I-14**{*1,1,1*}. Unfortunately, the following TFA-mediated transformation of the intermediate to benzoxazino-thiadiazepine derivative **I-9**{*1,1,1*} failed. Finally, the method **d** was tested to obtain the product **I-15**{*1,1,1*} in good crude purity (87%, calculated from HPLC-UV traces at 205–400 nm, Table 2, highlighted in bold), but the compound did not undergo further cyclization to fused oxazine derivative **I-9**{*1,1,1*}.

Scheme 29. The synthesis to fused oxazine derivative **I-9**{*1,1,1*} *via* various carboxylic acid derivatives[a]

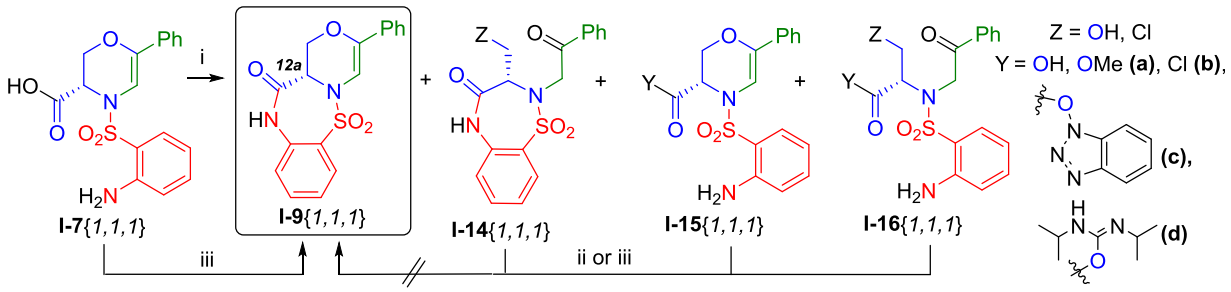

[a]Reagents and conditions: (i) **(a)** CH_2N_2, 10% NaOH (aq), 1 h, 0 °C, then add to an evaporator, 25 h, rt; **(b)** oxalyl chloride, DMF (cat.), anhydrous DCM, 2-24 h, rt; **(c)** HOBt, DIC, DMF, 24 h, rt; **(d)** DIC, DMAP, DMF, 24 h, rt; (ii) 50% TFA/DCM, 24 h, rt; (iii) PTSA, anhydrous $PhCH_3$, 24 h, 3.5 h, 110 °C or PTSA, anhydrous DCE, 5.5 h, 90 °C.

Table 2. The synthesis of oxazine-3-carboxylic acid derivatives **I-15**{*1,1,1*}[a-b]

neutralization after removal of a residual TFA using lyophilization	method[a]	time [h]	temp [°C]	Y	Z	crude purity of I-7 [%][b]	crude purity of I-9 [%][b]	crude purity of I-14 [%][b]	crude purity of I-15 [%][b]	crude purity of I-16 [%][b]
without	**a**	1	23	OMe	OH	9	0	0	0	88
		25	23	OMe	OH	0	0	0	0	78
without	**b**	2	23	Cl	Cl	67	0	0	0	26
		24	23	Cl	Cl	8	3	0	0	50
with TEA	**b**	2	23	Cl	Cl	35	17	0	0	37
		24	23	Cl	Cl	31	27	0	0	31
without	**c**	24	23	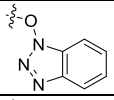	OH	20	7	40	0	0
with DIEA	**c**	24	23	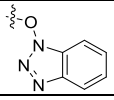	OH	0	8	60	0	0
with DIEA	**d**	**24**	**23**	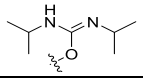	**-**	**3**	**0**	**0**	**87**	**0**
with NH_3/MeOH	**d**	24	23	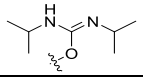	-	26	0	0	49	0

[a]The reaction conditions of the method are defined in Scheme 29; [b]Calculated from HPLC-UV traces at 205–400 nm.

After a number of unsuccessful experiments, we managed to accomplish the cyclization using PTSA in anhydrous toluene or anhydrous DCE. The reaction furnished the products **I-9**{*1,1,1*}^{tol} and **I-9**{*1,1,1*}^{DCE} under Dean-Stark conditions (in our case a collar flask was used). The impact of both solvents to crude purities, overall yields and the resulting configuration of C12*a* stereocenter was

compared. The use of DCE (90 °C) provided slightly better results in comparison to toluene (110 °C). The product **I-9**{*1,1,1*}^{DCE} was obtained in 81% crude purity (calculated from HPLC-UV traces at 205–400 nm) and 51% overall yield (calculated from the ^{1}H NMR spectrum of the purified product), whereas the product **I-9**{*1,1,1*}^{tol} was isolated in 77% crude purity (calculated from HPLC-UV traces at 205–400 nm) and 35% overall yield (calculated from the ^{1}H NMR spectrum of the purified product, Scheme 27, Table 7 for the final derivatives). Further, in the case of DCE, we observed a minor racemization (i.e. 8% of *R*-isomer) of the C12*a* stereocenter, whereas the cyclization in toluene afforded a higher proportion of *R*-isomer (i.e. 23% of *R*-isomer, Figure 9).

Figure 9. The comparison of chiral SFC chromatograms of both derivatives **9**{*1,1,1*}^{DCE} and **9**{*1,1,1*}^{tol}

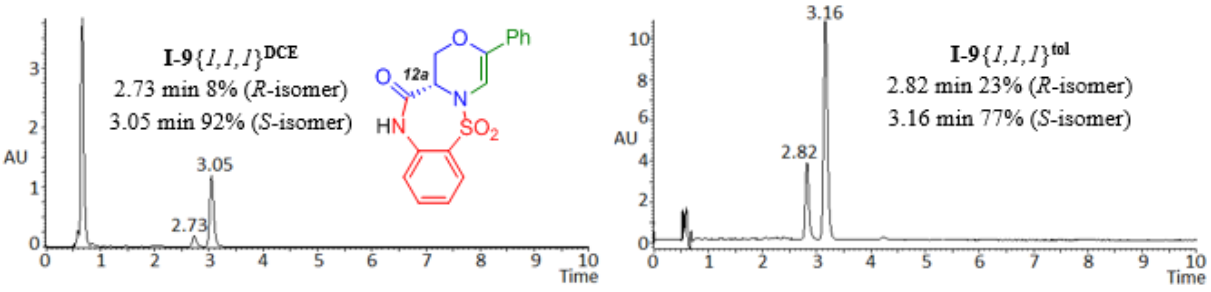

When TES was added into the cleavage cocktail after release of the product **I-6**{*1,1,1*} from the resin, the saturated analogue **I-8**{*1,1,1*} was obtained. Its cyclization to **I-10**{*1,1,1*} was again tested in toluene and DCE and gave similar results (i.e. 84-85% crude purities and 41-42% overall yields, Scheme 30, Table 7 for the final derivatives). The following NMR analysis of **I-10**{*1,1,1*}^{tol} and **I-10**{*1,1,1*}^{DCE} revealed the presence of both inseparable C12*a* *R,S* isomers in a ratio of 23:77 and 8:92, respectively. To clarify the formation of optical isomers, we decided to investigate the stereochemical outcome of critical steps of the reaction sequence using SFC and NMR studies. In the case of unsaturated intermediate **I-7**{*1,1,1*}, the C3 stereochemistry was studied in comparison to the racemic standard **I-7**^{RS}{*1,1,1*}. In accordance to our previously reported results,[2] we proved that the second enantiomer (*R*, 8%) was formed during the Fmoc-Ser(*t*Bu)-OH immobilization on the Wang resin (Figure 10-11). For TES-reduced intermediate **I-8**{*1,1,1*}, NMR analysis proved the stereoselective formation of C6 stereocenter and its configuration was determined as *R*. In the case of **I-9**{*1,1,1*} and later discussed related analogues **I-9**{R^1,R^2,R^3}, SFC analysis was used to detect the possible formation of C12*a* *R,S* isomers (enantiomers), whereas NMR analysis of saturated derivatives **I-10**{*1,1,1*} (Figure 12) and **I-10**{R^1,R^2,R^3} enabled a direct detection of both isomers (diastereomers) from the ^{1}H NMR spectra of the final products. The above-mentioned approaches allowed to conclude that DCE cyclization had no impact on the resulting stereochemistry of **I-10**{*1,1,1*}^{DCE}. In contrast, the use of toluene lowered diastereomeric purity as it yielded compound **I-10**{*1,1,1*}^{tol} as a mixture of the corresponding C12*a* *R,S* isomers in a ratio of 23:77 (Figure 9, 11). For this reason, cyclization using DCE was applied as the method of choice to synthesize and study other derivatives, except for threonine derivative **I-9**{*2,1,1*} discussed later in the thesis.

Scheme 30. The synthesis of saturated analogues **I-10**{*1,1,1*}[a]

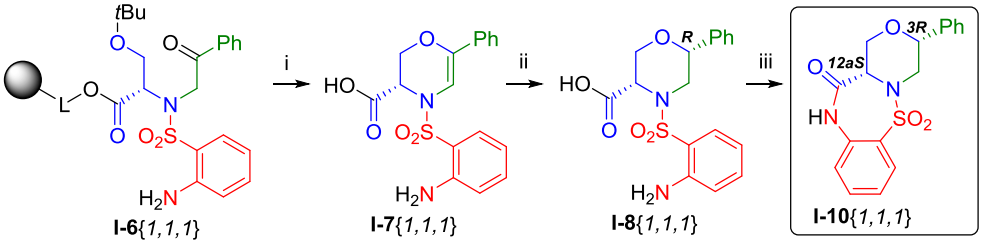

[a]Reagents and conditions: (i) 50% TFA/DCM, 3 h, rt; (ii) TES, 1 h, rt; (iii) PTSA, anhydrous $PhCH_3$, 4 h, 110 °C or PTSA, anhydrous DCE, 3 h, 90 °C.

Figure 10. Chiral SFC chromatograms of the starting racemic mixture and L-Fmoc-Ser(*t*Bu)-OH

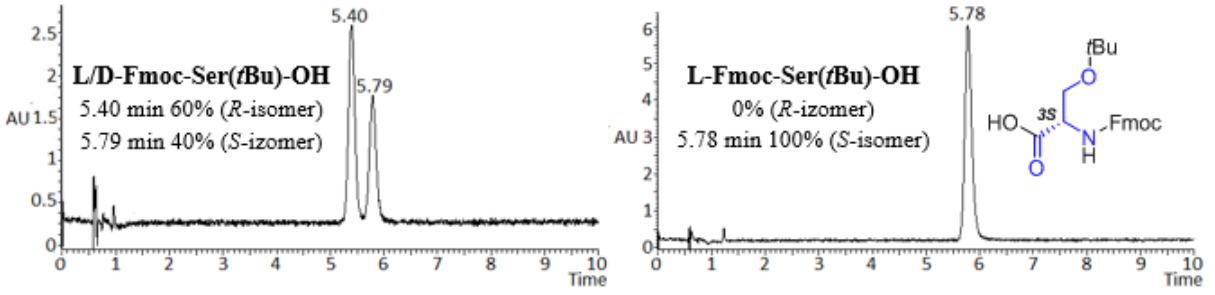

Figure 11. Chiral SCF chromatograms of the crude products **I-7**^{RS}{*1,1,1*} and **I-7**{*1,1,1*}

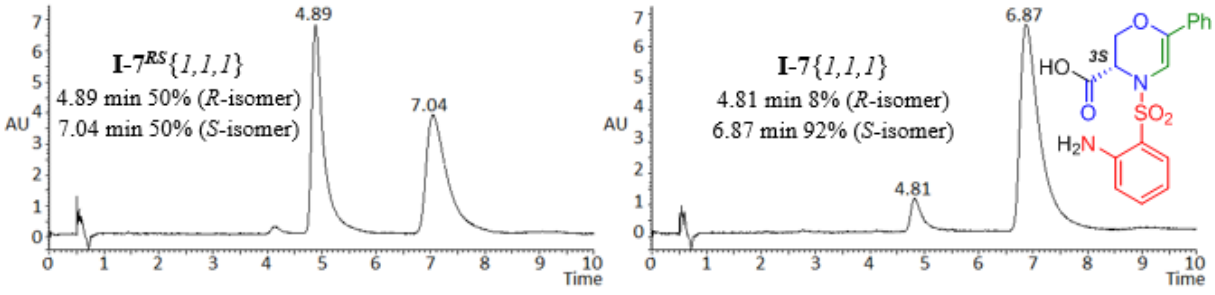

Figure 12. The ^{1}H NMR spectrum of saturated derivative **I-10**{*1,1,1*}^{DCE}

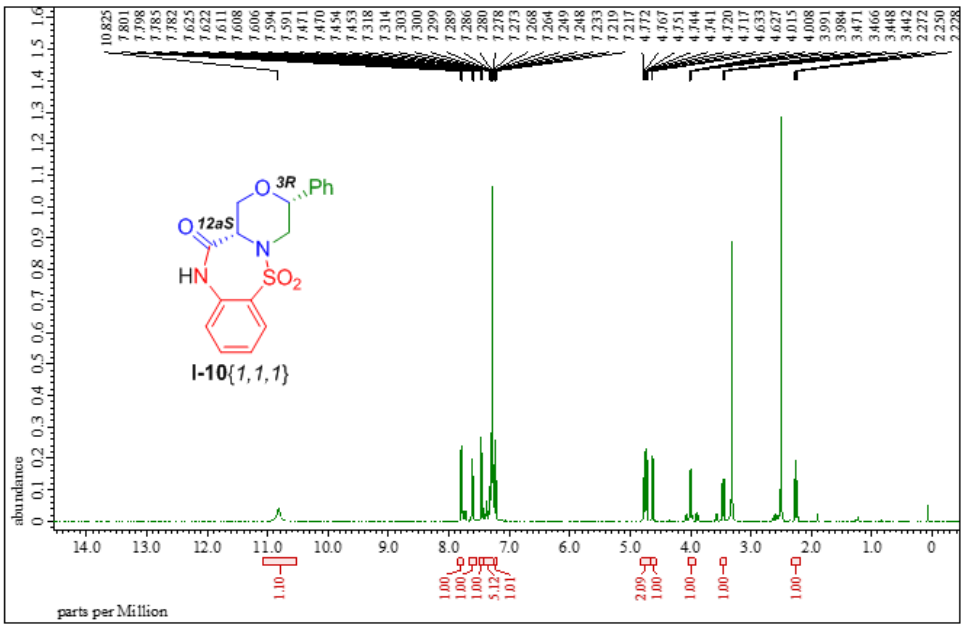

4.1.3 Limitations and scope

To determine the limitations and scope of the methodology, we tested a combination of three Fmoc-amino acids with the hydroxymethyl or sulfanylmethyl groups in a side chain, various 4-substituted 2-Nos-Cl and α-bromoketones containing both electron donating and electron withdrawing substituents (Figure 13).

Figure 13. The list of tested synthons for R^1, R^2 and R^3 substitution

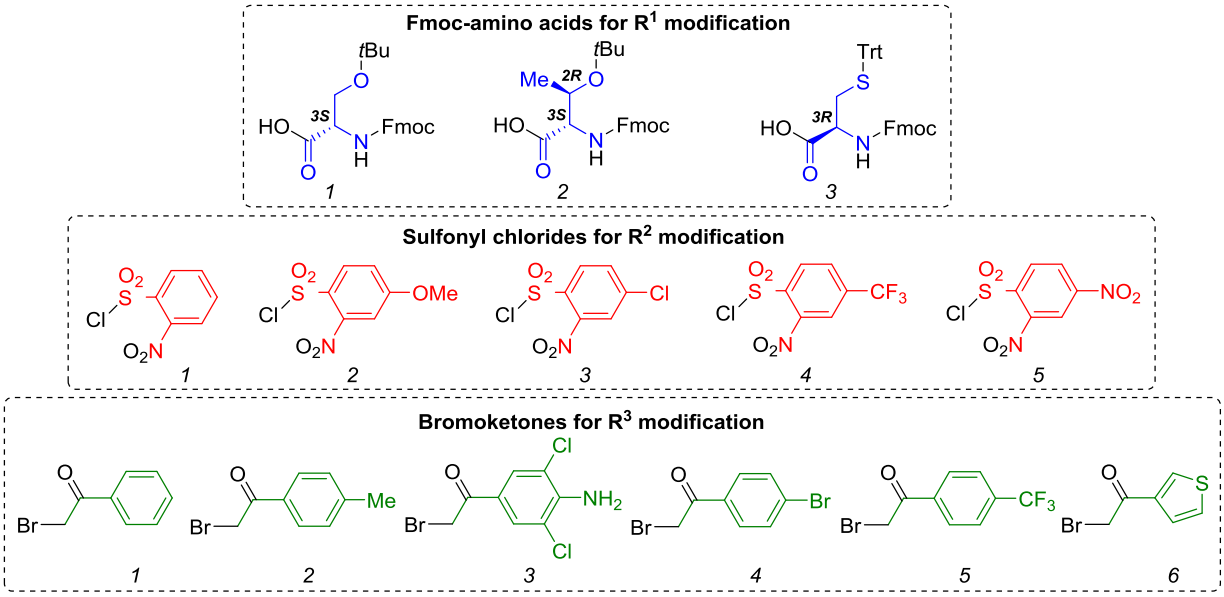

When immobilized Fmoc-Ser(*t*Bu)-OH was replaced with Fmoc-Thr(*t*Bu)-OH **I-2**{*2*}, the alkylation step required the use of longer reaction time (72 h) and a higher concentration of the alkylating agent and base to complete reaction. After that, the resulting *N*-phenacyl sulfonamide **I-5**{*2,1,1*} was reduced by sodium dithionite followed by release the product from the resin and its cyclization was tested in different cyclization solvents to evaluate the impact on reaction outcome (Scheme 31). Table 3 shows the unusability of polar aprotic solvents (e.g. NMP, DMF, DMSO and MeCN) and polar protic solvents (e.g. 2-isopropanol (IPA) and AcOH). We also tested various unpolar solvents (e.g. toluene, *n*-heptane and DCE). The seamless cyclization to derivative **I-9**{*2,1,1*} was accomplished in anhydrous DCE, whereas use of toluene or anhydrous toluene gave significantly different results and the reaction conversion was not completed even under microwave irradiation. Analogously to serine derivative **I-9**{*1,1,1*}, the fused derivative **I-9**{*2,1,1*} was cyclized in DCE and obtained in 92% crude purity (calculated from HPLC-UV traces at 205–400 nm) and 32% overall yield (calculated from ^{1}H NMR spectra of the purified product, Scheme 31). In this case, Figure 14 shows that the use of DCE as cyclization solvent did not affect the stereochemical outcome of C12*a* stereocenter and the final derivative was obtained as a diastereomerically pure compound using SFC analysis.

Scheme 31. The synthesis of threonine benzoxazino-thiadiazepinone derivative **I-9**{*2,1,1*}[a]

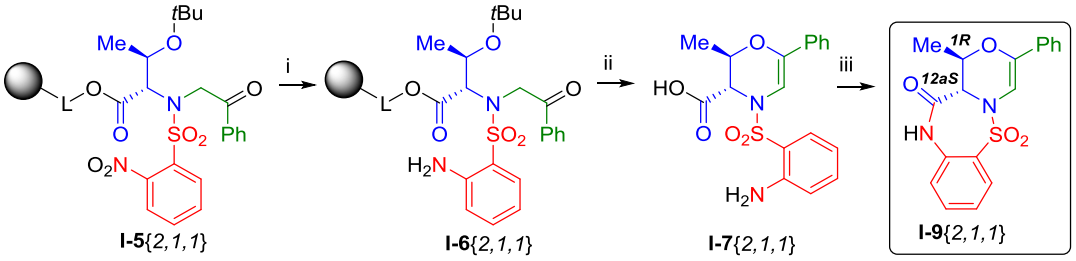

[a]Reagents and conditions: (i) $Na_2S_2O_4.2H_2O$, K_2CO_3, TBAHS, 50% DCM/H_2O, 3.5 h, rt (ii) 50% TFA/DCM, 4 h, rt; (iii) PTSA, solvent, time, temp, MW => PTSA, anhydrous DCE, 6 h, 90 °C (in preparative scale).

Table 3. The alternative solvent for the cyclization of threonine derivative **I-7**{*2,1,1*} (tested in analytical scale after the product **I-6**{*2,1,1*} cleavage from 50 mg of resin)[a]

solvent	time [h]	temp [°C]	MW [W]	crude purity of I-7 [%][a]	crude purity of I-9 [%][a]	ratio of I-7:9 [%][a]
$PhCH_3$	0.5	70	-	25	36	41:59
anhydrous $PhCH_3$	0.5	90	-	30	51	37:63
	0.5	90	200	20	20	50:50
n-heptane	0.5	90	-	5	30	14:86
anhydrous DCE	0.5	90	-	6	80	7:93
	1	**90**	**-**	**0**	**83**	**0:100**
diethylene glycol diethyl ether	0.5	90	-	3	4	43:57
NMP	0.5	90	-	76	12	86:14
DMF	0.5	90	-	78	4	95:5
anhydrous DMF	0.5	90	-	9	40	18:82
DMSO	0.5	90	-	75	10	88:12
anhydrous DMSO	0.5	90	-	76	10	88:12
MeCN	0.5	90	-	58	13	82:18
IPA	0.5	90	-	71	11	87:13
AcOH	0.5	90	-	52	23	69:31

[a]Calcualted from HPLC-UV traces at 205–400 nm.

Figure 14. SFC chromatograms of the representative derivatives **I-9**{*2,1,1*} and **I-9**{*3,1,1*}

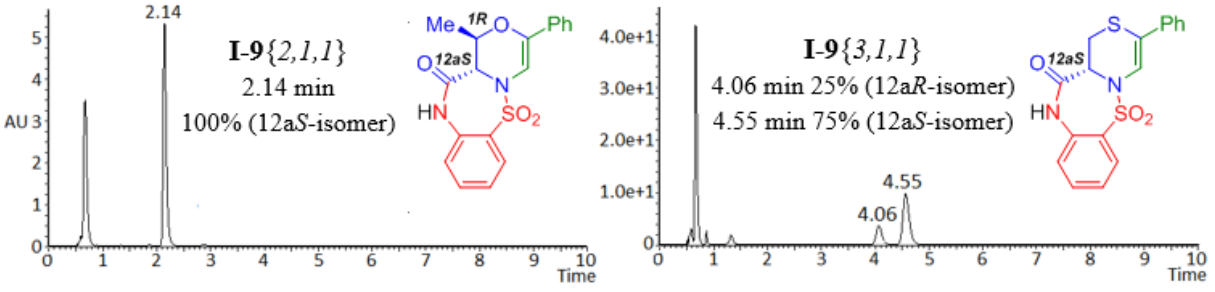

In the case of mehylmorpholine derivative **I-10**{*2,1,1*}, we observed a mixture of separable C3 *R,S* isomers **I-10a**{*2,1,1*} and **I-10b**{*2,1,1*} in a ratio of 63:47 (calculated from HPLC-UV traces at 205–400 nm, Scheme 32, Table 7 for the final derivatives). The non-stereoselective TES reduction of threonine-based intermediates is in accordance with our previous research.[1,2]

Scheme 32. The synthesis of benzo-methylmorpholino-thiadiazepinones **I-10a-b**{*2,1,1*} and their key NMR correlations used to identify both separated C3 diastereoisomers[a]

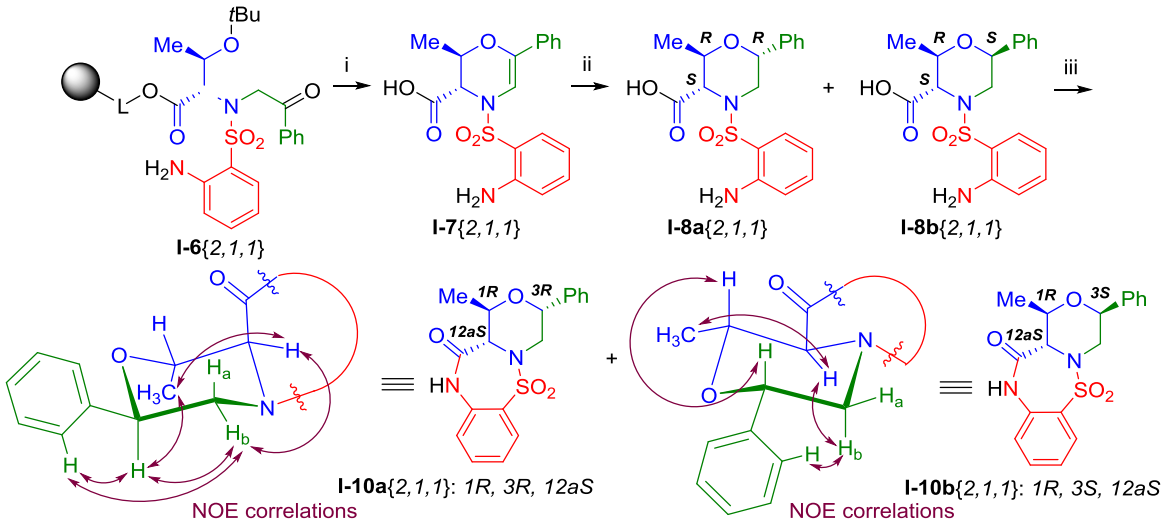

[a]Reagents and conditions: (i) 50% TFA/DCM, 4 h, rt; (ii) TES, 2 h, rt; (iii) PTSA, anhydrous DCE, 4 h, 90 °C.

In addition, the developed synthetic protocol was tested on Wang resin with immobilized Fmoc-Cys(Trt)-OH **I-2**{*3*} (Scheme 33). Interestingly, the synthesis of anilines **I-6**{*3,1,1*} using sodium dithionite failed in all tested cases (Table 4), but the use of tin(II) chloride dihydrate afforded the desired intermediate **I-6**{*3,1,1*} in excellent crude purity (94%, calculated from HPLC-UV traces at 205−400 nm). The final cyclization in anhydrous DCE provided desired product **I-9**{*3,1,1*} in 82% crude purity (calculated from HPLC-UV traces at 205−400 nm) and 27% overall yield (calculated from the ^{1}H NMR spectrum of the purified product). Nevertheless, the use of Fmoc-Cys(Trt)-OH instead of Fmoc-Ser(*t*Bu)-OH and Fmoc-Thr(*t*Bu)-OH affected a pronounced racemization on the C12*a* stereocenter and C12*a R,S* isomers were observed in a ratio of 25:75 (Figure 14). Furthermore, the TES reduction to **I-8**{*3,1,1*} was unsuccessful even at elevated temperature (50 °C) after 70 h (Table 6).

Scheme 33. The synthesis of cysteine-based derivatives **I-9**{*3,1,1*} and **I-10**{*3,1,1*}[a]

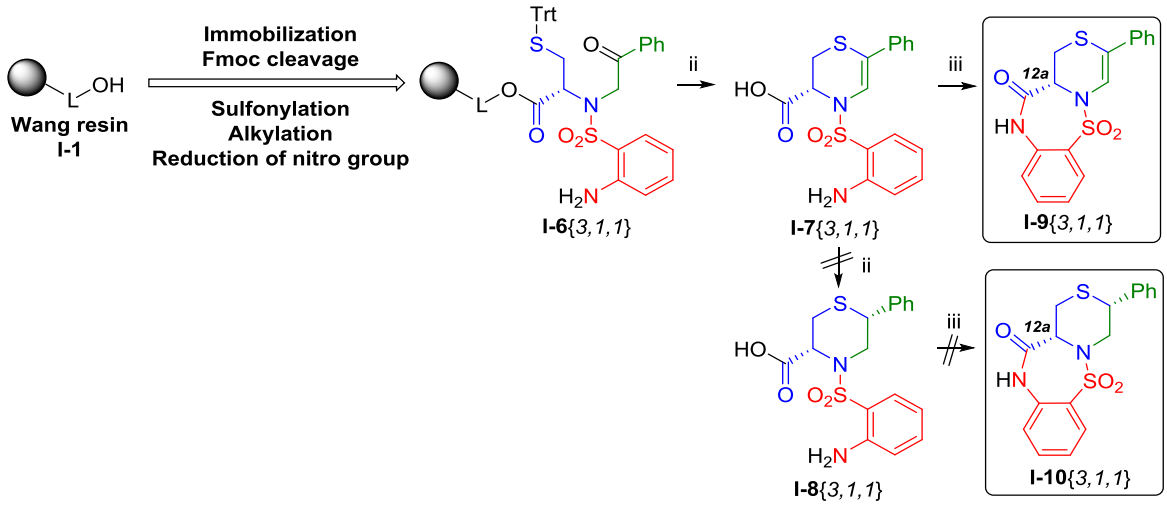

[a]Reagents and conditions: (i) 50% TFA/DCM, 3.5 h, rt; (ii) TES, 2-70 h, rt or 50 °C; (iii) PTSA, anhydrous DCE, 27 h, 90 °C.

To explore the diversification of R^2, all substituted 2-Nos-Cl were combined with immobilized Fmoc-Ser(*t*Bu)-OH and variously substituted *α*-bromoketones. In the case of electron donating group (MeO) in R^2 position, the sulfonylation and the subsequent alkylation step required longer reaction time (circa 2 days) to quantitative conversion. The reduction of all serine derivatives **I-5**{*1*,R^2,R^3} was performed with sodium dithionite and yielded compounds **I-6**{*1*,R^2,R^3} in good crude purities (82-98%, calculated from HPLC-UV traces at 205−400 nm, Scheme 34, Table 4).

Scheme 34. The reduction of nitro group of intermediates **I-5**{R^1,R^2,R^3}[a]

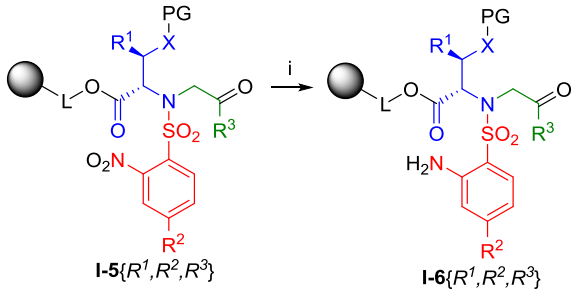

I-5{R^1,R^2,R^3} **I-6**{R^1,R^2,R^3}

[a]Reagents and conditions: (i) **(a)** $Na_2S_2O_4.2H_2O$, K_2CO_3, TBAHS, 50% DCM/H_2O, 2-5 h, rt; **(b)** $SnCl_2.2H_2O$, DIEA, DMF, 30 min, rt.

Table 4. The tested and final conditions for the reduction of nitro group of intermediates **I-5**{R^1,R^2,R^3}[a]

starting cmpd	X	R^1	R^2	R^3	method[a]	solvent	ratio of both solvents	time [h]	crude purity of I-5 [%][b]	crude purity of I-6 [%][b]	ratio of I-5:6 [%][b]
I-5{*1,1,1*}	O	H	H	Ph	**a**	DCM/H_2O	1:1	2.5	0	97	0:100
I-5{*1,2,1*}	O	H	MeO	Ph	**a**	DCM/H_2O	1:1	4	0	95	0:100
I-5{*1,3,1*}	O	H	Cl	Ph	**a**	DCM/H_2O	1:1	4	0	94	0:100
I-5{*1,4,1*}	O	H	CF_3	Ph	**a**	DCM/H_2O	1:1	2	0	82	0:100
I-5{*1,5,1*}	O	H	NO_2	Ph	**a**	DCM/H_2O	1:1	5	0	84	0:100
I-5{*1,1,2*}	O	H	H	4-Me-Ph	**a**	DCM/H_2O	1:1	2.5	0	90	0:100
I-5{*1,1,3*}	O	H	H	4-NH_2-3,5-diCl-Ph	**a**	DCM/H_2O	1:1	2.5	0	95	0:100
I-5{*1,1,4*}	O	H	H	4-Br-Ph	**a**	DCM/H_2O	1:1	2	0	95	0:100
I-5{*1,1,5*}	O	H	H	4-CF_3-Ph	**a**	DCM/H_2O	1:1	2.5	0	94	0:100
I-5{*1,1,6*}	O	H	H		**a**	DCM/H_2O	1:1	2	0	98	0:100
I-5{*2,1,1*}	O	Me	H	Ph	**a**	DCM/H_2O	1:1	3.5	0	94	0:100
I-5{*3,1,1*}	S	H	H	Ph	**a**	DCM/H_2O	1:1	0.5	0	23	0:100
							1:2	0.5	0	26	0:100
							1:0	0.5	34	39	47:53
							2:1	0.5	0	67	0:100
							4:1	0.5	0	47	0:100
							5:1	0.5	70	0	100:0
					b	**degassed DMF**	**-**	**0.5**	**0**	**94**	**0:100**

[a]The reaction conditions are defined in Scheme 34; [b]Calculated from HPLC-UV traces at 205–400 nm.

The product release from the resin as well as the subsequent TES reduction required different cleavage time (Table 5-6). In the case of **I-7**{*1,5,1*} and **I-7**{*1,1,5*} prepared from 2,4-dinitro-benzensulfonyl chloride and 2-bromo-1-(4-(trifluoromethyl)phenyl)ethan-1-one, respectively, expected

products were not detected by LC-MS analysis (Scheme 35, Table 5-6).

Scheme 35. The cleavage of intermediate **I-6**{R^1,R^2,R^3} from the resin[a]

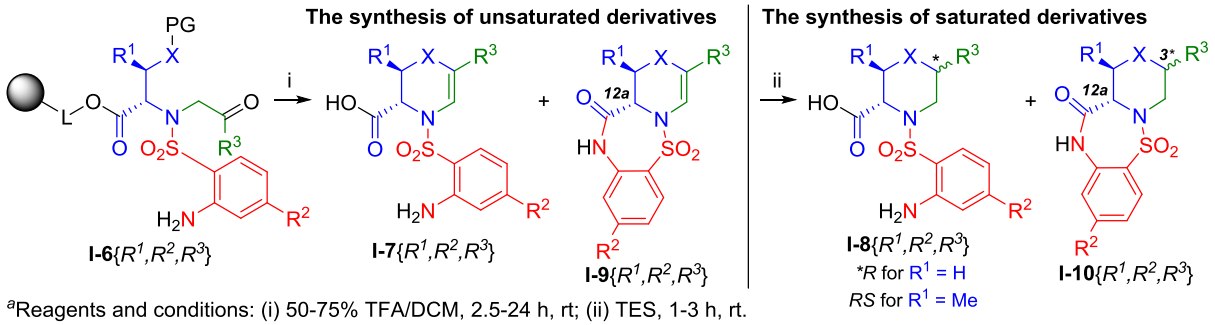

[a]Reagents and conditions: (i) 50-75% TFA/DCM, 2.5-24 h, rt; (ii) TES, 1-3 h, rt.

Table 5. Cleavage conditions for the preparation of unsaturated derivatives **I-7**{R^1,R^2,R^3} at rt[a]

starting cmpd	X	R^1	R^2	R^3	concentration of TFA/DCM	time [h]	crude purity of I-7 [%][a]	crude purity of I-9 [%][a]	ratio of I-7:9 [%][a]
6{*1,1,1*}	O	H	H	Ph	60%	3	92	3	97:3
6{*1,2,1*}	O	H	MeO	Ph	60%	7.5	91	4	96:4
6{*1,3,1*}	O	H	Cl	Ph	50%	4.5	67	16	81:19
6{*1,4,1*}	O	H	CF_3	Ph	50%	6	67	7	91:9
6{*1,5,1*}	O	H	NO_2	Ph	50%	2.5	64	0	100:0
6{*1,1,2*}	O	H	H	4-Me-Ph	50%	7	91	4	96:4
6{*1,1,3*}	O	H	H	4-NH_2-3,5-diCl-Ph	50%	5	97	1	99:1
6{*1,1,4*}	O	H	H	4-Br-Ph	75%	24	76	5	94:6
6{*1,1,5*}	O	H	H	4-CF_3-Ph	50%	7	94	1	99:1
6{*1,1,6*}	O	H	H		50%	24	76	0	100:0
6{*2,1,1*}	O	Me	H	Ph	50%	4	80	12	87:13
6{*3,1,1*}	S	H	H	Ph	50%	3.5	92	0	100:0

[a]Calculated from HPLC-UV traces at 205–400 nm.

Table 6. Cleavage conditions for the preparation of saturated **I-8**{R^1,R^2,R^3} at rt[a-b]

starting cmpd	X	R^1	R^2	R^3	concentration of TFA/DCM	time [h]	TES [h]	crude purity of I-8 [%][a]	crude purity of I-10 [%][a]	ratio of I-8:10 [%][a]
6{*1,1,1*}	O	H	H	Ph	50%	23	1	81	10	89:11
6{*1,2,1*}	O	H	MeO	Ph	60%	4	2	92	0	100:0
6{*1,3,1*}	O	H	Cl	Ph	50%	4.5	2	84	7	92:8
6{*1,4,1*}	O	H	CF_3	Ph	50%	4	2	58	0	100:0
6{*1,5,1*}	O	H	NO_2	Ph	50%	4.5	2	ND	ND	ND
6{*1,1,2*}	O	H	H	4-Me-Ph	50%	5.5	3	71	13	85:15
6{*1,1,3*}	O	H	H	4-NH_2-3,5-diCl-Ph	50%	5	1.5	97	1	99:1
6{*1,1,4*}	O	H	H	4-Br-Ph	60%	5	2	82	11	88:12
6{*1,1,6*}	O	H	H		50%	24	3	83	3	97:3
6{*2,1,1*}	O	Me	H	Ph	50%	4	2	74	16	82:18
6{*3,1,1*}	S	H	H	Ph	50%	4	2	ND	ND	ND
					50%	4	70[b]	ND	ND	ND

[a]Calculated from HPLC-UV traces at 205–400 nm; [b]The reaction tested at 50 °C; ND = not detected.

Although a minor formation of target products **I-9**{R^1,R^2,R^3} and **I-10**{R^1,R^2,R^3} was observed after the TFA-mediated cleavage of intermediates **I-7**{R^1,R^2,R^3} and **I-8**{R^1,R^2,R^3} from the resin (up to 16%), prolonged exposure to the cleavage cocktail did not lead to higher conversion (above mentioned in the thesis and Table 1), and heating in anhydrous DCE or anhydrous toluene with PTSA catalysis was required to completion (Scheme 36). However, the cyclization to saturated products **I-10**{R^1,R^2,R^3} required significantly longer time in comparison to the unsaturated analogous **I-9**{R^1,R^2,R^3} (Table 7 for the final derivatives).

Scheme 36. The final cyclization to fused derivatives **I-9**{R^1,R^2,R^3} and **I-10**{R^1,R^2,R^3}[a]

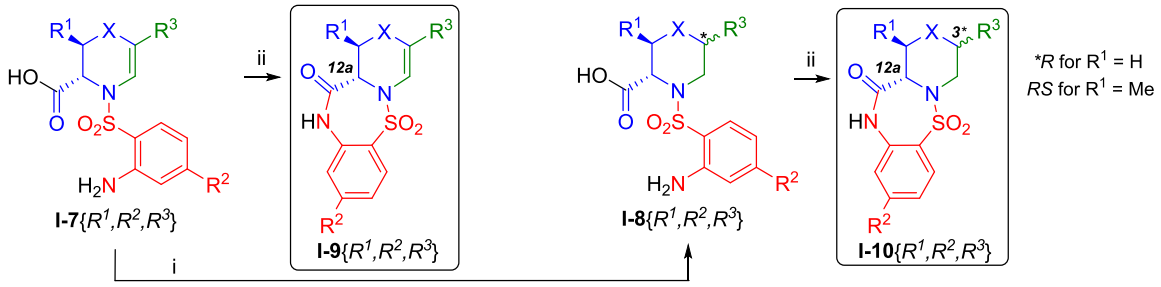

[a]Reagents and conditions: (i) TES, 1-3 h, rt; (ii) PTSA, anhydrous $PhCH_3$, 3.5-12 h, 110 °C or PTSA, anhydrous DCE, 1-144 h, 90 °C.

The synthesis of **I-9**{*1,1,3*}, prepared from 1-(4-amino-3,5-dichlorophenyl)-2-bromoethanone, failed in the stage of the final cyclization step. In contrast, the analogical saturated derivative **I-10**{*1,1,3*} was obtained in 82% crude purity (calculated from HPLC-UV traces at 205−400 nm) and 36% overall yield (calculated from the ^{1}H NMR spectrum of the purified product) as a mixture of C12a *R,S* isomers in a ratio of 29:71 detected in ^{1}H NMR spectrum of the purified product (Scheme 37, Table 7 for the final derivatives). In the case of crude product **I-9**{*1,5,1*}, the derivative decomposed during semipreparative reverse-phase HPLC purification. When TES was added to the crude derivative **I-7**{*1,5,1*}, the reduction failed, and no traces of product were detected by LC-MS analysis. These facts indicated that 2,4-dinitrobenzensulfonyl chloride is not compatible with the method.

Scheme 37. The synthesis of both derivatives **I-9**{*1,1,3*} and **I-10**{*1,1,3*} from 1-(4-amino-3,5-dichlorophenyl)-2-bromoethanone as an alkylating agent[a]

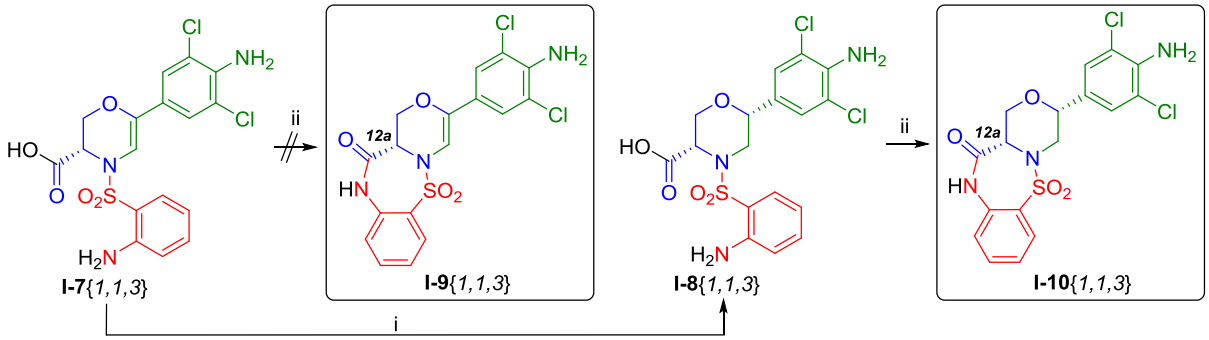

[a]Reagents and conditions: (i) TES, 1.5 h, rt; (ii) PTSA, anhydrous DCE, 1-42.5 h, 90 °C.

From the results, we concluded that the cyclization step partially affects the resulting C12*a* configuration. Although the model compounds **I-9**{*1,1,1*}^{DCE} and **I-10**{*1,1,1*}^{DCE} have been prepared without any conversion of the C12*a* stereocenter, their substituted analogues provided different results. In the case of unsaturated products **I-9**{R^1,R^2,R^3} cyclized in DCE, the detail SFC study revealed the presence of C12a *R* isomer in a quantity 8-28%, and in toluene, we obtained 23-37% of C2*a R*isomer. This indicates epimerization of C12*a* in a range of 0-20% after the cyclization step (8% was assigned to epimerization caused by the immobilization, as mentioned earlier in the thesis). In the case of saturated analogues **I-10**{R^1,R^2,R^3}, the detailed investigation of their ^{1}H NMR spectra after HPLC purification were performed. In accordance with our previous results,[1,2] the TES reduction of threonine-based derivative **I-7**{*2,1,1*} was non-stereoselective and its subsequent cyclization to benzo-methylmorpholino-thiadiazepinones gave a mixture of both separable C3 isomers **I-10a**{*2,1,1*} and **I-10b**{*2,1,1*} in the ratio of 63:47 (above mentioned in the thesis and Scheme 32). In contrast, the synthesis of serine-based morpholines **I-7**{*1*,R^2,R^3} was fully stereoselective and the final cyclization to required products **I-10**{*1*,R^2,R^3} furnished a mixture of both inseparable C12*a R* epimers in a range of 13-29% (in anhydrous DCE) and 23-50% (in anhydrous toluene) depending on R^3 substituent (calculated from ^{1}H NMR spectra of the purified products, Table 7 for the final derivatives).

4.1.4 Conclusion

To conclude, the developed methodology was applied to synthesize 20 diversely substituted compounds and two amino (un)saturated amino derivatives which were isolated and fully characterized. Notwithstanding minor limitations of the approach, the final products were observed in good crude purities and overall yields. Furthermore, the TES reduction was used to prepare benzomorpholino-thiadiazepines with a controlled 3D architecture and the detailed analysis of the C3 and C12*a* stereocenters was achieved using a combination of chiral SFC and advanced NMR experiments. According to our previous studies,[2] the formation of the C3 stereocenter (*R*) was fully stereoselective, except for threonine-based intermediates providing a mixture of separable 3C *R,S* isomers. The resulting C12*a* configuration was rather slightly influenced by the final cyclization and the use of DCE furnished the lower rate of epimerization in comparison to toluene.

Table 7. The used cyclization conditions leading to target compounds[a-d]

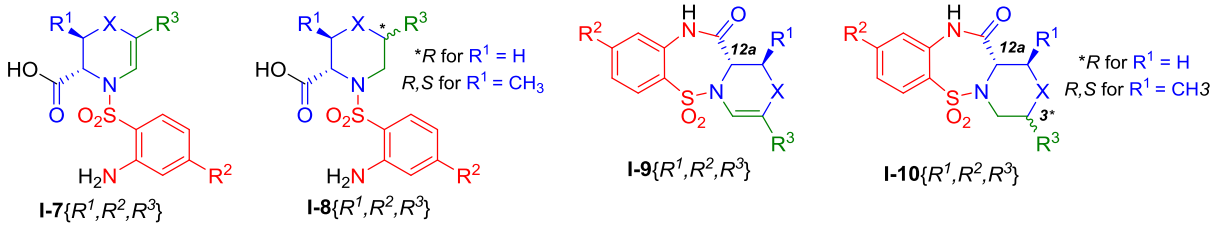

I-7{R^1,R^2,R^3} **I-8**{R^1,R^2,R^3} **I-9**{R^1,R^2,R^3} **I-10**{R^1,R^2,R^3}

cmpd	X	R^1	R^2	R^3	PTSA [equiv]	solvent	time [h]	temp [°C]	crude purity [%][a]	final purity [%][b]	overall yield [%][d]	ratio of *R:S* stereoisomers [%][c,d]
I-7{*1,1,4*}	O	-	H	4-Br-Ph	-	-	-	-	87	98	58	-
I-8{*1,1,1*}	O	-	H	Ph	-	-	-	-	83	95	77	-
I-9{*1,1,1*}^{tol}	O	H	H	Ph	2	$PhCH_3$	3.5	110	77	99	35	23:77[c]
I-9{*1,1,1*}^{DCE}	O	H	H	Ph	2	DCE	5.5	90	81	98	51	8:92[c]
I-9{*1,2,1*}	O	H	MeO	Ph	2	DCE	4.5	90	91	99	51	25:75[c]
I-9{*1,3,1*}	O	H	Cl	Ph	2	DCE	5	90	78	98	34	23:77[c]
I-9{*1,4,1*}	O	H	CF_3	Ph	2	DCE	4.5	90	70	99	42	27:73[c]
I-9{*1,5,1*}	O	H	NH_2	Ph	2	DCE	6	90	80	NI	NI	-
I-9{*1,1,2*}	O	H	H	4-Me-Ph	2	DCE	4.5	90	88	95	44	13:87[c]
I-9{*1,1,4*}^{tol}	O	H	H	4-Br-Ph	2	$PhCH_3$	1	90	65	97	40	37:63[c]
I-9{*1,1,5*}	O	H	H	4-CF_3-Ph	2	DCE	4.5	110	95	99	41	23:77[c]
I-9{*1,1,6*}	O	H	H		2	DCE	1	90	85	95	5	28:72[c]
I-9{*2,1,1*}	O	Me	H	Ph	2	DCE	6	90	92	99	32	0:100[c]
I-9{*3,1,1*}	S	H	H	Ph	2	DCE	27	90	82	90	27	25:75[c]
I-10{*1,1,1*}^{tol}	O	H	H	Ph	2	$PhCH_3$	4	110	84	95	41[e]	23:77[d]
I-10{*1,1,1*}^{DCE}	O	H	H	Ph	2	DCE	3	90	85	98	42[e]	8:92[d]
I-10{*1,2,1*}	O	H	MeO	Ph	2	DCE	5	90	90	98	39	0:100[d]
I-10{*1,3,1*}	O	H	Cl	Ph	2	DCE	144	90	70	99	38	0:100[d]
I-10{*1,4,1*}	O	H	CF_3	Ph	2	DCE	3	90	57	98	40	0:100[d]
I-10{*1,1,2*}	O	H	H	4-Me-Ph	2	DCE	25	90	91	99	42[e]	13:87[d]
I-10{*1,1,3*}	O	H	H	4-NH_2-3,5-diCl-Ph	4	DCE	42.5	90	82	97	36[e]	29:71[d]
I-10{*1,1,4*}^{tol}	O	H	H	4-Br-Ph	2	$PhCH_3$	12	110	84	98	10[e]	50:50[d]
I-10{*1,1,4*}^{DCE}	O	H	H	4-Br-Ph	2	DCE	4	90	87	95	44	0:100[d]
I-10{*1,1,6*}	O	H	H		2	DCE	21	90	85	95	44[e]	26:74[d]
I-10a{*2,1,1*}	O	Me	H	Ph	2	DCE	4	90	50	98	35[f]	0:100[d]
I-10b{*2,1,1*}	O	Me	H	Ph	2	DCE	4	90	30	98	17[g]	0:100[d]

[a]Overall purity after the entire reaction sequence calculated from HPLC-UV traces at 205–400 nm; [b]HPLC-UV traces at 205–400 nm after purification; [c]Ratio of C12*a R,S* enantiomers determined by SFC of the purified product; [d]Ratio of C12*a R,S* stereoisomers calculated from ^{1}H NMR of the purified product; [e]Inseparable C12*a R,S* isomers; [f]Separable C3 *R* isomer; [g]Separable C3 *S* isomer; NI: not isolated (decomposition during HPLC purification).

4.2 Stereoselective Synthesis of Benzo[*e*][1,4]oxazino[4,3-*a*][1,4]Diazepine-6,12-Diones with Two Diversity Positions

The results of this project were published in: Králová, P.; Maloň, M; Soural, M. *ACS Comb. Sci.* **2017**, *19* (12), 770–774.[39] The manuscript is attached in Appendix D (p. 172 – 176). The Supporting information is available at: https://pubs.acs.org/doi/suppl/10.1021/acscombsci.7b00134 and is attached as an electronic file on CD.

Numbering of the individual products in the subchapter does not correspond to the attached manuscript and Supporting information.

4.2.1 Brief introduction

The second project is devoted to the solid-phase synthetic strategy to prepare benzoxazino-diazepinones started from readily available synthons: Fmoc-L-serine, 2-nitrobenzoic acids and α-bromoketones. According to the previously reported results,[3,82] the reduction of nitro group of polymer-supported *N*-acyl intermediates and their cyclization yielded benzodiazepin-5-ones. For this reason, *N*-acyl intermediates were cleaved from the polymer support and then suggested to a post-cleavage modification consisting in three-step sequence (i.e. TES reduction, hydrogenation and acid-mediated cyclization) performed in solution phase. Importantly, only a simple work-up and isolation of reaction intermediates were used to keep applicability of the strategy using high-throughput synthesis concept (Figure 15). As in the previous case, we mainly focused on the study of target benzomorpholino-diazepinediones in terms of their configuration and optical purity.

Figure 15. The suggested synthesis of benzo[*e*][1,4]oxazino[4,3-*a*][1,4]diazepine-6,12-diones

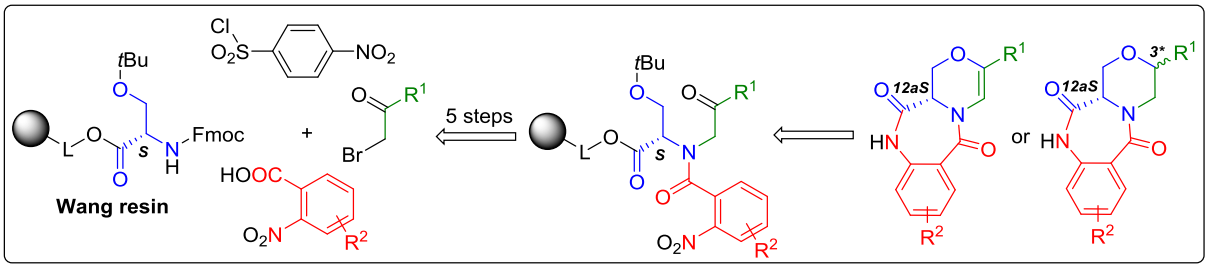

4.2.2 Synthesis

The synthesis of benzomorpholino-diazepinediones **II-8**{R^1,R^2} (Scheme 38) was performed using a combination of SPS and a three post-cleavage reactions (e.g. TES reduction, hydrogenation and a final cyclization) with a simple isolation of all cleaved intermediates using only evaporation under a stream of nitrogen or filtration. The proposed methodology was inspired by our previously reported research in the field of morpholine-3-carboxylic acid derivatives.[1,2] To develop the reaction sequence, we started with α-bromoacetophenone and 2-nitrobenzoic acid. The starting *N*-alkyl sulfonamide

II-2{*1*} was synthesized from the resin-bound Fmoc-Ser(*t*Bu)-OH on Wang resin **II-1** which was submitted to the Fmoc deprotection and an activation/protection of primary amine with 4-Nos-Cl followed by Fukuyama monoalkylation with *α*-bromoacetophenone. After cleavage of the 4-Nos protecting group using MCE/DBU, the key *α*-amino ketone **II-3**{*1*} was subjected to further acylation with 2-nitrobenzoic acid. In contrast to the previously reported synthesis of benzodiazepin-5-one derivatives,[3] no dealkylated product was obtained after the acylation step using LC-MS analysis, but the acylation required a longer reaction time (66 h, Table 10 later in the thesis) to complete conversion. The product **II-4**{*1,1*} was obtained in 88% crude purity (calculated from HPLC-UV traces at 205–400 nm). Obviously, the reduction of nitro group of polymer-supported intermediate **II-4**{*1,1*} triggered the reaction of the amino group with a ketone which, after TFA-mediated cleavage from the resin, yielded benzo[*e*][1,4]diazepin-5-one scaffold **II-10**{*1,1*}.[3,82] In this case the LC-MS analysis showed no traces of oxazine derivative **II-7a**{*1,1*}. The addition of TES into a cleavage cocktail commenced the reduction of imine to product **II-11**{*1,1*}, with a specific configuration of the newly formed C2 stereocenter (*R*) determined using 2D NMR spectra.

Scheme 38. The synthesis of benzomorpholino-diazepinediones **II-8**{R^1,R^2}[a]

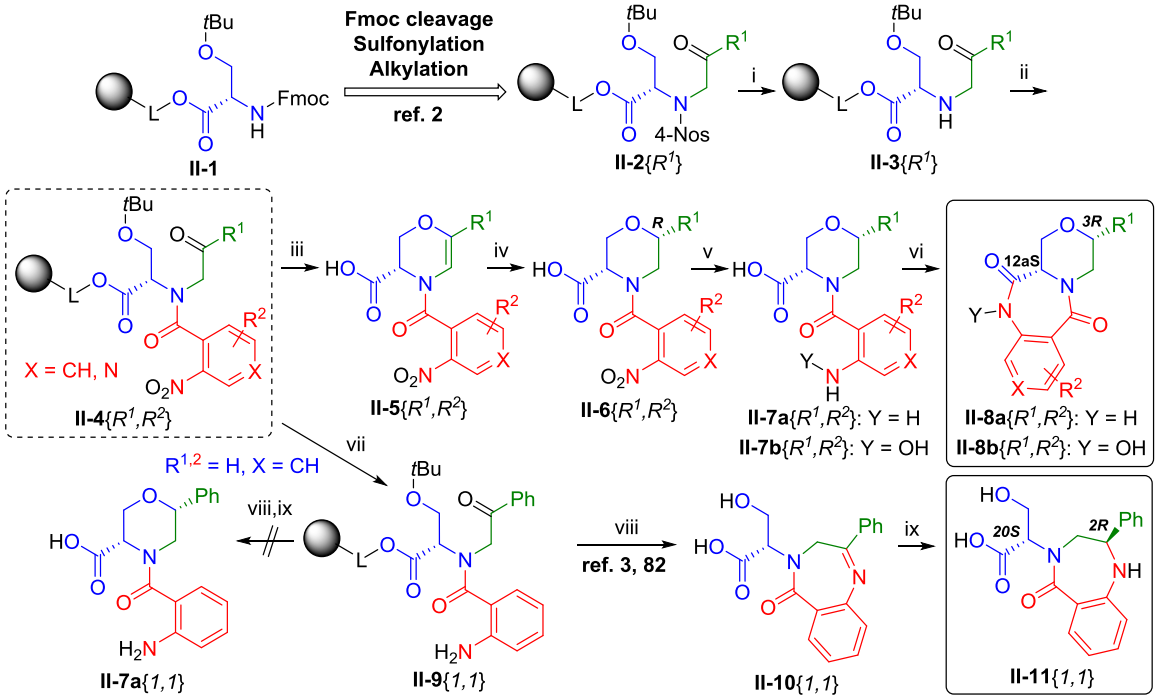

[a]Reagents and conditions: (i) MCE, DBU, DMF, 1.5 h, rt; (ii) 2-nitrobenzoic acid, DIC, deggased DMF, 48-96 h, rt; (iii) 50% TFA/DCM, 15-24 h, rt; (iv) TES, 2-21 h, rt; (v) **(a)** H_2, 10% Pd/C, IPA, 1-48 h, rt or **(b)** H_2, PtO_2, IPA, 2.5-48 h, rt (for derivatives **II-5**{*1,2*}, **II-5**{*1,4*}, **II-5**{*1,6*}, **II-5**{*1,7*}, **II-5**{*4,1*}, **II-5**{*5,6*} and **II-5**{*7,1*}); (vi) 10% TFA/DCM, 2-48 h, 50 °C; (vii) $Na_2S_2O_4.2H_2O$, K_2CO_3, TBAHS, 50% DCM/H_2O, 2 h, rt; (viii) 50% TFA/DCM, 3 h, rt; (ix) TES, 3 h, rt.

The structure elucidation was performed by means of ^1H, $^{13}C\{^1H\}$, ^1H-^1H COSY, ^1H-^1H NOESY, ^1H-^{13}C HSQC, ^1H-^{13}C HMBC, ^1H-^{15}N HMBC and ^1H-^{15}N HMQC data. The ^1H-^{15}N HMQC spectrum provided H^{23}-N1 correlation, whereas the ^1H-^{15}N HMBC spectrum gave interaction of the H^8-N1, and $H_{a\text{-}b}{}^3$ with both nitrogen atoms N1 and N4. The target structure **II-11**{*1,1*} was confirmed

using ^{1}H-^{13}C HMBC spectra, for instance, benzodiazepinone scaffold was proved by the correlations between H_a^3, H^8, H^{11}, H^{20}, H^{21} to C5 and also between H^{23} to C3, C6, C12, C16, C17. In the case of phenyl substituent, the protons H^2, $H_{a\text{-}b}^3$, $H^{12,16}$, H^{23} correlated to C17, whereas CH-(CH$_2$OH)-COOH moiety was detected using correlations of H^{20}, $H_{a\text{-}b}^{21}$ to C19, $H_{a\text{-}b}^{21}$ to C20 and H^{22} to C21 (Figure 16).

Figure 16. The detailed NOESY analysis of benzodiazepine analogue **II-11**{*1,1*}

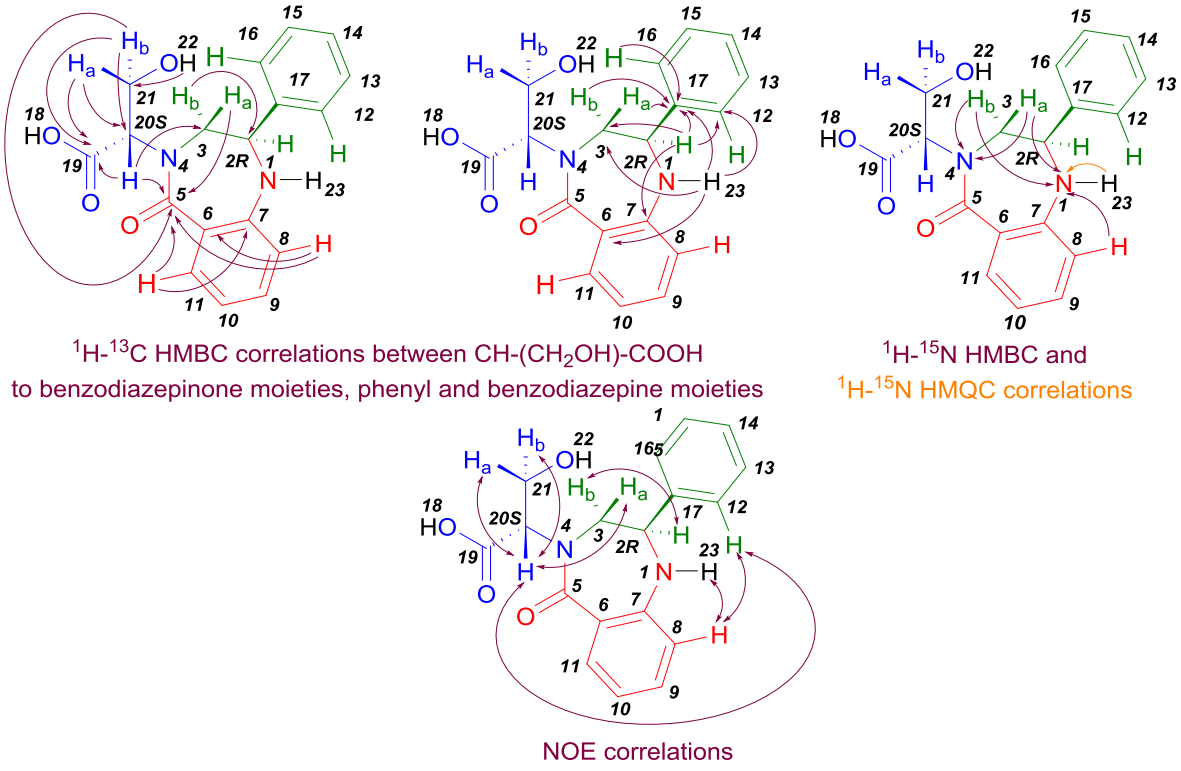

To avoid the formation of benzo[*e*][1,4]diazepin-5-one derivative **II-10**{*1,1*}, intermediate **II-4**{*1,1*} was subjected to TFA-mediated cleavage from the resin that enabled a further post-cleavage modification in solution. First, our attention was paid to the preparation of unsaturated derivative **II-13**{*1,1*} (Scheme 39, Table 8). In this stage, we tested five methods of reduction of nitro group: **(a)** hydrogenation with Pd/C, **(b)** hydrogenation with PtO_2, **(c)** sodium dithionite, **(d)** Fe, 1% AcOH in acetone and **(e)** Fe in AcOH. The hydrogenation of **II-5**{*1,1*} provided a mixture of amino-oxazine **II-7a**{*1,1*} with amino-morpholine **II-12**{*1,1*} and their corresponding lactams **II-8a**{*1,1*} and **II-13**{*1,1*}. In the case of method **(c)**, the reduction with sodium dithionite yielded desired product

Scheme 39. The reduction of *N*-acyl oxazine **II-5**{*1,1*}[a]

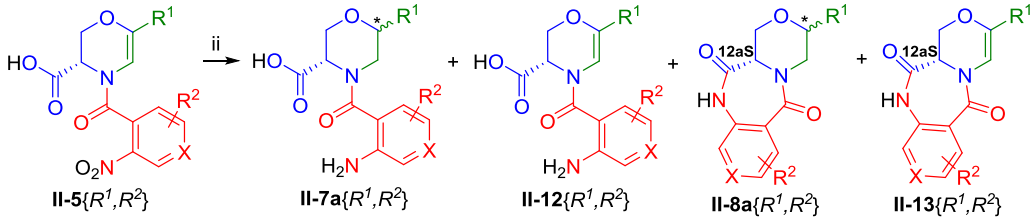

[a]Reagents and conditions: (i) 50% TFA/DCM, 22 h, rt; (ii) **(a)** H_2,10% Pd/C, IPA, 1-24 h, rt; **(b)** H_2, PtO_2, IPA,1-8 h, rt; **(c)** $Na_2S_2O_4$. $2H_2O$, K_2CO_3, EtOH, 30 min-1.5 h, rt; **(d)** Fe, 1% AcOH, aceton, 0.5-24 h, rt; **(e)** Fe, AcOH, 0.5-24 h, 110 °C.

II-7a{*1,1*} in a low crude purity (44%, calculated from HPLC-UV traces at 205–400 nm) and none of the optimizations tested gave better results. Similarly, the reduction with iron in AcOH failed in both tested cases **(d-e)**.

Table 8. Tested methods for the reduction of nitro group of **II-5**{*1,1*}[a-b]

method[a]	reaction conditions	time [h]	temp [°C]	crude purity of II-5 [%][b]	crude purity of II-7a [%][b]	crude purity of II-12 [%][b]	crude purity of II-8a [%][b]	crude purity of II-13 [%][b]	ratio of II-5:7a: 12:8a:13 [%][b]
a	H_2, 10% Pd/C, IPA	1	23	5	12	73	1	3	5:13:78:1:3
		24	23	0	4	22	14	54	0:4:23:15:58
b	H_2, PtO_2, IPA	1	23	0	25	21	0	31	0:33:27:0:40
		8	23	0	13	21	5	41	0:16:26:6:52
c	$Na_2S_2O_4.2H_2O$, K_2CO_3, EtOH	0.5	23	0	0	44	0	0	0:0:100:0:0
		1.5	23	0	0	43	0	0	0:0:100:0:0
d	Fe, 1% AcOH, acetone	0.5	23	80	0	0	0	0	100:0:0:0:0
		24	23	80	0	0	0	0	100:0:0:0:0
e	Fe, AcOH	0.5	110	75	0	0	0	0	100:0:0:0:0
		24	110	70	0	0	0	0	100:0:0:0:0

[a]The reaction conditions are defined in Scheme 39; [b]Calculated from HPLC-UV traces at 205–400 nm.

For these reasons, we attempted the stereoselective TES reduction of oxazine **II-5**{*1,1*} according to the previously reported protocol.[1,2] Similarly to our previous results,[2] the inseparable rotational isomers (rotamers) **II-6**{*1,1*} were obtained in a ratio of 74:26 (calculated from HPLC-UV traces at 205–400 nm, Figure 17, Table 10 later in the thesis). As it is already known, both isomers can rotate around amidic (CONH) bound, as previously observed for proline derivatives.[89] In the case of *N*-acyl morpholines, the presence of "*anti*" and "*syn*" rotamers were confirmed using ^{1}H NMR (doubled signals were detected) and NOESY experiments. The ratio of both rotamers was temperature-dependent, it means that increasing the temperature to 150 °C led to the gradual merging of the NMR signals followed by their refragmentation at 25 °C. According to these results, "*anti*" isomer was more stable than "*syn*" isomer at room temperature;[2] however, in the case of **II-6**{*1,1*}, the detailed NOESY assignment was not performed as the compound **II-6**{*1,1*} was just a synthetic intermediate.

Figure 17. The "*anti*" and "*syn*" rotamers of **II-6**{*1,1*}

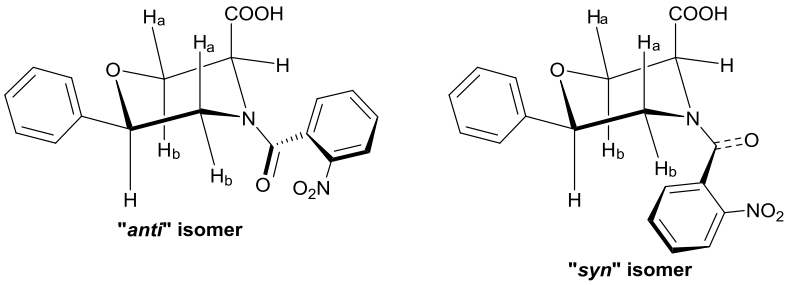

After TES reduction, a residual TFA/TES was removed **II-6**{*1,1*} using a combination of evaporation under a stream of nitrogen and freeze drying. The following catalytic hydrogenation using 10% Pd/C yielded desired amino compound **II-7a**{*1,1*} in excellent crude purity (90%, calculated from HPLC-UV traces at 205–400 nm). Interestingly, the LC-MS analysis confirmed an extinction of the rotational isomers after the reduction of nitro group and only one enantiomer was detected. Whereas the TFA-mediated cyclization at room temperature caused only a slow cyclization to product **II-8a**{*1,1*} (Scheme 38, Table 9), the quantitative conversion was achieved in 10% TFA/DCM at higher temperature (50 °C) for 41 h. The target derivative **II-8a**{*1,1*} was obtained in 92% crude purity (calculated from HPLC-UV traces at 205–400 nm after the entire reaction sequence) and 40% overall yield (calculated from ^{1}H NMR spectrum of the final product, Table 13 for the final derivatives) after semipreparative reversed-phase HPLC purification.

Table 9. The tested conditions for the final cyclization to **II-8a**{*1,1*}[a]

reaction conditions	ratio of reagents [%]	time [h]	temp [°C]	crude purity of II-7a [%][a]	crude purity of II-8a [%][a]	ratio of II-7a:8a [%][a]
TFA/DCM/IPA	1:1:1	4	23	52	32	63:37
		13.5	23	45	36	56:44
		4	50	39	39	50:50
		21	50	36	42	46:54
IPA	1	72	23	65	29	69:31
TFA	1	72	23	29	66	31:69
TFA/DCM	1:1	72	23	6	88	6:94
TFA/DCM	**1:10**	3.5	23	69	26	73:27
		7.5	23	43	49	47:53
		24	23	32	62	34:66
		72	23	4	92	4:96
		24	50	25	72	26:74
		41	**50**	**0**	**92**	**0:100**

[a]Calculated from HPLC-UV traces at 205–400 nm.

Finally, we evaluated the impact of TES reduction and TFA-mediated cyclization to the stereochemical outcome of both C3 and C12*a* stereocenters. Although the immobilization of Fmoc-Ser(*t*Bu)-OH on Wang resin to obtain resin **II-1** was performed using the convenient HOBt technique, it provided ~8% of the second enantiomer (detected by SFC chromatography).[38] Consequently, the cleavage and reduction of intermediate **II-5**{*1,1*} with TES afforded crude compound **II-6**{*1,1*} as a mixture of the corresponding diastereoisomers 3*R*, 12*aS* and 3*R*, 12*aR* in a ratio of 92:8. Similarly, the final cyclization yielded the crude compound **II-8a**{*1,1*} as two separable diastereomers in the same ratio. In this case (and for all analogues **II-8a**{R^1,R^2}), only the major diastereoisomer was isolated by semipreparative reverse-phase HPLC. The configuration of both stereocenters as 3*R*, 12*aS* was determined using the detailed 2D NMR analysis of two representative compounds **II-8a**{*2,3*} and **II-8b**{*5,6*} (depicted later in the thesis and in Figure 19). In contrast to previous research,[38,90–92] these results proved that the C12*a* configuration was not touched during the final cyclization.

4.2.3 Limitations and scope

To reveal the general applicability of our method, we tested a diverse combination of different *α*-bromoketones and 2-nitrobenzoic acids bearing both electron donating and electron withdrawing groups (Figure 18).

Figure 18. The list of tested building blocks for R^1 and R^2 substitution

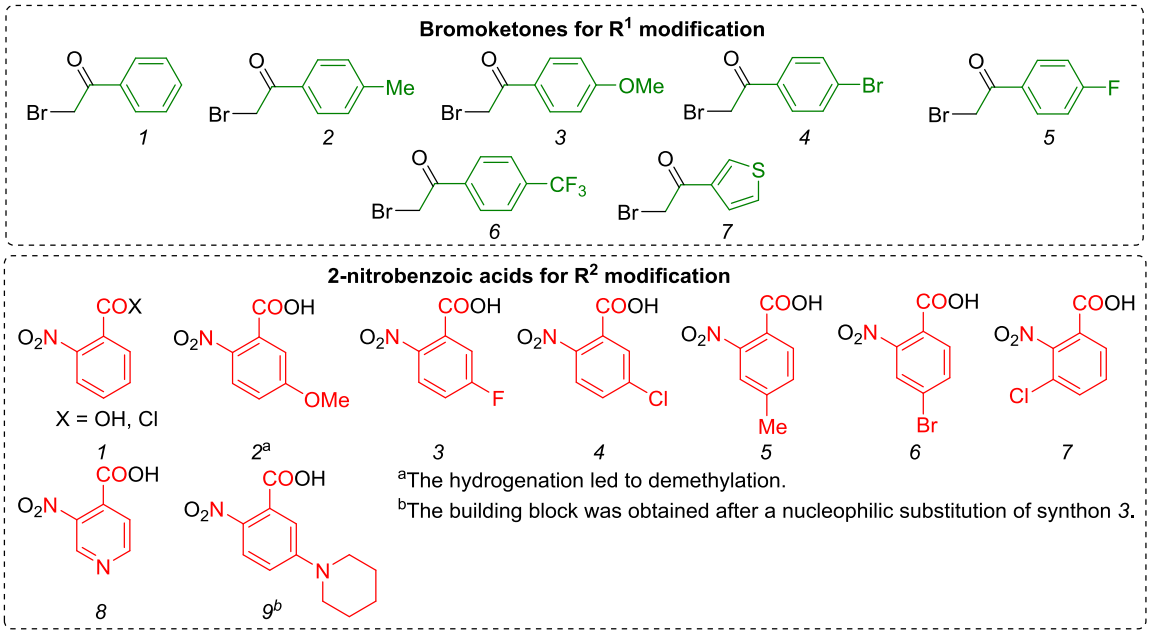

The key *N*-alkyl sulfonamides **II-2**{R^1} were observed in 72-98% crude purities (calculated from HPLC-UV traces at 205–400 nm after the product cleavage from the polymer support). In contrast to our previously reported results,[1,2] the quantitative cleavage of the 4-Nos protecting group needed longer deprotection time (1.5 h). The following acylation required 24-96 h to complete depending on the nucleophilicity of the amine **II-3**{R^1} and reactivity of acylation agents (R^2 modification, Table 10), but no mutual relationship of both R^1 and R^2 substituents was observed. In the case of low-reactive intermediate **II-2**{*6*} with strongly electron withdrawing group, the acylation with carboxylic acid in the presence of DIC, or even with the corresponding acyl chloride failed. The treatment of intermediates **II-4**{R^1,R^2} with TFA/TES resulted in a mixture of CONH rotamers observed in different ratios at room temperature (Scheme 40, Table 10).

Scheme 40. The acylation of **II-3**{R^1,R^2} with various agents and its subsequent cleavage from the resin[a]

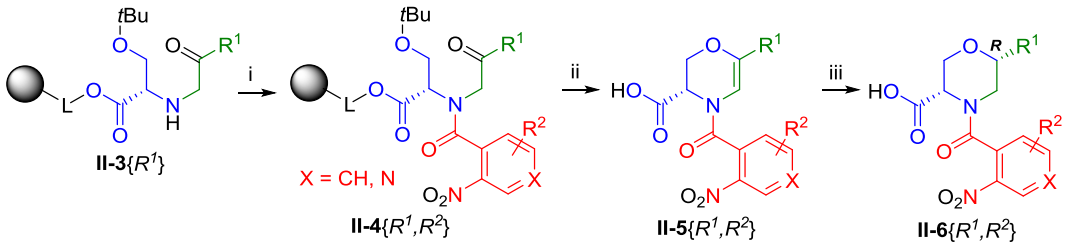

[a]Reagents and conditions: (i) **(a)** R^2-substituted 2-nitrobenzoic acid, DIC, deggased DMF, 48-96 h, rt or **(b)** 2-nitrobenzoyl chloride, 2,6-lutidine, DCM, 24 h, rt; (ii) 50% TFA/DCM, 15-24 h, rt; (iii) TES, 2-21 h, rt.

Table 10. The used reaction conditions for acylation of derivatives **II-3**{*R*[1]}[a]

starting cmpd	acylating agents {*R*[1]}	time [h]	temp [°C]	TFA cleavage time [h]	crude purity of II-4 [%][a]	TES reduction time [h]	crude purity of II-6 [%][a]	ratio of rotamers II-6 [%][a]
II-7{*1*}	2-NO_2-Ph-COOH {*1*}	66	25	22	88	3	90	74:26
II-7{*1*}	5-MeO-2-NO_2-Ph-COOH {*2*}	72	25	24	91	5	94	31:69
II-7{*1*}	5-F-2-NO_2-Ph-COOH {*3*}	24	25	24	91	5	88	36:64
II-7{*1*}	5-Cl-2-NO_2-Ph-COOH {*4*}	48	25	22	97	4.5	94	36:64
II-7{*1*}	4-Me-2-NO_2-Ph-COOH {*5*}	72	25	24	98	3	98	29:71
II-7{*1*}	4-Br-2-NO_2-Ph-COOH {*6*}	72	25	15	90	4	94	29:71
II-7{*1*}	3-Cl-2-NO_2-Ph-COOH {*7*}	48	25	22	94	4.5	89	29:71
II-7{*1*}	3-NO_2-4-Py-COOH {*8*}	72	25	24	96	5	91	49:51
II-7{*2*}	2-NO_2-Ph-COOH {*1*}	48	25	15	98	2	96	42:58
II-7{*2*}	5-MeO-2-NO_2-Ph-COOH {*2*}	72	25	15	98	4	97	40:60
II-7{*2*}	5-F-2-NO_2-Ph-COOH {*3*}	72	25	23	97	4	99	37:63
II-7{*3*}	2-NO_2-Ph-COOH {*1*}	48	25	23	95	2	70	35:65
II-7{*4*}	2-NO_2-Ph-COOH {*1*}	66	25	15	77	4	91	36:64
II-7{*5*}	2-NO_2-Ph-COOH {*1*}	66	25	18	84	4	94	36:64
II-7{*5*}	4-Me-2-NO_2-Ph-COOH {*5*}	72	25	18	82	21	97	40:60
II-7{*5*}	4-Br-2-NO_2-Ph-COOH {*6*}	72	25	15	92	21	90	41:59
II-7{*6*}	2-NO_2-Ph-COOH {*1*}	72	25	15	33	NP	NP	NP
		24	40	15	37	NP	NP	NP
	2-NO_2-Ph-COCl {*1*}	24	25	15	27	NP	NP	NP
II-7{*7*}	2-NO_2-Ph-COOH {*1*}	96	25	23	96	2	83	23:77

[a]Calculated from HPLC-UV traces at 205–400 nm; NP = not prepared.

Analogously to the derivative **II-6**{*1,1*}, the rotamery completely disappeared after the reduction of the nitro group. In general, the catalytic hydrogenation using Pd/C afforded desired derivatives **II-7a**{R^1,R^2} in 49-93% crude purities (calculated from HPLC-UV traces at 205–400 nm), however it led to cleavage of the C-Cl or C-Br bonds. To avoid the undesired hydrogenolysis, intermediates containing halogens were reduced using PtO_2. Furthermore, in the case of intermediates **II-6**{R^1,R^2} bearing halogens as the R^2 substituents (except for **II-6**{*1,7*}), the hydrogenation using PtO_2 afforded *N*-hydroxylamine intermediates **II-7b**{R^1,R^2} in the range of crude purities 7-83% (Scheme 41, Table 11). In the cases of **II-6**{*1,6*} and **II-6**{*5,6*}, the presence of 4-Br as R^2 substituent led to the predominant major formation of hydroxylamine **II-7b**{R^1,*6*} (crude purities above 80%, calculated from HPLC-UV traces at 205–400 nm). For this reason, the corresponding cyclic products **II-7b**{*1,6*} and **II-7b**{*5,6*}

Scheme 41. The hydrogenation of **II-6**{R^1,R^2} and their cyclization to final products **II-8a-b**{R^1,R^2}[a]

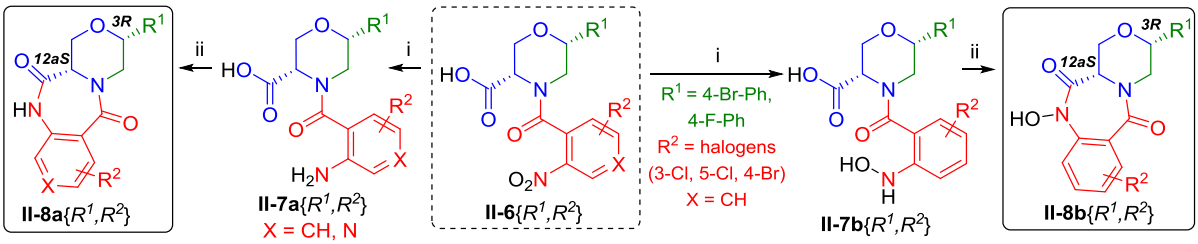

[a]Reagents and conditions: (i) **(a)** H_2,10% Pd/C, IPA, 1-48 h, rt or **(b)** H_2, PtO_2, IPA, 2.5-7.5 h, rt (for derivatives **II-5**{*1,4*}, **II-5**{*1,6*}, **II-5**{*1,7*}, **II-5**{*4,1*}, **II-5**{*5,6*} and **II-5**{*7,1*}); (ii) 10% TFA/DCM, 2-48 h, 50 °C.

were isolated and fully characterized. Figure 19 displays the key NOE correlations of both final derivatives **II-7a**{*2,3*} and **II-7b**{*5,6*}.

Table 11. Reaction conditions for hydrogenation of **II-6**{R^1,R^2}[a]

starting cmpd	R^1	R^2	X	catalyst	time [h]	crude purity of II-7a [%][a]	crude purity of II-7b [%][a]	ratio of II-7a:7b [%][a]
II-6{*1,1*}	Ph	H	CH	Pd/C	4	90	0	100:0
II-6{*1,3*}	Ph	5-F	CH	Pd/C	3	73	18	80:20
II-6{*1,4*}	Ph	5-Cl	CH	PtO_2	2.5	70	28	71:29
II-6{*1,5*}	Ph	4-Me	CH	Pd/C	12	90	0	100:0
II-6{*1,6*}	Ph	4-Br	CH	PtO_2	2.5	13	80	14:86
II-6{*1,7*}	Ph	3-Cl	CH	PtO_2	2.5	85	0	100:0
II-6{*1,8*}	Ph	H	N	Pd/C	3.5	89	0	100:0
II-6{*2,1*}	4-Me-Ph	H	CH	Pd/C	2.5	91	0	100:0
II-6{*2,3*}	4-Me-Ph	5-F	CH	Pd/C	1	83	7	92:8
II-6{*3,1*}	4-MeO-Ph	H	CH	Pd/C	2	87	0	100:0
II-6{*4,1*}	4-Br-Ph	H	CH	PtO_2	7.5	95	0	100:0
II-6{*5,1*}	4-F-Ph	H	CH	Pd/C	7.5	93	0	100:0
II-6{*5,5*}	4-F-Ph	4-Me	CH	Pd/C	8	49	0	100:0
II-6{*5,6*}	4-F-Ph	4-Br	CH	PtO_2	3.5	11	83	12:88
II-6{*7,1*}		H	CH	PtO_2	4	63	0	100:0

[a]Calculated from HPLC-UV traces at 205–400 nm.

Figure 19. The detail NOE NMR analyses of derivatives **II-7a**{*2,3*} and **II-7b**{*5,6*}

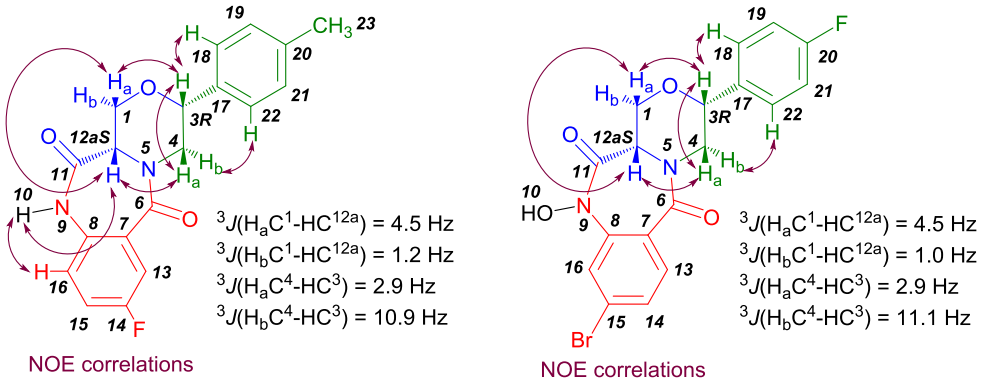

In addition, the catalytic hydrogenation of **II-6**{*1,2*} and **II-6**{*2,2*} with 5-methoxy group as the R^2 substituent caused demethylation using both Pd/C and PtO_2 catalysts (Scheme 42, Table 12). In the first case, the corresponding amine derivatives **II-7a**{*1,2*} or **II-7a-dem**{*1,2*} were not detected using LC-MS analysis, but the reaction led to a mixture of the final benzomorpholinediones **II-8a**{*1,2*} and **II-8a-dem**{*1,2*} in ratios 49:51 or 41:59 depending on the type of catalysts used. However, the presence of electron donating group (Me) in the R^1 position prevented the cyclization to the benzo-morfolino-diones and the demethylated aniline **II-7a-dem**{*2,2*} was obtained in 63% crude purity (calculated from HPLC-UV traces at 205–400 nm). Interestingly, the methoxy group as R^1 substituent (derivative **II-7a**{*3,1*}) did not undergo any demethylation.

Scheme 42. Demethylation of methoxy derivatives **II-6**{R^1,*2*} using catalytic hydrogenation[a]

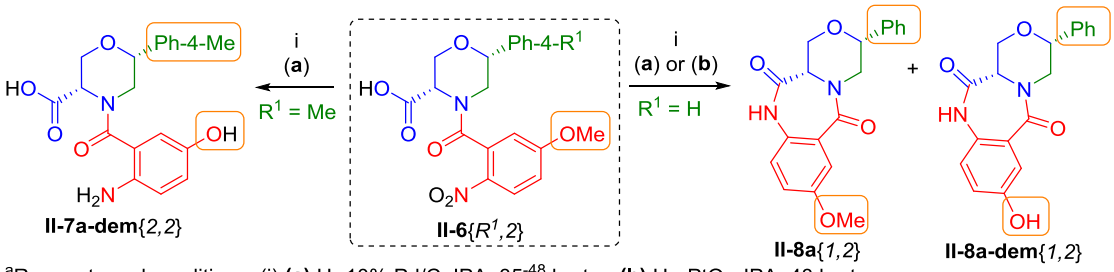

[a]Reagents and conditions: (i) **(a)** H_2, 10% Pd/C, IPA, 35-48 h, rt or **(b)** H_2, PtO_2, IPA, 48 h, rt.

Table 12. Demethylation of methoxy group in R^2 position of **II-6**{R^1,*2*} during hydrogentation[a-c]

starting cmpd	R^1	R^2	catalyst	time [h]	crude purity of II-7a-dem [%][a]	crude purity of II-8a [%][a]	crude purity of II-8a-dem [%][a]	ratio of II-8a: 8a-dem [%][a]
II-6{*1,2*}[b]	Ph	5-MeO	Pd/C	35	0	49	51	49:51
			PtO_2	48	0	38	54	41:59
II-6{*2,2*}[c]	4-Me-Ph	5-MeO	Pd/C	48	63	0	0	-

[a]Calculated from HPLC-UV traces at 205–400 nm; [b]Hydrogentation led to a mixture of product **8a** and its demethylated analogue **8a-dem**; [c]Hydrogenation led to demethylated product **7a-dem**.

In contrast to **8a**{*1,1*}, the cyclization to substituted analogues **II-8a**{R^1,R^2}, **II-8a-dem**{R^1,R^2} and **II-8b**{R^1,R^2} required significantly shorter cyclization time (2-24 h) depending on R^1 and R^2 substituents (Table 13). In the case of pyridine derivative **II-7a**{*1,8*}, the cyclization failed after 1 h and the corresponding derivative **II-8a**{*1,8*} was not prepared. The developed methodology provided 15 representative benzomorpholino-diazepinediones bearing CONH group **II-8a**{R^1,R^2} and **II-8a-dem**{R^1,R^2} in 49-92% crude purities (calculated from HPLC-UV traces at 205–400 nm) and 19-49% overall yields (calculated from ^{1}H NMR spectra of purified products), 2 derivatives with CON[9]-OH **II-8b**{R^1,R^2} in 82-83% crude purities and 49-50% overall yields (Figure 19), and one saturated analogue of benzodiazepin-5-one **II-11**{*1,1*} in 55% crude purity (calculated from HPLC-UV traces at 205–400 nm) and 30% overall yield (calculated from the ^{1}H NMR spectrum of purified product).

Table 13. List of synthesized and fully characterized compounds[a-d]

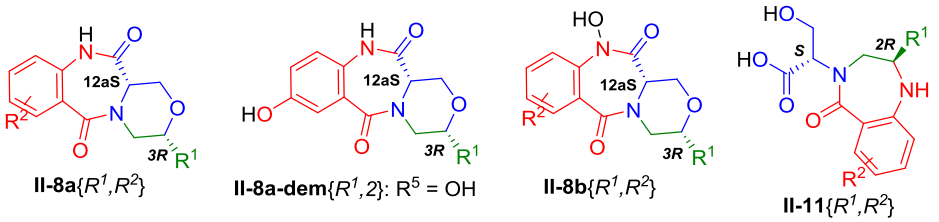

cmpd	R^1	R^2	cyclization time [h]	crude purity [%][a]	final purity [%][b]	overall yield [%][c]
II-8a{*1,1*}	Ph	H	41	92	98	40
II-8a{*1,2*}	Ph	5-MeO	-	49	98	19
II-8a{*1,3*}	Ph	5-F	2.5	66	99	43
II-8a{*1,4*}	Ph	5-Cl	5	70	99	35
II-8a{*1,5*}	Ph	4-Me	19	85	97	38
II-8a{*1,7*}	Ph	3-Cl	5	85	99	38
II-8a{*2,1*}	4-Me-Ph	H	22	75	98	49
II-8a{*2,3*}	4-Me-Ph	5-F	6	83	97	47
II-8a{*3,1*}	4-MeO-Ph	H	25	60	95	45
II-8a{*4,1*}	4-Br-Ph	H	24	85	98	43
II-8a{*5,1*}	4-F-Ph	H	24	86	99	41
II-8a{*5,5*}	4-F-Ph	4-Me	2.5	49	98	28
II-8a{*7,1*}		H	2.5	49	97	27
II-8a-dem{*1,2*}	Ph	5-OH	-	51	99	28
II-8a-dem{*2,2*}	4-Me-Ph	5-OH	5.5	61	98	46
II-8b{*1,6*}	Ph	4-Br	2	82	99	49
II-8b{*5,6*}	4-F-Ph	4-Br	3	83	98	50
II-11{*1,1*}	Ph	H	3+3[d]	55	99	30

[a]Overall purity after the entire reaction sequence calculated from HPLC-UV traces at 205–400 nm; [b]HPLC-UV traces at 205–400 nm after purification; [c]Calculated from the ^{1}H NMR spectrum of the purified product; [d]The cyclization was performed using a two-step cleavage consisted of 50% TFA/DCM for 3 h at rt and then an addition of TES into the cleavage cocktail and reaction for another 3 h at rt.

To extend the developed methodology, we tested the reaction of intermediate **II-4**{*1,3*}, bearing 5-fluoro substitution as R^2, with piperidine in anhydrous THF. The TFA/TES cleavage of the resulting intermediate **II-4**{*1,9*} from the resin yielded the corresponding morpholine **II-6**{*1,9*} in excellent crude purity (96%, calculated from HPLC-UV traces at 205–400 nm). Similarly to derivatives bearing C-halogens as R^2 substituent, further hydrogenation using Pd/C provided a mixture of both compounds

Scheme 43. The synthesis of piperidine analogue **II-8a-b**{*1,9*}[a]

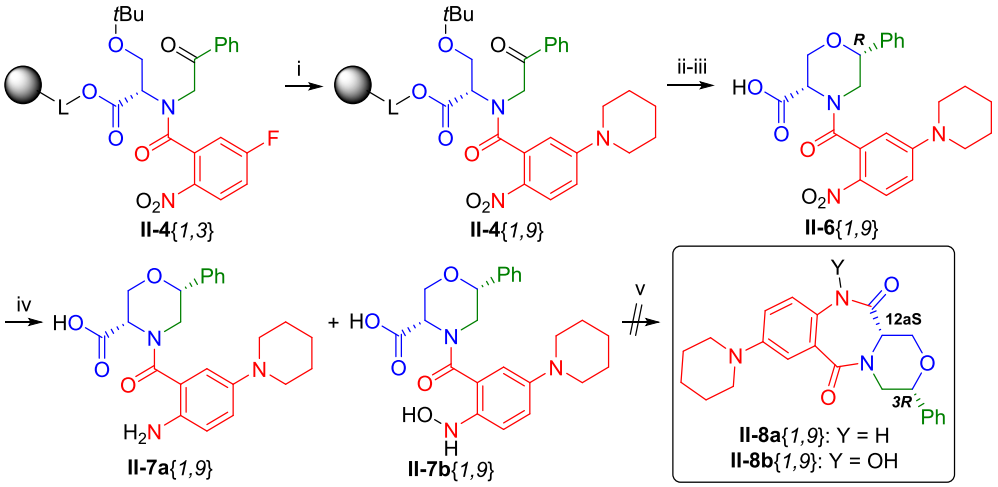

[a]Reagents and conditions: (i) PIP, anhydrous THF, 18 h, temp; (ii) 50% TFA/DCM, 24 h, rt; (iii) TES, 18 h, rt; (iv) **(a)** H_2,10% Pd/C, IPA, 1.5-168 h, rt or 15-44 h, 40 °C; (v) 10% TFA/DCM, 1 h, 50 °C.

II-7a{*1,9*} and **II-7b**{*1,9*} detected by LC-MS analysis in different ratios depending on reaction time and temperature used (Scheme 43, Table 14). First, the LC-MS analysis showed that the reaction conversion after 72 h was not complete and no hydroxylamine derivative **II-7b**{*1,9*} was observed. When the reduction time was extended to 94-168 h, both reduced derivatives **II-7a**{*1,9*} and **II-7b**{*1,9*} were obtained in a ratio of 46:54 (Table 14). To accelerate the transformation to one major product, the hydrogenation temperature was elevated to 40 °C that yielded hydroxylamine derivative **II-7b**{*1,9*} in 85% crude purity (calculated from HPLC-UV traces at 205–400 nm). Nevertheless, the final cyclization according to the above described conditions failed and the starting compound **II-7b**{*1,9*} decomposed.

Table 14. The ratio of **II-7a**{*1,9*} and **II-7b**{*1,9*} depending on the reduction conditions[a]

time [h]	temp [°C]	crude purity of II-4 [%][a]	crude purity of II-7a [%][a]	crude purity of II-7b [%][a]	ratio of II-4:7a:7b [%][a]
1.5	23	78	20	0	80:20:0
3.5	23	67	30	0	69:31:0
72	23	63	32	0	66:34:0
94	23	0	50	47	0:52:48
168	23	0	46	53	0:46:54
15	40	0	13	76	0:15:85
22	**40**	**0**	**10**	**85**	**0:11:89**
44	40	0	10	85	0:11:89

[a]Calculated from HPLC-UV traces at 205–400 nm.

4.2.4 Conclusion

The stereoselective synthesis of benzo[*e*][1,4]oxazino[4,3-*a*][1,4]diazepine-6,12-diones was developed and used to prepare 17 derivatives using a combination of both solid-phase and solution-phase techniques. Although the final steps of the reaction sequence (hydrogenation and cyclization) had to be performed after the product cleavage from the polymer support, the simple work up procedures (fast evaporation or filtration) make this method fully compatible with a high-throughput synthesis concept. The developed methodology has rather slight limitations and the synthesis with only two tested buildings block, e.g. 2-nitropyridin-4-yl and 2-nitro-5-(piperidin-1-yl)benzamide, failed in the stage of the cyclization step. Furthermore, we illustrated applicability of TES reduction for the stereoselective synthesis of benzodiazepine derivatives (e.g. saturated analogue of benzodiazepin-5-one and benzomorpholino-diazepine-diones).

4.3 Synthesis of Disubstituted Pyrazino-Oxazine Derivatives with Controlled Stereochemistry

The results of this project were published in: Ručilová, V.; Králová, P.; Soural, M. *Eur. J. Org. Chem.* **2017**, *2017* (47), 7034–7039.[40] The manuscript is attached in Appendix E (p. 179 – 182). The Supporting information is available at: https://onlinelibrary.wiley.com/doi/abs/10.1002/ejoc.201701448 and is attached as an electronic file on CD.

I participated in this project as a co-author, thus it will be discussed in lower details compared to other projects in this thesis. Numbering of the individual products in the subchapter does not correspond to the attached manuscript and Supporting information.

4.3.1 Brief introduction

To extend the previously reported results in the field of fused morpholine derivatives,[37,38] we decided to replace 2-nitrobenzoic acids with various Fmoc-amino acids. The key intermediates were prepared using a five-step sequence and then subjected to PIP-mediated deprotection which should trigger a spontaneous cyclative cleavage providing piperazine-2,5-dione intermediates. Their reaction with TFA to remove the *tert*-butyl protecting group followed by an acid-mediated cyclization should provide pyrazino-oxazines (Figure 20). In this project, we intended to test the suggested reaction sequence and reveal detailed limitations and scope using a set of natural Fmoc-amino acids with different substitution of a side chain.

Figure 20. The suggested synthesis of 1,7,8,9*a*-tetrahydropyrazino[2,1-*c*][1,4]oxazine-6,9-diones

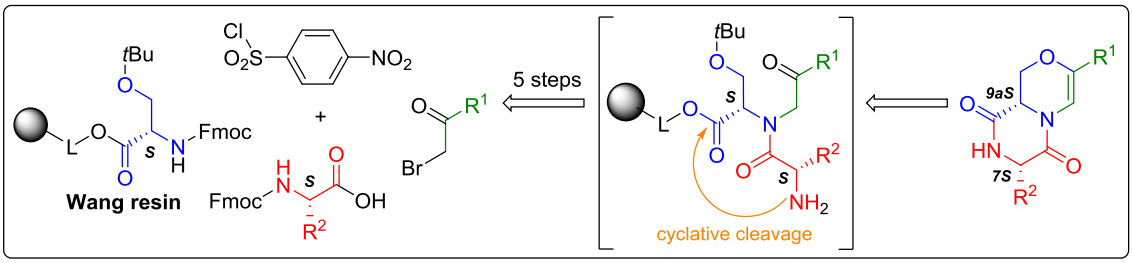

4.3.2 Synthesis

The synthesis of the key 4-Nos-amides **III-2**{R^1} was carried out according to the previously reported protocols[2] starting from immobilized Fmoc-Ser(*t*Bu)-OH on Wang resin **III-1**, 4-Nos-Cl and *α*-bromoketones with both electron donating and electron withdrawing groups as R^1 substituents (Figure 21). In all cases, desired *N*-alkyl-sulfonamides **III-2**{R^1} were observed in good crude purities (on average 90%, calculated from HPLC-UV traces at 205–400 nm). Unlike the previously reported procedure,[2] we had to increase the concentration of MCE (by 2.7 times more) and prolong the reaction time (to 1 h) to quantitatively remove the 4-Nos protecting group. After that, the acylation of the *α*-aminoketones **III-3**{R^1} with eleven different Fmoc-amino acids with various side chains (Figure 21,

R^2 modification) activated with DIC and HOBt yielded the resin-bound *N*-acyl derivatives **III-4**{R^1,R^2}. In some cases, the acylation step had to be repeated to reach completion. The piperidine-mediated deprotection of the Fmoc protecting group triggered a spontaneous cyclative cleavage that yielded piperazine-2,5-diones **III-6**{R^1,R^2}. After the cyclative cleavage, the residual cleavage cocktail was evaporated from intermediate **III-6**{R^1,R^2} followed by the post-cleavage modification consisting of the *tert*-butyl ether deprotection using 50% TFA/DCM yielded derivative **III-7**{R^1,R^2}. TFA should also trigger a spontaneous cyclization to target compounds **III-8**{R^1,R^2}.[2] However, the presence of the piperazine-2,5-dione moiety prevented the cyclization to oxazine derivatives according to previously reported conditions,[2,38,39] the intermediates **III-7**{R^1,R^2} underwent only the protective group cleavage and the cyclization did not proceed even at increased temperature. For this reason, the cleavage cocktail (TFA/DCM) was evaporated under a stream of nitrogen to dryness and the reaction was accomplished in MeCN at higher temperature (80-90 °C depending on both R^1 and R^2 substituent, Table 16 for the final derivatives). The crude pyrazino-oxazines **III-8**{R^1,R^2} were subjected to semipreparative reverse-phase HPLC purification to obtain 16 representative derivatives in 62-89% crude purities (calculated from HPLC-UV traces at 205–400 nm) and 5-46% overall yields (calculated after product cleavage from the resin and HPLC purification, Scheme 44, Table 16 for the final derivatives).

Scheme 44. Synthetic route leading to pyrazino-oxazines **III-8**{R^1,R^2}[a]

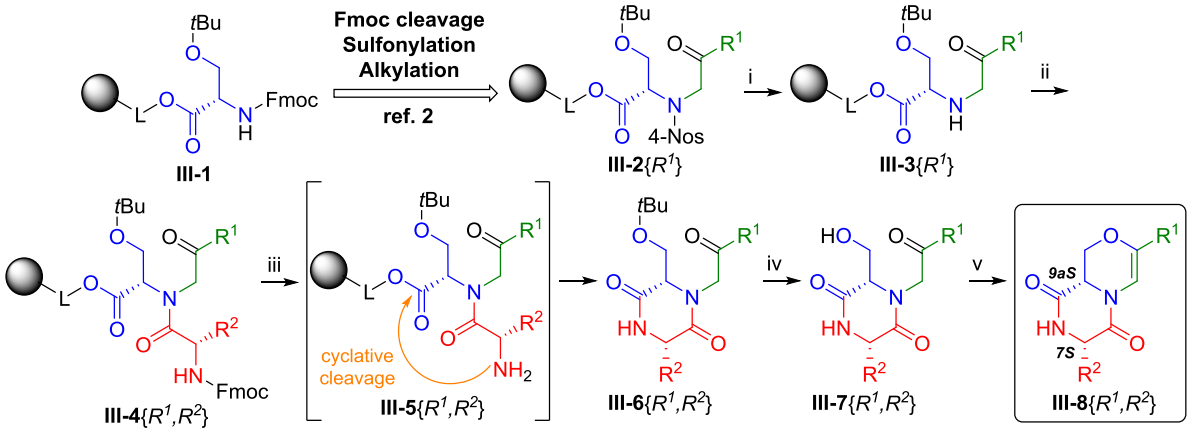

[a]Reagents and conditions: (i) MCE, DBU, DMF, 1 h, rt; (ii) **(a)** Fmoc-amino acids, HOBt, DIC, DCM, DMF, 24 h, rt, then repeat or **(b)** Fmoc-amino acids, DIC, DMF, 16 h, rt; (iii) 50% PIP/DMF, 30 min, rt, then lyophilization for 16 h; (iv) 50% TFA/DCM, 30 min, rt, then evaporation under stream of N_2; (v) MeCN, 1-8 h, 80 °C or 90 °C (for derivatives **III-8**{*1,2*} and **III-8**{*1,3*}, then evaporation under stream of N_2.

Figure 21. The list of tested synthons for R^1 and R^2 substituents

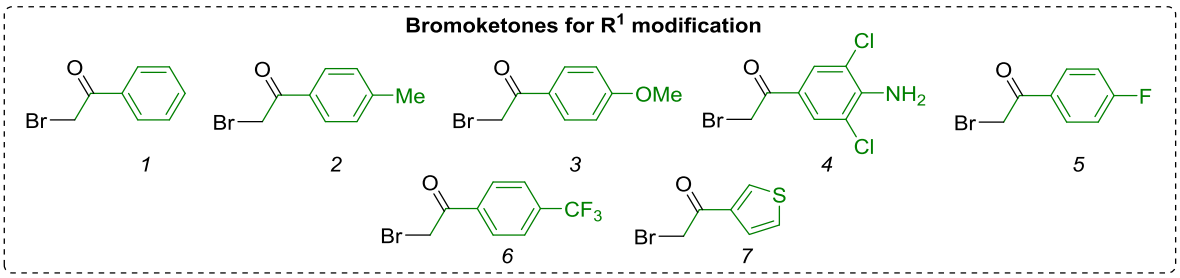

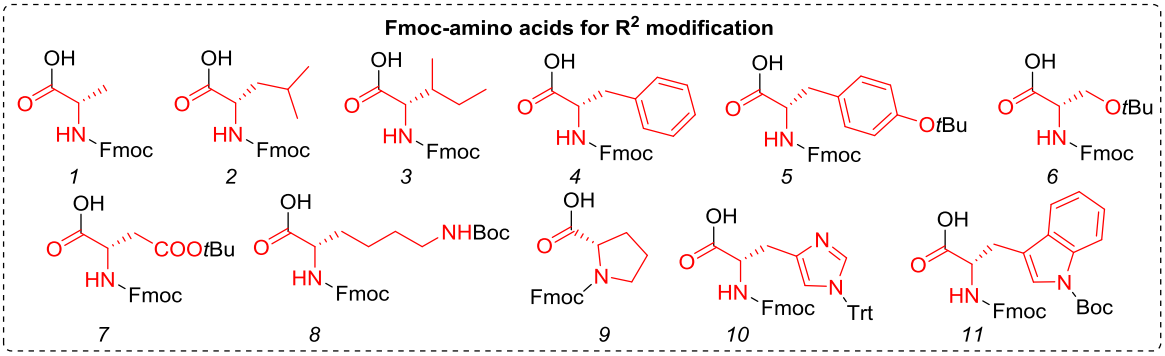

4.3.3 Limitations and scope

Since the reaction sequence afforded the final products **III-8**{R^1,R^2} in relatively limited overall yields, we investigated the reaction sequence in detail. In contrast to trouble-free acylation with 2-nitrobenzoic acid derivatives using the DIC technique discussed earlier in the thesis,[39] some by-products were detected after the acylation step which lowered yields of the final compounds **III-8**{R^1,R^2}. After further investigation, the LC-MS analysis confirmed the structure of the by-products as dealkylated derivatives **III-10**{-,R^2} (Scheme 45). The same behavior was previously reported for the acylation of similar intermediates with benzoic acids activated with DIC and HOBt.[3] To suppress undesired dealkylation, the use of HOBt was omitted, and acylation *via* a symmetrical anhydride using DIC technique was tested (procedure **(b)** in Scheme 45). In contrast to our previous results,[39] the dealkylated derivatives **III-10**{-,R^2} were detected again in considerably higher amount than in the case of DIC/HOBt activation. According to these facts, the formation of dealkylated products was dependent on the type of R^1 and R^2 substituents (i.e. the combination of α-bromoketones with 2-nitrobenzoic acid vs Fmoc-amino acids) and the type of acylation method used (i.e. acylation with DIC/HOBt **(a)** or with DIC **(b)**).

With these results in hands, we have concluded that the dealkylation did not occur during the deprotection of 4-Nos group since the control reactions of all immobilized α-amino ketones **III-3**{R^1} with Fmoc-OSu gave no dealkylated products (i.e. the starting Fmoc-serine **III-1**, Scheme 45). Furthermore, we evaluated a possible effect of the acid-mediated cleavage of **III-4**{R^1,R^2} from the resin on the dealkylation step (Scheme 45, Pathway A). In this case, we observed different ratios of *N*-acyl **III-9**{R^1,R^2} and dealkylated intermediates **III-10**{-,R^2} which indicated the influence of both the R^1 and R^2 substituents on the reaction outcome, but no systematic relationship was observed (Table 15). For this reason, we carried out the cyclative cleavage that yielded piperazine-2,5-diones **III-6**{R^1,R^2} and the corresponding by-products **III-12**{-,R^2}. The formation of **III-12**{-,R^2} clearly demonstrated that dealkylation occurred on the resin during the acylation step, otherwise product **III-12**{-,R^2} could not be detected. It is necessary to note that, in contrast to dealkylated intermediates **III-10**{-,R^2}, the quantities of the corresponding piperidin-2,5-diones **III-12**{-,R^2} for most of the amino acids could not be precisely determined using LC-UV due to the low UV-VIS activity of compounds **III-12**{-,R^2}

(Scheme 45, Pathway B).

Scheme 45. The formation of by-products **III-10**{-,R^2} and **III-12**{-,R^2}[a]

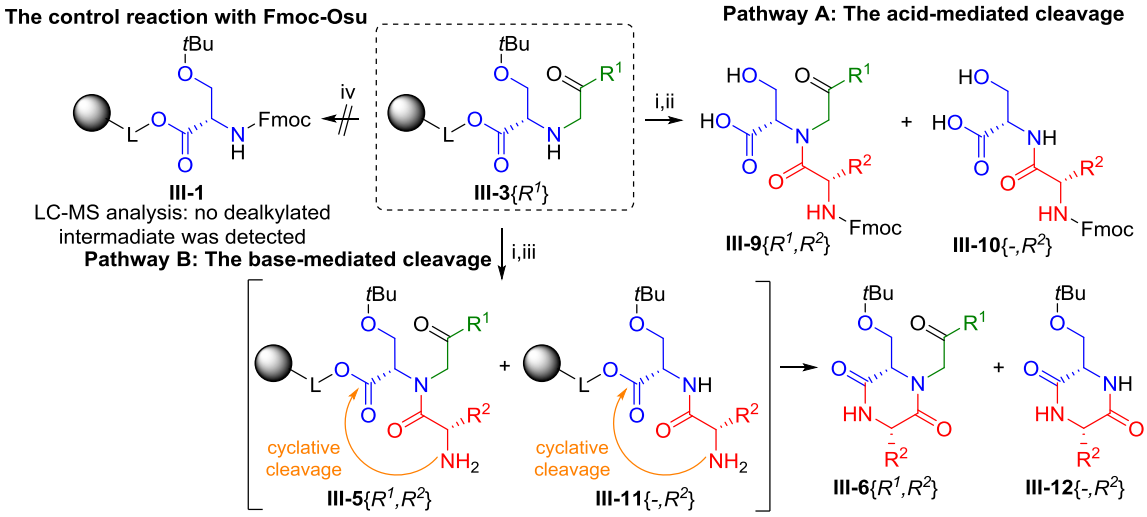

[a]Reagents and conditions: (i) **(a)** Fmoc-amino acids, HOBt, DIC, DCM, DMF, 24 h, rt, then repeat or **(b)** Fmoc-amino acids, DIC, DMF, 16 h, rt; (ii) 50% TFA/DCM, 30 min, rt; (iii) 50% PIP/DMF, 30 min, rt, then lyophilization for 16 h; (iv) Fmoc-OSu, DCM, 30 min, rt.

To substantiate these facts, we suggest the plausible mechanism of the dealkylation (Scheme 46). Appearance of the by-product **III-12**{-,R^2} can be caused by an intramolecular *trans*-alkylation as the side reaction to acylation. However, the formation of compounds **15a-c** (Scheme 46) was impossible to unambiguously detect in the reaction mixture using HPLC-UV-MS due to high excess of acylating agents (a typical feature of solid-supported reactions) and/or poor ionization of expected products.

Scheme 46. The plausible mechanism of dealkylation reaction

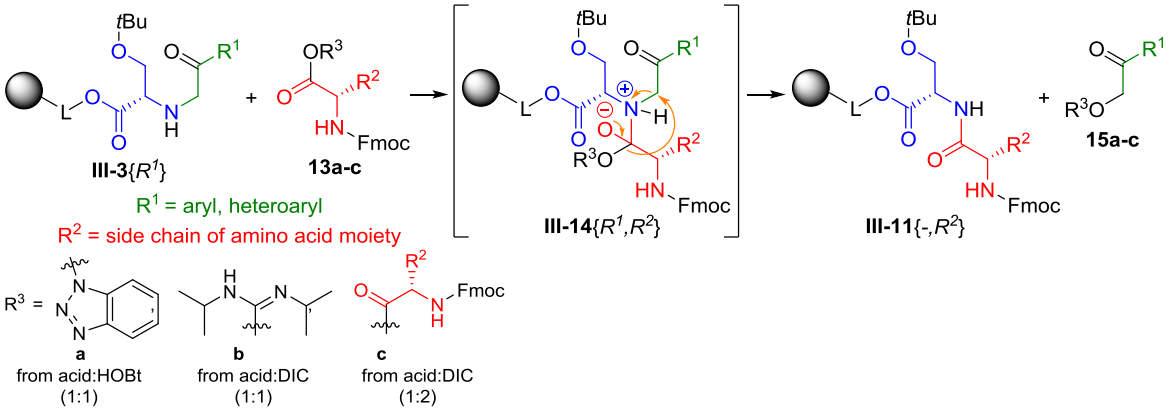

We tested 20 various combinations of seven *α*-bromoketones and eleven Fmoc-amino acids with different side chains to determine limitations and scope of the proposed methodology (Table 15). In the case of Fmoc-Pro-OH, the acylation was followed by quantitative dealkylation. Further, the target pyrazino-oxazines **III-8**{*1,7*} and **III-8**{*1,10*} starting from Fmoc-Asp(*t*Bu)-OH and Fmoc-His(Trt)-OH were accompanied with inseparable impurities and were not isolated (Table 15, highlighted in bold).

Table 15. Ratios of *N*-acyl derivatives **III-9**{R^1,R^2} and dealkylated products **III-10**{-,R^2} after acylation step[a]

cmpd {R^1}	**R^1**	**amino acid {R^2}**	**ratio of III-9{R^1,R^2}:III-10{-,R^2} [%][a]**
III-3{*1*}	Ph	Fmoc-Ala-OH {*1*}	88:12
III-3{*1*}	Ph	Fmoc-Leu-OH {*2*}	73:27
III-3{*1*}	**Ph**	**Fmoc-Ile-OH {*3*}**	**53:47**
III-3{*1*}	Ph	Fmoc-Phe-OH {*4*}	89:11
III-3{*1*}	Ph	Fmoc-Tyr(*t*Bu)-OH {*5*}	83:17
III-3{*1*}	Ph	Fmoc-Asp(*t*Bu)-OH {*7*}	79:21
III-3{*1*}	Ph	Fmoc-Lys(Boc)-OH {*8*}	84:16
III-3{*1*}	**Ph**	**Fmoc-Pro-OH {*9*}**	**0:100**
III-3{*1*}	**Ph**	**Fmoc-His(Trt)-OH {*10*}**	**45:55**
III-3{*1*}	Ph	Fmoc-Trp(Boc)-OH {*11*}	93:7
III-3{*2*}	4-Me-Ph	Fmoc-Ala-OH {*1*}	63:34
III-3{*2*}	4-Me-Ph	Fmoc-Phe(*t*Bu)-OH {*4*}	79:21
III-3{*2*}	4-Me-Ph	Fmoc-Ser(*t*Bu)-OH {*6*}	87:13
III-3{*2*}	4-Me-Ph	Fmoc-Lys(Boc)-OH {*8*}	85:15
III-3{*2*}	4-Me-Ph	Fmoc-Trp(Boc)-OH {*11*}	79:21
III-3{*3*}	4-MeO-Ph	Fmoc-Ala-OH {*1*}	86:14
III-3{*4*}	4-NH_2-3,5diCl-Ph	Fmoc-Ala-OH {*1*}	75:25
III-3{5}	4-F-Ph	Fmoc-Ala-OH {*1*}	69:31
III-3{*6*}	**4-CF_3-Ph**	**Fmoc-Ala-OH {*1*}**	**30:70**
III-3{7}		Fmoc-Ala-OH {*1*}	77:23

[a]Calculated from HPLC-UV traces at 205–400 nm.

The synthetic strategy was successfully applied to prepare 16 final derivatives in a range of 62-89% crude purities (calculated from HPLC-UV traces at 205–400 nm) and 5-46% overall yields (calculated from ^{1}H NMR spectra of the purified products), which were isolated and fully characterized (Table 16). Moreover, all prepared compounds **III-8**{R^1,R^2} were obtained as diastereomerically pure by NMR analysis, i.e. no diastereoisomers of intermediates **III-6-8**{R^1,R^2} were detected by LC-MS analysis. In this case, the cyclative cleavage of intermediates **III-4**{R^1,R^2} did not cause epimerization at C7 and C9*a* stereocenters within reaction sequence.

4.3.4 Conclusion

This project introduced a novel synthetic strategy to prepare rarely studied fused [6+6] morpholine derivatives started from readily available building blocks: Fmoc-*α*-amino acids and *α*-bromoketones. Although the developed methodology reported a minor shortcoming (i.e. dealkylation reaction), we synthesized 16 representative derivatives to determine limitations and scope depending on R^1 and R^2 substituents; however, no systematic relationship was found between substituents and yields. The target heterocycles were synthesized as diastereomerically pure compounds with specific configuration of both stereocenters and the synthesis did not provide no epimerization products.

Table 16. The list of final pyrazino-oxazine derivatives **III-8**{*R*[1],*R*[2]}[a-c]

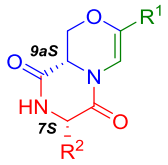

cmpd	R[1]	R[2]	cyclization time [h]	cyclization temp [°C]	crude purity [%][a]	final purity [%][b]	overall yield [%][c]
III-8{*1,1*}	Ph	Me	5	80	73	98	41
III-8{*1,2*}	Ph	$CH_2CH(CH_3)_2$	8	90	62	99	20
III-8{*1,3*}	Ph	$CH(CH_3)CH_2CH_3$	5	90	70	99	5
III-8{*1,4*}	Ph	CH_2Ph	8	80	89	98	31
III-8{*1,5*}	Ph	CH_2Ph-4-OH	8	80	86	97	34
III-8{*1,11*}	Ph	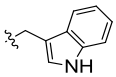	6	80	83	97	26
III-8{2,*1*}	4-Me-Ph	Me	2	80	82	98	18
III-8{*2,4*}	4-Me-Ph	CH_2Ph	1	80	84	98	23
III-8{*2,6*}	4-Me-Ph	CH_2OH	1	80	81	98	46
III-8{*2,8*}	4-Me-Ph	$CH_2(CH_2)_3NH_2$	2	80	76	99	32
III-8{*2,11*}	4-Me-Ph	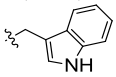	1	80	71	99	26
III-8{*3,1*}	4-MeO-Ph	Me	5	80	89	99	43
III-8{4,*1*}	4-NH_2-3,5-diCl-Ph	Me	1	80	78	98	32
III-8{5,*1*}	4-F-Ph	Me	5	80	82	99	21
III-8{6,*1*}	4-CF_3-Ph	Me	2	80	72	99	8
III-8{7,*1*}		Me	2	80	82	99	21

[a]Overall purity after the entire reaction sequence calculated from HPLC-UV traces at 205–400 nm; [b]HPLC-UV traces at 205–400 nm after purification; [c]Calculated from the ^{1}H NMR spectrum of the purified product.

More information is included in article by Ručilová, V.; Králová, P.; Soural, M. *Eur. J. Org. Chem.* **2017**, *2017* (47), 7034–7039[40] which is attached in Appendix E (p. 179 – 182).

4.4 Polymer-Assisted Synthesis of Single and Fused Diketomorpholines

The results of this project were published in: Králová, P.; Benická, S.; Soural, M. *ACS Comb. Sci.* **2019**, *21* (3), 154–157.[41] The manuscript is attached in Appendix F (p. 183 – 186). The Supporting information is available at: https://pubs.acs.org/doi/suppl/10.1021/acscombsci.8b00176 and is attached as an electronic file on CD.

Numbering of the individual products in the subchapter does not correspond to the attached manuscript and Supporting information.

4.4.1 Brief introduction

As a continuation of the formerly reported synthesis of pyrazino-oxazines,[40] we decided to replace Fmoc-amino acids with *α*-halocarboxylic acid derivatives. The resulting *N*-acyl intermediates should be treated with TFA to release the dihydrooxazine-3-carboxylic acid derivatives from the resin. Their post-cleavage modification consisting in a base-induced cyclization should yield the required diketomorpholines; however, except for desired oxazino[3,4-*c*][1,4]oxazine-diones, we obtained also 3-methylidene-diketomorpholines depending on the used reaction conditions (Figure 22). We decided to determine limitations and scope of the method for both types of compounds and in the case of oxazino-oxazines, to examine a stereoselectivity of the TES reduction.

Figure 22. The proposed synthesis of fused diketomorpholines

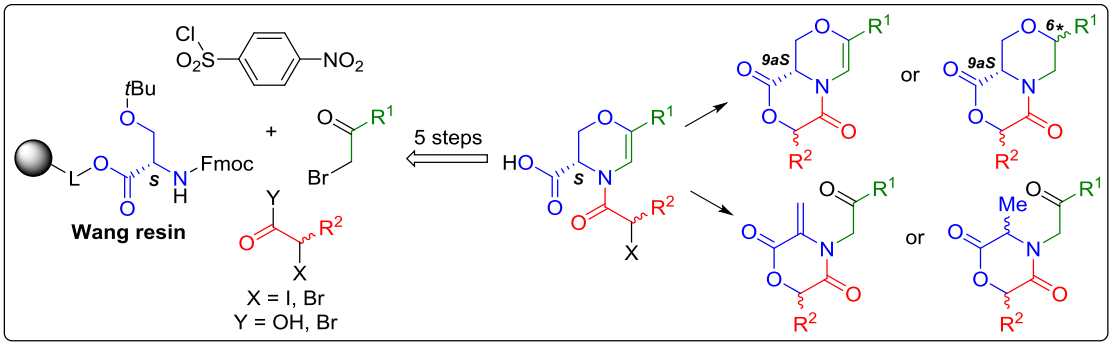

4.4.2 Synthesis

According to the previously reported conditions,[2] the key *α*-amino ketone **IV-2**{*1*} was prepared using a convenient SPS starting from the polymer-supported Fmoc-Ser(*t*Bu)-OH. The subsequent acylation with *α*-iodoacetic acid and TFA-mediated cleavage from the resin yielded dihydrooxazine-3-carboxylic acid **IV-4**{*1,1*}. After simple evaporation of the cleavage cocktail under a stream of nitrogen, we performed DIEA/DMSO-mediated post-cleavage cyclization of the crude evaporator **IV-4**{*1,1*} that yielded oxazino[3,4-*c*][1,4]oxazine-dione **IV-5**{*1,1*} or 3-methylidene-diketomorpholine **IV-6**{*1,1*} depending on the cyclization time. The quantitative conversion to fused [6+6] oxazine **IV-5**{*1,1*} was observed after only 20 min, whereas a longer reaction time (20 h) led

quantitatively to 3-methylidene-diketomorpholine **IV-6**{*1,1*} in 95% and 91% crude purities, respectively (calculated from HPLC-UV traces at 205–400 nm). After the removal of DIEA/DMSO by lyophilization, the crude products were isolated by semipreparative reverse-phase HPLC purification in 45 and 46% overall yields, respectively (calculated from ^{1}H NMR spectra of the purified products, Scheme 47, Table 20 for the purified products).

Scheme 47. The synthesis of final diketomorpholines *via* dihydrooxazine-3-carboxylic acids **IV-4**{R^1,R^2}[a]

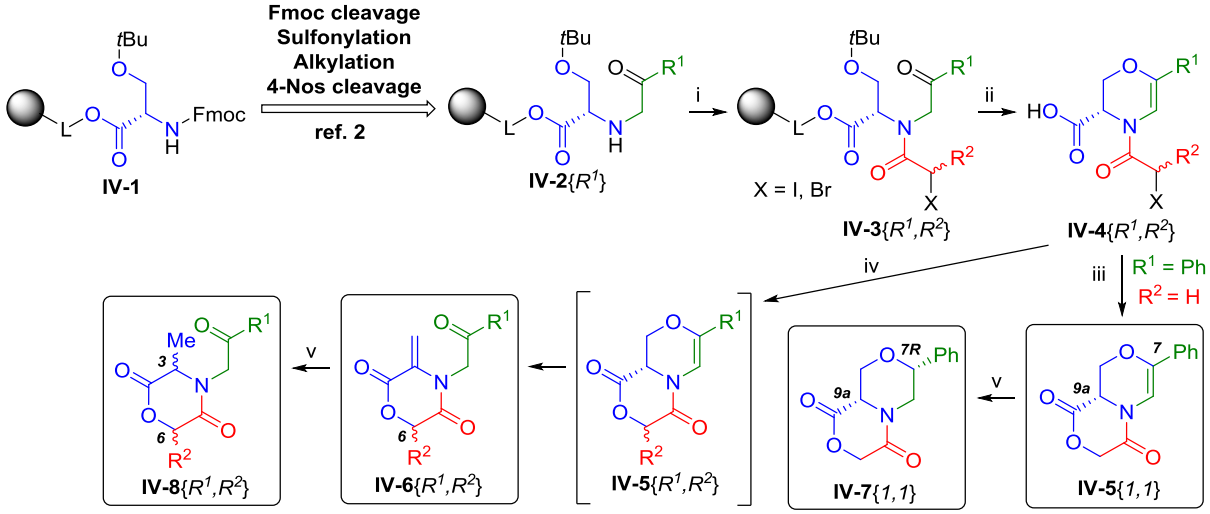

[a]Reagents and conditions: (i) halocarboxylic acid, DIC, DCM, 30 min, then added to resin, 24 h, rt; or 2-bromopropionyl bromide, 2,6-lutidine, DCM, 24 h, rt (ii) 50% TFA/DCM, 1 h or 4 h (for derivatives **IV-3**{R^1,*3*}), rt; (iii) DIEA, DMSO, 20 min (for **IV-4**{R^1,*1*}), rt; (iv) DIEA, DMSO, 20 h, rt (for **IV-4**{R^1,*1*} and **IV-4**{R^1,*3*}) or 1 h, 80 °C (for **IV-4**{R^1,*2*}); (v) TFA/TES/DCM (10:3:10), 24, rt.

After that, further reduction of crude lyophilized products **IV-5**{*1,1*} and **IV-6**{*1,1*} using TFA/TES provided the saturated analogs **IV-7**{*1,1*} and **IV-8**{*1,1*} in 74% and 89% crude purities (calculated from HPLC-UV traces at 205–400 nm) and 19% and 12% overall yields, respectively (calculated from ^{1}H NMR spectra of the purified products, Scheme 47, Table 20 for the final derivatives). Similarly to our formerly reported results,[2,38,39] the TES reduction to oxazino-morpholine derivatives **IV-7**{*1,1*} was fully stereoselective. The configuration of the newly formed C7 stereocenter was assigned as 7*R* based on NMR techniques. In contrast, the reduction of 3-methylidene-diketomorpholine **IV-6**{*1,1*} to 3-methyl-diketomorpholine **IV-8**{*1,1*} was not stereoselective and furnished a mixture of C3 *R,S* enantiomers in a ratio of 80:20 as detected by SFC analysis (Table 20 for the final derivatives).

In addition, the fused oxazine derivative **IV-5**{*1,1*} showed considerable instability and slowly converted to 3-methylidene-diketomorpholine **IV-6**{*1,1*}, when a sample was dissolved in different solvents (e.g. DMSO-d_6, MeOH-d_4, $CDCl_3$, and MeCN-d_3) for NMR analysis. In contrast, the saturated analogue **IV-7**{*1,1*} was completely stable, and it could be fully NMR characterized in MeOH-d_4.

4.4.3 Limitations and scope

To determine the limitations and scope, we tested a combination of three aromatic *α*-bromoketones with electron donating and electron withdrawing substituents, and eight *α*-halocarboxylic acid derivatives (Figure 23 for both R^1 and R^2 modifications). The resin-bound *N*-acyl compounds **IV-3**{*R*[1],*1-3*} were successfully synthesized for all tested *α*-bromoketones and four *α*-halocarboxylic acid derivatives (i.e. 2-iodoacetic acid, (*R*,*S*)-2-bromopropionyl bromide, (*S*)-(-)2-bromopropionic acid and (*R*,*S*)-2-bromo-2-phenylacetic acid). The following acid-mediated cleavage from the resin gave the products **IV-4**{*R*[1],*1-3*} in high crude purities (56-97%, calculated from HPLC-UV traces at 205–400 nm, Scheme 48, Table 17). However, in the case of phenylacetic acid derivatives, the release from the resin required the longer cleavage time (4 h instead of 1 h).

Figure 23. The list of tested synthons for R^1 and R^2 substituents

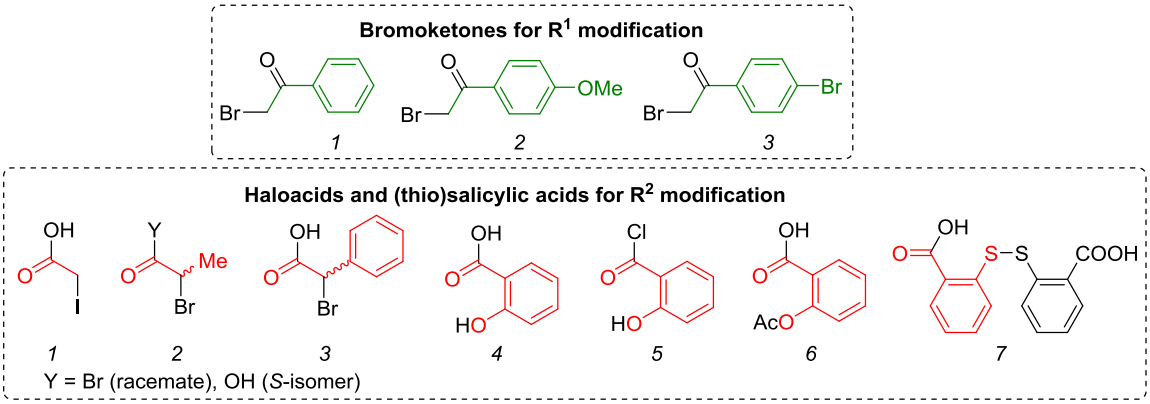

Scheme 48. The cyclization of intermediates **IV-3**{*R*[1],*R*[2]}[a]

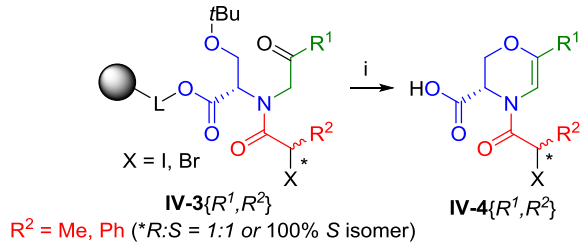

[a]Reagents and conditions: (i) 50% TFA/DCM, 1 h or 4 h (for derivatives **IV-3**{*R*[1],*3*}), rt.

Table 17. The crude purities of *N*-acyl-3,4-dihydro-2*H*-1,4-oxazine-3-carboxylic acids **IV-4**{*R*[1],*R*[2]}[a]

cmpd	R^1	R^2	crude purity [%][a]
IV-4{*1,1*}	Ph	H	97
IV-4{*1,2*}	Ph	Me	94
IV-4^S{*1,2*}	Ph	Me	96
IV-4{*1,3*}	Ph	Ph	91
IV-4{*2,2*}	4-MeO-Ph	Me	94
IV-4{*2,3*}	4-MeO-Ph	Ph	56
IV-4{*3,1*}	4-Br-Ph	H	94
IV-4{*3,2*}	4-Br-Ph	Me	85
IV-4{*3,3*}	4-Br-Ph	Ph	79

[a]Calculated from HPLC-UV traces at 205–400 nm.

Furthermore, the *α*-halocarboxylic acid derivatives were replaced with (thio)salicylic acid derivatives to attempt the preparation of benzoxazino-oxazinediones **IV-9**{R^1,*4-6*} or benzoxazino-thiazepinediones **IV-9**{R^1,*7*} (Scheme 49, Figure 23 for R^2 modifications *4-7*). Unfortunately, the acylation of *α*-amino ketones with *N*-(thio)salicylic derivatives **IV-4**{R^1,*4-7*} did not provide desired products under any tested conditions **a-e** and **g** after the cleavage from the resin (Scheme 49, Table 18). When acylation with acetylsalicylic acid activated with DIC and HOBt (conditions **f**) at room or higher temperatures (80 °C) was tested, the similar results were obtained in all cases, but the conversion was not quantitative (Table 18, highlighted in bold). Due to such unsatisfactory results, we left this alternative approach and focused on further modification of *N*-acyl derivatives **IV-4**{R^1,*1-3*}, synthesized from *α*-halocarboxylic acids.

Scheme 49. The acylation with (thio)salicylic acid derivatives to synthesize benzoxazino-oxazepine-diones **IV-9**{R^1,*4-6*} and benzoxazino-thiazinediones **IV-9**{R^1,*7*}[a]

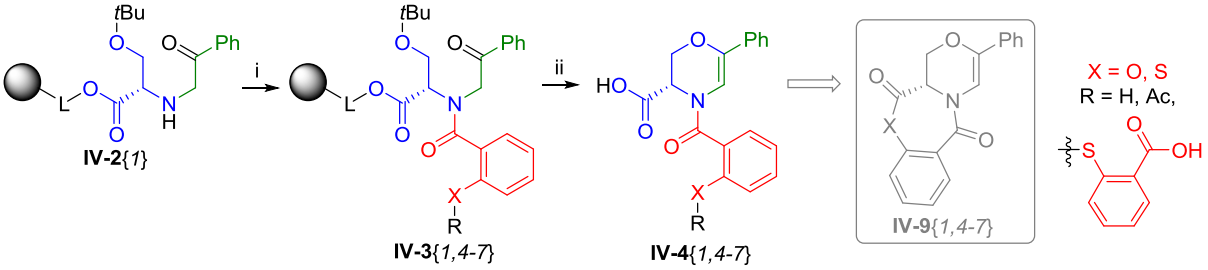

[a]Reagents and conditions: (i) **(a)** salicylic acid, DIC, DCM, 24 h, rt; **(b)** salicylic acid, DIC, DMF, 24 h, rt-80 °C; **(c)** salicylic acid, HOBt, DMAP, DIC, DMF, DCM, 24 h, rt; **(d)** salicyloyl chloride, 2,6-lutidine, DCM, 24 h, rt; **(e)** acetylsalicylic acid, DIC, DMF, 24 h, rt; **(f)** acetylsalicylic acid, HOBt, DIC, DMF, DCM, 24 h, rt-80 °C; **(g)** 2,2´-dithiodibenzoic acid, DIC, DMF, 24 h, rt; (ii) 50% TFA/DCM, 30 min, rt.

Table 18. The tested acylation conditions for *N*-acyl derivatives **IV-2**{R^1,*4-7*}[a-b]

starting cmpd	method[a]	acylating agent R^2 [concentration]	base other reagents [concentr.]	solvent	time [h]	temp [°C]	crude purity of IV-2 [%][b]	crude purity of IV-4 [%][b]	ratio of IV-2:4 [%][b]
IV-2{*1,4*}	**a**	2-OH-PhCOOH **{*4*}** (0.2 mmol)	DIC (0.1 mmol)	DCM	24	23	71	0	100:0
	b	2-OH-PhCOOH **{*4*}** (0.2 mmol)	DIC (0.1 mmol)	DMF	24 24	23 80	85 80	0 0	100:0 100:0
	c	2-OH-PhCOOH **{*4*}** (0.2 mmol)	DIC, HOBt (0.2 mmol) 5% DMAP	DCM/ DMF	24	23	82	0	100:0
IV-2{*1,5*}	**d**	2-OH-PhCOCl **{*5*}** (0.3 mmol)	2,6-lutidine (0.33 mmol)	DCM	24	23	60	0	100:0
IV-2{*1,6*}	**e**	2-OAc-PhCOOH **{*6*}** (0.2 mmol)	DIC (0.1 mmol)	DMF	24	23	70	0	100:0
	f	**2-OAc-PhCOOH {*6*} (0.2 mmol)**	**DIC, HOBt (0.2 mmol) 5% DMAP**	**DCM /DMF**	24 **24**	23 **80**	61 **54**	38 **44**	62:38 **55:45**
IV-2{*1,7*}	**g**	$(2\text{-S-PhCOOH})_2$ **{*7*}** (0.2 mmol)	DIC (0.1 mmol)	DMF	24	23	82	0	100:0

[a]The reaction conditions are defined in Scheme 49; [b]Calculated from HPLC-UV traces at 205–400 nm.

After that, the cleaved compounds **IV-4**{R^1,*1-3*} were subjected to the base-catalyzed cyclization to determine the limitations and scope (Scheme 50). To assess the solvent effect on the reaction outcome, we replaced DMSO with different solvents (e.g. DMF, MeCN, THF and acetone). In comparison to DMSO, the solvent exchange affected negatively the crude purities of both compounds **IV-5**{*1,1*} and **IV-6**{*1,1*} (Table 19). For this reason, the synthesis of other analogous **IV-5**{R^1,*1-3*} and **IV-6**{R^1,*1-3*} was performed using DMSO as the cyclization solvent. Except for the above-mentioned solvent effect, the cyclization required significantly different conditions depending on the R^2

Scheme 50. The cyclization of intermediates **IV-4**{R^1,*1-3*}[a]

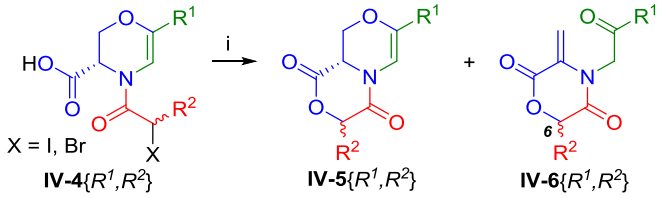

[a]Reagents and conditions: (i) DIEA, solvent, 20 min-120 h, rt-80 °C.

Table 19. The alternative solvents for cyclization of **IV-4**{*1,1*} and **IV-4**{*1,2*}[a]

starting cmpd	R^2	solvent	time [h]	temp [°C]	crude purity of IV-4 [%][a]	crude purity of IV-5 [%][a]	crude purity of IV-6 [%][a]	ratio of IV-4:5:6 [%][a]
IV-4{*1,1*}	H	**DMSO**	**0.33**	**23**	**0**	**95**	**0**	**0:100:0**
			20	**23**	**0**	**0**	**91**	**0:0:100**
		DMF	0.33	23	0	94	3	0:97:3
			20	23	0	27	68	0:28:72
		MeCN	0.33	23	0	70	2	0:97:3
		THF	0.33	23	0	80	0	0:100:0
		acetone	0.33	23	0	80	0	0:100:0
IV-4{*1,2*}	Me	**DMSO**	1	23	42	40	17	42:40:18
			2	23	41	38	19	41:39:20
			22	23	30	4	57	33:4:63
			44	23	20	0	70	22:0:78
			120	**23**	**0**	**0**	**85**	**0:0:100**
			0.08	50	40	55	2	41:57:2
			0.17	50	39	51	6	41:53:6
			0.5	50	35	42	22	35:42:23
			2	50	11	20	60	12:22:66
			20	**50**	**0**	**0**	**80**	**0:0:100**
			0.08	80	36	54	9	36:55:9
			0.17	80	32	50	14	33:52:15
			0.25	80	5	14	71	6:16:78
			0.33	80	0	3	85	0:3:97
			1	**80**	**0**	**0**	**88**	**0:0:100**
		DMF	0.17	80	18	50	20	20:57:23
			0.25	80	7	43	37	8:49:43
			0.58	80	2	24	60	2:29:69
			1	**80**	**0**	**0**	**86**	**0:0:100**

[a]Calculated from HPLC-UV traces at 205–400 nm.

substituent used. In the cases of intermediates **IV-4**{R^1,*1*} and **IV-4**{R^1,*3*}, prepared from 2-iodoacetic acid and 2-bromo-2-phenylacetic acid, the cyclization could be accomplished at room temperature for 20 h. In contrast, the room-temperature cyclization of intermediates **IV-4**{R^1,*2*}, prepared from 2-bromopropionyl bromide, was significantly slower and the conversion was achieved after 5 days. For this reason, the reaction was heated at 50 °C (for 20 h) or 80 °C (for 1 h) to accelerate the cyclization which was completed faster at higher temperature (Table 19, complete conversions are highlighted in black and bold, however the best results are highlighted in red and bold). According to these results, it was difficult to isolate corresponding fused oxazines **IV-5**{R^1,*2*} due to their thermal conversion to methylidene compounds **IV-6**{R^1,*2*}. For this reason, the project was primarily paid to the synthesis of 3-methylidene-diketomorpholines **IV-6**{R^1,R^2} along with other related analogues.

The developed synthetic route provided 12 final compounds: one fused derivative **IV-5**{*1,1*} and 9 derivatives **IV-6**{R^1,R^2}, **IV-7**{*1,1*} and **IV-8**{*1,1*} in 56-95% crude purities (calculated from HPLC-UV traces at 205–400 nm) and 12-46% overall yields (calculated from ^{1}H NMR spectra of the purified products, Table 20).

Table 20. The list of prepared and fully characterized products[a-e]

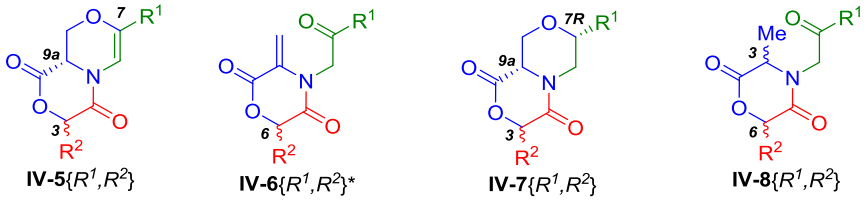

cmpd	R^1	R^2	crude purity [%][a]	final purity [%][b]	overall yield [%][c]	ratio of *R*:*S* enantiomers [%][d]
IV-5{*1,1*}	Ph	H	95	98	45[e]	6:94
IV-6{*1,1*}	Ph	H	91	99	46	-
IV-6{*1,2*}	Ph	Me	88	99	48	90:10
IV-6^R{*1,2*}	Ph	Me	67	99	24	85:15
IV-6{*1,3*}	Ph	Ph	66	98	27	100:0
IV-6{*2,2*}	4-MeO-Ph	Me	89	99	35	91:9
IV-6{*2,3*}	4-MeO-Ph	Ph	56	99	14	100:0
IV-6{*3,1*}	4-Br-Ph	H	90	98	30	-
IV-6{*3,2*}	4-Br-Ph	Me	90	96	22	87:13
IV-6{*3,3*}	4-Br-Ph	Ph	78	99	18	50:50
IV-7{*1,1*}	Ph	H	74	98	19	-
IV-8{*1,1*}	Ph	H	89	97	12	80:20

[a]Overall purity after the entire reaction sequence calculated from HPLC-UV traces at 205–400 nm; [b]HPLC-UV traces at 205–400 nm after purification; [c]Calculated from the ^{1}H NMR spectrum of the purified product; [d]Calculated from SFC-UV traces; [e]Dissolving the sample in MeCN-d_3 led to partial conversion of purified product **IV-5** to **IV-6** in a ratio of 83:17 as calculated from the ^{1}H NMR spectrum.

Finally, we decided to explore the 3D architecture of the target compounds using detailed SFC studies. In the case of **IV-4**{*1,1*} synthesized from iodoacetic acid, the reaction sequence resulted in a minor racemization on the C3 center (i.e. 6% of *R*-isomer was detected by SFC analysis). As mentioned in previous projects,[2] the minor enantiomer was formed during the immobilization of the enantiomerically pure (*S*)-Fmoc-Ser(*t*Bu)-OH to the Wang resin (Figure 24, on the left). Similarly, the same ratio of *R,S* isomer (6:94) was detected for fused derivative **IV-5**{*1,1*}, which indicated that the base (DIEA)-catalyzed cyclization did not affect the configuration of the chiral center C9*a* (Figure 24, on the right).

Figure 24. SFC chromatograms of crude intermediates **IV-4**{*1,1*} and **IV-4^{S}**{*1,2*}

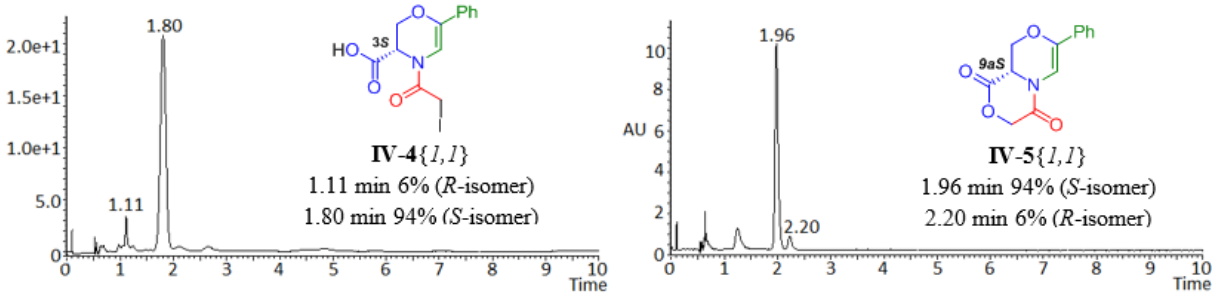

In the case of derivatives **IV-6**{*R^{1},2*}, prepared from racemic *α*-bromopropionyl bromide, the mixture of two enantiomers in a ratio of approximately 9:1 was detected. This fact points to the preferential formation of the more stable enantiomer, which was presumably promoted by the DIEA-catalyzed cyclization to the final derivatives. In this context, the compound **IV-4^{S}**{*1,2*} was synthesized from enantiomeric pure (*S*)-(-)-bromopropionic acid and subjected to base-cyclization under the same reaction conditions (DIEA, DMSO at 80 °C) as in the case of **IV-4**{*1,2*} to assess the effect of both R^1 and R^2 substituents on the stereochemical outcome. After cyclization of **IV-4^{S}**{*1,2*} at 80 °C for just 5 min, we observed a mixture of two enantiomers **IV-6^{R}**{*1,2*} and **IV-6^{S}**{*1,2*} in a ratio of 5:95. After additional 55 min, the ratio was changed to 81:19 indicating the slow conversion of the starting *S* isomer to the resulting *R* isomer (Scheme 51, Table 21).

Scheme 51. The DIEA-catalyzed cyclization of derivatives **IV-4**{*1,2*} and **IV-4^{S}**{*1,2*} at 80 °C[a]

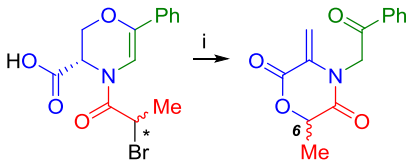

IV-4{*1,2*}: **R:S = 1:1*
IV-4^{S}{*1,2*}: **S = 100%*
IV-6^{RS}{*1,2*}

[a]Reagents and conditions: (i) DIEA, DMSO, 0-5 h, 80 °C.

Table 21. Detailed SFC studies of the cyclization step for derivatives **IV-4**{*1,2*}, **IV-4^{S}**{*1,2*} at 80 °C[a]

starting cmpd	time [min]	ratio of enantiomers IV-6$^{R:S}$ [%][a]
IV-4{*1,2*}	0	50:50
	5	22:78
	10	24:76
	15	46:54
	20	62:38
	25	74:26
	35	22:78
	40	20:80
	50	20:80
	60	**90:10**
	300	**90:10**

starting cmpd	time [min]	ratio of enantiomers IV-6$^{R:S}$ [%][a]
IV-4^{S}{*1,2*}	5	5:95
	10	17:83
	15	41:59
	20	47:53
	25	56:44
	30	64:36
	40	74:26
	50	79:21
	60	81:19
	75	81:19
	105	83:17
	135	**85:15**
	300	**85:15**

[a]Calculated from SFC spectra of the crude products.

To explain these results, Scheme 52 demonstrates the hypothetical mechanism of the diketomorpholine formation *via* oxazine-ring opening which afforded the 3-methylidene-diketomorpholine scaffold bearing the methyl group in C6 axial position (*S* isomer). The following deprotonation at the C6 center by DIEA proceeded through two diastereomeric transition states of unequal energy, i.e. *S* isomer was converted to more stable *R* isomer having an equatorial methyl group. According to these facts, we determined the preferable configuration of the C6 center on the diketomorpholine scaffold, but the longer cyclization (5 h) did not affected the conversion rate of *R,S* isomers, and we obtained a constant ratio of both *R,S* isomers (85:15). Moreover, the analogues **IV-6**{*1,3*} and **IV-6**{*2,3*} with identical R^2 groups (Ph), but different R^1 substituents (Ph or 4-MeO-Ph), were assembled as enantiomerically pure compounds, whereas **IV-6**{*3,3*} (R^1 = 4-Br-Ph) was obtained as the racemic mixture (50:50, Table 20). These results imply the substantial influence of R^1 substituent to the resulting stereochemical outcome.

Scheme 52. The hypothetical mechanism of the final cyclization to product **IV-6^{R}**{*1,2*}[a]

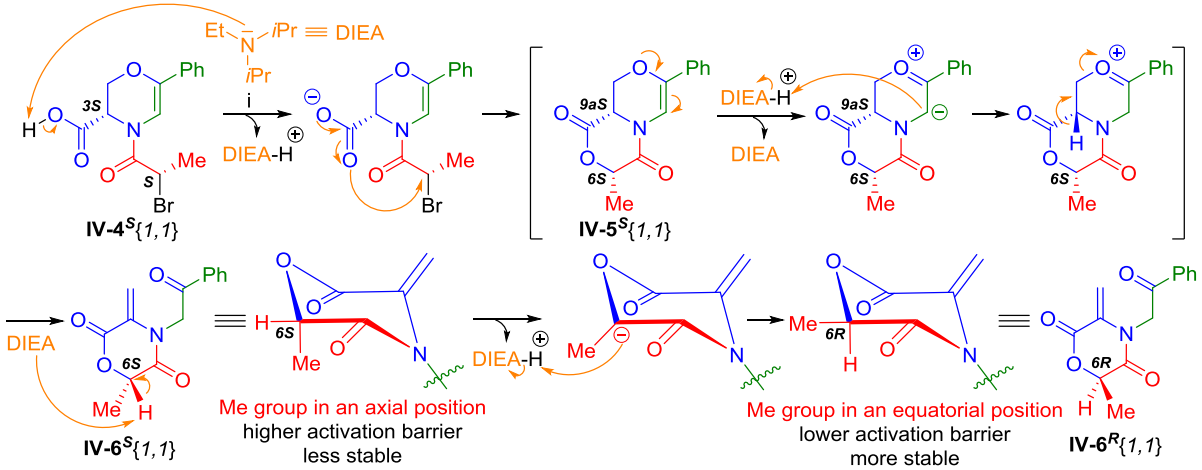

[a]Reagents and conditions: (i) DMSO,1 h, 80 °C.

4.4.4 Conclusion

In this project, we have developed the high-throughput synthetic protocol to prepare various diketomorpholine derivatives, including two post-cleavage modifications (i.e. final cyclization and TES reduction) with simple work-up based on evaporation of the reagents and solvents. Depending on the reaction conditions, the exposure to base resulted in cyclization to either fused [6+6] oxazines or 3-methylidene-diketomorpholines. In the case of oxazino-morpholine derivatives, the stereoselective TES reduction of olefins resulted in 7*R* isomer. In contrast, the TES reduction of 3-methylidene-diketomorpholines furnished the mixture of C3 *R*,*S* enantiomers in a ratio of 80:20. To determine the 3D architecture of 3-methylidene compounds with various R^2 substituent (R^2 = Me, Ph), the SFC studies were performed showing that the R^1 substituent influences the stereochemical resulting outcome and the final products were obtained as a mixture of 6*R*,*S* isomers in different ratios depending on R^1 substituent.

4.5 Convenient Synthesis of Thiohydantoins, Imidazole-2-Thiones and Imidazo[2,1-*b*]Thiazol-4-Iums from Polymer-Supported *α*-Acylamino Ketones

The results of this project were published in: Králová, P.; Maloň, M.; Koshino, H.; Soural, M. *Molecules* **2018**, *23* (4), 976–984.[42] The manuscript is attached in Appendix G (p. 187 – 194). The Supporting information is available at: https://www.mdpi.com/1420-3049/23/4/976 and is attached as an electronic file on CD.

Numbering of the individual products in the subchapter does not correspond to the attached manuscript and Supporting information.

4.5.1 Brief introduction

In this project, our attention was paid to Wang resin-immobilized Fmoc-thioureas to prepare fused [6+5] heterocycles bearing a thiohydantoin scaffold. The key intermediates were prepared from immobilized *α*-amino ketones and Fmoc/ *N*-alkylsubstituted-isothiocyanates. The corresponding thioureas should be subjected to cyclative cleavage conditions yielding thiohydantoin derivatives followed by an acid-mediated cyclization to receive thiohydantoin-oxazines derivatives. Alternatively, the reversed sequence should be tested, i.e. the immobilized thioureas should be treated with TFA providing expected oxazines followed by a base-catalyzed cleavage of the Fmoc protecting group and a cyclization to fused [6+5] derivatives (Figure 25). Eventually, the TES applicability for the stereoselective reduction of oxazine scaffold was suggested.

Figure 25. The considered synthesis of fused [6+5] morpholine derivatives

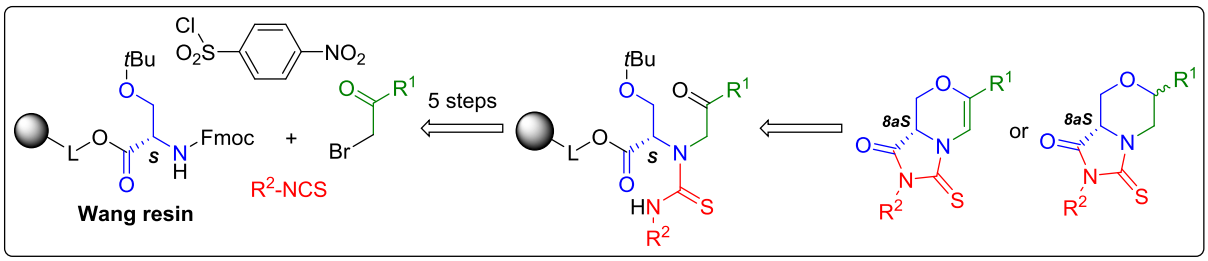

Interestingly, both tested synthetic strategies did not furnish expected fused [6+5] morpholines. In the first case, the cyclative cleavage reaction prompted the cyclization to the thiohydantoin scaffold followed by an acid-mediated cleavage of the *tert*-butyl protecting group and a spontaneous dehydration to 5-methylidene-thiohydantoins. Their TES reduction led to the corresponding methyl analogues. In contrast to Fmoc-thioureas, the *N*-substituted thioureas did not undergo the cyclative cleavage and TFA had to be used to release the intermediates from the resin. Further exposure to TFA under an elevated temperature enabled cyclization. Although the LC-MS data corresponded to the expected thiohydantoin-dihydrooxazine derivative (Figure 25), the careful structural NMR elucidation of the isolated compound revealed that the scaffold was not formed. The cyclization to imidazole-2-thiones

took place instead, followed by the dehydration and ring closure, which yielded an imidazo[2,1-*b*]thiazol-4-ium derivatives. Further, these compounds were prone to an isomerization to imidazole-2-thiones in DMSO-d_6 at room temperature, the rate of isomerization was temperature-dependent (Figure 26, Pathways A-B).

Figure 26. The developed methodology providing imidazole derivatives

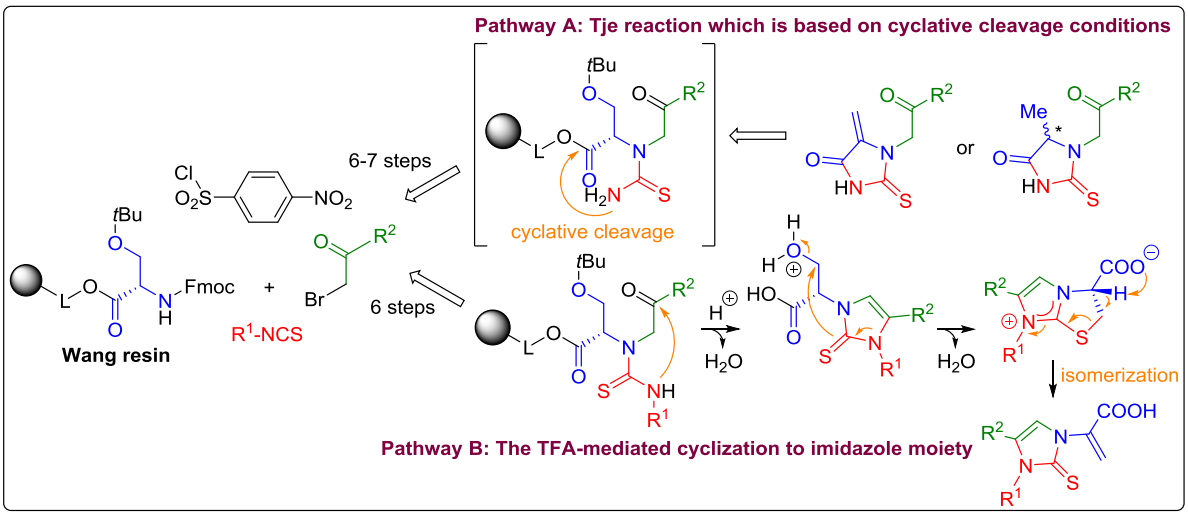

4.5.2 Synthesis

First, the suggested synthetic strategy (Scheme 53) was tested with *α*-bromoacetophenone and Fmoc-isothiocyanate (Fmoc-NCS) as representative synthons. The starting *α*-amino ketone **V-2**{*1*} was synthesized in four steps from Wang resin-supported Fmoc-Ser(*t*Bu)-OH **V-1** according to the previously reported protocol.[2] The reaction with Fmoc-NCS provided the corresponding Fmoc-thiourea **V-3**{*1,1*} followed by the Fmoc-protecting group release triggering a spontaneous cyclative cleavage of a liberated thiourea from the solid support to yield 2-thiohydantoin derivative **V-5**{*1,1*}. After the lyophilization of the cleavage cocktail (PIP/DMF), the crude residue **V-5**{*1,1*} was treated with TFA/DCM to remove the *tert*-butyl protecting group and eventually cyclize the fused [6+5] oxazine derivative **V-6**{*1,1*}. In contrast to our previous research,[2,38–41] the expected oxazine scaffold was not detected by the LC-MS analysis. In this case, the reaction resulted in the formation 5-methylidene-thiohydantoin **V-7**{*1,1*}. The following TES reduction provided the expected 5-methyl-thiohydantoin **V-8**{*1,1*} in excellent crude purity (85%, calculated from HPLC-UV traces at 205–400 nm) and 19% overall yield (calculated from the ^{1}H NMR spectrum of the purified product). Although the exact configuration on the newly formed C5 stereocenter of **V-8**{*1,1*} was not established, the structure was determined by means of ^{1}H, ^{13}C{^{1}H}, DEPT, ^{1}H-^{1}H COSY, ^{1}H-^{1}H NOESY, ^{1}H-^{13}C HSQC, ^{1}H-^{13}C HMBC, ^{1}H-^{15}N HMBC and ^{1}H-^{15}N HMQC. To confirm the structure, the ^{1}H-^{13}C HMBC analysis gave the correlations between methylene-phenylketone CH_2COPh and thiohydantoin moieties (i.e. H^5 and C2, C4, C15; H^{15} and C4 and C5; $H_{a,b}{}^6$ and C2, C5, C7). In ^{1}H-^{15}N HMBC and ^{1}H-^{15}N HMQC spectra, the nitrogen N1 correlated to H^5, $H_a{}^6$, $H_b{}^6$, H^{15} and methyl protons H^{14} to N3 (Figure 27).

Scheme 53. The synthesis of 5-methylidene and 5-methyl-thiohydantoins **V-7**{R^1,*1*} and **V-8**{R^1,*1*}[a]

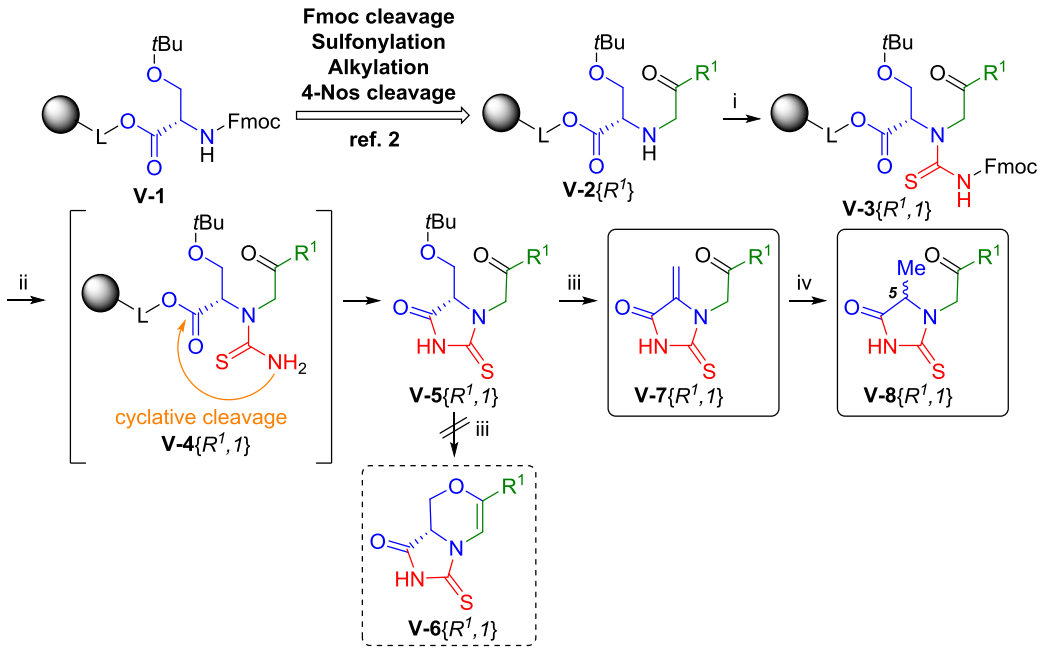

[a]Reagents and conditions: (i) Fmoc-NCS, anhydrous THF, 2 h, rt; (ii) 35% PIP/DMF or 10% PIP/DMF (for derivative **V-3**{*4,1*}), 24 h, rt; (iii) neat TFA, 20 h, 35 °C; (iv) TFA/TES/DCM (5:3:5), 24 h, rt.

Figure 27. The selected correlations of ^{1}H-^{15}N HMQC, ^{1}H-^{15}N HMBC, ^{1}H-^{13}C HMBC and NOESY analyses of derivative **V-8**{*1,1*}

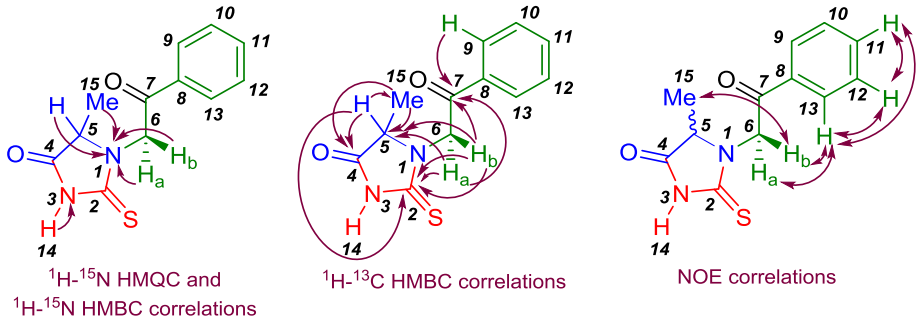

In addition, Fmoc-NCS was altered to *N*-alkyl-isothiocyanates to test the applicability of the reaction sequence for *N*-substituted analogues (Scheme 54). Since the corresponding *N*-benzylthiourea **V-3**{*1,2*}, prepared from benzyl-isothiocyanate, did not undergo the spontaneous cyclative cleavage from the resin, the resin was further exposed to TFA under elevated temperature (80 °C) to trigger the cyclization reaction (Table 22). Although the mass spectrometry data corresponded to expected thiohydantoin-dihydrooxazine derivative **V-6**{*1,2*}, the careful structural NMR elucidation of the isolated compound revealed that the scaffold was not formed. Interestingly, the reaction yielded no imidazole-2-thiones **V-9a-b**{*1,2*}, but the heating of **V-2**{*1,2*} in TFA enabled the dehydration and a ring closure that furnished imidazo[2,1-*b*]thiazol-4-ium derivative **V-10**{*1,2*}. The product was isolated and obtained in 80% crude purity (calculated from HPLC-UV traces at 205–400 nm) and 53% overall yield (calculated from the ^{1}H NMR spectrum of the purified product; Table 25 for the final

derivatives). The structure was carefully determined by means of ^{1}H, $^{13}C\{^{1}H\}$, DEPT, ^{1}H-^{1}H COSY, ^{1}H-^{1}H NOESY, ^{1}H-^{13}C HSQC, ^{1}H-^{13}C HMBC and ^{1}H-^{15}N HMBC. There were identified phenyl, benzyl and imidazo[2,1-*b*]thiazol-4-ium moieties. The ^{1}H-^{15}N HMBC spectrum provided correlation between benzyl protons H^{16} to N7, between imidazo[2,1-*b*]thiazol-4-ium proton H^{5} to N4, N7 and $H_{a,b}{}^{2}$ to N4. Figure 28 depicts the key ^{1}H-^{13}C HMBC correlations of $H_{a,b}{}^{2}$-C3, C8, C9; H^{3}-C2, C8, C9; H^{5}-C6, C8, C10 and H^{16}-C6, C8, C10, C14, C15, C17 to confirm the target structure.

Scheme 54. The applicability of *N*-substituted immobilized thioureas **V-3**{R^1,*2-6*}[a]

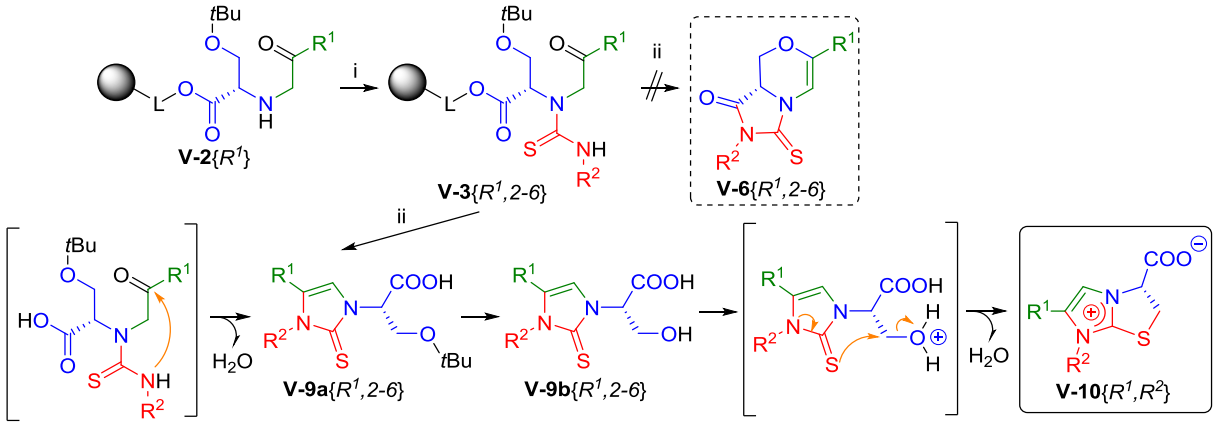

[a]Reagents and conditions: (i) R^2-NCS, anhydrous THF, 44 h or 20 h for derivatives **V-2**{R^1,*2*} and 72 h for derivatives **V-2**{R^1,*5*}, rt; (ii) a) neat TFA, 80 °C, 20 h or 48 h (for derivatives **V-3**{R^1,*3*}), b) evaporation of TFA, c) semipreparative reverse-phase HPLC purification using AmAc buffer, d) freeze-drying.

Table 22. The tested cyclization conditions for derivative **V-3**{*1,2*}[a]

cyclization cocktail	concentration of cyclization cocktail	time [h]	temp [°C]	crude purity of V-9a [%][a]	crude purity of V-9b [%][a]	crude purity of V-10 [%][a]	ratio of V-9a:9b:10 [%][a]
TFA/DCM	50%	13	23	12	58	1	17:82:1
TFA	**100%**	5	4	39	48	0	45:55:0
		13	23	3	70	1	4:95:1
		20	35	2	67	1	3:96:1
		13	50	44	2	41	51:2:47
		28	50	25	17	37	32:22:46
		48	50	22	0	58	28:0:72
		66	50	21	0	65	24:0:76
		90	50	17	0	72	19:0:81
		162	50	2	0	80	2:0:98
		20	**80**	**0**	**0**	**80**	**0:0:100**

[a]Calculated from HPLC-UV traces at 205–400 nm.

Figure 28. The key ^{1}H-^{15}N HMBC, ^{1}H-^{13}C HMBC and NOE correlation of **V-10**{*1*,*2*}

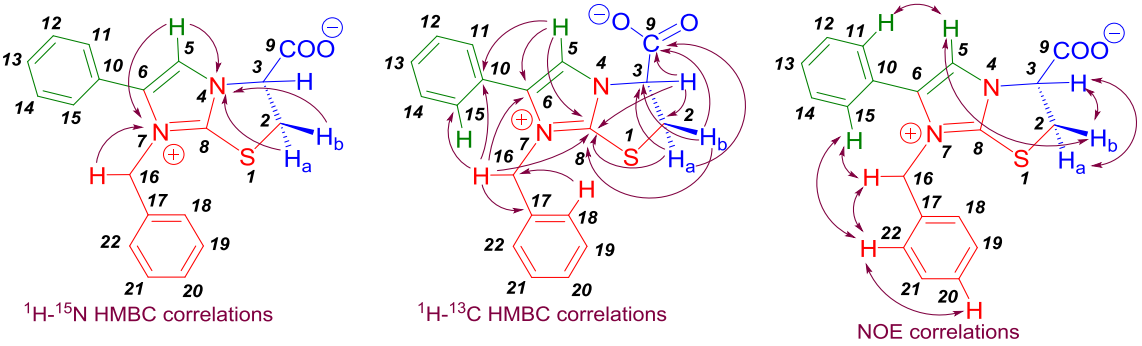

4.5.3 Limitations and scope

The applicability of the reaction sequence was tested for various *α*-bromoketones and isothiocyanates (Figure 29). Except for derivatives **V-3**{*2*,*5*}, **V-3**{*4*,*4*} and **V-3**{*4*,*5*}, prepared from building blocks bearing cyclohexylmethyl and 2-(4-morpholino)ethyl as R^2 substituent, the synthesis of key *α*-amino ketones **V-3**{R^1,R^2} was successful for all tested building blocks with electron donating and electron withdrawing substituents in R^1 position. The reaction time was dependent on a reactivity of the used isothiocyanate (Scheme 55, Table 23). In the case of resin-bound compounds **V-3**{R^1,*2*}, prepared from benzyl isothiocyanate, the formation of the corresponding thioureas was relatively fast, and the reaction time was just 20 h. In contrast, the reaction with allyl, 2-(4-morpholino)ethyl and cyclohexylmethyl isothiocyanates required noticeably longer time (44-72 h) to reach the completion. In the case of intermediates **V-3**{*2*,*5*}, **V-3**{*4*,*4*} and **V-3**{*4*,*5*}, the resulting thioureas were observed as a mixture with the starting material in a ratio of approximately 86:14 even if the reaction time was extended (44-72 h).

Figure 29. The list of tested building blocks for R^1 and R^2 substituents

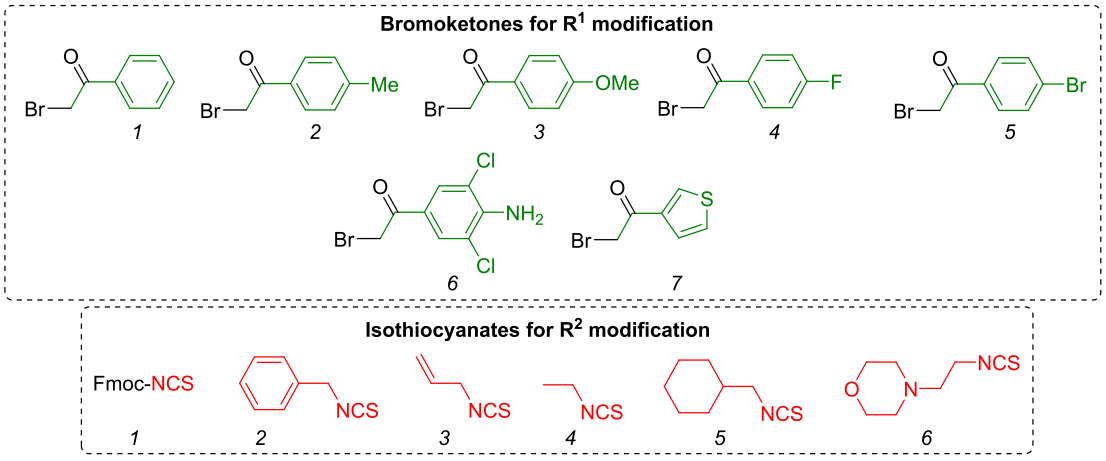

Scheme 55. The reaction of *α*-amino ketones **V-2**{*R*[1]} with R[2]-substituted isothiocyanates[a]

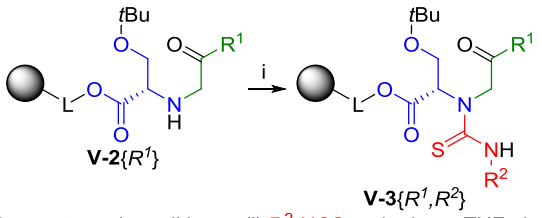

[a]Reagents and conditions: (i) R[2]-NCS, anhydrous THF, time, rt.

Table 23. The tested reaction conditions of **V-3**{*R*[1]} with various isothiocyanates[a]

starting cmpd	R[1]	isothiocyanates {R[2]}	time [h]	crude purity of V-2 [%][a]	crude purity of V-3 [%][a]	ratio of V-2:3 [%][a]
V-2{*1*}	Ph	Fmoc-NCS {*1*}	2	0	93	0:100
V-2{*4*}	4-F-Ph	Fmoc-NCS {*1*}	2	0	93	0:100
V-2{*5*}	4-Br-Ph	Fmoc-NCS {*1*}	2	0	98	0:100
V-2{*6*}	4-NH_2-3,5-diCl-Ph	Fmoc-NCS {*1*}	2	0	90	0:100
V-2{*7*}		Fmoc-NCS {*1*}	2	0	93	0:100
V-2{*1*}	Ph	Bn-NCS {*2*}	20	0	88	0:100
V-2{*1*}	Ph	allyl-NCS {*3*}	44	0	91	0:100
V-2{*1*}	Ph	Et-NCS {*4*}	44	0	98	0:100
V-2{*2*}	4-Me-Ph	Bn-NCS {*2*}	20	0	92	0:100
V-2{*2*}	4-Me-Ph	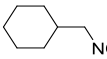 {*5*}	44 **72**	36 **15**	57 **79**	39:61 **16:84**
V-2{*3*}	4-MeO-Ph	allyl-NCS {*3*}	24 **44**	30 **0**	68 **90**	31:69 **0:100**
V-2{*3*}	4-MeO-Ph	Et-NCS {*4*}	24 **44**	14 **0**	84 **96**	14:86 **0:100**
V-2{*3*}	4-MeO-Ph	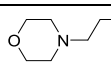 {*6*}	24 **44**	53 **0**	46 **97**	54:46 **0:100**
V-2{*4*}	4-F-Ph	Et-NCS {*4*}	**44**	**11**	**75**	**13:87**
V-2{*4*}	4-F-Ph	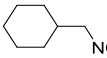 {*5*}	44 **72**	30 **15**	50 **79**	38:62 **16:84**
V-2{*5*}	4-Br-Ph	Bn-NCS {*2*}	20	0	90	0:100
V-2{*5*}	4-Br-Ph	allyl-NCS {*3*}	44	0	95	0:100
V-2{*5*}	4-Br-Ph	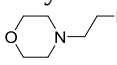 {*6*}	44	0	94	0:100
V-2{*7*}		Bn-NCS {*2*}	20	0	96	0:100
V-2{*7*}		allyl-NCS {*3*}	44	0	93	0:100
V-2{*7*}		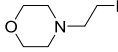 {*6*}	44	0	94	0:100

[a]Calculated from HPLC-UV traces at 205–400 nm.

Analogously to *N*-unsubstituted-isothiocyanates, the synthesis of other thiohydantoins **V-7**{*R*[1],*1*} and **V-8**{*R*[1],*1*} gave desired products in 68-85% crude purities (calculated from HPLC-UV traces at 205–400 nm) and 7-19% overall yields (calculated from ^{1}H NMR spectra of the purified products, Scheme 53, Table 25 for the final derivatives).

In the case of *N*-alkyl-thioureas **V-3**{*R*[1],*2-6*}, the subsequent TFA-mediated cyclization was dependent on the type of *N*-substituent, and for allyl derivatives **8**{*R*[1],*3*}, the reaction time had to be

prolonged from 20 to 48 h. In total, this second strategy enabled the synthesis of 16 final compounds **V-10**{R^1,*2-6*} using combination of various *α*-bromoketones and isothiocyanates, which were obtained in 69-97% crude purities (calculated from HPLC-UV traces at 205–400 nm) and 17-59% overall yields (calculated from ^{1}H NMR spectra of the purified products; Scheme 54, Table 25 for the final derivatives).

Although the target products **V-10**{R^1,*2-6*} were obtained as highly pure compounds (97-99%, calculated from HPLC-UV traces at 205–400 nm after HPLC purification), the ^{1}H NMR spectra of some derivatives (measured in deuterated DMSO) showed the presence of an impurity **V-11**{R^1,*2-6*} in quantities of up to 18%. When the samples **V-10**{*1,4*}, **V-10**{*3,6*} and **V-10**{*4,5*} were shortly heated prior to NMR analysis to dissolve, the quantity of the impurities rapidly increased by 40-92% (calculated from the ^{1}H NMR spectra of the purified products). For this reason, the compound **V-10**{*3,3*} synthesized from allyl isothiocyanate (16% of impurity was detected after dissolving the sample in DMSO-d_6), was subjected to detailed NMR elucidation. According to obtained data, the formation of the impurity **V-11**{*3,3*} was proved as a product of isomerization in DMSO-d_6 (Figure 30). To prove the isomerism, the compound **V-10**{*3,3*} was analysed using variable-temperature ^{1}H NMR experiments gradually at 80 °C, 100 °C, 120 °C, 140 °C and after cooling to 27 °C. The data indicated that almost full conversion to the by-product **V-11**{*3,3*} (97%) was observed at 120 °C. However, cooling the sample to 27 °C did not affect the conversion of the isomer (Table 24).

Figure 30. Isomerization of imidazo[2,1-*b*]thiazol-4-iums **V-10**{R^1,*2-6*} to imidazole-2-thiones **V-11**{R^1,*2-6*}

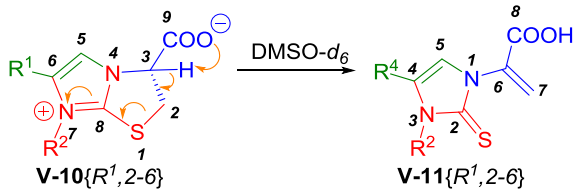

Table 24. The ratios of both forms **V-10**{R^1,R^2} and **V-11**{R^1,R^2} depending on temperature used[a-d]

starting cmpd	R¹	R²	temp [°C]	ratio of V-10:11 [%][a]
V-10{*1,2*}	Ph	Bn	27	93:7
			27[b]	76:24
			27[c]	46:54
			120	**0:100**
			140	0:100
			27[d]	0:100

starting cmpd	R¹	R²	temp [°C]	ratio of V-10:11 [%][a]
V-10{*3,3*}	4-MeO-Ph	allyl	27	84:16
			80	57:43
			100	16:84
			120	**3:97**
			140	3:97
			27[d]	3:97

[a]Calculated from the ^{1}H NMR spectrum of the purified product; [b,c]The sample was remeasured after 8 days[(b)] or 61 days[(c)]; [d]The sample was heated at 140 °C for 30 min and measured after cooling to 27 °C again.

Further NMR investigation of derivative **V-11**{*3,3*} using 2D spectroscopy confirmed the structure through the identification of 4-methoxyphenyl, allyl, 2-aminoacrylic acid and imidazole-2-

thione moieties *via* characteristic signals. The structure was determined by means of ^{1}H, ^{13}C{^{1}H}, DEPT, ^{1}H-^{1}H COSY, ^{1}H-^{1}H NOESY, ^{1}H-^{13}C HSQC, ^{1}H-^{13}C HMBC and ^{1}H-^{15}N HMBC. The ^{1}H-^{13}C HMBC spectrum provided the key correlations of H^{5} with C2, C4, C6, C10 and C13. Concomitantly in the ^{1}H-^{15}N HMBC, we observed the correlation of H^{5} to N1, N3 and further two-bond correlation between allyl protons H^{10}, H^{11} and N3, and between 2-aminoacrylic acid protons H$_{a\text{-}b}$^{7} and N1. Finally, the structure was confirmed by NOE correlations between phenyl and allyl protons (i.e. H^{14,18} to H^{10}, H^{11}, H$_{a}$^{12} and H$_{b}$^{12}), between imidazole-2-thione and protons of acrylic acid (H^{5} to H$_{a}$^{7} and H$_{b}$^{7}) and also the phenyl moiety (H^{5} to H^{18}; Figure 31).

Figure 31. The key ^{1}H-^{15}N HMBC, ^{1}H-^{13}C HMBC and NOE correlations of **V-11**{*3,3*}

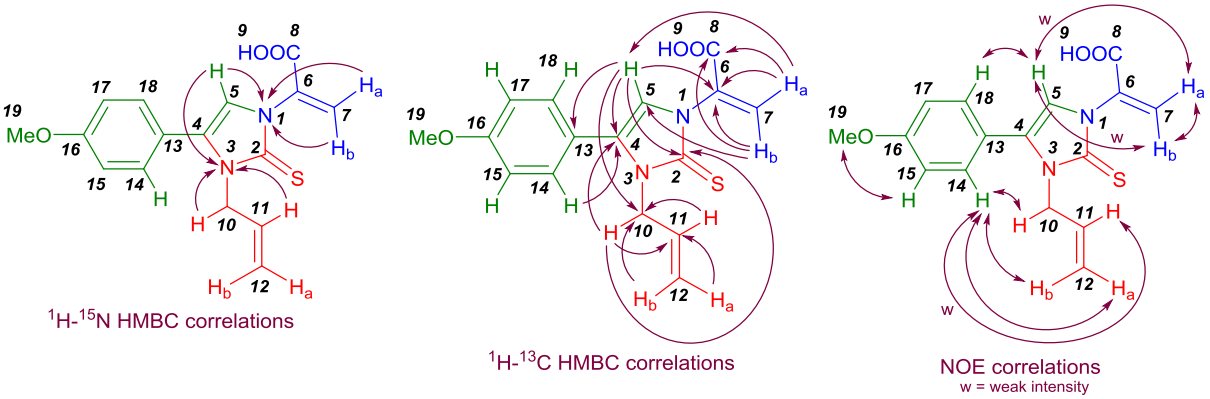

In the case of compound **V-10**{*1,2*}, which was synthesized from benzyl isothiocyanate, the slow conversion to **V-11**{*1,2*} was observed already at 27 °C in DMSO-d_6, and again, the reaction quickly reached full conversion to derivative **V-11**{*1,2*} at higher temperature (120 °C, Table 24). In most cases, heating of derivatives **V-10**{R^1,*2-6*} for 30 min provided compounds **V-11**{R^1,*2-6*} as major isomers (71-100%, calculated from ^{1}H NMR spectra of the purified products; Table 25 for the final derivatives). If the conversion to imidazole-2-thiones **V-11**{R^1,R^2} was not quantitative, the compounds were heated for longer time, but the ratio of both isomers **V-10**{R^1,R^2} and **V-11**{R^1,R^2} remained unchanged and only slow decomposition of products was observed. In just one case, heating of derivative **V-10**{*7,6*} did not change the initial ratio of isomers, even after prolonged time (17 h).

4.5.4 Conclusion

To conclude, we developed the solid-phase synthetic strategies to prepare three types of imidazole derivatives depending on the type of isothiocyanate and cleavage conditions used. In this context, we prepared more than 36 original compounds (e.g. thiohydantoins, imidazole-2-thiones and imidazo[2,1-*b*]thiazol-4-iums) in high crude purities (68-96%, calculated from HPLC-UV traces at 205–400 nm) and 7-59% overall yields (calculated from ^{1}H NMR spectra of the purified products). All structures of the final derivatives were confirmed by advanced NMR experiments and all of them were fully characterized. In addition, the plausible mechanism of isomerization of imidazo[2,1-*b*]thiazol-4-iums to imidazole-2-thiones was explained.

Table 25. List of prepared and fully characterized compounds[a-e]

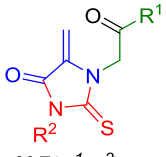
V-7{*R*^{1},*R*^{2}}

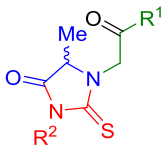
V-8{*R*^{1},*R*^{2}}

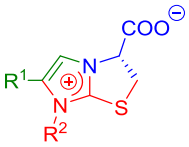
V-10{*R*^{1},*R*^{2}}

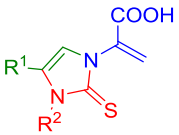
V-11{*R*^{1},*R*^{2}}

cmpd	R^1	R^2	cyclization time [h]	crude purity [%][a]	final purity [%][b]	overall yield [%][c]	ratio of V-10:11 at 27 °C [%][c]	ratio of V-10:11 after heating [%][c,d]
V-7{*1,1*}	Ph	H	20	80	99	11	-	-
V-7{*4,1*}	4-F-Ph	H	20	69	98	11	-	-
V-7{*5,1*}	4-Br-Ph	H	20	75	97	7	-	-
V-7{*6,1*}	4-NH_2-3,5-diCl-Ph	H	20	68	98	8	-	-
V-7{*7,1*}		H	20	85	97	8	-	-
V-8{*1,1*}	Ph	H	20	85	99	19	-	-
V-8{*5,1*}	4-Br-Ph	H	20	71	98	16	-	-
V-8{*7,1*}		H	20	72	99	15	-	-
V-10{*1,2*}	Ph	Bn	20	80	98	53	93:7	0:100
V-10{*1,3*}	Ph	allyl	48	90	98	34	100:0	8:92
V-10{*1,4*}	Ph	Et	20	91	99	23	45:55[e]	11:89
V-10{*2,2*}	4-Me-Ph	Bn	20	96	99	38	97:3	3:97
V-10{*2,5*}	4-Me-Ph		20	77	99	49	100:0	NT
V-10{*3,3*}	4-MeO-Ph	allyl	48	87	99	32	84:16	3:97
V-10{*3,4*}	4-MeO-Ph	Et	20	92	99	59	100:0	13:87
V-10{*3,6*}	4-MeO-Ph	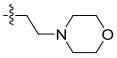	20	95	99	39	60:40[e]	0:100
V-10{*4,4*}	4-F-Ph	Et	20	85	99	57	100:0	16:84
V-10{*4,5*}	4-F-Ph		20	70	99	19	8:92[e]	8:92
V-10{*5,2*}	4-Br-Ph	Bn	20	91	98	28	98:2	9:91
V-10{*5,3*}	4-Br-Ph	allyl	48	69	99	18	100:0	29:71
V-10{*5,6*}	4-Br-Ph	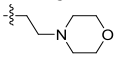	20	90	98	17	88:12	0:100
V-10{*7,2*}		Bn	20	97	98	26	97:3	0:100
V-10{*7,3*}		allyl	48	83	98	24	89:11	0:100
V-10{*7,6*}		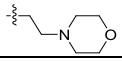	20	95	98	39	82:18	82:18

[a]Overall purity after the entire reaction sequence calculated from HPLC-UV traces at 205–400 nm; [b]HPLC-UV at 205–400 nm after purification; [c]Calculated from the ^{1}H NMR spectrum of the purified products; [d]Sample heated at 120 °C for 30 min and measured after cooling to 27 °C; [e]The sample was shortly heated prior to NMR analysis to dissolve; NT – not tested.

4.6 Synthesis of 2-Alkylsulfonyl-Imidazoles with Three Diversity Positions from Immobilized *α*-Acylamino Ketones

The results of this project were published in: Králová, P.; Soural, M. *ACS Comb. Sci.* **2018**, *20* (8), 467–471.[43] The manuscript is attached in Appendix H (p. 195 – 199). The Supporting information is available at: https://pubs.acs.org/doi/suppl/10.1021/acscombsci.8b00075 and is attached as an electronic file on CD.

Numbering of the individual products in the subchapter does not correspond to the attached manuscript and Supporting information.

4.6.1 Brief introduction

To avoid the above reported formation of thiohydantoins formed *via* cyclative cleavage of thioureas,[42] we decided to replace Wang resin with Wang-piperazine resin to stabilize the linkage to the support (i.e. to replace ester with the amide functionality). The synthesis of the corresponding thioureas was performed according to the previously developed protocols.[2,42] Theoretically, the resulting Fmoc-thioureas could undergo a base-mediated Fmoc-deprotection followed by immediate *S*-alkylation with *α*-bromoketones and a spontaneous cyclization to thiazole moiety, inspired by the known procedures.[62,63] In such a case, the treatment with TFA could yield *N*-thiazolo-oxazines (Figure 32, The original strategy). However, the suggested methodology was not feasible due to spontaneous attack of ketone by amine giving imidazolo-thiones. Their *S*-alkylation and oxidation yielded 2-alkylsulfonyl-imidazoles (Figure 32, The alternative strategy). The main aims of the project were determination of the limitations and scope using various Fmoc-amino acids, *α*-bromoketones and alkylating agents and development of suitable conditions to oxidize sulfides to corresponding sulfones or sulfoxides.

Figure 32. The proposed synthesis of *N*-thiazolo-oxazines and the actual formation of 2-alkylsulfonyl-imidazoles

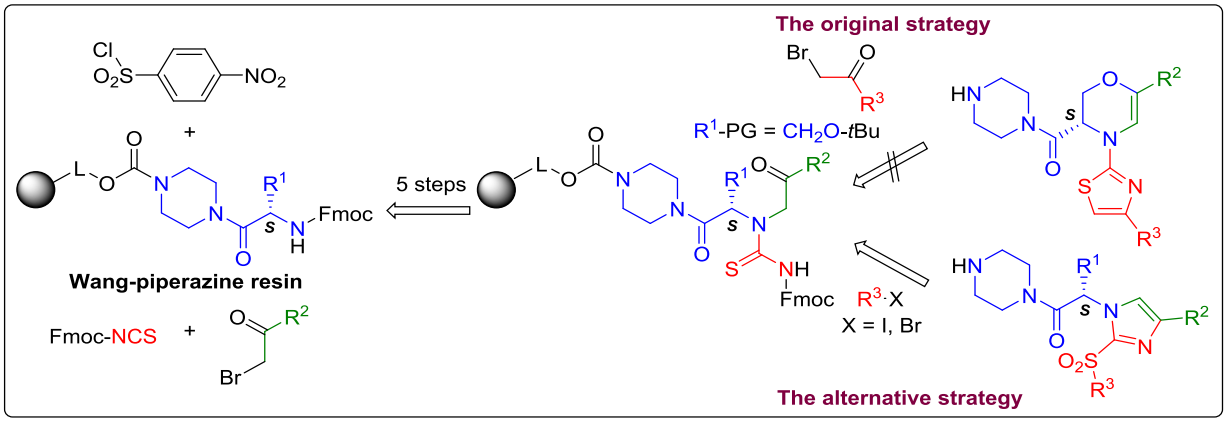

4.6.2 Synthesis

First, the synthesis of *N*-thiazolo-oxazines was tested using a combination of Wang-piperazine resin-immobilized Fmoc-Ser(*t*Bu)-OH **VI-3**{*2*} and *α*-bromoacetophenone. The key *α*-amino ketone **VI-3**{*2,1*} was synthesized in five steps according to our previously reported protocol.[2] The reaction with Fmoc-NCS under previously developed conditions[42] yielded desired thiourea derivative **VI-4**{*2,1*} in excellent crude purity (90%, calculated from HPLC-UV traces at 205–400 nm). After the removal of the Fmoc protecting group, the check of reaction solution (PIP/DMF) by LC-MS analysis confirmed that the cyclative cleavage has not taken place from the resin. The subsequent *S*-alkylation with *α*-bromoacetophenone and TFA treatment should afford (after the product cleavage from the resin and cyclization) *N*-thiazolo-oxazines **VI-5**{*2,1,4*} (Scheme 56).[62,63] However, the measured LC-MS data did not correspond to the mass of the product, but it indicated the previously reported formation of imidazole-2-thione scaffold **VI-7**{*2,1,4*}. To confirm the assumption, we performed the detailed NMR investigation of the product. The structure was determined by means of ^{1}H, ^{13}C{^{1}H}, DEPT, ^{1}H-^{1}H COSY, ^{1}H-^{1}H NOESY, ^{1}H-^{13}C HSQC, ^{1}H-^{13}C HMBC and ^{1}H-^{15}N HMBC. There were identified piperazine, CO-CH(CH$_2$OH), imidazole, phenyl and methylene-phenylketone moieties. Figure 33 displays the key interaction in the ^{1}H-^{13}C HMBC spectrum, e.g. H^4 correlated to C2, C5; H^7 to C2, C8; H^{10,14} to C8, C9, C11,13 and H^{15} to C2, C4, C16 and C18. The further investigation of NOE spectra gave mutual correlations between both diverse phenyl protons H^{10,14}-H^{26,30}, between phenyl protons to imidazole proton H^{26,30}-H^4, between imidazole proton to methylene protons H^4-H$_{a\text{-}b}$^{16} and between piperazine protons to CO-CH proton H^{20,24}-H^{15}. Since the detailed NMR analysis confirmed the imidazole-2-thione arrangement **VI-8**{*2,1,4*}, we designed the synthetic route to prepare novel 2-alkyl-sulfonyl-imidazoles **VI-11**{R^1,R^2,R^3} which should be based on a formation of sulfides and their oxidation to either sulfoxides or sulfones depending on the oxidizing conditions used.

Figure 33. The detailed ^{1}H-^{15}N HMBC, ^{1}H-^{13}C HMBC and NOE analysis of **VI-8**{*2,1,4*}

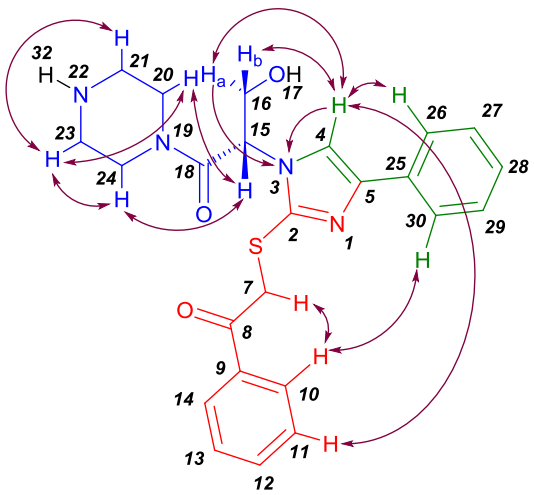

^{1}H-^{15}N HMBC and NOE correlations

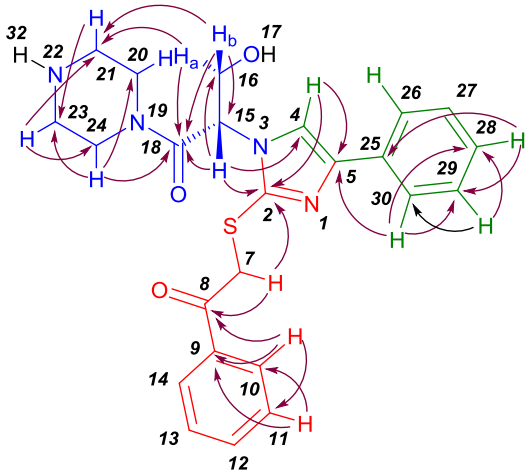

^{1}H-^{13}C HMBC correlations

Scheme 56. The synthesis of *N*-thiazolo-oxazines **VI-5**{*2*,R^2,*4*} and imidazoles **VI-10**{R^1,R^2,R^3}[a]

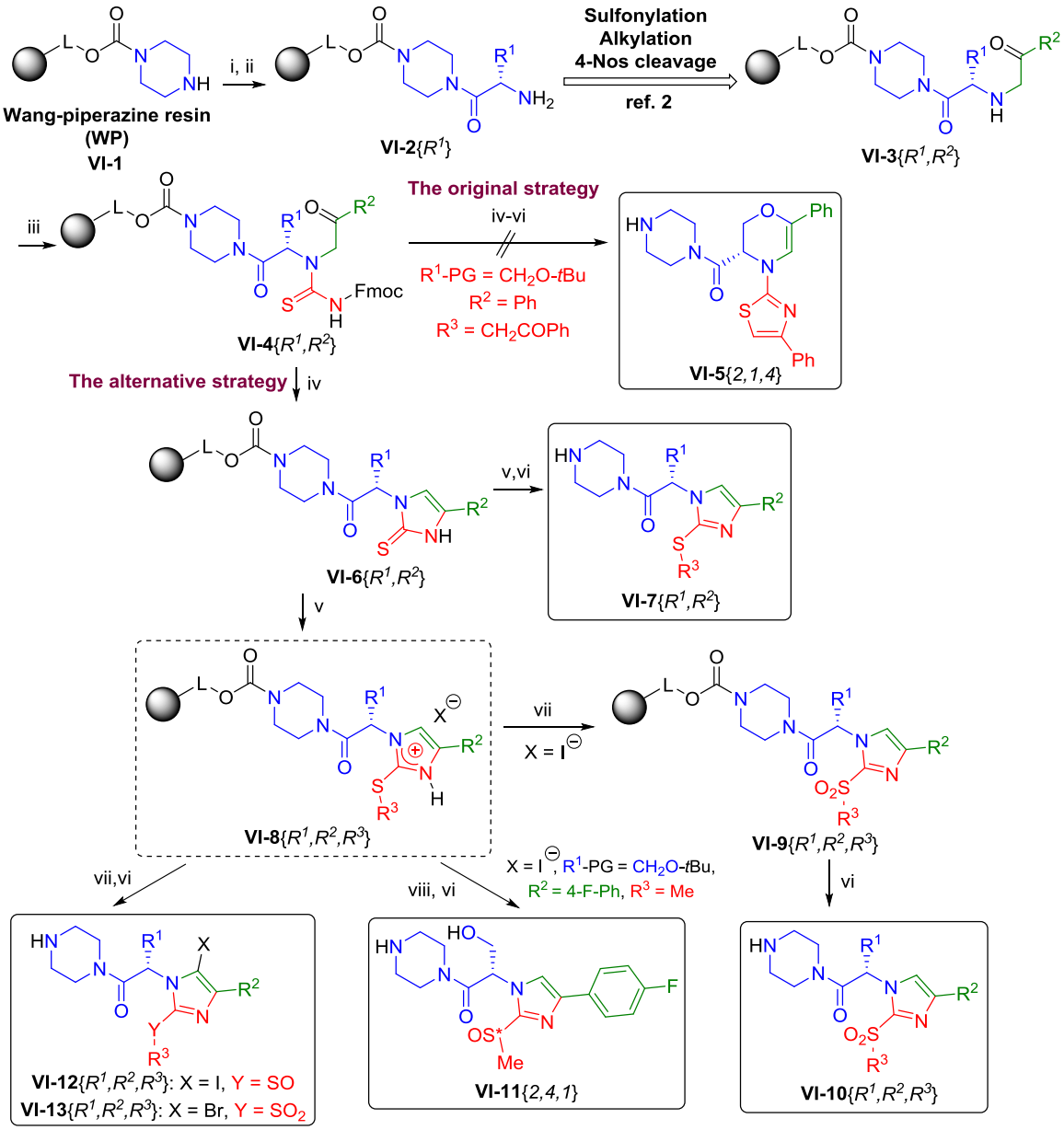

[a]Reagents and conditions: (i) Fmoc-amino acid, HOBt, DIC, DCM, DMF, 24 h, rt; (ii) 50% PIP/DMF, 30 min, rt; (iii) Fmoc-NCS, anhydrous THF, 2 h, rt; (iv) 50% PIP/DMF, 15 min, rt; (v) R^3X (X = I, Br), anhydrous DCM, 2 h, rt; (vi) neat TFA, on, rt; (vii) *m*CPBA, anhydrous DCM, 5 h, rt; (viii) *m*CPBA, anhydrous DCM, 30 min, rt.

The immobilized imidazole-2-thione **VI-8**{*1,1,1*} was obtained in seven-step reaction sequence according to the above described protocol started from Fmoc-Ala-OH immobilized on Wang-piperazine resin, *α*-bromoacetophenone and methyl iodide (Scheme 56). Then the sulfide **VI-8**{*1,1,1*} was oxidized with *meta*-chloroperoxybenzoic acid (*m*CPBA) using previously published conditions.[93] The TFA-mediated product cleavage from the resin afforded the final sulfone **VI-10**{*1,1,1*} in an excellent crude purity (95%, calculated from HPLC-UV traces at 205–400 nm) and 10% overall yield (calculated from the ^{1}H NMR spectrum of the purified product, Table 29 for the final derivatives).

4.6.3 Limitations and scope

The applicability of this synthetic approach was evaluated using a combination of different Fmoc-amino acids with functionalized side chains, *α*-bromoketones with electron donating and electron withdrawing substituents and various alkylating agents (Figure 34). The synthesis of all thiourea derivatives **VI-4**{R^1,R^2} was successful for all tested combinations of the synthons and the derivatives were obtained in 72-85% crude purities (calculated from HPLC-UV traces at 205–400 nm). After the deprotection of the Fmoc protecting group which triggered a formation of imidazole-2-thiones **VI-6**{R^1,R^2}, the alkylation was tested with alkyl iodides (ethyl iodoacetate, benzyl iodide, phenacyl iodide, allyl iodide) and alkyl bromides (ethyl bromoacetate, benzyl bromide, phenacyl bromide). Except for phenacyl iodide which afforded a mixture of unknown products, the resulting sulfides **VI-8**{R^1,R^2,*1-4*} were obtained in 57-94% crude purities (calcultated from HPLC-UV traces at 205–400 nm). In the case of sulfide **VI-8**{*1*,*1*,*6*}, the alkylation with 3-(bromomethyl)pyridine hydrobromide required the presence of base (DBU, 1 equiv to alkylating agent) to the reaction completion; however, the subsequent oxidation failed and only the starting material was detected in the LC-MS spectrum.

Figure 34. List of tested synthons for R^1, R^2 and R^3 substituents

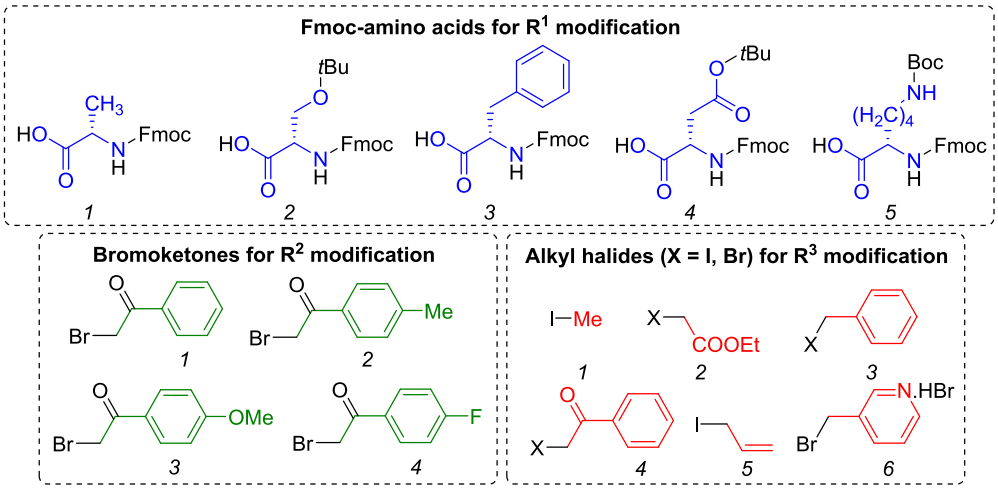

To extend the developed methodology, we tested different oxidation methods of intermediate **VI-8**{*2*,*4*,*1*} (Scheme 57). According to the results in Table 26, either sulfoxide or sulfone were obtained after the oxidation using *m*CPBA depending on the oxidation time (highlighted in bold). The oxidation for only 30 min afforded the corresponding sulfoxide **VI-11**{*2*,*4*,*1*}, which was obtained as a mixture of two inseparable diastereoisomers in a ratio of 68:32 (calculated from the ^{1}H NMR spectrum of the purified product). When the oxidation time was extended to 5 h, the reaction furnished sulfone **VI-11**{*2*,*4*,*1*}. However, in the case of other sulfide analogous **VI-8**{R^1,R^2,R^3}, the isolation of sulfoxides was impossible due to immediate oxidation to sulfones by the excess of *m*CPBA.

Scheme 57. The oxidation of sulfide **VI-8**{*2,4,1*}[a]

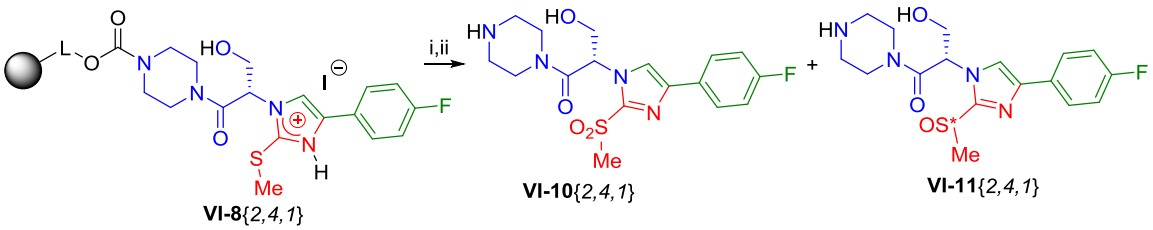

[a]Reagents and conditions: (i) **(a)** *m*CPBA, anhydrous DCM, 0.5-4 h, rt-(-20 °C); **(b)** H_5IO_6, $FeCl_3$, THF, 0.5-2.5, rt; **(c)** H_5IO_6, CrO_3, THF/H_2O, 1, rt; **(d)** oxone, DCM/H_2O, 1-19 h, rt-40 °C; **(e)** H_2O_2, $CF_3(CH_2)_2OH$, 4-18 h, rt; (ii) neat TFA, 2 h, rt.

Table 26. The tested oxidation conditions for sulfide **VI-8**{*2,4,1*}[a]

oxidizing agent	conc. ox. agents [mmol]	solvent	time [h]	temp [°C]	crude purity of VI-8 [%][a]	crude purity of VI-10 [%][a]	crude purity of VI-11 [%][a]	ratio of VI-8:10:11 [%][a]
			0.5	**23**	**0**	**65**	**0**	**0:100:0**
***m*CPBA**	**0.5**	**DCM**	**5**	**23**	**0**	**0**	**81**	**0:0:100**
			4	-20	0	34	30	0:53:47
H_5IO_6	0.1	THF	0.5	23	31	42	0	43:57:0
$FeCl_3$	0.035		2.5	23	0	0	3	0:0:100
H_5IO_6	0.1	THF/H_2O	1	23	90	0	0	100:0:0
CrO_3	0.039							
			1	23	65	17	0	79:21:0
			4	23	33	46	0	42:58:0
oxone	0.5	DCM/ H_2O	5	23	0	52	41	0:56:44
			19	23	0	28	67	0:29:71
			1	40	72	8	0	90:10:0
H_2O_2	1.0	$CF_3(CH_2)_2OH$	4	23	59	18	0	77:23:0
			18	23	20	53	0	27:73:0

[a]Calculated from HPLC-UV-MS traces at 205–400 nm.

The oxidation of sulfide **VI-8**{*1,3,2*}, prepared from ethyl iodoacetate, and the subsequent product release from the resin yielded neither the expected sulfone **VI-10**{*1,3,2*} nor sulfoxide **VI-11**{*1,3,2*}. In this case, a by-product with a molecular weight corresponding to an iodinated sulfoxide **VI-12**{*1,3,2*} was detected by LC-MS analysis (Scheme 58, Table 29 for the final derivatives). To determine the structure, the by-product was isolated by semipreparative reverse-phase HPLC and subjected to the detailed NMR analysis that confirmed the suggested structure. According to the ^{1}H NMR spectrum, the by-product was observed as a mixture of two inseparable diastereoisomers in a ratio of 86:14 (calculated from the ^{1}H NMR spectrum of the purified product, Figure 35). In contrast, the oxidation of sulfide **VI-8**{*1,1,3*}, prepared from benzyl iodide or then from benzyl bromide, resulted in either sulfone **VI-10**{*1,1,3*} or brominated sulfone **VI-13**{*1,1,3*} which were determined using HPLC-UV-MS analysis. The comparison of ^{1}H NMR spectra of all three compounds indicated that iodination or bromination took place on the imidazole scaffold based on the disappearance of the corresponding aromatic signal HC^4 (Figure 36-37). Surprisingly, the oxidation of other sulfides **VI-8**{R^1,R^2,R^3}, prepared from the corresponding alkyl iodides (e.g. methyl iodide, ethyl iodoacetate,

Scheme 58. The oxidation of sulfides **VI-8**{R^1,R^2,R^3}[a]

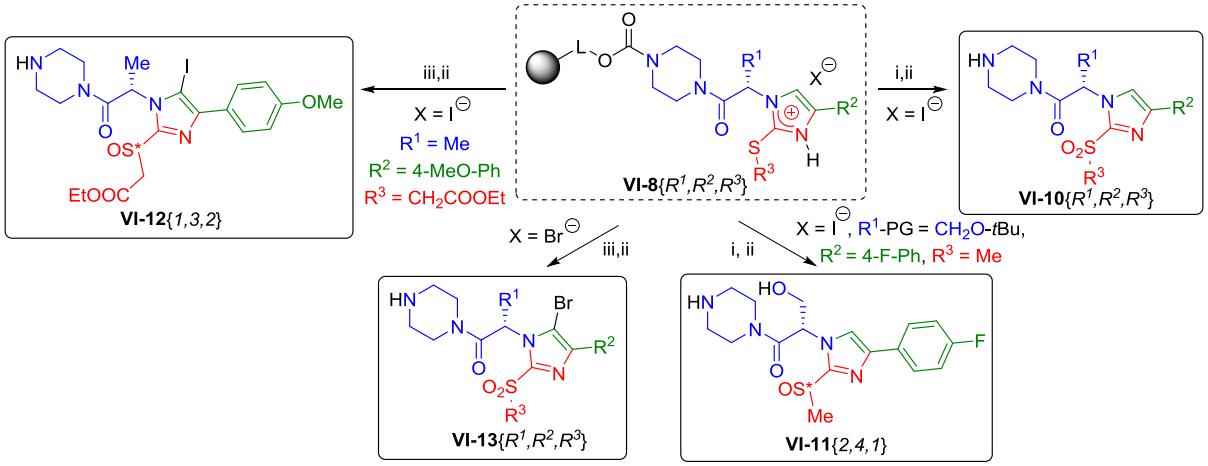

[a]Reagents and conditions: (i) *m*CPBA, anhydrous DCM, 30 min, rt; (ii) neat TFA, on, rt; (iii) *m*CPBA, anhydrous DCM, 5 h, rt.

Figure 35. Disappearance of the HC[4] signal of imidazole **VI-12**{*1,3,2*} after oxidation to sulfoxides observed as a mixture of two diastereoisomers in a ratio of 14:86

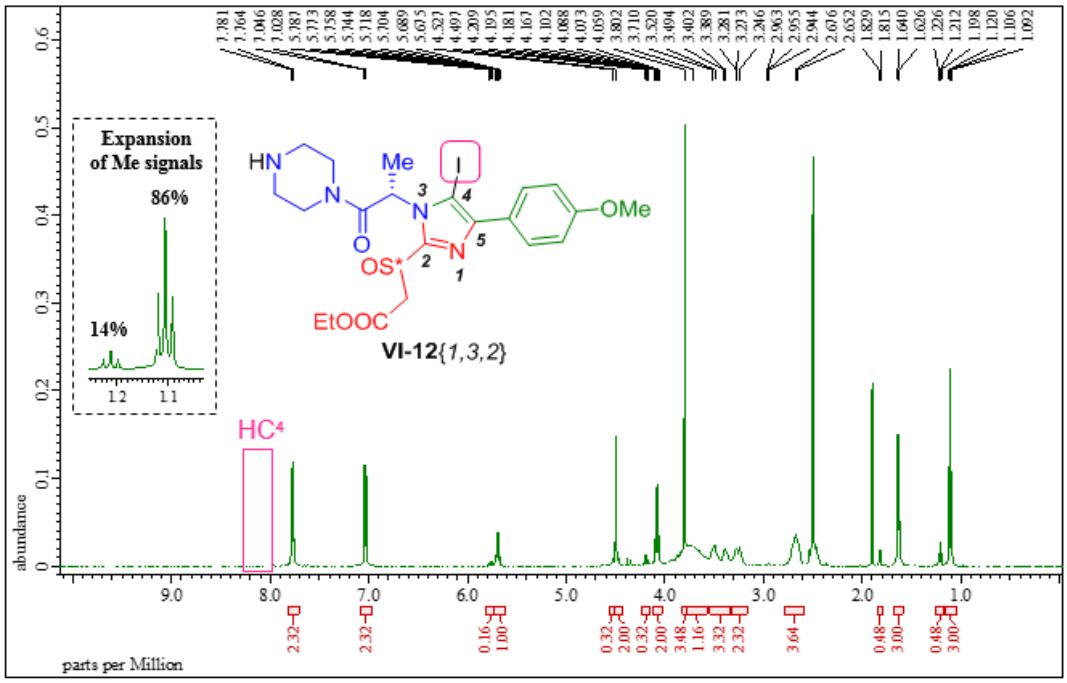

benzyl iodide) afforded predominantly sulfones **VI-10**{R^1,R^2,R^3} and no iodinated analogues **VI-12**{R^1,R^2,R^3} were detected (Table 29 for the final derivatives). However, the oxidation of sulfides **VI-8**{R^1,R^2,R^3}, prepared from the corresponding alkyl bromides (e.g. ethyl bromoacetate, benzyl bromide and phenacyl bromide), caused always the bromination. In some cases, the resulting brominated sulfones **VI-13**{R^1,R^2,R^3} were detected as a mixture of sulfones **VI-10**{R^1,R^2,R^3} in different ratios of both derivatives depended on overall substitution (Table 27).

Table 27. Ratios of **VI-10**{*R*[1],*R*[2],*R*[3]} and **VI-13**{*R*[1],*R*[2],*R*[3]} depending on *R*[1], *R*[2] and *R*[3] substituents[a]

starting cmpd	R[1]	R[2]	R[3]	ratio of VI-10:13 [%][a]
VI-8{*1,1,3*}	Me	Ph	Bn	0:1
VI-8{*1,2,4*}	Me	4-Me-Ph	CH_2COPh	1:2
VI-8{*2,1,2*}	CH_2OH	Ph	CH_2COOEt	1:1
VI-8{*2,2,2*}	CH_2OH	4-Me-Ph	CH_2COOEt	0:1
VI-8{*2,2,4*}	CH_2OH	4-Me-Ph	CH_2COPh	1:2
VI-8{*3,1,3*}	CH_2Ph	Ph	Bn	1:2
VI-8{*3,1,4*}	CH_2Ph	Ph	CH_2COPh	1:1
VI-8{*5,1,3*}	$(CH_2)_4NH_2$	Ph	Bn	1:3

[a]Calculated from HPLC-UV-MS traces at 205–400 nm.

Figure 36. The ^{1}H NMR spectrum of sulfone **VI-10**{*1,1,3*}

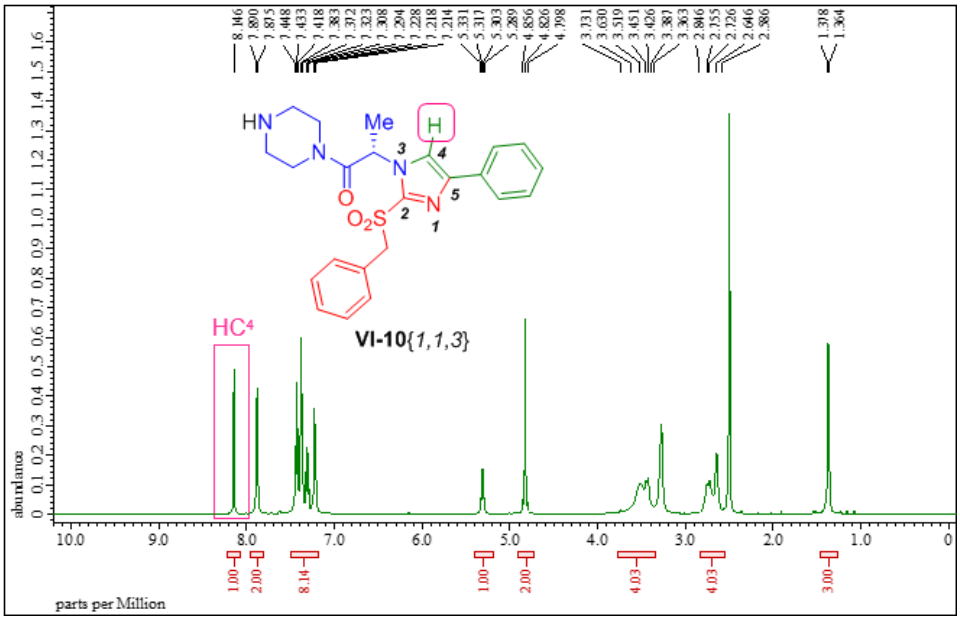

Figure 37. Disappearance of the HC^4 signal of imidazole **VI-13**{*1,1,3*} after oxidation

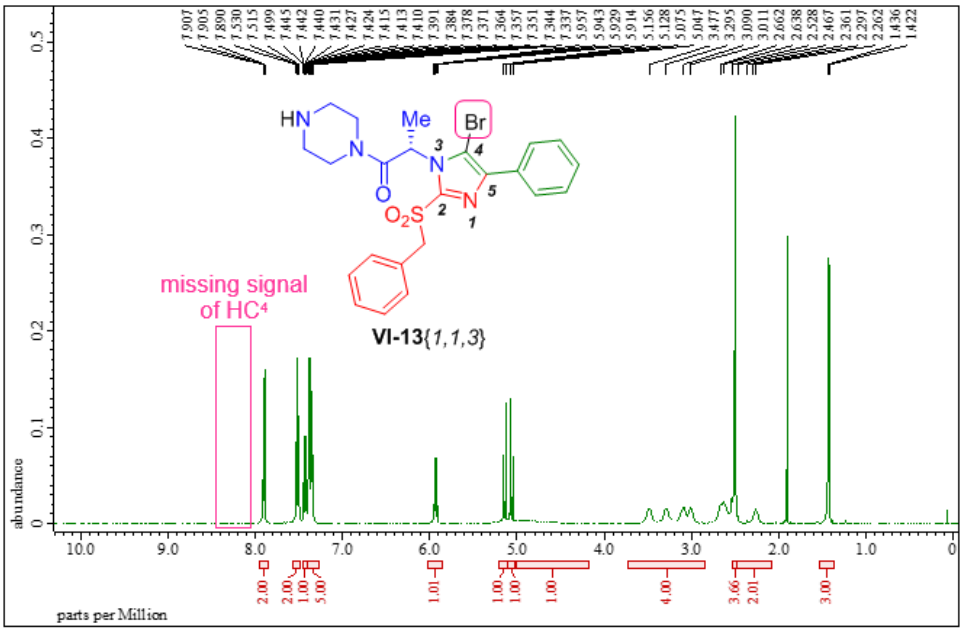

The unexpected halogenation can be explained by the formation of imidazole-hydrohalogenides (X = Br, I) at the stage of intermediates **VI-8**{R^1,R^2,R^3} as a result of the generation of HBr/HI and its capture after the alkylation step (Scheme 58). Subsequent treatment with *m*CPBA may oxidize the bromide/iodide anions to bromine/iodine followed by bromination/iodination of the imidazole scaffold by radical mechanism. The crucial role of *m*CPBA is evident from the cleavage and analysis of sulfides **VI-8**{R^1,R^2,R^3}, which showed no traces of the brominated/iodinated sulfides. According to these facts, the following oxidation leading to four diverse imidazoles **VI-10-13**{R^1,R^2,R^3} was dependent on overall substitution of the starting sulfides **VI-8**{R^1,R^2,R^3} and the type of alkylating agents used (e.g. alkyl iodide or alkyl bromide; Table 29 for the final derivatives).

In total, we prepared 20 final compounds **VI-10-13**{R^1,R^2,*1-4*} in 65-95% crude purities (calculated from HPLC-UV traces at 205–400 nm) and 10-36% overall yields (calculated from ^{1}H NMR spectra of the purified products; Table 29).

Table 28. The list of synthesized and fully characterized compounds[a-d]

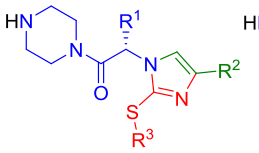

VI-7{R^1,R^2,R^3}

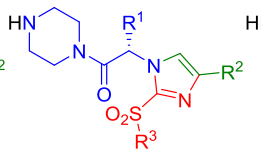

VI-10{R^1,R^2,R^3}

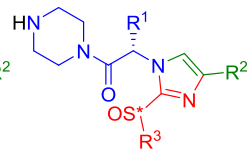

VI-11{R^1,R^2,R^3}

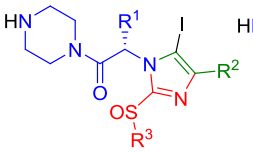

VI-12{R^1,R^2,R^3}

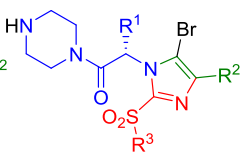

VI-13{R^1,R^2,R^3}

cmpd	R^1	R^2	R^3	type of alkylating agent X = Br, I[a]	crude purity [%][b]	final purity [%][c]	overall yield [%][d]
VI-7{*4,1,4*}	CH_2COOH	Ph	CH_2COPh	Br	75	99	11
VI-7{*2,1,4*}	CH_2OH	Ph	CH_2COPh	Br	82	99	16
VI-10{*1,1,1*}	Me	Ph	Me	I	75	98	10
VI-10{*1,1,3*}	Me	Ph	Bn	I	84	99	14
VI-10{*2,1,1*}	CH_2OH	Ph	Me	I	94	98	36
VI-10{*2,2,3*}	CH_2OH	4-Me-Ph	Bn	I	74	99	10
VI-10{*2,2,5*}	CH_2OH	4-Me-Ph	allyl	Br	88	98	26
VI-10{*2,3,1*}	CH_2OH	4-MeO-Ph	Me	I	72	98	23
VI-10{*2,4,1*}	CH_2OH	4-F-Ph	Me	I	81	97	21
VI-10{*3,1,1*}	CH_2Ph	Ph	Me	I	95	99	20
VI-10{*3,4,2*}	CH_2Ph	4-F-Ph	CH_2COOEt	I	69	99	17
VI-10{*3,4,3*}	CH_2Ph	4-F-Ph	Bn	I	65	99	16
VI-10{*4,1,1*}	CH_2COOH	Ph	Me	I	71	99	13
VI-10{*4,4,3*}	CH_2COOH	4-F-Ph	Bn	I	63	98	22
VI-10{*5,1,1*}	$(CH_2)_4NH_2$	Ph	Me	I	87	99	15
VI-11{*2,4,1*}	CH_2OH	4-F-Ph	Me	I	65	99	12
VI-12{*1,3,2*}	Me	4-MeO-Ph	CH_2COOEt	I	63	99	14
VI-13{*1,1,3*}	Me	Ph	Bn	Br	76	99	15
VI-13{*3,1,2*}	CH_2Ph	Ph	CH_2COOEt	Br	58	98	11
VI-13{*5,1,3*}	$(CH_2)_4NH_2$	Ph	Bn	Br	80	99	16

[a]The structure of alkylating agents is shown in Figure 34; [b]Overall crude purity after the entire reaction sequence calculated from HPLC-UV traces at 205–400 nm; [c]Purity calculated from HPLC-UV traces at 205–400 nm after purification; [d]Calculated from the ^{1}H NMR spectrum of the purified product.

In addition, the purified brominated sulfone **VI-13**{*1,1,3*} was subjected to the Suzuki-Miyaura coupling with phenylboronic acid to eventually form new C^4-C bond to obtain the product **VI-14**{*1,1,3*} (Scheme 59). Table 28 shows several tested conditions for the coupling in combination with different solvents, Pd-ligands and temperatures; however, all tested experiments failed and the desired product **VI-14**{*1,1,3*} was not obtained, probably due to low reactivity of the starting material **VI-13**{*1,1,3*} and/or undesired debromination providing the sulfone **VI-10**{*1,1,3*}.

Scheme 59. The attempted Suzuki-Miyaura coupling for the formation of C^4-C bond **VI-14**{*1,1,3*}[a]

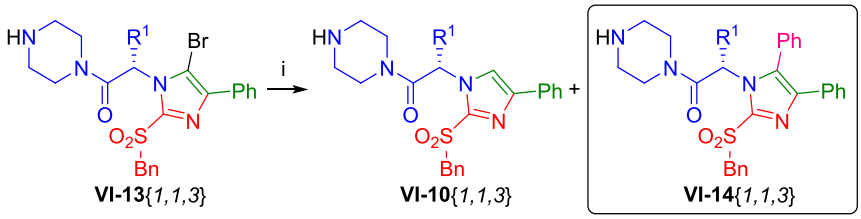

[a]Reagents and conditions: (i) $PhB(OH)_2$, Na_2CO_3, Pd-ligand, solvent, time, temp.

Table 29. The tested conditions for Suzuki-Miyaura coupling of **VI-13**{*1,1,3*} with phenylboronic acid[a]

Pd-ligand	solvent	time [h]	temp [°C]	crude purity of VI-13 [%][a]	crude purity of VI-10 [%][a]	crude purity of VI-14 [%][a]	ratio of VI-13:10:14 [%][a]
$Pd(PPh_3)_4$	$EtOH/H_2O$ (4:1)	24	90	95	0	0	100:0:0
$Pd(PPh_3)_4$	$PhCH_3$/EtOH (9:1)	24	90	90	0	0	100:0:0
XPhos Pd G2	$PhCH_3$/ H_2O (9:1)	0.67	120	0	96	0	0:100:0

[a]Calculated from HPLC-UV-MS traces at 205–400 nm.

Further attention was paid to on-resin nucleophilic substitution of sulfone **VI-9**{*1,1,1*} with various amines that could eventually yield the corresponding *N*-alkylamine-imidazole **VI-15**{*1,1,1*} (Scheme 60). In this case, we tested the reaction with four amines (e.g. cyclohexylamine, piperidine, benzylamine and isobutylamine) in combination with different base (e.g. TEA, DIEA, BTPP, DBU), solvents (e.g. DMSO, NMP, MeCN, DCE or EtOH), temperatures and time (23-160 °C for 0.5-24 h) or even under microwave irradiation;[94,95] however, in all tested cases, we detected only the starting material using the LC-MS analysis.

Scheme 60. The attempted nucleophilic substitution of sulfone **VI-9**{*1,1,1*} with amines[a]

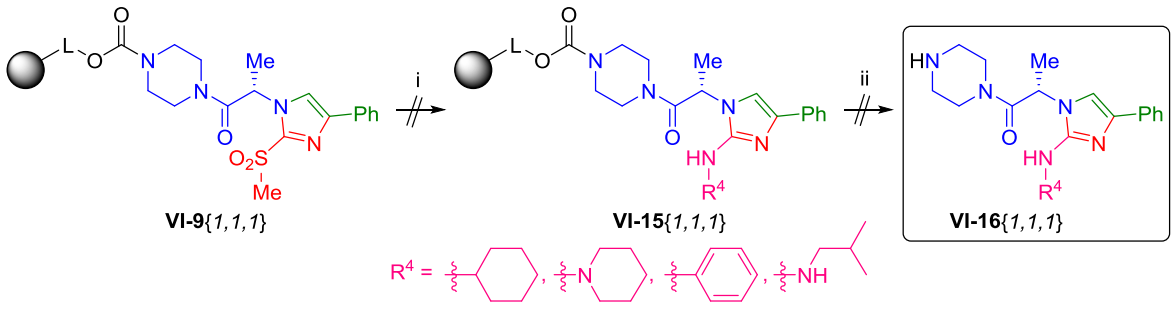

[a]Reagents and conditions: (i) R^4NH_2, base, solvent, time, temp, (MW); (ii) neat TFA, 2 h, rt.

Finally, we tested the possible alteration of the amidic moiety. Surprisingly, when the Wang-ethylenediamine resin (WED) was used instead of Wang-piperazine resin (WP), the reaction pathway failed at the stage of Fmoc-thiourea formation. Similar results were obtained when Rink amide resin (RA) and aminomethyl resin with immobilized secondary amines (AM) were used as the starting materials (Scheme 61).

Scheme 61. The possible diversification of the amidic moiety instead of Wang-piperazine linker[a]

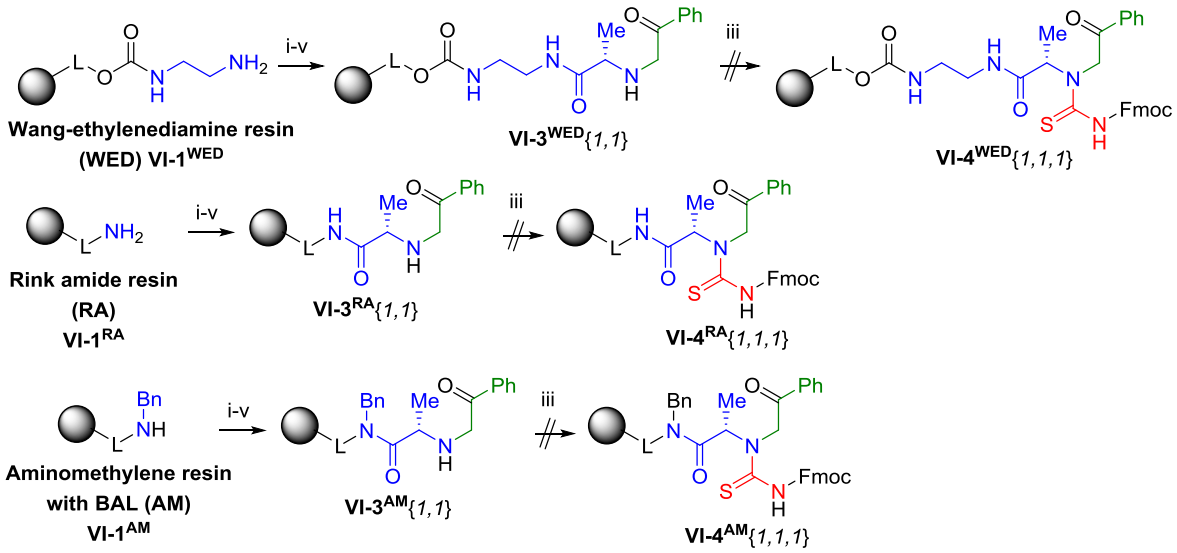

[a]Reagents and conditions: (i) Fmoc-Ala-OH, HOBt, DIC, DCM, DMF, 24 h, rt; (ii) 50% PIP/DMF, 30 min, rt; (iii) 4-Nos-Cl, 2,6-lutidine, DCM, 24 h, rt; (iv) $PhCOCH_2Br$, DIEA, DMF, 24 h, rt; (v) MCE, DBU, degassed DMF, 1.5 h, rt; (vi) Fmoc-NCS, anhydrous THF, 2 h, rt.

4.6.4 Conclusion

To conclude, the simple synthesis of 2-alkylsulfonyl-imidazoles with three diversity positions was developed. In some cases (started from immobilized L-alanine, L-phenylalanine and L-lysine), the C4 halogenated products were obtained depending on the combination of R^1, R^2 and R^3 substituents and type of the alkylating agents used. The developed strategy can be applied for combinatorial synthesis of chemical libraries using a large number of readily available building blocks.

4.7 Rearrangement of Threonine and Serine-Based *N*-(3-Phenylprop-2-yn-1-yl) Sulfonamides Yields Chiral Pyrrolidin-3-ones

The results of this project were published in: Králová, P.; Maloň, M; Pospíšil, J.; Soural, M. *J. Org. Chem.* **2020**, *85* (2), 985–993.[96] The manuscript is attached in Appendix I (p. 200 – 208). The Supporting information is available at: https://pubs.acs.org/doi/pdf/10.1021/acs.joc.9b02932 and is attached as an electronic file on CD.

Numbering of the individual products, linkers and building blocks used in the subchapter is adapted to Chemset Numbering System for the combinatorial chemistry and it does not correspond to the attached manuscript and Supporting information.

4.7.1 Brief introduction

This subchapter continues to our previous results[2,38–43] which describes the stereoselective synthesis of chiral morpholine or imidazole derivatives synthesized from immobilized *N*-phenacyl-2/4-Nos-amides. In the following research, *N*-phenacyl intermediates were replaced with internal alkynols by switching from haloketones to phenylakynols as the alkylating agents. The polymer-supported intermediates were subjected to TFA-mediated cleavage from the resin and then modified by an internal post-cleavage hydroxyalkoxylation-reduction using trimethylsilyl trifluoromethanesulfonate (TMSOTf) and TES. The reaction should result in a formation of 1,4-oxazepane scaffold according to the previously reported results.[4] The main aim of this project was development of a methodology to synthesize functionalized 1,4-oxazepanes amenable for further diversification, e.g. preparation of fused oxazepanes (Figure 38, The original strategy). However, the ^{1}H and $^{13}C\{^{1}H\}$ NMR spectra were not consistent with the 1,4-oxazepane structure and therefore, we performed detailed NMR investigation of the product which confirmed the pyrrolidin-3-one scaffold (Figure 38, The actual results).

Figure 38. The proposed synthetic strategy to prepare single and fused 1,4-oxazepanes

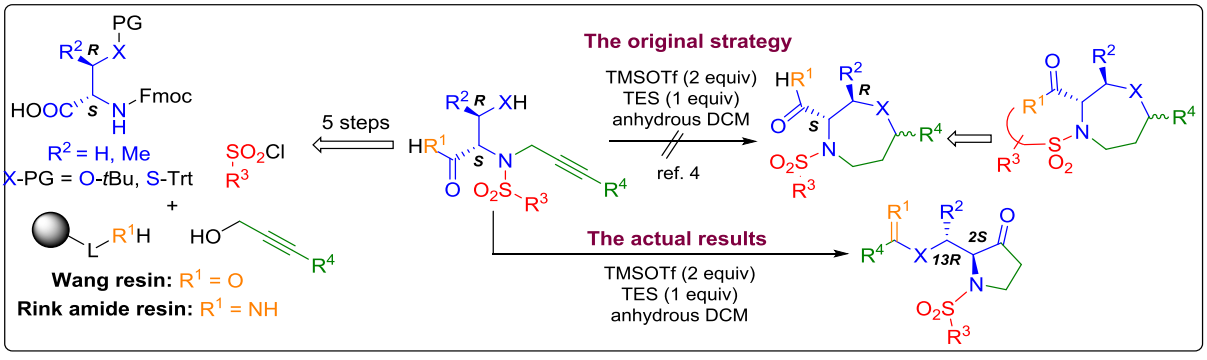

4.7.2 Synthesis

First, Wang resin and Rink amide resin **VII-1**{R^1} were acylated with Fmoc-amino acids, subjected to the Fmoc-cleavage, and reacted with sulfonyl chlorides (e.g. 2-NosCl, 4-NosCl, Ms-Cl and Ts-Cl) according to the previously reported procedure.[2] The resulting *N*-sulfonamides **VII-2**{R^1,R^2,R^3} were alkylated with different alkynols using a Mitsunobu alkylation (Figure 39, alkynols *1-6* for R^4 modification). For these purposes, *para*-substituted phenylalkynols bearing electron donating (Me and MeO) and electron withdrawing (CF_3) group were prepared from the corresponding aryl iodides and propargyl alcohol in 51-97% overall yields *via* Sonogashira coupling (calculated after purification by silica gel chromatography; the experimental conditions are attached as an electronic file

Figure 39. The list of tested building blocks for R^1, R^2, R^3 and R^4 substituents

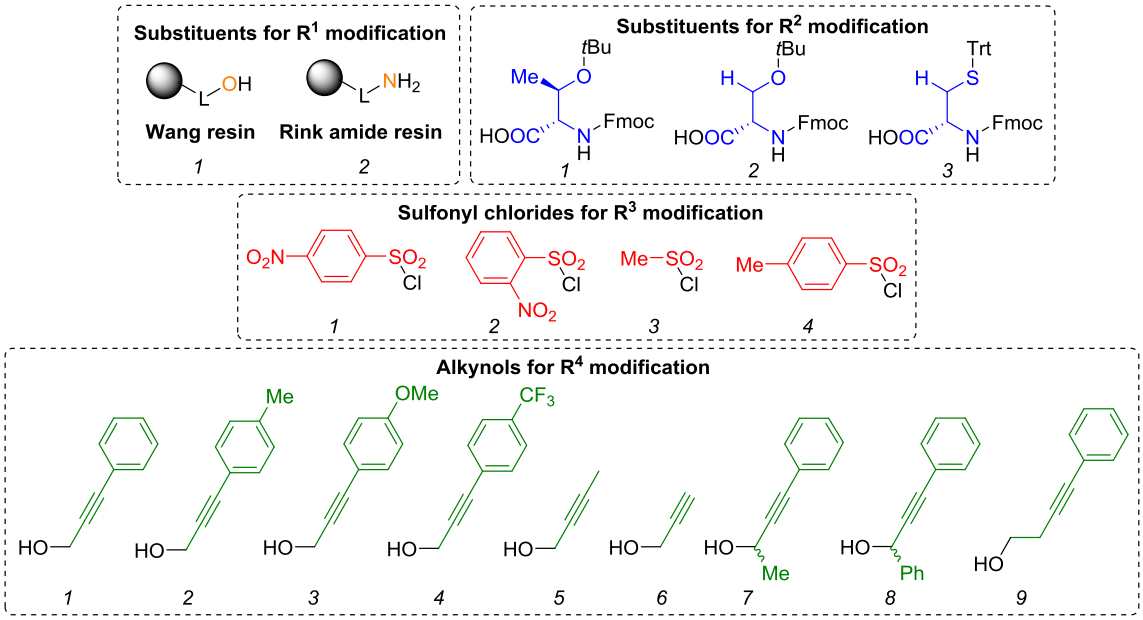

Scheme 62. The synthesis of alkynols **VII-4** and their TMSOTf-mediated rearrangement to **VII-5**[a]

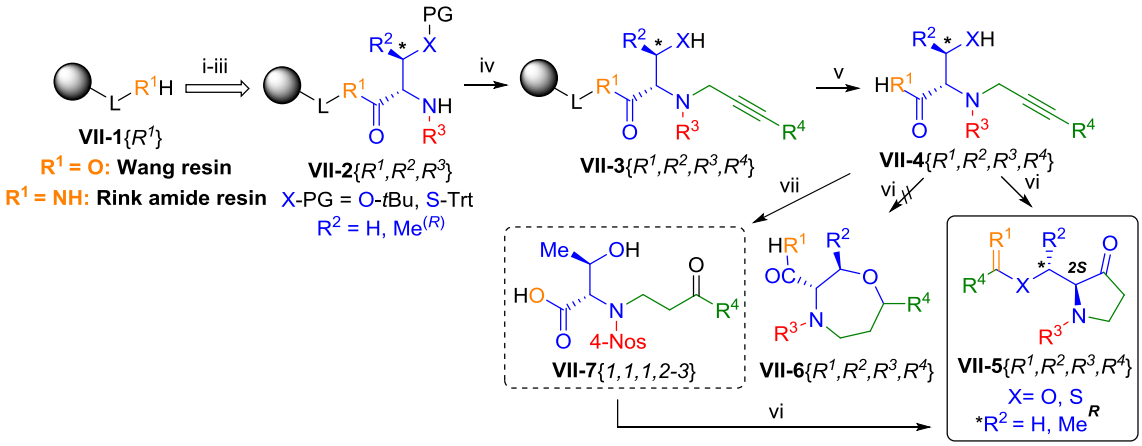

[a]Reagents and conditions: (i) Fmoc-amino acid, HOBt, DMAP, DIC, DMF, DCM, 24 h, rt; (ii) 50% PIP/DMF, 30 min, rt; (iii) R^3-sulfonyl chlorides, 2,6-lutidine, DCM, 24 h, rt; (iv) alkynol, TPP, DIAD, anhydrous THF, 24 h, rt; (v) 50% TFA/anhydrous DCM, 1 h, rt; (vi) TMSOTf/TES (2:1), anhydrous DCM, 24 h, 0 °C or TMSOTf, anhydrous DCM, 24-72 h, 23-40 °C; (vii) HPLC MeCN/H_2O or HPLC MeCN/10 *m*M AmAc, 0.08 h, rt (for derivative **VII-7**{*1,1,1,3*}) or HPLC MeCN/AmAc, 1440 h, rt (for derivative **VII-7**{*1,1,1,2*}).

on CD or in Supporting Information). Cleavage from resin **VII-3**{*R*[1],*R*[2],*R*[3],*R*[4]} with TFA was followed by spontaneous cleavage of the *tert*-butyl ether. The resulting intermediates **VII-4**{*R*[1],*R*[2],*R*[3],*R*[4]} were purified by semipreparative reverse-phase HPLC or by silica gel chromatography and 9 representative compounds were obtained in 40-95% crude purities (calculated from HPLC-UV traces at 205–400 nm) and 21-82% overall yields (calculated after cleavage of products from the resin and their HPLC purification; Scheme 62, Table 30).

Table 30. The list of synthesized intermediates **VII-4**{*R*[1],*R*[2],*R*[3],*R*[4]} and **VII-7**{*R*[1],*R*[2],*R*[3],*R*[4]}[a-e]

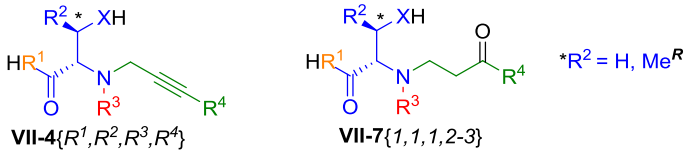

final cmpd	X	R[1]	R[2]	R[3]	R[4]	crude purity [%][a]	final purity [%][b]	yield [%][c]
VII-4{*1,1,1,1*}	O	O	Me	4-Nos	Ph	90	98	82
VII-4{*1,1,2,1*}	O	O	Me	2-Nos	Ph	90	98	21
VII-4{*1,1,3,1*}	O	O	Me	Ms	Ph	95	99	30
VII-4{*1,1,4,1*}	O	O	Me	Ts	Ph	86	99	31
VII-4{*1,1,1,2*}	O	O	Me	4-Nos	4-Me-Ph	NI[d]	NI	NI
VII-4{*1,1,1,3*}	O	O	Me	4-Nos	4-MeO-Ph	NI[d]	NI	NI
VII-4{*1,1,1,4*}	O	O	Me	4-Nos	4-CF_3-Ph	90	99	69
VII-4{*1,1,1,5*}	O	O	Me	4-Nos	Me	93	99	73
VII-4{*1,1,1,6*}	O	O	Me	4-Nos	H	90	99	33
VII-4{*1,2,1,1*}	O	O	H	4-Nos	Ph	87	98	30
VII-4{*1,3,1,1*}	S	O	H	4-Nos	Ph	40	NI	NI
VII-4{*2,1,1,1*}	O	NH	Me	4-Nos	Ph	95	99	30
VII-7{*1,1,1,2*}	O	O	Me	4-Nos	4-Me-Ph	80[e]	NI	NI
VII-7{*1,1,1,3*}	O	O	Me	4-Nos	4-MeO-Ph	90	98	41

[a]Overall crude purity after the entire reaction sequence calculated from HPLC-UV traces at 205–400 nm; [b]Calculated from HPLC-UV traces at 205–400 nm after purification; [c]Calculated after cleavage of products from the resin and their HPLC purification; [d]The hydrolysis of alkynes **VII-4** to ketones **VII-7** during HPLC purification; [e]The inseparable mixture of starting alkyne **VII-4** and ketone **VII-7** in a ratio of 10:90 after hydrolysis in AmAc/HPLC MeCN; NI = not isolated.

The purification of *N*-alkyl-sulfonamides **VII-4**{*1,1,1,2*} and **VII-4**{*1,1,1,3*} bearing electron donating (Me and MeO) substituents did not furnish expected alkynes due to their hydrolysis to the corresponding ketones **VII-7**{*1,1,1,2*} and **VII-7**{*1,1,1,3*} during their HPLC purification (Scheme 63, Table 30-31). The rate of the hydrolysis was dependent on the R^4 substitution. The hydrolysis to ketone was noticeably faster in the case of MeO group. Although the rate of hydrolysis to *p*-methoxybenzophenone **VII-7**{*1,1,1,3*} was comparable in both tested solvents (AmAc/MeCN vs H_2O/MeCN), the better results were achieved in 10 *m*M AmAc in MeCN. On the other hand, Me substitution slowed the conversion to *p*-methylbenzophenone **VII-7**{*1,1,1,2*}. Finally, the ketone **VII-7**{*1,1,1,3*} was purified by semipreparative reverse-phase HPLC and subjected to NMR experiments to check the characteristic signals of ketone **VII-7**{*1,1,1,3*}. The comparison of the $^{13}C\{^1H\}$

NMR spectra of alkyne **VII-4**{*1,1,3,1*} with ketone **VII-7**{*1,1,1,3*} (Figure 40-41) shows that two carbon signals of alkyne moiety at 85.0 ppm and 85.8 ppm (Figure 41) were replaced by three signals at 199.3 ppm, 44.5 ppm and 39.2 ppm indicating the carbonyl group and two methylene groups, respectively. Additionally, the ^{1}H NMR spectrum of ketone shows two methylene groups at 3.42 ppm and 3.60 ppm (Figure 42).

Scheme 63. The acidic hydrolysis of **VII-4**{*1,1,1,2-3*} to **VII-7**{*1,1,1,2-3*}[a]

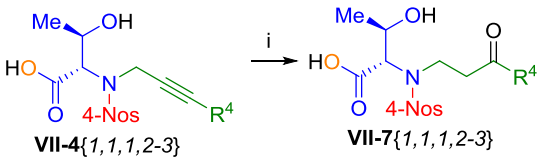

VII-4{*1,1,1,2-3*} **VII-7**{*1,1,1,2-3*}

[a]Reagents and conditions: (i) HPLC MeCN/H_2O or HPLC MeCN/AmAc, 5 min-60 days (1440 h), rt.

Table 31. The tested conditions for acidic hydrolysis of **VII-4**{*1,1,1,2-3*} to **VII-7**{*1,1,1,2-3*}[a-c]

starting cmpd	R^4	conditions (1:1)	time [h]	temp [°C]	crude purity of VII-4 [%][a]	crude purity of VII-7 [%][a]	ratio of VII-4:7 [%][a]
VII-4{*1,1,1,2*}	4-Me-Ph	water/MeCN	0.08	23	80	17	82:18
			1-12	23	33	65	34:66
		AmAc/MeCN	0.08	23	38	54	41:59
			1	23	35	62	36:64
			1440	**23**	**9**	**80**[b]	**10:90**
VII-4{*1,1,1,3*}	4-MeO-Ph	water/MeCN	0.08[c]	23	0	81	0:100
		AmAc/MeCN	**0.08**[c]	**23**	**0**	**95**	**0:100**

[a]Overall crude purity after rearrangement calculated from HPLC-UV traces (205–400 nm); [b]Observed as an inseparable mixture of the starting alkyne **VII-4** and the ketone **VII-7**; [c]Immediate conversion of alkyne **VII-4**{*1,1,1,3*} to ketone **VII-7**{*1,1,1,3*} in AmAc/MeCN or water/MeCN.

Figure 40. The ^{13}C{^{1}H} NMR spectrum of ketone **VII-7**{*1,1,1,3*}

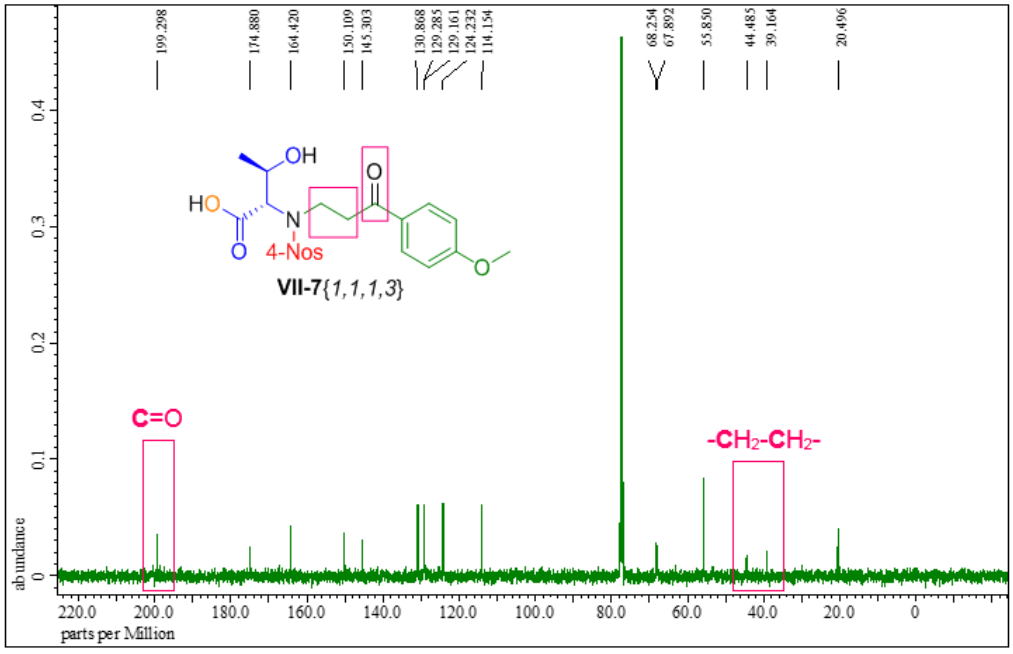

Figure 41. The $^{13}C\{^{1}H\}$ NMR spectrum of alkyne **VII-4**{*1,1,4,1*}

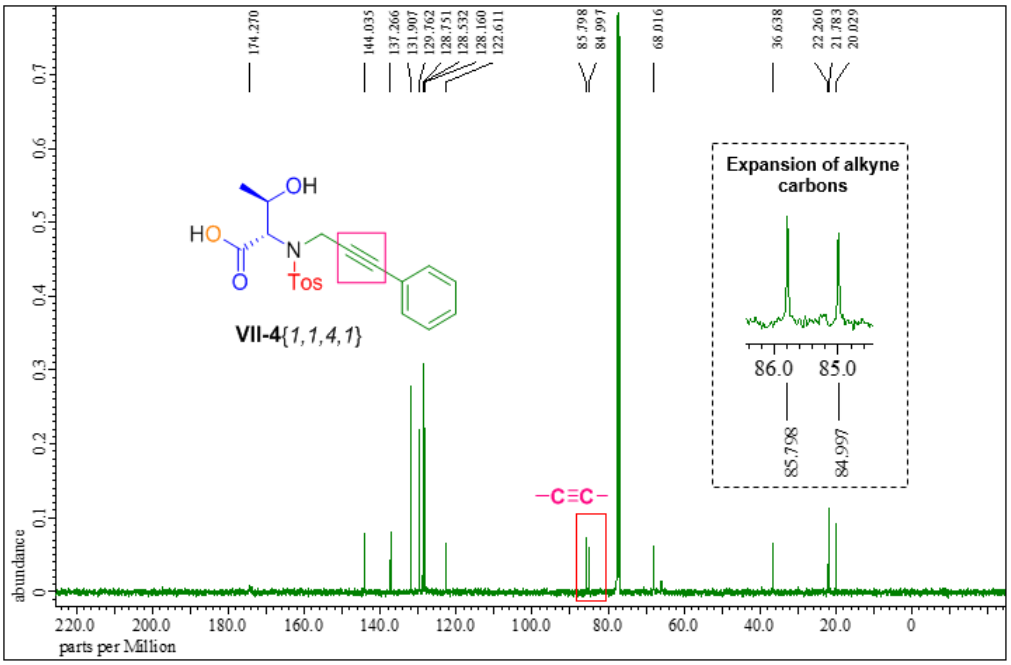

Figure 42. The ^{1}H NMR spectrum of ketone **VII-7**{*1,1,1,3*}

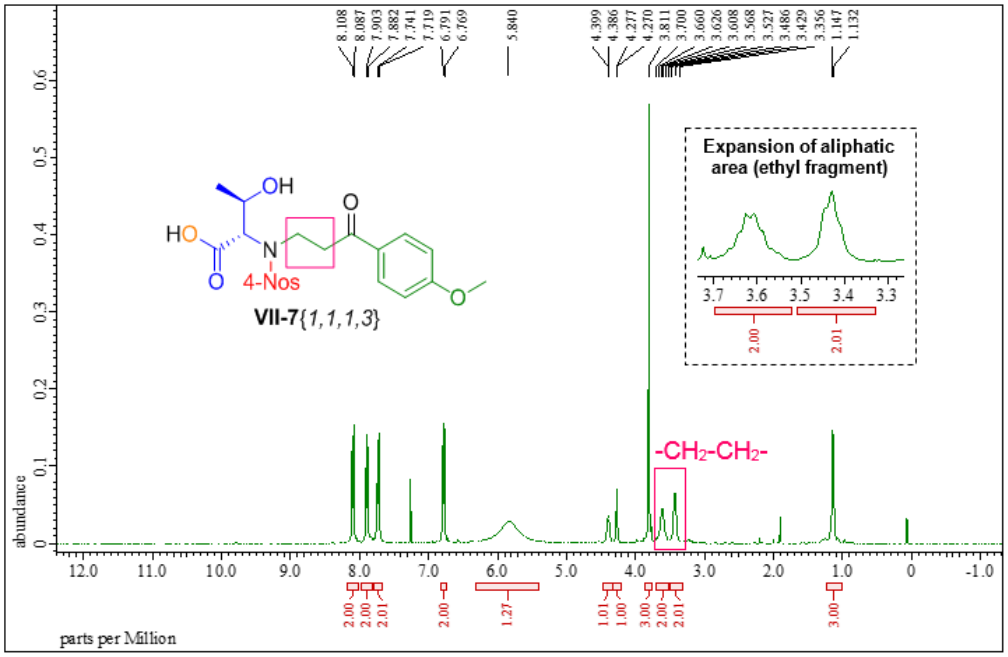

In addition, *N*-alkyl-sulfonamides **VII-2**{*1,1,1*} were alkylated with sterically bulky racemic alcohols (e.g. 4-phenylbut-3-yn-2-ol and 1,3-diphenylprop-2-yn-1-ol; Figure 39, modification *7-8* for R^4 substitution). The alkylation with 4-phenylbut-3-yn-2-ol required repetition twice times for the full conversion to product **VII-3**{*1,1,1,7*} which was obtained in 95% crude purity as a mixture of inseparable diastereoisomers (calculated from HPLC-UV traces at 205–400 nm). In the case of 1,3-diphenylprop-2-yn-1-ol, the alkylation conditions were extensively optimized; however, we

observed an incomplete conversion to the product **VII-3**{*1,1,1,8*} in only 56% crude purity (calculated from HPLC-UV traces at 205–400 nm; Scheme 64, Table 32).

Scheme 64. The alkylation of sulfonamide **VII-2**{*1,1,1*} with 1,3-diphenylprop-2-yn-1-ol[a]

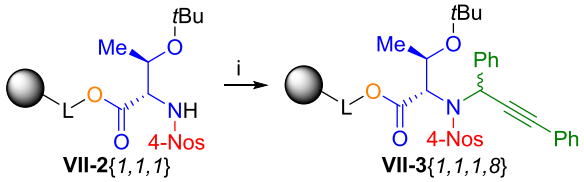

VII-2{*1,1,1*} **VII-3**{*1,1,1,8*}

[a]Reagents and conditions: (i) 1,3-diphenylprop-2-yn-1-ol, phosphine, DIAD, solvent, 24 h, rt-60°C.

Table 32. The tested alkylation conditions for intermediate **VII-2**{*1,1,1*} prepared in analytical scale[a]

phosphine	solvent	time [h]	temp [°C]	crude purity of VII-2 [%][a]	crude purity of VII-3 [%][a]	ratio of VII-2:3[a]
TPP	anhydrous THF	24	23	46	47	50:50
		24	50	28	56	33:67
TPP	anhydrous DCE	24	23	64	28	70:30
TPP	**anhydrous DME**	**24**	**23**	**18**	**58**	**24:76**
		24	60	18	58	24:76
TBP	anhydrous THF	24	23	62	0	100:0
		24	40	51	18	74:26

[a]Calculated from HPLC-UV traces at 205–400 nm.

After that, intermediate **VII-4**{*1,1,1,1*} was reacted with TMSOTf (2 equiv) and TES (1 equiv) in anhydrous DCM according to the previously reported conditions[4] to obtain 1,4-oxazepane **VII-6**{*1,1,1,1*} (Scheme 65). The reaction generated a highly pure compound with a molecular mass corresponding to the expected product **VII-6**{*1,1,1,1*}. However, its ^{1}H and ^{13}C{^{1}H} NMR spectra were not fully consistent with the structure of product **VII-6**{*1,1,1,1*}. For example, the ^{13}C{^{1}H} signal at 210.6 ppm indicating a carbonyl group (highlighted in pink in Figure 43 for the derivative **VII-5**{*1,1,1,1*}) could not be assigned to any carbon atom in **VII-6**{*1,1,1,1*}. For this reason, a set of 1D and 2D NMR spectra, including ^{1}H-^{15}N HMBC, were collected and carefully analyzed (Figure 44-45). It confirmed the formation of pyrrolidin-3-one **VII-5**{*1,1,1,1*}. The structure was determined by means of ^{1}H, ^{13}C{^{1}H}, APT, ^{1}H-^{1}H COSY, ^{1}H-^{1}H NOESY, ^{1}H-^{13}C HSQC, ^{1}H-^{13}C HMBC and ^{1}H-^{15}N HMBC. There were identified benzoyl, 4-Nosyl, pyrollidin-3-onyl and CH_3-CH-O moieties. The ^{1}H-^{13}C HMBC spectrum provided H^{13}-C14 correlation. At the same time, H^{13} was also correlated to C3 and N1 of pyrollidin-3-one moiety. Although ^{1}H-^{15}N four-bond correlation was not observed between 4-Nosyl protons and N1, the scaffold structure was confirmed by NOE correlations between 4-Nosyl protons and protons H^2, H_a^4, H_b^4, H_a^5, H_b^5 and H^{21}. NOE correlations were also observed between benzoyl protons and protons H^2, H_b^4, H_b^5 and H^{21}.

Scheme 65. The rearrangement of intermediates **VII-4**{R^1,R^2,R^3,R^4}[a]

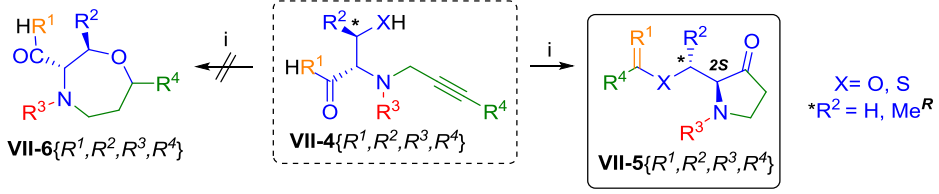

[a]Reagents and conditions: (i) TMSOTf/TES (2:1), anhydrous DCM, 24 h, 0 °C or TMSOTf, anhydrous DCM, 24-72 h, 23-40 °C.

Figure 43. The $^{13}C\{^1H\}$ NMR spectrum of product **VII-5**{*1,1,1,1*}

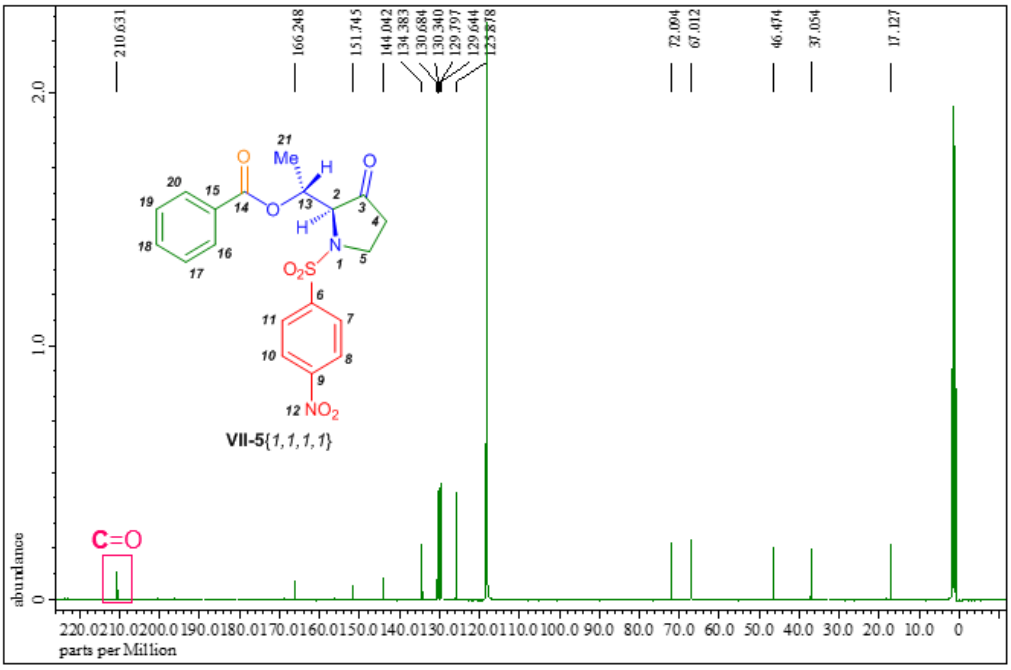

Figure 44. The detailed COSY, NOE and ^1H-^{15}N HMBC NMR analysis of product **VII-5**{*1,1,1,1*}

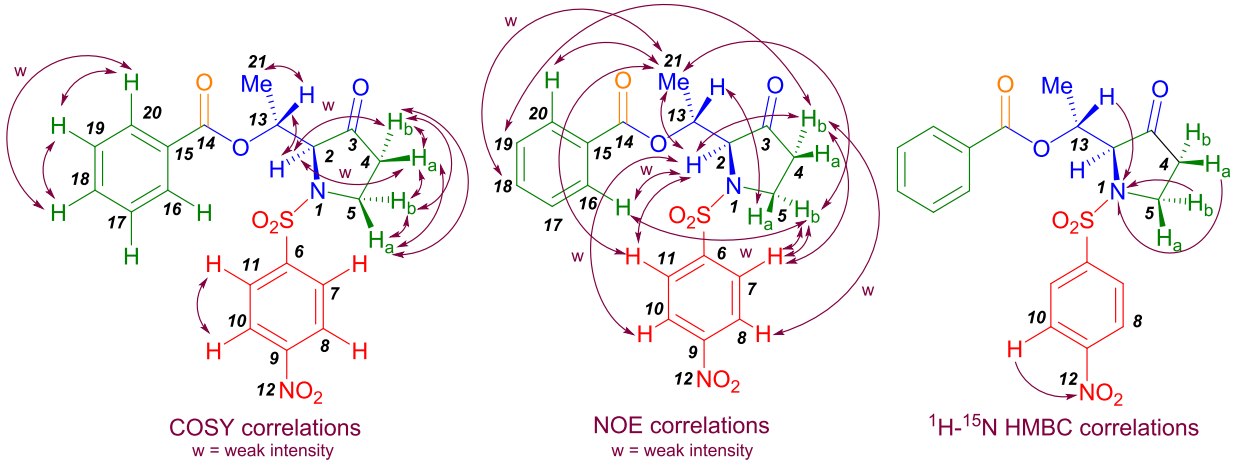

Figure 45. The detailed ^{1}H-^{13}C HMBC NMR analysis of product **VII-5**{*1,1,1,1*}

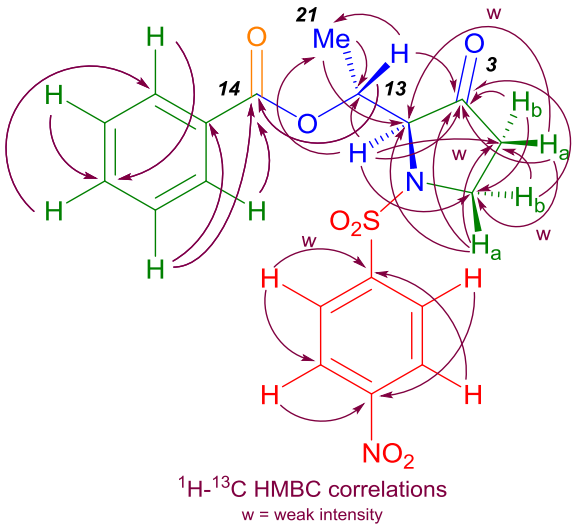

4.7.3 Limitations and scope

The reaction conditions were modified to further investigate their impact on the reaction outcome (Scheme 66). First, we added the same reagents in the same ratio (2 equiv TMSOTf and 1 equiv TES) but in the opposite order; then we performed the reaction at 0 °C and 23 °C and in all cases the reaction gave the same results (Table 33, highlighted in bold). The exchange of the ratio of these reagents (1 equiv TMSOTf and 2 equiv TES) led only to a mixture of the corresponding enol triflate **VII-8**{*1,1,1,1*} and the reduced analogues of compound **VII-4**{*1,1,1,1*} with double (**VII-9**{*1,1,1,1*}; at room temperature) or single bonds (**VII-10**{*1,1,1,1*}; at 0 °C). The same results were obtained when we used an equimolar ratio of reagents (1 equiv TMSOTf and 1 equiv TES). Nevertheless, the elimination of TES from the reaction mixture (only 2 equiv TMSOTf was used) yielded expected product **VII-5**{*1,1,1,1*} in 90% crude purity (calculated from HPLC-UV traces at 205–400 nm, Table 33). This last experiment showed that TES is not involved in the conversion of **VII-4**{*1,1,1,1*} to **VII-5**{*1,1,1,1*} (Table 33, highlighted in red and in bold); thus, it was omitted from the reaction mixture in further studies. Finally, the reaction of compound **VII-4**{*1,1,1,1*} was tested with $TiCl_4$ and $BF_3{\cdot}OEt_2$ as the alternative Lewis acids. When $TiCl_4$ was reacted with the starting material, no product was observed. The treatment with $BF_3{\cdot}OEt_2$ yielded desired derivative **VII-5**{*1,1,1,1*}; however, the conversion was only 10% after 48 h and it was slower in comparison with the TMSOTf-promoted rearrangement.

Scheme 66. The reaction of **VII-4**{*1,1,1,1*} with alternative Lewis acids[a]

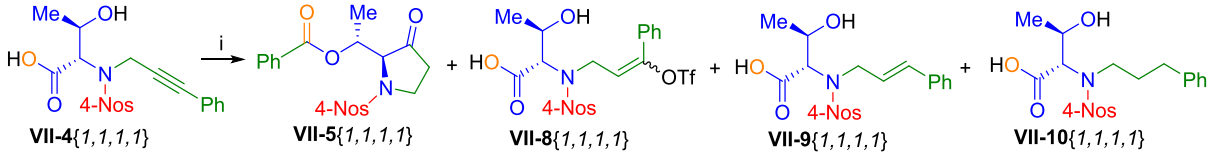

VII-4{*1,1,1,1*} **VII-5**{*1,1,1,1*} **VII-8**{*1,1,1,1*} **VII-9**{*1,1,1,1*} **VII-10**{*1,1,1,1*}

[a]Reagents and conditions: (i) Lewis acid (equiv), (TES, equiv), anhydrous DCM, 2.5-48 h, 0 °C-rt.

Table 33. Tested Lewis acids to promote rearrangement of **VII-4**{*1,1,1,1*}[a-c]

Lewis acid	Lewis acid [equiv]	TES [equiv]	time [h]	temp [°C]	VII-4 [%][a]	VII-5 [%][a]	VII-8 [%][a]	VII-9 [%][a]	VII-10 [%][a]
TMSOTf	1	1	2.5	0	0	0	31	35	19
			24	0	0	0	28	23	38
TMSOTf	1	1	2.5	23	0	0	22	65	5
			24	23	0	0	15	42	30
TMSOTf	1	2	2.5	0	0	0	45	0	38
			24	0	0	0	11	0	79
TMSOTf	1	2	2.5	23	0	0	21	69	0
			24	23	0	0	13	74	0
TMSOTf	**2**	**1**	2.5	0	14	63	11	0	0
			24	**0**	**0**	**89**	**0**	**0**	**0**
TMSOTf	**2**	**1**	2.5	23	18	60	11	0	0
			24	**23**	**1**	**90**	**0**	**0**	**0**
TMSOTf	2	-	2.5	0	31	38	19	0	0
			24	0	0	83	3	0	0
TMSOTf	**2**	**-**	2.5	23	25	40	22	0	0
			24	**23**	**0**	**90**	**0**	**0**	**0**
$BF_3.Et_2O$	1	-	2.5	23	86	3	10	0	0
			24	23	86	10	2	0	0
			48	23	86	10[b]	2	0	0
$TiCl_4$	1	-	2.5	23	0[c]	0	0	0	0
			24	23	0[c]	0	0	0	0

[a]Overall crude purities calculated from HPLC-UV traces at 205–400 nm; [b]The observed crude purity was 10% after 48 h calculated from HPLC-UV traces at 205–400 nm; [c]The desired intermediate was not detected.

The structure-reactivity relationship of the rearrangement was further studied deeply for all prepared *N*-alkynol-sulfonamides **VII-4**{R^1,R^2,R^3,R^4} (Scheme 67, Table 34). Generally, the rearrangement conditions (reaction time and temperature) were typically dependent on the type of the starting materials **VII-4**{R^1,R^2,R^3,R^4}. The electron withdrawing effect of R^4 substituent (CF_3) slowed the conversion to the product **VII-5**{*1,1,1,4*} and thus higher temperature (40 °C) was necessary to push the conversion of the starting material to the final product. In the cases of alkyl-alkynols bearing methyl or hydrogen group in R^4 position **VII-4**{*1,1,1,5*} and **VII-4**{*1,1,1,6*} and serine-based intermediates **VII-4**{*1,2,1,1*}, the rearrangement required longer reaction times (72 h) to completion. To compare the threonine/serine-based intermediates **VII-4**{*1,1,1,1*} and **VII-4**{*1,2,1,1*}, the slower rearrangement rate was expected because of lacking the Thorp-Ingold effect in serine-based precursor.[97] Similarly, replacement of carboxylic acid with the corresponding amide **VII-4**{*2,1,1,1*} also led to the slow transformation. In all above-mentioned cases, the corresponding enol triflates **VII-8**{R^1,R^2,R^3,R^4} were detected in the reaction mixtures in a ratio of 2-28% depending on R^1, R^2 and primarily on R^4 substituents (calculated from HPLC-UV traces at 205–400 nm). The isolated yields were somewhat compromised in several cases, which were caused by difficult chromatography and careful removal of impurities with similar retention times to products. Finally, to further extend the applicability of the disclosed reaction sequence, the sulfanyl analogue **VII-4**{*1,3,1,1*} was prepared from protected cysteine, however

no traces of the desired pyrrolidinone **VII-5**{*1,3,1,1*} were detected.

Scheme 67. The rearrangement conditions for intermediate **VII-4**{R^1,R^2,*1*,R^4}[a]

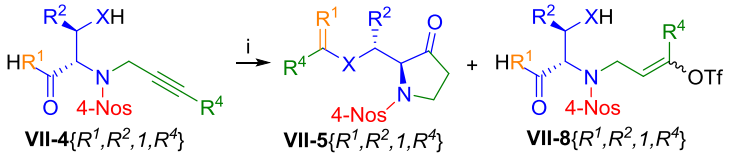

VII-4{R^1,R^2,*1*,R^4} **VII-5**{R^1,R^2,*1*,R^4} **VII-8**{R^1,R^2,*1*,R^4}

[a]Reagents and conditions: (i) TMSOTf, anhydrous DCM, 24-72 h, rt-40 °C.

Table 34. Optimization of rearrangement conditions for intermediate **VII-4**{R^1,R^2,*1*,R^4}[a]

starting cmpd	X	R^1	R^2	R^4	time [h]	temp [°C]	crude purity of VII-4 [%][a]	crude purity of VII-5 [%][a]	crude purity of VII-8 [%][a]	ratio of VII-4:5:8 [%][a]
VII-4{*1,1,1,4*}	O	O	Me	4-CF_3-Ph	24	23	56	18	19	60:19:21
					24	**40**	**0**	**56**	**28**	**0:67:33**
					48	40	0	56	28	0:67:33
VII-4{*1,1,1,5*}	O	O	Me	Me	24	23	26	43	2	37:60:3
					72	**23**	**0**	**75**	**12**	**0:86:14**
VII-4{*1,1,1,6*}	O	O	Me	H	**72**	**23**	**24**	**43**	**9**	**33:52:15**
					24	40	24	32	9	37:49:14
VII-4{*1,2,1,1*}	O	O	H	Ph	**72**	**23**	**0**	**51**	**12**	**0:81:19**
VII-4{*1,3,1,1*}	S	O	H	Ph	24	23	40	0	0	100:0:0
VII-4{*2,1,1,1*}	O	NH	Me	Ph	**72**	**23**	**0**	**60**	**21**	**0:74:26**

[a]Calculated from HPLC-UV traces at 205–400 nm.

In the case of **VII-4**{*1,1,1,7*}, the rearrangement at higher temperature (40 °C) gave a mixture of product **VII-5**{*1,1,1,7*} and the corresponding enol triflate **VII-8**{*1,1,1,7*} in a ratio of 36:64 (calculated from HPLC-UV traces at 205–400 nm, in 26% and 47% crude purities, respectively; Scheme 68). When the mixture was subjected to semipreparative reverse-phase HPLC purification and dissolved in initial mobile phase containing HPLC water and MeCN, it proved to be unstable for longer time needed to HPLC purification.

Scheme 68. Rearrangement conditions for intermediate **VII-4**{*1,1,1,7*}[a]

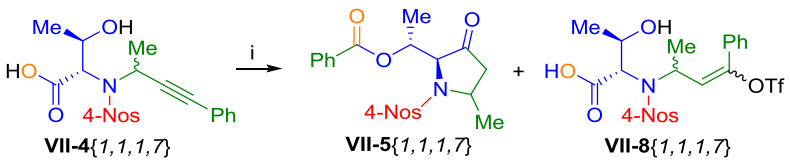

VII-4{*1,1,1,7*} **VII-5**{*1,1,1,7*} **VII-8**{*1,1,1,7*}

[a]Reagents and conditions: (i) TMSOTf, anhydrous DCM, 24 h, 40 °C.

To conclude, the rearrangement of alkynes **VII-4**{R^1,R^2,R^3,R^4} was successfully applied to prepare ten final compounds **VII-5**{R^1,R^2,R^3,R^4} synthesized from diverse synthons in 43-96% crude purities (calculated from HPLC-UV traces at 205–400 nm) and 14-71% overall yields (calculated after

cleavage of products from the resin and their HPLC purification) (Figure 39, Table 35). In addition, one representative compound **VII-5**{*1,1,1,3*} was synthesized from the corresponding ketone **VII-7**{*1,1,1,3*} by TMSOTf-promoted rearrangement in 93% crude purity (calculated from HPLC-UV traces at 205–400 nm) and 38% overall yield (calculated after cleavage of the product from the resin and its HPLC purification) according to the previously developed conditions.

Table 35. The analytical data for products **VII-5**{R^1,R^2,R^3,R^4}[a-e]

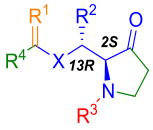

final cmpd	X	R^1	R^2	R^3	R^4	time [h]	temp [°C]	crude purity [%][a]	final purity [%][a]	yield [%][b]
VII-5{*1,1,1,1*}	O	O	Me	4-Nos	Ph	24	23	96	99	71
VII-5{*1,1,2,1*}	O	O	Me	2-Nos	Ph	24	23	96	99	41
VII-5{*1,1,3,1*}	O	O	Me	Ms	Ph	24	23	92	99	40
VII-5{*1,1,4,1*}	O	O	Me	Ts	Ph	24	23	80	99	50
VII-5{*1,1,1,2*}	O	O	Me	4-Nos	4-Me-Ph	24	23	76	99	30
VII-5{*1,1,1,3*}[c]	O	O	Me	4-Nos	4-MeO-Ph	24	23	81	99	42
VII-5{*1,1,1,3*}[d]	O	O	Me	4-Nos	4-MeO-Ph	24	23	93	99	38
VII-5{*1,1,1,4*}	O	O	Me	4-Nos	4-CF_3-Ph	24	40	56	98	18
VII-5{*1,1,1,5*}	O	O	Me	4-Nos	Me	72	23	75	98	33
VII-5{*1,1,1,6*}	O	O	Me	4-Nos	H	72	23	43[e]	NI	NI
VII-5{*1,2,1,1*}	O	O	H	4-Nos	Ph	72	23	51	97	14
VII-5{*1,3,1,1*}	S	O	H	4-Nos	Ph	24	23	NP	NP	NP
VII-5{*2,1,1,1*}	O	NH	Me	4-Nos	Ph	72	23	60	99	14

[a]Overall crude purity determined by HPLC after the entire reaction sequence prior to final purification; [b]Isolated overall yield calculated from the loading of the starting resin; [c]The product **VII-5**{*1,1,1,3*} was prepared from the starting alkyne **VII-4**{*1,1,1,3*}; [d]The product **VII-5**{*1,1,1,3*} was prepared from the starting ketone **VII-7**{*1,1,1,3*}; [e]The compound proved to be unstable during the HPLC purification process; NI = not isolated; NP = not prepared.

Scheme 69 depicts the plausible mechanism of TMSOTf-promoted rearrangement running certainly through the ketone intermediate **D**. Briefly to the mechanism, the reaction between TMSOTf and carboxylic acid or carboxamide **VII-4**{R^1,R^2,R^3,R^4} generated *in situ* triflic acid (TfOH) which triggered the addition of triflate OTf^- (intermediate **A**) to alkyne and yielded the resulting enol triflate **B**. The structure of intermediate **B** was suggested according to its molecular mass detected by HPLC-MS analysis. Then hydroxy group of the enol triflate **B** reacted with the second equivalent of TMSOTf to give silylated alcohol **C**. Another equivalent of formed TfOH mediated the conversion of **C** to intermediate **D** that further underwent the intramolecular 7-*exo-trig* cyclization to yield, upon TMS group release, the key oxonium intermediate **F**. *Trans*-annular addition of carboxylic acid to oxonium yielded strained acetal intermediate **G** that was well organized for Lewis acid promoted C-C bond fragmentation reaction. Finally, rearranged hemiacetal intermediate **H** opened up to yield the desired product **VII-5**{R^1,R^2,R^3,R^4}.

Scheme 69: The plausible mechanism of the rearrangement of **VII-4**{R^1,R^2,R^3,R^4}

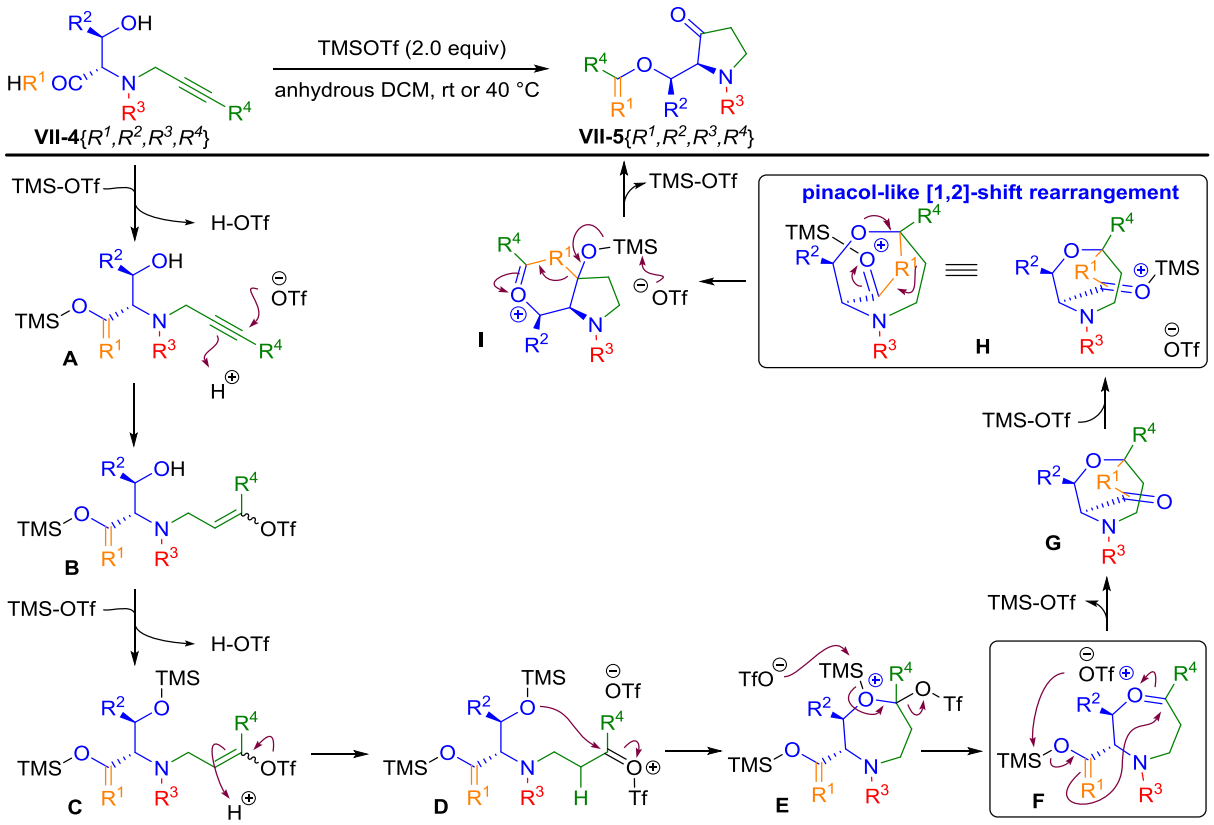

More detailed information is included in article by Králová, P.; Maloň, M; Pospíšil, J.; Soural, M. *J. Org. Chem.* **2020**, *85* (2), 985–993[96] which is attached in Appendix I (p. 200 – 208).

4.7.4 Biological screening

All purified compounds were subjected to antimicrobial and cytotoxic tests on representative cancer cell lines. In the case of derivative **VII-5**{*1,2,1,1*}, the compound showed low micromolar toxicity to T-lymphoblastic leukemia (CCRF-CEM) and good selectivity when compared to human fibroblasts (BJ). The therapeutic index (TI_{50}) was calculated to 31 as a BJ proportion to CCRF-CEM (Table 36).

Table 36. Cytotoxic tests on representative cancer cell lines for derivative **VII-5**{*1,2,1,1*}

cell lines		IC_{50} [μM]
A549	human lung adenocarcinoma	43.13
CCRF-CEM	**T-lymphoblastic leukemia**	**1.60**
CEM-DNR	T-lymphoblastic leukemia, daunorubicin resistant	24.41
HCT116	human colorectal cancer	16.56
HCT116p53-/-	human colorectal cancer, p53 deficient	16.98
K562	acute myeloid leukemia	15.13
K562-TAX	acute myeloid leukemia, paclitaxel resistant	19.43
MRC-5	diploid human fibroblast derived from lung tissue	41.32
BJ	human fibroblast	49.77

4.7.5 Alternative application of pinacol-like rearrangement to prepare piperidin-3-ones

This brief subchapter contains unpublished results from the synthetic trials to apply the above reported rearrangement to obtain piperidin-3-one scaffold. First, the starting *N*-sulfonamide **VII-2**{*1,1,1*} was subjected to the Mitsunobu alkylation with 4-phenylbut-3-yn-1-ol (Figure 39, building block *9* for R^4 substitution which was synthesized using Sonogashira coupling) according to the previously reported conditions in subchapter 4.7.2. The release of the polymer-supported intermediate from the resin yielded the corresponding phenylalkynol **VII-4**{*1,1,1,9*} in excellent crude purity (94%, calculated from HPLC-UV traces at 205–400 nm). When the product was dissolved in mobile phase and subjected to semipreparative reverse-phase HPLC purification, we found out that the compound is prone to hydrolysis to corresponding ketone **VII-7**{*1,1,1,9*}. An increase of ketone in the mixture was noticeably slow (from 3% to only 39% within one hour at room temperature; calculated from HPLC-UV traces at 205–400 nm, Scheme 70) in comparison to derivatives **VII-7**{*1,1,1,2-3*} bearing phenylalkynols with electron donating groups (Me and MeO). As a result of this phenomenon, the compound **VII-4**{*1,1,1,9*} could not be purified, thus it was directly submitted to rearrangement conditions.

Scheme 70. The use of 4-phenylbut-3-yn-1-ol for Mitsunobu alkylation and applicability of rearrangement conditions to obtain **VII-5**{*1,1,1,9*}[a]

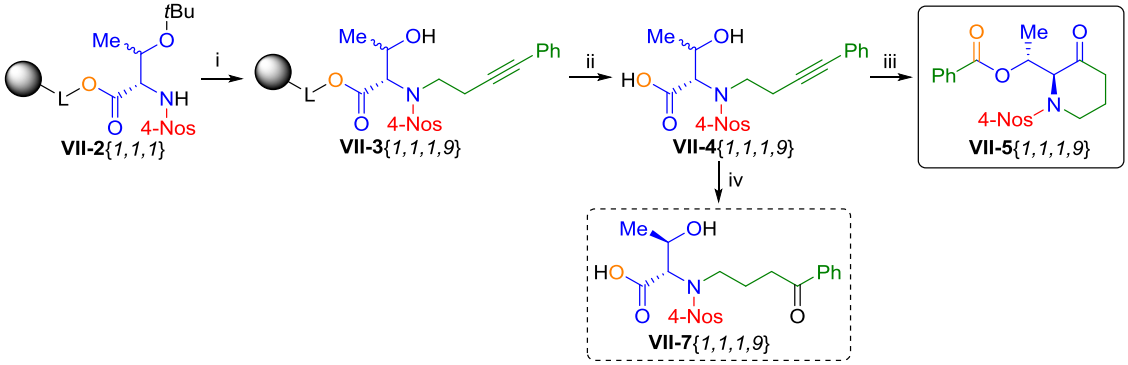

[a]Reagents and conditions: (i) 4-phenylbut-3-yn-1-ol, TPP, DIAD, anhydrous THF, 24 h, rt; (ii) 50% TFA/anhydrous DCM, 1 h, rt; (iiii) TMSOTf, anhydrous DCM, 24 h, rt; (iv) HPLC MeCN/H_2O, 5 min-1 h, rt.

To test the rearrangement of intermediate **VII-4**{*1,1,1,9*}, Lewis acids (e.g. TMSOTf, TMSOTf/TES, $TiCl_4$ and $BF_3{\cdot}OEt_2$) in different ratios and different reaction temperature were tested (Scheme 71, Table 37). The reaction did not work properly and in all cases, analysis with LC-MS detected a presence of the starting material **VII-4**{*1,1,1,9*}, the compound with molecular weight corresponding to rearrangement product **VII-5**{*1,1,1,9*} and the ketone **VII-7**{*1,1,1,9*} (Scheme 71). Due to its low content (Table 37), the product was not isolated thus its structure was not confirmed by NMR.

Scheme 71. The reactivity of **VII-4**{*1,1,1,9*} with various Lewis acids[a]

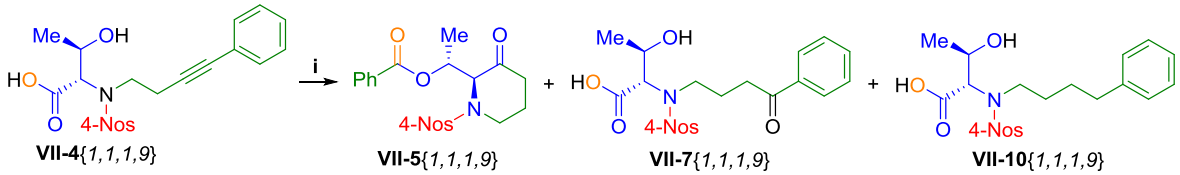

VII-4{*1,1,1,9*} **VII-5**{*1,1,1,9*} **VII-7**{*1,1,1,9*} **VII-10**{*1,1,1,9*}

[a]Reagents and conditions: (i) Lewis acid (2.0-4.0 equiv), (TES, 1.0 equiv), anhydrous or extra anhydrous DCM, 2-72 h, 0 °C-rt.

Table 37. Tested Lewis acids for intermediate **VII-4**{*1,1,1,9*}[a-d]

Lewis acid	Lewis acid [equiv]	TES [equiv]	solvent	time [h]	temp [°C]	VII-4 [%][a]	VII-5 [%][a]	VII-7 [%][a]	VII-10 [%][a]
TMSOTf	2	-	anhydrous DCM	2	23	12	18	57	0
			anhydrous DCM	72	23	0	0	0	0
			extra anhydrous DCM	24	23	19	0	55	0
			extra anhydrous DCM	**24**	**0**	**2**	**29**[b]	**20**	**0**
	4	-	extra anhydrous DCM	24	23	0	20	18	0
TMSOTf	2	1	anhydrous DCM	2	23	6	0	4	46
$BF_3.Et_2O$	1	-	anhydrous DCM	2	23	9	4	4	0
			anhydrous DCM	72	23	0	11[c]	29	0
$TiCl_4$	1	-	anhydrous DCM	2	23	0	0[d]	31	0

[a]Overall crude purity calculated from HPLC-UV traces at 205–400 nm; [b]The observed conversion was 57% (calculated from HPLC-UV traces at 205–400 nm); [c]The observed conversion was 28% (calculated from HPLC-UV traces at 205–400 nm); [d]The desired product was not detected.

4.7.6 Conclusion

The unexpected rearrangement of *N*-alkyl-sulfonamides to novel chiral derivatives of pyrrolidin-3-ones was discovered while the synthesis of single 1,4-oxazepanes according to the previously reported conditions failed. The reaction was studied in detail to find optimal rearrangement conditions using various Lewis acids, Fmoc-amino acids, sulfonyl chlorides and alkynols to determine limitations and scope of the proposed methodology. The synthetic strategy was applied to synthesize 10 representative pyrrolidin-3-ones whereas the extension of the methodology to prepare piperidin-3-ones was not applicable due to low purity of desired product.

4.8 The synthesis of fused 1,4-oxazepanes

This project contains only unpublished results. The Supporting information is attached as an electronic file on CD under name Appendix J_SI.

4.8.1 Brief introduction

The above attempted preparation of oxazepanes from alkynols was unsuccessful,[96] thus this subchapter describes efforts to develop an alternative synthetic strategies (Figure 46). Inspired by our previous results in the field of morpholine chemistry, the first part of the project was paid to the solid-phase synthesis of immobilized *N*-alkenyl (cinnamyl) or *N*-phenacyl-sulfonamides which are placed in a dashed rectangle in Figure 46. The preparation of such intermediates was suggested either from immobilized Fmoc-L-serine/L-threonine (**Scenarios A-B**) or Fmoc-L-homoserine (**Scenario C**). These key intermediates should be modified with various acylating or alkylating agents to yield the resulting *α*-amino ketones. Their acid-mediated cleavage from the resin and/or a subsequent post-cleavage modification should yield functionalized 1,4-oxazepanes which could be further converted to fused 1,4-oxazepanes similarly to the previously reported protocols.[38–43]

Figure 46. The tested synthetic routes to prepare single and fused 1,4-oxazepane derivatives

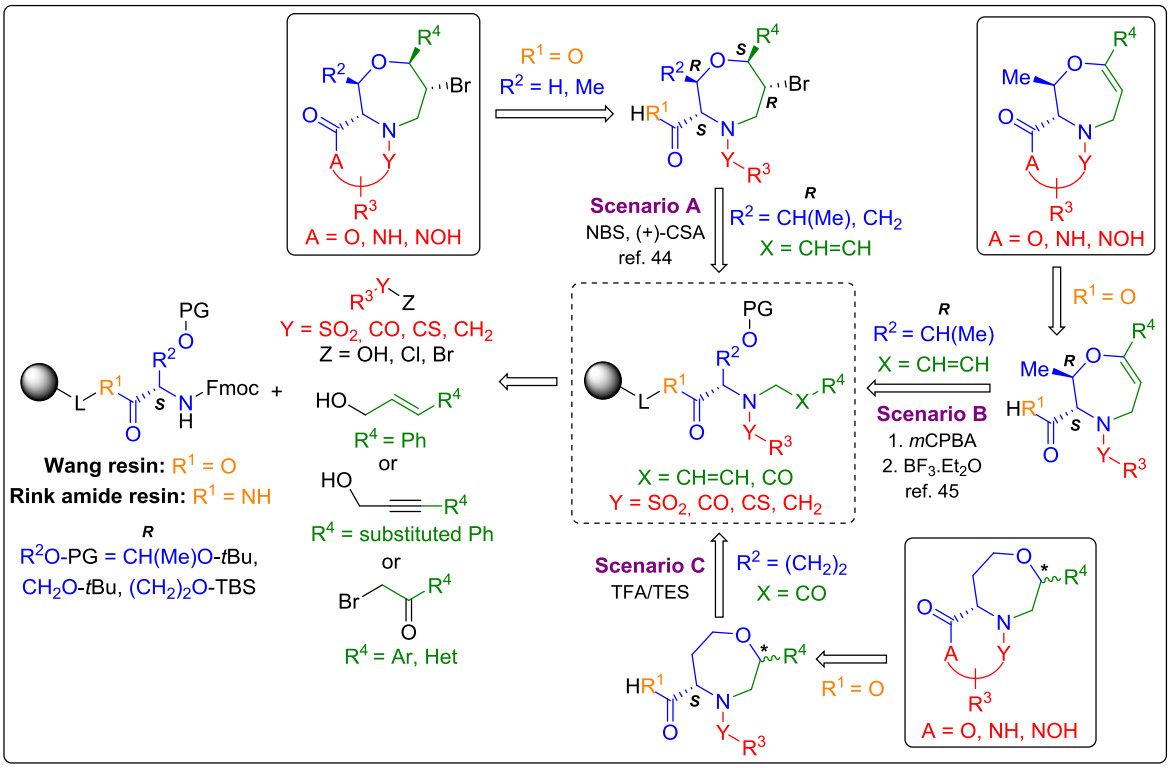

The aim of the project was to test three alternative routes **A-C** to obtain the 1,4-oxazepane or 1,4-oxazepine derivatives. In specific cases, the TES applicability for the stereoselective reduction of 1,4-oxazepines to 1,4-oxazepanes was suggested. Similarly to our previous projects, we also intended to determine limitations and scope of the proposed methodologies for various building blocks.

4.8.2 Synthesis, limitations and scope

The synthesis of immobilized 2-Nos-amides and/or *α*-amino ketones was performed using a combination of different Fmoc-amino acids (e.g. L-serine, L-threonine and L-homoserine), various 2/4-Nos-Cl, alkylating agents (e.g. cinnamyl alcohols and α-bromoketones) and acylating agents (e.g. 2-nitrobenzoic acids, Fmoc-amino acids, iodoacetic acid, Fmoc-NCS) or 2-nitrobenzyl bromide (Figure 47). Unless otherwise stated, the synthesis was accomplished exactly according to the above disassembled protocols.[2,38–43] For this reason, these procedures are not discussed in the text. The following three subchapters are classified according to the type of synthetic pathway used.

Figure 47. The list of tested building blocks for R^1, R^2, R^3 and R^4 substituents

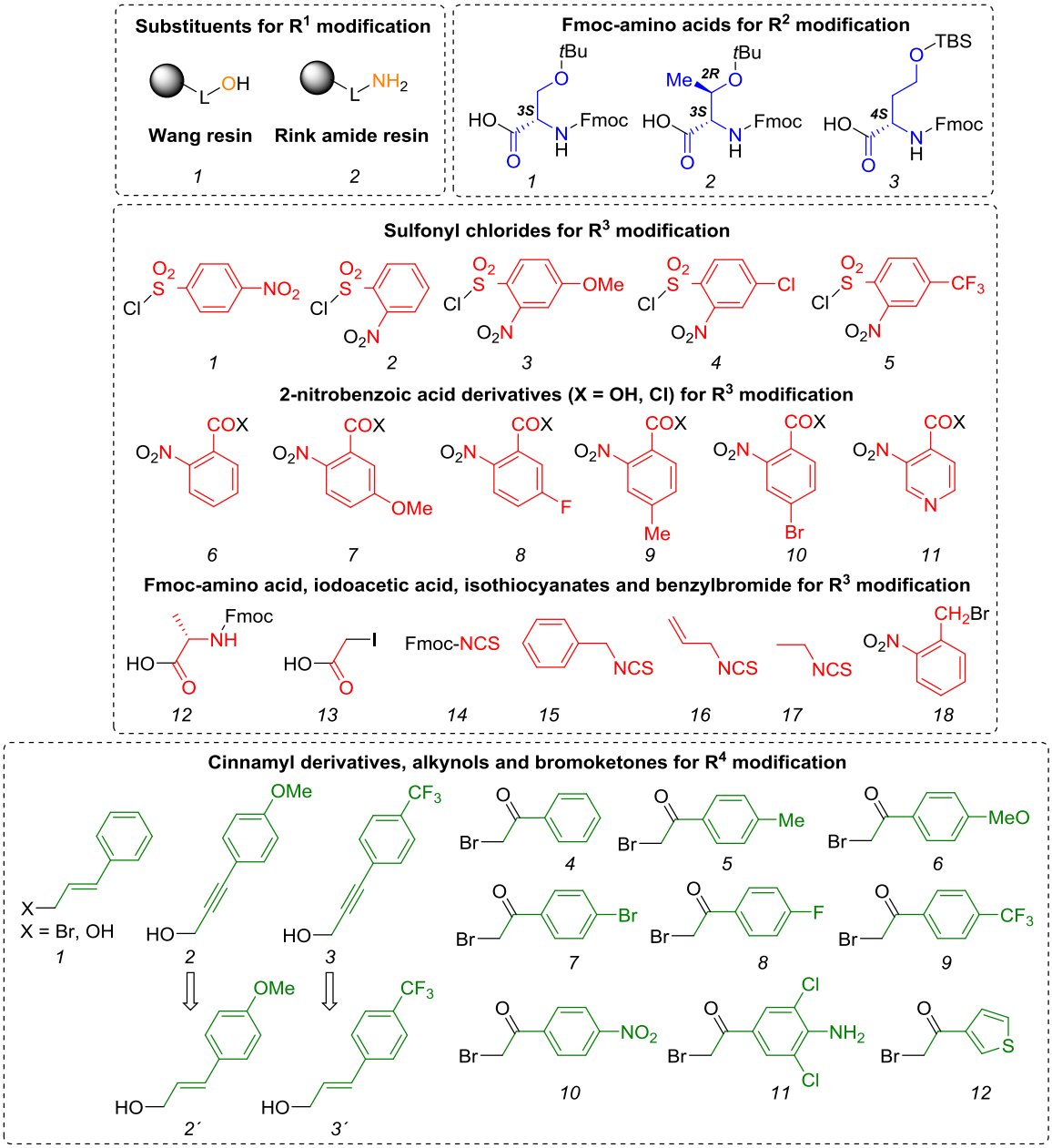

Note: The synthesis of 4-substituted-*trans*-cinnamyl alcohols *2´-3´* was performed according to the previously reported protocols based on a $LiAlH_4$-promoted reduction of the corresponding alkynols *2-3* (Figure 47).[98,99]

4.8.2.1 Scenario A

In this scenario, the synthesis of 1,4-oxazepane derivatives was tested in parallel for immobilized Fmoc-Ser(*t*Bu)-OH and Fmoc-Thr(*t*Bu)-OH **VIII-2**{*1,1*} and **VIII-2**{*1,2*}, respectively. Fmoc-deprotected amino acids were reacted with 4-Nos-Cl followed by alkylation with cinnamyl bromide. In contrast to the alkylation with α-bromoketones,[2,38–43] the reaction required a repetition of the alkylation step to completion. When a Mitsunobu alkylation using cinnamyl alcohol was used, the serine and threonine-based derivatives **VIII-5**{*1,1,1,1*} and **VIII-5**{*1,2,1,1*} were obtained in 90% and 96% crude purities (calculated from HPLC-UV traces at 205–400 nm after the product cleavage from the resin). After the cleavage from the polymer support, the residual TFA was evaporated under a stream of nitrogen to dryness and lyophilized overnight. The crude intermediates were cyclized using NBS and (1*S*)-(+)-10-camphorsulfonic acid ((+)-CSA) to desired 1,4-oxazepane scaffold **VIII-6**{*1,1,1,1*} and **VIII-6**{*1,2,1,1*} (Scheme 72, Pathway B).[44]

Scheme 72. The synthesis of immobilized *α*-amino ketones **VIII-4**{*1,1-2,1-5,1*} and their post-cleavage modification to benzoxazepino-thiadiazepinone 7,7-dioxides **VIII-10**{*1,2,2-5,1*}[a]

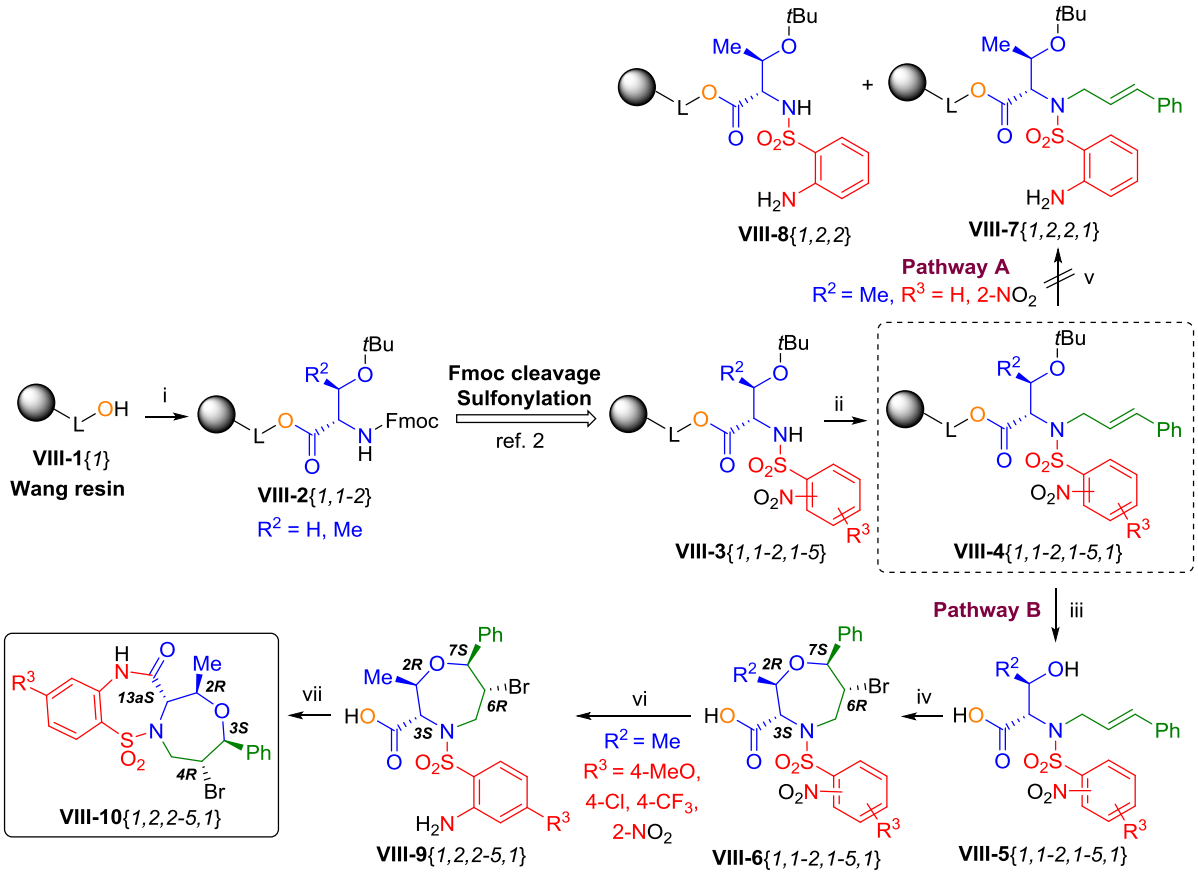

[a]Reagents and conditions: (i) Fmoc-amino acid, HOBt, DMAP, DIC, DCM, DMF, 24 h, rt; (ii) $R^4CH{=}CHCH_2OH$, TPP, DIAD, anhydrous THF, 24 h, rt or anhydrous dioxane, 5 days, 100 °C (for derivative **VIII-4**{*1,2,3,1*}); (iii) 50% TFA/DCM, 1 h, rt; (iv) NBS, (+)-CSA, DMF or MeCN, 24 h, 0 °C, then 5-20 h, rt; (v) $Na_2S_2O_4.2H_2O$, K_2CO_3, TBAHS, 50% DCM/H_2O, 2 h, rt; (vi) H_2, 10% Pd/C, EA, 20 h, rt (for derivative **VIII-9**{*1,2,2,1*}) or 19-23 h, 4 bar (for derivatives **VIII-9**{*1,2,3-5,1*}); (vi) PTSA, anhydrous DCE, 3.5-23 h, 90 °C.

Similarly to reported results,[44] the short cyclization (5 h) of serine analogue **VIII-5**{*1,1,1,1*} gave a mixture of inseparable 6*R*,7*S* and 6*S*,7*R* diastereoisomers in a ratio of 1:1 and in low overall crude purity (43%, calculated from HPLC-UV traces at 205–400 nm). The prolongation of the cyclization time (20 h) did not affect the ratio of both diastereoisomers (Table 38, later in the text), therefore, the synthesis of other serine analogues **VIII-5**{*1,1,1-5,1*} was not tested. In the case of threonine product **VIII-6**{*1,2,1,1*}, the desired oxazepane derivative was obtained in 86% crude purity (calculated from HPLC-UV traces at 205–400 nm) and 26% overall yield in excellent diastereomeric purity (diastereomeric ratio = dr.r. 98.8:1.2, calculated from the ^{1}H NMR spectrum of the purified product, Scheme 72, Table 45 for the final derivatives). Despite the previously reported NOE investigation which determined the configuration of all stereocenters at 1,4-oxazepane derivative bearing methyl ester,[44] we performed the detailed NMR elucidation for our free carboxylic acid. Since the synthesis of 1,4-oxazepane scaffold started from Fmoc-L-threonine (2*R* and 3*S*) we assumed that the configuration of both stereocenters remained the same (2*R* and 3*S*) after the entire reaction sequence. The structure was confirmed by means of ^{1}H, ^{13}C{^{1}H}, APT, ^{1}H-^{1}H COSY, ^{1}H-^{1}H NOESY, ^{1}H-^{13}C HSMC and ^{1}H-^{13}C HMBC analysis. The ^{1}H-^{13}C HMBC analysis provided key correlations in the 1,4-oxazepane scaffold as H^{3}-C2, C5, C8, C9, H_a^{5}-C3, C6, C7, C18 and H^{7}-C2, C6, C18, C19, C23. Similarly to the previous research,[44] the configuration of both newly formed stereocenters at the C6 and C7 was determined by NOE spectrum as 6*R* and 7*S*. In NOE spectrum, the interactions between methyl and phenyl signals H^{8}-$H^{19,23}$, between $H^{19,23}$ and H^{3}, H^{6}, H^{8}, between H_a^{5} and methyl signals H^{8}, and finally between H_a^{5} and H^{6}, $H^{12,16}$ were observed (Figure 48). The obtained data indicated that the methodology was almost fully diastereostereoselective and that the synthesis might be further applied to prepare fused oxazepane analogues with the specific configuration of four stereocenters.

Figure 48. The detailed NMR analysis of 1,4-oxazepane **VIII-10**{*1,2,1,1*}

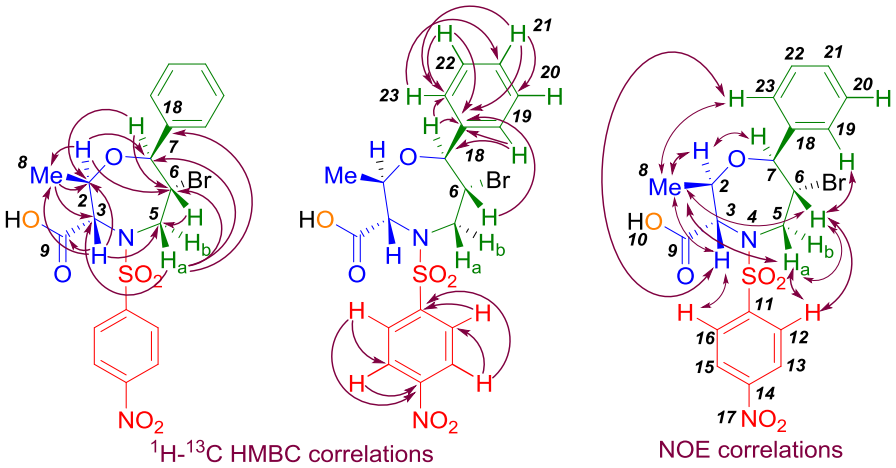

First, we focused on the synthesis of benzoxazepino-thiadiazepinone 7,7-dioxides **VIII-10**{*1,2,2,1*}. In contrast to our previous research,[38] the on-resin reduction of nitro group by sodium dithionite gave a mixture of amino derivative **VIII-7**{*1,2,2,1*} and dealkylated by-product **VIII-8**{*1,2,2*}

in a ratio of 1:2 (Scheme 73).

Scheme 73. The on-resin reduction of *N*-cinnamylsulfonamides **VIII-4**{*1,2,2,1*}[a]

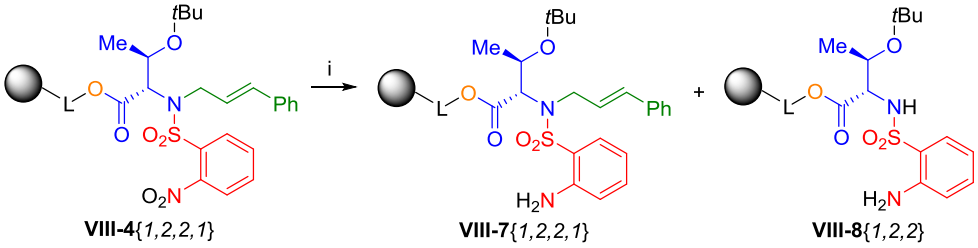

VIII-4{*1,2,2,1*} **VIII-7**{*1,2,2,1*} **VIII-8**{*1,2,2*}

[a]Reagents and conditions: (i) $Na_2S_2O_4.2H_2O$, K_2CO_3, TBAHS, 50% DCM/H_2O, 2 h, rt.

For this reason, the intermediate **VIII-4**{*1,2,2,1*} was first cleaved from the resin, then subjected to a post-cyclization to oxazepane scaffold **VIII-6**{*1,2,2,1*} and a subsequent hydrogenation of the nitro group. In contrast to compound **VIII-6**{*1,2,1,1*}, prepared from 4-Nos-Cl, the cyclization of 2-Nos-amide in DMF provided the desired product in worse crude purity (64%, calculated from HPLC-UV traces at 205–400 nm). When MeCN was used instead of previously reported DMF, the product **VIII-6**{*1,2,2,1*} was obtained in better crude purity (85%, calculated from HPLC-UV traces at 205–400 nm). Although the solvent exchange had rather a minor impact to diastereoselectivity (dr.r 87:13, calculated from the ^{1}H NMR spectrum of the purified product as a ratio of both 6*R*,7*S* and 6*S*,7*R* isomers), also MeCN was later tested for synthesis of all other 2-Nos-amides **VIII-6**{*1,2,3-5,1*} (*R^3 = 4-MeO, Cl, CF_3-2-NO_2-$PhSO_2$;* Scheme 74 – highlighted in dashed frame, Table 38). After that, the reduction of nitro group was achieved using a catalytical hydrogenation with Pd/C in ethyl acetate (EA) that yielded the amino compound **VIII-9**{*1,2,2,1*} in 72% crude purity (calculated from HPLC-UV traces at 205–400 nm), in a dr.r. of 91:9 and 9% overall yield (calculated from the ^{1}H NMR spectrum of the purified product as a ratio of both inseparable 6*R*,7*S* and 6*S*,7*R* diastereoisomers, Table 45 for the synthesized derivatives). Finally, the cyclization to derivative **VIII-10**{*1,2,2,1*} was performed according to the previously reported protocol[38] that yielded fused [7+7] oxazepane derivative in 64% crude purity (calculated from HPLC-UV traces at 205–400 nm) and 12% overall yield (calculated from the ^{1}H NMR spectrum after its HPLC purification that enabled separation of the major diastereoisomer

Scheme 74. The cyclization of *N*-cinnamylsulfonamides **VIII-5**{*1,1-2,1-5,1*} and their further modification[a]

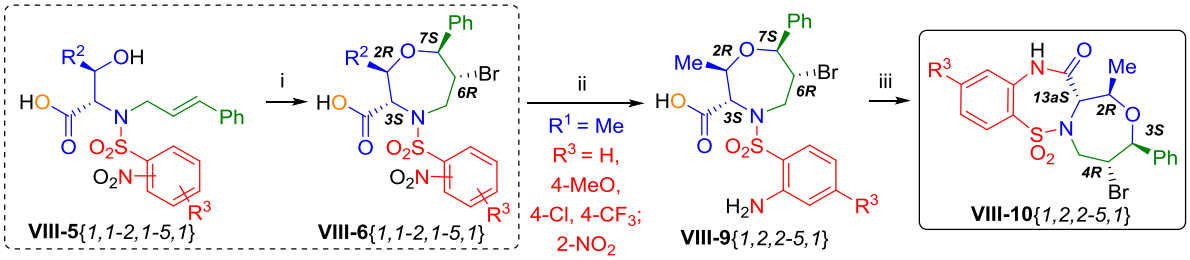

VIII-5{*1,1-2,1-5,1*} **VIII-6**{*1,1-2,1-5,1*} **VIII-9**{*1,2,2-5,1*} **VIII-10**{*1,2,2-5,1*}

[a]Reagents and conditions: (i) NBS, (+)-CSA, DMF (for derivative **VIII-6**{*1,1-2,1,1*} or MeCN (for derivatives **VIII-6**{*1,2,2-5,1*} 24 h, 0 °C, then 5-20 h, rt; (ii) H_2, Pd/C, EA, 20 h (for derivative **VIII-9** {*1,2,2,1*}) or 19-23 h, rt, 4 bar (for derivatives **VIII-9**{*1,2,3-5,1*}); (iii) PTSA, anhydrous DCE, 3.5-23 h, 90 °C.

Scheme 74, Table 45 for the synthesized derivatives).

Table 38. The used conditions for cyclization to oxazepanes **VIII-6**{*1,R²,R³,1*}[a-c]

starting cmpd	R^2	R^3	position of NO_2	cyclization solvent	time [h]	crude purity of VIII-6 [%][a]	ratio of diastereoisomers VIII-6 6*R*,7*S*:6*S*,7*R* [%][b,c]
VIII-5{*1,1,1,1*}	H	H	4-NO_2	DMF	5	47	1:1[b]
					20	47	1:1[b]
VIII-5{*1,2,1,1*}	Me	H	4-NO_2	DMF	20	86	98.8:1.2[c]
VIII-5{*1,2,2,1*}	Me	H	2-NO_2	DMF	5	64	-
				MeCN	**5**	**85**	**87:13**[c]
VIII-5{*1,2,3,1*}	Me	4-MeO	2-NO_2	MeCN	5	61	-
VIII-5{*1,2,4,1*}	Me	4-Cl	2-NO_2	MeCN	5	67	-
VIII-5{*1,2,5,1*}	Me	4-CF_3	2-NO_2	MeCN	7.5	86	-

[a]Calculated from HPLC-UV traces at 205–400 nm; [b]Ratio of 6*R*,7*S* and 6*S*,7*R* diastereoisomers calculated from HPLC-UV traces at 205–400 nm; [c]Ratio of 6*R*,7*S* and 6*S*,7*R* diastereoisomers calculated from the ^{1}H NMR spectrum of the crude or purified products.

To determine limitations and scope, the suggested methodology was further tested for immobilized threonine-based sulfonamides **VIII-4**{*1,2,3-5,1*} (Figure 47 for R^3 modification), prepared from the 2-Nos-Cls bearing electron donating (MeO, Cl) and electron withdrawing (CF_3) groups and from cinnamyl alcohol (Scheme 74). The TFA-promoted product cleavage from the resin provided desired sulfonamides **VIII-5**{*1,2,4-5,1*} in excellent crude purities (91-93%, calculated from HPLC-UV traces at 205–400 nm), except for derivative **VIII-5**{*1,2,3,1*} bearing electron donating group (MeO) as R^3 substituent (71% crude purity). In this case, the alkylation of intermediate **VIII-3**{*1,2,3,1*} was incomplete even using a combination of different phosphines (e.g. TPP, TBP), solvents (e.g. anhydrous THF, DCM, DMF, dioxane), reaction time and temperatures (Scheme 75, Table 39, the best results are highlighted in bold). Despite the incomplete conversion, the following cyclization in MeCN gave the required oxazepane **VIII-6**{*1,2,3,1*} in 61% crude purity (calculated from HPLC-UV traces at 205–400 nm). Analogously, the synthesis of derivatives **VIII-6**{*1,2,4,1*} and **VIII-6**{*1,2,5,1*} prepared from 4-chloro and 4-trifluoromethyl-2-Nos-Cls, was accomplished in MeCN, but in the case of **VIII-6**{*1,2,5,1*}, it required longer cyclization time (7.5 h, Scheme 74, Table 38).

Scheme 75. The alkylation of intermediate **VIII-3**{*1,2,3*} bearing electron donating group (MeO) as R^3 substituent and its cleavage from the resin[a]

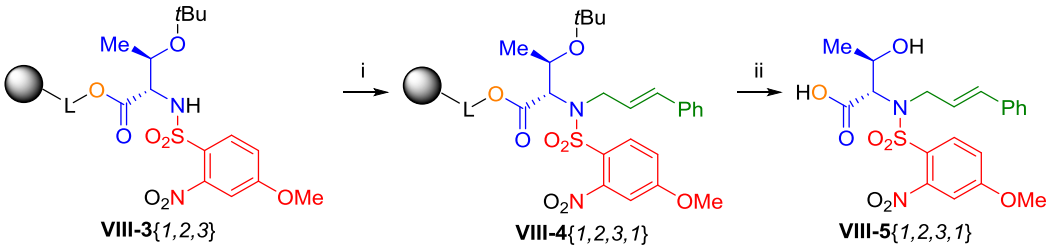

VIII-3{*1,2,3*} **VIII-4**{*1,2,3,1*} **VIII-5**{*1,2,3,1*}

[a]Reagents and conditions: (i) phosphine, DIAD, anhydrous solvent, 19-144 h, rt-110 °C; (ii) 50% TFA/DCM, 1 h, rt.

Table 39. The tested alkylation conditions for intermediate **VIII-3**{*1,2,3,1*}[a-c]

solvent	phosphine	concentration of all reagents [mmol][a]	time [h]	temp [°C]	crude purity of VIII-3 [%][b]	crude purity of VIII-5 [%][b]	ratio of VIII-3:5 [%][b]
anhydrous THF	TPP	0.4	22	23	33	54	38:62
	TPP	0.4[c]	19	23	33	54	38:62
	TPP	0.8	22	23	58	41	59:41
	TPP	0.4	22	66	30	60	33:67
	TPP	0.8	72	66	43	47	48:52
	TBP	0.4	22	23	35	54	39:61
anhydrous dioxane	TPP	0.4	22	23	46	53	43:57
	TPP	0.4	22	80	34	56	38:62
	TPP	0.4	88	100	26	70	27:73
	TPP	**0.4**	**144**	**100**	**25**	**71**	**26:74**
	TPP	**0.4**	**88**	**110**	**21**	**71**	**23:67**
anhydrous DCM	TPP	0.4	22	23	47	43	52:48
anhydrous DCM/THF	TPP	0.4	22	23	46	48	47:53
anhydrous DCM/DMF	TPP	0.4	22	23	44	45	49:51

[a]Reagents are meant cinnamyl alcohol, TPP or TBP and DIAD; [b]Calculated from HPLC-UV traces at 205–400 nm; [c]The reaction was repeated twice.

The catalytic hydrogenation of 2-Nos oxazepanes **VIII-6**{*1,2,3-5,1*} was dependent on the R^3 substitution. In the case of 4-substituted-2-Nos-amides, the reaction required a higher pressure (4 bar) to quantitative conversion to anilines **VIII-9**{*1,2,3-5,1*}. In contrast, the compound **VIII-6**{*1,2,2,1*}, prepared from 2-Nos-Cl was reduced at atmospheric pressure (Scheme 76, Table 40).

Scheme 76. The hydrogenation of intermediates **VIII-6**{*1,2,2-5,1*}[a]

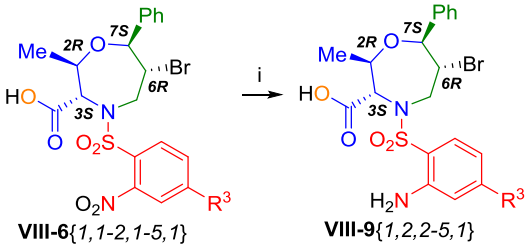

VIII-6{*1,1-2,1-5,1*} **VIII-9**{*1,2,2-5,1*}

[a]Reagents and conditions: (i) H_2, 10% Pd/C, EA, 20 h, rt (for derivative **VIII-9**{*1,2,2,1*}) or 19-23 h, rt, 4 bars (for derivatives **VIII-9**{*1,2,3-5,1*}.

Table 40. The tested conditions for hydrogenation of **VIII-6**{*1,2,R^3,1*}[a]

starting cmpd	R^3	time [h]	pressure [bar]	crude purity of VIII-6 [%][a]	crude purity of VIII-9 [%][a]	ratio of VIII-6:9 [%][a]
VIII-6{*1,2,2,1*}	H	2.5	1	60	3	95:5
		20	**1**	**0**	**64**	**0:100**
VIII-6{*1,2,3,1*}	MeO	20	1	67	5	93:7
		44	1	60	11	85:15
		19	3	19	68	22:78
		19	**4**	**0**	**71**	**0:100**

		20	1	47	30	61:39
VIII-6{*1,2,4,1*}	Cl	44	1	47	30	61:39
		19	**4**	**0**	**62**	**0:100**
VIII-6{*1,2,5,1*}	CF_3	**23**	**4**	**0**	**76**	**0:100**

[a]Calculated from HPLC-UV traces at 205–400 nm.

Similarly to our previous results,[38] the final cyclization step affected the resulting configuration of C13*a* stereocenter. In the case of aniline **VIII-9**{*1,2,5,1*} bearing electron withdrawing group (CF_3) as R^3 substituent, a ratio of *R,S* isomers changed during the cyclization (Scheme 77, Table 41). Consequently, after 3.5 h, the product **VIII-10**{*1,2,5,1*} was detected as a mixture of diastereomers and it was not purified. In the cases of **VIII-10**{*1,2,3-4,1*}, the final cyclization was not tested.

Scheme 77. The final cyclization to benzoxazepino-thiadiazepinone 7,7-dioxides **VIII-10**{*1,2,2-5,1*}[a]

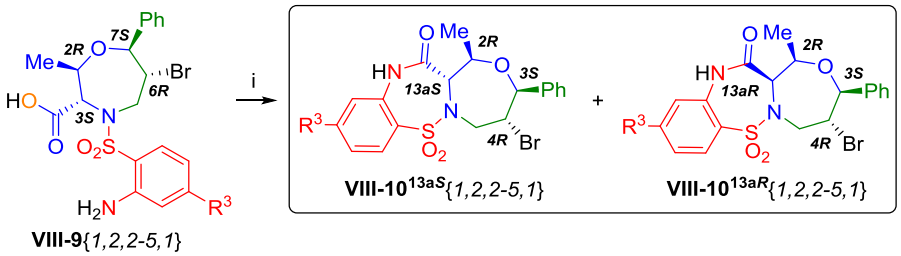

[a]Reagents and conditions: (i) PTSA, anhydrous DCE, 3.5-23 h, 90 °C.

Table 41. The cyclization conditions for derivatives **VIII-9**{*1,2,2-5,1*}[a]

starting cmpd	**R^3**	**time [h]**	**crude purity of VIII-9 [%]**[a]	**crude purity of VIII-10 [%]**[a]	**ratio of VIII-9:10 [%]**[a]	**ratio of VIII-10^{13a} *R:S* isomers [%]**[a]
		2	15	43	26:74	0:100
VIII-9{*1,2,2,1*}	H	4.5	30	31	49:51	0:100
		23	**0**	**64**	**0:100**	**0:100**
		1.5	34	53	39:61	31:69
VIII-9{*1,2,5,1*}	CF_3	**3.5**	**0**	**80**	**0:100**	**49:51**

[a]Calculated from HPLC-UV traces at 205–400 nm.

The second part of the Scenario A was devoted to the synthesis of fused *N*-acyl/*N*-alkyl oxazepanes. After the 4-Nos-cleavage of intermediate **VIII-4**{*1,2,1,1*}, the key α-amino ketone **VIII-11**{*1,2,-,1*} was subjected to further modification according to our previously reported procedures (Scheme 78, Pathway A-D).[39–43] After many unsuccessful attempts, the proposed methodologies did not give any fused oxazepane derivatives in good crude and diastereoemeric purities; however, some reaction intermediates were isolated and fully characterized.

The first limitation of the synthetic route was observed during the acylation/alkylation step with various agents *6-18* (Figure 47 for R^3 modification, Scheme 78). In the case of intermediate **VIII-12**{*1,2,6,1*}, the acylation step was accomplished using 2-nitrobenzoyl chloride in pyridine instead of the previously used 2-nitrobenzoic acid. The synthesis of related chlorides with various YR^3 substitu-

Scheme 78. The attempted synthesis of fused oxazepanes starting from one common *α*-amino ketone **VIII-11**{*1,2,-,1*}[a]

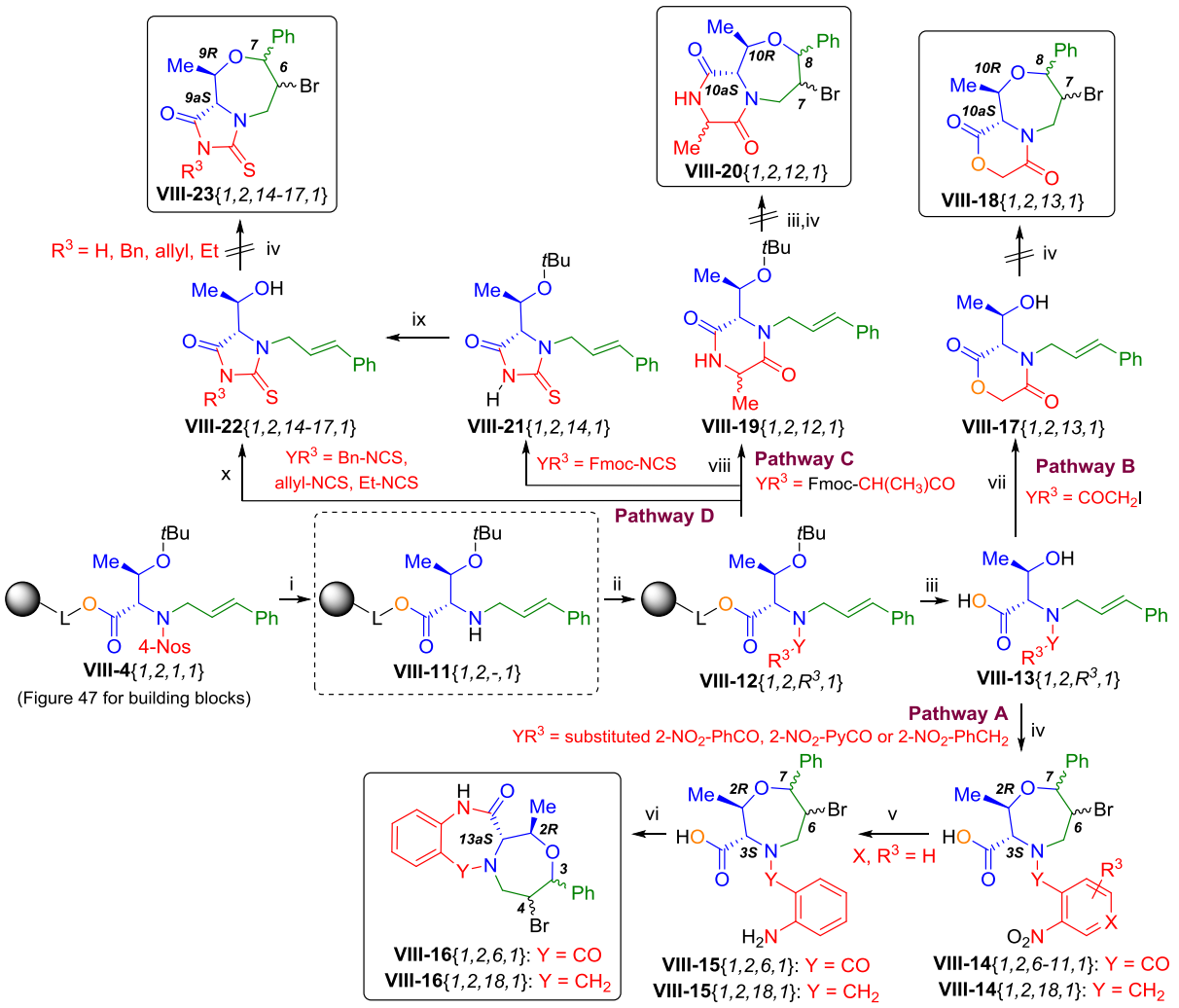

[a]Reagents and conditions: (i) MCE, DBU, 1.5 h, rt; (ii) **(a)** R^3-substituted 2-NO_2PhCOCl, Py, anhydrous DCM, 24-168 h, rt; **(b)** Fmoc-Ala-OH, HOBt, DIC, DMAP, DMF, DCM, 24 h, rt or Fmoc-Ala-OH, DIC, DMF, 24 h, rt; **(c)** ICH_2COOH, DIC, DCM, 30 min, rt; then add to the resin, 24 h, rt; **(d)** Fmoc-NCS, anhydrous THF, 3 h, rt or R^3-NCS, anhydrous THF, 72 h, rt; **(e)** DIEA, anhydrous DMF, 5 min, rt; then add to the resin 2-NO_2BnBr, anhydrous DMF, 48 h, 80 °C; (iii) Y = CO: 50% TFA/DCM, 1 h, rt; Y = CH_2: neat TFA, 1 h, 40 °C; (iv) NBS, (+)-CSA, MeCN (for derivative **VIII-15**{*1,2,6,1*}) or DMF (for derivatives **VIII-18**{*1,2,13,1*} and **VIII-23**{*1,2,14-17,1*}) or $CHCl_3$ (for derivative **VIII-15**{*1,2,18,1*}), 24 h, 0 °C, then 5 h, rt; (v) H_2, 10% Pd/C, IPA, 18 h, rt; (vi) 10% TFA/DCE, 24 h, 50 °C; (vii) DIEA, DMSO, 20 min, rt; (viii) 50% PIP/DMF, 30 min, rt; (ix) 50% MeOH.HCl/DCM, 24 h, rt; (x) neat TFA, 1 h, rt.

ents *7-11* (e.g. 5-MeO/5-F/4-Me/4-Br-2-NO_2-PhCO or 2-NO_2-PyCO) was accomplished using DMF-catalyzed chlorination of the appropriate 2-nitrobenzoic acids using thionyl chloride. The resulting chlorides *7-11* were directly used in the acylation step without further purification (e.g. after evaporation of dryness). The acylation with 5-fluoro-nitrobenzoyl chloride in lower scale (100 mg of the resin used) was successful although it required longer reaction time (7 days) in comparison to the derivative **VIII-12**{*1,2,6,1*}, prepared from 2-nitrobenzoyl chloride. Unfortunately, the reaction scale-up (500 mg of the resin used) completely failed and the product **VIII-12**{*1,2,8,1*} was observed as a part of a mixture containing unknown by-products. When the reaction was heated at 50 °C in anhydrous DCM in a pressure ampoule or in anhydrous DCE, no product was detected (Scheme 79).

Scheme 79. The acylation of *α*-amino ketone **VIII-11**{*1,2,-,1*} using various benzoyl chlorides[a]

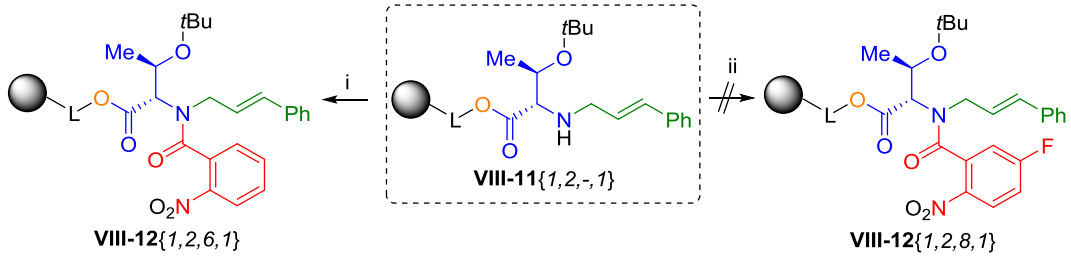

[a]Reagents and conditions: (i) 2-NO_2PhCOCl, Py, anhydrous DCM, 24 h, rt; (ii) **(a)** 5-F-2-NO_2PhCOCl, Py, anhydrous DCM, 168 h, rt; **(b)** anhydrous DCM, 24 h, 50 °C in a pressure ampoule; **(c)** anhydrous DCE, 24 h, 50 °C.

Similarly, the acylation of **VIII-11**{*1,2,-,1*} with Fmoc-Ala-OH did not work using DIC activation and/or DIC, HOBt technique. When the Fmoc-Ala-OH was replaced with iodoacetic acid and Fmoc-NCS, the expected intermediates **VIII-12**{*1,2,13,1*} and **VIII-12**{*1,2,14,1*} were obtained in 90% and 91% crude purities (calculated from HPLC-UV traces at 205–400 nm). The reaction with *N*-substituted-isothiocyanates *15-17* (e.g. benzyl, allyl and ethyl) required longer reaction time (72 h) to give the corresponding thioureas **VIII-12**{*1,2,15-17,1*}. In the case of intermediate **VIII-12**{*1,2,18,1*} prepared from 2-nitrobenzyl bromide, the complete alkylation required heating (80 °C) for 2 days (Scheme 80).

Scheme 80. The acylation/alkylation of *α*-amino ketone **VIII-11**{*1,2,-,1*}[a]

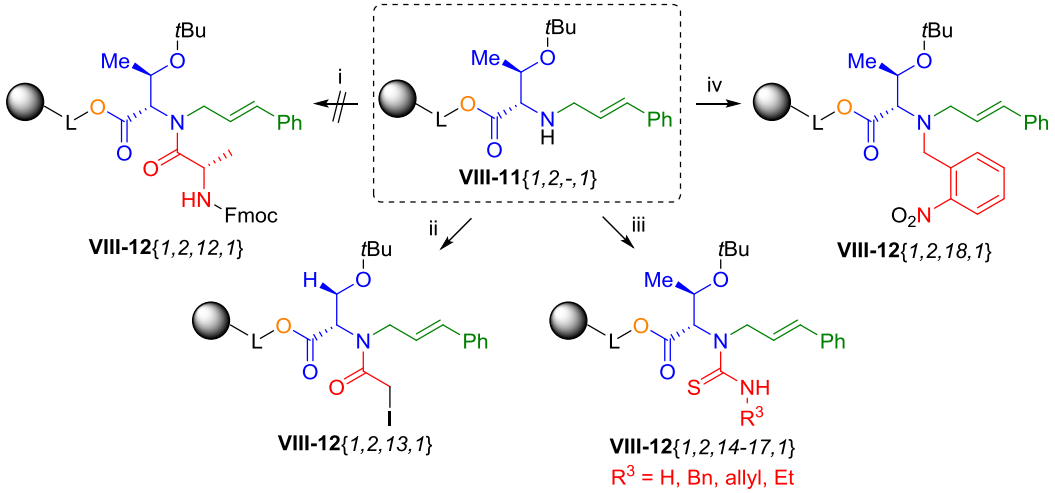

[a]Reagents and conditions: (i) **(a)** Fmoc-Ala-OH, HOBt, DIC, DMAP, DMF, DCM, 24 h, rt or **(b)** Fmoc-Ala-OH, DIC, DMF, 24 h, rt; (ii) ICH_2COOH, DIC, DCM, 30 min, rt; then add to the resin, 24 h, rt; (iii) **(a)** Fmoc-NCS, anhydrous THF, 3 h, rt or **(b)** R^3-NCS, anhydrous THF, 72 h, rt; (iv) DIEA, anhydrous DMF, 5 min, rt; then add to the resin 2-NO_2BnBr, anhydrous DMF, 48 h, 80 °C.

After that, the resulting *α*-amino ketones **VIII-12**{*1,2,6,1*} and **VIII-12**{*1,2,18,1*} prepared from 2-nitrobenzoyl chloride and 2-nitrobenzyl bromide, respectively, were treated with 50% TFA/DCM to release the products from the resin. In the case of **VIII-12**{*1,2,18,1*} prepared using 2-nitrobenzyl bromide, the quantitative removal of *tert*-butyl group required a slight heating (40 °C) in neat TFA. To further test the methodology, the crude compounds **VIII-13**{*1,2,6,1*} and **VIII-13**{*1,2,18,1*} were cyclized to receive 1,4-oxazepane derivatives **VIII-14**{*1,2,6,1*}

and **VIII-14**{*1,2,18,1*} (Scheme 81). Since the cyclization in DMF totally failed in both cases, the different cyclization solvents were tested to find the optimal cyclization conditions (Table 42). In the case of **VIII-13**{*1,2,18,1*} bearing 2-nitrobenzyl substituent, the product **VIII-14**{*1,2,18,1*} was obtained in 64% crude purity (calculated from HPLC-UV traces at 205–400 nm) using chloroform as the cyclization solvent. In contrast, the reaction of intermediate **VIII-13**{*1,2,6,1*} bearing 2-nitrobenzoyl substituent, gave a mixture of two inseparable diastereoisomers **VIII-14**{*1,2,6,1*} in 72% overall crude purity (calculated from HPLC-UV traces at 205–400 nm) in different ratios depending on the type of cyclization solvents used (MeCN vs $CHCl_3$, Table 42). Despite the lower crude purity of product **VIII-14**{*1,2,6,1*}, the reaction sequence was further tested to prepare fused [7+7] oxazepanes in two steps (e.g. hydrogenation and acid-mediated cyclization) according to the previously reported conditions[39] that yielded the target product **VIII-16**{*1,2,6,1*} in 70% crude purity (dr.r. 19:81) (tested for only 100 mg of resin). The reaction scale-up (500 mg of the resin used) completely failed in the cyclization step to 1,4-oxazepane scaffold **VIII-14**{*1,2,6,1*}, and the product was not isolated.

Scheme 81. The synthesis of 1,4-oxazepanes **14**{*1,2,R*^{3}*,1*} and their futher modificafation[a]

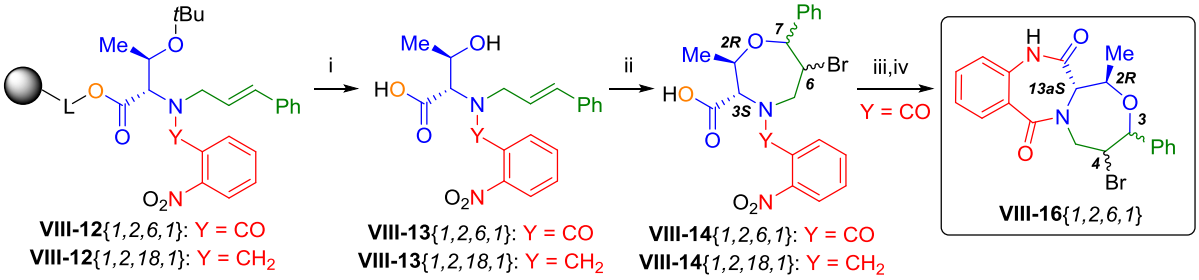

VIII-12{*1,2,6,1*}: Y = CO
VIII-12{*1,2,18,1*}: Y = CH_2

VIII-13{*1,2,6,1*}: Y = CO
VIII-13{*1,2,18,1*}: Y = CH_2

VIII-14{*1,2,6,1*}: Y = CO
VIII-14{*1,2,18,1*}: Y = CH_2

[a]Reagents and conditions: (i) Y = CO: 50% TFA/DCM, 1 h, rt; Y = CH_2: neat TFA, 1 h, 40 °C; (ii) NBS, (+)-CSA, solvent, 24 h, 0 °C, then 5 h, rt; (iii) H_2, 10% Pd/C, IPA, 18 h, rt; (iv) 10% TFA/DCE, 24 h, 50 °C.

Table 42. The tested cyclization conditions for intermediates **VIII-13**{*1,2,6,1*} and **VIII-13**{*1,2,18,1*}[a]

starting cmpd	Y	solvent	crude purity of VIII-14 [%][a]	ratio of diastereoisomers VIII-14[13a] [%][a]
VIII-13{*1,2,6,1*}	CO	**MeCN**	**72**	**32:68**
		DMF	4	100:0
		toluene	0	-
		EA	7	100:0
		THF	2	100:0
		$CHCl_3$	**72**	**50:50**
VIII-13{*1,2,18,1*}	CH_2	DMF	0	-
		MeCN	0	-
		acetone	0	-
		*i*PrOH	0	-
		$PhCH_3$	0	-
		$CHCl_3$	**64**	**100:0**

[a] Calculated from HPLC-UV traces at 205–400 nm.

In the case of benzyl analogue **VIII-14**{*1,2,18,1*}, the catalytic hydrogenation using 10% Pd/C caused debenzylation to product **VIII-24**{*1,2,-,1*} (Scheme 82, Pathway A), whereas in the case

of immobilized intermediate **VIII-12**{*1,2,18,1*}, the reduction of nitro group using sodium dithionite (at 23 °C; Scheme 82, Pathway B) failed. Similarly to the catalytic hydrogenation, increasing the temperature (80 °C) caused a slow debenzylation to an undesired product **VIII-11**{*1,2,-,1*} and any aniline **VIII-25**{*1,2,-,1*} was not detected (Scheme 82, Pathway B).

Scheme 82. The reduction of nitro group of derivatives **VIII-14**{*1,2,18,1*} and **VIII-12**{*1,2,18,1*}[a]

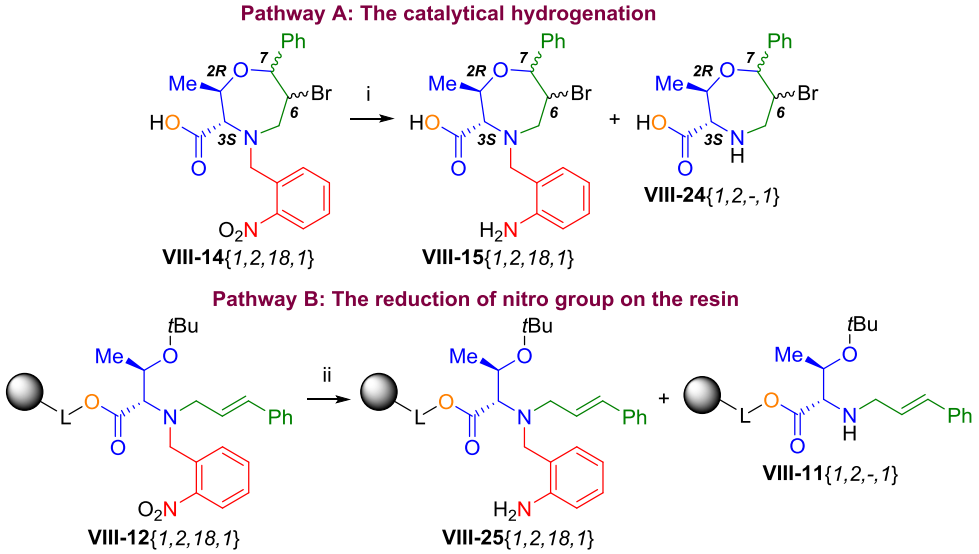

[a]Reagents and conditions: (i) H_2, 10% Pd/C, EA, 18 h, rt; (ii) $Na_2S_2O_4.2H_2O$, K_2CO_3, TBAHS, 50% DCM/H_2O, 2-24 h, rt-80 °C.

In addition, the synthesis of diketomorpholine **VIII-17**{*1,2,13,1*} was attempted (Scheme 83) according to the previously reported protocol.[41] The desired product was obtained in 89% crude purity (calculated from HPLC-UV traces at 205–400 nm) and 62% overall yield (calculated from the ^{1}H NMR spectrum of the purified product, Table 45 for the synthesized derivatives). According to the ^{1}H NMR spectrum, the product was detected as a mixture of 10*a R,S* diastereomers in a ratio of 6:94. These results corresponded to our previous findings,[2,41] in which HOBt-mediated immobilization of Fmoc-amino acid on the Wang resin resulted in a minor racemization (approximately ±8% of the second isomer). Since 6% of *R* isomer was observed in the ^{1}H NMR spectrum at the end of the reaction sequence, the obtained data indicated that the cyclization to diketomorpholine **VIII-17**{*1,2,13,1*} did not influence the optical purity. Unfortunately, when the compound **VIII-17**{*1,2,13,1*} was further cyclized using NBS and (+)-CSA in both solvents (e.g. DMF or MeCN), the reaction did not produce the desired [7+6] oxazepane (Scheme 83).

Scheme 83. The synthesis of diketomorpholine **VIII-17**{*1,2,13,1*} and its further modification[a]

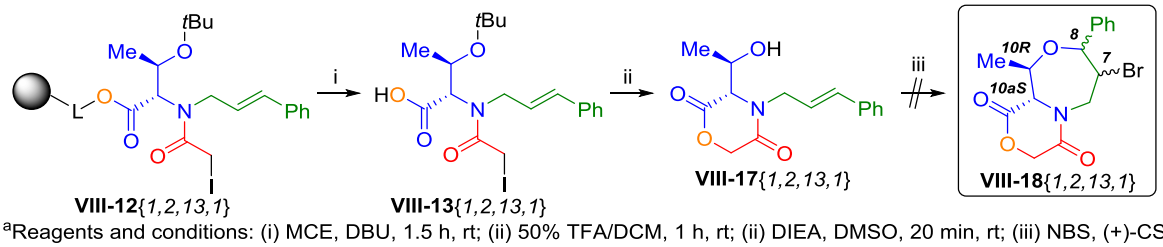

[a]Reagents and conditions: (i) MCE, DBU, 1.5 h, rt; (ii) 50% TFA/DCM, 1 h, rt; (ii) DIEA, DMSO, 20 min, rt; (iii) NBS, (+)-CSA, DMF or MeCN, 24 h, 0 °C, then 5 h, rt.

Then, we focused on the preparation of fused [7+5] oxazepanes started from the immobilized Fmoc-thiourea intermediate **VIII-12**{*1,2,14,1*}. Its base-mediated Fmoc-deprotection triggered a spontaneous cyclative cleavage from the resin that yielded the corresponding 2-thiohydantoin derivative **VIII-21**{*1,2,14,1*} in 92% crude purity (calculated from HPLC-UV traces at 205–400 nm). Similarly to our previous results,[42] the subsequent TFA-promoted cleavage of the *tert*-butyl group caused an undesired dehydration to olefin **VIII-26**{*1,2,14,1*}, which was obtained in 76% crude purity (calculated from HPLC-UV traces at 205–400 nm). The structure **VIII-26**{*1,2,14,1*} was suggested only from HPLC-MS analysis, the product was not purified thus the structure was not confirmed by NMR. To avoid undesired dehydration, TFA was replaced to 50% methanolic hydrochloric acid in DCM. These conditions caused removal of the *tert*-butyl group without elimination and yielded the expected alcohol **VIII-22**{*1,2,14,1*} in 56% crude purity (calculated from HPLC-UV traces at 205–400 nm). However, its semipreparative reverse-phase HPLC purification using AmAc buffer led to dehydration and the desired product was not isolated. For this reason, we tested the cyclization of the crude product **VIII-22**{*1,2,14,1*} to fused derivative **VIII-23**{*1,2,14,1*}; however, the final product was not detected which shows the suggested methodology is not feasible (Scheme 84).

Scheme 84. The cleavage of *tert*-butyl group of **VIII-21**{*1,2,14,1*} and its final cyclization[a]

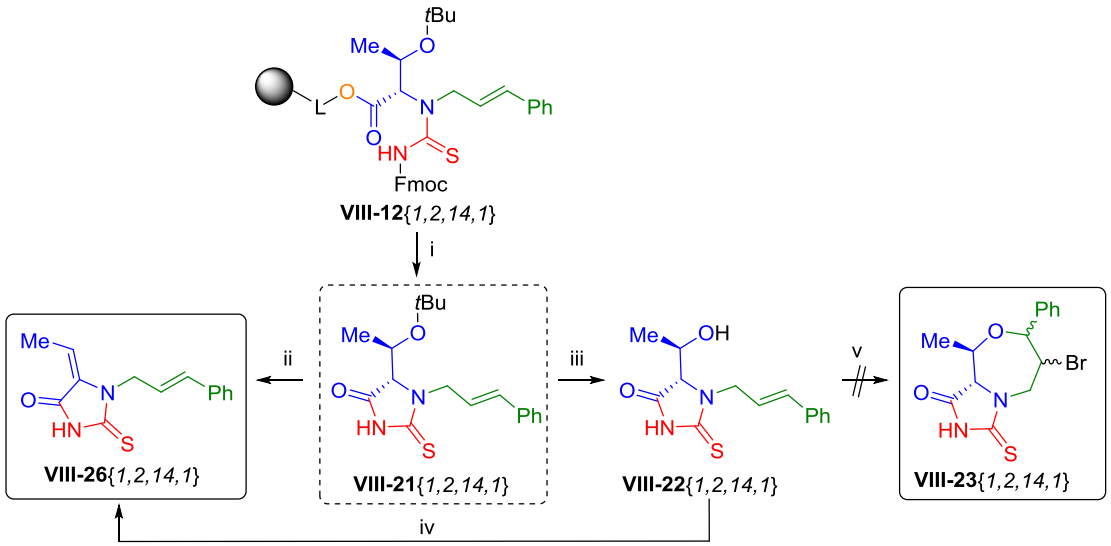

[a]Reagents and conditions: (i) 50% PIP/DMF, 30 min, rt; (ii) neat TFA, 1.5 h, rt; (iii) 50% MeOH.HCl/DCM, 24 h, rt; (iv) semi preparative reverse-phase HPLC purification using AmAc buffer; (v) NBS, (+)-CSA, DMF or MeCN, 24 h, 0 °C, then 5 h, rt.

In the case of *N*-substituted-thioureas **VIII-12**{*1,2,15-17,1*} prepared from benzyl, allyl and ethyl isothiocyanates, TFA-mediated cleavage the products from the resin provided the linear intermediates **VIII-27**{*1,2,15-17,1*} which slowly cyclized to thiohydantoins scaffold **VIII-22**{*1,2,15-17,1*}. The synthesis of thiohydantoin **VIII-22**{*1,2,15,1*} required heating in neat TFA for 1 h. However, subsequent cyclization to fused [7+5] derivative **VIII-23**{*1,2,15,1*} failed due to decomposition (Scheme 85, Table 43). For this reason, the synthesis of other *N*-substituted analogues was not performed.

Scheme 85. The cleavage and slow cyclization of *N*-substituted thioureas **VIII-12**{*1,2,15-17,1*}[a]

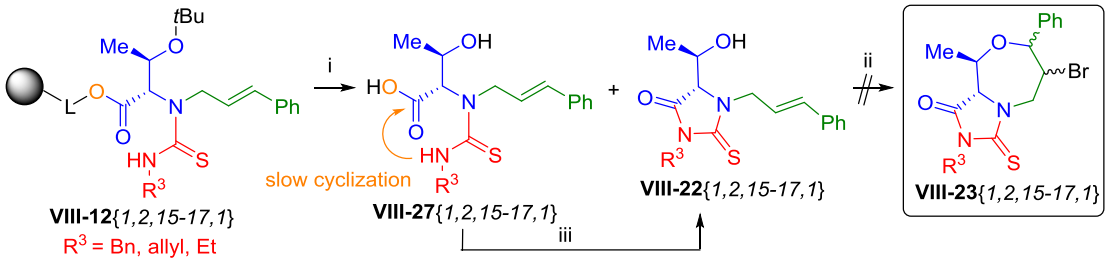

VIII-12{*1,2,15-17,1*}
R^3 = Bn, allyl, Et

VIII-27{*1,2,15-17,1*}

VIII-22{*1,2,15-17,1*}

VIII-23{*1,2,15-17,1*}

[a]Reagents and conditions: (i) TFA cleavage, time, rt; (ii) NBS, (+)-CSA, DMF or MeCN, 24 h, 0 °C, then 5 h, rt; (iii) 50% TFA/DCM, 0.5-24 h, rt or neat TFA, 12 h, rt.

Table 43. The tested cyclization conditions for derivatives **VIII-12**{*1,2,15-17,1*}[a]

starting cmpd	R^3	cleavage conditions	time [h]	crude purity of VIII-27 [%][a]	crude purity of VIII-22 [%][a]	ratio of VIII-27:22 [%][a]
VIII-12{*1,2,15,1*}	Bn	50% TFA/DCM	0.5	65	6	92:8
			2	44	23	66:34
			24	32	35	48:52
		TFA	**1**	**0**	**67**	**0:100**
VIII-12{*1,2,16,1*}	allyl	50% TFA/DCM	2	44	22	67:33
			24	27	38	42:58
VIII-12{*1,2,17,1*}	Et	50% TFA/DCM	2	72	10	88:12
			24	39	44	47:53

[a] Calculated from HPLC-UV traces at 205–400 nm.

Finally, Wang resin **VIII-1**{*1*} was replaced with Rink amide resin **VIII-1**{*2*} and the reaction sequence was tested with Fmoc-Thr(*t*Bu)-OH, 2/4-Nos-Cls and cinnamyl alcohol. However, the final cyclization of intermediates **VIII-5**{*2,2,1-2,1*} to oxazepanes **VIII-6**{*2,2,1-2,1*} completely failed (Scheme 86). Since the methodologies reported above did not provide satisfactory results, we continued to develop an alternative approach leading to fused derivatives using the Scenario B.

Scheme 86. The synthesis of oxazepane derivatives **VIII-6**{*2,2,1-2,1*} started from Rink amide resin[a]

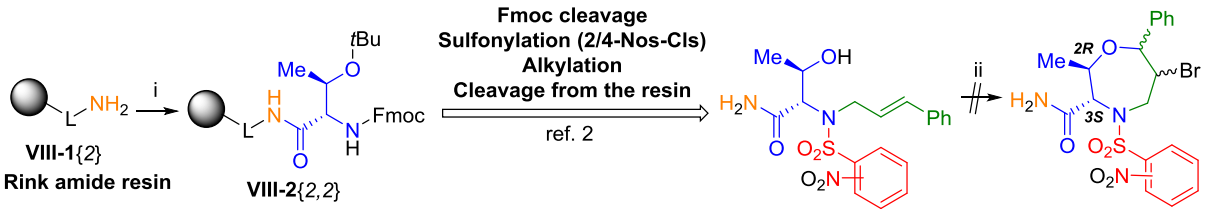

VIII-1{*2*}
Rink amide resin

VIII-2{*2,2*}

VIII-5{*1,2,1,1*}: 4-NO_2
VIII-5{*1,2,2,1*}: 2-NO_2

VIII-6{*1,2,1,1*}: 4-NO_2
VIII-6{*1,2,2,1*}: 2-NO_2

[a]Reagents and conditions: (i) Fmoc-Thr(*t*Bu)-OH, HOBt, DIC, DCM, DMF, 24 h, rt; (ii) NBS, (+)-CSA, DMF or MeCN, 24 h, 0 °C, then 5-20 h, rt.

4.8.2.2 Scenario B

The key *N*-cinnamyl-2-Nos-amide **VIII-4**{*1,2,2,1*} was prepared from Wang resin-immobilized Fmoc-Thr(*t*Bu)-OH, 2-Nos-Cl and cinnamyl alcohol. The resulting intermediate **VIII-4**{*1,2,2,1*} was

further oxidized using *m*CPBA and cleaved from the solid support using Lewis acid ($BF_3.Et_2O$).[45] In contrast to previous results,[45] the expected 6-hydroxy-1,4-oxazepane derivative **VIII-29**{*1,2,2,1*} was not isolated, but the reaction furnished the compound **VIII-30**{*1,2,2,1*} as a result of dehydration caused by TFA. The unsaturated product **VIII-30**{*1,2,2,1*} was isolated in 55% crude purity (calculated from HPLC-UV traces at 205–400 nm) and 19% overall yield (calculated from the ^{1}H NMR spectrum of the purified product, Scheme 87, Table 45 for the synthesized derivatives).

Scheme 87. The synthesis of 1,4-oxazepine derivatives **VIII-30**{*1,2,2,1*} *via* immobilized 2-Nos-amide[a]

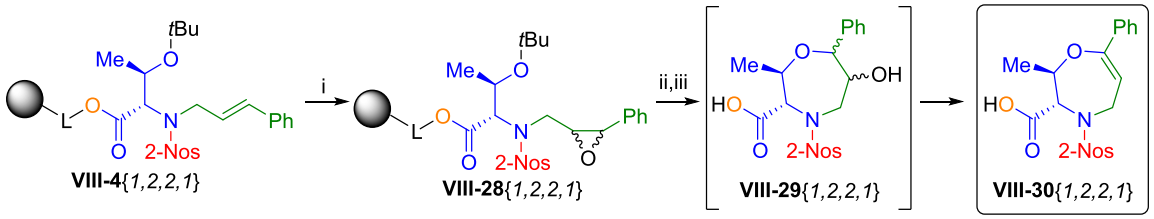

[a]Reagents and conditions: (i) *m*CPBA, anhydrous DCM, 15 h, rt; (ii) $BF_3.Et_2O$, DCM, rt, 6.5 h; (iii) HPLC MeCN/H_2O (HPLC purification using AmAc buffer).

Similarly, this methodology was tested for *N*-acyl derivatives (Scheme 88). In the Pathway A, the oxidation of intermediate **VIII-4**{*1,2,1,1*} using *m*CPBA yielded the corresponding oxirane **VIII-28**{*1,2,1,1*} in 85% crude purity (calculated from HPLC-UV traces at 205–400 nm after the product cleavage from the resin). The following 4-Nos cleavage and acylation with 2-nitrobenzoyl chloride gave the resulting intermediate **VIII-31**{*1,2,6,1*}. To compare the results, the product was cleaved from the resin using both Brønsted and Lewis acids (e.g. 50% TFA/DCM and $BF_3.Et_2O$). Both alternatives provided the same results; however, oxazepane derivative **VIII-30**{*1,2,6,1*} was not observed, but the reaction furnished a linear intermediate **VIII-32**{*1,2,6,1*} in relatively low crude purity (45%, calculated from HPLC-UV traces at 205–400 nm). In the second stage (Pathway B), the oxidation of *N*-acyl intermediate **VIII-12**{*1,2,6,1*} (95% crude purity, calculated from HPLC-UV traces (at 205–

Scheme 88. The synthesis of 1,4-oxazepanes from the immobilized *α*-amino ketone **VIII-4**{*1,2,1,1*}[a]

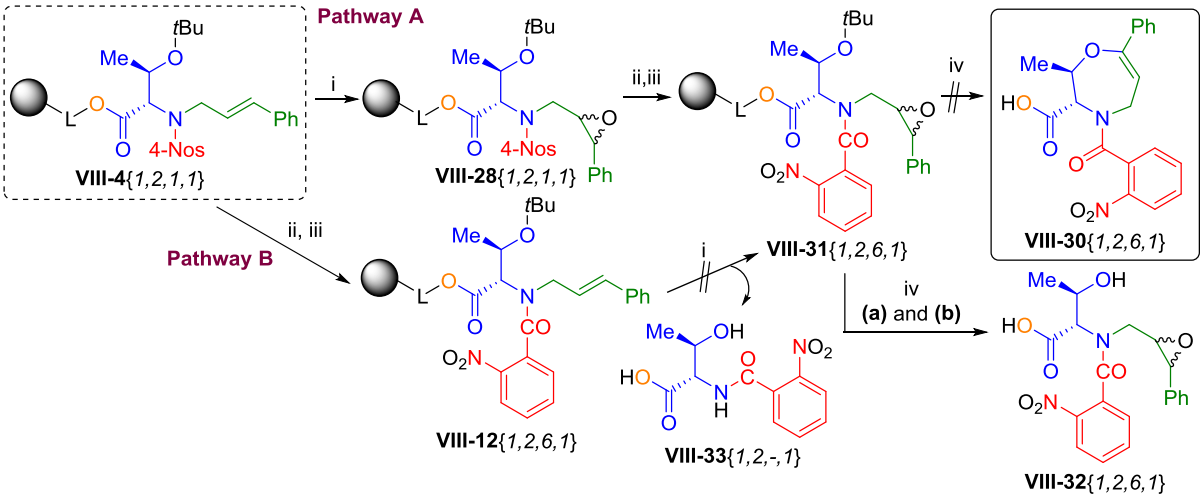

[a]Reagents and conditions: (i) *m*CPBA, anhydrous DCM, 15 h, rt; (ii) MCE, DBU, degassed DMF, 1.5 h, rt; (iii) 2-NO_2PhCOCl, Py, anhydrous DCM, 24 h, rt; (iv) **(a)** 50% TFA/DCM, 1 h, rt or **(b)** $BF_3.Et_2O$, DCM, 6.5 h, rt.

400 nm) completely failed and only the starting material **VIII-12**{*1,2,6,1*} was observed in a mixture with dealkylated product **VIII-33**{*1,2,-,1*} in a ratio of 34:66, respectively. According to these unsatisfactory results, we decided to continue in the synthesis of 1,4-oxazepane derivatives using Scenario C, started from Fmoc-HSe(TBS)-OH.

4.8.2.3 Scenario C

In the third suggested approach, Fmoc-Thr(*t*Bu)-OH was replaced with Fmoc-HSe(TBS)-OH **VIII-35**, prepared from commercially available Fmoc-homoserine using a two-step procedure,[100,101] Fmoc-HSe(TBS)-OH **VIII-35** was anchored to Wang resin **VIII-1**{*1*} which yielded the intermediate **VIII-2**{*1,3*}. The key *N*-phenacyl sulfonamide **VIII-4**{*1,3,2,4*} was then synthesized using 2-Nos-Cl and *α*-bromoacetophenone in three steps according to the previously reported protocols.[2] The acid-mediated cleavage from the resin gave the compound with a molecular mass corresponding to the desired oxazepine derivative **VIII-36**{*1,3,2,4*} in 87% crude purity (calculated from HPLC-UV traces at 205–400 nm) and 74% overall yield (calculated from the ^{1}H NMR spectrum of the purified product; Scheme 89, Pathway A; Table 45 for the synthesized derivatives). However, its ^{13}C{^{1}H} NMR spectrum provided signals of both carbonyl and carboxyl/ester groups at 194.7 ppm and 174.3 ppm (Figure 49). According to these facts, we assumed that product cleavage from the resin triggered an immediate lactonization[100] and yielded the product **VIII-37**{*1,3,2,4*} instead of 1,4-oxazepine **VIII-36**{*1,3,2,4*}

Scheme 89. The synthesis of 1,4-oxazepanes **VIII-39**{R^1,3,R^3,R^4} and lactones **VIII-37**{R^1,3,R^3,R^4} started from the immobilized Fmoc-HSe(TBS)-OH[a]

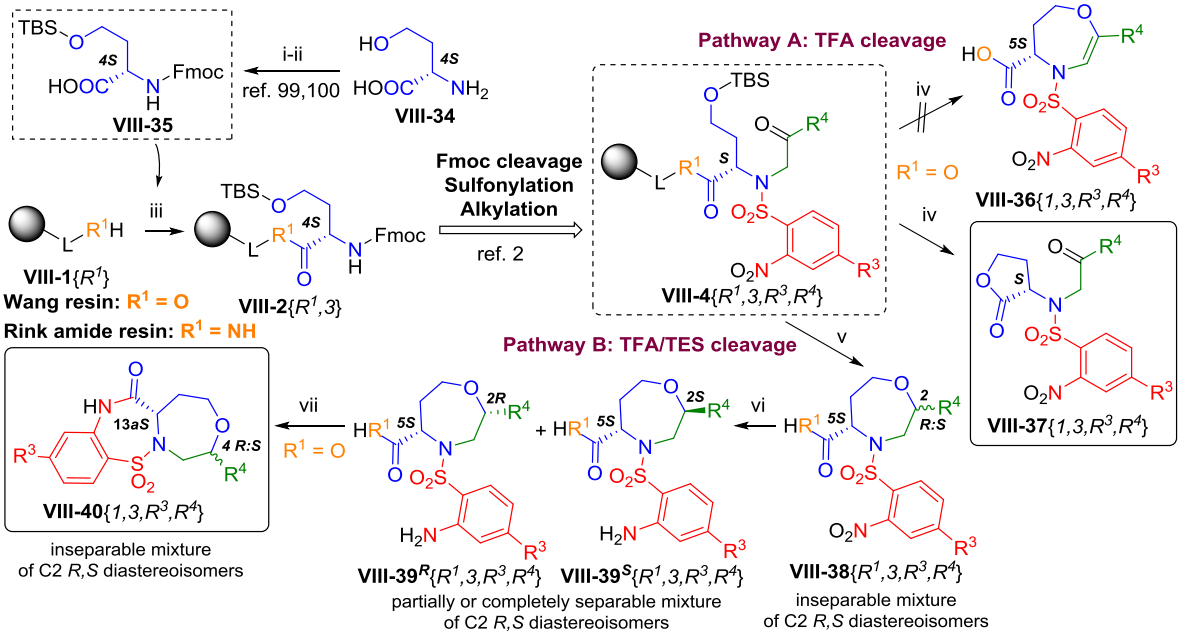

[a]Reagents and conditions: (i) Fmoc-OSu, 5% $NaHCO_3$, MeCN, 2 h, rt; (ii) TBS-Cl, imidazole, anhydrous DMF, 2 h, rt; (iii) HOBt, DMAP, DIC, DCM, DMF, 24 h, rt; (iv) 50% TFA/DCM, 1 h, rt; (v) TFA/TES/DCM (10:1:9), 30 min, rt; (vi) H_2, 10% Pd/C or PtO_2 (for derivatives **VIII-39**{*1,3,2,7*}, **VIII-39**{*1,3,2,12*} **VIII-39**{*1,3,3,4*}, **VIII-39**{*1,3,4,4*}), IPA, 1 h (prepared after the cleavage from 100 mg of the resin) or 24 h (prepared after the cleavage from 500 mg of the resin), rt; (vii) PTSA, anhydrous DCE, 1-96 h, 90 °C.

(Scheme 90, Pathway A). To prove this assumption, we performed the detailed structural elucidation of product **VIII-37**{*1,3,2,4*} using ^{1}H, ^{13}C{^{1}H}, APT, ^{1}H-^{1}H COSY, ^{1}H-^{1}H NOESY, ^{1}H-^{13}C HMQC, ^{1}H-^{13}C HMBC and ^{1}H-^{15}N HMBC experiments (Figure 50).

Figure 49. The ^{13}C{^{1}H} NMR spectrum of lactone **VIII-37**{*1,3,2,4*} with characteristic C=O signals

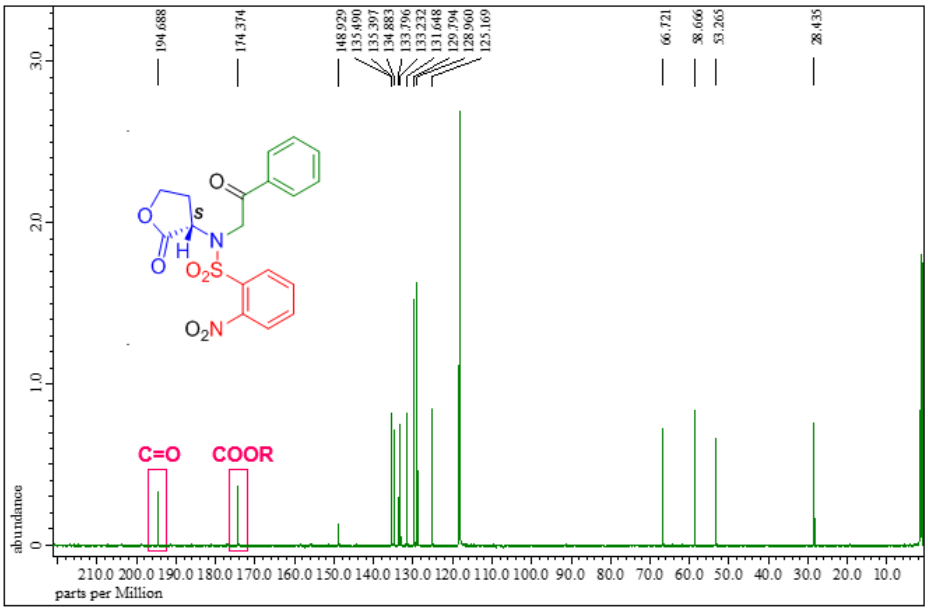

Figure 50. The detailed NMR elucidation of the structure **VIII-37**{*1,3,2,4*}

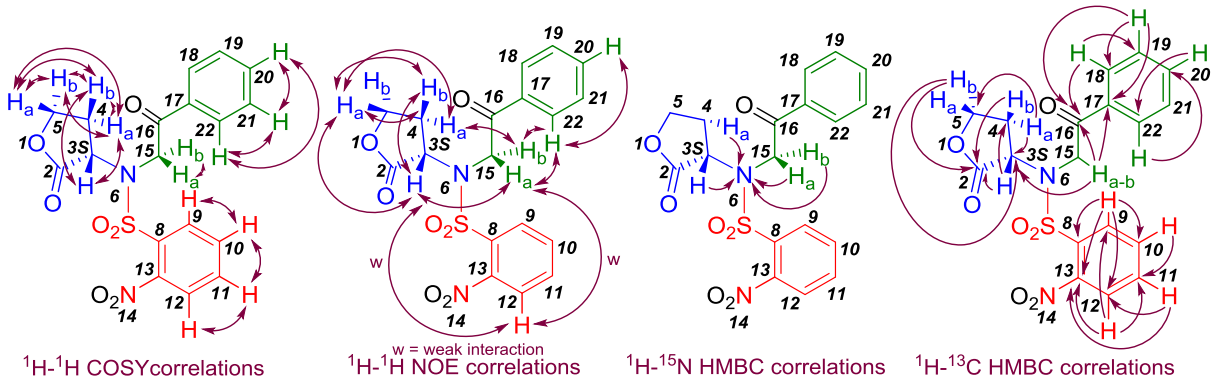

Interestingly, the addition of TES into the cleavage cocktail changed the course of reaction and yielded the 1,4-oxazepane **VIII-38**{*1,3,2,4*} in 85% crude purity (calculated from HPLC-UV traces at 205–400 nm) as an inseparable mixture of C2 *R,S* diastereoisomers which were detected by HPLC-UV analysis. The catalytic hydrogenation of **VIII-38**{*1,3,2,4*} using Pd/C in IPA[39] afforded the aniline **VIII-39**{*1,3,2,4*}. This compound was obtained in 91% crude purity as a mixture of C2 *R,S* diastereomers in a ratio of 56:44 (calculated from HPLC-UV traces at 205–400 nm; Scheme 89, Pathway B). At this stage, HPLC analysis indicated that both isomers could be partially separated using reverse-phase HPLC chromatography, thus the major isomer was successfully isolated in 34% overall yield (calculated from the ^{1}H NMR spectrum of the purified product, Table 45 for the synthesized derivatives). The detailed NMR elucidation of product **VIII-39**{*1,3,2,4*} confirmed the presumed 1,4-oxazepane

scaffold in which the key correlations were determined from ^{1}H, ^{13}C{^{1}H}, APT, ^{1}H-^{1}H COSY, ^{1}H-^{1}H NOESY, ^{1}H-^{13}C HMQC, ^{1}H-^{13}C HMBC and ^{1}H-^{15}N HMBC NMR spectra (Figure 51) and the configuration of the newly formed stereocenter C2 was assigned by NOE spectrum as *R*.

Figure 51. The key correlations of oxazepane derivative **VIII-39**{*1,3,2,4*}

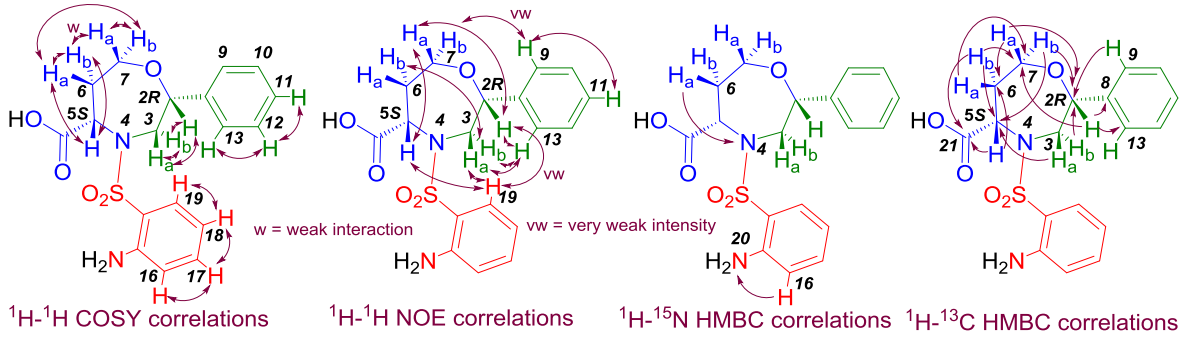

To explain the role of TES in a preferential formation of oxazepane over the lactone scaffold, we suggested the plausible mechanism (Scheme 90). In the presence of TES, an intermediate **E** is reduced to the stable oxazepane scaffold, thus it does not undergo *trans*-annular ring-opening by the carboxylate which (without the presence of TES) gives lactone **VIII-37**{*1,3,2,4*}. However, any of suggested intermediates **A-F** were not detected in the reaction mixture using the LC-MS analysis.

Scheme 90. The plausible mechanism of oxazepane formation **VIII-38**{*1,3,2,4*}

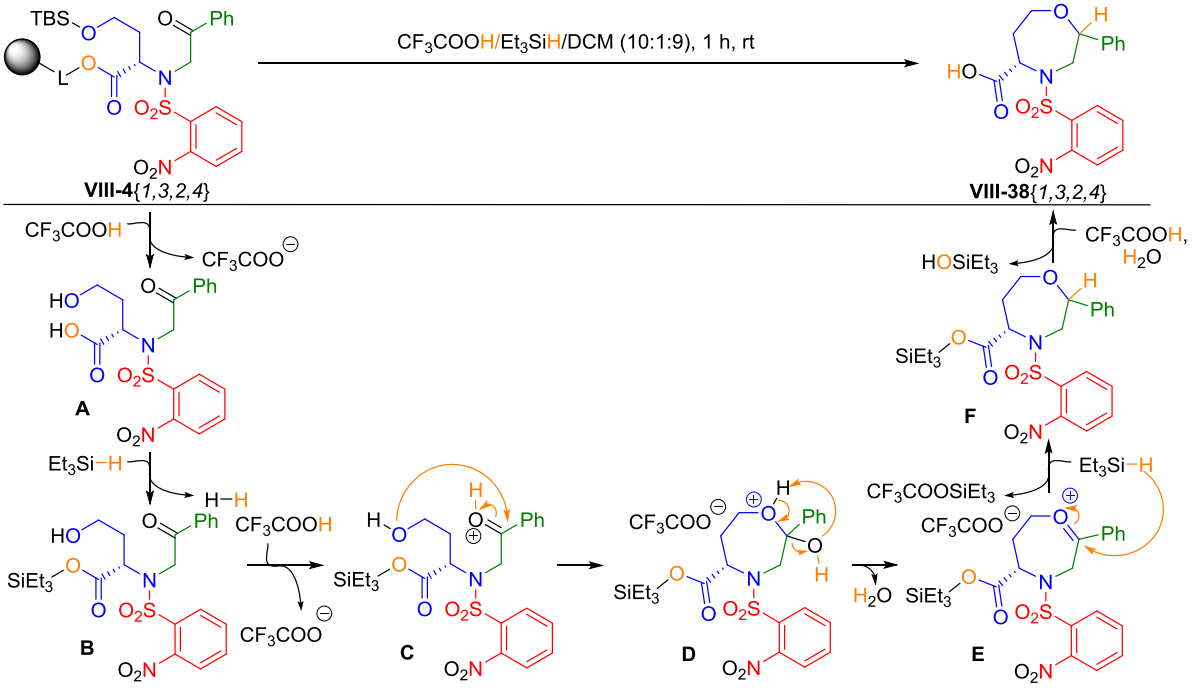

We also tested the cyclization of aniline **VIII-39**{*1,3,2,4*} using PTSA in anhydrous DCE at reflux.[38] The final product **VIII-40**{*1,3,2,4*} was obtained in limited crude purity (31%, calculated from HPLC-UV traces at 205–400 nm, Scheme 91) as an inseparable mixture of C4 *R,S* diastereoisomers and therefore it was not isolated.

Scheme 91. The final cyclization to fused derivative **VIII-40**{*1,3,2,4*}[a]

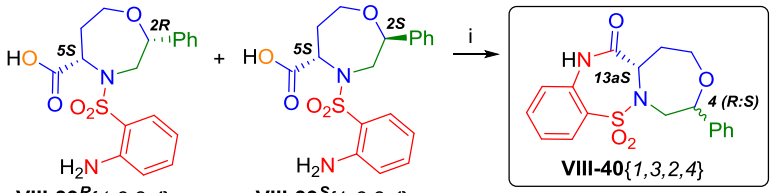

[a]Reagents and conditions: (i) PTSA, anhydrous DCE, 1-96 h, 90 °C.

We further decided to determine the impact of R^1, R^3 and R^4 substitution on the stereoselectivity of TES reduction (Scheme 92). The reaction sequence was tested on Wang resin (R^1= O) and Rink amide resin (R^1 = NH) in combination with various electron donating and electron withdrawing building blocks for R^3 and R^4 modifications. After TFA/TES cleavage of 2-Nos-amides **VIII-4**{R^1,*3*,R^3,R^4} from the resin, we obtained an inseparable mixture of C2 *R,S* diastereoisomers **VIII-38**{R^1,*3*,R^3,R^4} in 23-92% crude purities (calculated from HPLC-UV traces at 205–400 nm, Table 44).

Scheme 92. The synthesis of substituted 1,4-oxazepanes **VIII-38**{R^1,*3*,R^3,R^4} and **VIII-39**{R^1,*3*,R^3,R^4}[a]

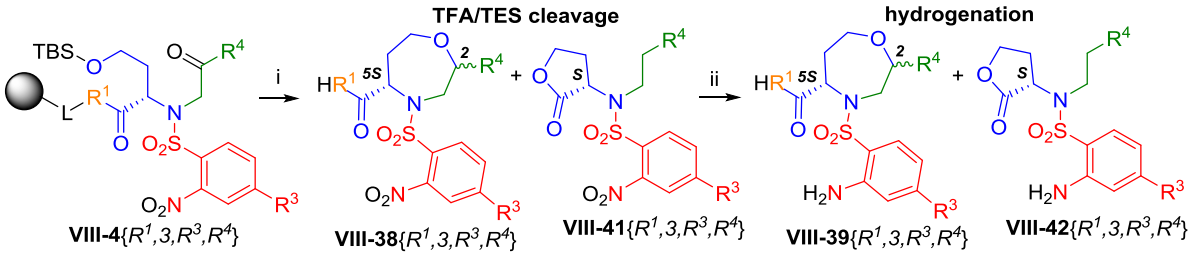

[a]Reagents and conditions: (i) TFA/TES/DCM (10:1:9), 30 min-24 h, rt; (iii) H_2, Pd/C or PtO_2, IPA, 1 h, rt.

Table 44. The ratios of both C2 *R,S* isomers depending on R^1, R^3 and R^4 substitution[a-h]

starting cmpd	R^1	R^3	R^4	TFA/TES cleavage		hydrogenation			
				crude purity of VIII-38 [%][a,b,g-h]	crude purity of VIII-41 [%][a]	cata-lyst	crude purity of VIII-39 [%][a,c-f]	ratio of C2 *R:S* isomers VIII-39 [%][a,c]	crude purity of VIII-42 [%][a]
VIII-4{*1,3,2,4*}	O	H	Ph	85	0	**Pd/C**	**91**[d]	**56:44**	**0**
VIII-4{*1,3,2,5*}	O	H	4-Me-Ph	80	0	**Pd/C**	**91**	**75:25**	**0**
VIII-4{*1,3,2,6*}	O	H	4-MeO-Ph	2	77	Pd/C	0	-	77
VIII-4{*1,3,2,7*}	O	H	4-Br-Ph	80	0	Pd/C	23[e]	65:35	0
						PtO_2	**80**	**59:41**	**0**
VIII-4{*1,3,2,8*}	O	H	4-F-Ph	80	0	**Pd/C**	**96**	**70:30**	**0**
VIII-4{*1,3,2,9*}	O	H	4-CF_3-Ph	55	0	**Pd/C**	**65**	**57:43**	**0**
VIII-4{*1,3,2,10*}	O	H	4-NO_2-Ph	82	0	**Pd/C**	**0**[d,f]	-	**0**
VIII-4{*1,3,2,11*}	O	H	4-NH_2-3,5-diCl-Ph	23	61	Pd/C	8	-	61
VIII-4{*1,3,2,12*}	O	H		80	0	**PtO_2**	**71**	**85:15**	**0**
VIII-4{*1,3,3,4*}	O	OMe	Ph	92[g]	0	**PtO_2**	**92**	**62:38**	**0**
VIII-4{*1,3,4,4*}	O	Cl	Ph	63	0	Pd/C	52[e]	69:31	0
						PtO_2	**60**	**69:31**	**0**
VIII-4{*2,3,2,4*}	NH	H	Ph	76[h]	0	**Pd/C**	**65**	**49:51**	**0**

[a]Calculated from HPLC-UV traces at 205–400 nm; [b]Inseparable mixture of C2 *R,S* diastereoisomers; [c]Partially se-

parable mixture of C2 *R,S* diastereoisomers; [d]The hydrogenation required 24 h for derivatives **VIII-38**{*1,3,2,4*} and **VIII-38**{*1,3,2,10*} to complete reduction of nitro group in a preparative scale (cleaved from 500 mg of the resin); [e]The hydrogenation led to undesired dehalogenation; [f]The derivative **VIII-43**{*1,3,2,10*} was obtained in 82% crude purity; [g]The alkylation required 2 days to complete reaction; [h]Repetition of the alkylation step to complete conversion; Note: All reactions were performed from 100 mg of the starting resin.

After hydrogenation step, the anilines **VIII-39**{R^1,*3*,R^3,R^4} were detected as a mixture of diastereomers in different ratios depending on the overall substitution (Scheme 92, Table 44). In the case of **VIII-39**{*1,3,2,7*} bearing 4-Br-Ph as R^4 substituent, hydrogenation triggered the competitive debromination to derivative **VIII-39**{*1,3,2,4*} obtained in 63% crude purity (calculated from HPLC-UV traces at 205–400 nm). Similarly, the undesired dehalogenation was observed in the case of derivative **VIII-39**{*1,3,4,4*} bearing 4-Cl as R^3 substituent. To suppress the dehalogenation, Pd/C was replaced to PtO_2 that yielded the required products **VIII-39**{*1,3,2,7*} and **VIII-39**{*1,3,4,4*}. In contrast, the dehalogenated product was not detected in the case of 4-F-Ph as R^4 substituent. In the case of oxazepane **VIII-38**{*1,3,2,10*} bearing 4-nitrophenyl rest as R^4 substituent, the hydrogenation led to undesired debenzylation to sulfonamide **VIII-43**{*1,3,2,10*}. The isolated sulfonamide was obtained in 82% crude purity (calculated from HPLC-UV traces at 205–400 nm) and 50% overall yield (calculated from the ^{1}H NMR spectrum of the purified product; Scheme 93).

Scheme 93. The undesired debenzylation of oxazepane **VIII-38**{*1,3,2,10*} during hydrogenation[a]

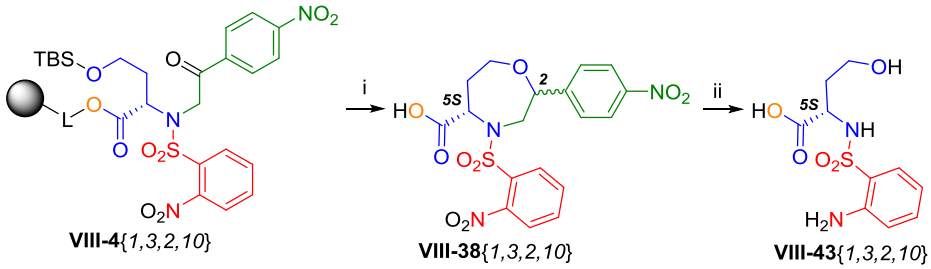

VIII-4{*1,3,2,10*} **VIII-38**{*1,3,2,10*} **VIII-43**{*1,3,2,10*}

[a]Reagents and conditions: (i) TFA/TES/DCM (10:1:9), 30 min, rt; (iii) H_2, Pd/C, IPA, 1-24h, rt.

Surprisingly, in the case of derivatives **VIII-4**{*1,3,2,6*} and **VIII-4**{*1,3,2,11*} synthesized from 2-bromo-1-(4-methoxyphenyl)ethanone and 1-(4-amino-3,5-dichlorophenyl)-2-bromo-ethanone, the TFA/TES cleavage gave preferably lactone derivatives **VIII-41**{*1,3,2,6*} and **VIII-41**{*1,3,2,11*} (Scheme 92) in 77% and 61% crude purities (calculated from HPLC-UV traces at 205–400 nm), respectively. In the case of lactone **VIII-41**{*1,3,2,6*}, its semipreparative reverse-phase HPLC chromatography yielded the product in 33% overall yield (calculated from the ^{1}H NMR spectrum of the purified product). In contrast to the ^{13}C{^{1}H} NMR spectrum of lactone **VIII-37**{*1,3,2,4*} (Figure 49), the signal of ketone at 194.7 ppm disappeared and the corresponding carbon of newly formed methylene -CH_2- group was obtained at 36.1 ppm (Figure 52).

The hydrogenation of both obtained derivatives **VIII-41**{*1,3,2,6*} and **VIII-41**{*1,3,2,11*} provided the corresponding anilines **VIII-42**{*1,3,2,6*} and **VIII-42**{*1,3,2,11*} in 77% and 61% crude purities (calculated from HPLC-UV traces at 205–400 nm; Scheme 92, Table 44).

Figure 52. Disappearance of the C=O signal of lactone **VIII-41**{*1,3,2,6*} in $^{13}C\{^{1}H\}$ NMR spectrum

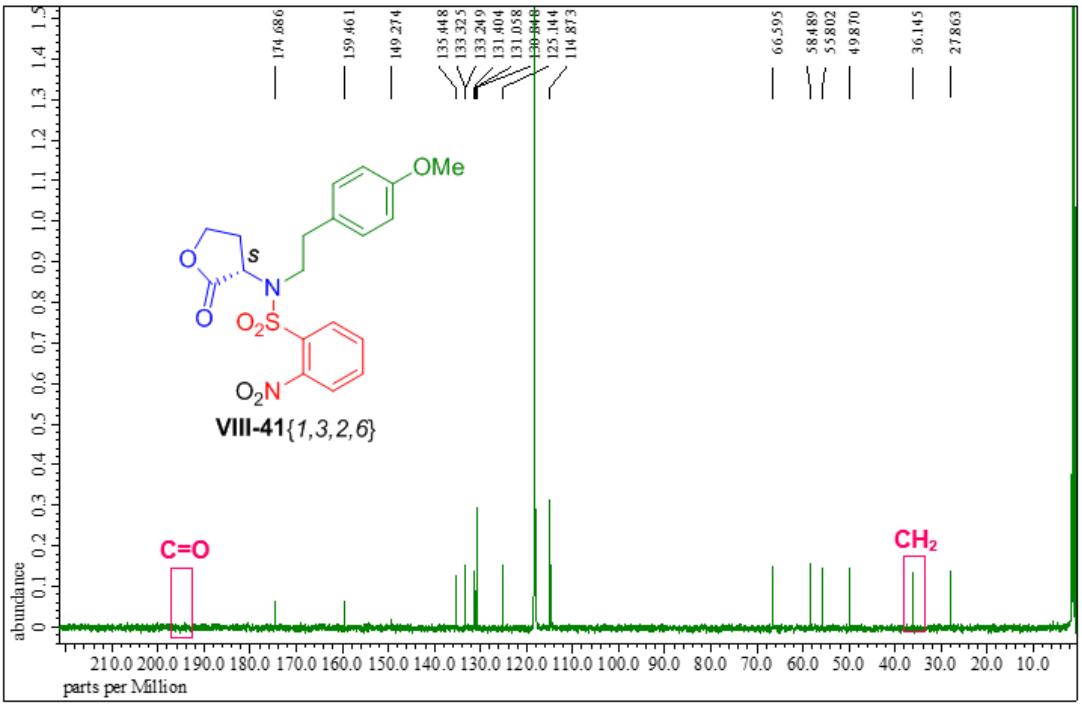

In addition, we decided to investigate the stereochemical outcome of the reaction sequence using SFC studies. In the case of Fmoc-HSe-OH and Fmoc-HSe(TBS)-OH, the C4 stereochemistry was studied in comparison to their racemic standards. Despite the spontaneous lactonization of Fmoc-HSe-OH during analysis, the both compounds (Figure 53-54), were obtained as enantiomerically pure derivatives. Similarly to our previous results reported for Fmoc-Ser(O*t*Bu)-OH,[38] the immobilization of Fmoc-HSe-TBS **VIII-35** to Wang resin **VIII-1**{*1*} yielded only a minor racemization on the C4 stereocenter (6% of *R* isomer, Figure 55). Taking this fact in account, we can state that formation of C2 *R,S* isomers of compound **VIII-39**{*1,3,2,4*} (56:44, calculated from HPLC-UV traces at 205–400 nm) has to be caused by non-stereoselective TES reduction. As only 6% of the second diastereoisomer can be assigned to epimerization within immobilization, the stereoselectivity of TES reduction in the series of derivatives **VIII-39**{R^1,*3*,R^3,R^4} was in the range of 15-51% (calculated from HPLC-UV traces at 205–400 nm without separation). After HPLC purification, the product **VIII-39**{*1,3,2,4*} was detected as a mixture of C2 *R,S* isomers in a ratio of 98:2 in comparison to its racemic standard (Figure 56).

Figure 53. Chiral SFC chromatograms of the crude racemic mixture and L-Fmoc-HSe-OH

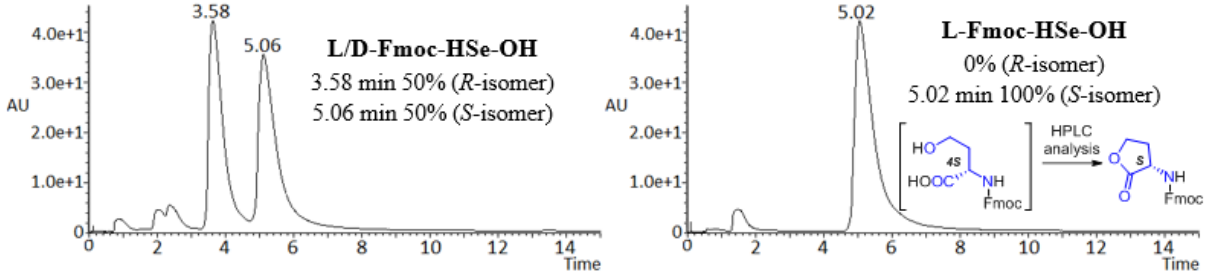

Figure 54. Chiral SFC chromatograms of the crude racemic mixture and L-Fmoc-HSe(TBS)-OH

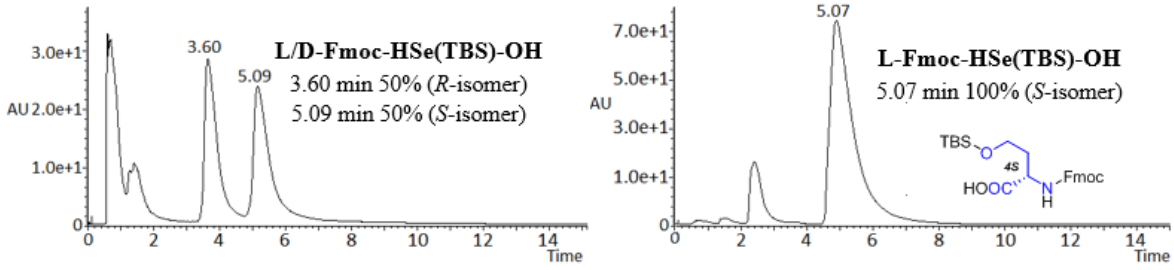

Figure 55. Chiral SFC chromatograms of Fmoc-HSe-OH **VIII-2**{*1,3*}$^{\text{after cleavage}}$ after immobilization on Wang resin and subsequent cleavage

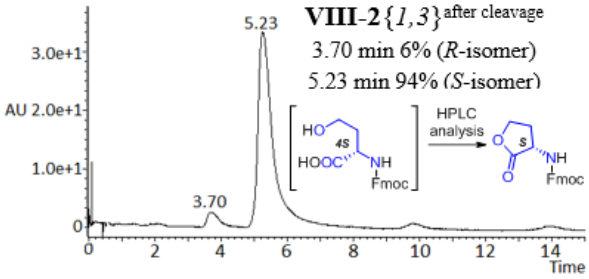

Figure 56. Chiral SFC chromatograms of racemic mixture and purified derivative **VIII-39**{*1,3,2,4*}

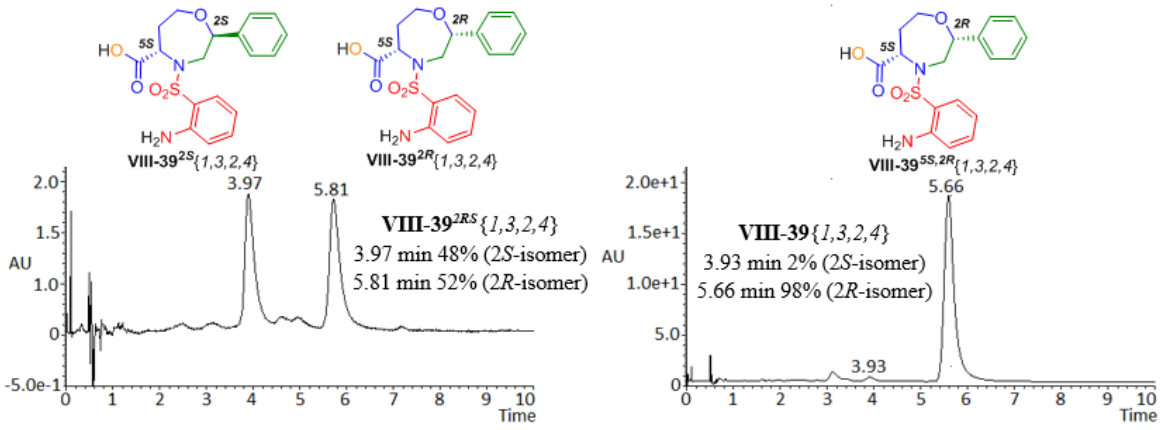

Scheme 94. The reactivity of key *α*-amino ketone **VIII-11**{*1,3,-,4*} with different agents[a]

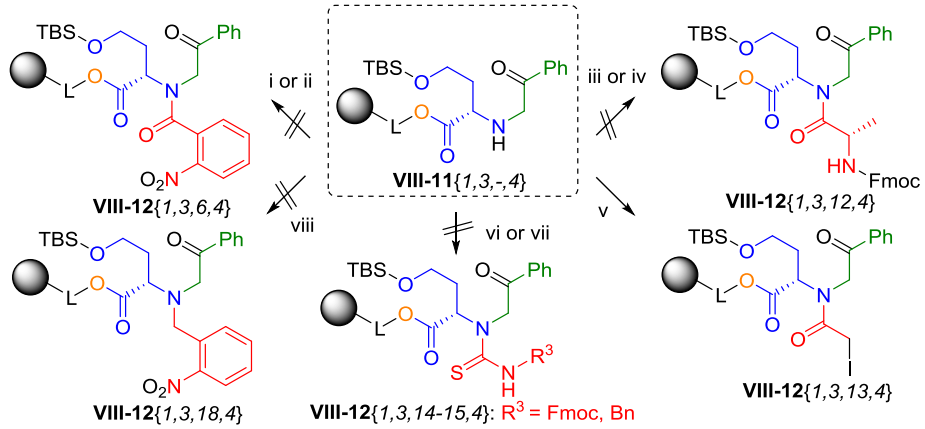

[a]Reagents and conditions: (i) 2-NO_2PhCOOH, DIC, DMF, 24-48 h, rt; (ii) 2-NO_2PhCOCl, Py, anhydrous DCM, 24-48 h, rt; (iii) Fmoc-Ala-OH, DIC, DMF, 24-48 h, rt; (iv) Fmoc-Ala-OH, HOBt, DIC, DMF/DCM, 24-48 h, rt; (v) ICH_2COOH, DIC, DCM, 30 min, rt; then add to the resin, 24 h, rt; (vi) Fmoc-NCS, anhydrous THF, 2-48 h, rt; (vii) BnNCS, anhydrous THF, 24-48 h, rt; (viii) DIEA, anhydrous DMF, 5 min, rt; then add 2-NO_2-BnBr, anhydrous DMF, 24-48 h, rt-80 °C.

Further, our attention was paid to the reaction of key *α*-amino ketone **VIII-11**{*1,3,-,4*} with different electrophiles to eventually access different fused 1,4-oxazepane derivatives. The cleavage of the 4-Nos group was performed according to the previously reported protocol[2] and yielded required *α*-amino ketone in 70% crude purity (calculated from HPLC-UV traces at 205–400 nm). The key intermediate **VIII-11**{*1,3,-,4*} was reacted with 2-nitrobenzoic acid derivatives,[39] Fmoc-Ala-OH,[3,40] Fmoc/benzyl-isothiocyanate[42,43] and 2-nitrobenzyl bromide; however, no traces of desired products **VIII-12**{*1,3,R*^{3}*,4*} were detected (Scheme 94). The only promising result was obtained after acylation with iodoacetic acid *via* the corresponding anhydride[41] which furnished the desired product **VIII-12**{*1,3,13,4*} in limited crude purity (31%, calculated from HPLC-UV traces at 205–400 nm).

4.8.3 Conclusion

In this subproject, we focused on the development of synthetic route applicable to fused 1,4-oxazepane derivatives based on previously reported procedures for fused morpholines.[2,38–43] Although we tested many different approaches, the proposed synthetic strategies were rather unsuccessful. So far, only the preparation of benzoxazepino-thiadiazepinone 7,7-dioxides by Scenario **A** seems to be feasible. All isolated and fully characterized reaction intermediates are summarized in Table 45.

Table 45. The list of synthesized and fully characterized compounds[a-e]

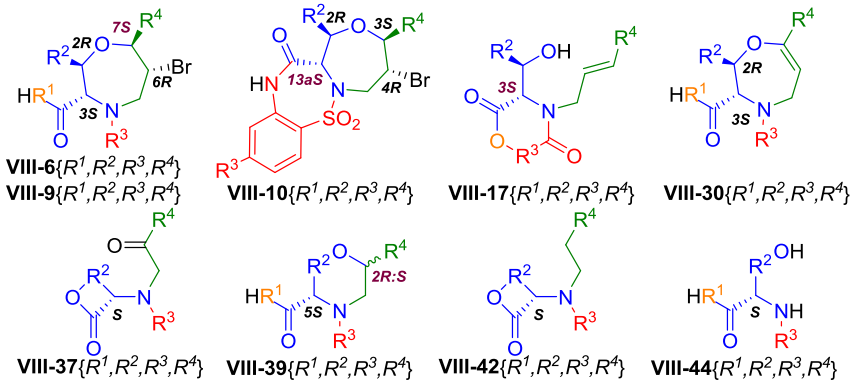

cmpd	R^1	R^2	R^3	R^4	crude purity [%][a]	final purity [%][b]	overall yield [%][c]	ratio of *R:S* stereoisomers [%][d,e]
VIII-6{*1,2,1,1*}	O	Me	4-NO_2-Ph-SO_2	Ph	86	98	26	1:99[d]
VIII-9{*1,2,2,1*}	O	Me	2-NH_2Ph-SO_2	Ph	72	95	9	9:91[d]
VIII-10{*1,2,2,1*}	O	Me	H	Ph	64	98	12	0:100[d]
VIII-17{*1,2,13,1*}	O	Me	CH_2	Ph	89	99	62	6:94[d]
VIII-30{*1,2,2,1*}	O	Me	2-NO_2Ph-SO_2	Ph	55	99	19	-
VIII-37{*1,3,2,4*}	O	$(CH_2)_2$	2-NO_2Ph-SO_2	Ph	87	99	74	-
VIII-39{*1,3,2,4*}	O	$(CH_2)_2$	2-NH_2Ph-SO_2	Ph	51	97	34	98:2[e]
VIII-42{*1,3,2,6*}	O	$(CH_2)_2$	2-NO_2Ph-SO_2	4-MeO-Ph	77	99	33	-
VIII-44{*1,3,2,10*}	O	$(CH_2)_2$	2-NO_2Ph-SO_2	4-NO_2-Ph	82	99	50	-

[a]Overall crude purity after the entire reaction sequence calculated from HPLC-UV traces at 205–400 nm; [b]Purity calculated from HPLC-UV traces at 205–400 nm after purification; [c]Calculated from the ^{1}H NMR spectrum of the purified product; [d]Ratio of *R,S* stereoisomers calculated from ^{1}H NMR of the purified product; [e]Ratio of C2 *R,S* stereoisomers calculated from SFC analysis of the purified products.

5. CONCLUSION

This thesis is devoted to the applicability of the polymer-supported 2/4-Nos-amides in the preparation of different heterocycles. 2/4-Nos-amides are readily available precursors of α-amino ketones that represent a multireactive compounds to prepare various heterocyclic scaffolds using a solid-phase synthetic strategy (SPS). To summarize the field, a general application of polymer-supported α-amino ketones was described in the *State of the art* followed by our contribution to this area, as reported in the part of *Results and discussion*. In our case, the starting compounds were synthesized from Fmoc-amino acids containing functionalized side chain to prepare imidazole, fused morpholine and oxazepane derivatives. We have been using a combination of both SPS and a post-cleavage (solution-phase) modification and our procedures are fully compatible with the high-throughput synthetic concept. The general principle of the developed methodologies was based on a denosylation of the immobilized 2/4-Nos-amides that yielded the key α-amino ketones which were further modified with various electrophiles to provide the suitable intermediates which yielded, after post-cleavage modification, the corresponding heterocycles. In this context, we have developed different protocols that were verified by the synthesis and full characterization of more than 130 fused morpholines **I-IV**, imidazoles **V-VI** and pyrrolidinones **VII** (Figure 57). Importantly, the TES applicability for the reduction to provide new stereocenters with controlled configuration was successfully tested in majority of projects. Except for threonine-based benzomorpholino-thiadiazepine and 3-methyl-diketo-morpholines, the TES reduction was fully stereoselective as proven by SFC and advanced NMR experiments.

In the first project, we studied the impact of the final cyclization step to the resulting configuration of the C12*a* stereocenter of benzomorpholino-thiadiazepinone derivatives. The reaction outcome was investigated with respect to the configuration of C3 stereocenter formed after the TES reduction. TES reduction of threonine-based intermediates gave a mixture of separable *R,S* diastereoisomers, whereas the reduction of serine/cysteine-based intermediates was fully stereoselective and provided *R* isomer. According to obtained results, the final cyclization rather slightly influenced the resulting C12*a* configuration and the epimerization rate on the stereocenter was dependent on R^2 substituent and the type of cyclization solvent used (DCE vs toluene).

Further, we compared the effect of carbonyl group instead of sulfonyl group to the stereoselectivity outcome. This distinct exchange did not affect the stereoselectivity (probably due to milder conditions required in the cyclization step) and the benzomorpholino-diazepinediones were obtained as pure 12*aS* and 3*R* isomers.

Similarly, no 9*a* epimerization was observed during the synthesis of pyrazino-oxazine and fused diketomorpholine derivatives. In the case of pyrazino-oxazines, the configuration of both stereocenters was determined as 7*S* and 9*aS* with respect to the configuration of the starting Fmoc-amino acids as R^2 substituent in C7 position. Analogously, the stereoselective TES reduction was achieved for oxazino-

morpholines, prepared from iodoacetic acid (R^2 = H). In this case, the configuration of both stereocenters was determined as 7*R*, 9*aS* by a combination of both SFC and 2D NMR analysis.

In addition, the SFC analysis helped to establish the configuration of 3-methylidene-diketomorpholines with different R^2 substituent (R^2 = Me, Ph) located at the C6 center. According to analytical data, the final products were obtained as a mixture of 6*R* and 6*S* isomers in different ratios depending on R^1 substituent. To explain the resulting C6 epimerization, we designed the hypothetical mechanism of the cyclization step, which was based on the DIEA-mediated formation of diketomorpholine scaffold bearing various R^2 substituent in C6 position (*S* isomer). The following deprotonation at the C6 center by DIEA and the reaction of intermediate carbanion with proton from DIEA-H^+ yielded the more stable C6*R* isomer having the bulky substituent (e.g. Me, Ph) in equatorial position. In the case of 3-methylene-diketomorpholines, the TES reduction was not stereoselective and furnished the mixture of C3 *R,S* enantiomers of 3-methyl-diketomorpholines in a ratio of 80:20.

Other project was devoted to possible synthesis of thiohydantoin-oxazine derivatives; however, the expected derivatives were not obtained. For this reason, the detailed NMR studies were performed to determine the structure of isolated compounds (thiohydantoins, imidazole-2-thiones and imidazo [2,1-*b*]thiazol-4-iums) by advanced NMR spectroscopy. According to obtained data, we devised the plausible mechanism of isomerization of imidazo[2,1-*b*]thiazol-4-iums to imidazole-2-thiones. To extend the tested methodology, the synthesis was done on the Wang-piperazine resin instead of Wang resin to access 2-alkylsulfonyl-imidazoles.

In the penultimate contribution, we focused on the synthesis of 1,4-oxazepane derivatives using the previously developed conditions. In contrast to published outcomes, we have witnessed the pinacol-like rearrangement [1,2]-shift of serine/threonine-based alkynols which yielded the chiral pyrrolidin-3-ones. The final compounds were obtained as diastereomerically pure products.

The last project was devoted to methodologies to prepare fused 1,4-oxazepane derivatives **VIII**. In this case, three alternative synthetic approaches were tested, but each of them suffered from certain limitations. Despite a series of unsuccessful attempts, we managed to prepare benzoxazepino-thiadiazepinone 7,7-dioxide derivatives, single 1,4-oxazepanes and also some reaction intermediates were isolated and fully characterized. As in the previous projects, the target products were subjected to detailed NMR analysis to determine the resulting configuration of all stereocenters. In this regard, both applied scenarios (A and C) had the distinct impact to the stereochemical outcome. In the case of threonine-immobilized intermediates (Scenario A), the cyclization to 1,4-oxazepane scaffold was dependent on R^3 substitution and concurrently on the type of cyclization solvent used which influenced diastereoselectivity of the reaction. Despite these facts (and similarly to our above-mentioned research of benzomorpholino-thiadiazepinone 6,6-dioxides), the PTSA-mediated cyclization to the fused oxazepanes affected the resulting configuration of C13*a* stereocenter and yielded a mixture of C13*aR* and C13*aS* isomers in different ratios depending on the R^3 substitution. In contrast to threonine-based intermediates, the release of Nos-amides prepared from the immobilized Fmoc-HSe(TBS)-OH on Wang

resin provided the lactone derivative. To suppress the undesired lactonization, the TFA/TES was applied to release the Nos-amides from the resin that yielded the required 1,4-oxazepane derivative. In this case, the TES reduction was non-stereoselective and gave the inseparable separable mixture of C2 *R,S* diastereoisomers in different ratios depending on R^1, R^3 and R^4 substitution. However, hydrogenation to the corresponding anilines enabled the separation of C2 *R,S* diastereoisomers. The structure of 1,4-oxazepane derivative was confirmed using detailed NMR analysis. In contrast to Scenario A, the final cyclization to benzoxazepino-thiadiazepinone 7,7-dioxides yielded the expected product in limited crude purity and therefore the compound was not isolated.

To sum up, we developed methodologies applicable for the preparation of different heterocycles starting from immobilized 2/4-Nos-amides and α-acylamino ketones derived from amino acids with functionalized side chains. These methodologies can be used for diversity-oriented reagent-based synthesis of different scaffolds with further extensive substitution. Figure 57 shows the final overview of synthons and more than 28 multifarious structures (including the previously reported single morpholine **IX** and unsaturated benzodiazepin-5-one derivatives **X**) accessible from the key intermediates. Consequently, considering number of readily available building blocks, the developed protocols enable quick synthesis of sizable chemical libraries of drug-like molecules for their subsequent pharmacological evaluation.

Figure 57. Immobilized 2-Nos-amides and/or α-amino ketones and their conversion to diverse types of heterocycles **I-X**

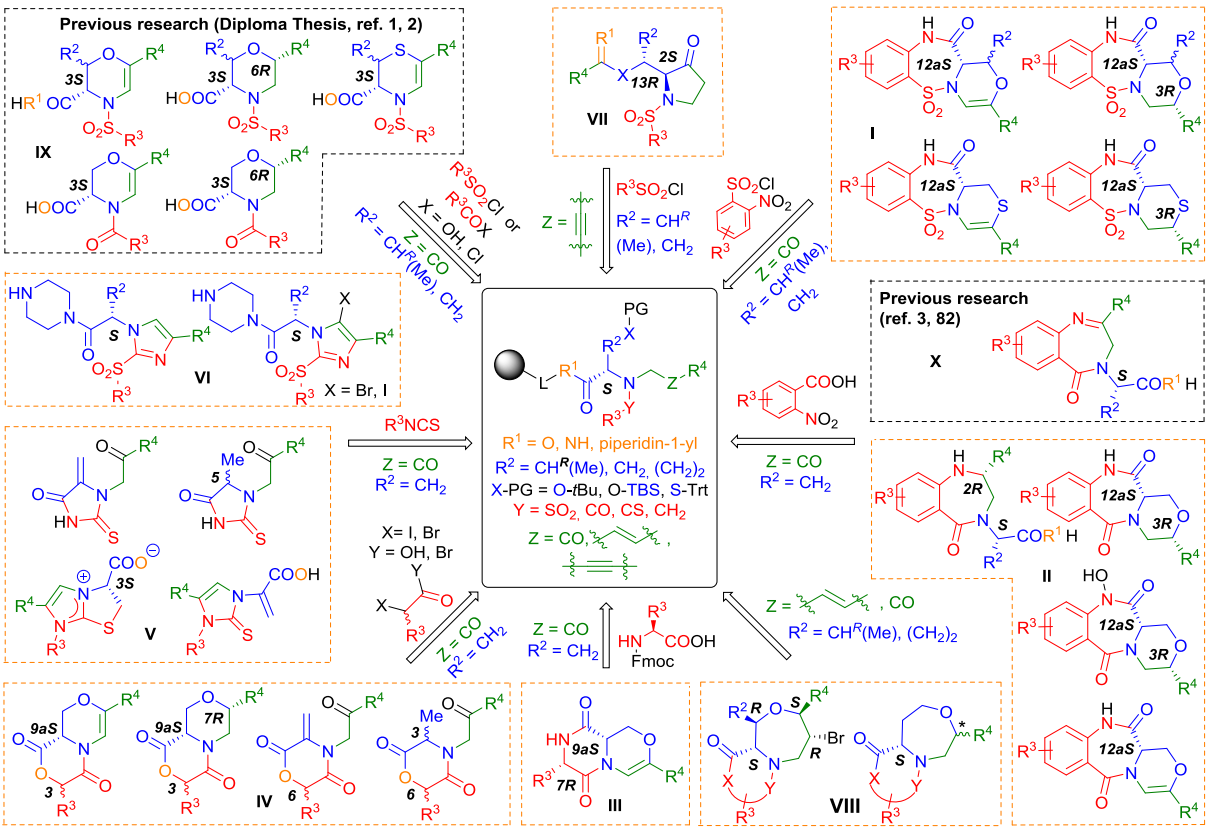

6. REFERENCES

(1) Králová, P. Solid-Phase Synthesis of Novel Morpholine/Thiomorpholine-3-Carboxylic Acid Derivatives. The Diploma Thesis, **2016**.

(2) Králová, P.; Fülöpová, V.; Maloň, M.; Volná, T.; Popa, I.; Soural, M. *ACS Comb. Sci.* **2017**, *19* (3), 173–180.

(3) Fülöpová, V.; Gucký, T.; Grepl, M.; Soural, M. *ACS Comb. Sci.* **2012**, *14* (12), 651–656.

(4) Gharpure, S. J.; Vishwakarma, D. S.; Nanda, S. K. *Org. Lett.* **2017**, *19* (24), 6534–6537.

(5) Galloway, W. R. J. D.; Isidro-Llobet, A.; Spring, D. R. *Nat. Commun.* **2010**, *1*, 80.

(6) Itoh, H.; Inoue, M. *Org. Biomol. Chem.* **2019**, *17* (27), 6519–6527.

(7) Beaucage, S. L.; Iyer, R. P. *Tetrahedron* **1992**, *48* (12), 2223–2311.

(8) Branderhorst, H. M.; Liskamp, R. M. J.; Pieters, R. J. *Tetrahedron* **2007**, *63* (20), 4290–4296.

(9) Seeberger, P. H.; Haase, W.-C. *Chem. Rev.* **2000**, *100* (12), 4349–4394.

(10) Fülöpová, V.; Soural, M. *ACS Comb. Sci.* **2015**, *17* (10), 570–591.

(11) Králová, P.; Ručilová, V.; Soural, M. *ACS Comb. Sci.* **2018**, *20* (9), 529–543.

(12) Cankařová, N.; Schütznerová, E.; Krchňák, V. *Chem. Rev.* **2019**.

(13) Soural, M.; Hlaváč, J.; Krchňák, V. Linkers for Solid-Phase Peptide Synthesis. In *Amino Acids, Peptides and Proteins in Organic Chemistry*; Wiley Online Books; **2011**.

(14) Lemrová, B.; Fülöpová, V. *Praktické Aspekty Syntézy Na Pevné Fázi. Skripta.*; Zatloukal, M., Soural, M., Eds.; UP Olomouc, **2015**.

(15) Guillier, F.; Orain, D.; Bradley, M. *Chem. Rev.* **2000**, *100* (10), 3859.

(16) Gutte, B.; Merrifield, R. B. *J. Biol. Chem.* 1971, pp 1922–1941.

(17) Merrifield, R. B. *J. Am. Chem. Soc.* **1963**, *85* (14), 2149–2154.

(18) Minta, E.; Boutonnet, C.; Boutard, N. et al. *Tetrahedron Lett.* **2005**, *46* (11), 1795–1797.

(19) Rich, D. H.; Gurwara, S. K. *J. Am. Chem. Soc.* **1975**, *97* (6), 1575–1579.

(20) ten Holte, P.; Thijs, L.; Zwanenburg, B. *Tetrahedron Lett.* **1998**, *39* (40), 7407–7410.

(21) Wang, S.-S. *J. Am. Chem. Soc.* **1973**, *95* (4), 1328–1333.

(22) Rodebaugh, R.; Fraser-Reid, B.; Mario Geysen, H. *Tetrahedron Lett.* **1997**, *38* (44), 7653–7656.

(23) Hammer, R. P.; Albericio, F.; Gera, L.; Barany, G. *Int. J. Pept. Protein Res.* **1990**, *36* (1), 31–45.

(24) Suntornchashwej, S.; Chaichit, N.; Isobe, M.; Suwanborirux, K. *J. Nat. Prod.* **2005**, *68* (6), 951–955.

(25) Wijtmans, R.; Vink, M. K. S.; Schoemaker, H. E. et al. *Synthesis (Stuttg).* **2004**, *2004* (5), 641–662.

(26) Carr, G.; Williams, D. E.; Diaz-Marrero, A. R.; et al. *J. Nat. Prod.* **2010**, *73* (3), 422–427.

(27) Davis, R. A.; Duffy, S.; Fletcher, S. et al. *J. Org. Chem.* **2013**, *78* (19), 9608–9613.

(28) Gardelli, C.; Nizi, E.; Muraglia, E.; Crescenzi, B. et al. *J. Med. Chem.* **2007**, *50* (20), 4953–4975.

(29) Bryan, D. B.; Hall, R. F.; Holden, K. G. et al. *J. Am. Chem. Soc.* **1977**, *99* (7), 2353–2355.

(30) McGuire R.G. A4 - Dimitroglou, D.A., R. G. A.-M. *Biocontrol. Sci. Techn.* **1999**, *9* (1), 53-65.

(31) Hanawalt, J. D.; Rinn, H. W.; Frevel, L. K. **1938**, *10* (9), 457–512.

(32) Ohlow, M. J.; Moosmann, B. *Drug Discov. Today* **2011**, *16* (3–4), 119–131.

(33) Moellering, R. C. *Ann. Intern. Med.* **2003**, *138* (2), 135–142.
(34) Ahmadi, A.; Khalili, M.; Hajikhani, R.; Naserbakht, M. *Pharmacol. Biochem. Behav.* **2011**, *98* (2), 227–233.
(35) Moss, M. L.; Sklair-Tavron, L.; Nudelman, R. *Nat. Clin. Pr. Rheumatol.* **2008**, *4* (6), 300–309.
(36) Fülöpová, V.; Krchňák, V. *ACS Comb. Sci.* **2014**, *16* (8), 412–420.
(37) Schutznerova, E.; Krchnak, V. *ACS Comb. Sci.* **2015**, *17* (2), 137–146.
(38) Králová, P.; Maloň, M.; Volná, T.; Ručilová, V.; Soural, M. *ACS Comb. Sci.* **2017**, *19* (10), 670–674.
(39) Králová, P.; Maloň, M.; Soural, M. *ACS Comb. Sci.* **2017**, *19* (12), 770–774.
(40) Ručilová, V.; Králová, P.; Soural, M. *Eur. J. Org. Chem.* **2017**, *2017* (47), 7034–7039.
(41) Králová, P.; Benická, S.; Soural, M. *ACS Comb. Sci.* **2019**, *21* (3), 154–157.
(42) Králová, P.; Maloň, M.; Koshino, H.; Soural, M. *Molecules* **2018**, *23* (4), 976–984.
(43) Králová, P.; Soural, M. *ACS Comb. Sci.* **2018**, *20* (8), 467–471.
(44) Bezanson, M.; Pottel, J.; Bilbeisi, R. et al. *J. Org. Chem.* **2013**, *78* (3), 872–885.
(45) Ghosh, P.; Deka, M. J.; Saikia, A. K. *Tetrahedron* **2016**, *72* (5), 690–698.
(46) Kumar, D.; Sundaree, S.; Patel, G.; Rao, V. S. A *Tetrahedron Lett.* **2008**, *49* (5), 867–869.
(47) Popovici, D.; Maior, O.; Schiketanz, A. R.; Balaban, A. T. *Analele Univ. Bucuresti, Chim.* **2000**, *9*, 75–81.
(48) Bigot, A.; Blythe, J.; Pandya, C.; Wagner, T.; Loiseleur, O. *Org. Lett.* **2011**, *13* (2), 192–195.
(49) Koshelev, V. M.; Vasil'ev, N. V; Gontar, A. F. US 1648947 A1, May 15, **1991**.
(50) Metze, R. 1,2,4-Triazines. VIII. *Chem. Ber.* **1958**, *91*, 1863–1866.
(51) Anselmi, C.; Camparini, A.; Scotton, M. *J. Heterocycl. Chem.* **1983**, *20* (3), 687–689.
(52) Pudelová, N.; Krchňák, V. *J. Comb. Chem.* **2009**, *11* (5), 851–859.
(53) Miller, P. C.; Owen, T. J.; Molyneaux, J. M. et al. *J. Comb. Chem.* **1999**, *1* (3), 223–234.
(54) Fülöpová, V.; Cziesla, L.; Fleming, M.; Lu, Y.; Voelker, A.; Krchňák, V. *ACS Comb. Sci.* **2015**, *17* (8), 470–473.
(55) Hamdan, F.; Tahoori, F.; Balalaie, S. *RSC Adv.* **2018**, *8* (59), 33893–33926.
(56) Pudelová, N.; Krchňák, V. *J. Comb. Chem.* **2009**, *11* (3), 370–374.
(57) Mjalli, A. M. M. WO 2000023487 A1., April 27, **2000**.
(58) Kočí, J.; Pudelová, N.; Krchňák, V. *J. Comb. Chem.* **2009**, *11* (3), 397–402.
(59) Garcia, J.; Mata, E. G.; Tice, C. M.; Hormann, R. E. et al. *J. Comb. Chem.* **2005**, *7* (6), 843–863.
(60) Tice, C. M.; Michelotti, E. L.; Mata, E. G. et al. *Tetrahedron Lett.* **2002**, *43* (42), 7491–7494.
(61) Pulici, M.; Quartieri, F.; Felder, E. R. *J. Comb. Chem.* **2005**, *7* (3), 463–473.
(62) Arutyunyan, S.; Nefzi, A. *J. Comb. Chem.* **2010**, *12* (3), 315–317.
(63) Murru, S.; Nefzi, A. *ACS Comb. Sci.* **2014**, *16* (1), 39–45.
(64) Wallace, O. B. *Tetrahedron Lett.* **1997**, *38* (28), 4939–4942.
(65) Dinh, T. Q.; Armstrong, R. W. *Tetrahedron Lett.* **1996**, *37* (8), 1161–1164.
(66) Lalli, C.; Trabocchi, A.; Sladojevich, F. et al. *Chem. Eur. J.* **2009**, *15* (32), 7871–7875.
(67) Humphrey, J. M.; Chamberlin, A. R. *Chem. Rev.* **1997**, *97* (6), 2243–2266.

(68) Garcia, J.; Nicolàs, E.; Albericio, F.; Michelotti, E. L.; Tice, C. M. *Tetrahedron Lett.* **2002**, *43* (42), 7495–7498.
(69) Vlattas, I.; Dellureficio, J.; Dunn, R.; Sytwu, I. I. et al. *Tetrahedron Lett.* **1997**, *38* (42), 7321–7324.
(70) Camarero, J. A.; Adeva, A.; Muir, T. W. *Lett. Pept. Sci.* **2000**, *7* (1), 17–21.
(71) Solmaz, R.; Kardaş, G. *Prog. Org. Coat.* **2009**, *64* (1), 81–88.
(72) Leznoff, C.; Fyles, T.; Weatherston, J. *Can. J. Chem.* **2011**, *55*, 1143–1153.
(73) Cheng, J. F.; Chen, M.; Nadzan, A. M. WO 2002034728 A1, **2002**.
(74) Schunk, S.; Enders, D. *Org. Lett.* **2001**, *3* (20), 3177–3180.
(75) Ručilová, V.; Maloň, M.; Soural, M. *Eur. J. Org. Chem.* **2018**, *2018* (4), 564–570.
(76) Meldal, M. *Tetrahedron Lett.* **1992**, *33* (21), 3077–3080.
(77) Strohmeier, G. A.; Kappe, C. O. *Angew. Chem. Int. Ed.* **2004**, *43* (5), 621–624.
(78) Fülöpová, V.; Krchňáková, A.; Schütznerová, E.; Zajíček, J.; Krchňák, V. *J. Org. Chem.* **2015**, *80* (3), 1795–1801.
(79) Lee, T.; Park, J.-H.; Jeon, M.-K.; Gong, Y.-D. *J. Comb. Chem.* **2009**, *11* (2), 288–293.
(80) Bouillon, I.; Zajíček, J.; Pudelová, N.; Krchňák, V. *J. Org. Chem.* **2008**, *73* (22), 9027–9032.
(81) Křupková, S.; Slough, G. A.; Krchňák, V. *J. Org. Chem.* **2010**, *75* (13), 4562–4566.
(82) Králová, P. Solid-Phase Synthesis of Some Novel Benzo[1,4]Diazepin-5-One Derivates. The Bachelor Thesis, Palacký University Olomouc, **2014**.
(83) Kočí, J.; Krchňák, V. *J. Comb. Chem.* **2010**, *12* (1), 168–175.
(84) Komnatnyy, V. V; Givskov, M.; Nielsen, T. E. *Chem. Eur. J.* **2012**, *18* (52), 16793–16800.
(85) Trabocchi, A.; Menchi, G.; Guarna, F.; Machetti, F.; Scarpi, D.; Guarna, A. *Synlett* **2006**, *2006* (03), 331–353.
(86) Kaplánek, R.; Krchňák, V. *Tetrahedron Lett.* **2013**, *54* (21), 2600–2603.
(87) Carminati, P.; Gallo, G.; Fanto', N.; Ruggiero, V. et al. US 20080064643 A1, June 29, **2006**.
(88) Montalbetti, C.; Falque, V. *Tetrahedron* **2005**, *61*, 10827–10852.
(89) Stein, R. L. *Adv. Protein. Chem.*; Anfinsen, C. B. et al. Eds.; Academic Press, **1993**; 44, 1–24.
(90) Trapani, P.; Volná, T.; Soural, M. *ACS Comb. Sci.* **2016**, *18* (6), 349–354.
(91) McMaster, C.; Fülöpová, V.; Popa, I.; Grepl, M.; Soural, M. *ACS Comb. Sci.* **2014**, *16* (5), 221–224.
(92) Messina, I.; Popa, I.; Maier, V.; Soural, M. *ACS Comb. Sci.* **2014**, *16* (1), 33–38.
(93) Drábiková, M.; Krajčovičová, S.; Soural, M. *Tetrahedron* **2017**, *73* (44), 6296–6306.
(94) Lee, D.; Lee, S.; Liu, K.-H.; Bae, J.-S.; Baek, D. J.; Lee, T. *ACS Comb. Sci.* **2016**, *18* (1), 70–74.
(95) Lukasik, P. M.; Elabar, S.; Lam, F.; Shao, H. et al. *Eur. J. Med. Chem.* **2012**, *57*, 311–322.
(96) Králová, P.; Maloň, M.; Pospíšil, J.; Soural, M. *J. Org. Chem.* **2020**, *85* (2), 985–993.
(97) Beesley, R. M.; Ingold, C. K.; Thorpe, J. F. *J. Chem. Soc., Perkin Trans. 1*. **1915**, *107*, 1080–1106.
(98) Paraskar, A. S.; Sudalai, A. *Tetrahedron* **2006**, *62* (24), 5756–5762.
(99) Mojr, V.; Svobodová, E.; Strakova, K.; Neveselý, T. et al. *Chem. Commun.* **2015**, *51*, 12036–12039.
(100) Filira, F.; Biondi, B.; Biondi, L.; Giannini, E. et al. *Org. Biomol. Chem.* **2003**, *1* (17), 3059–3063.
(101) Zwick, C. R.; Renata, H. *Tetrahedron* **2018**, *74* (45), 6469–6473.

7. APPENDICES

7.1 List of publications

Appendix A (144 – 151)

Králová, P.; Fülöpová, V.; Maloň, M.; Volná, T.; Popa, I.; Soural, M. *ACS Comb. Sci.* **2017**, 19 (3), 173–180.

Appendix B (152 – 166)

Králová, P.; Ručilová, V.; Soural, M. *ACS Comb. Sci.* **2018**, *20* (9), 529–543.

Appendix C (167 – 171)

Králová, P.; Maloň, M; Ručilová, V.; Volná, T.; M.; Soural, M. *ACS Comb. Sci.* 2017, *19* (10), 670–674.

Appendix D (172 – 176)

Králová, P.; Maloň, M; Soural, M. *ACS Comb. Sci.* **2017**, *19* (12), 770–774.

Appendix E (177 – 182)

Ručilová, V.; Králová, P.; Soural, M. *Eur. J. Org. Chem.* **2017**, *2017* (47), 7034–7039.

Appendix F (183 – 186)

Králová, P.; Benická, S.; Soural, M. *ACS Comb. Sci.* **2019**, *21* (3), 154–157.

Appendix G (187 – 194)

Králová, P.; Maloň, M.; Koshino, H.; Soural, M. *Molecules* **2018**, *23* (4), 976–984.

Appendix H (195 – 199)

Králová, P.; Soural, M. *ACS Comb. Sci.* **2018**, *20* (8), 467–471.

Appendix I (200 – 208)

Králová, P.; Maloň, M; Pospíšil, J.; Soural, M. *J. Org. Chem.* **2020**, *85* (2), 985–993.

ACS Combinatorial Science

Research Article

pubs.acs.org/acscombsci

Stereoselective Polymer-Supported Synthesis of Morpholine- and Thiomorpholine-3-carboxylic Acid Derivatives

Petra Králová,[†,∥] Veronika Fülöpová,[‡,∥] Michal Maloň,[§] Tereza Volná,[†] Igor Popa,[†] and Miroslav Soural*[,‡]

[†]Department of Organic Chemistry, Faculty of Science, Palacký University, 17. listopadu 12, 771 46 Olomouc, Czech Republic

[‡]Institute of Molecular and Translation Medicine, Faculty of Medicine and Dentistry, Palacký University, Hněvotínská 5, 779 00 Olomouc, Czech Republic

[§]JEOL Resonance Inc., Musashino 3-1-2, Akishima, Tokyo 196-8558, Japan

Supporting Information

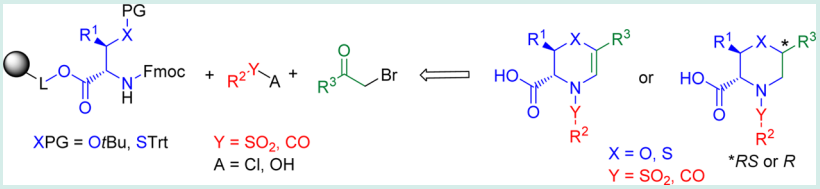

ABSTRACT: Herein we report the polymer-supported synthesis of 3,4-dihydro-2*H*-1,4-oxazine-3-carboxylic acid derivatives using immobilized Fmoc-Ser(*t*Bu)-OH and Fmoc-Thr(*t*Bu)-OH as the starting materials. After the solid-phase-synthesis of *N*-alkyl-*N*-sulfonyl/acyl intermediates, the target dihydrooxazines were obtained using trifluoroacetic acid-mediated cleavage from the resin. This approach was also studied for the preparation of dihydrothiazines from immobilized Fmoc-Cys(Trt)-OH. Inclusion of triethylsilane in the cleavage cocktail resulted in the stereoselective formation of the corresponding morpholine/thiomorpholine-3-carboxylic acids. Stereochemical studies revealed the specific configuration of the newly formed stereocenter and also the formation of stable *N*-acylmorpholine rotamers.

KEYWORDS: *amino acid, bromoketone, morpholine, thiazine, thiomorpholine, oxazine, nitrobenzenesulfonyl chloride, solid-phase synthesis, stereoselective synthesis*

INTRODUCTION

Aliphatic six-membered heterocyclic rings are frequently occurring structural motifs in both synthetic and natural drugs. In this context, the most common motifs are piperazines followed by morpholine derivatives. Morpholine and thiomorpholine scaffolds can be found in a broad array of biologically active compounds[1−9] with applications in industrial,[10] agricultural,[11,12] and pharmaceutical fields.[13−17] The specific class of (thio)morpholine derivatives is represented by compounds bearing the carbonyl group at the C^3 position (Figure 1).

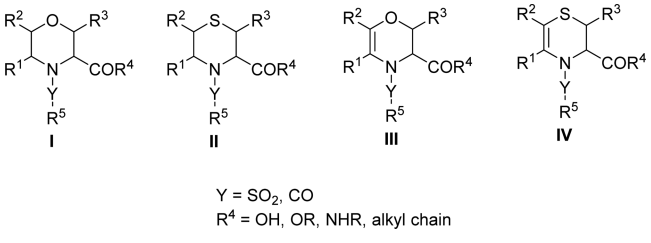

Figure 1. Morpholine and thiomorpholine compounds resembling the target scaffolds.

Derivatives **I** (Y = SO_2, CO), **II** (Y = SO_2, CO), and **III** (Y = CO) have been studied in medicinal chemistry as potential inhibitors of tumor necrosis factor α converting enzyme (TACE), tumor necrosis factor (TNF),[18−20] thrombin,[21] and matrix metalloproteinases (MMPs).[22−24] The specific derivatives **I** (Y = SO_2) and **II** (Y = SO_2) also act as agonists of the very late antigen (VLA-4)[25] and as drugs for the potential treatment of neurodegenerative diseases.[26] In contrast, the biological properties of compounds **III** (Y = SO_2) and **IV** (Y = SO_2, CO) have not been reported, and only a few articles on their synthesis have been published.[27−31]

Previous reports have described the preparation of the scaffolds depicted in Figure 1 using traditional solution-phase chemistry and various methods such as (i) direct cyclization of suitable linear intermediates,[19,32−36] (ii) heterocycle formation followed by substitution of the nitrogen atom,[37−40] and (iii) heterocycle formation and subsequent reduction or elimination to yield the desired saturated/unsaturated analogues.[22,41,42] The selection of a suitable approach (i)−(iii) depends on the type of scaffold being made. With this in mind, we have been searching for a general synthetic strategy for all of the scaffolds. Recent research on the solid-phase synthesis of thiadiazepine

Received: November 30, 2016
Revised: January 10, 2017
Published: January 13, 2017

DOI: 10.1021/acscombsci.6b00178
ACS Comb. Sci. 2017, 19, 173−180

1,1-dioxides[28] showed that polymer-supported O-protected *N*-sulfonylserine underwent acid-mediated cyclization, leading to the formation of the dihydro-1,4-oxazine scaffold **III**. This reaction inspired us to develop a general method that is applicable for the preparation of variously substituted compounds **I**–**IV** simply by changing the building blocks and reagents. Herein we report the optimization of the reaction conditions, the limitations and scope of the method, and detailed stereochemical studies of the final compounds to determine their absolute and geometric configurations.

RESULTS AND DISCUSSION

The general solid-phase synthesis of *N*-sulfonylmorpholine/thiomorpholine-3-carboxylic acid derivatives is displayed in Scheme 1. To verify the synthetic route, we employed Wang resin and three representative building blocks included in Figure 2: Fmoc-Ser(*t*Bu)-OH, 4-nitrobenzenesulfonyl chloride (NsCl), and 2-bromo-4′-methylacetophenone. After immobilization of Fmoc-Ser(*t*Bu)-OH and cleavage of the Fmoc protecting group, the intermediate **3**(*1*) was protected/activated by sulfonylation with NsCl according to a previously published procedure.[43] Subsequent Fukuyama monoalkylation[44] of the corresponding sulfonamide **4**(*1,1*) with 2-bromo-4′-methylacetophenone provided the intermediate **5**(*1,1,1*) with excellent crude purity of 92% as measured by LC-UV traces at 205–400 nm after cleavage from the resin (the purity was determined as a sum of compounds **5** and partially cyclized products **6**). Quantitative conversion to the product **6**(*1,1,1*) was observed after longer exposure to the cleavage cocktail. Alternatively, addition of triethylsilane (TES) to the cleavage cocktail resulted in the formation of morpholine **7**(*1,1,1*). Both compounds were isolated with excellent crude purity (82% and 93%, respectively) after cleavage from the polymer support and in good overall yield (46% and 90%) after reversed-phase semipreparative HPLC purification.

Encouraged by these results, we tested the applicability of this synthetic route to the preparation of *N*-acyl analogues (Scheme 2). In the first step of this route, the nosyl group was cleaved from resin **5**(*1,1,1*). The resulting secondary amine **8**(*1,H,1*) was acylated using various reagents (Figure 2, R^2, building blocks 5–10) under different conditions (see the Supporting Information) with high conversion ranging from 73% to 85% as measured by LC-UV traces at 205–400 nm after cleavage from the resin. The purity was determined as a sum of compounds **9** and partially cyclized products **10**. In the case of Fmoc-Gly-OH, the purity was only 34% employing activation with *N*,*N*′-diisopropylcarbodiimide (DIC), and therefore, the corresponding product **10**(*1,8,1*) was finally not prepared. The acid-mediated cleavage with trifluoroacetic acid (TFA)/dichloromethane (DCM) or TFA/TES/DCM gave products **10**(*1*,R^2,*1*) or **11**(*1*,R^2,*1*), respectively, which were obtained with acceptable crude purity and overall yield (Table 1).

To determine the scope and limitations of our method, we selected diverse building blocks bearing both electron-withdrawing and electron-donating substituents (Figure 2). First, we performed the sulfonylation of intermediate **3**(*1*) with various sulfonyl chlorides (Figure 2, R^2, building blocks 2–4). For all of these reagents, the reaction yielded compounds **4**(*1*,R^2) with good crude purity (56–92%, LC-UV traces at 205–400 nm). However, the subsequent alkylation step was difficult for bromoacetophenones bearing *p*-Me and *p*-OMe groups. In addition, the alkylation of **4**(*1,2*) with 4′-amino-2-bromo-3′,5′-dichloroacetophenone resulted in a mixture of compound **5**(*1,2,3*) and an unknown byproduct (30%, LC-UV traces at 205–400 nm) that was unstable under semipreparative HPLC conditions. To suppress the formation of the byproduct, the concentration of the base was decreased from 3.0 to 1.5 mM (for the detailed procedure, see the Supporting Information). Additionally, we found that the sulfonamide **4**(*1,4*) was resistant to alkylation.

We also attempted to synthesize carboxamides by using polymer-supported amines different from Wang resin (Scheme 3).

Scheme 1. Synthesis of *N*-Sulfonyl Derivatives[a]

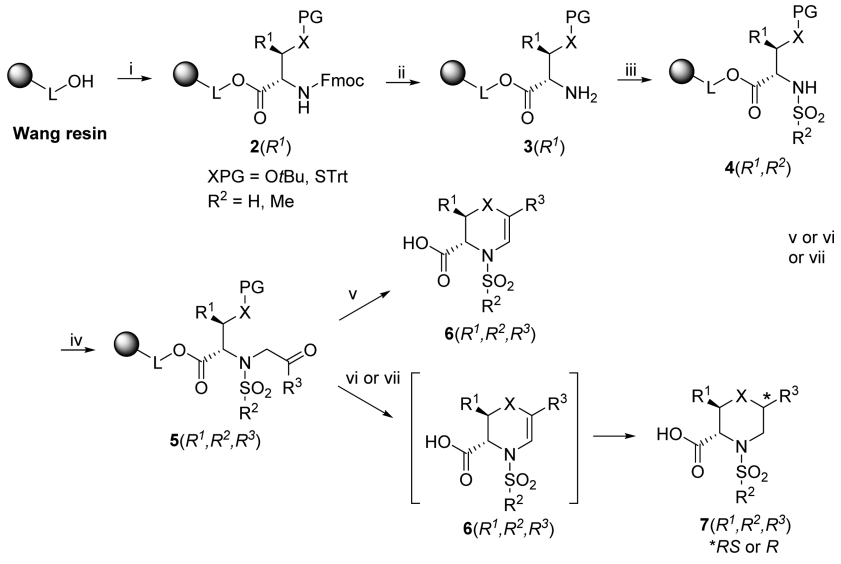

[a]Reagents and conditions: (i) Fmoc-amino acid, HOBt, DMAP, DIC, DMF, DCM, 24 h, rt; (ii) 50% piperidine/DMF, 30 min, rt; (iii) sulfonyl chloride, 2,6-lutidine, DCM, 24 h, rt; (iv) 2-bromoacetophenone, DIEA, DMF, 24 h, rt; (v) 50% TFA/DCM, 24 h, rt (for serine, threonine derivatives and for **6**(*2,3,2*)) or 25% TFA/DCM, 24 h, rt (for **6**(*1,1,S*)) or neat TFA (for cysteine derivatives), 6–9 h, rt; (vi) TFA/TES/DCM (10:1:9), 5–8 h, rt; (vii) 50% TFA/DCM, 24 h, rt, then TES, 1 h, rt.

DOI: 10.1021/acscombsci.6b00178
ACS Comb. Sci. 2017, 19, 173–180

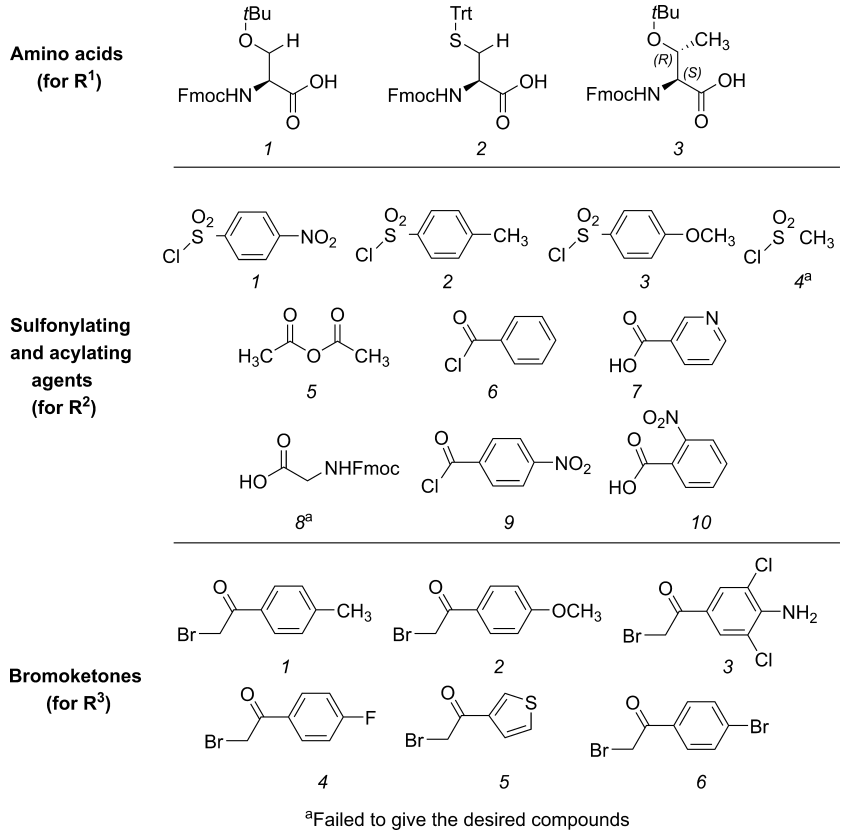

Figure 2. List of tested building blocks.

Scheme 2. Synthesis of *N*-Acyl Derivatives[a]

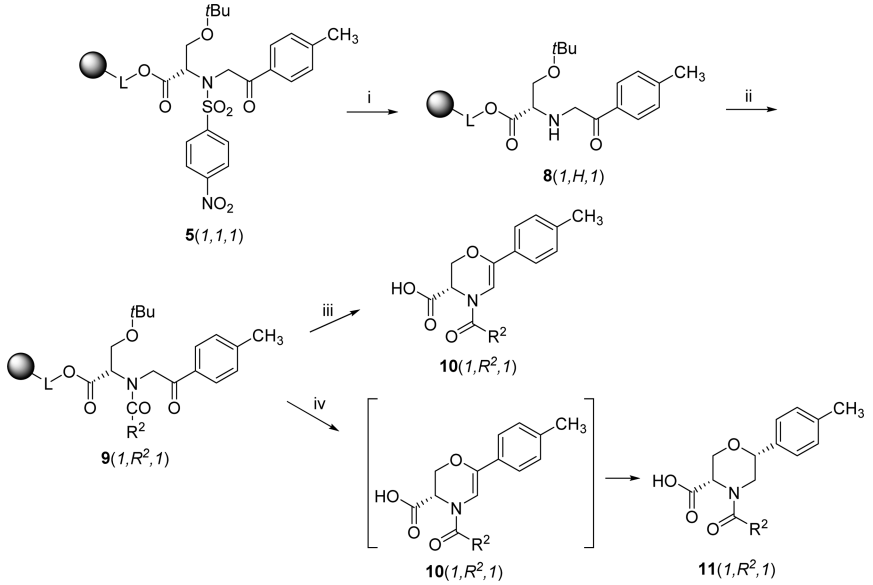

[a]Reagents and conditions: (i) mercaptoethanol, DBU, DMF, 30 min, rt; (ii) acylating agent, DIC or 2,6-lutidine, DMF or DCM, 24 h, rt; (iii) 50% TFA/DCM, 24 h, rt; (iv) TFA/TES/DCM (10:1:9), 7 h, rt.

When intermediate $\mathbf{4}^{\mathbf{WP}}(1,1)$ made from Wang-piperazine resin was alkylated with 4′-methylbromoacetophenone followed by the TFA cleavage, the expected final product $\mathbf{12}(1,1,1)$ was obtained in high crude purity (75%, LC-UV traces at 205−400 nm). In contrast, the alkylations of $\mathbf{4}^{\mathbf{RA}}(1,1)$ made from Rink-amide resin and $\mathbf{4}^{\mathbf{BAL}}(1,1)$ made from BAL resin with immobilized propylamine led to the formation of unknown compounds (45−51%, LC-UV traces at 205−400 nm). The molecular masses obtained from LC−MS traces corresponded to the C/N-arylated products, as reported previously by Krchňák for similar nitrobenzenesulfonamides.[43,45] Despite our efforts to optimize the reaction conditions by changing the base or temperature or by using the microwave reactor, the desired products were not prepared.

DOI: 10.1021/acscombsci.6b00178
ACS Comb. Sci. 2017, 19, 173−180

Table 1. List of Synthesized Morpholine/Thiomorpholine-3-carboxylic Acid Derivatives

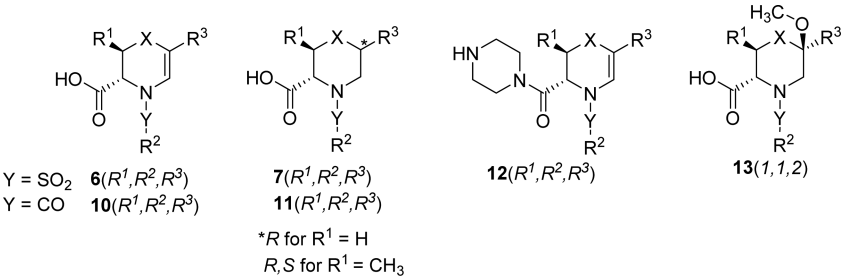

compd	X	Y	R^1	R^2	R^3	purity [%] crude[a]	purity [%] final[b]	yield [%][c]
6(*1,1,1*)	O	SO_2	H	4-NO_2-Ph	4-Me-Ph	82	99	46
6(*1,1,2*)	O	SO_2	H	4-NO_2-Ph	4-OMe-Ph	51	97	40
6(*1,1,3*)	O	SO_2	H	4-NO_2-Ph	3,5-Cl_2-4-NH_2-Ph	72	97	82
6(*1,1,4*)	O	SO_2	H	4-NO_2-Ph	4-F-Ph	81	99	44
6(*1,1,5*)	O	SO_2	H	4-NO_2-Ph	thiophen-3-yl	92	99	96
6(*2,1,1*)	S	SO_2	H	4-NO_2-Ph	4-Me-Ph	98	99	83
6(*2,1,2*)	S	SO_2	H	4-NO_2-Ph	4-OMe-Ph	69	99	30
6(*3,1,1*)	O	SO_2	Me	4-NO_2-Ph	4-Me-Ph	60	90	41
6(*1,2,3*)	O	SO_2	H	4-Me-Ph	3,5-Cl_2-4-NH_2-Ph	72	97	40
6(*1,2,4*)	O	SO_2	H	4-Me-Ph	4-F-Ph	73	99	52
6(*1,2,6*)	O	SO_2	H	4-Me-Ph	4-Br-Ph	92	99	44
6(*1,3,1*)	O	SO_2	H	4-OMe-Ph	4-Me-Ph	79	98	51
6(*1,3,4*)	O	SO_2	H	4-OMe-Ph	4-F-Ph	65	98	50
6(*2,3,2*)	S	SO_2	H	4-OMe-Ph	4-OMe-Ph	56	99	72
6(*2,3,4*)	S	SO_2	H	4-OMe-Ph	4-F-Ph	81	99	50
7(*1,1,1*)	O	SO_2	H	4-NO_2-Ph	4-Me-Ph	93	99	90
7a(*3,1,1*)	O	SO_2	Me	4-NO_2-Ph	4-Me-Ph	49	99	22
7b(*3,1,1*)	O	SO_2	Me	4-NO_2-Ph	4-Me-Ph	43	99	20
7(*1,2,4*)	O	SO_2	H	4-Me-Ph	4-F-Ph	72	97	72
7(*1,1,4*)	O	SO_2	H	4-NO_2-Ph	4-F-Ph	75	95	80
10(*1,5,1*)	O	CO	H	Me	4-Me-Ph	57	98	50
10(*1,6,1*)	O	CO	H	Ph	4-Me-Ph	91	99	21
10(*1,7,1*)	O	CO	H	pyridin-3-yl	4-Me-Ph	48	97	32
10(*1,9,1*)	O	CO	H	4-NO_2-Ph	4-Me-Ph	52	99	51
10(*1,10,1*)	O	CO	H	2-NO_2-Ph	4-Me-Ph	72	99	72
11(*1,6,1*)	O	CO	H	Ph	4-Me-Ph	88	99	45
12(*1,1,1*)	O	SO_2	H	4-NO_2-Ph	4-Me-Ph	75	99	63
13(*1,1,2*)	O	SO_2	H	4-NO_2-Ph	4-OMe-Ph	43	98	68

[a]HPLC-UV (205−400 nm). [b]HPLC-UV after purification (205−400 nm). [c]Overall yields after purification, calculated from ^{1}H NMR analyses.

The final cyclization using 50% TFA in DCM for 24 h was applicable for morpholines **6**(*1,*R^2,R^3) and **6**(*3,1,1*) and for thiomorpholine **6**(*2,3,2*), whereas the quantitative ring closure of thiomorpholines **6**(*2,*R^2,R^3) was achieved with neat TFA for 6−9 h. In the case of the reduced morpholines **7**(R^1,R^2,R^3), 10% TES was either included directly in the cleavage cocktail or added to the cleavage cocktail after 24 h (for the detailed procedure, see the Supporting Information). We also tested the reduction method to prepare saturated thiomorpholines (Scheme 4), but an inseparable mixture of **6**(*2,1,1*) and **7**(*2,1,1*) was recovered. In the case of intermediate **5**(*3,1,1*) made from threonine, the cyclization and reduction afforded two separable compounds that were identified as C^6 epimers (Scheme 5) (see the stereochemical studies later in the text).

To perform the semipreparative HPLC purification, the cleaved products **6**(R^1,*1,*R^3) were initially dissolved in MeOH. However, LC−MS analysis revealed instability of some cysteine derivatives **6**(*2,*R^2,R^3) resulting in decomposition that was probably triggered by residual TFA. We also detected partial conversion of morpholines **6**(*1,1,*R^3) to the corresponding ketals **13**(*1,1,*R^3) (Scheme 6). This fact was confirmed by the two-dimensional (2D) NMR structure elucidation of isolated compound **13**(*1,1,2*) (see the Supporting Information). The formation of ketals (>60%, LC-UV traces at 205−400 nm) was also observed for derivatives bearing electron-donating substituents at the para position (R^2 = 4-OMe-Ph, 4-NH_2-3,5-Cl_2-Ph) as a consequence of increased olefin reactivity. In the case of the 4-fluorophenyl group, only a 10% yield of **13**(*1,1,4*) was detected. Interestingly, the formation of **13**(*1,1,2*) was fully stereoselective, which makes the reaction applicable for the preparation of analogous (6*R*)-ketals **13** by the use of different alcohols. To avoid undesirable structural changes in the cleaved products, we replaced MeOH with a mixture of MeCN in water (1:1). This mixture was applied to dissolve all of the prepared compounds, including **10**(*1,*R^3,*1*) and **11**(*1,6,1*).

Although we began the synthetic route with enantiomerically pure *α*-amino acids (L isomers), we considered possible

DOI: 10.1021/acscombsci.6b00178
ACS Comb. Sci. 2017, 19, 173−180

Scheme 3. Attempts To Synthesize the Corresponding Carboxamides (See Scheme 1 for Reaction Conditions)

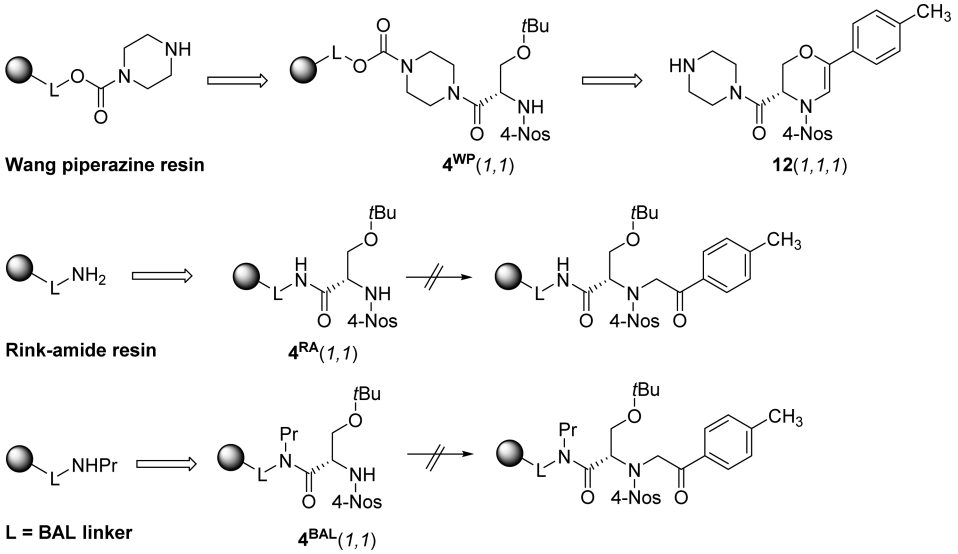

Scheme 4. Nonquantitative Conversion of 5(2,1,1) to 7(2,1,1)[a]

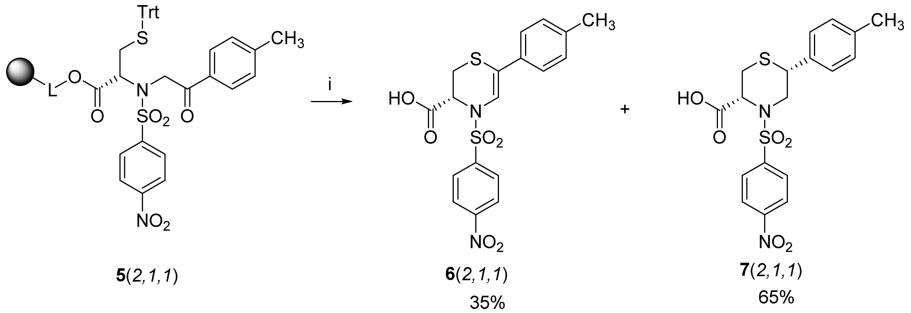

[a]Reagents and conditions: (i) TFA/TES/DCM (10:1:9), 8 h, rt.

Scheme 5. Formation of Diastereomers 7a(3,1,1) and 7b(3,1,1)[a]

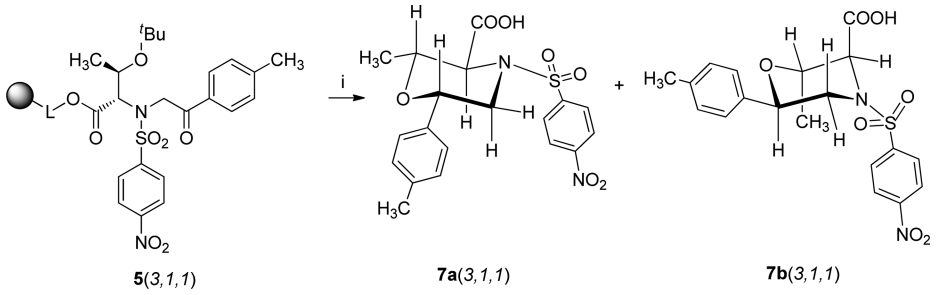

[a]Reagents and conditions: (i) TFA/TES/DCM (10:1:9), 8 h, rt.

racemization within the reaction sequence. In our recent articles, we demonstrated that the original configuration is maintained if the amino acid is immobilized using the HOBt/DIC coupling strategy.[46,47] In contrast, full[47,48] or partial[47,49] racemization of the α-amino acid stereocenter can occur during the following reaction sequence. To reveal possible racemization, we studied the resulting configuration of the C^3 stereocenter. For this study, we selected two representative products, **6**(*1,1,1*) and **10**(*1,6,1*). For both compounds, we synthesized the corresponding racemic standards $\mathbf{6}^{RS}$(*1,1,1*) and $\mathbf{10}^{RS}$(*1,6,1*) using racemic Fmoc-Ser(*t*Bu)-OH as the starting material. Compounds **6**(*1,1,1*) and **10**(*1,6,1*) were analyzed by chiral supercritical fluid chromatography (SFC), and as can be clearly concluded from the SFC-UV traces (see Figure 3 and 4), the C^3 stereocenter underwent only negligible conversion (up to 5%) in both cases. To evaluate the quality of the starting material, we also tested the enantiomeric purity of Fmoc-Ser(*t*Bu)-OH. However, the absence of its *R* isomer (see the Supporting Information) proved that the *R* isomers of **6**(*1,1,1*) and **10**(*1,6,1*) appeared during the reaction sequence, presumably during the immobilization on Wang resin.

Next, using the known C^3 configuration as the reference point and 2D NMR experiments (ROESY; see the Supporting Information), we determined the configuration of the C^6 stereocenter in morpholine **7**(*1,1,1*) and thiomorpholine **7**(*2,1,1*) as 6*R*. In the case of the two epimers separated after the cyclization

DOI: 10.1021/acscombsci.6b00178
ACS Comb. Sci. 2017, 19, 173−180

Scheme 6. Conversion of the Final Products into the Compounds 13(*1,1,R*^{3})[a]

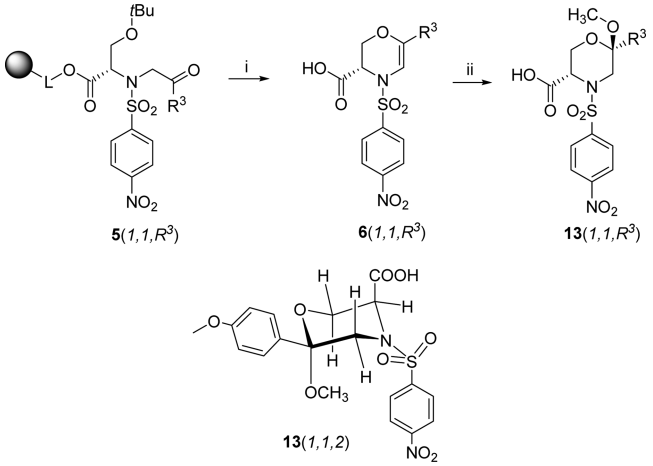

[a]Reagents and conditions: (i) 50% TFA/DCM, 24 h, rt; (ii) MeOH.

and reduction of intermediate **5**(*3,1,1*) (Scheme 4), the NMR elucidation confirmed the formation of the 2*R*,6*S* product **7a**(*3,1,1*) and the 2*R*,6*R* product **7b**(*3,1,1*) (Figure 5). From the stereochemical studies, it can be concluded that the synthetic route gives the stereoselective formation of the newly introduced C^6 stereocenter for compounds synthesized from cysteine and serine. Similar stereoselectivity of TES/TFA reduction has been previously described and discussed for indole derivatives.[50] In contrast, the stereoselectivity is lost in the case of compounds with C^2-methyl substitution.

NMR studies of the *N*-acyl derivative **10**(*1,10,1*) revealed the presence of double signals in the ^{1}H NMR spectrum (Figure 6). This fact was explained by the formation of inseparable rotational isomers,[51,52] as previously observed for proline derivatives.[53] Further ^{1}H NMR and ROESY investigations of analogous *N*-acylmorpholines **10**(1,*R*^{3},*1*) confirmed the presence of "anti" and "syn" rotamers in different ratios at room temperature (Table 2). Increasing the temperature to 150 °C led to the gradual merging of the NMR signals, followed by their refragmentation at 25 °C (see the Supporting Information).

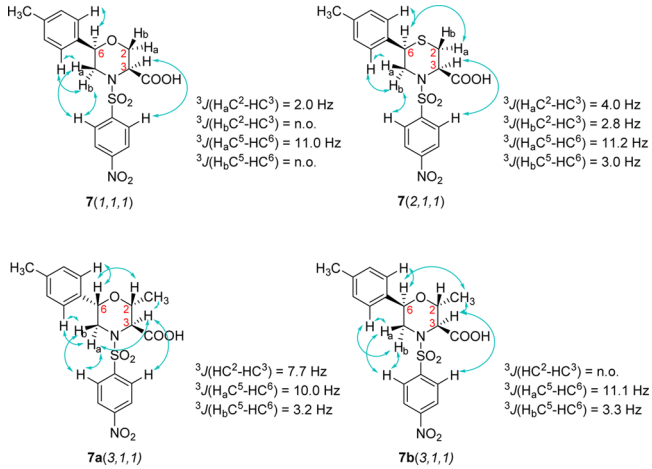

Figure 5. Configurations at C^2, C^3, and C^6 in the representative compounds 7(*1,1,1*), 7(*2,1,1*), and 7(3,1,1) with the selected ROESY correlations and vicinal coupling constants.

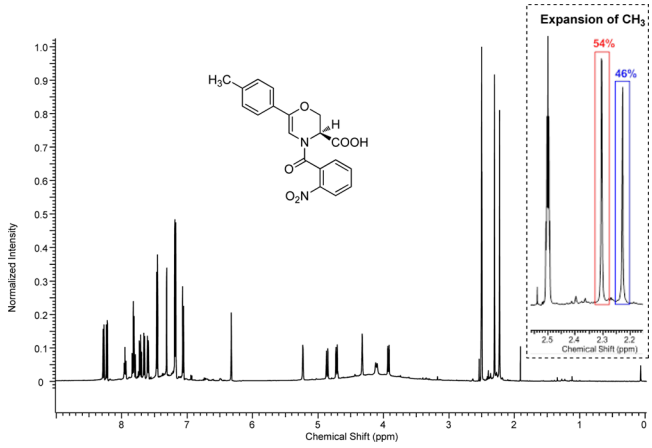

Figure 6. ^{1}H NMR spectrum of rotamers **10**(*1,10,1*).

CONCLUSION

We have introduced a simple and fast solid-phase synthesis strategy to prepare saturated and unsaturated morpholine/

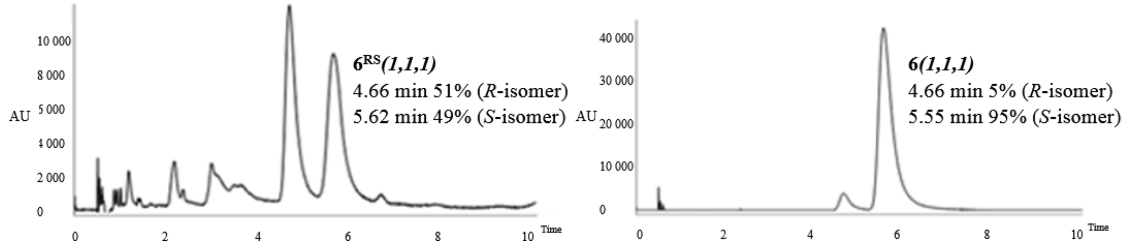

Figure 3. Chiral SFC separation of crude **6**^{RS}(*1,1,1*) and **6**(*1,1,1*).

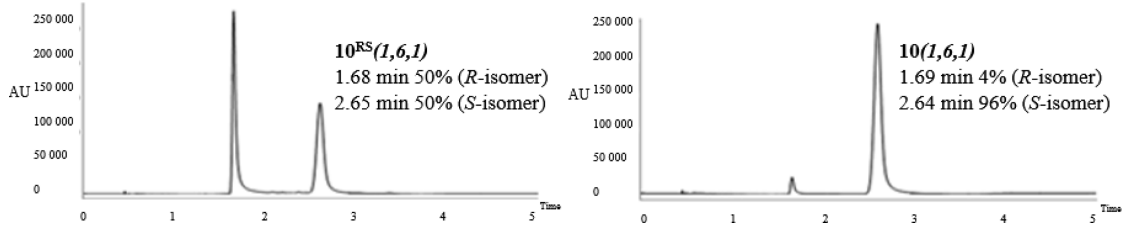

Figure 4. Chiral SFC separation of **10**^{RS}(*1,6,1*) and **10**(*1,6,1*).

DOI: 10.1021/acscombsci.6b00178
ACS Comb. Sci. 2017, 19, 173−180

Table 2. Ratios of "Anti" and "Syn" Rotamers Observed at Room Temperature

compd	R^2	anti:syn ratio[a]
10(*1,5,1*)	Me	57:43
10(*1,6,1*)	Ph	61:39
10(*1,7,1*)	pyridin-3-yl	55:45
10(*1,9,1*)	4-NO_2-Ph	35:65
10(*1,10,1*)	2-NO_2-Ph	54:46
11(*1,6,1*)	Ph	63:37

[a]Calculated from ^{1}H NMR analyses; "anti" and "syn" rotamers were assigned employing ROESY (see the Supporting Information).

thiomorpholine-3-carboxylic acid derivatives with three diversity positions. Only some minor limitations have been observed, and the developed method provided 28 final compounds in good overall yields. Full characterization of the target products, including the detailed determination of individual stereocenters and rotamers of *N*-acyl derivatives, was achieved using chiral SFC followed by NMR experiments. The developed protocols allow for the preparation of diverse enantiomerically pure target compounds using common coupling reagents and conditions and readily available building blocks. Further application of the method to prepare fused heterocycles is under development.

■ ASSOCIATED CONTENT

Supporting Information

The Supporting Information is available free of charge on the ACS Publications website at DOI: 10.1021/acscombsci.6b00178.

Details of experimental, synthetic, and analytical procedures along with spectroscopic data for synthesized compounds (PDF)

■ AUTHOR INFORMATION

Corresponding Author

*E-mail: miroslav.soural@upol.cz.

ORCID

Miroslav Soural: 0000-0001-7288-8617

Author Contributions

‖P.K. and V.F. contributed equally to this work.

Notes

The authors declare no competing financial interest.

■ ACKNOWLEDGMENTS

The authors are grateful to Project CZ.1.07/2.3.00/20.0009 from the European Social Fund and the National Program of Sustainability (Project LO1304).

■ REFERENCES

(1) Suntornchashwej, S.; Chaichit, N.; Isobe, M.; Suwanborirux, K. Hectochlorin and Morpholine Derivatives from the Thai Sea Hare, Bursatella Leachii. *J. Nat. Prod.* **2005**, *68* (6), 951−955.

(2) Wijtmans, R.; Vink, M. K. S.; Schoemaker, H. E.; van Delft, F. L.; Blaauw, R. H.; Rutjes, F. P. J. T. Biological Relevance and Synthesis of C-Substituted Morpholine Derivatives. *Synthesis* **2004**, *2004* (05), 641−662.

(3) Carr, G.; Williams, D. E.; Díaz-Marrero, A. R.; Patrick, B. O.; Bottriell, H.; Balgi, A. D.; Donohue, E.; Roberge, M.; Andersen, R. J. Bafilomycins Produced in Culture by Streptomyces spp. Isolated from Marine Habitats are Potent Inhibitors of Autophagy. *J. Nat. Prod.* **2010**, *73* (3), 422−427.

(4) Cavallini, D.; Ricci, G.; Dupre, S.; Pecci, L.; Costa, M.; Matarese, R. M.; Pensa, B.; Antonucci, A.; Solinas, S. P.; Fontana, M. Sulfur-Containing Cyclic Ketimines and Imino Acids: A Novel Family of Endogenous Products in the Search for a Role. *Eur. J. Biochem.* **1991**, *202*, 217−223.

(5) Davis, R. A.; Duffy, S.; Fletcher, S.; Avery, V. M.; Quinn, R. J. Thiaplakortones A-D: Antimalarial Thiazine Alkaloids from the Australian Marine Sponge Plakortis Lita. *J. Org. Chem.* **2013**, *78* (19), 9608−9613.

(6) Armani, E.; Amari, G.; Carzaniga, L.; Capaldi, C.; Esposito, O.; Villetti, G.; De, F. R. Derivatives of 1-Phenyl-2-pyridinyl Alkyl Alcohols as Phosphodiesterase Inhibitors. WO 2012168226 A1, Dec 13, 2012.

(7) Gardelli, C.; Nizi, E.; Muraglia, E.; Crescenzi, B.; Ferrara, M.; Orvieto, F.; Pace, P.; Pescatore, G.; Poma, M.; Rico Ferreira, M. d. R.; Scarpelli, R.; Homnick, C. F.; Ikemoto, N.; Alfieri, A.; Verdirame, M.; Bonelli, F.; Gonzalez Paz, O.; Taliani, M.; Monteagudo, E.; Pesci, S.; Laufer, R.; Felock, P.; Stillmock, K. A.; Hazuda, D.; Rowley, M.; Summa, V. Discovery and Synthesis of HIV Integrase Inhibitors: Development of Potent and Orally Bioavailable *N*-Methyl Pyrimidones. *J. Med. Chem.* **2007**, *50* (20), 4953−4975.

(8) Grisar, J. M. Novel Antihypertensive Agent. U.S. Patent 4,221,808 A, Sept 9, 1980.

(9) Bryan, D. B.; Hall, R. F.; Holden, K. G.; Huffman, W. F.; Gleason, J. G. Nuclear Analogs of β-Lactam Antibiotics. 2. The Total Synthesis of 8-Oxo-4-thia-1-azabicyclo[4.2.0]oct-2-ene-2-carboxylic Acids. *J. Am. Chem. Soc.* **1977**, *99* (7), 2353−2355.

(10) Amar, H.; Braisaz, T.; Villemin, D.; Moreau, B. Thiomorpholin-4-ylmethyl-phosphonic Acid and Morpholin-4-methyl-phosphonic Acid as Corrosion Inhibitors for Carbon Steel in Natural Seawater. *Mater. Chem. Phys.* **2008**, *110* (1), 1−6.

(11) McGuire, R. G.; Dimitroglou, D. A. Evaluation of Shellac and Sucrose Ester Fruit Coating Formulations that Support Biological Control of Post-Harvest Grapefruit Decay. *Biocontrol Sci. Technol.* **1999**, *9* (1), 53−65.

(12) Smith, L. E. Analysis of Commercial Phenothiazine Used as an Insecticide. *Ind. Eng. Chem., Anal. Ed.* **1938**, *10* (2), 60.

(13) Ohlow, M. J.; Moosmann, B. Phenothiazine: The Seven Lives of Pharmacology's First Lead Structure. *Drug Discovery Today* **2011**, *16* (3−4), 119−131.

(14) Zhou, D.; Harrison, B. L.; Shah, U.; Andree, T. H.; Hornby, G. A.; Scerni, R.; Schechter, L. E.; Smith, D. L.; Sullivan, K. M.; Mewshaw, R. E. Studies Toward the Discovery of the Next Generation of Antidepressants. Part 5:3,4-Dihydro-2*H*-benzo[1,4]oxazine Derivatives with Dual 5-HT1A Receptor and Serotonin Transporter Affinity. *Bioorg. Med. Chem. Lett.* **2006**, *16* (5), 1338−1341.

(15) Moellering, R. C. Linezolid: The First Oxazolidinone Antimicrobial. *Ann. Intern. Med.* **2003**, *138* (2), 135−142.

(16) Ahmadi, A.; Khalili, M.; Hajikhani, R.; Naserbakht, M. New Morpholine Analogues of Phencyclidine: Chemical Synthesis and Pain Perception in Rats. *Pharmacol., Biochem. Behav.* **2011**, *98* (2), 227−233.

(17) Kardile, D. P.; Kalyane, N. V. Synthesis and Antimicrobial Activity of 4−Thiomorpholine-4-yl Benzohydrazide Derivatives. *Int. J. Appl. Biol. Pharm.* **2010**, *1* (3), 1021−1031.

(18) Moss, M. L.; Sklair-Tavron, L.; Nudelman, R. Drug Insight: Tumor Necrosis Factor-Converting Enzyme as a Pharmaceutical Target for Rheumatoid Arthritis. *Nat. Clin. Pract. Rheumatol.* **2008**, *4* (6), 300−309.

(19) Levin, J. I.; Chen, J. M.; Laakso, L. M.; Du, M.; Du, X.; Venkatesan, A. M.; Sandanayaka, V.; Zask, A.; Xu, J.; Xu, W.; Zhang, Y.; Skotnicki, J. S. Acetylenic TACE Inhibitors. Part 2: SAR of Six-Membered Cyclic Sulfonamide Hydroxamates. *Bioorg. Med. Chem. Lett.* **2005**, *15* (19), 4345−4349.

(20) Chupak, L. S.; Letavic, M. A.; McClure, K. F.; Noe, M. C. Tace Inhibitors. WO 2000009492 A1, Feb 24, 2000.

(21) Blizzard, T. A.; Biftu, T. Thrombin Inhibitors. WO 2013148478 A1, Oct 3, 2013.

(22) Lalli, C.; Trabocchi, A.; Sladojevich, F.; Menchi, G.; Guarna, A. Diversity-Oriented Synthesis of Morpholine-Containing Molecular Scaffolds. *Chem. - Eur. J.* **2009**, *15* (32), 7871−7875.

DOI: 10.1021/acscombsci.6b00178
ACS Comb. Sci. 2017, 19, 173−180

(23) Almstead, N. G.; Bradley, R. S.; Pikul, S.; De, B.; Natchus, M. G.; Taiwo, Y. O.; Gu, F.; Williams, L. E.; Hynd, B. A.; Janusz, M. J.; Dunaway, C. M.; Mieling, G. E. Design, Synthesis, and Biological Evaluation of Potent Thiazine- and Thiazepine-Based Matrix Metalloproteinase Inhibitors. *J. Med. Chem.* **1999**, *42* (22), 4547−4562.
(24) Almstead, N. G.; Cheng, M.; De, B.; Matthews, R. S.; Natchus, M. G.; Pikul, S.; Taiwo, Y. O. 1,4-Heterocyclic Metalloprotease Inhibitors. WO 1998008825 A1, Mar 5, 1998.
(25) Cheung, M.; Eidam, H. S.; Fox, R. M.; Manas, E. S. TRPV4 Antagonists. WO 2009146182 A1, Dec 3, 2009.
(26) Nie, A.; Xiao, J.; Wang, L.; Liao, G.; Liu, H.; Ren, S.; Li, S. Drug Discovery Based on the Structure of FKBP12: Design, Synthesis and Evaluation of L-1, 4-Thiazane-3-carboxylic Acid Derivatives as Neuroimmunophilin Ligands. *Sci. China, Ser. B: Chem.* **2007**, *50* (3), 405−417.
(27) Guarna, A.; Trabocchi, A.; Menchi, G.; Lalli, C.; Sladojevich, F.; Cini, N. Heterocyclic Compounds Containing the Morpholine Nucleus Their Preparation and Use. WO 2008129004 A2, Oct 30, 2008.
(28) Fülöpová, V.; Krchňák, V. Solid-Phase Synthesis of Trisubstituted 2,5-Dihydrobenzo[*f*][1,2,5]thiadiazepine 1,1-Dioxide Derivatives. *ACS Comb. Sci.* **2014**, *16* (8), 412−420.
(29) Tokitoh, N.; Igarashi, Y.; Ando, W. Silicon Pummerer Reaction of Thiazolidine S-Oxides; A New Method for Stereospecific c-5 Functionalization of Thiazolidines. *Tetrahedron Lett.* **1987**, *28* (47), 5903−5906.
(30) Joseph, J. T.; Elmore, J. D.; Wong, J. L. Comparative Sulfhydryl Reaction Pathways of Chlorooxirane and Chloroacetaldehyde. *J. Org. Chem.* **1990**, *55* (2), 471−474.
(31) Shimozu, Y.; Shibata, T.; Ojika, M.; Uchida, K. Identification of Advanced Reaction Products Originating from the Initial 4-Oxo-2-nonenal-cysteine Michael Adducts. *Chem. Res. Toxicol.* **2009**, *22* (5), 957−964.
(32) Bagnoli, L.; Scarponi, C.; Rossi, M. G.; Testaferri, L.; Tiecco, M. Synthesis of Enantiopure 1,4-Dioxanes, Morpholines, and Piperazines from the Reaction of Chiral 1,2-Diols, Amino Alcohols, and Diamines with Vinyl Selenones. *Chem. - Eur. J.* **2011**, *17* (3), 993−999.
(33) Dyatkin, A. B.; Hoekstra, W. J.; Maryanoff, B. E.; Matthews, J. M. Tricyclic Benzodiazepines as Vasopressin Receptor Antagonists. WO 2000043398 A3, Jan 11, 2001.
(34) Larsson, U.; Carlson, R. Synthesis of Amino Acids with Modified Principal Properties 3: Sulfur-Containing Amino Acids. *Acta Chem. Scand.* **1994**, *48*, 517.
(35) Foschi, F.; Albanese, D.; Pecnikaj, I.; Tagliabue, A.; Penso, M. Regioselective *O*-Sulfonylation of *N*,*N*-Bis(2-hydroxyalkyl)tosylamides as a Synthetic Key Step to Enantiopure Morpholines. *Org. Lett.* **2017**, *19* (1), 70−73.
(36) Penso, M.; Foschi, F.; Pellegrino, S.; Testa, A.; Gelmi, M. L. Diastereoselective Protocols for the Synthesis of 2,3-trans- and 2,3-cis-6-Methoxy-morpholine-2-carboxylic Acid Derivatives. *J. Org. Chem.* **2012**, *77* (7), 3454−3461.
(37) Josien, H. B.; Clader, J. W.; Bara, T. A.; Xu, R.; Li, H.; Pissarnitski, D.; Zhao, Z. Substituted *N*-Arylsulfonylheterocyclic Amines as gamma-Secretase Inhibitors. WO 2006004880 A2, Jan 12, 2006.
(38) Chenard, B. L.; Ge, P.; Hodgetts, K. J.; Ihle, D. C.; Li, G.; Wustrow, D. J. Spirocyclic Sulfonamides and Related Compounds. WO 2007140383 A2, Dec 6, 2007.
(39) Ge, P.; Guo, Q.; Hodgetts, K. J.; Hutchison, A. J.; Ihle, D. C.; Li, G.; Peterson, J. M. Aryl Sulfonyl Heterocycles. WO 2007101007 A2, Sept 7, 2007.
(40) Guo, C.; Dong, L.; Kephart, S.; Hou, X. An Efficient Synthesis of Sulfamides. *Tetrahedron Lett.* **2010**, *51* (21), 2909−2913.
(41) Sladojevich, F.; Guarna, A.; Trabocchi, A. Evaluation of Stereochemically Dense Morpholine-Based Scaffolds as Proline Surrogates in *β*-turn peptides. *Org. Biomol. Chem.* **2010**, *8* (4), 916−924.
(42) Lenci, E.; Innocenti, R.; Menchi, G.; Faggi, C.; Trabocchi, A. Two-Step One-Pot Synthesis of Dihydropyrazinones as Xaa-Ser Dipeptide Isosteres Through Morpholine Acetal Rearrangement. *Org. Biomol. Chem.* **2015**, *13* (25), 7013−7019.
(43) Fülöpová, V.; Soural, M. Mining the Chemical Space: Application of 2/4-Nitrobenzenesulfonamides in Solid-Phase Synthesis. *ACS Comb. Sci.* **2015**, *17* (10), 570−591.
(44) Fukuyama, T.; Jow, C. K.; Cheung, M. 2- and 4-Nitrobenzenesulfonamides: Exceptionally Versatile Means for Preparation of Secondary Amines and Protection of Amines. *Tetrahedron Lett.* **1995**, *36* (36), 6373−6374.
(45) Smyslová, P.; Kisseljova, K.; Krchňák, V. *Base-Mediated Intramolecular C- and N-Arylation of N,N-Disubstituted 2-Nitrobenzenesulfonamides: Advanced Intermediates for the Synthesis of Diverse Nitrogenous Heterocycles*. *ACS Comb. Sci.* **2014**, *16* (9), 500−505.
(46) Vanda, D.; Jorda, R.; Lemrová, B.; Volná, T.; Kryštof, V.; McMaster, C.; Soural, M. *Synthesis of Novel N^9-Substituted Purine Derivatives from Polymer Supported α-Amino Acids*. *ACS Comb. Sci.* **2015**, *17* (7), 426−432.
(47) Trapani, P.; Volná, T.; Soural, M. *Solid-Phase Synthesis of 2,3-Dihydrobenzo[f]thiadiazepin-4(5H)-one 1,1-Dioxides with Three Diversity Positions*. *ACS Comb. Sci.* **2016**, *18* (6), 349−354.
(48) Messina, I.; Popa, I.; Maier, V.; Soural, M. *Solid-Phase Synthesis of 5-Noranagrelide Derivatives*. *ACS Comb. Sci.* **2014**, *16* (1), 33−38.
(49) McMaster, C.; Fülöpová, V.; Popa, I.; Grepl, M.; Soural, M. *Solid-Phase Synthesis of Anagrelide Sulfonyl Analogues*. *ACS Comb. Sci.* **2014**, *16* (5), 221−224.
(50) Lanzilotti, A. E.; Littell, R.; Fanshawe, W. J.; McKenzie, T. C.; Lovell, F. M. Stereoselective Reduction of Some Indoles with Triethylsilane-Trifluoroacetic Acid. *J. Org. Chem.* **1979**, *44* (26), 4809−4813.
(51) Matthews, J. M.; Dyatkin, A. B.; Evangelisto, M.; Gauthier, D. A.; Hecker, L. R.; Hoekstra, W. J.; Liu, F.; Poulter, B. L.; Sorgi, K. L.; Maryanoff, B. E. Synthesis, Resolution, and Absolute Configuration of Novel Tricyclic Benzodiazepines. *Tetrahedron: Asymmetry* **2004**, *15* (8), 1259−1267.
(52) Sladojevich, F.; Trabocchi, A.; Guarna, A. Stereoselective Cyclopropanation of Serine- and Threonine-Derived Oxazines to Access New Morpholine-Based Scaffolds. *Org. Biomol. Chem.* **2008**, *6* (18), 3328−3336.
(53) Stein, R. L. Mechanism of Enzymatic and Nonenzymatic Prolyl *Cis-Trans* Izomerization. *Adv. Protein Chem.* **1993**, *44*, 1−24.

DOI: 10.1021/acscombsci.6b00178
ACS Comb. Sci. 2017, 19, 173−180

ACS Combinatorial Science

Review

Cite This: ACS Comb. Sci. 2018, 20, 529−543

pubs.acs.org/acscombsci

Polymer-Supported Syntheses of Heterocycles Bearing Oxazine and Thiazine Scaffolds

Petra Králová,[†,§] Veronika Ručilová,[‡,§] and Miroslav Soural*[,‡]

[†]Department of Organic Chemistry, Faculty of Science, Palacký University, 17. listopadu 12, 771 46 Olomouc, Czech Republic

[‡]Institute of Molecular and Translational Medicine, Faculty of Medicine and Dentistry, Palacký University, Hněvotínská 5, 779 00, Olomouc, Czech Republic

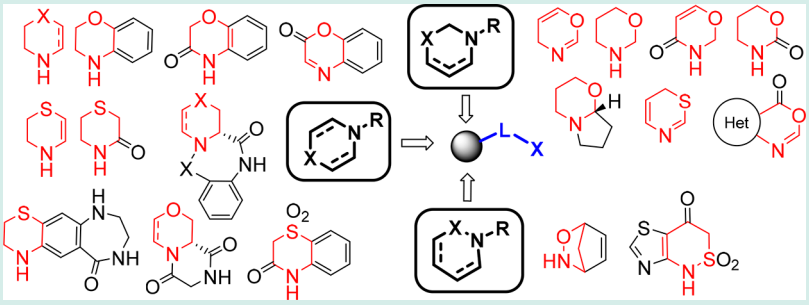

ABSTRACT: In this review, we summarize synthetic approaches to preparing single or fused oxazine and thiazine derivatives using solid-phase synthesis (SPS). The literature survey revealed that diverse compounds bearing variously functionalized 1,2-oxazine, 1,3-oxazine, or 1,4-oxazine scaffolds and the corresponding thiazines are accessible by SPS. The latest contributions involving the stereoselective polymer-supported syntheses of morpholines indicate that the field is continuing to expand.

KEYWORDS: *oxazine, thiazine, morpholine, thiomorpholine, solid-phase synthesis*

INTRODUCTION

Aliphatic, six-membered heterocycles are attractive and frequently studied moieties in medicinal chemistry and chemical biology.[1−3] Piperazines are clearly a privileged scaffold as they can be found in a large number of biologically active compounds and synthetic drugs.[4,5] Oxazines are slightly less common, but they also received considerable attention as either core scaffolds or a peripheral substituent because of their polarity and hydrogen bond acceptor (HBA) properties. Consequently, oxazine scaffold-containing compounds and thiazine scaffold-containing compounds have been identified as pharmacologically interesting molecules with a wide range of biological effects.[6−12]

In general, aliphatic, six-membered heterocycles possessing one nitrogen and one oxygen or sulfur atom can be divided into three structural classes: 1,2-oxazines, 1,3-oxazines, and 1,4-oxazines and the analogous thiazines (Figure 1).

In the late 1990s, Merrifield's SPS[13] expanded from the field of peptide and oligonucleotide synthesis to the synthesis of small molecules. Polymer-supported chemistry quickly became a useful tool for synthesizing diverse drug-like compounds using combinatorial chemistry because of its many advantages.[14] To date, a wide range of heterocyclic scaffolds have been synthesized using SPS. Not surprisingly, the preparation of various oxazines and thiazines has also received significant attention from synthetic chemists studying polymer-supported reactions. In this review, we summarize all reported approaches. Only methodologies based on the cyclization of the heterocyclic scaffold on-resin or immediately after the cleavage of linear intermediates from the polymer matrix are reported; the immobilization of presynthesized heterocycles and their further modification is not included. The individual approaches are sorted according to the target scaffold, and the overall list of accessible structures is summarized in Figure 2.

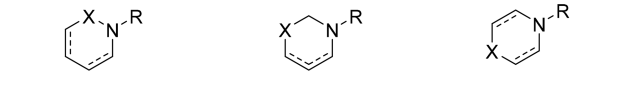

Figure 1. Classification of oxazines and thiazines.

1,2-OXAZINES/THIAZINES

The solid-phase synthesis of 1,2-oxazines was extensively studied using different immobilized dienophiles amenable to hetero-Diels−Alder cycloadditions. The first report in this field was published in 2002 by Faita.[15] Wang resin-supported nitrile-oxides **1** were oxidized by *N*-methylmorpholine *N*-oxide (NMO) to acyl-nitroso intermediates **2**. The reaction of **2** with cyclohexadiene resulted in the formation of cycloadducts **3** (Scheme 1). Because of the acidic lability of products, which

Received: May 30, 2018
Revised: July 18, 2018
Published: July 24, 2018

DOI: 10.1021/acscombsci.8b00076
ACS Comb. Sci. 2018, 20, 529−543

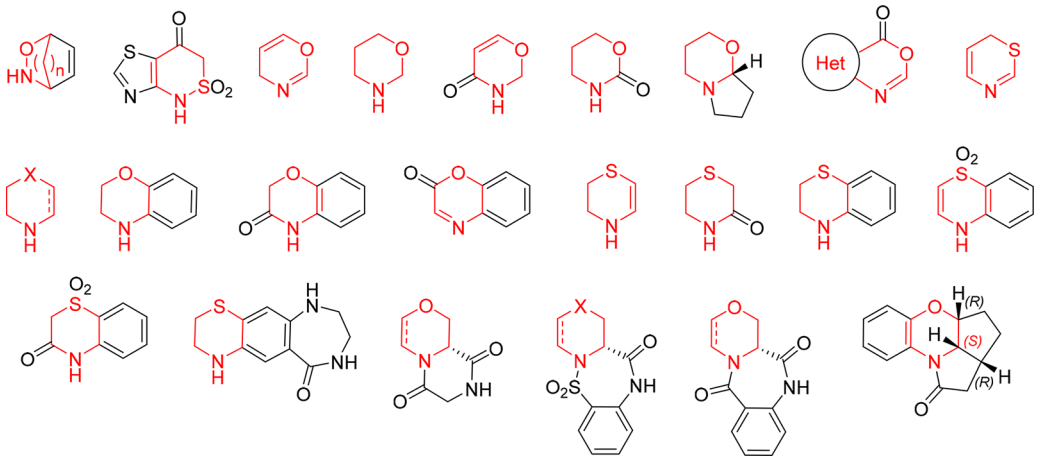

Figure 2. List of oxazines and thiazines accessible by SPS (potential substitutions of the scaffolds are not shown).

Scheme 1. Hetero-Diels–Alder Cycloaddition Using Immobilized Nitrile-oxides

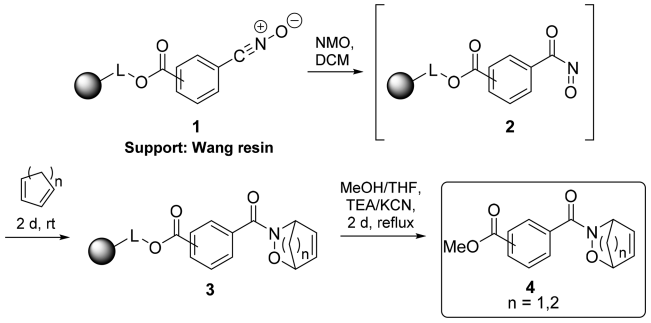

resulted in the cleavage of the N–O bond, trifluoroacetic acid (TFA – a typical reagent for liberating products from Wang resin) was omitted, and the final compounds **4** were cleaved from the polymer matrix using a base-catalyzed transesterification with methanol. The isolated yields were moderate which indicated the acylnitroso species **2** were not stable.

Solid-supported hetero-Diels–Alder reactions (HDA reactions) leading to 1,2-oxazines **6** and **7** were further investigated by Krchňák. In this case, the dienophile was generated from hydroxamate **5** by oxidation with tetrabutylammonium periodate. Because of the instability of acylnitroso species, the oxidation was performed in the presence of the diene to generate polymer-supported products (Scheme 2).[16] A wide range of dienes and different resin attachments were successfully tested. In the case of hydroxamates immobilized directly to Wang resin ($R^1 = CH_2$), the *N*-unsubstituted products **7** were obtained after TFA mediated cleavage from the resin. In contrast, use of Rink amide resin acylated with 4-hydroxymethylbenzoic acid ($R^1 = 4\text{-}CONH_2\text{–}Ph\text{–}CH_2$) or the application of diisopropylsilyl linker cleavable with tetabutylammonium fluoride (TBAF) yielded *N*-substituted oxazines **6**. The instability of the resulting oxazines **6** and **7** toward TFA was resolved by using 2,3-dichloro-5,6-dicyano-1,4-benzoquinone (DDQ) to cleave the products from Wang resin. In addition, a dual linker strategy consisting of a diisopropylsilyl linker conjugated with a Wang linker was applied to study the stability of the target oxazines toward TFA in greater detail. Furthermore, arylnitroso dienophiles prepared from *N*-hydroxyanilines were reported as suitable reagents for cycloaddition reactions.[17] Finally, it was discovered that the acid-instability of dihydro-[1,2]oxazines **6** or **7** prepared from the acyl and arylnitroso HDA reactions is influenced by three factors: substituents at the C^3 and C^6 carbons, the presence of a bridge between the C^3 and C^6 carbons and, to a lesser extent, the identity of the *N*-substituent.[18]

Later, the stereochemical outcome of the solid-phase HDA reactions leading to 3,6-dihydro-2*H*-1,2-oxazines was studied in detail by Hlavac et al. using chiral supercritical fluid chromatography (SFC).[19,20]

The only report on the solid-phase synthesis of compounds bearing the 1,2-thiazine scaffold was by Lee.[21] First, thiazole intermediate **10** was synthesized from chloromethyl resin **8** in two steps. After sulfonylation followed by Mitsunobu alkylation, intermediate **12** was cyclized to thiazolo[4,5-*c*][1,2]thiazin-4(3*H*)one-2,2-dioxide **13** using sodium hydride as the base (Scheme 3). The oxidation of sulfide **13** to sulfone **14** released the products by aminolysis, thus giving the target compound **15** in a traceless manner. The thiazolo[4,5-*c*][1,2]thiazines **15** were isolated in high purities (>95%). This strategy enabled the

Scheme 2. Hetero-Diels–Alder Cycloaddition Starting from Immobilized Hydroxamates

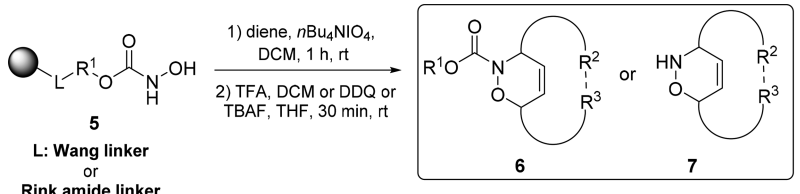

5

L: Wang linker
or
Rink amide linker
or
diisopropylsilyl linker

Diene: e.g. 1,3-cyclohexadiene, α–terpinene, 9,10-dimethylanthracene, 2,4-hexadiene, sorbic acid, ethyl sorbate, 1,3,5,5-tetramethyl-CHD, *trans,trans*-2,4-hexadien-1-ol, 4-methyl-penta-1,3-diene

DOI: 10.1021/acscombsci.8b00076
ACS Comb. Sci. 2018, 20, 529–543

Scheme 3. Solid-Phase Synthesis of 1,3,6-Trisubstituted-1*H*-thiazolo[4,5-*c*][1,2]thiazin-4(3*H*)one-2,2-dioxides

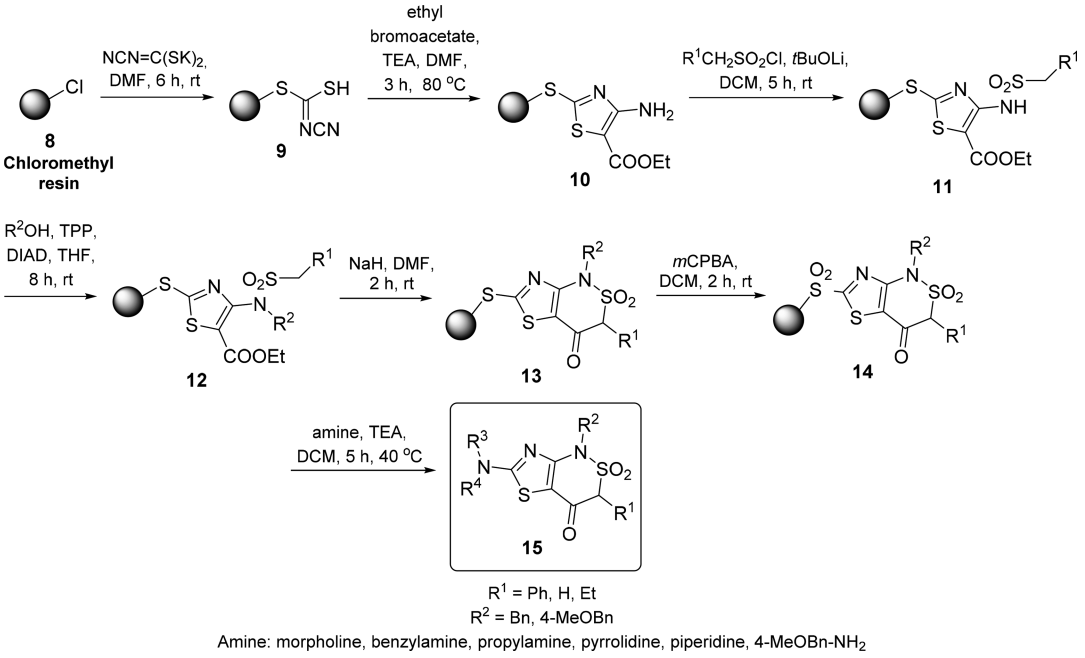

Scheme 4. Polymer-Supported Synthesis of 1,3-Oxazinan-2-ones via Cyclative Cleavage of Resin-Bound Amino Alcohols

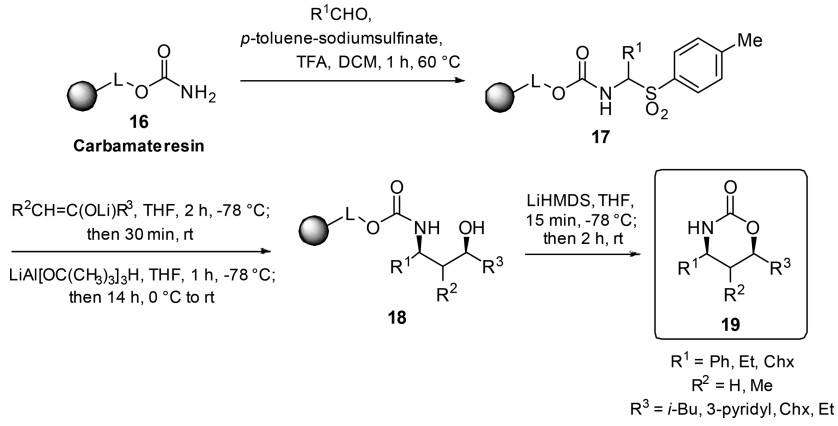

Scheme 5. Polymer-Supported 1,3-Oxazines as Intermediates for High-Throughput Synthesis of Pyrazoles

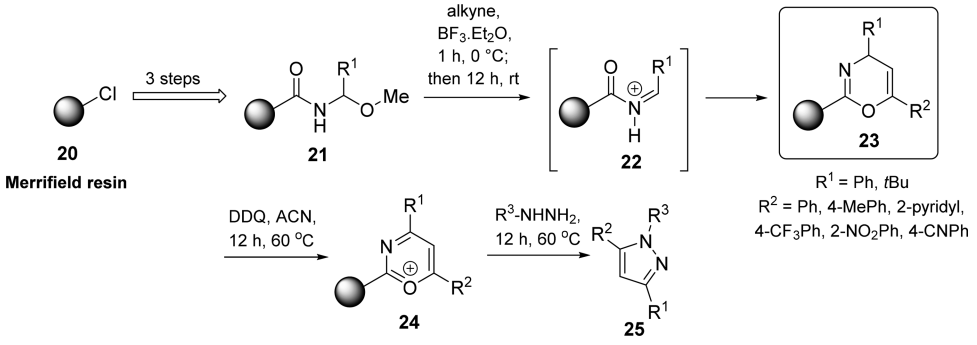

construction of a chemical library from readily available sulfonyl chlorides, alcohols and amines.

1,3-OXAZINES/THIAZINES

In 2001, Enders and Schunk reported the first solid-phase synthesis of 1,3-oxazinan-2-ones **19** starting from carbamate resin **16**[22] (Scheme 4). Because of the TFA-promoted formation of the intermediate, benzyl alcohol resin was used instead of Wang resin to prevent premature cleavage from the polymer support. After the formation of intermediates **18**, their cyclative cleavage using lithium bis(trimethylsilyl)amide (LiHDMS) gave the final products **19**[23] in excellent purities and diastereomeric excesses. The relative configuration of carbamates **19** was established as cis via NMR analysis. Later, the undesired

DOI: 10.1021/acscombsci.8b00076
ACS Comb. Sci. 2018, 20, 529−543

Scheme 6. Solid-Phase Synthesis of Tetrasubstituted 1,3-Thiazines

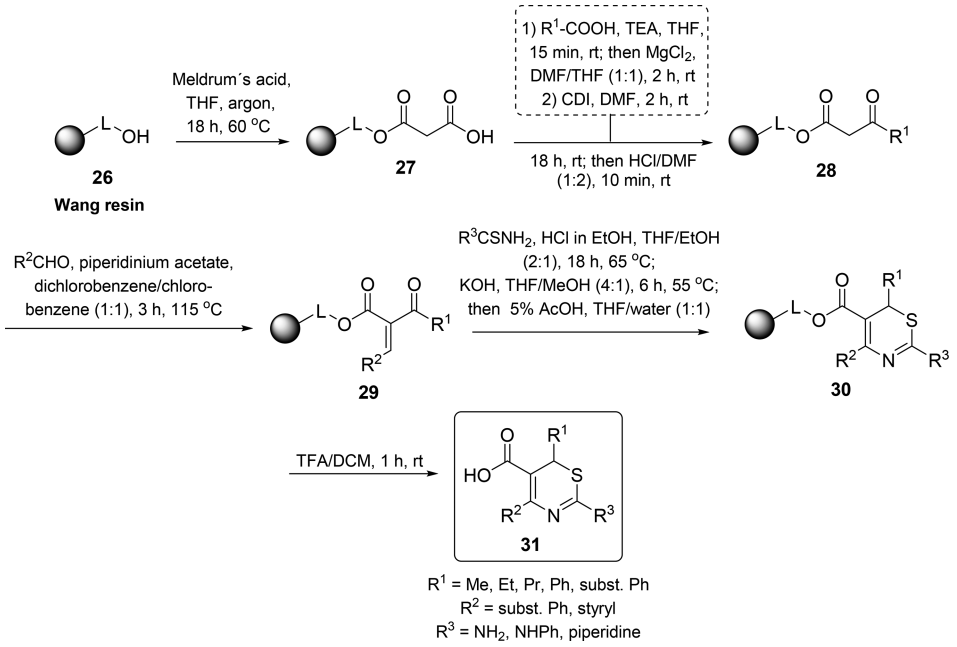

Scheme 7. Formation of 1,3-Oxazines Using Iminium Chemistry

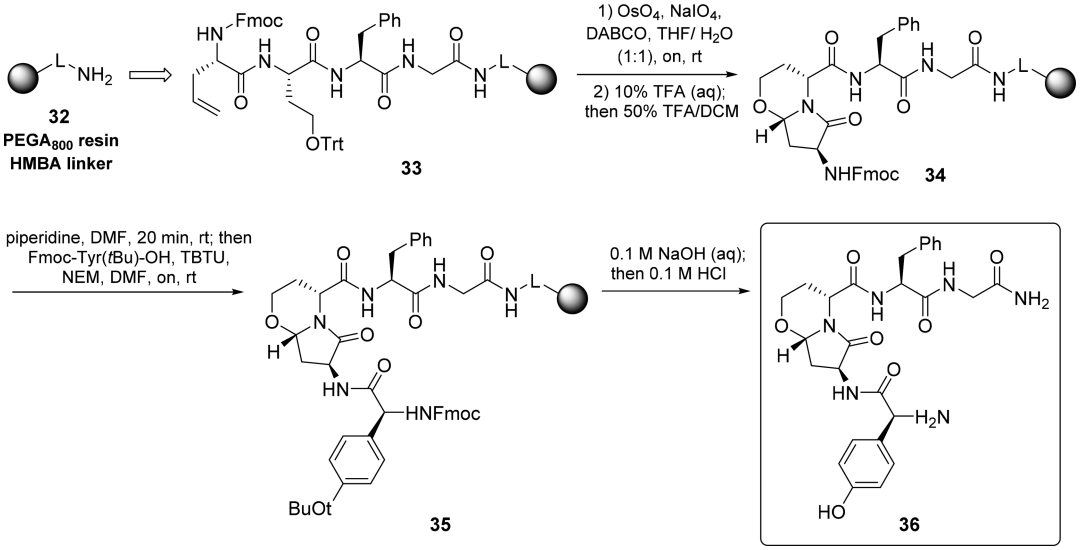

formation of the 1,3-oxazinan-2-one scaffold **19** based on the cyclative cleavage of immobilized amino alcohol mesylates was reported by Uriac.[24]

Polymer-supported 1,3-oxazines **23** were synthesized as efficient intermediates for the preparation of other heterocycles such as **25**.[25] Merrifield resin (**20**) was converted in three steps to resin-bound *N*-(*R*-methoxyalkyl)-amides **21**, which, after reaction with alkynes, yielded the corresponding oxazines **23** (Scheme 5). Oxidation with DDQ followed by treatment with hydrazines led to the formation of trisubstituted pyrazoles **25**. The removal of the excess insoluble DDQ from the 1,3-oxazinium salts **24** still linked to the resin by washing prevented a tremendously tedious purification of the final pyrazoles **25**. Furthermore, the whole process could be readily automated.

A solid-phase synthesis strategy for the generation of combinatorial libraries of 2-amino-1,3-thiazine-5-carboxylates **31** was developed by Kappe.[26] Wang resin **26** was reacted with Meldrum's acid, and immobilized malonic acid (**27**) was converted to *β*-ketoester **28**. Subsequently, Knoevenagel condensations with aldehydes furnished polymer-bound enols **29**, which were cyclized to thiazines **30** by acid-catalyzed ring closures with thiourea building blocks (Scheme 6). The ring closure reactions were more tedious than were the solution-phase alternatives.[27] Hydrochloric acid was found to be the best catalyst, and notably, the acid-labile Wang linker survived the procedure without any undesired cleavage of the product. To increase the purity of resin-bound thiazines **30**, an on-bead purification method was used to eliminate unreacted intermediates from the support before the cleavage step.[28]

The preparation of 6 + 5 fused 1,3-oxazine derivatives **36** using solid-phase iminium chemistry was reported by Meldal.[29a] Starting from amino-functionalized $PEGA_{800}$ resin **32**[30] equipped with a base-labile hydroxymethyl-benzoic acid (HMBA) linker, masked aldehyde-containing intermediate **33**

DOI: 10.1021/acscombsci.8b00076
ACS Comb. Sci. 2018, 20, 529−543

Scheme 8. Solid-Phase Synthesis of Fused 1,3-Oxazin-6-ones

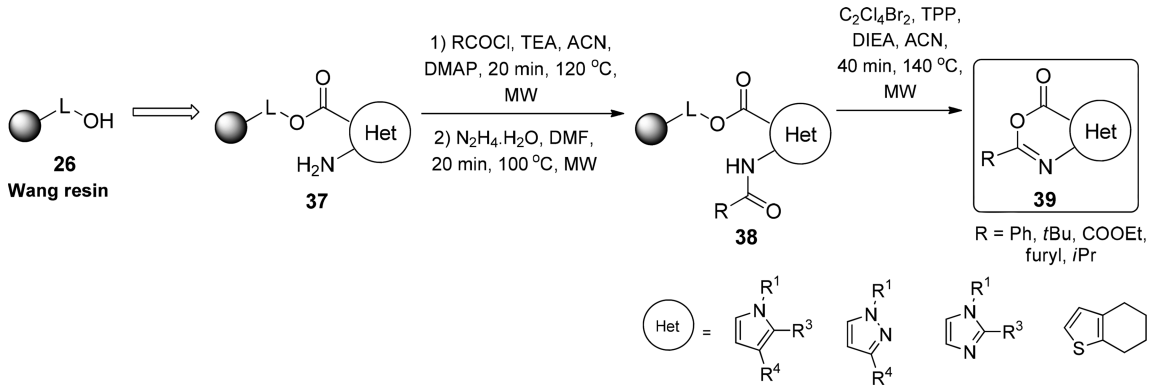

Scheme 9. Unexpected Formation of Oxazinone Using a Solid-Phase Staudinger Reaction

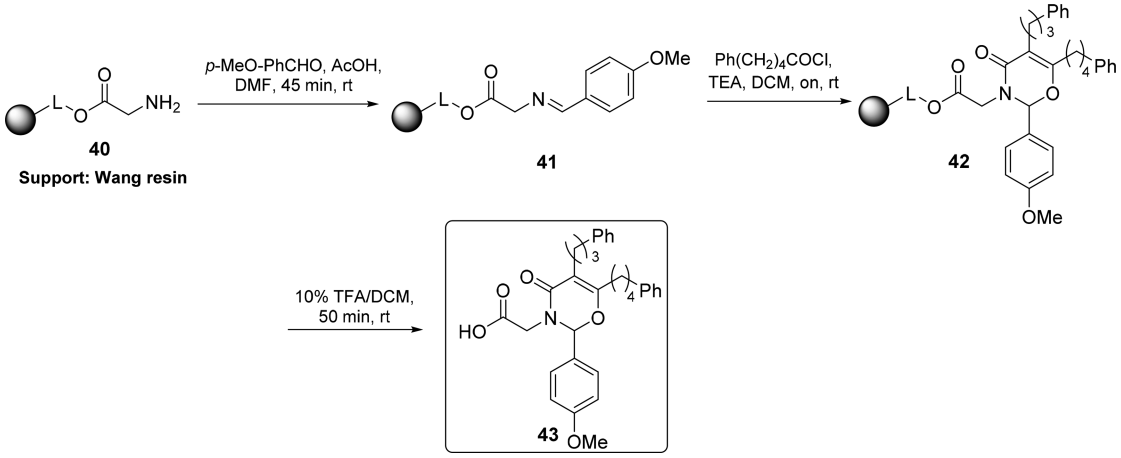

Scheme 10. Reaction Sequence for the Soluble Polymer-Supported Flow Synthesis of 1,3-Oxazines

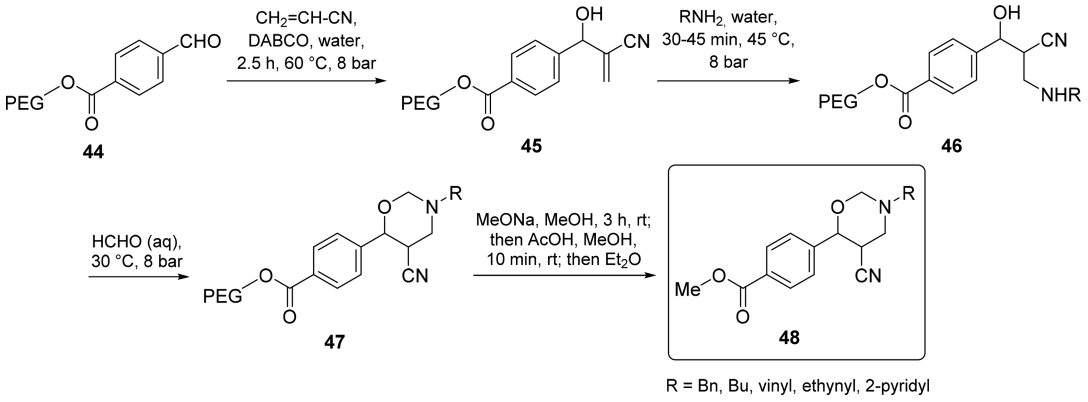

was obtained. Scheme 7 depicts an example of this chemistry for the synthesis of constrained enkephalin analogue **36**. In this particular case, the aldehyde was generated by oxidation of terminal alkene **33**. The ring closure to afford oxazine scaffold **34** was accomplished via the subsequent formation of the *N*-acyliminium intermediate using TFA and intramolecular attack by the neighboring hydroxy functionality. The desired bicyclic hexahydro-pyrrolo[2,1-*b*][1,3]oxazine **36** was obtained in excellent purity and diastereoselectivity (both >90%). In addition to the preparation of enkephalin analogue **36**, the authors used this solid-phase approach to prepare similar (5,6)-, (6,5)-, and (6,6)-fused ring systems. Recently, the preparation of fused heterocycles containing the [1,3]oxazine scaffold using the concept of iminium chemistry was also reported by Krchňák.[29b]

The solid-phase synthesis of 1,3-oxazin-6-ones **39** fused with pyrrole, pyrazole, imidazole, and thiophene moieties was developed by Lam.[31] First, monocyclic intermediates **37** were synthesized using Wang resin **26** in two steps and subjected to acylation with aroyl chlorides (Scheme 8). The reaction yielded diacylated byproducts even under mild conditions, and for this reason, a deacylation step using hydrazine had to be included. The final cyclization of intermediates **38** proceeded with dibromotetrachloroethane and triphenylphosphine (TPP) in the presence of DIEA. Optimization of the reaction conditions showed that the best overall yields were obtained when the

DOI: 10.1021/acscombsci.8b00076
ACS Comb. Sci. 2018, 20, 529−543

Scheme 11. First Solid-Phase Synthesis of Thiomorpholines

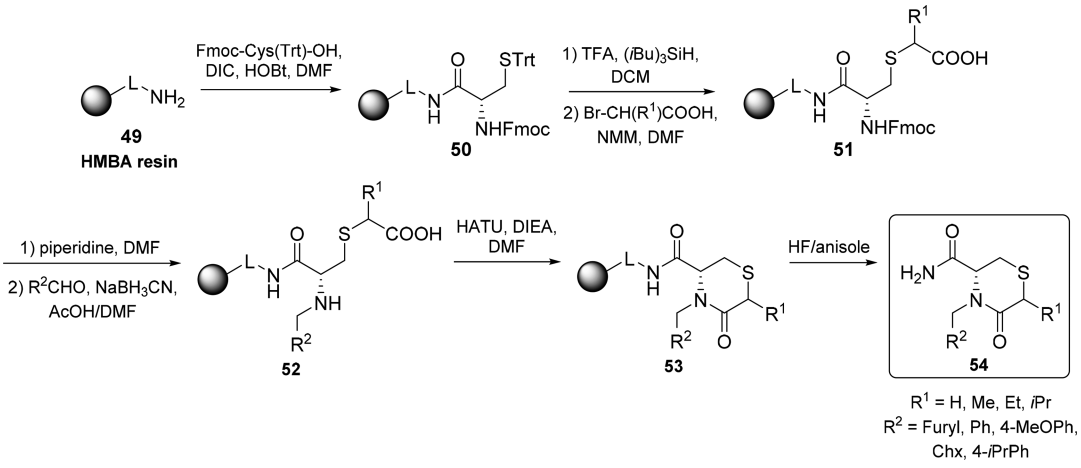

Scheme 12. Dess–Martin Periodinane-Mediated Formation of a Polycyclic Morpholine Derivative

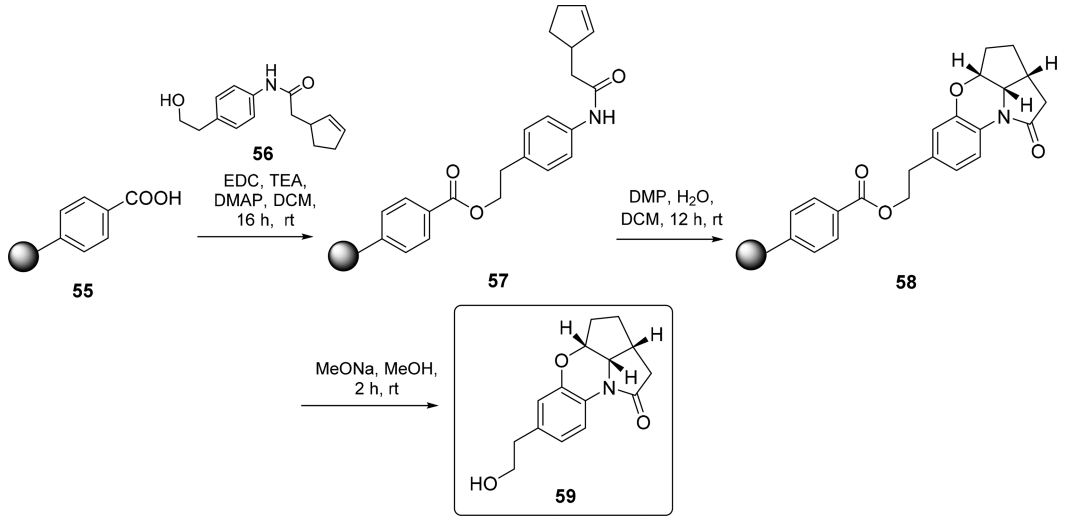

reaction mixture was subjected to microwave irradiation. A representative set of 20 bi- and tricyclic heteroannulated 1,3-oxazin-6-ones **39** was prepared in 16–36% overall yield, indicating an average yield of at least 70% for each step of the reaction.

The unexpected formation of oxazinone product **43** was reported by Mata in a study targeting the solid-phase synthesis of β-lactams.[32] Fmoc-Gly-OH was immobilized on Wang resin **40** and converted to imine **41** in two steps (Scheme 9). Resin **41** was then subjected to a solid-phase Staudinger reaction[33,34] involving the generation of ketenes from a large excess of alkanoyl chlorides and TEA. Surprisingly, oxazinone **43** was obtained instead of the expected β-lactam. The authors explained the result by the tendency of ketenes to dimerize to acylketenes and their subsequent reaction with resin **41**, which gives the [4 + 2] Diels–Alder adducts.

Recently, the preparation of 1,3-oxazines **48** using a soluble polymer-supported flow method was developed by Scherrmann[35] starting from PEG-linked aldehyde **44**. 1,3-Oxazines **48** were prepared via a four-step synthesis, namely, a Baylis–Hillman reaction, Michael addition of a range of amines, cyclization with formaldehyde and hydrolysis of the PEG linkage (Scheme 10). An aqueous solution of the desired amine was added to the PEG-linked Baylis–Hillman adduct **45** without additives. The aqueous solutions obtained under flow conditions were directly mixed with an aqueous formaldehyde solution to cyclize the oxazine scaffold **47**. Finally, the tetrahydro-1,3-isoxazines **47** were released from the PEG by treatment with sodium methoxide to obtain the corresponding methyl ester derivatives **48** as the mixture of diastereoisomers. The developed methodology is a nice example of a green process for the preparation of heterocycles using solid-supported synthesis.

1,4-OXAZINES/THIAZINES

One of the first reports on the solid-phase synthesis of 1,4-oxazines/thiazines was published by Houghten.[36] The key building block was *N*-Fmoc-*S*-trityl-L-cysteine immobilized on *p*-methylbenzhydrylamine (MBHA) resin **49**. Cleavage of the trityl protecting group was followed by alkylation of the thiol with α-halocarboxylic acids to yield resin **51**. Following the removal of the Fmoc protecting group, reductive alkylation of the free amine occurred in the presence of an aldehyde without racemization in the reduction step. The formation of thiomorpholin-3-one **53** was completed via an intramolecular acylation (Scheme 11).

The alkylation step was problematic for bulkier R^1 substituents, and for this reason, an alternative synthetic route

DOI: 10.1021/acscombsci.8b00076
ACS Comb. Sci. 2018, 20, 529–543

Scheme 13. Resin-Bound Pseudo-oxazolones in the Synthesis of Benzoxazine-2-ones

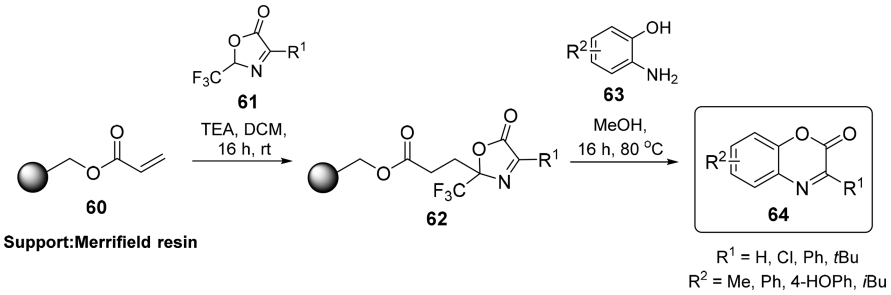

Scheme 14. Resin-Bound Benzoxazin-2-ones Using BOMBA Resin

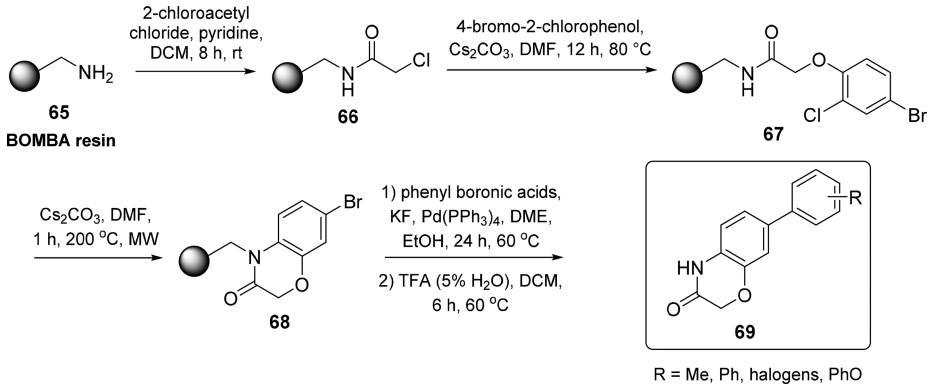

Scheme 15. Formation of Benzoxazines via a Benzyne Intermediate

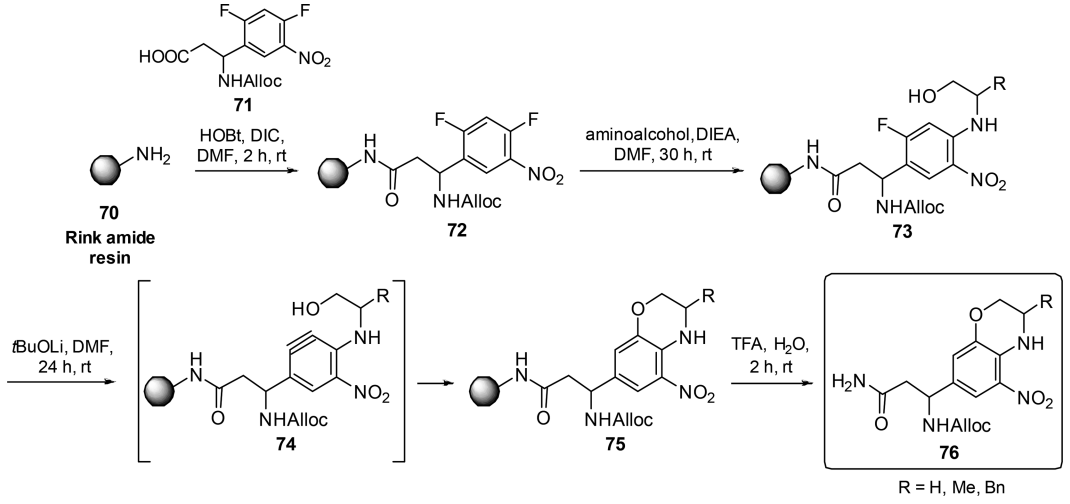

was developed. The alternative consisted of the reverse reaction sequence. First, the resin-bound secondary amine was obtained using reductive amination, the secondary amine was then acylated with an α-halocarboxylic acid, and thiomorpholine ring closure occurred after cleavage of the Trt group. One year later, the same approach was applied to synthesize trisubstituted thiomorpholines starting from TentaGel-S-OH resin,[37] and in 2012, Nefzi used a similar strategy to synthesize spirocyclic morpholine derivatives on *p*-methylbenzhydrylamine (MBHA) resin using an Ugi four-center three-component reaction.[38] Finally, an analogous approach for the traceless synthesis of oxazines was reported by Saruta starting from a mercapto alcohol immobilized via a sulfidic functionality.[39]

The unexpected formation of fused morpholines **59** using Dess-Martin periodinane (DMP) was reported by Nicolaou. Immobilization of presynthesized alcohol **56** via esterification of polymer-supported benzoic acid **55** led to intermediate **57**, which was subjected to DMP oxidation and afforded polycyclic compound **58**. Product **59** was cleaved from the resin via the hydrolysis of the ester functionality with sodium methoxide (Scheme 12).[40]

An interesting solid-phase synthesis of benzoxazinones **64** via cyclative cleavage of resin-bound pseudo-oxazolones **62** was reported by Jung and Bräse.[41] Merrifield resin was equipped with acrylic linker **60**, which was subjected to Michael addition by oxazolones **61** in the 2-position (Scheme 13). Target compounds **64** were prepared by the reaction of resins **62** with different 2-amino-phenols **63**. The average yield of isolated benzoxazolones **64** was dependent on the identity of both the aminophenol and the immobilized oxazolone. Good results were

DOI: 10.1021/acscombsci.8b00076
ACS Comb. Sci. 2018, 20, 529−543

Scheme 16. Formation of Benzothiazines via the Mesylate

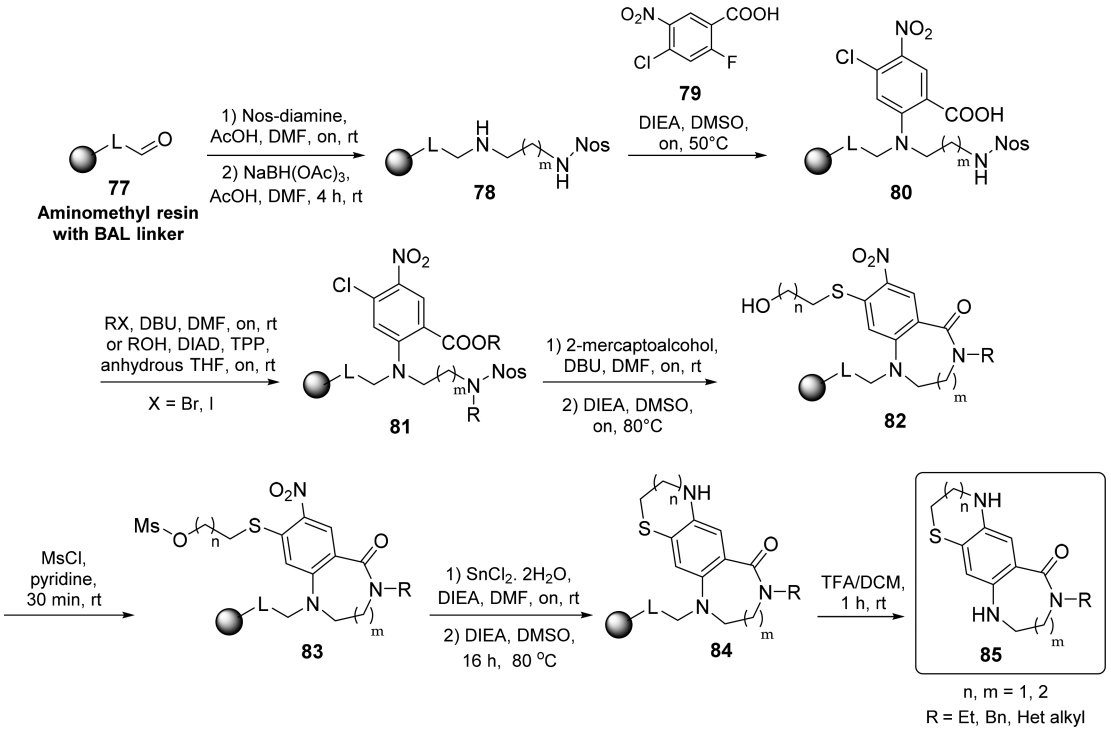

Scheme 17. Solid-Phase Synthesis of 3,4-Dihydro-1,4-benzothiazines from Polymer-Supported Aminothiophenols

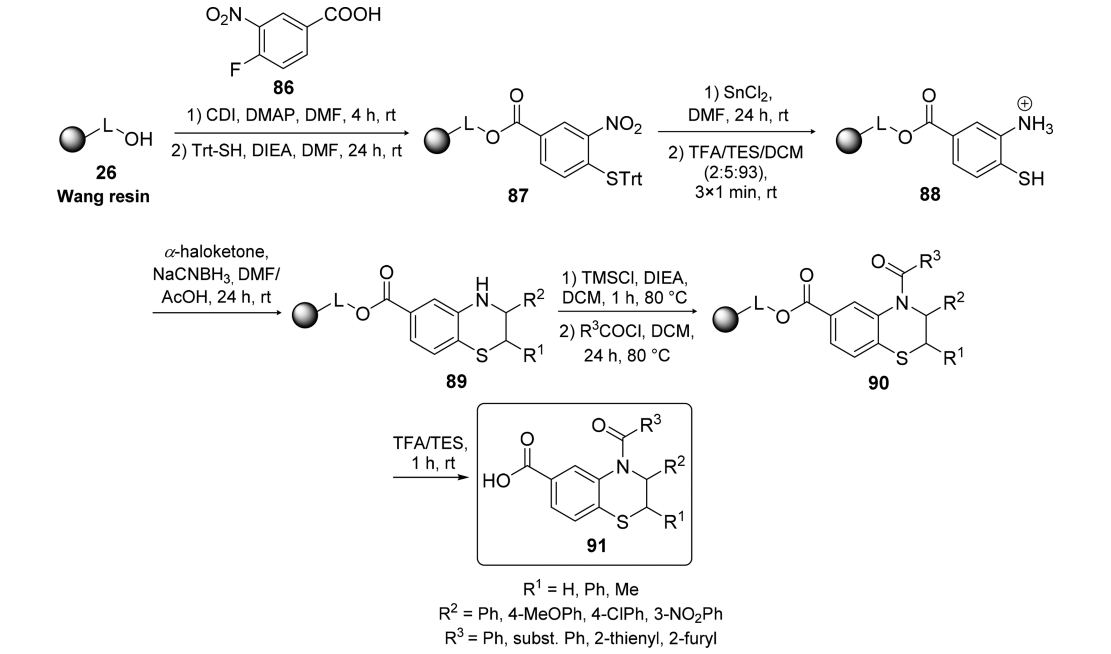

obtained for all compounds cleaved from the hydroxyphenylglycine-derived oxazolone **62** (R^1 = 4-HOPh); however, benzoxazolone-forming reactions with the phenylglycine-derived oxazolone resin **62** (R^1 = Ph) or alanine-derived oxazolone resin **62** (R^1 = Me) generally resulted in lower yields.

A reaction sequence to prepare the α-chloroacetamide resin employing the 4-benzyloxy-2-methoxybenzylamine (BOMBA) resin **65** as the starting polymer support was developed by Gong.[42] Treatment of the BOMBA resin **65** with α-chloroacetyl chloride led to the corresponding α-chloroacetamide resin **66** (Scheme 14). After the reaction with 4-chloro-2-bromophenol, the corresponding resin-bound α-(2-chloro-4-bromophenoxy)-acetamide **67** was subjected to a Smiles-cyclization reaction promoted by cesium carbonate under microwave conditions. Prior to cleavage from the polymer support, intermediate **68** was further modified via a Suzuki reaction.

The solid-phase synthesis of benzoxazines **76** via benzyne intermediate **74** was described by Kurth.[43] *N*-Alloc-3-amino-3-(2,4-difluoro-5-nitrophenyl)propanoic acid **71** was immobilized by acylation of Rink amide resin **70**. After substitution of the fluorine atom with an amino alcohol, the reaction of intermediate **73** with lithium *t*-butoxide triggered the formation

DOI: 10.1021/acscombsci.8b00076
ACS Comb. Sci. 2018, 20, 529−543

Scheme 18. Solid-Phase Synthesis of Benzothiazines from Polymer-Supported Iodoacetic Acid

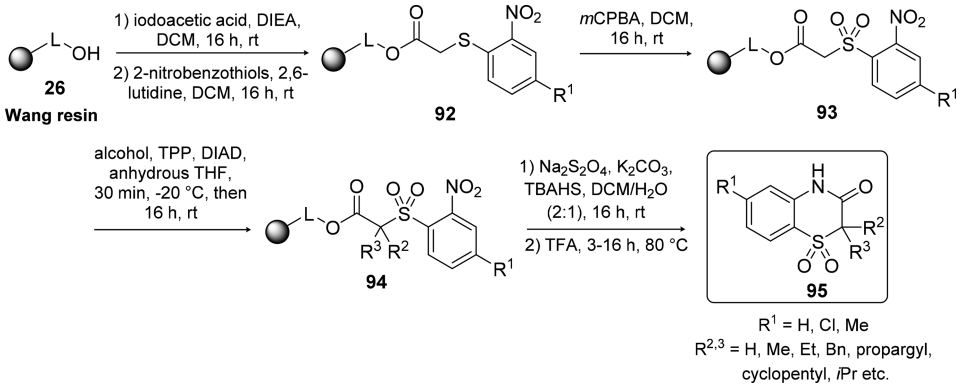

Scheme 19. Synthesis of Benzothiazines from Polymer-Bound 1,2-Diaza-1,3-butadienes

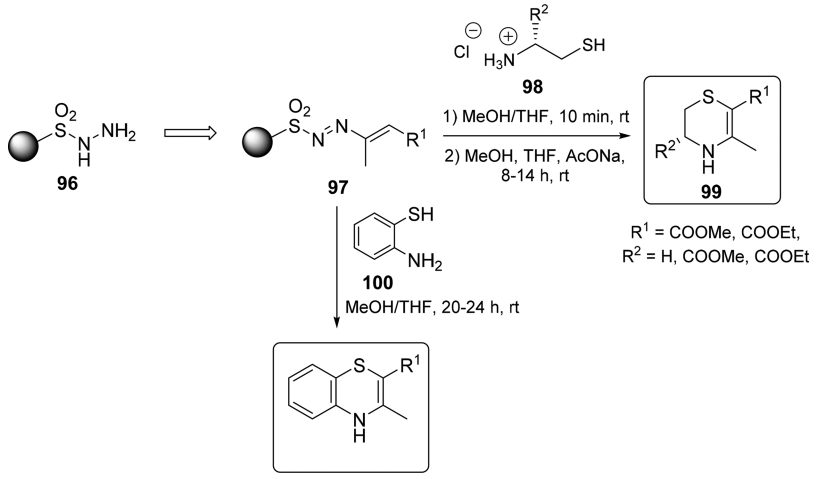

of benzyne **74**, which underwent spontaneous intramolecular addition (Scheme 15).

The use of mercaptoethanol to prepare benzene-fused thiomorpholines **85** was reported by Lemrová in 2012.[44] In this case, 2-fluoro-4-chloro-5-nitrobenzoic acid **79** was used as the key building block. Starting from aminomethyl resin equipped with benzaldehyde linker **77**, linear intermediate **81** was synthesized in three steps (Scheme 16). Replacement of the chloride of **81** with 2-mercaptoalcohol led to spontaneous cleavage of the Nos group and cyclization to benzodiazepinones **82**. Morpholine scaffold **84** was then formed via the subsequent conversion of alcohol **82** to the corresponding mesylate **83** followed by reduction of the nitro group and cyclization. In addition to 2-mercaptoethanol, 3-mercaptopropanol was successfully used to prepare the seven-membered ring. In contrast, 4-mercaptobutanol was not tolerated in the cyclization step.

The preparation of 3,4-dihydro-1,4-benzothiazines **91** from polymer-supported 2-aminothiophenols **88** was reported by Barany.[45] Immobilized 2-amino-4-carboxythiophenol **88** was synthesized from Wang resin **26** and 4-fluoro-3-nitrobenzoic acid **86** in four steps (Scheme 17). The cyclization to the thiazine scaffold **89** was accomplished by the reaction with α-haloketones or α-bromo methyl esters and reductive amination. Prior to cleavage from the polymer support, an additional diversification position was introduced via *N*-acylation with acyl chlorides. Alternatively, the same reaction sequence was successfully applied to the preparation of 3,4-dihydro-3-oxo-1,4-benzothiazines using esters of α-halocarboxylic acids instead of haloketones. In this case, oxidation of the sulfides with *m*-chloroperbenzoic acid (*m*CPBA) to obtain 3,4-benzothiazine-1,1-dioxides was also possible.

In this context, the reversed approach was recently developed by Drábiková.[46] The approach consisted of immobilization of α-halocarboxylic acids, followed by nucleophilic substitution with *o*-nitrothiophenols. After oxidation of **92** to sulfones **93**, the acidic SO_2CH_2CO methylene groups were alkylated with alcohols using Mitsunobu reactions (Scheme 18). Interestingly, the reaction outcome was heavily dependent on the structure of the alcohols, which could generate mono- or dialkylated intermediates **94** regioselectively. Reduction of the nitro group and cyclization using TFA afforded the final benzothiazine-1,1-dioxides **95**.

A different approach to the synthesis of thiazines **99** and benzothiazines **101** was developed by Palacios et al.[47] Polymer-bound 1,2-diaza-1,3-butadienes **97** were prepared from polymer-bound *p*-toluenesulfonyl hydrazide **96**[48] and were reacted with 2-mercaptoethylamine hydrochloride or L-cysteine ethyl ester hydrochloride. Resin **97** was treated with sodium acetate in MeOH/THF to directly obtain 3,4-dihydro-2*H*-1,4-thiazines **99** in solution in a satisfactory degree of purity. Similarly, polymer-bound 1,2-diaza-1,3-butadienes **97** reacted with 2-aminothiophenol **100** to directly afford 2-substituted-1,4-benzothiazines **101** (Scheme 19). The overall yields refer to the multistep-process of the solid-phase reactions and are comparable to the corresponding yields obtained in solution.

DOI: 10.1021/acscombsci.8b00076
ACS Comb. Sci. 2018, 20, 529−543

Scheme 20. Solid-Phase Synthesis of 4*H*-benzo[*b*][1,4]thiazine 1,1-dioxides

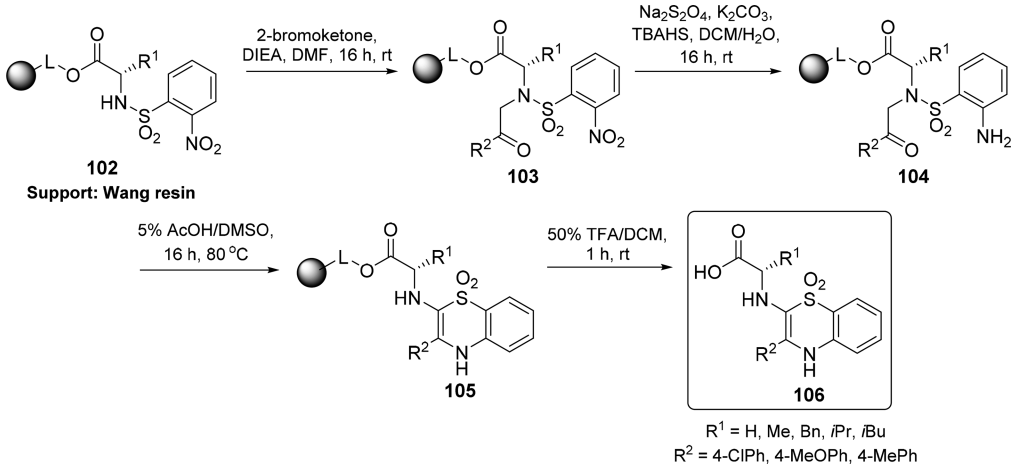

Scheme 21. Stereoselective Solid-Phase Synthesis of *N*-Benzensufonyl Morpholines and Thiomorpholines

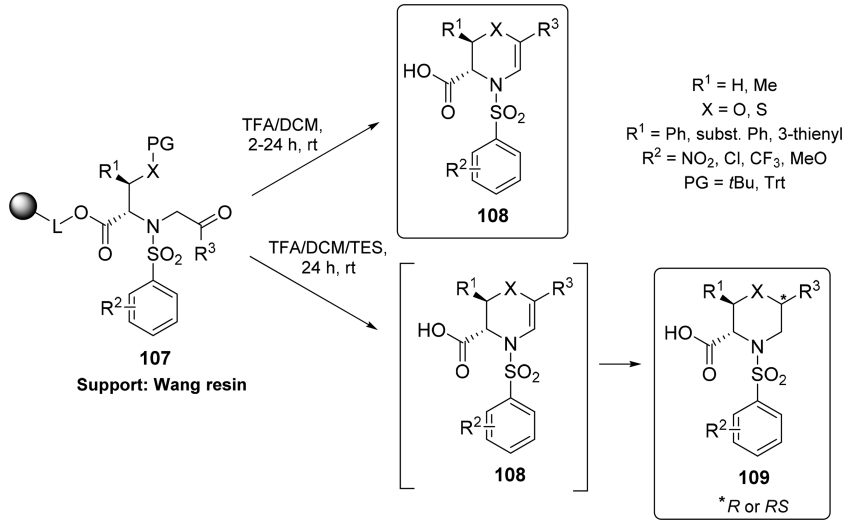

Scheme 22. Stereoselective Solid-Phase Synthesis of *N*-Acetyl Oxazines and Morpholines

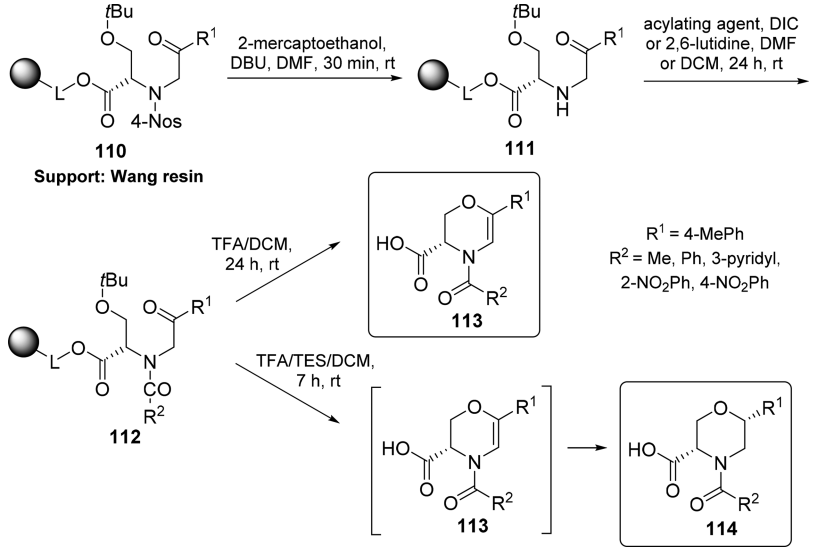

An interesting solid-phase synthesis of benzothiazines 1,1-dioxides based on the rearrangement of benzothiadiazepine 1,1-dioxides **106** was reported by Krchňák.[49] The polymer-supported amino acids were sulfonylated with various 2-nitrobenzensulfonyl chlorides to prepare resin **102** (Scheme 20). After alkylation with various α-haloketones and reduction

DOI: 10.1021/acscombsci.8b00076
ACS Comb. Sci. 2018, 20, 529−543

Scheme 23. Stereoselective Solid-Phase Synthesis of Benzoxazino[4,3-*b*][1,2,5]thiadiazepinone 6,6-Dioxides

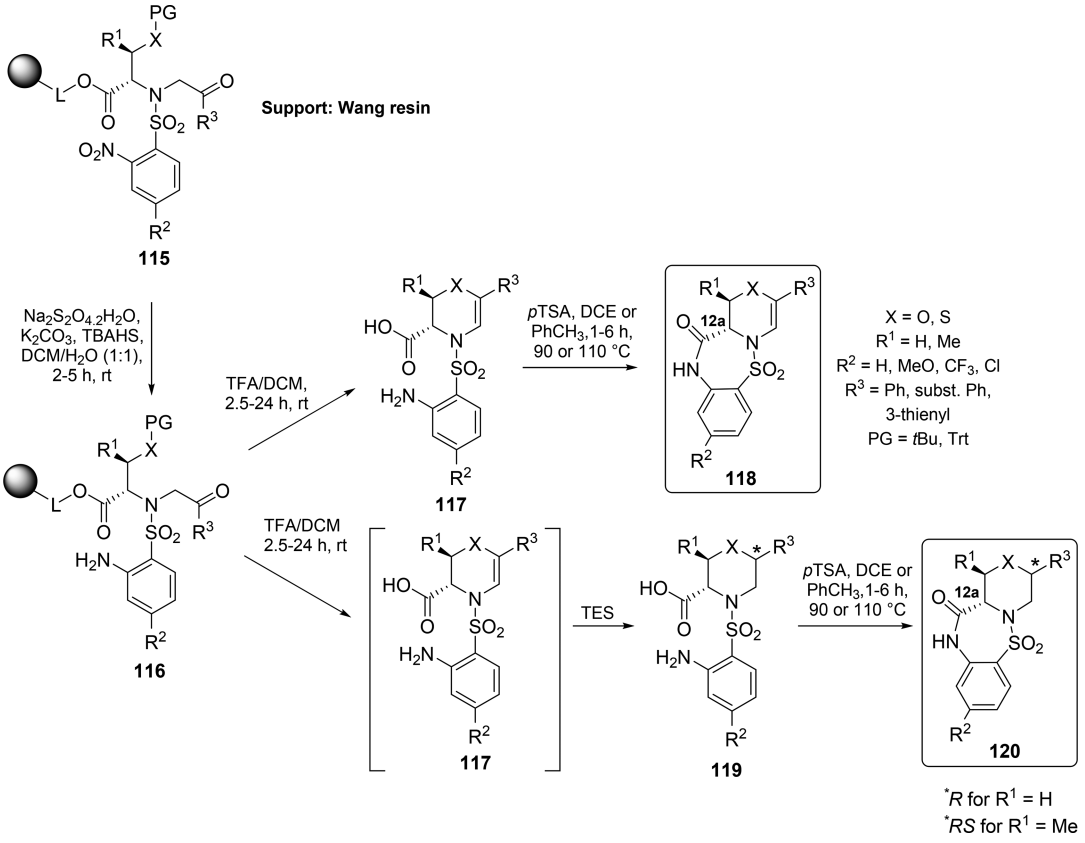

Scheme 24. Stereoselective Solid-Phase Synthesis of benzo[*e*][1,4]oxazino[4,3-*a*][1,4] diazepine-6,12-diones

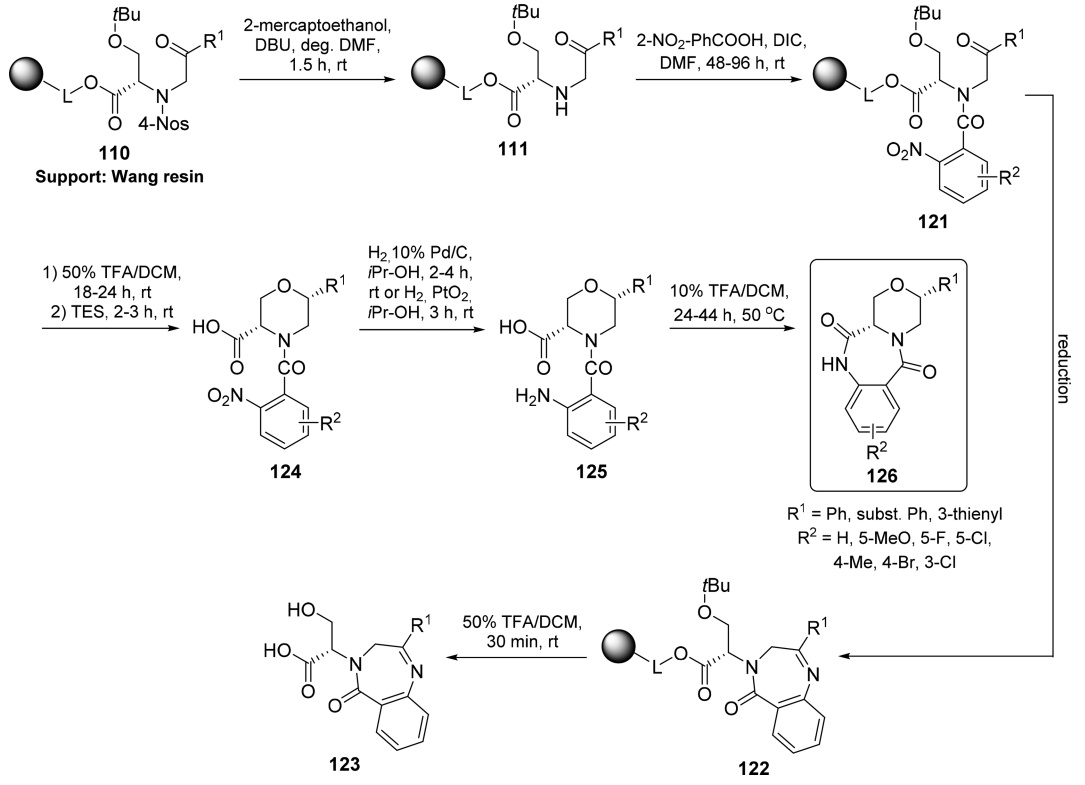

of the nitro group, linear intermediates **104** were converted to benzothiazines **105** using acetic acid in DMSO. Previous experiments using solution-phase synthesis revealed the prior formation of benzothiadiazepine intermediates, which underwent ring contraction to generate six-membered ring scaffolds.

DOI: 10.1021/acscombsci.8b00076
ACS Comb. Sci. 2018, 20, 529−543

Scheme 25. Polymer-Supported Synthesis of Pyrazino-oxazines

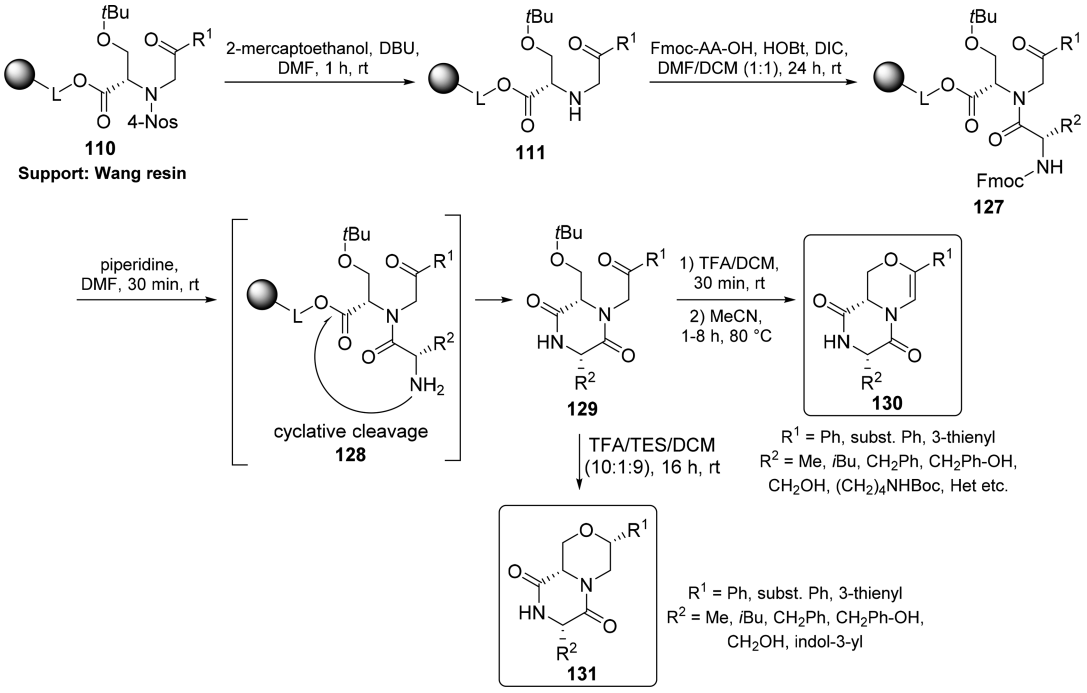

When intermediates **107** synthesized from polymer-supported Ser(*t*Bu)OH or Thr(*t*Bu)OH (X = O) were subjected to TFA-mediated cleavage from the resin, the corresponding 3,4-dihydro-2*H*-1,4-oxazines **108** (X = O) were formed (Scheme 21).[50,51] The same reaction outcome was observed when intermediates **107**, which were made from Cys(Trt)OH (X = S), were used to prepare thiazine scaffold **108** (X = S). If triethylsilane (TES) was added to the cleavage cocktail, olefin **108** (R^1 = H) was stereoselectively reduced to give the *R* configuration of the newly formed sp^3 carbon.[51] However, in the case of compounds **109** (R^1 = Me) made from Thr(*t*Bu)OH, the stereoselectivity was lost.

Desulfonylation of intermediates **110** followed by acylation with different carboxylic acids afforded intermediates **112**, which after treatment with TFA or TFA/TES, yielded the corresponding *N*-acyl dihydroxazines **113** and morpholines **114** (Scheme 22). Application of TES for the solid-phase synthesis of morpholine-3-ones **114** using intermediates acylated with α-halocarboxylic acids was previously reported by Krchňák; however, the resulting stereochemistry was not specified.[52]

Alternatively, intermediates **115** synthesized from *o*-nitrobenzenesulfonyl chlorides were reduced to the corresponding anilines **116** and cleaved from the polymer support to yield desired morpholines **117**. The final cyclization required harsher conditions and afforded benzoxazino[4,3-*b*][1,2,5]-thiadiazepinone 6,6-dioxides **118** (Scheme 23).[53] While the reduction of olefins **117** with TES was stereoselective, the cyclization to afford seven-membered scaffolds **120** led to a partial inversion of the resulting C^{12a} stereocenter (up to 20%). However, no racemization was observed for compounds with $R^{1,2}$ = H and R^3 = Ph.

The method was further extended to the acylation of intermediates **111** with *o*-nitrobenzoic acids. The solid-phase reduction led to spontaneous on-resin cyclization to benzodiazepinones **123**.[54] For this reason, intermediates **121** were subjected to cleavage and cyclization to morpholines **124**. After subsequent in situ reduction and cyclization, the target benzo[*e*][1,4]oxazino[4,3-*a*][1,4]diazepine-6,12-diones **126** were obtained (Scheme 24).[55] In this case, the cyclization of the seven-membered scaffold could be achieved under milder conditions, and for this reason, the resulting configuration remained unchanged, giving the final compounds **126** with full control of the stereocenters.

Acylation of intermediates **111** with Fmoc-amino acids yielded resin **127**, which upon deprotection with piperidine, underwent spontaneous cyclative cleavage, leading to the release of the corresponding piperazin-1,4-dione intermediates **129** from the polymer support (Scheme 25).[56] Subsequent cyclization in TFA afforded pyrazino-oxazines **130** with two controlled stereocenters. The use of TFA/TES/DCM cocktail led to the saturated derivatives **131** with the newly formed stereocenter.[57] The yields of the target compounds were slightly decreased due to unexpected dealkylation after the acylation step.

CONCLUSION

In the field of oxazine and thiazine scaffold-containing compounds, solid-phase synthesis has been proven to be an efficient tool for the synthesis of diverse derivatives using different starting materials, a wide range of coupling reactions, and a number of readily available building blocks. Synthesis of 1,2-dioxazines on solid-phase is practically limited to the application of hetero-Diels–Alder reaction and due to limited stability of 1,2-dioxazines toward strong acids, it requires a careful approach to the cleavage of products from polymer matrix. Synthetic strategies to prepare 1,3-dioxazines/thiazines are considerably more rich. 1,3-Dioxazine scaffold is typically constructed from immobilized propanolamines, taking advantage of nucleophilic addition of the hydroxy group to different electrofiles, such as iminiums or various oxo-derivatives. Similarly to solution-phase synthesis, the most frequently studied and diverse synthetic strategies can be found in the field of 1,4-oxazines/thiazines and benzoxazines/benzothiazines. Using SPS, these compounds have been traditionally

DOI: 10.1021/acscombsci.8b00076
ACS Comb. Sci. 2018, 20, 529–543

synthesized from polymer-supported ethanolamines/*o*-aminophenols or aminoethanethiols/2-aminothiophenols. Various compounds containing the mentioned structural unit, for example, trifunctional building blocks cysteine or serine, were immobilized to common supports (Wang or Rink amide or MBHA resin) and transformed to the target heterocycles. Recent progress in the field indicates that polymer-supported chemistry still offers interesting methodologies amenable to the production of novel drug-like oxazine and thiazine derivatives using high-throughput synthesis techniques. With respect to current trends in medicinal chemistry and specifically to the preparation of chiral compounds and scaffold with the 3D architecture, it is expected that further strategies suitable for the preparation of chiral oxazines/thiazines will be reported in the near future.

AUTHOR INFORMATION

Corresponding Author

*E-mail: miroslav.soural@upol.cz.

ORCID

Miroslav Soural: 0000-0001-7288-8617

Author Contributions

§P.K. and V.R. contributed equally to this work.

Notes

The authors declare no competing financial interest.

ACKNOWLEDGMENTS

The authors are grateful to National Program of Sustainability (project LO1304).

ABBREVIATIONS

ACN, acetonitrile; Alloc, allyloxycarbonyl; BAL, backbone amide linker; BOMBA resin, 4-benzyloxy-2-methoxybenzylamine resin; CDI, 1′-carbonyldiimidazole; Chx, cyclohexyl; DABCO, 1,4-diazabicyclo[2.2.2]octane; DBU, 1,8-diazabicyclo(5.4.0)undec-7-ene; DCE, 1,2-dichloroethane; DCM, dichloromethane; DDQ, 2,3-dichloro-5,6-dicyano-1,4-benzoquinone; DIAD, diisopropyl azocarboxylate; DIC, *N*,*N*′-diisopropylcarbodiimide; DIEA, *N*,*N*′-diisopropylethylamine; DMAP, 4-(dimethylamino)pyridine; DME, dimethoxyethane; DMF, *N*,*N*′-dimethylformamide; DMP, Dess−Martin periodinane; DMSO, dimethyl sulfoxide; EDC, 1-ethyl-3-(3-(dimethylamino)propyl)carbodiimide; Fmoc-AA-OH, Fmoc-amino acid; Fmoc-Ser(*t*Bu)-OH, Fmoc-O-*terc*-butyl-L-serine; Fmoc-Thr(*t*Bu)-OH, Fmoc-O-*terc*-butyl-L-threonine; Fmoc-Cys(Trt)-OH, Fmoc-O-trityl-L-cysteine; HATU, 1-[bis(dimethylamino)methylene]-1*H*-1,2,3-triazolo[4,5-*b*]pyridinium 3-oxide hexafluorophosphate; HBA, hydrogen bond acceptor; HDA, hetero-Diels−Alder; Het, heteroaromate or heteroaromatic substitution; HMBA linker, 4-hydroxymethylbenzoic acid linker; HOBt, 1-hydroxybenzotriazole; *i*Bu, isobutyl; *i*Pr, isopropyl; LiHDMS, lithium bis(trimethylsilyl)amide; MBHA, *p*-methylbenzhydrylamine; *m*CPBA, *m*-chloroperoxybenzoid acid; Ms, mesylate; MW, microwave; NEM, *N*-ethylmaleimide; NMM, *N*-methylmorpholine; NMO, *N*-methylmorpholine *N*-oxide; NMR, nuclear magnetic resonance; Nos, nitrobenzenesulfonyl; on, overnight; PEG, polyethylene glycol; $PEGA_{800}$ resin, 2-acrylamidoprop-1-yl-(2-aminoprop-1-yl)-polyethylene $glycol_{800}$; $Pd(PPh)_3$, tetrakis(triphenylphosphine)palladium(0); PIP, piperidine; *p*TSA, *p*-toluenesulfonic acid; rt, room temperature; SFC, supercritical fluidic chromatography; SPS, solid-phase synthesis; TBAF, tetra-*n*-butylammonium fluoride; TBAHS, tetrabutylammonium hydrogensulfate; TBTU, *N*,*N*,*N*′,*N*′-tetramethyl-*O*-(1*H*-benzotriazol-1-yl)uronium hexafluorophosphate; *t*Bu, *terc*-butyl; TEA, triethylamine; TES, triethylsilane; TFA, trifluoroacetic acid; THF, tetrahydrofuran; TMSCl, trimethylsilyl chloride; TPP, triphenylphosphine; Trt, trityl

REFERENCES

(1) Pal'chikov, V. A. Morpholines. Synthesis and Biological Activity. *Russ. J. Org. Chem.* **2013**, *49* (6), 787−814.

(2) Xu, Z.; Tice, C. M.; Zhao, W.; Cacatian, S.; Ye, Y. J.; Singh, S. B.; Lindblom, P.; McKeever, B. M.; Krosky, P. M.; Kruk, B. A.; Berbaum, J.; Harrison, R. K.; Johnson, J. A.; Bukhtiyarov, Y.; Panemangalore, R.; Scott, B. B.; Zhao, Y.; Bruno, J. G.; Togias, J.; Guo, J.; Guo, R.; Carroll, P. J.; McGeehan, G. M.; Zhuang, L.; He, W.; Claremon, D. A. Structure-Based Design and Synthesis of 1,3-Oxazinan-2-one Inhibitors of 11-*β*-Hydroxysteroid Dehydrogenase Type 1. *J. Med. Chem.* **2011**, *54* (17), 6050−6062.

(3) Kim, D. K.; Ryu, D. H.; Lee, J. Y.; Lee, N.; Kim, Y. W.; Kim, J. S.; Chang, K.; Im, G. J.; Kim, T. K.; Choi, W. S. Synthesis and Biological Evaluation of Novel A-Ring Modified Hexacyclic Camptothecin Analogues. *J. Med. Chem.* **2001**, *44* (10), 1594−1602.

(4) Gaggini, F.; Laleu, B. t.; Orchard, M.; Fioraso-Cartier, L.; Cagnon, L.; Houngninou-Molango, S.; Gradia, A.; Duboux, G.; Merlot, C.; Heitz, F.; Szyndralewiez, C.; Page, P. Design, Synthesis and Biological Activity of Original Pyrazolo-Pyrido-diazepine, -pyrazine and -oxazine Dione Derivatives as Novel Dual Nox4/Nox1 Inhibitors. *Bioorg. Med. Chem.* **2011**, *19* (23), 6989−6999.

(5) Shaquiquzzaman, M.; Verma, G.; Marella, A.; Akhter, M.; Akhtar, W.; Khan, M. F.; Tasneem, S.; Alam, M. M. Piperazine Scaffold: A Remarkable Tool in generation of Diverse Pharmacological Agents. *Eur. J. Med. Chem.* **2015**, *102* (Suppl C), 487−529.

(6) Breschi, M. C.; Calderone, V.; Digiacomo, M.; Manganaro, M.; Martelli, A.; Minutolo, F.; Rapposelli, S.; Testai, L.; Tonelli, F.; Balsamo, A. Spirocyclic Benzopyran-Based Derivatives as New Anti-ischemic Activators of Mitochondrial ATP-Sensitive Potassium Channel. *J. Med. Chem.* **2008**, *51* (21), 6945−6954.

(7) Kourounakis, A. P.; Charitos, C.; Rekka, E. A.; Kourounakis, P. N. Lipid-Lowering (Hetero)Aromatic Tetrahydro-1,4-Oxazine Derivatives with Antioxidant and Squalene Synthase Inhibitory Activity. *J. Med. Chem.* **2008**, *51* (18), 5861−5865.

(8) Bobek, M.; Kuhar, S.; Bloch, A. Synthesis and Biological Activity of 5-Fluoro- and 5-Methyl-1,3-oxazine-2,6(3*H*)-dione. *J. Med. Chem.* **1979**, *22* (5), 592−594.

(9) Jabeen, I.; Wetwitayaklung, P.; Klepsch, F.; Parveen, Z.; Chiba, P.; Ecker, G. F. Probing the Stereoselectivity of P-glycoprotein-synthesis, Biological Activity and Ligand Docking Studies of a Set of Enantiopure Benzopyrano[3,4-*b*][1,4]oxazines. *Chem. Commun.* **2011**, *47* (9), 2586−2588.

(10) Das, B. C.; Madhukumar, A. V.; Anguiano, J.; Mani, S. Design, Synthesis and Biological Evaluation of 2*H*-Benzo[*b*][1,4]oxazine Derivatives as Hypoxia Targeted Compounds for Cancer Therapeutics. *Bioorg. Med. Chem. Lett.* **2009**, *19* (15), 4204−4206.

(11) Gaster, L. M.; Wyman, P. A.; Ellis, E. S.; Brown, A. M.; Young, T. J. 5-HT_4 Receptor Antagonists: Oxazolo, Oxazino and Oxazepino[3,2-*a*]indole Derivatives. *Bioorg. Med. Chem. Lett.* **1994**, *4* (5), 667−668.

(12) San Feliciano, A.; Caballero, E.; Puebla, P.; Pereira, J. A. P.; Gras, J.; Valenti, C. Synthesis and Pharmacological Activities of Some Pyrido[2,1-*b*]oxazines. *Eur. J. Med. Chem.* **1992**, *27* (5), 527−535.

(13) Merrifield, R. B. Solid Phase Peptide Synthesis. I. The Synthesis of a Tetrapeptide. *J. Am. Chem. Soc.* **1963**, *85* (14), 2149−2154.

(14) Hlaváč, J.; Soural, M.; Krchňák, V. Practical Aspects of Combinatorial Solid-Phase Synthesis. In *Solid-Phase Organic Synthesis*; John Wiley & Sons, Inc., 2011; pp 95−130.

(15) Faita, G.; Mella, M.; Mortoni, A.; Paio, A.; Quadrelli, P.; Seneci, P. Solid-Supported Nitrile Oxides as Stable and Valuable Reactive Intermediates. *Eur. J. Org. Chem.* **2002**, *2002* (7), 1175−1183.

(16) Krchňák, V.; Moellmann, U.; Dahse, H. M.; Miller, M. J. Solid-Supported Nitroso Hetero Diels−Alder Reactions. 1. Acylnitroso Dienophiles: Scope and Limitations. *J. Comb. Chem.* **2008**, *10* (1), 94−103.
(17) Krchňák, V.; Moellmann, U.; Dahse, H. M.; Miller, M. J. Solid-Supported Nitroso Hetero Diels−Alder Reactions. 2. Arylnitroso Dienophiles: Scope and Limitations. *J. Comb. Chem.* **2008**, *10* (1), 104−111.
(18) Krchňák, V.; Moellmann, U.; Dahse, H. M.; Miller, M. J. Solid-Supported Nitroso Hetero-Diels−Alder Reactions. 3. Acid-Mediated Transformation of Cycloadducts by Scission of the Oxazine C−O Bonds. *J. Comb. Chem.* **2008**, *10* (1), 112−117.
(19) Harrison, A.; Melchionna, M.; Franco, P.; Hlavac, J. Solid-Phase Synthesis and Analysis of 3,6-Dihydro-2*H*-1,2-oxazines in Their Stereo- and Regioisomer Mixtures. *New J. Chem.* **2014**, *38* (11), 5491−5499.
(20) Krupkova, S.; Aguete, G. P.; Kocmanova, L.; Volna, T.; Grepl, M.; Novakova, L.; Miller, M. J.; Hlavac, J. Solid-Phase Synthesis of γ-Lactone and 1,2-Oxazine Derivatives and Their Efficient Chiral Analysis. *PLoS One* **2016**, *11* (11), No. e0166558.
(21) Lee, T.; Park, J. H.; Jeon, M. K.; Gong, Y. D. Solid-Phase Synthesis of 1,3,6-Trisubstituted-1*H*-thiazolo[4,5-*c*][1,2]thiazin-4-(3*H*)one-2,2-dioxide Derivatives Using Traceless Linker. *J. Comb. Chem.* **2009**, *11* (2), 288−293.
(22) Meester, W. J. N.; Rutjes, F. P. J. T.; Hermkens, P. H. H.; Hiemstra, H. Synthesis of Homoallylic Amines *via* *N*-Acyliminium Ion Reactions on Solid Support. *Tetrahedron Lett.* **1999**, *40* (8), 1601−1604.
(23) Schunk, S.; Enders, D. Solid-Phase Synthesis of β-Amino Ketones and Six-Ring Carbamates *via* Immobilized α-Alkoxycarbonylamino Sulfones. *Org. Lett.* **2001**, *3* (20), 3177−3180.
(24) Picard, S.; Le Roch, M.; Renault, J.; Uriac, P. Parallel Supported Synthesis of Polyamine−Imidazole Conjugates. *Org. Lett.* **2004**, *6* (25), 4711−4714.
(25) Vanier, C.; Wagner, A.; Mioskowski, C. Resin-Bound 4*H*-1,3-Oxazine-Masked β-Diketones for Functionalizing Cleavage Strategy. *J. Comb. Chem.* **2004**, *6* (5), 846−850.
(26) Strohmeier, G. A.; Haas, W.; Kappe, C. O. Synthesis of Functionalized 1,3-Thiazine Libraries Combining Solid-Phase Synthesis and Post-Cleavage Modification Methods. *Chem. Eur. J.* **2004**, *10* (12), 2919−2926.
(27) Strohmeier, G. A.; Kappe, C. O. Combinatorial Synthesis of Functionalized 1,3-Thiazine Libraries Using a Combined Polymer-Supported Reagent/Catch-and-Release Strategy. *Angew. Chem., Int. Ed.* **2004**, *43* (5), 621−624.
(28) Breitenbucher, J. G.; Figliozzi, G. Solid-Phase Synthesis of 4-Aryl-1,4-dihydropyridines *via* the Hantzsch Three Component Condensation. *Tetrahedron Lett.* **2000**, *41* (22), 4311−4315.
(29) (a) Le Quement, S. T.; Nielsen, T. E.; Meldal, M. Scaffold Diversity through Intramolecular Cascade Reactions of Solid-Supported Cyclic *N*-Acyliminium Intermediates. *J. Comb. Chem.* **2007**, *9* (6), 1060−1072. (b) Ventosa-Andres, P.; La-Venia, A.; Ripoll, C. A. B.; Hradilova, L.; Krchnak, V. Synthesis of nature-inspired medium-sized fused heterocycles from amino acids. *Chem. - Eur. J.* **2015**, *21* (37), 13112−13119.
(30) Meldal, M. PEGA: A Flow Stable Polyethylene Glycol Dimethyl Acrylamide Copolymer for Solid-Phase Synthesis. *Tetrahedron Lett.* **1992**, *33* (21), 3077−3080.
(31) Che, J.; Raghavendra, M. S.; Lam, Y. Traceless Solid-Phase Synthesis of Heteroannulated 1,3-Oxazin-6-ones. *J. Comb. Chem.* **2009**, *11* (3), 378−384.
(32) Delpiccolo, C. M. L.; Testero, S. A.; Leyes, F. N.; Boggián, D. B.; Camacho, C. M.; Mata, E. G. Stereoselective, Solid Phase-Based Synthesis of *trans* 3-Alkyl-Substituted β-Lactams as Analogues of Cholesterol Absorption Inhibitors. *Tetrahedron* **2012**, *68* (52), 10780−10786.
(33) Delpiccolo, C. M. L.; Méndez, L.; Fraga, M. A.; Mata, E. G. Exploring the Solid-Phase Synthesis of 3,4-Disubstituted β-Lactams: Scope and Limitations. *J. Comb. Chem.* **2005**, *7* (2), 331−344.
(34) Delpiccolo, C. M. L.; Mata, E. G. Stereoselective Solid-Phase Synthesis of 3,4-Substituted Azetidinones as Key Intermediates for Mono- and Multicyclic β-Lactam Antibiotics and Enzyme Inhibitors. *Tetrahedron: Asymmetry* **2002**, *13* (9), 905−910.
(35) Prosa, N.; Turgis, R.; Piccardi, R.; Scherrmann, M. C. Soluble Polymer-Supported Flow Synthesis: A Green Process for the Preparation of Heterocycles. *Eur. J. Org. Chem.* **2012**, *2012* (11), 2188−2200.
(36) Nefzi, A.; Giulianotti, M.; Houghten, R. A. Solid Phase Synthesis of 2,4,5-Trisubstituted Thiomorpholin-3-ones. *Tetrahedron Lett.* **1998**, *39* (22), 3671−3674.
(37) Mortezaei, R.; Ida, S.; Campbell, D. A. Preparation of *N*-Alkylated 5-Oxo-3-carboxamyl-1,4-thiazinanes on Solid Support. *Mol. Diversity* **1998**, *4* (2), 143−148.
(38) Liu, Z.; Nefzi, A. Ugi Four-Center Three-Component Reaction for the Parallel Solid-Phase Synthesis of *N*-Substituted Thiomopholinones. *Tetrahedron Lett.* **2012**, *53* (9), 1013−1014.
(39) Saruta, K.; Ogiku, T. A Traceless Solid Phase Synthesis of Thiomorpholin-3-ones. *Tetrahedron Lett.* **2008**, *49* (3), 424−427.
(40) Nicolaou, K. C.; Baran, P. S.; Zhong, Y. L.; Sugita, K. Iodine(V) Reagents in Organic Synthesis. Part 1. Synthesis of Polycyclic Heterocycles *via* Dess−Martin Periodinane-Mediated Cascade Cyclization: Generality, Scope, and Mechanism of the Reaction. *J. Am. Chem. Soc.* **2002**, *124* (10), 2212−2220.
(41) Gräßle, S.; Vanderheiden, S.; Hodapp, P.; Bulat, B.; Nieger, M.; Jung, N.; Bräse, S. Solid Phase Synthesis of (Benzannelated) Six-Membered Heterocycles *via* Cyclative Cleavage of Resin-Bound Pseudo-Oxazolones. *Org. Lett.* **2016**, *18* (15), 3598−3601.
(42) Lee, J. M.; Yu, E.-A.; Park, J. Y.; Ryu, I. A.; Shin, D. S.; Gong, Y.-D. Solid-phase synthesis of 7-aryl-benzo[b][1,4]oxazin-3(4H)-one derivatives on a BOMBA resin utilizing the Smiles rearrangement. *Bull. Korean Chem. Soc.* **2009**, *30* (6), 1325−1330.
(43) Dixon, S.; Wang, X.; Lam, K. S.; Kurth, M. J. Solid-Phase Synthesis of Quinoxaline, Thiazine, and Oxazine Analogs through a Benzyne Intermediate. *Tetrahedron Lett.* **2005**, *46* (43), 7443−7446.
(44) Lemrová, B.; Soural, M. Solid-Phase Synthesis of 4,7,8-Trisubstituted 1,2,3,4-Tetrahydro-benzo[*e*][1,4]diazepin-5-ones. *ACS Comb. Sci.* **2012**, *14* (12), 645−650.
(45) Yokum, T. S.; Alsina, J.; Barany, G. Solid-Phase Syntheses of Heterocycles Containing the 2-Aminothiophenol Moiety. *J. Comb. Chem.* **2000**, *2* (3), 282−292.
(46) Drábiková, M.; Krajčovičová, S.; Soural, M. Mitsunobu C-Alkylation of β-Alkoxycarbonyl 2-Nitrobenzenesulfones and its Use for the Rapid Synthesis of Novel Benzothiazine Derivatives. *Tetrahedron* **2017**, *73* (44), 6296−6306.
(47) Attanasi, O. A.; Filippone, P.; Lillini, S.; Mantellini, F.; Nicolini, S.; de los Santos, J. S. M.; Ignacio, R.; Aparicio, D.; Palacios, F. Reactions of 1,2-Diaza-1,3-dienes with Thiol Derivatives: A Versatile Construction of Nitrogen/Sulfur Containing Heterocycles. *Tetrahedron* **2008**, *64* (39), 9264−9274.
(48) Attanasi, O. A.; De Crescentini, L.; Filippone, P.; Mantellini, F.; Santeusanio, S. Improved Synthesis of Substituted Quinoxalines from New N = N-Polymer-bound 1,2-Diaza-1,3-butadienes. *Synlett* **2003**, *2003* (08), 1183−1185.
(49) Fülöpová, V.; Krchňáková, A.; Schütznerová, E.; Zajíček, J.; Krchňák, V. Ring Contraction of 2,5-Dihydrobenzo[*f*][1,2,5]-thiadiazepine 1,1-Dioxides: Access to 4*H*-Benzo[*b*][1,4]thiazine 1,1-Dioxides. *J. Org. Chem.* **2015**, *80* (3), 1795−1801.
(50) Fülöpová, V.; Krchňák, V. Solid-Phase Synthesis of Trisubstituted 2,5-Dihydrobenzo[*f*][1,2,5]thiadiazepine 1,1-Dioxide Derivatives. *ACS Comb. Sci.* **2014**, *16* (8), 412−420.
(51) Králová, P.; Fülöpová, V.; Maloň, M.; Volná, T.; Popa, I.; Soural, M. Stereoselective Polymer-Supported Synthesis of Morpholine- and Thiomorpholine-3-carboxylic Acid Derivatives. *ACS Comb. Sci.* **2017**, *19* (3), 173−180.
(52) Pudelova, N.; Krchnak, V. Multiplicity of Diverse Heterocycles from Polymer- Supported α-Acylamino Ketones. *J. Comb. Chem.* **2009**, *11* (5), 851−859.

DOI: 10.1021/acscombsci.8b00076
ACS Comb. Sci. 2018, 20, 529−543

(53) Králová, P.; Maloň, M.; Volná, T.; Ručilová, V.; Soural, M. Polymer-Supported Stereoselective Synthesis of Benzoxazino[4,3-*b*][1,2,5]thiadiazepinone 6,6-dioxides. *ACS Comb. Sci.* **2017**, *19* (10), 670−674.
(54) Fülöpová, V.; Gucký, T.; Grepl, M.; Soural, M. Solid-Phase Synthesis of Trisubstituted Benzo[1,4]-Diazepin-5-one Derivatives. *ACS Comb. Sci.* **2012**, *14* (12), 651−656.
(55) Králová, P.; Maloň, M.; Soural, M. Stereoselective Synthesis of Benzo[*e*][1,4]oxazino[4,3-*a*][1,4]diazepine-6,12-diones with Two Diversity Positions. *ACS Comb. Sci.* **2017**, *19* (12), 770−774.
(56) Ručilová, V.; Králová, P.; Soural, M. Synthesis of Disubstituted Pyrazino-Oxazine Derivatives with Controlled Stereochemistry. *Eur. J. Org. Chem.* **2017**, *2017* (47), 7034−7039.
(57) Ručilová, V.; Maloň, M.; Soural, M. Use of Triethylsilane for Directed Enantioselective Reduction of Olefines: Synthesis of Pyrazino[2,1-*c*][1,4]oxazine-6,9-diones with Full Control of the Absolute Configuration. *Eur. J. Org. Chem.* **2018**, *2018* (4), 564−570.

DOI: 10.1021/acscombsci.8b00076
ACS Comb. Sci. 2018, 20, 529−543

ACS Combinatorial Science

Research Article

pubs.acs.org/acscombsci

Polymer-Supported Stereoselective Synthesis of Benzoxazino[4,3-*b*][1,2,5]thiadiazepinone 6,6-dioxides

Petra Králová,[†] Michal Maloň,[‡] Tereza Volná,[†] Veronika Ručilová,[§] and Miroslav Soural*[,§]

[†]Department of Organic Chemistry, Faculty of Science, Palacký University, 771 46 Olomouc, Czech Republic

[‡]JEOL Resonance, Inc., Musashino 3-1-2, Akishima, Tokyo 196-8558, Japan

[§]Institute of Molecular and Translational Medicine, Faculty of Medicine and Dentistry, Palacký University, Hněvotínská 5, 779 00 Olomouc, Czech Republic

Supporting Information

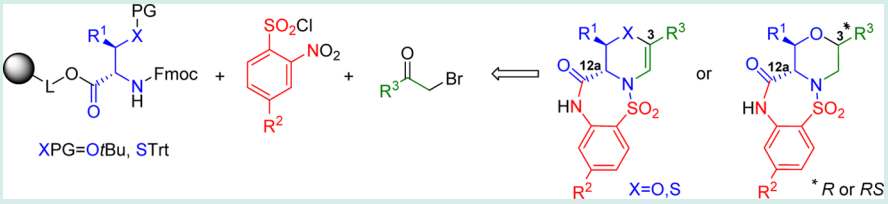

ABSTRACT: Herein, we report the stereoselective synthesis of trisubstituted benzoxazino[4,3-*b*][1,2,5]thiadiazepinone 6,6-dioxides from polymer-supported Fmoc-Ser(*t*Bu)-OH and Fmoc-Thr(*t*Bu)-OH. After the solid-phase synthesis of *N*-alkylated-*N*-sulfonylated intermediates using various 2-nitrobenzenesulfonyl chlorides and bromoketones, the target compounds were obtained via trifluoroacetic acid (TFA)-mediated cleavage from the resin, followed by cyclization of the diazepinone scaffold. Except for the threonine-based intermediates, the inclusion of triethylsilane (TES) in the cleavage cocktail yielded a specific configuration of the newly formed C^3 chiral center. The final cyclization resulted in minor or no inversion of the C^{12a} stereocenter configuration.

KEYWORDS: *serine, cysteine, threonine, morpholine, thiomorpholine, benzoxazinothiadiazepinone, nitrobenzenesulfonyl chloride, bromoketone, solid-phase synthesis, triethylsilane, stereoselective synthesis*

INTRODUCTION

2/4-Nitrobenzenesulfonyl chlorides (NosCls) are efficient starting materials to prepare diverse, pharmacologically promising heterocycles, and for this reason, their use in organic synthesis has received considerable attention over the past decade.[1] Readily available, polymer-supported nitrobenzenesulfonamides (NosAs) were subjected to Fukuyama alkylation,[2] followed by base-mediated *C*/*N*-arylations with the concomitant cleavage of sulfur dioxide, which yielded various scaffolds, such as indazoles,[3] quinazolines,[4] or indoles.[5] Alternatively, 2-nitrobenzensulfonamides were reduced to 2-aminobenzensulfonamides and converted to different fused bicyclic[6−9] or tricyclic[10−12] compounds, including scaffolds with sp^3 carbons and 3D architecture.[11,12] In this context, compounds with 6 + 6 or 5 + 6 fused rings were reported. Considering the interesting physicochemical and biological properties of seven-membered cycles, we applied NosAs chemistry to prepare fused 7 + 6 heterocycles containing the benzodiazepine scaffold. 1,4-Benzodiazepines with fused heterocycles have been reported as highly potent ligands for different molecular targets. For instance, anxiolytic triazolobenzodiazepinones[13] and imidazolobenzodiazepinones,[14] antitumor pyrrolobenzodiazepinones,[15] vasopressin receptor antagonists oxazinobenzodiazepines,[16] thiazinobenzodiazepines,[16] and pyrazinobenzodiazepines[17] or dopamine D2 receptor antagonists thiazolobenzodiazepinones[18] have been reported.

Recently, we applied 2-nitrobenzensulfonamides to the synthesis of trisubstituted morpholines and thiomorpholines.[19] Herein, we describe the further extension of this chemistry to prepare structurally novel heterocycles—morpholinobenzothiadiazepines. The important feature is the stereoselective control of the newly formed C^3 chiral center and only minor inversion of the C^{12a} configuration in the majority of tested examples.

RESULTS AND DISCUSSION

The suggested synthetic approach (Scheme 1) was initially tested with Wang resin-immobilized Fmoc-Ser(*t*Bu)-OH **1**{*1*} and two representative building blocks: 2-nitrobenzenesulfonyl chloride and 2-bromoacetophenone. The synthesis of *N*-alkyl 2-nitrobenzenesulfonamide was performed according to the protocols we reported recently,[19] which provided the resin-bound intermediate **5**{*1,1,1*} in an excellent crude purity of 99% (evaluated from the LC-UV trace after cleavage from the resin). The nitro group was reduced using the sodium dithionate method,[20] followed by the acid-mediated cleavage

Received: July 25, 2017
Revised: August 15, 2017
Published: August 21, 2017

DOI: 10.1021/acscombsci.7b00115
ACS Comb. Sci. 2017, 19, 670−674

Scheme 1. General Synthesis of Final Compounds 9 and 10[a]

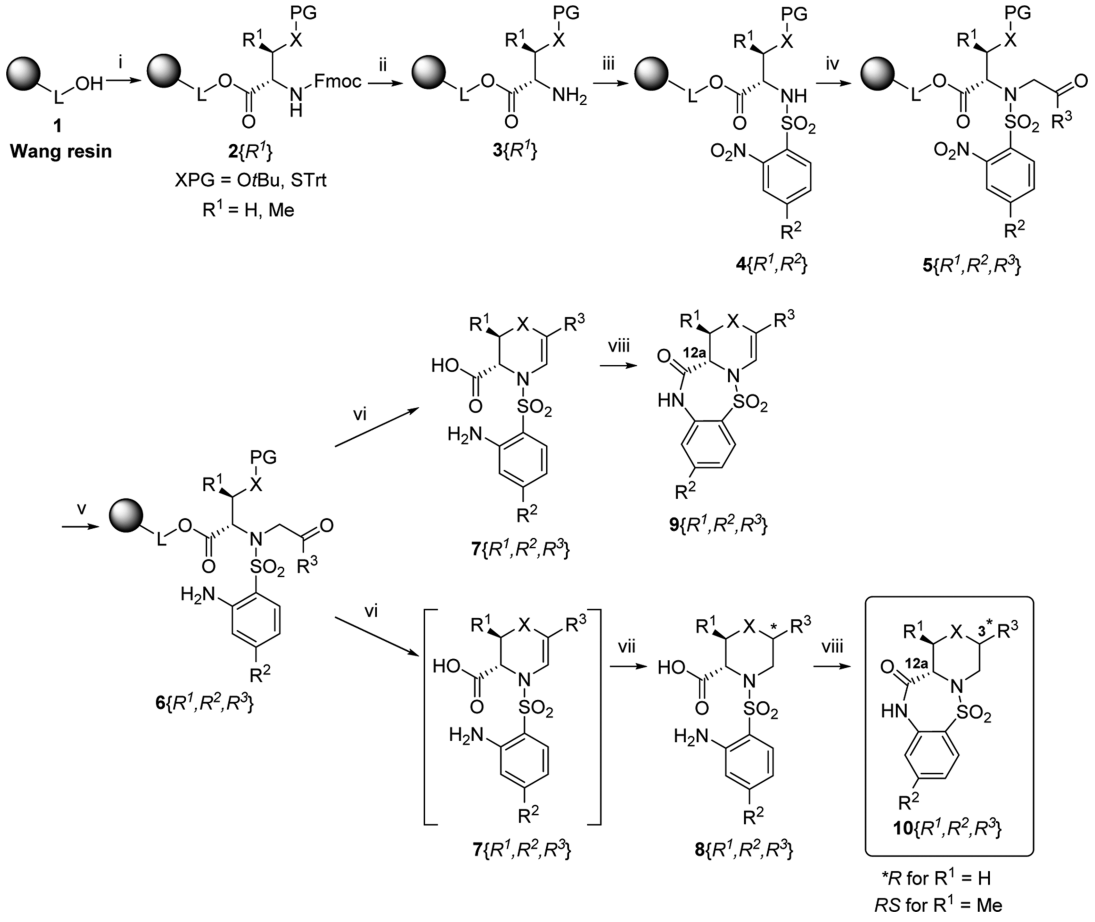

[a]Reagents and conditions: (i) Fmoc-amino acid, HOBt, DMAP, DIC, DMF, DCM, 24h, rt; (ii) 50% piperidine/DMF, 30 min, rt; (iii) 4-substituted 4-Nos-Cl, 2,6-lutidine, DCM, 24h (for derivative 7{1,2} 44 h), rt; (iv) R^3COCHBr, DIEA, DMF, 24 h, rt(for derivative 7{1,2,1} 43h, rt and for derivative 7{2,1,1} 72 h, rt); (v) Na_2S_2O, K_2CO_3, TBAHS, 50% DCM/H_2O, 2−5 h, rt (for serine and threonine derivative) or $SnCl_2.2H_2O$, DIEA, degassed DMF, 30 min, rt (for cysteine derivatives); (vi) TFA/DCM, 2.5−24 h, rt; (vii) *p*TSA, anhydrous $PhCH_3$, 3.5−12 h, 110 °C or *p*TSA, anhydrous DCE, 1−144 h, 90 °C.

of intermediate **6**{*1,1,1*} from the resin. Although TFA cleavage of analogous compounds was previously described to yield benzodiazepines via the attack of the ketone by an amino group,[7,22] we achieved the preferential formation of the morpholine scaffold and intermediate **7**{*1,1,1*} in high crude purity. Potential formation of benzodiazepine derivative was not detected in LC-UV-MS traces.

After a number of unsuccessful attempts, the cyclization of intermediate **7**{*1,1,1*} to the final compound was accomplished via reflux in anhydrous toluene or anhydrous 1,2-dichloroethane (DCE) in the presence of *p*-toluenesulfonic acid (*p*TSA) under Dean−Stark conditions. The corresponding product **9**{*1,1,1*}^{tol} was obtained in a crude purity of 77% and an overall yield of 35%, whereas the use of DCE provided slightly better results (**9**{*1,1,1*}^{DCE} in a crude purity of 81%, overall yield of 51%). On the other hand, the cyclization methods had significantly different influences on the resulting configuration of the resulting C^{12a} stereocenter (see later in the text). The addition of TES into the cleavage cocktail led to the formation of saturated intermediate **8**{*1,1,1*}, which finally afforded the saturated product **10**{*1,1,1*}^{DCE} in a crude purity of 85% and overall yield of 42%. NMR analysis of **10**{*1,1,1*}^{DCE} revealed the presence of C^{12a} *S,R* isomers in a ratio of 92:8. To clarify the formation of the minor stereoisomer, we investigated the stereochemical outcome of each step of the reaction sequence using chiral supercritical fluidic chromatography (SFC). It was discovered that the second stereoisomer was already formed after the immobilization of Fmoc-Ser(*t*Bu)-OH on the Wang resin. This fact indicated that DCE cyclization had no impact on the resulting stereochemistry of **10**{*1,1,1*}^{DCE}. In contrast, the use of toluene yielded compound **10**{*1,1,1*}^{tol} as a mixture of the corresponding C^{12a} *S,R* isomers in a ratio of 77:23. For this reason, cyclization using DCE was applied as the method of choice to synthesize and study other derivatives.

When immobilized Fmoc-Thr(*t*Bu)-OH was used instead of Fmoc-Ser(*t*Bu)-OH, the corresponding methylmorpholine products **9**{*2,1,1*} and **10**{*2,1,1*} were obtained. The threonine-based intermediates exhibited different behavior than the serine analogues: the alkylation of intermediate **4**{*2,1*} required an increased concentration of the alkylating species and base (see Supporting Information for more details). The resulting methylmorpholine product **10**{*2,1,1*} was detected as a mixture of separable C^3 *R,S* isomers **10a**{*2,1,1*} and **10b**{*2,1,1*} in a ratio of 63:37 (calculated from the crude LC-UV trace). Such nonstereoselective TES reduction of threonine-based intermediates **7** is in accordance with our previous results.[19] As for unsaturated products **9**, the final cyclization method of **10**{*1,1,4*}^{tol} using toluene led to C^{12a} full

DOI: 10.1021/acscombsci.7b00115
ACS Comb. Sci. 2017, 19, 670−674

Table 1. List of Synthesized and Fully Characterized Products

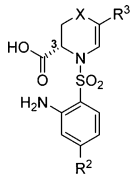

7{*R*[1],*R*[2],*R*[3]}

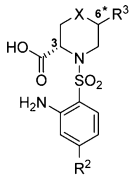

8{*R*[1],*R*[2],*R*[3]}
R for R[1] = H
R,*S* for R[1] = CH3

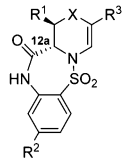

9{*R*[1],*R*[2],*R*[3]}

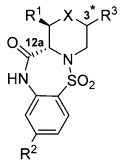

10{*R*[1],*R*[2],*R*[3]}
R for R[1] = H
R,*S* for R[1] = CH3

Entry	cmpd	X	R[1]	R[2]	R[3]	crude purity [%][a]	purity [%][b]	overall yield [%][c]	ratio of stereoisomers [%][c,d]
1	**7**{*1,1,4*}	O	-	H	4-Br-Ph	87	98	58	-
2	**8**{*1,1,1*}	O	-	H	Ph	83	95	77	-
3	**9**{*1,1,1*}^{tol}	O	H	H	Ph	77	99	35	77:23[d]
4	**9**{*1,1,1*}^{DCE}	O	H	H	Ph	81	98	51	92:8[d]
5	**9**{*1,1,2*}	O	H	H	4-Me-Ph	88	95	44	87:13[d]
6	**9**{*1,2,1*}	O	H	MeO	Ph	91	99	51	75:25[d]
7	**9**{*1,3,1*}	O	H	Cl	Ph	78	98	34	77:23[d]
8	**9**{*1,4,1*}	O	H	CF_3	Ph	70	99	42	73:27[d]
9	**9**{*1,5,1*}	O	H	NH_2	Ph	80	NI	NI	-
10	**9**{*1,1,4*}^{tol}	O	H	H	4-Br-Ph	65	97	40	63:37[d]
11	**9**{*1,1,5*}	O	H	H	4-CF_3-Ph	95	99	41	77:23[d]
12	**9**{*1,1,6*}	O	H	H		85	95	5	72:28[d]
13	**9**{*2,1,1*}	O	Me	H	Ph	92	99	32	100:0[d]
14	**9**{*3,1,1*}	S	H	H	Ph	82	90	27	25:75[d]
15	**10**{*1,1,1*}^{tol}	O	H	H	Ph	84	95	41 inseparable C^{12a} *S,R* isomers	77:23[c]
16	**10**{*1,1,1*}^{DCE}	O	H	H	Ph	85	98	42 inseparable C^{12a} *S,R* isomers	92:8[c]
17	**10**{*1,2,1*}	O	H	MeO	Ph	90	98	39	100:0[c]
18	**10**{*1,3,1*}	O	H	Cl	Ph	70	99	38	100:0[c]
19	**10**{*1,4,1*}	O	H	CF_3	Ph	57	98	40	100:0[c]
20	**10**{*1,1,2*}	O	H	H	4-Me-Ph	91	99	42 inseparable C^{12a} *S,R* isomers	87:13[c]
21	**10**{*1,1,3*}	O	H	H	4-NH_2-3,5-diCl-Ph	82	97	36 inseparable C^{12a} *S,R* isomers	71:29[c]
22	**10**{*1,1,4*}^{tol}	O	H	H	4-Br-Ph	84	98	10 inseparable C^{12a} *S,R* isomers	50:50[c]
23	**10**{*1,1,4*}^{DCE}	O	H	H	4-Br-Ph	87	95	44	100:0[c]
24	**10**{*1,1,6*}	O	H	H		85	95	44 inseparable C^{12a} *S,R* isomers	74:26[c]
25	**10a**{*2,1,1*}	O	Me	H	Ph	50	98	35 separable C^3 *R* isomer	100:0[c]
26	**10b**{*2,1,1*}	O	Me	H	Ph	30	98	17 separable C^3 S isomer	100:0[c]

[a]Overall purity after the entire reaction sequence calculated from HPLC-UV (205−400 nm). [b]HPLC-UV after purification (205−400 nm). [c]Ratio of C^{12a} *S,R* stereoisomers calculated from ^{1}H NMR of the purified product. [d]Ratio of C^{12a} *S,R* enantiomers determined by SFC of the purified product. NI: Not isolated (decomposition during HPLC purification).

racemization, whereas the use of DCE did not change the resulting configuration of **10**{*1,1,4*}^{DCE} (see Table 1).

Analogously, use of Fmoc-Cys(Trt)-OH yielded thiomorpholine product **9**{*3,1,1*}. It is worth mentioning that the reduction of cysteine intermediate **5**{*3,1,1*} with sodium dithionate failed, and only a mixture of unknown products was obtained. In contrast, the use of tin(II)chloride dihydrate afforded the desired intermediate **6**{*3,1,1*} in excellent crude purity (94%, LC-UV trace at 205−400 nm). However, subsequent TES reduction was unsuccessful even at elevated temperature.

To evaluate the limitation and scope of the method, we tested various 2-nitrobenzenesulfonyl chlorides and bromoketones containing both electron-donating and electron-withdrawing groups (see Figure 1 for the list of tested building blocks and Table 1 for the list of synthesized compounds). All substituted sulfonyl chlorides were used in combination with Fmoc-Ser(*t*Bu)-OH and unsubstituted bromoacetophenone. In each case, the corresponding intermediates **5**{*1,R*[2],*R*[3]} were obtained in excellent crude purity (95−99%, LC-UV trace at 205−400 nm). However, sulfonylation with a methoxy derivative and the subsequent alkylation step required longer reaction times due to the electron-donating effect. The

DOI: 10.1021/acscombsci.7b00115
ACS Comb. Sci. 2017, 19, 670−674

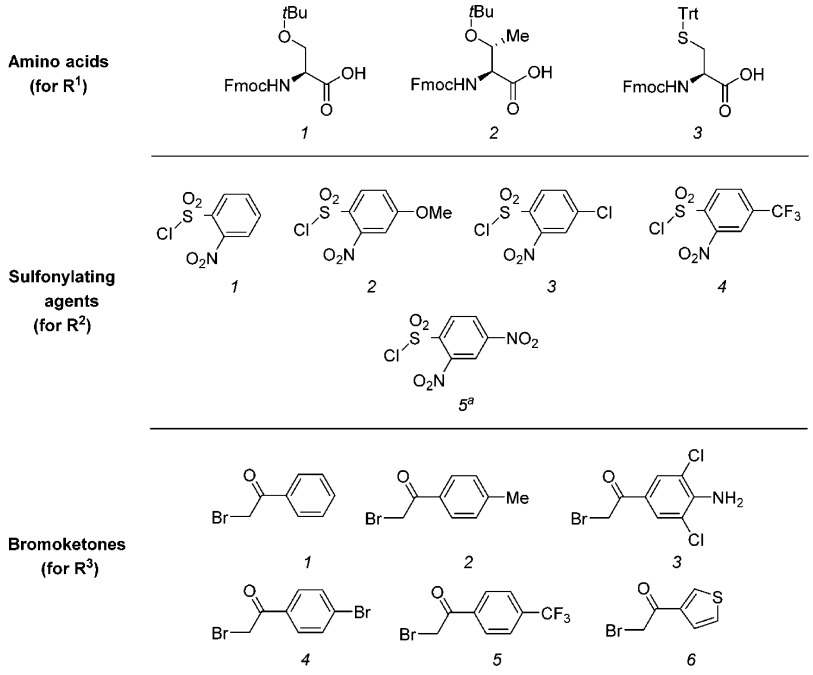

Figure 1. List of tested building blocks.

reduction of derivatives **5**{R^1,R^2,R^3} required a different reaction time and yielded compounds **6**{R^1,R^2,R^3} with very good crude purity (82−98%, LC-UV trace at 205−400 nm). As for the model compounds described earlier in the text, the intermediates **6**{R^1,R^2,R^3} were cleaved from the resin in a mixture of TFA in DCM, and for saturated derivatives **8**{R^1,R^2,R^3}, TES was subsequently added into the cleavage cocktail (see Supporting Information for details). Although the minor formation of target compounds **9** and **10** was observed after the acidic release of intermediates **7** and **8** from the resin (up to 10%), prolonged exposure to the cleavage cocktail did not lead to higher conversion, and heating in anhydrous DCE or toluene with *p*TSA catalysis was required for completion. The cyclization time for almost all of the saturated products **10**{R^1,R^2,R^3} was significantly longer compared to unsaturated derivatives **9**{R^1,R^2,R^3} (see Supporting Information for details). The synthesis of **9**{*1*,*1*,*3*} failed in the stage of the final cyclization step. Unsaturated product **9**{*1*,*5*,*1*} was prepared as a crude compound, but it decomposed during purification using reverse-phase HPLC. Furthermore, crude product **8**{*1*,*5*,*1*} decomposed after the addition of TES, and the corresponding saturated product **10**{*1*,*5*,*1*} was not detected, which indicates that 2,4-dinitrobenzenesulfonyl chloride is not compatible with this method.

Considering the sp^3 carbons in the final scaffold, the key goal was to evaluate the stereochemical outcome of the method. According to our previous report on single (thio)morpholines, the synthesis of intermediates **8** from serine or cysteine was expected to yield the 3*S* and 6*R* configuration, whereas analogous threonine intermediates have been reported to yield C^6 racemization after TES reduction.[19] For the unsaturated intermediates **7**, we studied the C^3 stereochemistry using the representative compound **7**{*1*,*1*,*1*} in comparison to the racemic standard $\mathbf{7}^{RS}${*1*,*1*,*1*}. Its analysis with SFC confirmed the retention of the C^3 configuration (*S*); however, the formation of the second enantiomer (8%) was observed as a consequence of immobilization on Wang resin leading to 8% racemization of **2**{*1*} (see the Supporting Information). In the case of Fmoc-Thr(*t*Bu)-OH, the racemization of **2**{*2*} was not observed. For TES-reduced intermediates **8**, NMR analysis of **8**{*1*,*1*,*1*} proved the stereoselective formation of C^6 in the serine intermediate (*R*). The final task was to study the impact of *p*TSA cyclization on the overall stereochemistry. In the past, we observed partial[21] or full[10] racemization when the amino acid carboxylate was further subjected to cyclization, yielding the imidazole scaffold. More importantly, substrate-dependent racemization was recently observed after the cyclization of structurally analogous dihydrobenzo[f][1,2,5]thiadiazepin-4(5*H*)-one 1,1-dioxides.[9] For this reason, we decided to systematically investigate the stereochemical outcome of DCE cyclization through the detailed structural analysis of all prepared compounds. For unsaturated compounds **9**{R^1,R^2,R^3}, SFC was used to detect the possible formation of C^{12a} *R*,*S* isomers. For saturated compounds **10**{R^1,R^2,R^3}, the possible formation of the corresponding diastereomers was evaluated using NMR. From the results, we can conclude that the cyclization partially affects the resulting C^{12a} configuration. Although the model compounds **9**{*1*,*1*,*1*}^{DCE} and **10**{*1*,*1*,*1*}^{DCE} have been prepared without any conversion of the C^{12a} stereocenter, their substituted analogues provided different results. SFC analysis of products **9**{R^1,R^2,R^3} cyclized in DCE revealed the presence of the C^{12a} *R* isomer in a quantity 8−27%. This indicates C^{12a} 0−19% epimerization after the cyclization step (8% was assigned to epimerization caused by the immobilization, as mentioned earlier in the text). The similar results were observed for crude saturated products **10**{R^1,R^2,R^3}, their subsequent semipreparative HPLC purification allowed for isolation of major diastereomer. However, in some cases the separation of C^{12a} *R*,*S* isomers was not possible (see Table 1).

CONCLUSION

In conclusion, we reported the use of triethylsilane for the preparation of structurally novel morpholinobenzothiadiaze-

DOI: 10.1021/acscombsci.7b00115
ACS Comb. Sci. 2017, 19, 670−674

pines with a controlled 3D architecture. Only minor limitations were observed, and the developed method provided 21 diversely substituted derivatives with good overall yields and crude purities. Analysis of the C^3 and C^{12a} stereocenters was achieved using a combination of chiral SFC and advanced NMR experiments. The formation of the C^3 stereocenter was fully stereoselective, except for compounds synthesized from threonine. The resulting C^{12a} configuration was rather slightly influenced by the final cyclization. The best results were obtained using dichloroethane, whereas the cyclization in toluene led to higher level of racemization. The developed protocols allow for the simple preparation of target compounds with a specific configuration using common coupling reagents and conditions and readily available starting material.

■ ASSOCIATED CONTENT

Supporting Information

The Supporting Information is available free of charge on the ACS Publications website at DOI: 10.1021/acscombsci.7b00115.

Details of experimental, synthetic, and analytical procedures, along with spectroscopic data for synthesized compounds (PDF)

■ AUTHOR INFORMATION

Corresponding Author

*E-mail: miroslav.soural@upol.cz.

ORCID

Miroslav Soural: 0000-0001-7288-8617

Notes

The authors declare no competing financial interest.

■ ACKNOWLEDGMENTS

The authors are grateful to project CZ.1.07/2.3.00/20.0009 from the European Social Fund, the National Program of Sustainability (project LO1304) and an internal grant from Palacký University IGA_PrF_2017_009 and IGA_LF_2017_028.

■ REFERENCES

(1) Fulopova, V.; Soural, M. Mining the Chemical Space: Application of 2/4-Nitrobenzenesulfonamides in Solid-Phase Synthesis. *ACS Comb. Sci.* **2015**, *17*, 570−591.

(2) Fukuyama, T.; Jow, C. K.; Cheung, M. 2- and 4-nitrobenzenesulfonamides: exceptionally versatile means for preparation of secondary amines and protection of amines. *Tetrahedron Lett.* **1995**, *36*, 6373−6374.

(3) Bouillon, I.; Zajicek, J.; Pudelova, N.; Krchnak, V. Remarkably Efficient Synthesis of 2H-Indazole 1-Oxides and 2H-Indazoles via Tandem Carbon-Carbon Followed by Nitrogen-Nitrogen Bond Formation. *J. Org. Chem.* **2008**, *73*, 9027−9032.

(4) Fulopova, V.; Cziesla, L.; Fleming, M.; Lu, Y.; Voelker, A.; Krchnak, V. Traceless Solid-Phase Synthesis of Trisubstituted Quinazolines. *ACS Comb. Sci.* **2015**, *17*, 470−473.

(5) Schutznerova, E.; Krchnak, V. Solid-Phase Synthesis of 2-Aryl-3-alkylamino-1H-indoles from 2-Nitro-N-(2-oxo-2-arylethyl)-benzenesulfonamides via Base-Mediated C-Arylation. *ACS Comb. Sci.* **2015**, *17*, 137−146.

(6) Makino, S.; Nakanishi, E.; Tsuji, T. Efficient Synthesis of 2,4-Disubstituted 1,2,4-Benzothiadiazin-3-one 1,1-Dioxides on Solid Support. *J. Comb. Chem.* **2003**, *5*, 73−78.

(7) Fulopova, V.; Krchnak, V. Solid-Phase Synthesis of Trisubstituted 2,5-Dihydrobenzo[f][1,2,5]thiadiazepine 1,1-Dioxide Derivatives. *ACS Comb. Sci.* **2014**, *16*, 412−420.

(8) Fulopova, V.; Krchnakova, A.; Schutznerova, E.; Zajicek, J.; Krchnak, V. Ring Contraction of 2,5-Dihydrobenzo[f][1,2,5]-thiadiazepine 1,1-Dioxides: Access to 4H-Benzo[b][1,4]thiazine 1,1-Dioxides. *J. Org. Chem.* **2015**, *80*, 1795−1801.

(9) Trapani, P.; Volna, T.; Soural, M. Solid-phase synthesis of 2,3-dihydrobenzo[f][1,2,5]thiadiazepin-4(5H)-one 1,1-dioxides with three diversity positions. *ACS Comb. Sci.* **2016**, *18*, 349−354.

(10) McMaster, C.; Fulopova, V.; Popa, I.; Grepl, M.; Soural, M. Solid-Phase Synthesis of Anagrelide Sulfonyl Analogues. *ACS Comb. Sci.* **2014**, *16*, 221−224.

(11) Schutznerova, E.; Verdia, P.; Krchnak, V. Fused Ring Molecular Scaffold with 3D Architecture for Constrained Peptidomimetics: Polymer-Supported Stereoselective Synthesis of Tetrahydrobenzo[e]-pyrazino[2,1-c][1,2,4]thiadiazinone 6,6-dioxide *via* N-Acyl Iminiums. *ACS Comb. Sci.* **2016**, *18*, 655−659.

(12) Cankarova, N.; La Venia, A.; Krchnak, V. Polymer-Supported Stereoselective Synthesis of Tetrahydrobenzopyrazino-thiadiazinone Dioxides via N-Sulfonyl Iminiums. *ACS Comb. Sci.* **2014**, *16*, 293−302.

(13) Mandrioli, R.; Mercolini, L.; Raggi, M. A. Benzodiazepine metabolism: an analytical perspective. *Curr. Drug Metab.* **2008**, *9*, 827−44.

(14) Olkkola, K. T.; Ahonen, J. Midazolam and Other Benzodiazepines. In *Handbook of Experimental Pharmacology*, Modern Anesthetics, Vol *182*; Schüttler, J., Schwilden, H., Eds.; Springer: Berlin, 1985; pp 446−472.

(15) Thurston, D. E.. Advances in the Study of Pyrrolo[2,1-c][1,4]benzodiazepine (PBD) Antitumour Antibiotics. In *Molecular Aspects of Anticancer Drug-DNA Interactions*; Neidle, S., Waring, M. J., Eds.; Macmillan. Education UK: London, 1993; pp 54−88.

(16) Matthews, J. M.; Hoekstra, W. J.; Dyatkin, A. B.; Hecker, L. R.; Hlasta, D. J.; Poulter, B. L.; Andrade-Gordon, P.; de Garavilla, L.; Demarest, K. T.; Ericson, E.; et al. Potent nonpeptide vasopressin receptor antagonists based on oxazino- and thiazinobenzodiazepine templates. *Bioorg. Med. Chem. Lett.* **2004**, *14*, 2747−2752.

(17) Matthews, J. M.; Hlasta, D. J.; Andrade-Gordon, P.; Demarest, K. T.; Ericson, E.; Gunnet, J. W.; Hageman, W.; Look, R.; Moore, J. B.; Maryanoff, B. E. Pyrazinobenzodiazepines as potent nonpeptide vasopressin receptor antagonists. *Lett. Drug Des. Discovery* **2005**, *2*, 219−223.

(18) Aicher, T. D.; Chen, Z.; Chen, Y.; Faul, M. M.; Krushinski, J. H.; Le, H. Y.; Pineiro-Nunez, M. M.; Rocco, V. P.; Ruley, K. M.; Schaus, J. M. Preparation of piperazine-substituted aryl-fused benzodiazepines as dopamine D2 receptor antagonists for treating psychosis and bipolar disorders. WO 2003082877 A1, Oct 9, 2003.

(19) Králová, P.; Fülöpová, V.; Maloň, M.; Volná, T.; Popa, I.; Soural, M. Stereoselective Polymer-Supported Synthesis of Morpholine- and Thiomorpholine-3-carboxylic Acid Derivatives. *ACS Comb. Sci.* **2017**, *19*, 173−180.

(20) Kaplánek, R.; Krchňák, V. Fast and effective reduction of nitroarenes by sodium dithionite under PTC conditions: application in solid-phase synthesis. *Tetrahedron Lett.* **2013**, *54*, 2600−2603.

(21) Messina, I.; Popa, I.; Maier, V.; Soural, M. Solid-Phase Synthesis of 5-Noranagrelide derivatives. *ACS Comb. Sci.* **2014**, *16*, 33−38.

(22) Fülöpová, V.; Gucký, T.; Grepl, M.; Soural, M. Solid-Phase Synthesis of Trisubstituted Benzo[1,4]-Diazepin-5-one Derivatives. *ACS Comb. Sci.* **2012**, *14*, 651−656.

DOI: 10.1021/acscombsci.7b00115
ACS Comb. Sci. 2017, 19, 670−674

ACS Combinatorial Science

Research Article

pubs.acs.org/acscombsci

Stereoselective Synthesis of Benzo[*e*][1,4]oxazino[4,3-*a*][1,4]diazepine-6,12-diones with Two Diversity Positions

Petra Králová,[†] Michal Maloň,[‡] and Miroslav Soural*[,§]

[†]Department of Organic Chemistry, Faculty of Science, Palacký University, 771 46 Olomouc, Czech Republic

[‡]JEOL Resonance Inc., Musashino 3-1-2, Akishima, Tokyo 196-8558, Japan

[§]Institute of Molecular and Translational Medicine, Faculty of Medicine and Dentistry, Palacký University, Hněvotínská 5, 779 00, Olomouc, Czech Republic

Supporting Information

ABSTRACT: Herein, we report a stereoselective formation of tetrahydro-6*H*-benzo[*e*][1,4]oxazino[4,3-*a*][1,4]diazepine-6,12-(11*H*)-diones. Their preparation consisted in solid-phase synthesis of linear intermediates starting from polymer-supported Ser(*t*Bu)-OH. Using various 2-nitrobenzoic acids and bromoketones, the key intermediates were obtained in five steps and subjected to trifluoroacetic acid-mediated cleavage from the resin, followed by stereoselective reduction with triethylsilane. Subsequent catalytic hydrogenation of the nitro group and cyclization yielded the target compounds with full retention of the C^{12a} stereocenter configuration.

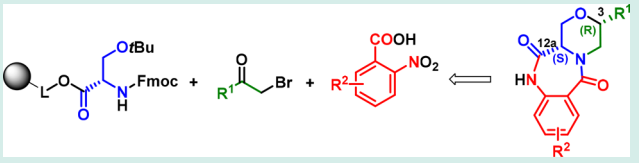

KEYWORDS: *morpholine, oxazine, benzodiazepine, solid-phase synthesis, triethylsilane, stereoselective synthesis*

INTRODUCTION

Synthetic benzo[1,4]diazepines are interesting molecules for drug discovery, especially as potent central nervous system (CNS) agents.[1] Although this effect is considered the most important, there are also other diverse properties, such as antiarrhythmic effects,[2] antagonism of cholecystokinin receptor activity,[3] HIV-1 reverse transcriptase inhibition,[4] opioid receptor activity,[5] anticancer,[6] and anti-inflammatory[7] properties. For these reasons, benzodiazepines are conventionally classified as "privileged scaffolds." Along with CNS-active 1,3-dihydro-2*H*-benzo[*e*][1,4]diazepin-2-ones, benzo[*e*][1,4]-diazepine-2,5-diones are the most frequently reported [1,4]-diazepines in the field of organic synthesis.[8] Their preparation frequently starts from α-amino acids, which, upon acylation with *o*-nitrobenzoic acids followed by reduction and cyclization, affords the benzodiazepine scaffold.[9−14] Herein, we report a further extension of this approach toward fused heterocycles, benzoxazinodiazepinediones, with 3D architectures and specific configurations of the two stereocenters, which possess great importance for the discovery of novel pharmacologically relevant molecules.[15,16] In the literature, there have been only two reports on the preparation of similar molecules using traditional solution-phase synthesis.[17,18] Taking the limitations of both methods into account, we focused on the development of a novel approach compatible with a high-throughput synthetic concept using common coupling reagents and procedures and readily available building blocks. It is worth mentioning that tricyclic benzodiazepines have been reported as compounds of high medicinal interest, which have been documented by anxiolytic triazolobenzodiazepinones[19] and imidazolobenzodiazepinones;[20] antitumor pyrrolobenzodiazepinones;[21] vasopressin receptor antagonists oxazinobenzodiazepines,[22] thiazinobenzodiazepines[22] and pyrazinobenzodiazepines;[23] and dopamine D2 receptor antagonists thiazolobenzodiazepinones (Figure 1).[24]

RESULTS AND DISCUSSION

Synthetic Pathway. The synthetic approach was inspired by our previous report on the preparation of morpholine-3-carboxylic acid derivatives.[25] The reaction sequence was tested using two representative building blocks: 2-bromoacetophenone and *o*-nitrobenzoic acid. First, Fmoc-Ser(*t*Bu)-OH was immobilized on Wang resin, followed by the cleavage of the Fmoc-protecting group and activation/protection of the liberated amino group with 4-nitrobenzensulfonyl chloride (4-Nos-Cl) to obtain intermediate **4**. Alkylation with 2-bromoacetophenone yielded *N*-alkyl 4-nitrobenzensulfonamide **6**{*1*} (see Figure 2 for the numbering of compounds hereafter) in an excellent crude purity of 98%, as measured by LC-UV traces at 205−400 nm after cleavage from the polymer support. Subsequently, the Nos group was cleaved, and aminoketone **7**{*1*} was acylated using 2-nitrobenzoic acid (Scheme 1). In the manipulation of the polymer-supported intermediate **9**{*1,1*}, the reduction of the nitro group was followed by reaction of the amino group with a ketone, which, after TFA-mediated cleavage from the resin, yielded benzo[*e*][1,4]diazepin-5-one

Received: September 13, 2017
Revised: October 15, 2017
Published: October 19, 2017

DOI: 10.1021/acscombsci.7b00134
ACS Comb. Sci. 2017, 19, 770−774

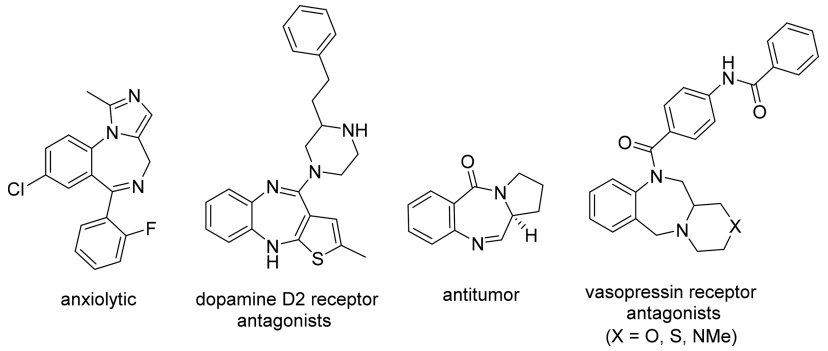

Figure 1. Pharmacologically relevant tricyclic benzodiazepines.

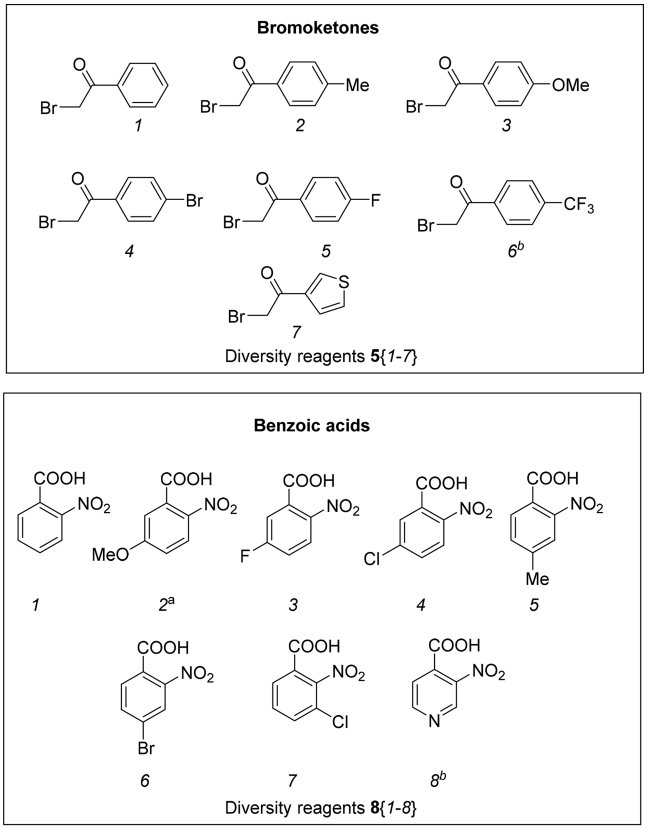

[a]The hydrogenation step led to demethylation.
[b]Failed to yield the final compounds.

Figure 2. Building blocks employed in the synthesis of benzoxazinodiazepinediones.

14{*1,1*}, as reported previously.[26] Interestingly, the inclusion of TES in the cleavage cocktail led to the formation of compound **15**{*1,1*} with a specific configuration of the newly formed C^2 stereocenter (*R*, see Supp. Information for 2D NMR analysis). To avoid the formation of compound **14**{*1,1*}, intermediate **9**{*1,1*} was subjected to acid-mediated cleavage from the resin followed by the addition of triethylsilane, which stereoselectively yielded the corresponding morpholine derivative **10**{*1,1*}. The subsequent nitro group reduction was performed by catalytic hydrogenation using Pd/C. Finally, the cyclization of morpholine compound **11**{*1,1*} was accomplished using a mixture of 10% TFA in DCM at 50 °C. Target product **12**{*1,1*} was obtained in 92% crude purity after the entire reaction sequence, and an overall yield of 40% was obtained after reversed-phase semipreparative HPLC purification.

Limitation and Scope. To determine the general applicability of our method, we tested a diverse combination of different bromoketones and *o*-nitrobenzoic acids bearing both electron-donating and electron-withdrawing groups (see Figure 2). The preparations of intermediates **6**{*1*−*7*} were successful for all tested bromoketones and provided the corresponding derivatives in high crude purities (evaluated by LC-UV after cleavage from the polymer support). The following acylation required 24−96 h to complete depending on the nucleophilicity of the amine and reactivity of acylation species (see Supporting Information for details). In the case of the low-reactive intermediate **7**{*6*}, acylation with carboxylic acid in the presence of carbodiimide or even with the corresponding acyl chloride failed. After acid-mediated cleavage and TES reduction, intermediates **10** were obtained as mixtures of stable CONH rotamers, which is in accordance with our previous report (see Supp. Information for details).[25] However, the rotamery completely disappeared after the reduction of the nitro group. Catalytic hydrogenation using Pd/C afforded desired intermediates **11**, but it led to cleavage of the C−Cl or C−Br bonds. To avoid the undesired hydrogenolysis, intermediates containing halogens were reduced using PtO_2. Furthermore, in the case of intermediates **10** bearing halogens as the R^2 substituents (except for **10**{R^1,*7*}), the hydrogenation using Pd/C or PtO_2 afforded *N*-hydroxyaniline intermediates **16** in range of crude purities 7−83% (Scheme 2, highlighted in red). The presence of 4-Br as R^2 led to predominant major formation **16** (over 80%). Therefore, products **17**{*1,6*} and **17**{*5,6*} were isolated and fully characterized (see Supporting Information for details).

Similarly, the presence of a 5-methoxy group as R^2 led to demethylation using both Pd/C and PtO_2 (Scheme 3, highlighted in red) and yielded products **12**{*1,2-dem*} and **12**{*2,2-dem*}, respectively. Interestingly, the methoxy group as the R^1 substituent was not affected by the hydrogenation. In general, the reduced intermediates **11** were obtained in good to excellent crude purities ranging from 49% to 95%. However, the preparation of **12**{*1,8*} using a pyridine building block failed in the cyclization stage.

Stereochemistry. Although the immobilization of Fmoc-Ser(*t*Bu)-OH on Wang resin to obtain resin **2** was performed using the convenient HOBt technique, it provided ∼8% of the second enantiomer (detected by chiral supercritical fluidic chromatography).[30] Consequently, the cleavage and reduction of intermediates **9** with TES afforded crude compounds **10** as a mixture of the corresponding diastereomers 3*R*/12[a]*S* and 3*R*/12[a]*R* in a ratio of 92:8. Similarly, according to LC-UV-MS, the final cyclization yielded crude compounds **12** as two separable

DOI: 10.1021/acscombsci.7b00134
ACS Comb. Sci. 2017, 19, 770−774

Scheme 1. General Synthesis of Target Benzoxazinodiazepinediones 12[a]

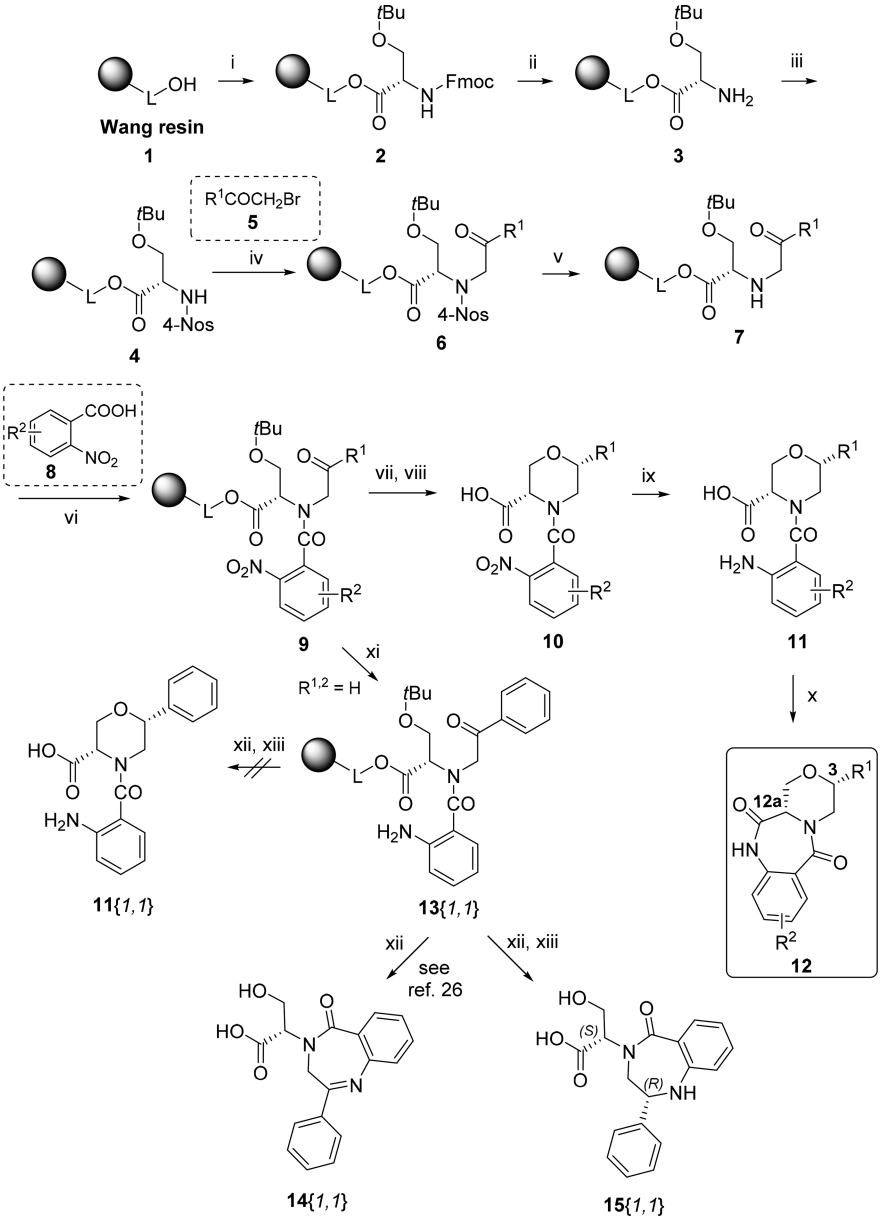

[a]Reagents and conditions: (i) Fmoc-Ser(tBu)-OH, HOBt, DMAP, DIC, DMF, DCM, 24 h, rt; (ii) 50% piperidine/DMF, 30 min, rt; (iii) 4-Nos-Cl, 2,6-lutidine, DCM, 24 h, rt; (iv) DIEA, DMF, 24 h, rt; (v) 2-mercaptoethanol, DBU, degassed DMF, 1.5 h, rt; (vi) DIC, deggased DMF, 24−96 h, rt; (vii) 50% TFA/DCM, 15−24 h, rt; (viii) TES, 2−21 h, rt; (ix) H_2,10% Pd/C, propan-2-ol, 1−48 h, rt or H_2, PtO_2, propan-2-ol, 2.5−48 h, rt (for derivatives **10**{*1,2*}, **10**{*1,4*}, **10**{*1,6*}, **10**{*1,7*}, **10**{*4,1*}, **10**{*5,6*}, and **10**{*7,1*}); (x) 10% TFA/DCM, 1−48 h, 50 °C; (xi) $Na_2S_2O_4$, K_2CO_3, TBAHS, 2 h, rt; (xii) 50% TFA/DCM, 3 h, rt; (xiii) TES, 3 h, rt.

Scheme 2. Reduction of 10 to *N*-Hydroxyanilines and Their Cyclization[a]

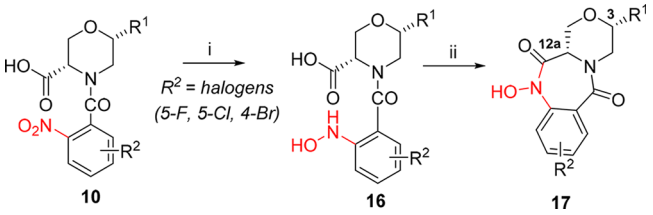

[a]Reagents and conditions: (i) H_2, Pd/C, propan-2-ol (for derivatives **10**{*1,3*} and **10**{*2,3*}) or H_2, PtO_2, propan-2-ol, rt (for derivatives **10**{*1,4*}, **10**{*1,6*}, and **10**{*5,6*}); (ii) 10% TFA/DCM, 1−48 h, 50 °C.

diastereomers in the same ratio. In each case, the major diastereomer was isolated by semipreparative HPLC, and one representative compound was subjected to 2D NMR analysis, which proved the configuration of the stereocenters as 3*R*, 12a*S* (see Supporting Information). In contrast to previous reports,[27−30] these results indicated that the amino acid configuration was not influenced by the stereochemistry of the final cyclization.

CONCLUSION

In conclusion, we report a stereoselective formation of benzo[*e*][1,4]oxazino[4,3-*a*][1,4]diazepine-6,12-diones using a combination of both solid-phase and solution-phase techniques.

DOI: 10.1021/acscombsci.7b00134
ACS Comb. Sci. 2017, 19, 770−774

Scheme 3. Demethylation of Methoxy Derivatives 10 Using Catalytic Hydrogenation[a]

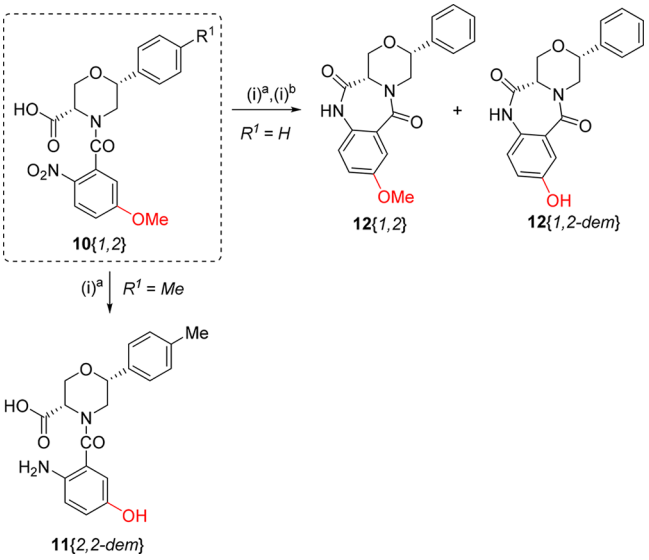

[a]Reagents and conditions: (i) (a) H_2,10% Pd/C, propan-2-ol, 35−48 h, rt; (b) H_2, PtO_2, propan-2-ol, 48 h, rt.

Table 1. List of Synthesized and Fully Characterized Benzoxazinodiazepinediones

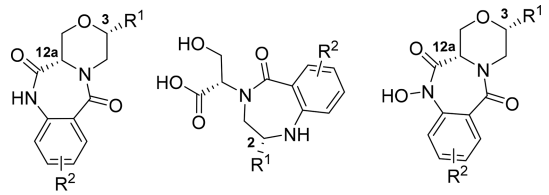

cmpd	R^1	R^2	crude purity (%)[a]	purity (%)[b]	overall yield (%)[c]
12{*1,1*}	Ph	H	92	98	40
12{*1,2*}	Ph	5-MeO	49	98	19
12{*1,2-dem*}	Ph	5-OH	51	99	28
12{*1,3*}	Ph	5-F	66	99	43
12{*1,4*}	Ph	5-Cl	70	99	35
12{*1,5*}	Ph	4-Me	85	97	38
12{*1,7*}	Ph	3-Cl	85	99	38
12{*2,1*}	4-Me-Ph	H	75	98	49
12{*2,2-dem*}	4-Me-Ph	5-OH	61	98	46
12{*2,3*}	4-Me-Ph	5-F	83	97	47
12{*3,1*}	4-MeO-Ph	H	60	95	45
12{*4,1*}	4-Br-Ph	H	85	98	43
12{*5,1*}	4-F-Ph	H	86	99	41
12{*5,5*}	4-F-Ph	4-Me	49	98	28
12{*7,1*}	S	H	49	97	27
15{*1,1*}	Ph	H	55	99	30
17{*1,6*}	Ph	4-Br	82	99	49
17{*5,6*}	4-F-Ph	4-Br	83	98	50

[a]Overall purity after the entire reaction sequence calculated from HPLC-UV (205−400 nm). [b]HPLC-UV after purification (205−400 nm). [c]Calculated from the ^{1}H NMR spectrum of the purified product.

Although the final steps of the reaction sequence (hydrogenation and cyclization) had to be performed after cleavage from the polymer support, the simple procedures (fast evaporation or filtration workup) make this method fully compatible with a high-throughput synthesis concept. With respect to the number of readily available building blocks (bromoketones and 2-nitrobenzoic acids), the method can be used for the on demand, time efficient synthesis of the chemical libraries of corresponding fused heterocycles using parallel or combinatorial chemistry. Furthermore, it was demonstrated that reduction with TES is applicable also for the stereoselective synthesis of benzodiazepine compounds **15**.

■ ASSOCIATED CONTENT

Supporting Information

The Supporting Information is available free of charge on the ACS Publications website at DOI: 10.1021/acscombsci.7b00134.

Details of experimental, synthetic, and analytical procedures, along with spectroscopic data for synthesized compounds (PDF)

■ AUTHOR INFORMATION

Corresponding Author

*E-mail: miroslav.soural@upol.cz.

ORCID

Miroslav Soural: 0000-0001-7288-8617

Notes

The authors declare no competing financial interest.

■ ACKNOWLEDGMENTS

The authors are grateful to project CZ.1.07/2.3.00/20.0009 from the European Social Fund, the National Program of Sustainability (project LO1304) and an internal grant from Palacký University (IGA_PrF_2017_009 and IGA_LF_2017_028).

■ REFERENCES

(1) Hadjipavlou-Litina, D.; Hansch, C. Quantitative Structure-Activity Relationships of the Benzodiazepines. A Review and Reevaluation. *Chem. Rev.* **1994**, *94* (6), 1483−1505.

(2) Butcher, J. W.; Liverton, N. J.; Claremon, D. A.; Freidinger, R. M.; Jurkiewicz, N. K.; Lynch, J. J.; Salata, J. J.; Wang, J.; Dieckhaus, C. M.; Slaughter, D. E.; Vyas, K. Novel 5-cyclopropyl-1,4-benzodiazepin-2-ones as potent and selective I_{Ks}-blocking class III antiarrhythmic agents. *Bioorg. Med. Chem. Lett.* **2003**, *13* (6), 1165−1168.

(3) Haynes, S. W.; Gao, X.; Tang, Y.; Walsh, C. T. Assembly of Asperlicin Peptidyl Alkaloids from Anthranilate and Tryptophan: A Two-Enzyme Pathway Generates Heptacyclic Scaffold Complexity in Asperlicin E. *J. Am. Chem. Soc.* **2012**, *134* (42), 17444−17447.

(4) Breslin, H. J.; Kukla, M. J.; Kromis, T.; Cullis, H.; De Knaep, F.; Pauwels, R.; Andries, K.; De Clercq, E.; Janssen, M. A. C.; Janssen, P. A. J. Synthesis and anti-HIV activity of 1,3,4,5-tetrahydro-2*H*-1,4-benzodiazepin-2-one (TBO) derivatives. Truncated 4,5,6,7-tetrahydro-5-methylimidazo[4,5,1-*jk*][1,4]benzodiazepin-2(1*H*)-ones (TIBO) analogues. *Bioorg. Med. Chem.* **1999**, *7* (11), 2427−2436.

(5) Anzini, M.; Canullo, L.; Braile, C.; Cappelli, A.; Gallelli, A.; Vomero, S.; Menziani, M. C.; De Benedetti, P. G.; Rizzo, M.; Collina, S.; Azzolina, O.; Sbacchi, M.; Ghelardini, C.; Galeotti, N. Synthesis, Biological Evaluation, and Receptor Docking Simulations of 2-[(Acylamino)ethyl]-1,4-benzodiazepines as κ-Opioid Receptor Agonists Endowed with Antinociceptive and Antiamnesic Activity. *J. Med. Chem.* **2003**, *46* (18), 3853−3864.

(6) Chen, C. Y.; Lee, P. H.; Lin, Y. Y.; Yu, W. T.; Hu, W. P.; Hsu, C. C.; Lin, Y. T.; Chang, L. S.; Hsiao, C. T.; Wang, J. J.; Chung, M. I. Synthesis, DNA-binding abilities and anticancer activities of triazole-

pyrrolo[2,1-*c*][1,4]benzodiazepines hybrid scaffolds. *Bioorg. Med. Chem. Lett.* **2013**, *23* (24), 6854−6859.
(7) Cortes Eduardo, C.; Simon, H. O.; Apan Teresa, R.; Camacho Antonio, N.; Lijanova, I. V.; Marcos, M.-G. Anticancer Activity and Anti-inflammatory Studies of 5-Aryl-1,4-benzodiazepine Derivatives. *Anti-Cancer Agents Med. Chem.* **2012**, *12* (6), 611−618.
(8) Fulopova, V.; Soural, M. Solid-Phase Synthesis of Seven-Membered Heterocycles with Two Nitrogen Atoms. In *Solid-Phase Synthesis of Nitrogenous Heterocycles*; Krchnak, V., Ed.; Springer International Publishing, 2017; Vol. *52*, pp 23−63.
(9) Goff, D. A.; Zuckermann, R. N. Solid-phase synthesis of defined 1,4-benzodiazepine-2,5-dione mixtures. *J. Org. Chem.* **1995**, *60* (18), 5744−5745.
(10) Verdié, P.; Subra, G.; Feliu, L.; Sanchez, P.; Berge, G.; Garcin, G.; Martinez, J. On-Line Synthesis of Pseudopeptide Library Incorporating a Benzodiazepinone Turn Mimic: Biological Evaluation on MC1 Receptors. *J. Comb. Chem.* **2007**, *9* (2), 254−262.
(11) Mayer, J. P.; Zhang, J.; Bjergarde, K.; Lenz, D. M.; Gaudino, J. J. Solid phase synthesis of 1,4-benzodiazepine-2,5-diones. *Tetrahedron Lett.* **1996**, *37* (45), 8081−8084.
(12) Hulme, C.; Ma, L.; Kumar, N. V.; Krolikowski, P. H.; Allen, A. C.; Labaudiniere, R. Novel applications of resin bound α-amino acids for the synthesis of benzodiazepines (via Wang resin) and ketopiperazines (via hydroxymethyl resin). *Tetrahedron Lett.* **2000**, *41* (10), 1509−1514.
(13) Jeon, M. K.; Kwon, J. J.; Kim, M. S.; Gong, Y. D. A Novel Solid-Phase Synthetic Method for 1,4-Benzodiazepine-2,5-dione Derivatives. *Synlett* **2008**, *2008* (11), 1651−1656.
(14) Boojamra, C. G.; Burow, K. M.; Ellman, J. A. An expedient and high-yielding method for the solid-phase synthesis of diverse 1,4-benzodiazepine-2,5-diones. *J. Org. Chem.* **1995**, *60* (18), 5742−5743.
(15) Roughley, S. D.; Jordan, A. M. The Medicinal Chemistry Toolbox: An Analysis of Reactions Used in the Pursuit of Drug Candidates. *J. Med. Chem.* **2011**, *54*, 3451−3479.
(16) Walters, W. P.; Green, J.; Weiss, J. R.; Murcko, M. A. What Do Medicinal Chemists Actually Make? A 50-Year Retrospective. *J. Med. Chem.* **2011**, *54*, 6405−6416.
(17) Lalli, C.; Trabocchi, A.; Sladojevich, F.; Menchi, G.; Guarna, A. Diversity-Oriented Synthesis of Morpholine-Containing Molecular Scaffolds. *Chem. - Eur. J.* **2009**, *15*, 7871−7875.
(18) Matthews, J. M.; Dyatkin, A. B.; Evangelisto, M.; Gauthier, D. A.; Hecker, L. R.; Hoekstra, W. J.; Liu, F.; Poulter, B. L.; Sorgi, K. L.; Maryanoff, B. E. Synthesis, resolution, and absolute configuration of novel tricyclic benzodiazepines. *Tetrahedron: Asymmetry* **2004**, *15*, 1259−1267.
(19) Mandrioli, R.; Mercolini, L.; Raggi, M. A. Benzodiazepine metabolism: an analytical perspective. *Curr. Drug Metab.* **2008**, *9* (8), 827−44.
(20) Olkkola, K. T.; Ahonen, J. Midazolam and other benzodiazepines. *Handb. Exp. Pharmacol.* **2008**, *182*, 335−60.
(21) Thurston, D. E. Advances in the Study of Pyrrolo[2,1-c][1,4]benzodiazepine (PBD) Antitumour Antibiotics. In *Molecular Aspects of Anticancer Drug−DNA Interactions*; Neidle, S., Waring, M. J., Eds.; Macmillan Education: London, 1993; pp 54−88.
(22) Matthews, J. M.; Hoekstra; William, J.; Dyatkin, A. B.; Hecker, L. R.; Hlasta, D. J.; Poulter, B. L.; Andrade-Gordon, P.; de Garavilla, L.; Demarest, K. T.; Ericson, E.; et al. Potent nonpeptide vasopressin receptor antagonists based on oxazino- and thiazinobenzodiazepine templates. *Bioorg. Med. Chem. Lett.* **2004**, *14* (11), 2747−2752.
(23) Matthews, J. M.; Hlasta, D. J.; Andrade-Gordon, P.; Demarest, K. T.; Ericson, E.; Gunnet, J. W.; Hageman, W.; Look, R.; Moore, J. B.; Maryanoff, B. E. Pyrazinobenzodiazepines as potent nonpeptide vasopressin receptor antagonists. *Lett. Drug Des. Discovery* **2005**, *2* (3), 219−223.
(24) Aicher, T. D.; Chen, Z.; Chen, Y.; Faul, M. M.; Krushinski, J. H.; Le, H. Y.; Pineiro-Nunez, M. M.; Rocco, V. P.; Ruley, K. M.; Schaus, J. M. Preparation of piperazine-substituted aryl-fused benzodiazepines as dopamine D2 receptor antagonists for treating psychosis and bipolar disorders. Int. Patent WO 2003082877A1, Oct 9, 2003.
(25) Kralova, P.; Fulopova, V.; Malon, M.; Volna, T.; Popa, I.; Soural, M. Stereoselective Polymer-Supported Synthesis of Morpholine- and Thiomorpholine-3-carboxylic Acid Derivatives. *ACS Comb. Sci.* **2017**, *19* (3), 173−180.
(26) Fulopova, V.; Gucky, T.; Grepl, M.; Soural, M. Solid-Phase Synthesis of Trisubstituted Benzo[1,4]-Diazepin-5-one Derivatives. *ACS Comb. Sci.* **2012**, *14* (12), 651−656.
(27) Trapani, P.; Volna, T.; Soural, M. Solid-phase synthesis of 2,3-dihydrobenzo[f][1,2,5]thiadiazepin-4(5H)-one 1,1-dioxides with three diversity positions. *ACS Comb. Sci.* **2016**, *18* (6), 349−354.
(28) McMaster, C.; Fulopova, V.; Popa, I.; Grepl, M.; Soural, M. Solid-Phase Synthesis of Anagrelide Sulfonyl Analogues. *ACS Comb. Sci.* **2014**, *16* (5), 221−224.
(29) Messina, I.; Popa, I.; Maier, V.; Soural, M. Solid-Phase Synthesis of 5-Noranagrelide derivatives. *ACS Comb. Sci.* **2014**, *16*, 33−38.
(30) Kralova, P.; Malon, M.; Volna, T.; Rucilova, V.; Soural, M. Polymer-Supported Stereoselective Synthesis of Benzoxazino[4,3-b][1,2,5]thiadiazepinone 6,6-dioxides. *ACS Comb. Sci.* **2017**, *19*, 670.

DOI: 10.1021/acscombsci.7b00134
ACS Comb. Sci. 2017, 19, 770−774

ChemPubSoc Europe

DOI: 10.1002/ejoc.201701448

EurJOC European Journal of Organic Chemistry

Full Paper

Stereocontrolled Heterocycles

Synthesis of Disubstituted Pyrazino-Oxazine Derivatives with Controlled Stereochemistry

Veronika Ručilová,[b] Petra Králová,[b] and Miroslav Soural*[a]

Abstract: Herein, we report a simple synthesis of disubstituted pyrazino-oxazines with controlled stereochemistry using readily available building blocks: *N*-Fmoc-protected α-amino acids and 2-bromo ketones. The convenient solid-phase synthesis afforded polymer-supported derivatives of *N*-alkylated *N*-acylated *tert*-butylserine, which were subjected to spontaneous cyclative cleavage to yield the corresponding pyrazine intermediates. The target 1,7,8,9*a*-tetrahydropyrazino[2,1-*c*][1,4]oxazine-6,9-diones were obtained in two steps by acid-mediated cleavage of the *tert*-butyl group followed by cyclization of the oxazine scaffold.

Introduction

Amino acids (AAs) have a unique bifunctional structure that serves to conveniently form peptides, peptidomimetics and proteins.[1,2] As a result of the presence of these compounds or their fragments in a large number of bioactive natural products,[3–6] AAs have also been frequently used as benign and readily available synthons to prepare variously sized heterocycles with promising pharmacological properties.[7–11] In the field of drug discovery, enantiomerically pure heterocycles bearing more than one stereocentre are very attractive. However, researchers have struggled to develop approaches to achieve such scaffolds.[12–15] Owing to their optical purity, synthetically transformable structure/functionality[16–23] and chiral centres, AAs have also become an important tool for asymmetric synthesis and chiral catalysis.[24–27]

The specific class of heterocycles accessible from AAs are piperazine-2,5-diones (also termed diketopiperazines, DKPs).[28–33] DKPs represent a rich source of biologically interesting compounds exhibiting a broad spectrum of pharmacological activities, for example, antiviral, antifungal, antitumour, antithrombic and antibacterial.[34,35] Such scaffolds have been shown to inhibit enzymes and control the activity of many receptors;[31,36] therefore they have widespread applications in organic, medicinal and supramolecular chemistry.[37] DKPs are typically synthesized from dipeptides in solution or on the solid phase, followed by subsequent derivatization and cyclization under various conditions.[38–43] Piperazinediones have also been synthesized by an Ugi multi-component reaction[44,45] or aza-Wittig cyclization.[34] In 2011, Svete and co-workers reported a three-step method based on the *N*-alkylation of an amino acid ester hydrochloride, chloroacetylation and cyclization in methanolic ammonia.[37] Although there have been numerous reports on the synthesis of piperazine-2,5-diones fused with additional heterocyclic moieties, only a few have addressed the preparation of pyrazino[2,1-*c*][1,4]oxazines. DesMarteau et al. developed a method for the formation of a novel chromophore from 6-benzyl-1-(3,3,3-trifluoropropyl)piperazine-2,5-dione by its deprotonation with NaH in DMF.[46] In the same year, Trabocchi et al. published the reaction of dimethoxyacetaldehyde and β-hydroxy-α-amino acid bearing an Fmoc-protecting group.[47] The cyclization of dihydro-oxazine, prepared from the coupling of morpholine with the appropriate Fmoc-amino acid chloride, was carried out in the same manner.[48] As a continuation of our previous research in the field of chiral morpholines,[13] we herein describe a novel approach for the modular synthesis of pyrazino-oxazines starting from immobilized serine. The key features of this method are 1) the simple and rapid reactions using only common coupling reactions and reagents, 2) a large number of readily available building blocks to introduce diverse substituents and 3) fully controlled configurations of both stereocentres in the final scaffold.

Results and Discussion

The synthesis of 1,7,8,9*a*-tetrahydropyrazino[2,1-*c*][1,4]oxazine-6,9-dione derivatives was carried out according to Scheme 1. The first step of the reaction was the immobilization of Fmoc-Ser(*t*Bu)-OH on the commercially available Wang resin. After cleavage of the Fmoc-protecting group, the liberated amino derivative **2** was treated with 4-nitrobenzenesulfonyl chloride (4-NsCl) to give intermediate **3** in excellent crude purity of 94 % (calculated from LC–UV traces at 205–400 nm). Subsequent Fukuyama alkylation[49–51] with various aromatic 2-bromo ketones (Figure 1) yielded the corresponding sulfonamides **4**(R^1) in high crude purity (88–94 %, LC–UV traces at 205–400 nm). Unlike the previously reported procedure,[13] we had to increase the concentration of mercaptoethanol/DBU (1,8-diazabicyclo-

[a] *Department of Organic Chemistry, Faculty of Science, Palacký University, 77146 Olomouc, Czech Republic*
E-mail: miroslav.soural@upol.cz
https://www.orgchem.upol.cz/koch/en/
[b] *Institute of Molecular and Translational Medicine, Faculty of Medicine and Dentistry, Palacký University, Hněvotínská 5, 77900 Olomouc, Czech Republic*

Supporting information and ORCID(s) from the author(s) for this article are available on the WWW under https://doi.org/10.1002/ejoc.201701448.

ChemPubSoc Europe

EurJOC European Journal of Organic Chemistry
Full Paper

[5.4.0]undec-1-ene) and prolong the reaction time to cleave the 4-Ns group quantitatively (see the Supporting Information). To test the applicability of the designed synthetic route, Fmoc-Ala-OH (see Figure 1) was initially selected as the amino acid for the acylation reaction. Its activation with diisopropylcarbodiimide (DIC) and *N*-hydroxybenzotriazole (HOBt) led to the conversion of intermediate **5**(*2*) (see Figure 1 for numbering, Chemset Numbering System used) into the resin-bound compound **6**(*2,1*). However, in some cases, the acylation step had to be repeated to reach completion. The piperidine-mediated deprotection of the Fmoc group triggered a spontaneous cyclative cleavage (see Scheme 1, red arrow) that yielded piperazinedione **8**(*2,1*). To determine whether the possible side-reaction took place (see Scheme 1, blue arrow), residual resin was subjected to acid-mediated cleavage using a 50 % solution of trifluoroacetic acid (TFA) in dichloromethane (DCM). Interestingly, only a trace amount of the expected product was detected, which indicates the regioselective amination of the ester functionality. After the cyclative cleavage, the cleavage cocktail consisting of piperidine and dimethylformamide (DMF) was removed from **8**(*2,1*) by lyophilization, and the resulting material was treated with 50 % TFA/DCM to trigger the cleavage of the *t*Bu group and subsequent cyclization of the morpholine scaffold.[13] Surprisingly, intermediate **9**(*2,1*) underwent only the protective group cleavage, and the spontaneous cyclization was only partially observed, even at increased temperature. For this reason, a change of solvent was considered, and the TFA/DCM was evaporated in a stream of nitrogen. The oily material containing residual TFA was heated in acetonitrile to successfully yield the desired product. The target compound **10**(*2,1*) was isolated with a high overall crude purity of 82 % (LC–UV traces at 205–400 nm) and an acceptable overall yield of 18 % after the entire reaction sequence and purification by semi-preparative HPLC.

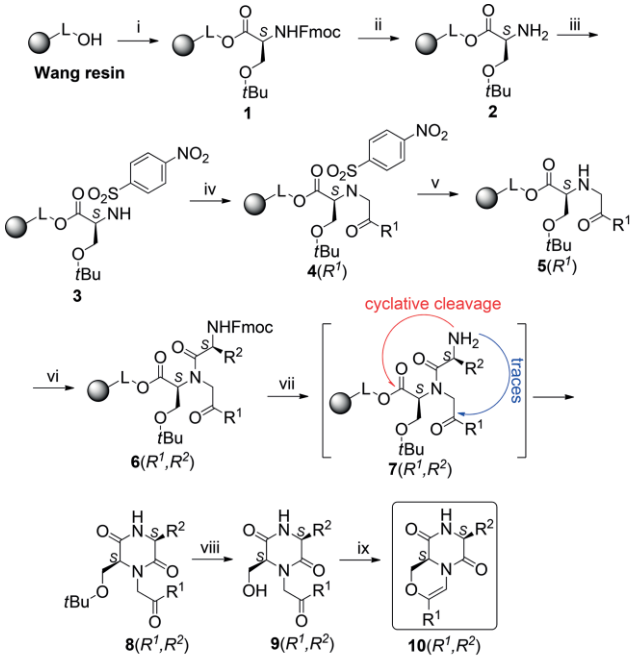

[a]Reagents: (i) Fmoc-Ser(*t*Bu)-OH, HOBt, DIC, DMAP, DMF/DCM (1:1), 24 h, r.t.; (ii) piperidine/DMF (1:1), 30 min, r.t.; (iii) 4-NsCl, 2,6-lutidine, DCM, 24 h, r.t.; (iv) 2-bromoketone (Figure 1), EDIPA, DMF, 24 h, r.t.; (v) 2-mercaptoethanol, DBU, DMF, 1 h, r.t.; (vi) Fmoc-AA-OH (Figure 1), HOBt, DIC, DMF/DCM (1:1), 24 h, r.t., then repeat 1x or 2x (see the Supporting Information); (vii) piperidine/DMF (1:1), 30 min, r.t., then lyophilization for 16 h; (viii) TFA/DCM (1:1), 30 min, r.t., then stream of N_2; (ix) MeCN, 1-8 h, 80 °C or 90 °C (see the Supporting Information), then stream of N_2.

Scheme 1. Synthetic pathway leading to the target pyrazino-oxazines **10**(R^1,R^2).

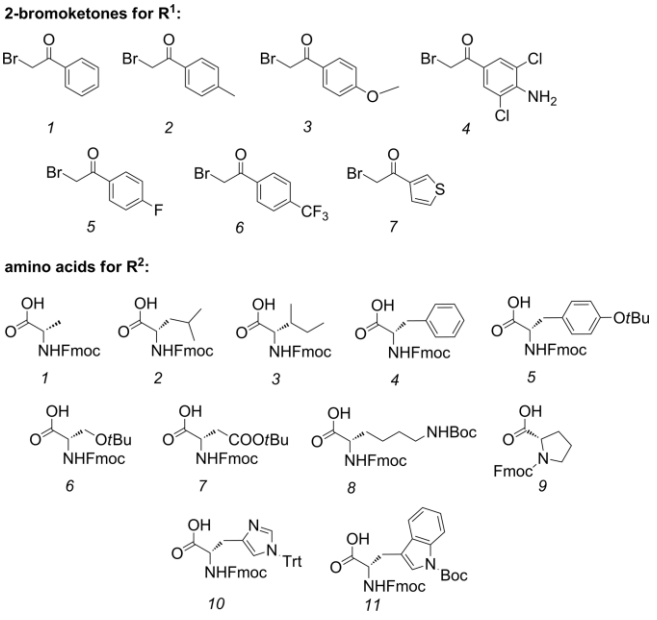

Figure 1. List of building blocks used for R^1 and R^2 substitutions.

To evaluate the limitation and scope of the method, we subsequently tested seven bromo ketones with both electron-donating and -withdrawing groups. Similarly, 11 diverse Fmoc-amino acids with various side-chains were selected. All the tested building blocks are depicted in Figure 1. In terms of R^1 substitution, the reaction sequence was applicable for all the used bromo ketones. In contrast, Fmoc-Pro-OH could not be used due to quantitative dealkylation in the acylation step (see below). Also, the use of Fmoc-Asp(*t*Bu)-OH and Fmoc-His(Trt)-OH yielded the desired intermediates, but the corresponding target compounds were accompanied with inseparable impurities and were not isolated. The list of successfully synthesized, isolated and fully characterized compounds is presented in Table 1. Importantly, no diastereomers of intermediates **8** and **9** were detected by LC–MS analysis, and also the final compounds **10** were identified as diastereomerically pure by NMR analysis. For this reason, it can be concluded that the amino acids did not undergo epimerization within the reaction sequence.

In some cases, the reaction sequence afforded the target compounds in relatively limited overall yields. After further investigation, we discovered the formation of side-products that appeared after the acylation of intermediates **5**(R^1), which were responsible for lowering the yields. LC–MS analysis suggested the structure of the side-products as dealkylated compounds **12**(H,R^2) (Scheme 2). The same behaviour was previously reported for the acylation of similar intermediates with benzoic acids.[52] Because different ratios of **11**(R^1,R^2) and **12**(H,R^2) (see

ChemPubSoc Europe

EurJOC European Journal of Organic Chemistry
Full Paper

Table 1. List of synthesized pyrazino-oxazine derivatives **10**(R^1,R^2).

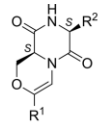

10(R^1,R^2)

Cmpd	R^1	R^2	Purity [%] Crude[a]	Purity [%] Final[b]	Yield [%][c]
10(*1*,*1*)	Ph	Me	73	98	41
10(*1*,*2*)	Ph	$CH_2CH(CH_3)_2$	62	99	20
10(*1*,*3*)	Ph	$CH(CH_3)CH_2CH_3$	70	99	5
10(*1*,*4*)	Ph	CH_2Ph	89	98	31
10(*1*,*5*)	Ph	CH_2Ph-4-OH	86	97	34
10(*1*,*11*)	Ph		83	97	26
10(*2*,*1*)	Ph-4-Me	Me	82	98	18
10(*2*,*4*)	Ph-4-Me	CH_2Ph	84	98	23
10(*2*,*6*)	Ph-4-Me	CH_2OH	81	98	46
10(*2*,*8*)	Ph-4-Me	$CH_2(CH_2)_3NH_2$	76	99	32
10(*2*,*11*)	Ph-4-Me		71	99	26
10(*3*,*1*)	Ph-4-OMe	Me	89	99	43
10(*4*,*1*)	Ph-2,5-diCl-4-NH_2	Me	78	98	32
10(*5*,*1*)	Ph-4-F	Me	82	99	21
10(*6*,*1*)	Ph-4-CF_3	Me	72	99	8
10(*7*,*1*)		Me	82	99	21

[a] Crude purity after the entire reaction sequence determined by HPLC-UV (205–400 nm). [b] Final purity determined by HPLC-UV (205–400 nm) after purification. [c] Overall yields of the isolated products after the entire reaction sequence and HPLC purification.

Table 2) were observed, it can be concluded that dealkylation did not occur during the deprotection of the 4-Ns group. Furthermore, we considered the dealkylation to be possibly caused by the acid-mediated release of **6**(R^1,R^2) from the resin, which was performed for LC–MS analysis purposes. However, the cyclative cleavage of **6**(R^1,R^2) also furnished the desired compounds **8**(R^1,R^2) accompanied by side-products **14**(H,R^2), as detected by LC–MS. The formation of **14**(H,R^2) clearly demonstrates that dealkylation occurred on the resin during the acylation step, otherwise product **14**(H,R^2) could not be detected. It is necessary to note that, in contrast to **12**(H,R^2), the quantities of **14**(H,R^2) for most of the amino acids could not be precisely determined by LC–UV analysis due to the low UV/Vis activity of compounds **14**(H,R^2). The ratio of **11**(R^1,R^2) to **12**(H,R^2) indicates the influence of both the R^1 and R^2 groups on the reaction outcome, but no systematic relationship was observed (see Table 2).

Table 2. Ratio of **11**(R^1,R^2)/**12**(H,R^2) after the acylation step.

Cmpd.(R^1)	Amino acid (R^2)	**11**(R^1,R^2)/**12**(R^1,R^2) [%][a]
5(*1*)	Fmoc-Ala-OH (*1*)	88:12
5(*1*)	Fmoc-Leu-OH (*2*)	73:27
5(*1*)	Fmoc-Ile-OH (*3*)	53:47
5(*1*)	Fmoc-Phe-OH (*4*)	89:11
5(*1*)	Fmoc-Tyr(*t*Bu)-OH (*5*)	83:17
5(*1*)	Fmoc-Asp(*t*Bu)-OH (*7*)	79:21
5(*1*)	Fmoc-Lys(Boc)-OH (*8*)	84:16
5(*1*)	Fmoc-Pro-OH (*9*)	0:100
5(*1*)	Fmoc-His(Trt)-OH (*10*)	45:55
5(*1*)	Fmoc-Trp(Boc)-OH (*11*)	93:07
5(*2*)	Fmoc-Ala-OH (*1*)	63:34
5(*2*)	Fmoc-Phe(*t*Bu)-OH (*4*)	79:21
5(*2*)	Fmoc-Ser(*t*Bu)-OH (*6*)	87:13
5(*2*)	Fmoc-Lys(Boc)-OH (*8*)	85:15
5(*2*)	Fmoc-Trp(Boc)-OH (*11*)	79:21
5(*3*)	Fmoc-Ala-OH (*1*)	86:14
5(*4*)	Fmoc-Ala-OH (*1*)	75:25
5(*5*)	Fmoc-Ala-OH (*1*)	69:31
5(*6*)	Fmoc-Ala-OH (*1*)	30:70
5(*7*)	Fmoc-Ala-OH (*1*)	77:23

[a] Calculated from LC-UV traces at 205–400 nm.

To suppress the undesired dealkylation, the use of HOBt was omitted (see step ii in Scheme 2), and acylation via a symmetrical anhydride using the DIC technique was also tested. Again, the formation of compound **12**(H,*1*) was detected and, moreover, the overall crude purity of product **11**(*2*,*1*) was considerably lower. In Scheme 3, we demonstrate a hypothetical mechanism to explain the dealkylation reaction. The appearance of side-products **12**(H,R^2) can be caused by the intramolecular transalkylation that takes place in the intermediate of the acylation step. However, the formation of compounds **16**

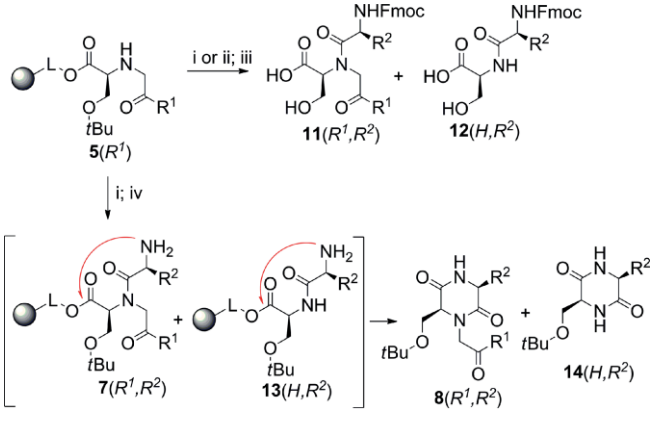

[a]Reagents: (i) Fmoc-AA-OH, HOBt, DIC, DMF/DCM (1:1), 24 h, r.t., then repeat; (ii) acylating agent:DIC (2:1), DMF, 16 h, r.t.; (iii) TFA/DCM (1:1), 30 min, r.t.; (iv) PIP/DMF (1:1), 30 min,r.t..

Scheme 2. Formation of side-products **12**(H,R^2) and **14**(H,R^2).

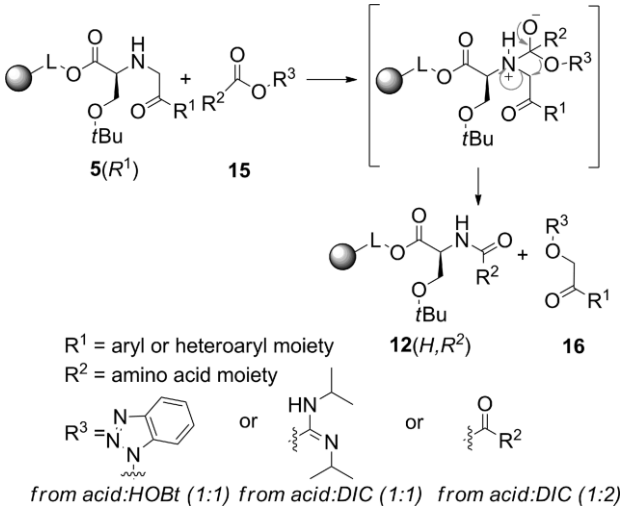

Scheme 3. Plausible mechanism for the formation of **12**(H,R^2) during the acylation step.

ChemPubSoc Europe

EurJOC European Journal of Organic Chemistry
Full Paper

was impossible to unambiguously detect in the reaction mixture by using LC–UV–MS due to a high excess of the acylating agents (a typical feature of solid-supported reactions) and/or poor ionization of the expected products.

Conclusions

We have developed a novel strategy for the synthesis of the rarely studied pyrazino[2,1-*c*][1,4]oxazine-6,9-dione derivatives using readily available building blocks: Fmoc-α-amino acids and 2-bromo ketones. Although a minor limitation (namely, dealkylation) was observed, the reported protocol provided 16 model compounds with high crude purities and good overall yields. The developed strategy allows for the simple preparation of target heterocycles with 3D architectures and specific configurations of the two resulting stereocentres, which is of great importance for the discovery of novel pharmacologically relevant molecules.[53,54] Moreover, the developed method is not limited only to solid-phase synthesis, although this does provide significant benefits such as fast and simple isolation of intermediates/products and minimum hands-on-time. If necessary, the synthetic approach can be performed by using traditional liquid-phase chemistry and an Fmoc-Ser(*t*Bu)-OH aliphatic ester as the starting material.

Experimental Section

General: Solvents and chemicals were purchased from Aldrich (Milwaukee, IL, www.sigmaaldrich.com) and Acros (Geel, Belgium, www.acros.cz). The Wang resin (100–200 mesh, 1 % DVB, 0.9 mmol/g) was obtained from AAPPTec (Louisville, KY, www.aapptec.com). Solid-phase synthesis was carried out in plastic reaction vessels (syringes, each equipped with a porous disk) using a manually operated synthesizer (Torviq, Niles, MI, www.torviq.com). The volume of wash solvent was 10 mL per 1 g of resin. For washing, the resin slurry was shaken with the fresh solvent for at least 1 min before changing the solvent. Resin-bound intermediates were dried with a stream of nitrogen for prolonged storage and/or quantitative analysis. For the LC–MS analysis, a sample of resin (ca. 5 mg) was treated with TFA in DCM (1:1), the cleavage cocktail was evaporated in a stream of nitrogen and the cleaved compounds extracted into MeCN/H_2O (1 mL, 1:1). All the reactions were carried out at ambient temperature (21 °C) unless stated otherwise. The LC–MS analyses were performed with a UHPLC–MS system consisting of an Acquity UHPLC chromatograph equipped with a photodiode array detector and single quadrupole mass spectrometer (Waters) using an X-Select C18 column at 30 °C and a flow rate of 600 µL/min. The mobile phase was 0.01 M ammonium acetate in H_2O (A) and MeCN (B) linearly programmed from 20 to 80 % B over 2.5 min and then solvent B for 1.5 min. The column was re-equilibrated with 20 % of solution B for 1 min. The ESI I source was operated at a discharge current of 5 µA, a vaporizer temperature of 350 °C and a capillary temperature of 200 °C. Purification was carried out on a C18 reversed-phase column (YMC Pack ODS-A, 20 × 100 mm, 5 µm particles) with a gradient formed from 10 mM aqueous ammonium acetate and MeCN at a flow rate of 15 mL/min. For lyophilization of the residual solvents (H_2O, ammonium acetate buffer, DMSO, DMF) at –110 °C, the ScanVac Coolsafe 110-4 instrument was used. All ^1H, ^{13}C and 2D NMR experiments were performed with a JEOL ECA400II or ECX500 spectrometer at magnetic field strengths of 9.39 or 11.75 T, corresponding to ^1H and ^{13}C resonance frequencies of 399.78 or 500.16 MHz and 100.53 or 125.77 MHz, respectively, at ambient temperature (25 °C). The chemical shifts (δ) are reported in parts per million [ppm] and the coupling constants (J) are reported in Hertz [Hz]. The signal of [D_6]DMSO was set at δ = 2.50 ppm in the ^1H NMR spectra and at δ = 39.5 ppm in the ^{13}C NMR spectra. The acetate salt (residual agent from the semi-preparative HPLC purification) exhibited a singlet at 1.89–1.90 ppm in the ^1H NMR spectrum and two resonances at 21.1–21.3 and 172.0–172.1 ppm in the ^{13}C NMR spectrum. HRMS analysis was performed by LC–MS using an Orbitrap Elite high-resolution mass spectrometer (Dionex Ultimate 3000, Thermo Exactive plus, MA, USA) operating in positive full scan mode (120000 FWMH) in the m/z range of 100–1000. The settings for electrospray ionization were as follows: oven temperature of 150 °C and source voltage of 3.6 kV. The acquired data were internally calibrated with phthalate as a contaminant in MeOH (m/z = 297.15909). Samples were diluted to a final concentration of 0.1 mg/mL in H_2O and MeOH (50:50, v/v). Before HPLC separation (column Phenomenex Gemini, 50 × 2.00 mm, 3 µm particles, C18), the samples were injected by direct infusion into the mass spectrometer using an autosampler. The mobile phase was isocratic MeCN/IPA/0.01 M ammonium acetate (40:5:55) at a flow rate of 0.3 mL/min.

Experimental Procedures

Immobilization of Fmoc-Ser(*t*Bu)-OH on Wang Resin — Synthesis of 1: Wang resin (1 g, 0.9 mmol/g) was washed three times with DCM. A solution of Fmoc-Ser(*t*Bu)-OH (767 mg, 2.0 mmol), HOBt (306 mg, 2.0 mmol), DMAP (61 mg, 0.5 mmol) and DIC (312 µL, 2.0 mmol) in DMF/DCM (10 mL, 50 %) was added to the resin and the slurry was shaken for 24 h at ambient temperature. The resin was then washed three times with DMF and three times with DCM.

Quantification of Resin 1: A sample of resin **1** (ca. 40 mg) was washed three times with DCM, five times with MeOH, dried and divided into two samples (2 × 13 mg). Both samples were cleaved from the resin using TFA in DCM (0.5 mL, 50 %) for 30 min at ambient temperature. The cleavage cocktail was evaporated in a stream of nitrogen and the oily residue was extracted into MeCN/H_2O (1 mL, 50 %) and analysed by HPLC–UV–MS. The loading of the resin was calculated with the use of an external standard (Fmoc-Ala-OH, 0.5 mg/mL).

Deprotection of the Fmoc Group and Reaction with 4-NsCl — Synthesis of 3: Resin **1** (960 mg) was shaken with piperidine in DMF (10 mL, 50 %) for 30 min at room temperature. The resulting resin **2** was washed three times with DMF, three times with DCM and then a solution of 4-NsCl (798 mg, 3.6 mmol) and 2,6-lutidine (456 µL, 3.9 mmol) in DCM (10 mL) was added. The resin slurry was shaken for 24 h at room temperature and then washed three times with DCM. Quantitative conversion of this reaction was confirmed by derivatization of the resin sample with Fmoc-OSu followed by LC–MS analysis.

Alkylation with Bromoacetophenones — Synthesis of 4(R^1): Resin **3** (460 mg) was washed three times with DMF and a solution of bromoacetophenone (3.0 mmol) and EDIPA (522 µL, 3.0 mmol) in DMF (5 mL) was added. The reaction mixture was shaken for 24 h at room temperature and then washed three times with DMF and three times with DCM.

Deprotection of the 4-Ns Group — Synthesis of 5(R^1): A solution of 2-mercaptoethanol (504 µL, 7.2 mmol) and DBU (120 µL, 2.4 mmol) in DMF (5 mL) was added to the resin **4**(R^1) (450 mg), previously washed three times with DMF, and the slurry was shaken for 1 h at room temperature. Finally, the resin was washed three times with DMF and three times with DCM.

ChemPubSoc Europe

EurJOC European Journal of Organic Chemistry
Full Paper

Acylation with Fmoc-Amino Acids — Synthesis of 6(R^1,R^2): A solution of Fmoc-amino acid (1.5 mmol), HOBt·H_2O (230 mg, 1.5 mmol) and DIC (232 μL, 1.5 mmol) in DMF/DCM (5 mL, 50 %) was added to the resin **5**(R^1) (440 mg). The reaction mixture was shaken for 24 h at room temperature and the resin was subsequently washed three times with DCM and the reaction was then repeated once more. In the case of acylation with Fmoc-Ile-OH, the reaction was repeated twice.

Cyclative Cleavage — Synthesis of 8(R^1,R^2): Resin **6**(R^1,R^2) (430 mg) was exposed to a solution of piperidine/DMF (5 mL, 50 %) for 30 min at room temperature. The resin was then separated from the reaction solution and washed seven times with DMF. All the obtained fractions were collected and added to the separated solution. The residual piperidine/DMF was removed by lyophilization for 16 h at –110 °C.

Deprotection of *t*Bu Group and FInal Cyclization — Synthesis of 10(R^1,R^2): A solution of TFA in DCM (5 mL, 50 %) was added to the residue **8**(R^1,R^2) and then the reaction mixture was stirred for 30 min at ambient temperature to remove the *t*Bu group. The TFA solution was then concentrated in a stream of nitrogen. The residual material **9**(R^1,R^2) was dissolved in neat MeCN (5 mL) and the solution was stirred for different reaction times (see Table 3) at 80 °C, and at 90 °C for **10**(*1*,*2*) and **10**(*1*,*3*). The resulting material was submitted to semi-preparative HPLC purification.

Table 3. Reaction time for cyclization of **9**(R^1,R^2) to **10**(R^1,R^2).

Cmpd.	Reaction time [h]
10(*1*,*1*)	5
10(*1*,*2*)	8
10(*1*,*3*)	5
10(*1*,*4*)	8
10(*1*,*5*)	8
10(*1*,*11*)	6
10(*2*,*1*)	2
10(*2*,*4*)	1
10(*2*,*6*)	1
10(*2*,*8*)	2
10(*2*,*11*)	1
10(*3*,*1*)	5
10(*4*,*1*)	1
10(*5*,*1*)	5
10(*6*,*1*)	2
10(*7*,*1*)	2

Acknowledgments

The authors are grateful to the European Social Fund (project CZ.1.07/2.3.00/20.0009), the National Program of Sustainability (project LO1304), and IGA_LF_2017_028.

Keywords: Heterocycles · Amino acids · Solid-phase synthesis · Stereochemistry

[1] A. La-Venia, P. Ventosa-Andrés, V. Krchňák in *Peptidomimetics II* (Ed. W. Lubell), Springer International Publishing, Cham, **2017**, pp. 105–126.
[2] J. L. Räber, S. A. Stoykova, C. Strässler, H. Heimgartner, *Phosphorus Sulfur Silicon Relat. Elem.* **2013**, *188*, 441–445.
[3] L. Kiss, F. Fülöp, *Chem. Rev.* **2014**, *114*, 1116–1169.
[4] C. Agami, F. Couty, M. Poursoulis, J. Vaissermann, *Tetrahedron* **1992**, *48*, 431–442.
[5] J. M. Humphrey, A. R. Chamberlin, *Chem. Rev.* **1997**, *97*, 2243–2266.
[6] R. A. Hughes, C. J. Moody, *Angew. Chem. Int. Ed.* **2007**, *46*, 7930–7954; *Angew. Chem.* **2007**, *119*, 8076.
[7] F. J. Sardina, H. Rapoport, *Chem. Rev.* **1996**, *96*, 1825–1872.
[8] Z. Li, M. Giulianotti, W. Chen, R. A. Houghten, Y. Yu, *Solid-Phase Organic Synthesis*, Wiley, Hoboken, New Jersey, **2011**, pp. 269–318.
[9] T. Liu, R. Wang, H. Yang, H. Fu, *Chem. Eur. J.* **2011**, *17*, 6765–6771.
[10] M. Tisler, P. Kolar, *Adv. Heterocycl. Chem.* **1995**, *64*, 2–81.
[11] M. M. Heravi, V. Fathi Vavsari, *Adv. Heterocycl. Chem.* **2015**, *114*, 77–145.
[12] A. Bhavini, T. Vanraj, H. Jagruti, B. Fenil, N. Malleshappa, *J. Med. Pharm. Allied Sci.* **2014**, *3*, 12.
[13] P. Králová, V. Fülöpová, M. Maloň, T. Volná, I. Popa, M. Soural, *ACS Comb. Sci.* **2017**, *19*, 173–180.
[14] M. I. Calaza, C. Cativiela, *Amino Acids, Peptides and Proteins in Organic Chemistry*, Wiley-VCH, Weinheim, **2010**, pp. 83–114.
[15] R. B. Hamed, J. Mecinovic, C. Ducho, T. D. W. Claridge, C. J. Schofield, *Chem. Commun.* **2010**, *46*, 1413–1415.
[16] X. H. Cai, B. Xie, *ARKIVOC* **2014**, *1*, 205–248.
[17] S. Kotha, V. B. Bandarugattu, N. G. Krishna, *Tetrahedron* **2014**, *70*, 5361–5384.
[18] See ref.[3]
[19] G. Prabhu, N. Narendra, Basavaprabhu, V. Panduranga, V. V. Sureshbabu, *RSC Adv.* **2015**, *5*, 48331–48362.
[20] L. Kiss, F. Fülöp, *Synlett* **2010**, 1302–1314.
[21] C. Rochais, S. Rault, P. Dallemagne, *Curr. Med. Chem.* **2010**, *17*, 4342–4369.
[22] J. Heinicke, J. Lach, K. R. Basvani, N. Peulecke, P. G. Jones, M. Köckerling, *Phosphorus Sulfur Silicon Relat. Elem.* **2011**, *186*, 666–677.
[23] H. Waldmann, *Synlett* **1995**, 133–141.
[24] P. Singh, K. Samanta, S. K. Das, G. Panda, *Org. Biomol. Chem.* **2014**, *12*, 6297–6339.
[25] M. Shamszad, M. T. Crimmins, *Comprehensive Chirality*, Elsevier, Amsterdam, **2012**, pp. 19–41.
[26] D. L. Priebbenow, S. G. Stewart, F. M. Pfeffer, *Tetrahedron Lett.* **2012**, *53*, 1468–1471.
[27] M. M. Heravi, M. H. Tehrani, K. Bakhtiari, H. A. Oskooie, *Catal. Commun.* **2007**, *8*, 1341–1344.
[28] R. M. Williams, T. Glinka, E. Kwast, *J. Am. Chem. Soc.* **1988**, *110*, 5927–5929.
[29] W. R. Li, S. Z. Peng, *Tetrahedron Lett.* **1998**, *39*, 7373–7376.
[30] K. M. Depew, S. P. Marsden, D. Zatorska, A. Zatorski, W. G. Bornmann, S. J. Danishefsky, *J. Am. Chem. Soc.* **1999**, *121*, 11953–11963.
[31] A. Bianco, C. P. Sonksen, P. Roepstorff, J. P. Briand, *J. Org. Chem.* **2000**, *65*, 2179–2187.
[32] W. R. Li, J. H. Yang, *J. Comb. Chem.* **2002**, *4*, 106–108.
[33] N. Deppermann, A. H. G. P. Prenzel, A. Beitat, W. Maison, *J. Org. Chem.* **2009**, *74*, 4267–4271.
[34] K. C. Majumdar, K. Ray, S. Ganai, *Synlett* **2010**, 2122–2124.
[35] M. Tullberg, M. Grotli, K. Luthman, *J. Org. Chem.* **2007**, *72*, 195–199.
[36] M. Tullberg, K. Luthman, M. Grotli, *J. Comb. Chem.* **2006**, *8*, 915–922.
[37] Č. Malavašič, U. Grošelj, A. Golobič, J. Bezenšek, B. Stanovnik, K. Stare, J. Wagger, J. Svete, *Tetrahedron: Asymmetry* **2011**, *22*, 629–640.
[38] C. L. L. Chai, A. R. King, *Tetrahedron Lett.* **1995**, *36*, 4295–4298.
[39] D. W. Gordon, J. Steele, *Bioorg. Med. Chem. Lett.* **1995**, *5*, 47–50.
[40] J. Kowalski, M. A. Lipton, *Tetrahedron Lett.* **1996**, *37*, 5839–5840.
[41] R. A. Smith, M. A. Bobko, W. Lee, *Bioorg. Med. Chem. Lett.* **1998**, *8*, 2369–2374.
[42] D. X. Wang, M. T. Liang, G. J. Tian, H. Lin, H. Q. Liu, *Tetrahedron Lett.* **2002**, *43*, 865–867.
[43] J. J. N. Veerman, R. S. Bon, B. T. B. Hue, D. Girones, F. P. J. T. Rutjes, J. H. van Maarseveen, H. Hiemstra, *J. Org. Chem.* **2003**, *68*, 4486–4494.
[44] Q. Lin, H. E. Blackwell, *Chem. Commun.* **2006**, *27*, 2884–2886.
[45] M. Nikulnikov, A. Shumsky, M. A. Krasavin, *Synthesis* **2010**, 2527–2532.
[46] D. D. DesMarteau, C. Lu, D. Vanderveer, *Tetrahedron Lett.* **2009**, *50*, 3741–3745.
[47] C. Lalli, A. Trabocchi, F. Sladojevich, G. Menchi, A. Guarna, *Chem. Eur. J.* **2009**, *15*, 7871–7875.
[48] L. Ciofi, M. Morvillo, F. Sladojevich, A. Guarna, A. Trabocchi, *Tetrahedron Lett.* **2010**, *51*, 6282–6285.
[49] T. Fukuyama, C. K. Jow, M. Cheung, *Tetrahedron Lett.* **1995**, *36*, 6373–6374.

ChemPubSoc Europe

EurJOC European Journal of Organic Chemistry
Full Paper

[50] T. Fukuyama, M. Cheung, C. K. Jow, Y. Hidai, T. Kan, *Tetrahedron Lett.* **1997**, *38*, 5831–5834.
[51] V. Fülöpová, M. Soural, *ACS Comb. Sci.* **2015**, *17*, 570–591.
[52] V. Fülöpová, T. Gucký, M. Grepl, M. Soural, *ACS Comb. Sci.* **2012**, *14*, 651–656.
[53] S. D. Roughley, A. M. Jordan, *J. Med. Chem.* **2011**, *54*, 3451–3479.
[54] W. P. Walters, J. Green, J. R. Weiss, M. A. Murcko, *J. Med. Chem.* **2011**, *54*, 6405–6416.

Received: October 18, 2017

ACS Combinatorial Science

Letter

Cite This: ACS Comb. Sci. 2019, 21, 154−157

pubs.acs.org/acscombsci

Polymer-Assisted Synthesis of Single and Fused Diketomorpholines

Petra Králová,[†] Sandra Benická,[†] and Miroslav Soural*[,‡]

[†]Department of Organic Chemistry, Faculty of Science, Palacký University, 771 46 Olomouc, Czech Republic

[‡]Institute of Molecular and Translational Medicine, Faculty of Medicine and Dentistry, Palacký University, Hněvotínská 5, 779 00, Olomouc, Czech Republic

Supporting Information

ABSTRACT: The synthesis of different diketomorpholines via *N*-acyl-3,4-dihydro-2*H*-1,4-oxazine-3-carboxylic acids is reported in this article. The key intermediates were prepared using a convenient solid-phase synthesis starting from polymer-supported Ser(*t*Bu)-OH. After subsequent sulfonylation with 4-nitrobenzenesulfonyl chloride (4-Nos-Cl), alkylation with an α-bromoketone, cleavage of the 4-Nos group and acylation with an α-halocarboxylic acids, acid-mediated cleavage from the resin yielded dihydrooxazine-3-carboxylic acids in high crude purities. Depending on the reaction conditions, exposure to base resulted in cyclization to either oxazino[3,4-*c*][1,4]oxazine-diones or 3-methylidenemorpholine-2,5-diones. Further reaction with triethylsilane-trifluoroacetic acid (TES/TFA) led to olefin reduction, in the case of oxazino[3,4-*c*][1,4]oxazine-dione with full control of the newly formed stereocenter.

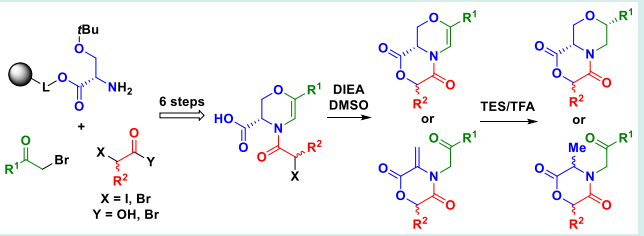

KEYWORDS: *serine, bromoketone, morpholine, diketomorpholine, solid-phase synthesis*

Diketomorpholines (DKMs) represent an interesting group of biologically active heterocycles. Although diketomorpholine scaffolds appear less frequently in both natural and synthetic derivatives than isosteric diketopiperazines, both simple and complex DKMs have been synthesized or isolated from different natural sources and identified as potent ligands of various biomolecular targets (see Figure 1).[1−12]

In the past, the synthesis of DKMs has been reported using traditional solution-phase synthesis with various approaches. The most convenient strategy consisted of the acylation of α-amino acids with α-hydroxycarboxylic acids[13] or α-halocarboxylic acids,[14,15] followed by an acid-mediated or a base-promoted cyclization, respectively. Alternatively, a hypervalent iodine-mediated spirocyclization of methyl 2-(4-hydroxybenzamido)acrylate was recently reported by Hempel et al.[16] In contrast to single DKMs, the number of synthetic strategies reported for the preparation of these compounds fused to additional heterocycles is significantly limited. For this reason, we suggested the use of polymer-supported aminoketones[17−20] to synthesize novel oxazine−oxazine systems (see Figure 1) from readily available building blocks. The solid-phase synthesis strategy was chosen because of its well-known advantages, especially the fast and simple isolation of the reaction intermediates, which allows the quick production of collections of compounds for biological screening.

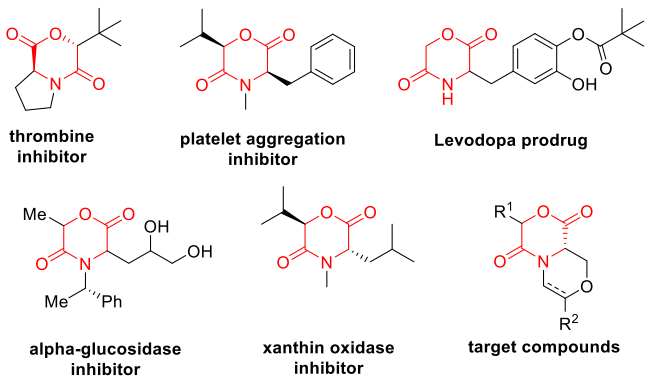

Figure 1. Representative examples of pharmacologically relevant compounds bearing the DKM scaffold.

The solid-phase synthesis of intermediate **1**{*1*} (Chemset numbering system is used hereafter) was performed according to our previous report (see Scheme 1).[17] The Wang resin was acylated with Fmoc-Ser(*t*Bu)-OH, and this was followed by cleavage of the Fmoc-protecting group, sulfonylation with 4-nitrobenzenesulfonyl chloride and alkylation with 2-bromoacetophenone. Cleavage of the 4-Nos group using mercaptoethanol/DBU yielded immobilized aminoketone **1**{*1*}, which was acylated with iodoacetic acid using DIC activation[21] to afford resin **2**{*1,1*}. TFA-mediated cleavage from the polymer matrix triggered cyclization of the oxazine scaffold, and dihydrooxazine-3-carboxylic acid (**3**{*1,1*}) was obtained in excellent crude purity (97%, measured by LC-UV traces at 205−400 nm). After simple evaporation of the cleavage

Received: November 21, 2018
Revised: January 7, 2019
Published: January 14, 2019

DOI: 10.1021/acscombsci.8b00176
ACS Comb. Sci. 2019, 21, 154−157

Scheme 1. Synthetic Route to Final Products[a]

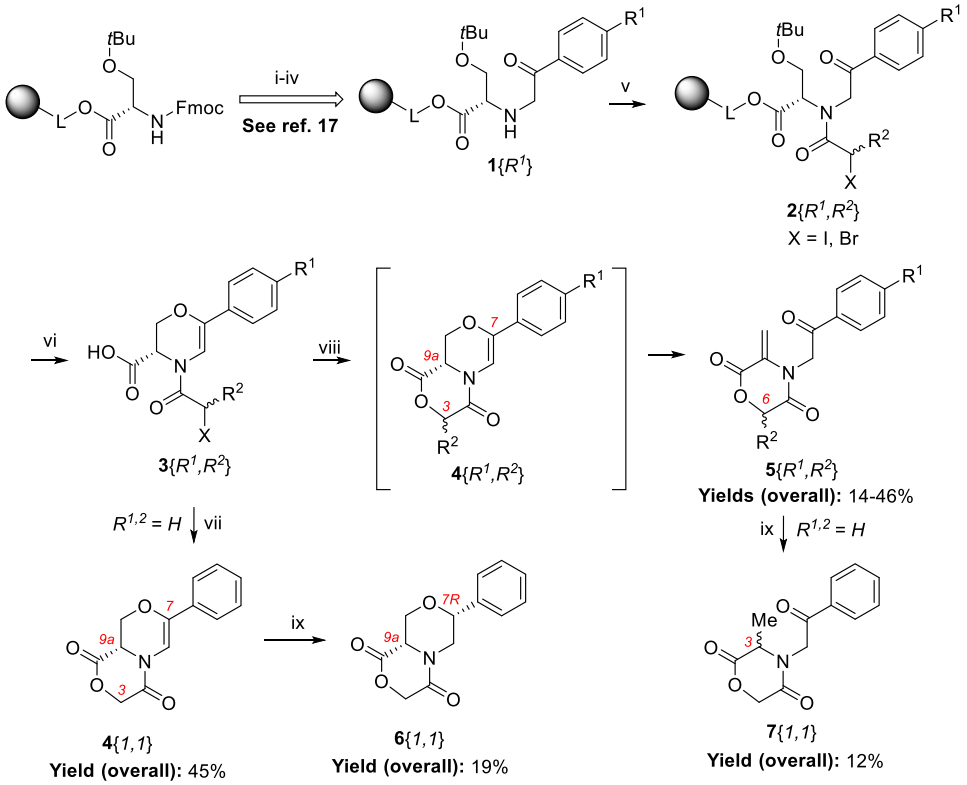

[a]Reagents and conditions: (i) 50% piperidine/DMF, 30 min, rt; (ii) 4-nitrobenzenesulfonyl chloride, 2,6-lutidine, DCM, 24 h, rt; (iii) 2-bromoacetophenone, DIEA, DMF, 24 h, rt; (iv) mercaptoethanol, DBU, DMF, 30 min, rt; (v) halocarboxylic acid, DIC, DCM, 30 min, then added to resin, 24 h, rt; or 2-bromopropionyl bromide, 2,6-lutidine, DCM, 24 h, rt (vi) 50% TFA/DCM, 1 or 4 h (for derivatives 2{R^1,3}), rt; (vii) DIEA, DMSO, 20 min (for 4{R^1,1}), rt; (viii) DIEA, DMSO, 20 h, rt (for 5{R^1,1} and 5{R^1,3}) or 1 h, 80 °C (for 5{R^1,2}); (ix) TFA/TES/DCM (10:3:10), 24, rt.

cocktail, crude intermediate 3{*1,1*} was subjected to base-catalyzed cyclization using *N,N*-diisopropylethylamine (DIEA) in DMSO. After only 20 min, the quantitative formation of expected oxazino[3,4-*c*][1,4]oxazine-dione 4{*1,1*} was observed, whereas a longer reaction time (20 h) led to quantitative conversion of 4{*1,1*} to 3-methylidenemorpholine-2,5-dione 5{*1,1*}. Products 4{*1,1*} or 5{*1,1*} were obtained in excellent crude purities (91% or 95%, as measured by LC-UV traces at 205−400 nm) and overall yields (45% or 46%, after reversed-phase semipreparative HPLC purification). After it was freeze-dried from DMSO/DIEA, crude 4{*1,1*} was further reduced by TES/TFA to the corresponding saturated analogue 6{*1,1*}. In accordance with our previous reports,[17−19] the reduction of the dihydroxazine scaffold was fully stereoselective. In contrast, the TES/TFA-mediated reduction of 5{*1,1*} to 7{*1,1*} afforded a mixture of enantiomers (see the stereochemical studies later in the text).

To determine the scope and limitations of our synthetic pathway, we tested a combination of different aromatic bromoketones with electron-donating and electron-withdrawing substituents and some α-halocarboxylic acids or acyl halides (see Figure 2).

Resin-bound intermediates 2{R^1,R^2} were successfully synthesized for all tested α-bromoketones and α-halocarboxylic acids or acyl halides, that is, 2-iodoacetic acid, (*R,S*)-2-bromopropionyl bromide, (*S*)-(−)-2-bromopropionic acid, and (*R,S*)-2-bromo-2-phenylacetic acid. TFA-mediated cleavage yielded the corresponding *N*-acyl-3,4-dihydro-2*H*-1,4-

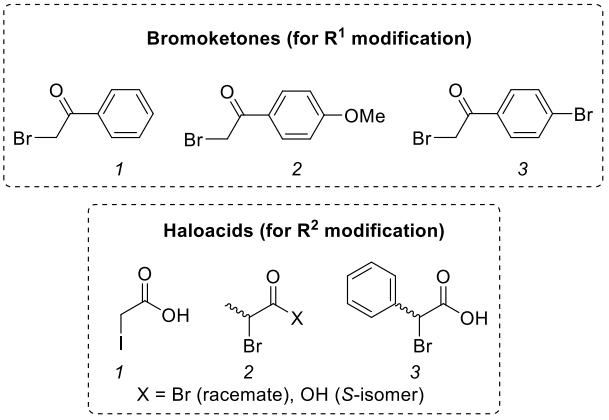

Figure 2. Tested building blocks used to obtain different R^1 and R^2 substituents

oxazine-3-carboxylic acids 3{R^1,R^2} in good to excellent crude purities (56−97%, as measured by LC-UV traces at 205−400 nm). The cyclization of the cleaved compounds required different conditions. In the cases of intermediates 3{R^1,1} and 3{R^1,3} prepared from 2-iodoacetic acid and 2-bromo-2-phenylacetic acid, the cyclization could be achieved at room temperature using quite short reaction times (see conditions in Scheme 1 and the Supporting Information for more details). In contrast, the room-temperature cyclization of intermediates 3{R^1,2}, prepared from 2-bromopropionyl bromide, was very slow, and only small quantities of products were

DOI: 10.1021/acscombsci.8b00176
ACS Comb. Sci. 2019, 21, 154−157

detected after several days; however, heating to 80 °C accelerated the conversion, and the reaction was completed in 1 h. Consequently, it was difficult to isolate corresponding fused morpholines **4**{R^1,2} because of their thermal conversion to methylidene compounds **5**{R^1,2}. Furthermore, it is worth mentioning that the conversion of **4**{1,1} to **5**{1,1} (as an example) was observed when a sample of **4**{1,1} was prepared for NMR analysis. Even the use of different solvents such as DMSO-d_6, MeOH-d_4, $CDCl_3$, and MeCN-d_3 caused slow conversion, which highlights generally low stability of compounds **4**{R^1,R^2} bearing the unsaturated oxazine scaffold. In contrast, reduced compound **6**{1,1} was completely stable, and it could undergo full NMR characterization in MeOH-d_4.

To determine the 3D structures of the final compounds, NMR and chiral supercritical fluid chromatography (SFC) were used to study the configurations in detail. In the case of reduced compound **6**{1,1}, the configuration of the newly formed C7 stereocenter was assigned as (*R*) based on NMR techniques, and this configuration is in accordance with our previous findings.[17−20] In contrast, the reduction of **5**{1,1} to **7**{1,1} was not stereoselective and yielded a mixture of C3 enantiomers in a ratio of 20:80 as detected by SFC analysis. In the case of **5**{R^1,2}, prepared from racemic α-bromopropionyl bromide, the final compounds were not obtained as racemates but as mixtures of two enantiomers in a ratio of approximately 9:1. This fact points to the preferential formation of the more stable enantiomer, which was presumably promoted by the base (DIEA) used in the final cyclization step. In this context, we synthesized compound **3**^{S}{1,2} using (*S*)-(−)-bromopropionic acid. After cyclization of **3**^{S}{1,2} at 80 °C for just 5 min, two enantiomers **5**^{S}{1,2} and **5**^{R}{1,2} in a ratio of 95:5 were detected. Interestingly, after an additional 45 min, the ratio changed to 21:79, which demonstrates the slow conversion of the starting *S*-isomer to the *R*-isomer. This nonracemic outcome could be explained by deprotonation at C^3 from both faces by DIEA, which proceeded through two diastereomeric transition states of unequal energy. Further, two analogues, **5**{1,3} and **5**{2,3}, with identical R^2 groups (Ph) but different R^1 groups (H or MeO), were produced as the enantiomerically pure compounds, and **5**{3,3}, where R^2 = Br, was obtained as the racemic mixture (50:50). This shows that R^1 substitution also influences the stereochemical outcome.

In conclusion, we have developed a simple synthetic approach leading to novel diketomorpholines by taking advantage of the convenience of solid-phase synthesis. Although the final cyclization (and subsequent TES reduction) had to be performed after cleavage from the polymer support, the procedure is still compatible with high-throughput synthesis, as the workup in the last two steps is based on simple evaporation of the reagents and solvents. Twelve representative derivatives from structurally distinct building blocks were synthesized and fully characterized. The method can be applied in combination with previously reported procedures[17−20] to synthesize diverse drug-like oxazine derivatives using diversity oriented, reagent-based synthesis starting from immobilized aminoketones. Importantly, due to the recent attention paid to Michael acceptors,[22−24] compounds **5** can be considered attractive derivatives for drug discovery in the field of covalent inhibitors.

Table 1. List of Prepared and Fully Characterized Compounds

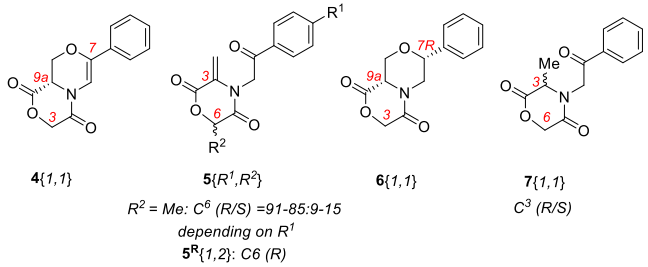

cmpd	R^1	R^2	crude purity [%][a]	final purity [%][b]	overall yield [%][c]	ratio of *R*/*S* enantiomers [%][e]
4{1,1}	H	H	95	98	45[d]	6:94
5{1,1}	H	H	91	99	46	
5{1,2}	H	Me	88	99	48	90:10
5^R{1,2}	H	Me	67	99	24	85:15
5{1,3}	H	Ph	66	98	27	100:0
5{2,2}	MeO	Me	89	99	35	91:9
5{2,3}	MeO	Ph	56	99	14	100:0
5{3,1}	Br	H	90	98	30	
5{3,2}	Br	Me	90	96	22	87:13
5{3,3}	Br	Ph	78	99	18	50:50
6{1,1}	H	H	74	98	19	
7{1,1}	H	H	89	97	12	80:20

[a]Overall purity after the entire reaction sequence calculated from the HPLC-UV traces (205−400 nm). [b]Determined from the HPLC-UV traces after purification (205−400 nm). [c]Calculated from the ^{1}H NMR spectrum of the purified products (see the Supporting Information for general procedure); [d]Dissolving the sample in MeCN-d_3 led to partial conversion of purified products **4** and **5** in ratio 83:17 as calculated from the ^{1}H NMR spectrum. [e]Calculated from chiral SFC-UV traces.

■ ASSOCIATED CONTENT

Supporting Information

The Supporting Information is available free of charge on the ACS Publications website at DOI: 10.1021/acscombsci.8b00176.

Details of experimental, synthetic, and analytical procedures, along with spectroscopic data for synthesized compounds (PDF)

■ AUTHOR INFORMATION

Corresponding Author

*E-mail: miroslav.soural@upol.cz.

ORCID

Miroslav Soural: 0000-0001-7288-8617

Notes

The authors declare no competing financial interest.

■ ACKNOWLEDGMENTS

Supported by the European Regional Development Fund, Project ENOCH (No. CZ.02.1.01/0.0/0.0/16_019/0000868), and internal grants from Palacký University (IGA_PrF_2018_29 and IGA_LF_2018_032). Authors are also grateful to Soňa Krajčovičová for measuring NMR data.

REFERENCES

(1) Khalil, Z. G.; Huang, X.; Raju, R.; Piggott, A. M.; Capon, R. J. Shornephine A: Structure, chemical stability, and P-glycoprotein inhibitory properties of a rare diketomorpholine from an Australian marine-derived Aspergillus sp. *J. Org. Chem.* **2014**, *79* (18), 8700−8705.

(2) Cheng, S.-M.; Huang, J.; Wang, H.-Y.; Li, G.-Y.; Lin, R.-C.; Wang, J.-H. Two new compounds from Bombyx batryticatus. *J. Asian Nat. Prod. Res.* **2014**, *16* (8), 825−829.

(3) Aparicio-Cuevas, M. A.; Rivero-Cruz, I.; Sánchez-Castellanos, M.; Menéndez, D.; Raja, H. A.; Joseph-Nathan, P.; González, M. d. C.; Figueroa, M. Dioxomorpholines and Derivatives from a Marine-Facultative Aspergillus Species. *J. Nat. Prod.* **2017**, *80* (8), 2311−2318.

(4) Smelcerovic, A.; Rangelov, M.; Smelcerovic, Z.; Veljkovic, A.; Cherneva, E.; Yancheva, D.; Nikolic, G. M.; Petronijevic, Z.; Kocic, G. Two 6-(propan-2-yl)-4-methyl-morpholine-2,5-diones as new non-purine xanthine oxidase inhibitors and anti-inflammatory agents. *Food Chem. Toxicol.* **2013**, *55*, 493−497.

(5) Suntornchashwej, S.; Chaichit, N.; Isobe, M.; Suwanborirux, K. Hectochlorin and Morpholine Derivatives from the Thai Sea Hare, Bursatella leachii. *J. Nat. Prod.* **2005**, *68* (6), 951−955.

(6) Nakadate, S.; Nozawa, K.; Horie, H.; Fujii, Y.; Nagai, M.; Komai, S.; Hosoe, T.; Kawai, K.; Yaguchi, T.; Fukushima, K. New Dioxomorpholine Derivatives, Javanicunine A and B, from Eupenicillium javanicum. *Heterocycles* **2006**, *68* (9), 1969−1972.

(7) Nelson, T. D.; LeBlond, C. R.; Frantz, D. E.; Matty, L.; Mitten, J. V.; Weaver, D. G.; Moore, J. C.; Kim, J. M.; Boyd, R.; Kim, P.-Y.; Gbewonyo, K.; Brower, M.; Sturr, M.; McLaughlin, K.; McMasters, D. R.; Kress, M. H.; McNamara, J. M.; Dolling, U. H. Stereoselective Synthesis of a Potent Thrombin Inhibitor by a Novel P2-P3 Lactone Ring Opening. *J. Org. Chem.* **2004**, *69* (11), 3620−3627.

(8) Oh, H.; Kim, T.; Oh, G.-S.; Pae, H.-O.; Hong, K.-H.; Chai, K.-Y.; Kwon, T.-O.; Chung, H.-T.; Lee, H.-S. (3*R*,6*R*)-4-Methyl-6-(1-methylethyl)-3-phenylmethylperhydro-1,4-oxazine-2,5-dione: an apoptosis-inducer from the fruiting bodies of Isaria japonica. *Planta Med.* **2002**, *68* (04), 345−348.

(9) Cingolani, G. M.; Di Stefano, A.; Mosciatti, B.; Napolitani, F.; Giorgioni, G.; Ricciutelli, M.; Claudi, F. Synthesis of L-(+)-3-(3-hydroxy-4-pivaloyloxybenzyl)-2,5-diketomorpholine as potential pro-drug of L-Dopa. *Bioorg. Med. Chem. Lett.* **2000**, *10* (12), 1385−1388.

(10) Kagamizono, T.; Nishino, E.; Matsumoto, K.; Kawashima, A.; Kishimoto, M.; Sakai, N.; He, B. M.; Chen, Z. X.; Adachi, T.; Morimoto, S.; Hanada, K. Bassiatin, a new platelet aggregation inhibitor produced by Beauveria bassiana K-717. *J. Antibiot.* **1995**, *48* (12), 1407−1413.

(11) Hasumi, K.; Shinohara, C.; Iwanaga, T.; Endo, A. Lateritin, a new inhibitor of acyl-CoA: cholesterol acyltransferase produced by Gibberella lateritium IFO 7188. *J. Antibiot.* **1993**, *46* (12), 1782−1787.

(12) Arcelli, A.; Balducci, D.; Grandi, A.; Porzi, G.; Sandri, M.; Sandri, S. Chiral 1,4-Morpholine-2,5-Dione Derivatives as α-Glucosidase Inhibitors: Part 2. *Tetrahedron: Asymmetry* **2005**, *16* (8), 1495−1501.

(13) Segat-Dioury, F.; Lingibé, O.; Graffe, B.; Sacquet, M.-C.; Lhommet, G. A General Synthesis of Enantiopure 1,2-Aminoalcohols via Chiral Morpholinones. *Tetrahedron* **2000**, *56* (2), 233−248.

(14) Porzi, G.; Sandri, S. Enantioselective synthesis of (*R*)-and (*S*)-α-aminoacids using (6*S*)- and (6*R*)-6-methyl-morpholine-2,5-dione derivatives. *Tetrahedron: Asymmetry* **1996**, *7* (1), 189−196.

(15) Pfleger, R.; Markert, G. Über α-Acylamino-Acrylsäuren, IV. Der Einfluss Des Lösungsmittels Und Des an Der Kohlenstoff-Doppelbindung Stehenden Halogens Auf Die Halogenierung Der Methylgruppen Der α-Acetamino-Zimtsäure-Und Der α-p-Toluylamino-Zimtsäure-Azlactone. *Chem. Ber.* **1957**, *90* (8), 1482−1488.

(16) Hempel, C.; Weckenmann, N. M.; Maichle-Moessmer, C.; Nachtsheim, B. A Hypervalent Iodine-Mediated Spirocyclization of 2-(4-Hydroxybenzamido)Acrylates − Unexpected Formation of δ-Spirolactones. *Org. Biomol. Chem.* **2012**, *10* (47), 9325−9329.

(17) Králová, P.; Fülöpová, V.; Maloň, M.; Volná, T.; Popa, I.; Soural, M. Stereoselective Polymer-Supported Synthesis of Morpholine- and Thiomorpholine-3-Carboxylic Acid Derivatives. *ACS Comb. Sci.* **2017**, *19* (3), 173−180.

(18) Králová, P.; Maloň, M.; Volná, T.; Ručilová, V.; Soural, M. Polymer-Supported Stereoselective Synthesis of Benzoxazino[4,3-b][1,2,5]Thiadiazepinone 6,6-Dioxides. *ACS Comb. Sci.* **2017**, *19* (10), 670−674.

(19) Králová, P.; Maloň, M.; Soural, M. Stereoselective Synthesis of Benzo[e][1,4]Oxazino[4,3-a][1,4]Diazepine-6,12-Diones with Two Diversity Positions. *ACS Comb. Sci.* **2017**, *19* (12), 770−774.

(20) Ručilová, V.; Králová, P.; Soural, M. Synthesis of Disubstituted Pyrazino-Oxazine Derivatives with Controlled Stereochemistry. *Eur. J. Org. Chem.* **2017**, *2017* (47), 7034−7039.

(21) Drábiková, M.; Krajčovičová, S.; Soural, M. Mitsunobu C-Alkylation of β-Alkoxycarbonyl 2-Nitrobenzenesulfones and Its Use for the Rapid Synthesis of Novel Benzothiazine Derivatives. *Tetrahedron* **2017**, *73* (44), 6296−6306.

(22) Wang, L.; Zhao, J.; Yao, Y.; Wang, C.; Zhang, J.; Shu, X.; Sun, X.; Li, Y.; Liu, K.; Yuan, H.; Ma, X. Covalent Binding Design Strategy: A Prospective Method for Discovery of Potent Targeted Anticancer Agents. *Eur. J. Med. Chem.* **2017**, *142*, 493−505.

(23) De Cesco, S.; Kurian, J.; Dufresne, C.; Mittermaier, A. K.; Moitessier, N. Covalent Inhibitors Design and Discovery. *Eur. J. Med. Chem.* **2017**, *138*, 96−114.

(24) Lagoutte, R.; Patouret, R.; Winssinger, N. Covalent Inhibitors: An Opportunity for Rational Target Selectivity. *Curr. Opin. Chem. Biol.* **2017**, *39*, 54−63.

DOI: 10.1021/acscombsci.8b00176
ACS Comb. Sci. 2019, 21, 154−157

molecules

MDPI

Article

Convenient Synthesis of Thiohydantoins, Imidazole-2-thiones and Imidazo[2,1-*b*]thiazol-4-iums from Polymer-Supported α-Acylamino Ketones

Petra Králová [1], Michal Maloň [2], Hiroyuki Koshino [3] and Miroslav Soural [4,*]

1 Department of Organic Chemistry, Faculty of Science, Palacký University, 17. Listopadu 12, 771 46 Olomouc, Czech Republic; petra.kralova@upol.cz
2 JEOL Ltd., Musashino 3-1-2, Akishima, Tokyo 196-8558, Japan; mmichal@jeol.co.jp
3 RIKEN Center for Sustainable Resource Science, Hirosawa 2-1, Wako, Saitama 351-0198, Japan; koshino@riken.jp
4 Institute of Molecular and Translational Medicine, Faculty of Medicine and Dentistry, Palacký University, Hnevotinska 5, 779 00 Olomouc, Czech Republic
* Correspondence: miroslav.soural@upol.cz; Tel.: +420-585632196

Received: 10 April 2018; Accepted: 20 April 2018; Published: 23 April 2018

Abstract: The preparation of 5-methylene-thiohydantoins using solid-phase synthesis is reported in this paper. After sulfonylation of immobilized Ser (*t*-Bu)-OH with 4-nitrobenzenesulfonyl chloride followed by alkylation with various bromoketones, the 4-Nos group was removed and the resulting polymer-supported α-acylamino ketones reacted with Fmoc-isothiocyanate. Cleavage of the Fmoc protecting group was followed by the spontaneous cyclative cleavage releasing the 5-methylene-thiohydantoin derivatives from the polymer support. Reduction with triethylsilane (TES) yielded the corresponding 5-methyl-thiohydantoins. When Fmoc-isothiocyanate was replaced with alkyl isothiocyanates, the trifluoroacetic acid (TFA) mediated cleavage from the polymer support, which was followed by the cyclization reaction and the imidazo[2,1-*b*]thiazol-4-iums were obtained. Their conversion in deuterated dimethylsulfoxide led to imidazole-2-thiones.

Keywords: heterocycle; thiohydantoin; imidazole; serine; bromoketone; solid-phase synthesis

1. Introduction

The reaction of polymer-supported 2- or 4-nitrobenzensulfonamides with α-haloketones allows the simple production of many different heterocycles using the concept of diversity-oriented synthesis [1]. Recently, this chemistry was used to prepare morpholines and thiomorpholines from polymer-supported serine and cysteine via the corresponding α-acylamino ketones [2–4]. In addition, fused benzodiazepine-oxazines **I**, **II** [7 + 6] or pyrazino-oxazines **III** [6 + 6] were obtained via the acylation or sulfonylation of α-acylamino ketones with different reagents (see Scheme 1) [5–7]. As a continuation of our ongoing research in the field of solid-phase syntheses of pharmacologically promising heterocycles, we suggested the application of immobilized α-acylamino ketones for preparing novel fused [5 + 6] heterocycles bearing a thiohydantoin scaffold. 2-Thiohydantoins are present in the structure of many natural and synthetic compounds that can serve as antiandrogens [8], immunomodulators [9], or agricultural agents [10,11]. These derivatives also possess antimycobacterial [12], anti-inflammatory [13], anticonvulsant [14,15], antiarrhythmic [16], and anti-tumour properties [17,18]. A variety of approaches for accessing 2-thiohydantoins using both traditional solution-phase synthesis [10,19–22] and solid-phase synthesis [23–26] have been reported. In contrast, 2-thiohydantoins fused with morpholine or oxazine scaffolds and structurally related compounds have rarely been studied. Inspired by these findings, we attempted a simple synthesis to

prepare the desired heterocycles from polymer-supported α-acylamino ketones. The actual course of reaction based on careful structural elucidation of isolated products is reported in this paper.

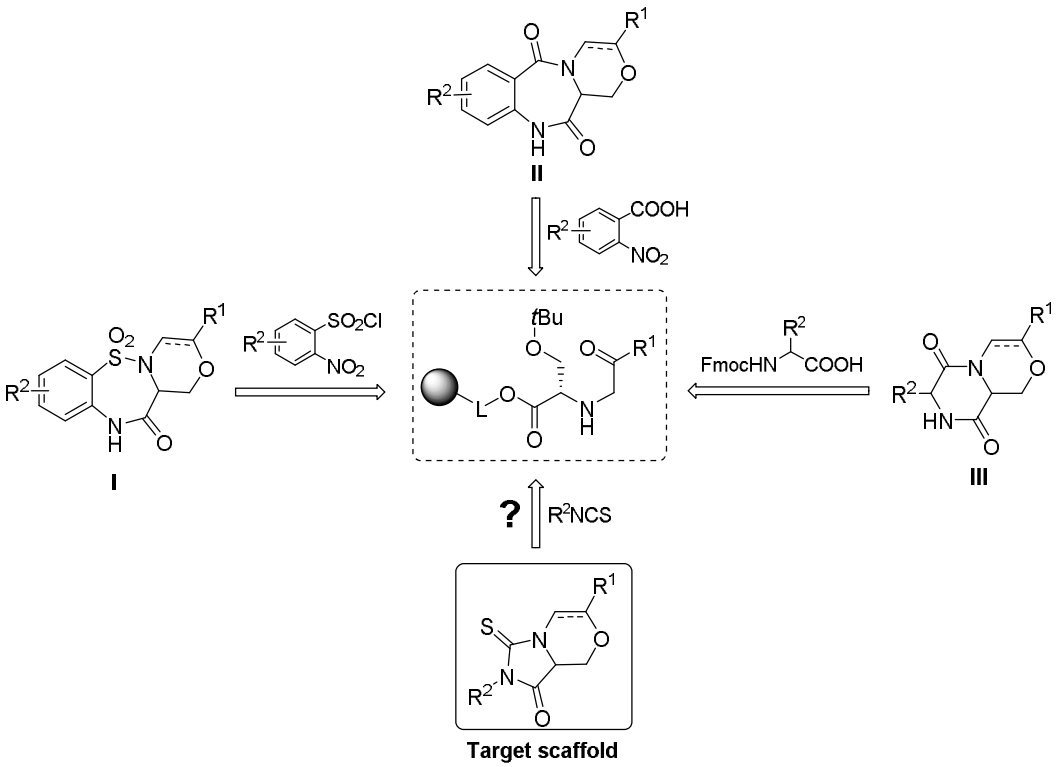

Scheme 1. Previous applications of serine-based immobilized α-acylamino ketones and the proposed [5 + 6] heterocyclic scaffold.

2. Results

The proposed synthetic pathway (see Scheme 2) was tested with 2-bromo-1-phenylethan-1-one and Fmoc-isothiocyanate as representative substrates. First, α-acylamino ketone **1**{*1*} (Chemset Numbering System is used hereafter) was synthetized in four steps from Wang resin-supported Fmoc-Ser(*t*-Bu)-OH based on previously reported procedures. [2] Reaction with Fmoc-NCS yielded the corresponding Fmoc-thiourea **2**{*1,1*}. After cleaving the Fmoc-protecting group, liberated thiourea **3**{*1,1*} underwent spontaneous cyclative cleavage, which released 2-thiohydantoin intermediate **3**{*1,1*} from the polymer matrix. The cleavage cocktail (DMF/piperidine) was freeze dried and the residual compound **4**{*1,1*} was subjected to TFA cyclization. However, the previously reported formation of the oxazine scaffold **5**{*1,1*} [7] was not observed and 5-methylidene-thiohydantoin **6**{*1,1*} was obtained in 80% crude purity (measured by LC-UV traces at 205–400 nm) as a result of the *t*-Bu protecting group cleavage and dehydration. We also tested TFA/TES reduction of the methylidene derivative **6**{*1,1*}, which was reported earlier to reduce dihydroxazines [2]. This provided 5-methyl-thiohydantoin **7**{*1,1*} in excellent crude purity (85%) and had an overall yield of 19%. Similar results were obtained for other 5-methyl-thiohydantoins **7**{R^1,*1*}, which were obtained in crude purities of 71% to 85% and overall yields of 15% to 19% (see Table 1).

Table 1. List of prepared compounds.

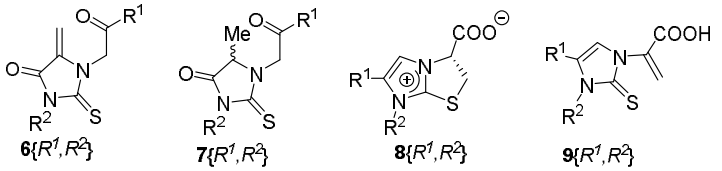

Cmpd	R^1	R^2	Crude Purity (%) [a]	Final Purity (%) [b]	Overall Yield (%) [c]	Ratio 8:9 At rt (%) [c]	Ratio 8:9 after Heating (%) [c,d]
6{1,1}	Ph	H	80	99	11	-	-
6{4,1}	4-F-Ph	H	69	98	11	-	-
6{5,1}	4-Br-Ph	H	75	97	7	-	-
6{6,1}	4-NH_2-3,5-diClPh	H	68	98	8	-	-
6{7,1}	3-thiophenyl	H	85	97	8	-	-
7{1,1}	Ph	H	85	99	19	-	-
7{6,1}	4-Br-Ph	H	71	98	16	-	-
7{7,1}	3-thiophenyl	H	72	99	15	-	-
8{1,2}	Ph	Bn	80	98	53	93:7	0:100
8{1,3}	Ph	allyl	90	98	34	100:0	8:92
8{1,4}	Ph	Et	91	99	23	45:55 [e]	11:89
8{2,2}	4-Me-Ph	Bn	96	99	38	97:3	3:97
8{2,5}	4-Me-Ph	cyclohexylmethyl	77	99	49	100:0	NT
8{3,3}	4-MeO-Ph	allyl	87	99	32	84:16	3:97
8{3,4}	4-MeO-Ph	Et	92	99	59	100:0	13:87
8{3,6}	4-MeO-Ph	2-(4-morpholino)ethyl	95	99	39	60:40 [e]	0:100
8{4,4}	4-F-Ph	Et	85	99	57	100:0	16:84
8{4,5}	4-F-Ph	cyclohexylmethyl	70	99	19	8:92 [e]	8:92
8{5,2}	4-Br-Ph	Bn	91	98	28	98:2	9:91
8{5,3}	4-Br-Ph	allyl	69	99	18	100:0	29:71
8{5,6}	4-Br-Ph	2-(4-morpholino)ethyl	90	98	17	88:12	0:100
8{7,2}	3-thiophenyl	Bn	97	98	26	97:3	0:100
8{7,3}	3-thiophenyl	allyl	83	98	24	89:11	0:100
8{7,6}	3-thiophenyl	2-(4-morpholino)ethyl	95	98	39	82:18	82:18

[a] Overall purity after the entire reaction sequence calculated from HPLC-UV (205–400 nm); [b] HPLC-UV after purification (205–400 nm); [c] Calculated from the ^{1}H-NMR spectrum of the purified product; [d] Sample heated at 120 °C for 30 min and measured after cooling to 27 °C; [e] Sample was shortly heated prior to NMR analysis to dissolve, NT—not tested.

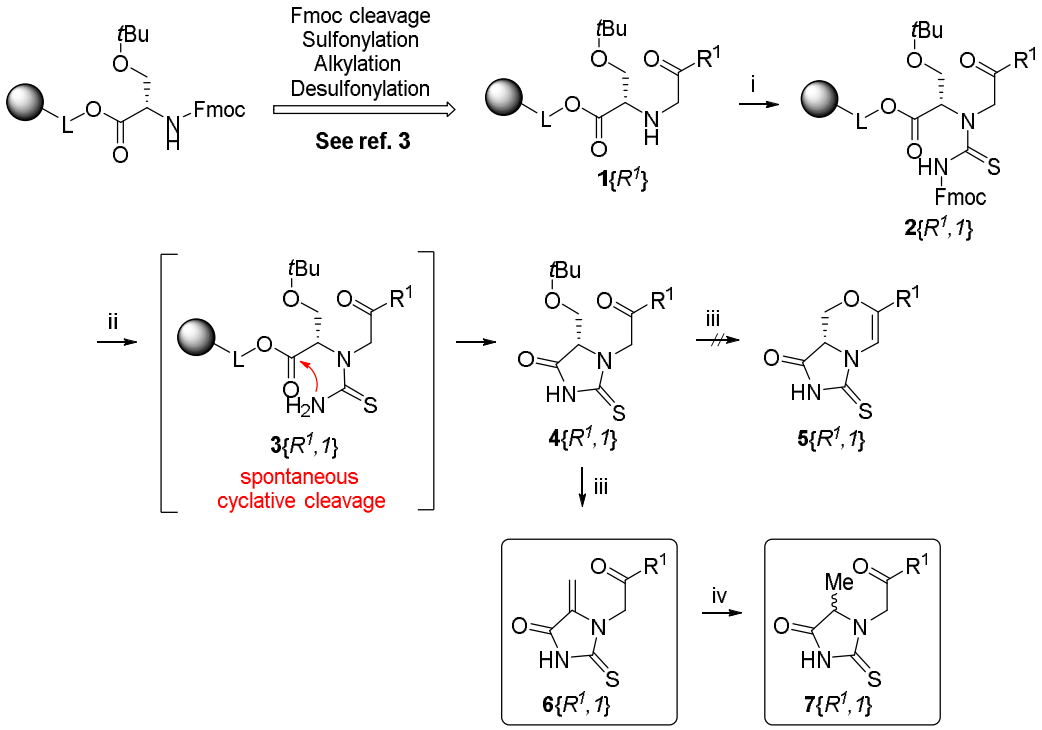

Scheme 2. Synthesis of 5-methylidene and 5-methyl-thiohydantoins. Reagents and conditions: (i) Fmoc-NCS, anhydrous THF, 2 h, rt; (ii) 35% piperidine/DMF, 24 h, rt (or 10% piperidine/DMF for derivative **2**{*4*,*1*}); (iii) neat TFA, 20 h, 35 °C; (iv) TFA/TES/DCM (5:3:5), 24 h, rt.

To test the applicability of the reaction sequence for *N*-substituted derivatives, we subsequently replaced Fmoc-NCS with alkyl-isothiocyanates. The reaction of **1**{*1*} with benzyl-isothiocyanate yielded the corresponding *N*-benzyl-thiourea **2**{*1,2*} (see Scheme 3). In contrast to intermediates **3**{R^1,*1*}, the immobilized *N*-benzyl-thiourea **2**{*1,2*} did not undergo the cyclative cleavage and trifluoroacetic acid (TFA) was used to release the compound from the resin. Further exposure to TFA under an elevated temperature led to a cyclization reaction. Although the mass spectrometry data corresponded to the expected thiohydantoin-dihydrooxazine derivative (see Scheme 3), the careful structural NMR elucidation of the isolated compound revealed that the scaffold was not formed. The cyclization to imidazole-2-thione took place followed by the dehydration and ring closure, which yielded an imidazo[2,1-*b*]thiazol-4-ium derivative **8**{*1,2*}. The product was obtained in an overall crude purity of 80% and overall yield of 53% (after semipreparative HPLC purification).

We further tested how applicable the reaction sequence is for various α-bromoketones and isothiocyanates. Structurally diverse building blocks (see Figure 1) with electron-donating and electron-withdrawing substituents were successfully used to prepare key intermediates **2**{R^1,*2*−*6*}. The reaction time was dependent on the reactivity of the used isothiocyanate. For instance, in the case of resin-bound compounds **2**{R^1,*2*}, which were prepared from benzyl isothiocyanate, the formation of the corresponding thioureas was relatively fast and the reaction time was only 20 h. However, the reaction with cyclohexylmethyl isothiocyanate required noticeably longer to reach quantitative conversion (see supplementary materials for more details). The subsequent TFA-mediated cyclization was also dependent on the type of *N*-substituent, and for allyl derivatives **8**{R^1,*3*}, the reaction time had to be extended from 20 h to 48 h. In total, 16 final compounds were synthesized by combining different α-bromoketones and isothiocyanates (see Table 1 for the list of products). The desired products were obtained and they had very good to excellent overall crude purities of 69% to 97% and good overall yields of 17% to 59%.

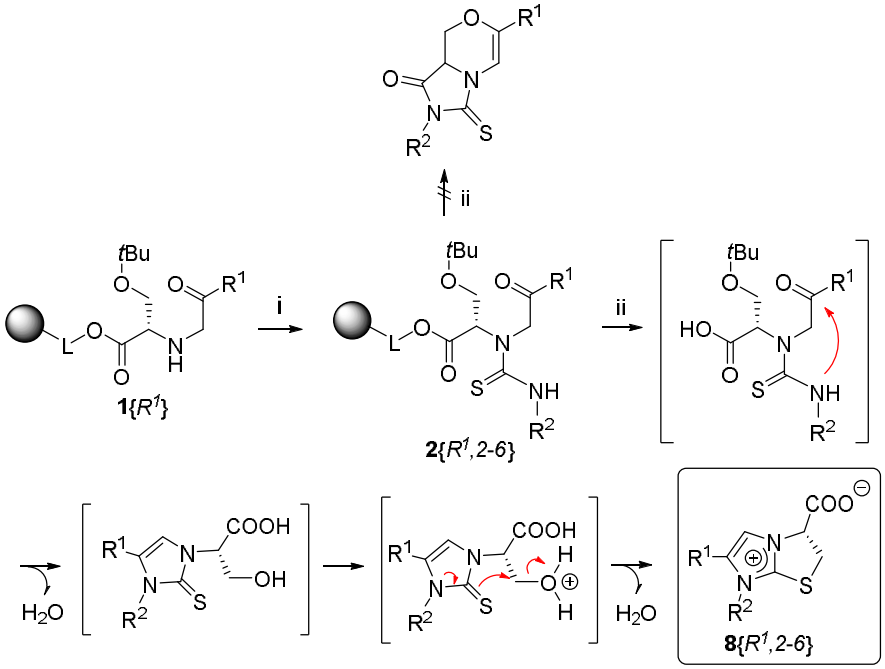

Scheme 3. Synthesis and applicability of *N*-substituted immobilized thioureas. Reagents and conditions: (i) R^2-NCS, anhydrous THF, 44 h, rt (or 20 h for derivatives 2{R^1,*2*} and 64 h for derivatives 2{R^1,*5*}); (ii) (a) neat TFA, 80 °C, 20 h (or 48 h for derivatives 2{R^1,*3*}), (b) evaporation of TFA, (c) reverse-phase HPLC purification using ammonium acetate buffer, (d) freeze-drying.

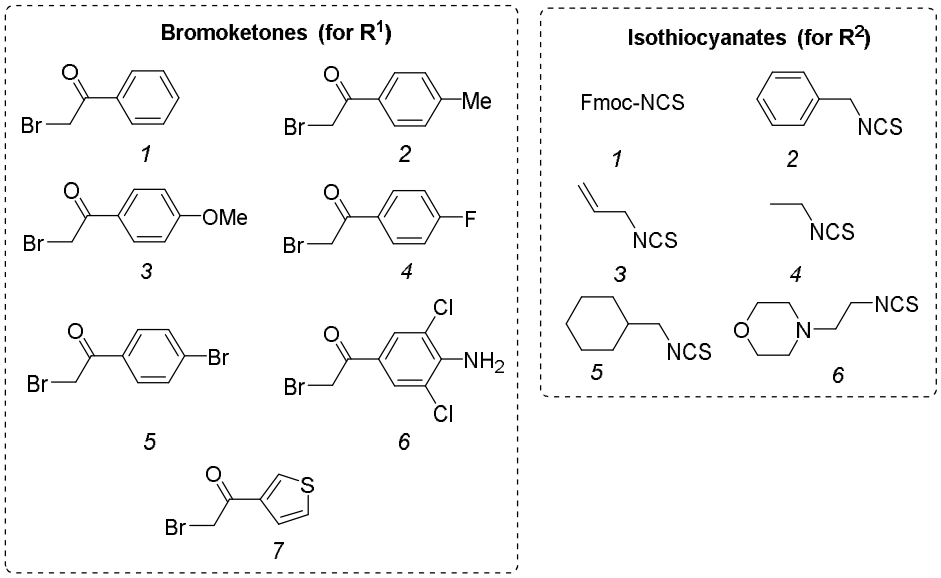

Figure 1. List of successfully tested building blocks.

When semipreparative HPLC purified compounds **8**{R^1,R^2} were submitted to NMR analysis in deuterated DMSO. ^{1}H-NMR spectra of some derivatives showed the presence of impurity in quantities up to 18%. Compound **8**{*3*,*3*}, which was synthesized from allyl isothiocyanate (16% of impurity detected), was subjected to detailed NMR characterization. The data indicated ring opening may have led to the formation of **9**{*3*,*3*} as the corresponding impurity (see Figure 2).

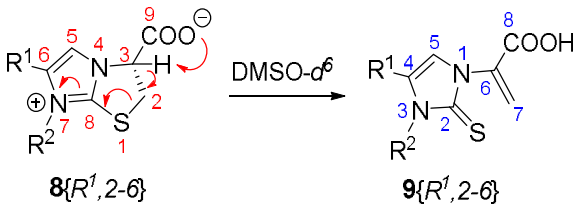

Figure 2. Isomerization of imidazo[2,1-b]thiazol-4-iums to imidazole-2-thiones.

To prove the structure, **8**{*3*,*3*} was analyzed using gradual increase temperature ^{1}H-NMR. Elevated temperatures led to a gradual increase in the content of the minor compound from 16% to 43% (80 °C) and 84% (100 °C). A nearly full conversion (97%) to the side product was observed at 120 °C. Cooling the sample to room temperature did not change the content of the new product. HPLC-MS analysis of the isolated compound confirmed its molecular weight was identical to that of the original product, which supported the putative formation of compound **9**{*3*,*3*} (see Figure 2). Further NMR investigations of both compounds (**8**{*3*,*3*} and **9**{*3*,*3*}) using 2D experiments confirmed their structures by identifying characteristic signals (see Figure 3).

In the case of compound **8**{*1*,*2*}, which was synthesized from benzyl isothiocyanate, the slow conversion to **9**{*1*,*2*} was observed at 27 °C in DMSO-d_6. The reaction quickly reached full conversion to **9**{*1*,*2*} at a higher temperature (see Supporting Information for more details). In most cases, the heating of derivatives **8**{R^1,*2*–*6*} for 30 min provided compounds **9**{R^1,*2*–*6*} as major products (71–100% as measured by ^{1}H NMR spectra; see Table 1). If the conversion to imidazole-2-thiones **9** was not quantitative, heating for a longer time was also tested and the ratio remained unchanged, but slow decomposition of products was observed. In just one case, heating of **8**{*7*,*6*} did not change the initial ratio of compounds even after a prolonged time of 17 h. In the cases of **8**{*1*,*4*}, **8**{*3*,*6*}, and **8**{*4*,*5*}, the solubilities of the purified samples in DMSO-d_6 at room temperature were limited. Therefore,

short heating to 50 °C was necessary to dissolve the material for analysis. For this reason, the NMR spectra of these products are significantly enriched in the compounds **9** (40% to 92%).

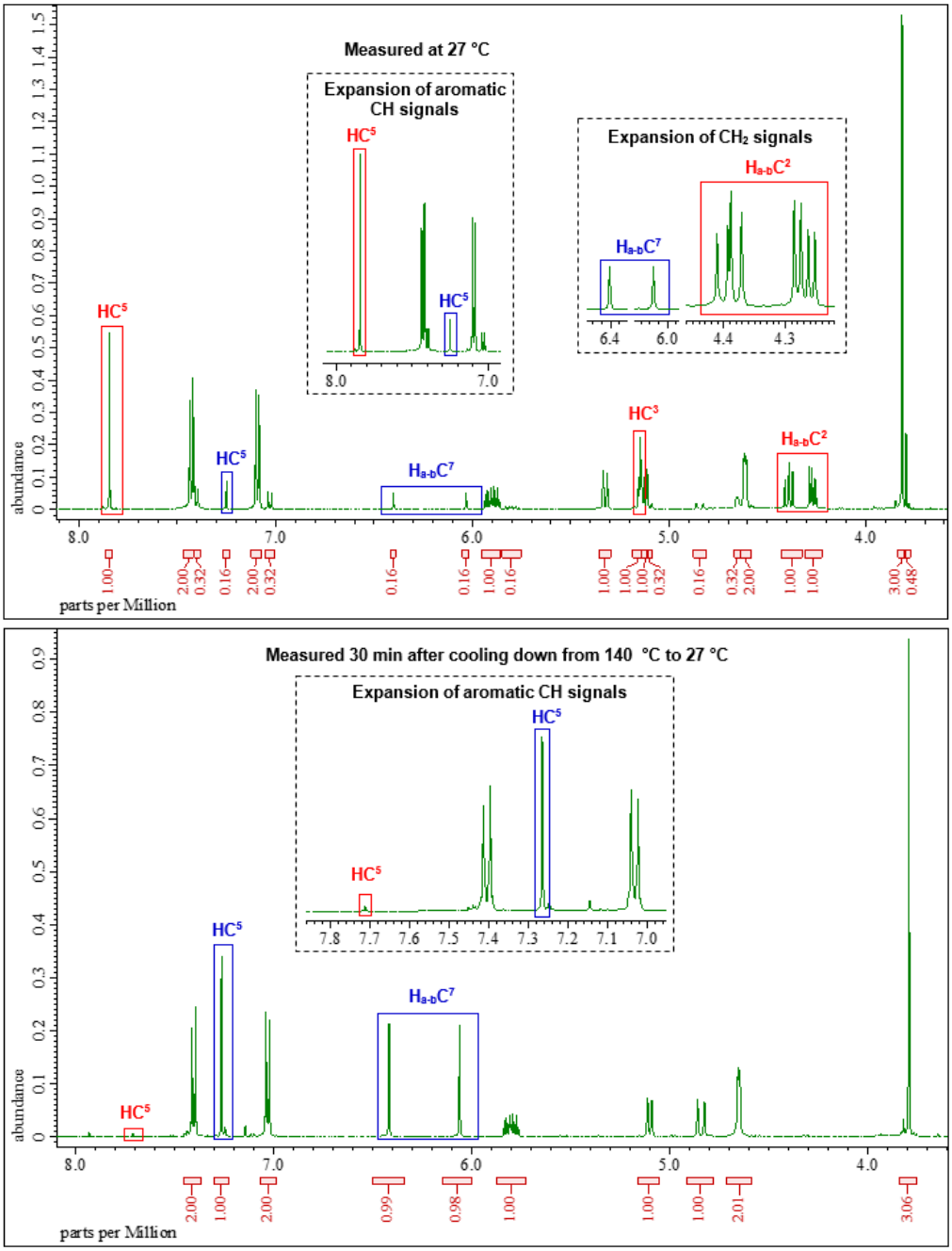

Figure 3. Characteristic signals of imidazo[2,1-*b*]thiazol-4-ium **8**{*3*,*3*} (highlighted in red) and imidazole-2-thione **9**{*3*,*3*} (highlighted in blue) (measured at 27 °C and after heating to 140 °C and cooling to 27 °C, respectively).

3. Conclusions

In conclusion, we have reported a convenient method for preparing novel thiohydantoins, imidazole-2-thiones, and imidazo[2,1-*b*]thiazol-4-iums using a solid-phase synthesis technique. Depending on the type of isothiocyanate and cleavage conditions used, different products were obtained. In total, we synthetized and fully characterized more than 36 original compounds, which were generally isolated and had very good overall purities and acceptable yields. The developed

strategy can be combined with previously reported protocols to synthesize different heterocycles starting from immobilized α-acylamino ketones by using diversity-oriented reagent-based synthesis. Derivatives **7** and **9** represent Michael acceptors and can be considered potential inhibitors of various enzymes through the irreversible Michael addition reaction, which currently represents an area of growing interest in the field of drug discovery and development [27–29].

Supplementary Materials: The following are available online: Experimental procedures and analytical data of products.

Acknowledgments: The authors are grateful to project CZ.1.07/2.3.00/20.0009 from the European Social Fund, the National Program of Sustainability (project LO1304), and an internal grant from Palacký University (IGA_LF_2018_32 and IGA_PrF_2018_29).

Author Contributions: P.K. performed all synthetic experiments and characterization of compounds; M.M. and H.K. analyzed NMR data and verified the target structures; M.S. supervised the project and wrote the paper.

Conflicts of Interest: The authors declare no conflict of interest. The founding sponsors had no role in the design of the study; in the collection, analyses, or interpretation of data; in the writing of the manuscript, and in the decision to publish the results.

References

1. Fülöpová, V.; Soural, M. Mining the Chemical Space: Application of 2/4-Nitrobenzenesulfonamides in Solid-Phase Synthesis. *ACS Comb. Sci.* **2015**, *17*, 570–591. [CrossRef] [PubMed]
2. Králová, P.; Fülöpová, V.; Maloň, M.; Volná, T.; Popa, I.; Soural, M. Stereoselective Polymer-Supported Synthesis of Morpholine- and Thiomorpholine-3-Carboxylic Acid Derivatives. *ACS Comb. Sci.* **2017**, *19*, 173–180. [CrossRef] [PubMed]
3. Pudelová, N.; Krchňák, V. Multiplicity of Diverse Heterocycles from Polymer-Supported α-Acylamino Ketones. *J. Comb. Chem.* **2009**, *11*, 851–859. [CrossRef] [PubMed]
4. Fülöpová, V.; Krchňák, V. Solid-Phase Synthesis of Trisubstituted 2,5-Dihydrobenzo[*f*][1,2,5]thiadiazepine 1,1-Dioxide Derivatives. *ACS Comb. Sci.* **2014**, *16*, 412–420. [CrossRef] [PubMed]
5. Králová, P.; Maloň, M.; Volná, T.; Ručilová, V.; Soural, M. Polymer-Supported Stereoselective Synthesis of Benzoxazino[4,3-*b*][1,2,5]thiadiazepinone 6,6-Dioxides. *ACS Comb. Sci.* **2017**, *19*, 670–674. [CrossRef] [PubMed]
6. Králová, P.; Maloň, M.; Soural, M. Stereoselective Synthesis of Benzo[*e*][1,4]oxazino[4,3-*a*][1,4]diazepine-6, 12-Diones with Two Diversity Positions. *ACS Comb. Sci.* **2017**, *19*, 770–774. [CrossRef] [PubMed]
7. Ručilová, V.; Králová, P.; Soural, M. Synthesis of Disubstituted Pyrazino-Oxazine Derivatives with Controlled Stereochemistry. *Eur. J. Org. Chem.* **2017**, *2017*, 7034–7039. [CrossRef]
8. Feldman, D.L. IBM PC Compatible Multi-Chip Module. U.S. Patent 5,742,844, 16 January 1998.
9. Blanc, M.; Cussac, M.; Boucherle, A.; Leclerc, G. Synthesis and Immunomodulating Activity of 1-Amino-2-Thiohydantoin Derivatives. *Eur. J. Med. Chem.* **1992**, *27*, 839–843. [CrossRef]
10. Janos, M.; Janos, E.; Sandor, H.; Tibor, T. Preparation and Fungicidal Activity of 5-Substituted Hydantoins and Their 2-Thio Analogs. *J. Agric. Food. Chem.* **1993**, *41*, 148–152.
11. Sauli, M. Fungicidal Hydantoins Derivatives. U.S. Patent 3,823,240, 9 July 1974.
12. Łażewska, D.; Maludziński, P.; Szymańska, E.; Kieć-Kononowicz, K. The Lipophilicity Estimation of 5-Arylidene Derivatives of (2-Thio)hydantoin with Antimycobacterial Activity. *Biomed. Chromatogr.* **2007**, *21*, 291–298. [CrossRef] [PubMed]
13. Santos, L.C.; Uchōa, F.T.; Canas, A.R.P.A.; Sousa, I.A.; Moura, R.O.; Lima, M.C.A.; Galdio, S.L.; Pitta, I.R.; Barbe, J. Synthesis and Anti-inflammatory Activity of New Thiazolidine-2,4-diones, 4-thioxothiazolidinones and 2-thioxoimidazolidinones. *Heterocycl. Commun.* **2005**, *11*, 121–128. [CrossRef]
14. Knoefel, P.K.; Lehmann, G. The Anticonvulsant Action of Diphenyl Hydantoin and Some Related Compounds. *J. Pharmacol. Exp. Ther.* **1942**, *76*, 194–201.
15. Habib, M.M.W.; Abdelfattah, M.A.O.; Abadi, A.H. Design and Synthesis of Novel Phenylpiperazine Derivatives as Potential Anticonvulsant Agents. *Arch. Pharm.* **2015**, *348*, 868–874. [CrossRef] [PubMed]
16. Havera, H.J.; Goshen, G. 3-Substituted-5-Phenyl-5-Pyridyl Hydantoins. U.S. Patent 3,994,904, 30 November 1976.
17. Tolman, R.L.; Gamsey, S.; Mehta, S.; Pongracz, K. Telomerase Inhibitors and Methods of Their Use. U.S. Patent 6,518,268, 11 February 2003.

18. Rodgers, T.R.; LaMontagne, M.P.; Markovac, A.; Ash, A.B. Hydantoins as Antitumor Agents. *J. Med. Chem.* **1977**, *20*, 591–594. [CrossRef] [PubMed]
19. Bell, C.; Conklin, G.L. Hydantoin Compounds and Methods of Preparation. U.S. Patent 3,452,041, 24 June 1969.
20. Kodama, S. Thiocarbimide Reaction. *J. Tokyo Chem. Soc.* **1920**, *41*, 951–965.
21. Reyes, S.; Burgess, K. On Formation of Thiohydantoins from Amino Acids under Acylation Conditions. *J. Org. Chem.* **2006**, *71*, 2507–2509. [CrossRef] [PubMed]
22. Johnson, T.B.; Renfrew, A.G. Reseaches on Hydantoins. XLIII. Synthesis of the Polypeptide-Hydantoin: "Hydantoin-3-Acetic Acid". *J. Am. Chem. Soc.* **1925**, *47*, 240–245. [CrossRef]
23. Siddiqui, I.R.; Yadav, S.; Shamim, S.; Shireen; Waseem, M.A.; Srivastava, A.; Srivastava, A. Solid-Supported Cyclocondensation of Arylglyoxal on Ribosylthiourea under Microwave Activation: A Novel and Efficient Synthesis of *N*-Glycosylated-2-Thiohydantoins. *Bull. Chem. Soc. Jpn.* **2014**, *87*, 506–510. [CrossRef]
24. Dadiboyena, S.; Nefzi, A. Parallel Solid-Phase Synthesis of Disubstituted 3-(1*H*-Benzo[d]imidazol-2-yl) imidazolidine-2,4-Diones and 3-(1*H*-Benzo[d]imidazol-2-yl)-2-Thioxoimidazolidin-4-Ones. *Tetrahedron Lett.* **2011**, *52*, 7030–7033. [CrossRef] [PubMed]
25. Jullian, M.; Hernandez, A.; Maurras, A.; Puget, K.; Amblard, M.; Martinez, J.; Subra, G. N-Terminus FITC Labeling of Peptides on Solid Support: The Truth behind the Spacer. *Tetrahedron Lett.* **2009**, *50*, 260–263. [CrossRef]
26. Lin, M.-J.; Sun, C.-M. Microwave-Assisted Traceless Synthesis of Thiohydantoin. *Tetrahedron Lett.* **2003**, *44*, 8739–8742. [CrossRef]
27. Wang, L.; Zhao, J.; Yao, Y.; Wang, C.; Zhang, J.; Shu, X.; Sun, X.; Li, Y.; Liu, K.; Yuan, H. Covalent binding design strategy: A prospective method for discovery of potent targeted anticancer agents. *Eur. J. Med. Chem.* **2017**, *142*, 493–505. [CrossRef] [PubMed]
28. De Cesco, S.; Kurian, J.; Dufresne, C.; Mittermaier, A.K.; Moitessier, N. Covalent inhibitors design and discovery. *Eur. J. Med. Chem.* **2017**, *138*, 96–114. [CrossRef] [PubMed]
29. Lagoutte, R.; Patouret, R.; Winssinger, N. Covalent inhibitors: An opportunity for rational target selectivity. *Curr. Opinion Chem. Biol.* **2017**, *39*, 54–63. [CrossRef] [PubMed]

Sample Availability: Samples of the compounds are not available from the authors.

ACS Combinatorial Science

Letter

Cite This: ACS Comb. Sci. 2018, 20, 467−471

pubs.acs.org/acscombsci

Synthesis of 2-Alkylsulfonyl-imidazoles with Three Diversity Positions from Immobilized α-Acylamino Ketones

Petra Králová[†] and Miroslav Soural*[,‡]

[†]Department of Organic Chemistry, Faculty of Science, Palacký University, 771 46 Olomouc, Czech Republic

[‡]Institute of Molecular and Translational Medicine, Faculty of Medicine and Dentistry,Palacký University, Hněvotínská 5, 779 00, Olomouc, Czech Republic

Supporting Information

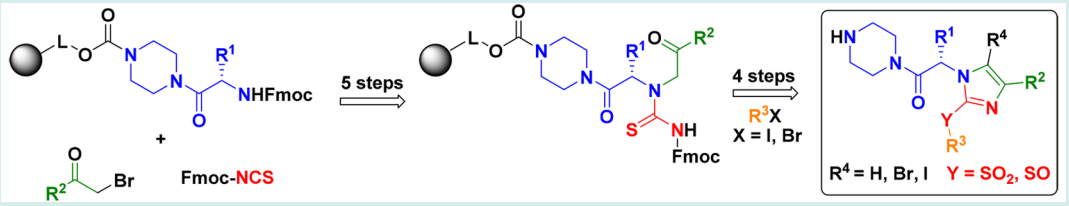

ABSTRACT: The synthesis of novel imidazole derivatives via immobilized α-acylamino ketones is reported in this article. The key intermediates were prepared from the Wang-piperazine resin-supported Fmoc-amino acids. After their sulfonylation with 4-nitrobenzenesulfonyl chloride (4-Nos-Cl), followed by alkylation with α-bromoketones and cleavage of Nos group, the resulting α-acylamino ketones were reacted with Fmoc-isothiocyanate. The corresponding Fmoc-thioureas were subjected to the Fmoc-cleavage and spontaneous ring-closure to imidazole scaffold. The resulting imidazole-thiones were alkylated with alkyl halides and oxidized using meta-chloroperbenzoic acid (*m*CPBA). Trifluoroacetic acid (TFA)-mediated cleavage yielded the corresponding trisubstituted 2-alkylsulfonyl imidazoles in good crude purity and acceptable overall yields. In the case of sulfides, prepared from alkyl bromides, the unexpected products brominated at the C^4 position of the imidazole were obtained.

KEYWORDS: *amino acid, bromoketone, imidazole, solid-phase synthesis*

α-Acylamino ketones are multireactive compounds readily available from primary amines and α-bromoketones. These versatile intermediates are applicable in the preparation of different nitrogen-containing heterocycles using traditional solution-phase[1−6] or solid-phase syntheses.[7−14] In the past decade, particular attention has been paid to α-acylamino ketones prepared from immobilized amino acids alkylated with bromoketones via activation with 2- or 4-nitrobenzenesulfonyl chloride.[15] In 2009, Krchnak et al. used such polymer-supported α-acylamino ketones for the reagent-based, diversity-oriented synthesis of morpholin-3-ones, pyrrol-2-ones, pyrazin-2-ones, imidazo-triazepines, 1*H*-imidazoles, and β-lactams.[7] More recently, the same intermediates have been used to prepare benzodiazepin-5-ones,[8] and serine-based Wang resin-supported α-acylamino ketones were used in the synthesis of chiral morpholines[9] and their derivatives bearing fused [6 + 6][10,11] or [7 + 6][12,13] heterocyclic scaffolds. The latest article in this field was devoted to the synthesis of 2-thiohydantoins, imidazo[2,1-*b*]thiazol-4-iums, and imidazole-2-thiones.[14] Inspired by the diversity of heterocycles accessible from polymer-supported α-acylamino ketones,[15] we suggested their use for the convenient synthesis of 2-alkylsulfonyl-imidazoles derived from natural amino acids. To avoid the spontaneous formation of thiohydantoins that has been reported previously,[14] the starting amino acids were not immobilized directly on Wang resin via the ester functionality, and instead, Wang-piperazine resin[16] was used to avoid the unwanted cyclative cleavage during the reaction sequence.

It is worth mentioning that 2-alkylsulfonyl-imidazoles and related compounds are pharmacologically attractive agents with diverse biological effects.[17−20] These derivatives serve as biocidal,[21] anti-HIV,[22] antibacterial,[23] antitrichomonal,[24] antiviral[25] and anti-inflammatory agents,[26] and selective COX-2 inhibitors[26] (see Figure 1 for representative examples). On the other hand, the target 2-alkylsulfonyl-imidazoles derived from natural amino acids are an unexplored class of derivatives.

The proposed synthetic route (see Scheme 1) was tested using a combination of Wang-piperazine resin-immobilized Fmoc-Ala-OH **1**(*1*), phenylethan-1-one, and methyl iodide. The key intermediate, α-acylamino ketone **2**{*1,1*}, was synthesized in three steps according to a previously reported protocol.[9] After the reaction of **2**{*1,1*} with Fmoc-isothiocyanate, the Fmoc protecting group was removed to afford imidazole-2-thione **4**{*1,1*}. The *S*-alkylation of this compound with methyl iodide yielded sulfide **5**{*1,1*}, which upon oxidation with *m*CPBA, followed by TFA-mediated cleavage from the resin, afforded final sulfone **7**{*1,1,1*} in an excellent crude purity (95%, measured by LC-UV traces at 205−400 nm).

To evaluate the applicability of this synthetic methodology for parallel/combinatorial synthesis of a library of target

Received: May 25, 2018
Revised: June 28, 2018
Published: July 3, 2018

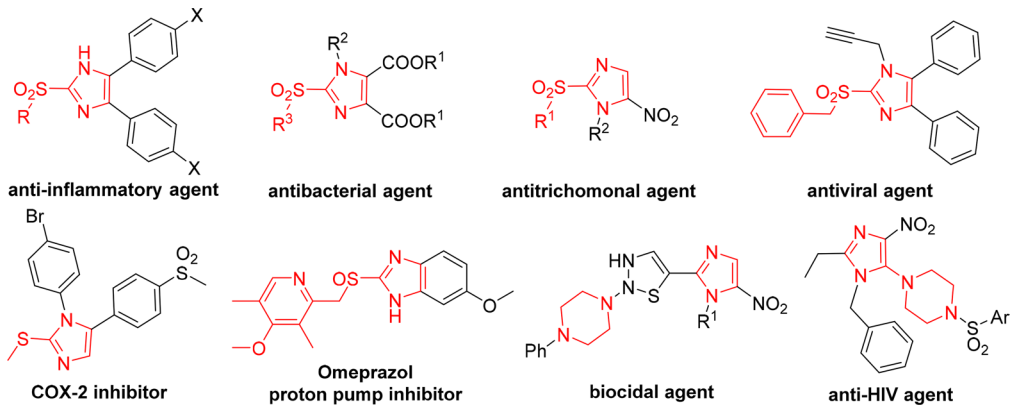

Figure 1. Pharmacologically relevant compounds structurally related to the target derivatives.

Scheme 1. Synthetic Pathway Leading to Target Imidazoles 7−10

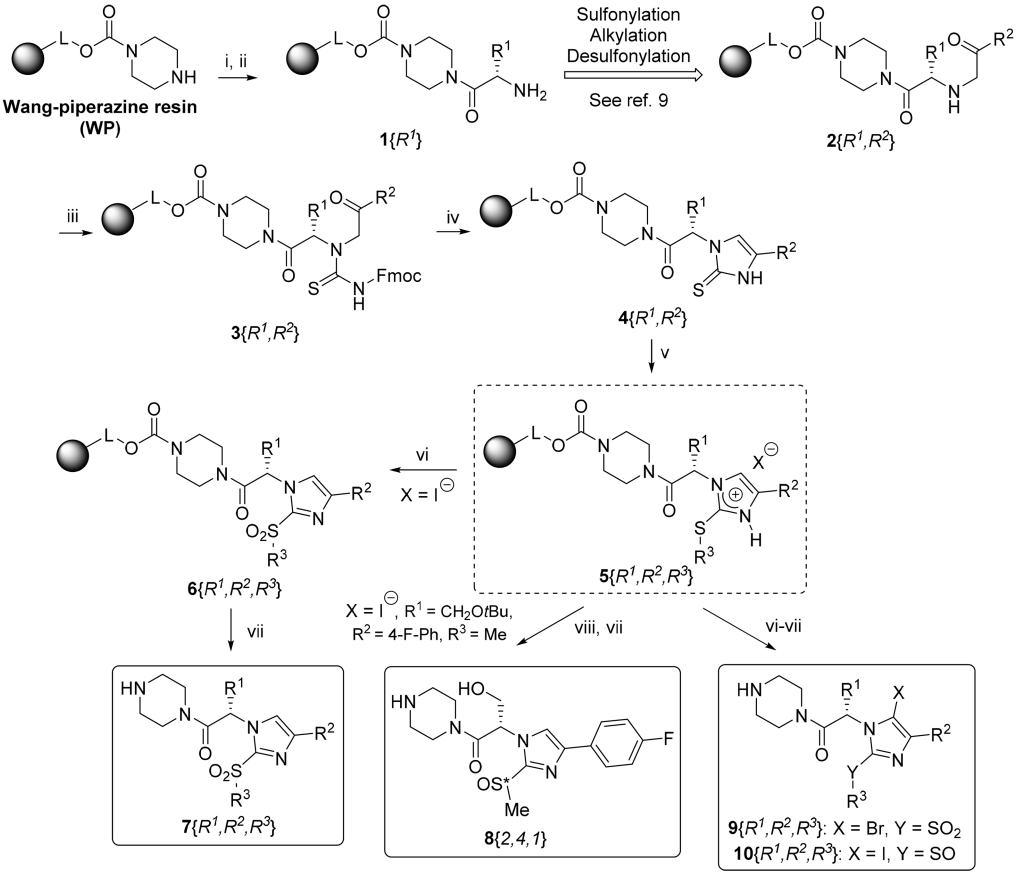

[a]Reagents and conditions: (i) Fmoc-AAs, HOBt, DIC, DCM, DMF, 24 h, rt; (ii) 50% piperidine/DMF, 30 min, rt; (iii) Fmoc-NCS, anhydrous THF, 2 h, rt; (iv) 50% piperidine/DMF, 15 min, rt; (v) R^3X(X = 1, Br), anhydrous DCM, 2 h, rt; (vi) *m*CPBA, anhydrous DCM, 5 h, rt; (vii) neat TFA, on, rt; (viii) *m*CPBA, anhydrous DCM, 30 min, rt.

compounds, different Fmoc-amino acids with functionalized side chains, bromoketones with electron-donating and electron-withdrawing substituents and various alkylating agents were tested (see Figure 2).

The preparation of α-acylamino ketones **2**{R^1,R^2} was successful for all building blocks in the various tested combinations. After the formation of intermediates **4**{R^1,R^2}, the alkylation of these compounds was tested with alkyl iodides (ethyl iodoacetate, benzyl iodide, phenacyl iodide, and allyl iodide) and alkyl bromides (ethyl bromoacetate, benzyl bromide, and phenacyl bromide). The resulting sulfides **5**{R^1,R^2,R^3} were obtained in good crude purities (57−94%, measured by LC−UV traces at 205−400 nm) with exception of phenacyl iodide, which afforded a mixture of unknown products. Subsequent oxidation with *m*CPBA and TFA-mediated cyclization furnished sulfones 7{R^1,R^2,R^3} in 55−97% crude purities and 10−36% overall yields (see Table 2); however, the reaction outcome was dependent on the substitution of the starting material. In the case of intermediate **5**{*2,4,1*}, we managed to isolate corresponding sulfoxide **8**{*2,4,1*} after adjusting the reaction time to only 30 min. The purified product was obtained as a mixture of two inseparable diastereoisomers in a

DOI: 10.1021/acscombsci.8b00075
ACS Comb. Sci. 2018, 20, 467−471

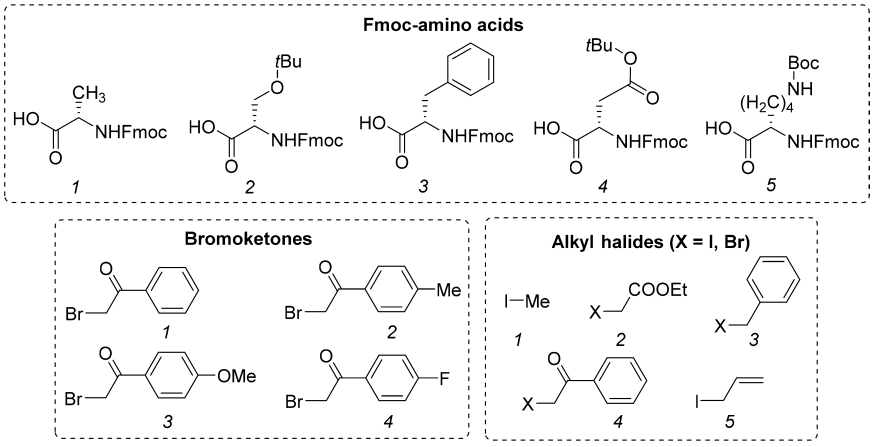

Figure 2. List of tested building blocks to obtain different R^1, R^2, and R^3 substituents.

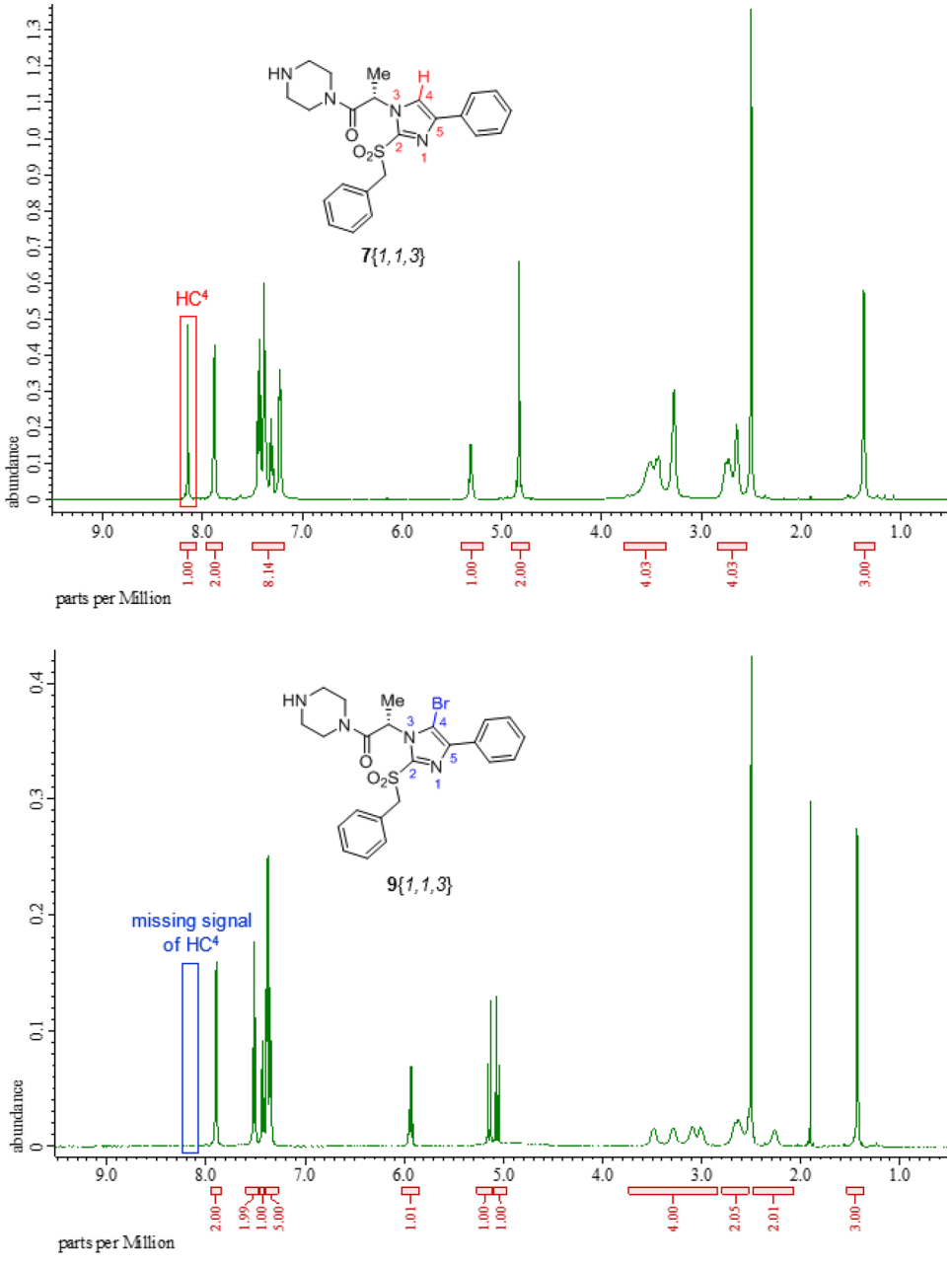

Figure 3. Disappearance of the HC^4 signal of imidazole 7{*1,1,3*} after oxidation.

DOI: 10.1021/acscombsci.8b00075
ACS Comb. Sci. 2018, 20, 467−471

68:32 ratio (calculated from the ^{1}H NMR spectrum). Prolonged oxidation (5 h) furnished corresponding sulfone **6**{*2,4,1*}. Similarly, oxidation and cleavage of **5**{*1,3,2*} yielded the iodinated sulfoxide **10**{*1,3,2*} (see later in the text). In the case of the other intermediates, the isolation of the sulfoxide was impossible due to their immediate oxidation in the presence of excess of *m*CPBA.

The oxidation of sulfide **5**{*1,1,3*}, prepared from benzyl bromide, resulted in expected sulfone **6**{*1,1,3*} along with a byproduct with a molecular weight corresponding to the oxidized and brominated product **9**{*1,1,3*}. The byproduct was isolated and investigated with NMR spectroscopy. The structural elucidation indicated that bromination took place on the imidazole scaffold based on the disappearance of the corresponding aromatic signal HC^4 (see Figure 3).

The similar behavior was observed using ethyl bromoacetate and phenacyl bromide; the corresponding brominated products were obtained. The ratios of sulfones **7**{R^1,R^2,R^3} and brominated analogues **9**{R^1,R^2,R^3} varied depending on the overall substitution; however, no systematic relationship was observed (see Table 1).

The unexpected bromination can be explained by the formation of imidazole-hydrobromides at the stage of intermediates **5**{R^1,R^2,R^3} as a result of the generation of HBr and its capture after the alkylation step (see Scheme 1, step v). Subsequent treatment with perbenzoic acid may oxidize the bromide anion followed by bromination of the imidazole scaffold by radical mechanism. The crucial role of *m*CPBA is evident from the cleavage and analysis of sulfides **5**{R^1,R^2,R^3}, which showed no trace of the brominated sulfides.

In the case of alkyl iodides, the halogenation of imidazole scaffold was generally not observed with the exception of intermediate **5**{*1,3,2*}, which afforded the iodinated sulfoxide **10**{*1,3,2*} (see Scheme 1 and Supporting Information for more details).

Table 1. Ratios of 7{R^1,R^2,R^3} and 9{R^1,R^2,R^3} Depended on R$^{1-3}$

starting cmpd	R^1	R^2	R^3	ratios 7:9[a]
5{*1,1,3*}	Me	Ph	Bn	0:1
5{*1,2,4*}	Me	4-Me-Ph	CH_2COPh	1:2
5{*2,1,2*}	CH_2OH	Ph	CH_2COOEt	1:1
5{*2,2,2*}	CH_2OH	4-Me-Ph	CH_2COOEt	0:1
5{*2,2,4*}	CH_2OH	4-Me-Ph	CH_2COPh	1:2
5{*3,1,3*}	CH_2Ph	Ph	Bn	1:2
5{*3,1,4*}	CH_2Ph	Ph	CH_2COPh	1:1
5{*5,1,3*}	$(CH_2)_4NH_2$	Ph	Bn	1:3

[a]Calculated from HPLC-UV-MS (205−400 nm).

Table 2. List of Synthesized and Fully Characterized Compounds 7−11

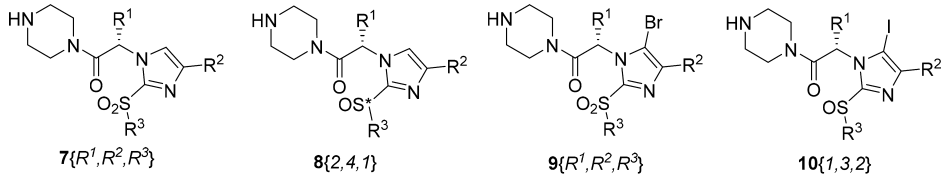

cmpd	R^1	R^2	R^3	crude purity [%][a]	final purity [%][b]	overall yield [%][c]
7{*1,1,1*}	Me	Ph	Me	75	98	10
7{*1,1,3*}	Me	Ph	Bn	84	99	14
7{*2,1,1*}	CH_2OH	Ph	Me	94	98	36
7{*2,2,5*}	CH_2OH	4-Me-Ph	allyl	88	98	26
7{*2,2,3*}	CH_2OH	4-Me-Ph	Bn	74	99	10
7{*2,3,1*}	CH_2OH	4-MeO-Ph	Me	72	98	23
7{*2,4,1*}	CH_2OH	4-F-Ph	Me	81	97	21
7{*3,1,1*}	CH_2Ph	Ph	Me	95	99	20
7{*3,4,2*}	CH_2Ph	4-F-Ph	CH_2COOEt	69	99	17
7{*3,4,3*}	CH_2Ph	4-F-Ph	Bn	65	99	16
7{*4,1,1*}	CH_2COOH	Ph	Me	71	99	13
7{*4,4,3*}	CH_2COOH	4-F-Ph	Bn	63	98	22
7{*5,1,1*}	$(CH_2)_4NH_2$	Ph	Me	87	99	15
8{*2,4,1*}	CH_2OH	4-F-Ph	Me	65	99	12
9{*1,1,3*}	Me	Ph	Bn	76	99	15
9{*3,1,2*}	CH_2Ph	Ph	CH_2COOEt	58	98	11
9{*5,1,3*}	$(CH_2)_4NH_2$	Ph	Bn	80	99	16
10{*1,3,2*}	Me	4-MeO-Ph	CH_2COOEt	63	99	14
11{*2,1,4*}	CH_2OH	Ph	CH_2COPh	82	99	16
11{*4,1,4*}	CH_2COOH	Ph	CH_2COPh	75	99	11

[a]Overall purity after the entire reaction sequence calculated from the HPLC-UV chromatogram (205−400 nm). [b]Purity determined from the HPLC-UV chromatogram after purification (205−400 nm). [c]Calculated from the ^{1}H NMR spectrum of the purified product (see Supporting Information for more details).

DOI: 10.1021/acscombsci.8b00075
ACS Comb. Sci. 2018, 20, 467−471

The product was obtained in good crude purity 63% and 14% yield as a mixture of two inseparable diastereoisomers in a ratio 86:14 (calculated from the ^{1}H NMR spectrum).

Finally, we tested the possible diversification of the amidic moiety. Surprisingly, when the Wang-piperazine resin was changed to Wang-ethylenediamine resin, the reaction pathway failed at the stage of Fmoc-thiourea formation. Similar results were obtained when Rink amide resin and BAL resin-immobilized secondary amines, respectively, were used as the starting materials.

In conclusion, we developed a simple synthesis of 2-alkylsulfonyl-imidazoles with three positions available for diversification using immobilized α-acylamino ketones as the key intermediates. The methodology can be used for combinatorial synthesis of chemical library using a large number of readily available building blocks. In total, we synthesized and fully characterized 20 representative compounds. Additionally, the C^4 halogenated products can be utilized for further diversification of the target scaffold using metal-catalyzed C−C couplings.

■ ASSOCIATED CONTENT

Supporting Information

The Supporting Information is available free of charge on the ACS Publications website at DOI: 10.1021/acscombsci.8b00075.

Details of experimental, synthetic, and analytical procedures, along with spectroscopic data for synthesized compounds (PDF)

■ AUTHOR INFORMATION

Corresponding Author

*E-mail: miroslav.soural@upol.cz.

ORCID

Miroslav Soural: 0000-0001-7288-8617

Notes

The authors declare no competing financial interest.

■ ACKNOWLEDGMENTS

The authors are grateful to the National Program of Sustainability (project LO1304) and an internal grants from Palacký University IGA_PrF_2018_29 and IGA_LF_2018_032.

■ REFERENCES

(1) Kumar, D.; Sundaree, S.; Patel, G.; Rao, V. S. A Facile Synthesis of Naturally Occurring 5-(3-Indolyl)oxazoles. *Tetrahedron Lett.* **2008**, *49* (5), 867−869.

(2) Bigot, A.; Blythe, J.; Pandya, C.; Wagner, T.; Loiseleur, O. DAST-Mediated Cyclization of α,α-Disubstituted-α-Acylaminoketones: Efficient and Divergent Synthesis of Unprecedented Heterocycles. *Org. Lett.* **2011**, *13* (2), 192−195.

(3) Popovici, D.; Maior, O.; Schiketanz, A. R.; Balaban, A. T. Aminoketone, Oxazole and Thiazole Synthesis Part XV. Acylaminoacylation with the Azlactone of Para-Benzoylhippuric Acid and Derived 2,5-Diaryloxazoles. *Analele Univ. Bucuresti, Chim.* **2000**, *9*, 75−81.

(4) Koshelev, V. M.; Vasil'ev, N. V.; Gontar, A. F. Preparation of Methyloxazoles by Cyclization of α-Acylaminoketones. SU1648947A1, 15 May 1991.

(5) Metze, R. 1,2,4-Triazines. VIII. A New Synthesis of the Fluorescent 1,2,4-Triazines. *Chem. Ber.* **1958**, *91*, 1863−1866.

(6) Anselmi, C.; Camparini, A.; Scotton, M. A One-Step Conversion of *N*-Acylaminoketones into 5-Alkylidene-3-Pyrrolin-2-Ones. *J. Heterocycl. Chem.* **1983**, *20* (3), 687−689.

(7) Pudelová, N.; Krchňák, V. Multiplicity of Diverse Heterocycles from Polymer-Supported α-Acylamino Ketones. *J. Comb. Chem.* **2009**, *11* (5), 851−859.

(8) Fülöpová, V.; Gucký, T.; Grepl, M.; Soural, M. Solid-Phase Synthesis of Trisubstituted Benzo[1,4]-Diazepin-5-One Derivatives. *ACS Comb. Sci.* **2012**, *14* (12), 651−656.

(9) Králová, P.; Fülöpová, V.; Maloň, M.; Volná, T.; Popa, I.; Soural, M. Stereoselective Polymer-Supported Synthesis of Morpholine- and Thiomorpholine-3-Carboxylic Acid Derivatives. *ACS Comb. Sci.* **2017**, *19* (3), 173−180.

(10) Ručilová, V.; Králová, P.; Soural, M. Synthesis of Disubstituted Pyrazino-Oxazine Derivatives with Controlled Stereochemistry. *Eur. J. Org. Chem.* **2017**, *2017* (47), 7034−7039.

(11) Ručilová, V.; Maloň, M.; Soural, M. Use of Triethylsilane for Directed Enantioselective Reduction of Olefines: Synthesis of Pyrazino[2,1-c][1,4]oxazine-6,9-Diones with Full Control of the Absolute Configuration. *Eur. J. Org. Chem.* **2018**, *2018* (4), 564−570.

(12) Králová, P.; Maloň, M.; Volná, T.; Ručilová, V.; Soural, M. Polymer-Supported Stereoselective Synthesis of Benzoxazino[4,3-b][1,2,5]thiadiazepinone 6,6-Dioxides. *ACS Comb. Sci.* **2017**, *19* (10), 670−674.

(13) Králová, P.; Maloň, M.; Soural, M. Stereoselective Synthesis of Benzo[e][1,4]oxazino[4,3-a][1,4]diazepine-6,12-Diones with Two Diversity Positions. *ACS Comb. Sci.* **2017**, *19* (12), 770−774.

(14) Králová, P.; Maloň, M.; Koshino, H.; Soural, M. Convenient Synthesis of Thiohydantoins, Imidazole-2-Thiones and Imidazo[2,1-B]thiazol-4-Iums from Polymer-Supported α-Acylamino Ketones. *Molecules* **2018**, *23* (4), 976−984.

(15) Fülöpová, V.; Soural, M. Mining the Chemical Space: Application of 2/4-Nitrobenzenesulfonamides in Solid-Phase Synthesis. *ACS Comb. Sci.* **2015**, *17* (10), 570−591.

(16) Neagoie, C.; Krchňák, V. Piperazine Amide Linker for Cyclative Cleavage from Solid Support: Traceless Synthesis of Dihydroquinoxalin-2-Ones. *ACS Comb. Sci.* **2012**, *14* (7), 399−402.

(17) Braendstroem, A. E. Method for Synthesis of Omeprazole. WO9118895 A1, 12 December 1991.

(18) Rajesh, R.; Manikandan, A.; Sivakumar, A.; Ramasubbu, C.; Nagaraju, N. Substituted Methoxybenzyl-Sulfonyl-1H-Benzo[d]-imidazoles Evaluated as Effective H+/K+-ATPase Inhibitors and Anti-Ulcer Therapeutics. *Eur. J. Med. Chem.* **2017**, *139*, 454−460.

(19) Anand, K.; Wakode, S. Development of Drugs Based on Benzimidazole Heterocycle: Recent Advancement and Insights. *Int. J. Chem. Stud.* **2017**, *5*, 350−362.

(20) Shivaprasad, C. M.; Kumar, S. M.; Manjunath, B. C.; Swaroop, T. R.; Rangappa, K. S.; Lokanath, N. K. Synthesis and Structural Studies of 2-((3-Methyl-4-(2,2,2-Trifluoroethoxy)pyridin-2-Yl)-methylthio)-1-(Methylsulfonyl)-1H-Benzo[d]imidazole. *X-Ray Struct. Anal. Online* **2013**, *29* (12), 47−48.

(21) Berkelhammer, G.; Asato, G. Biocidal 5-Nitro-2-Imidazoles. ZA6802863, 12 December 1968.

(22) Al-Soud, Y. A.; Al-Masoudi, N. A.; Hassan, H. G.; De Clercq, E.; Pannecouque, C. Nitroimidazoles. V. Synthesis and Anti-HIV Evaluation of New 5-Substituted Piperazinyl-4-Nitroimidazole Derivatives. *Acta Pharm. (Zagreb, Croatia)* **2007**, *57* (4), 379−393.

(23) Suresh, M.; Lavanya, P.; Rao, C. V. Synthesis, Antibacterial, Antifungal and Antioxidant Activity Studies on 2-Benzylthio- and 2-Benzylsulfonyl-1H-Imidazoles. *Pharm. Lett.* **2010**, *2* (4), 393−402.

(24) Henry, D. W. 2-Sulfonyl- and 2-Cyano-5-Nitroimidazoles. US3341549, 12 September 1967.

(25) Moore, T. W.; Sana, K.; Yan, D.; Krumm, S. A.; Thepchatri, P.; Snyder, J. P.; Marengo, J.; Arrendale, R. F.; Prussia, A. J.; Natchus, M. G.; Liotta, D. C.; Plemper, R. K.; Sun, A. Synthesis and Metabolic Studies of Host-Directed Inhibitors for Antiviral Therapy. *ACS Med. Chem. Lett.* **2013**, *4* (8), 762−767.

(26) Assadieskandar, A.; Amirhamzeh, A.; Salehi, M.; Ozadali, K.; Ostad, S. N.; Shafiee, A.; Amini, M. Synthesis, Cyclooxygenase Inhibitory Effects, and Molecular Modeling Study of 4-Aryl-5-(4-(Methylsulfonyl)phenyl)-2-Alkylthio and 2-Alkylsulfonyl-1H-Imidazole Derivatives. *Bioorg. Med. Chem.* **2013**, *21* (8), 2355−2362.

DOI: 10.1021/acscombsci.8b00075
ACS Comb. Sci. 2018, 20, 467−471

JOC The Journal of Organic Chemistry Article
Cite This: J. Org. Chem. 2020, 85, 985−993 pubs.acs.org/joc

Rearrangement of Threonine- and Serine-Based *N*-(3-Phenylprop-2-yn-1-yl) Sulfonamides Yields Chiral Pyrrolidin-3-ones

Petra Králová,[†] Michal Maloň,[‡] Jiří Pospíšil,[†,§] and Miroslav Soural*[,†,∥]

[†]Department of Organic Chemistry, Faculty of Science, Palacký University, Tr. 17 Listopadu 12, 771 46 Olomouc, Czech Republic
[‡]JEOL (United Kingdom) Limited, JEOL House, Silver Court, Watchmead, Welwyn Garden City, AL7 1LT Hertfordshire, United Kingdom
[§]Laboratory of Growth Regulators, The Czech Academy of Sciences, Institute of Experimental Botany & Palacký University, Šlechtitelů 27, 78371 Olomouc, Czech Republic
[∥]Institute of Molecular and Translational Medicine, Faculty of Medicine and Dentistry, Palacký University, Hněvotínská 5, 779 00 Olomouc, Czech Republic

Supporting Information

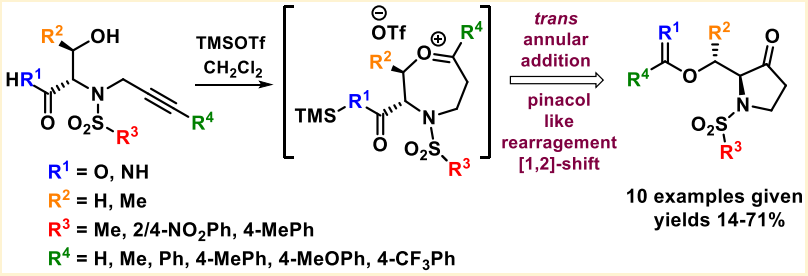

ABSTRACT: *N*-(3-Phenylprop-2-yn-1-yl)-sulfonamides derived from serine and threonine were synthesized using solid-phase synthesis and subjected to reaction with trimethylsilyl trifluoromethanesulfonate (TMSOTf). In contrast to the previously reported formation of 1,4-oxazepanes, this reaction afforded pyrrolidin-3-ones. A mechanistic explanation for this unexpected outcome is proposed, and the limitations and scope of the rearrangement are outlined.

INTRODUCTION

N-Substituted 2/4-nitrobenzenesulfonamides are excellent synthetic intermediates for preparing diverse nitrogenous heterocycles.[1,2] Recently, substantial attention has been paid to *N*-phenacyl-2/4-nitrobenzenesulfonamides derived from natural amino acids, especially serine and threonine, as the cyclization of these compounds stereoselectively yields various chiral morpholine derivatives.[3,4] On the basis of the synthetic potential of internal alkynols in the field of catalyzed intramolecular hydroalkoxylations,[5−10] we switched from *N*-phenacyl to *N*-(3-phenylprop-2-yn-1-yl) analogues and applied the previously reported reaction[11] to potentially synthesize functionalized 1,4-oxazepanes amenable to further diversification (Scheme 1).

Surprisingly, completely different reaction outcomes were obtained, and the isolated compounds were identified as pyrrolidin-3-one derivatives. Inspired by this unusual result and considering the limited number of synthetic routes leading to chiral pyrrolidin-3-ones despite their occurrence in biologically active compounds,[12−17] we decided to explore the limitations and scope of the rearrangement and provide insight into the reaction mechanism.

RESULTS AND DISCUSSION

By analogy to previously reported *N*-phenacyl analogues,[3] corresponding phenylalkynol **3a** was prepared using a convenient solid-phase synthesis process. Briefly, Wang resin was acylated with Fmoc-Thr-(O^{t}Bu)-OH, subjected to Fmoc-cleavage, and reacted with 4-nitrobenzenesulfonyl chloride (4-NsCl). Resulting sulfonamide **1a** was alkylated with 3-phenylprop-2-yn-1-ol using a Mitsunobu alkylation. Cleavage from resin **2a** with trifluoroacetic acid (TFA) was followed by spontaneous cleavage of the *tert*-butyl ether. Intermediate **3a** was obtained in excellent crude purity (≥90%, calculated from LC-UV traces), and prior to the final transformation, it was purified by semipreparative HPLC and fully characterized (Scheme 2). Even with the efficacy of solid-phase synthesis, consisting particularly in the rapid production of compounds via multistep reaction sequences with minimal hands-on time,[18] it should be noted that the corresponding intermediate **3a** can also be easily obtained using traditional solution-phase synthesis starting from threonine with a suitably protected carboxylic group. Intermediate **3a** was reacted with TMSOTf and Et_3SiH to obtain 1,4-oxazepane **5a**. We applied previously

Received: October 29, 2019
Published: December 6, 2019

DOI: 10.1021/acs.joc.9b02932
J. Org. Chem. 2020, 85, 985−993

Scheme 1. Different Reactivity of *N*-(3-Phenylprop-2-yn-1-yl)sulfonamides

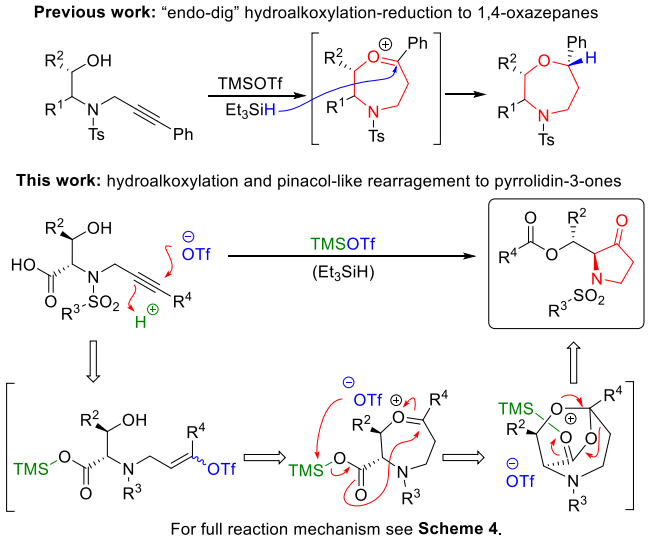

Scheme 2. Synthesis of Starting Material 3a and Its TMSOTf-Mediated Rearrangement to 4a[a]

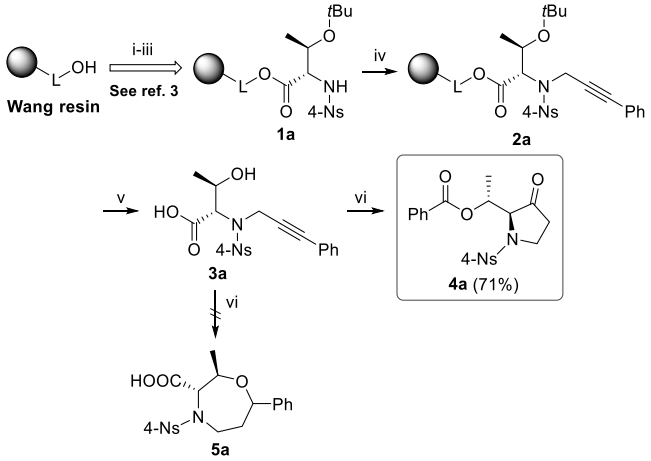

[a]Reagents and conditions: (i) Fmoc-Thr(O^{t}Bu)OH, 1-hydroxybenzotriazole (HOBt), 4-(dimethylamino)pyridine (DMAP), diisopropylcarbodiimide (DIC), dimethylformamide (DMF), CH_2Cl_2, 24 h, rt; (ii) 50% piperidine/DMF, 30 min, rt; (iii) 4-NsCl, 2,6-lutidine, CH_2Cl_2, 24 h, rt; (iv) 3-phenylprop-2-yn-1-ol, triphenylphosphine (TPP), diisopropyl azodicarboxylate (DIAD), tetrahydrofuran (THF), 24 h, rt; (v) 50% trifluoroacetic acid (TFA)/CH_2Cl_2, 1 h, rt; (vi) TMSOTf/Et_3SiH (2:1), anhydrous CH_2Cl_2, 24 h, 0 °C.

reported conditions[11] (i.e., 2 equiv of TMSOTf and 1 equiv of Et_3SiH in anhydrous CH_2Cl_2) and generated a highly pure compound (≥90%, LC-UV-MS traces) with a molecular mass corresponding to expected product **5a**. However, its ^1H and $^{13}C\{^1H\}$ NMR spectra were not consistent with the structure of **5a**. For example, the $^{13}C\{^1H\}$ signal at 210.6 ppm indicating a carbonyl group could not be assigned to any carbon atom in **5a**. For this reason, a set of 1D and 2D NMR spectra, including $^1H-^{15}N$ HMBC, was collected and carefully analyzed.

The structure of **4a** was determined by means of ^1H, $^{13}C\{^1H\}$, APT, $^1H-^1H$ COSY, $^1H-^1H$ NOESY, $^1H-^{13}C$ HSQC, $^1H-^{13}C$ HMBC, and $^1H-^{15}N$ HMBC. See the Supporting Information for the complete set of 1D and 2D spectra. Figure 1 summarizes $^1H-^{13}C\{^1H\}$ and $^1H-^{15}N$ long-range correlations. We identified benzoyl, 4-Nosyl, pyrollidin-3-onyl, and CH_3-CH-O moieties. The $^1H-^{13}C$ HMBC spectrum provided $H^{13}-C^{14}$ correlation. At the same time, H^{13} was also correlated to C3 and N1 of the pyrollidin-3-one moiety. Although $^1H-^{15}N$ four-bond correlation was not observed between 4-Nosyl protons and N1, the scaffold structure was confirmed by NOE correlations between 4-Nosyl protons and protons H^2, H_a^4, H_b^4, H_a^5, H_b^5, and H^{21} (see Supporting Information for more details). NOE correlations were also observed between benzoyl protons and protons H^2 and H^{21} (Figure 1).

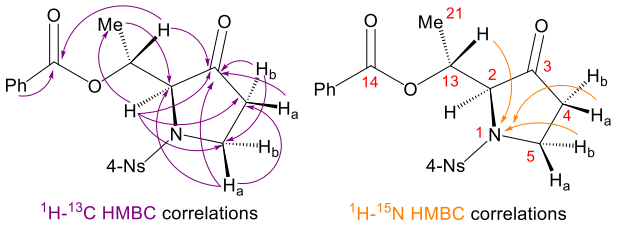

Figure 1. Selected correlations for 2D NMR analysis of rearrangement product **4a** (all correlations are displayed in Supporting Information, Figure S48 and S49).

The reaction conditions were further modified to investigate their impact on the reaction outcome (see Supporting Information for details, Table S3): (i) the same reagents in the same ratio (2 equiv of TMSOTf and 1 equiv of Et_3SiH) were added in the opposite order and gave the same results; (ii) the same reagents in the opposite ratio (1 equiv of TMSOTf and 2 equiv of Et_3SiH) led only to a mixture of the corresponding enol triflate and the reduced analogues of compound **3a** with double (at room temperature) or single (at 0 °C) bonds (Scheme 3); (iii) the same reagents in an equimolar ratio (1 equiv of TMSOTf and 1 equiv of Et_3SiH) again yielded a mixture of enol triflate, alkene, and alkane derivatives; (iv) reaction with 2 equiv of TMSOTf gave solely compound **4a**. The last experiment shows that Et_3SiH is not involved in the conversion of **3a** to **4a**; thus, it was omitted from the reaction mixture in further studies. Finally, we tested the reaction of compound **3a** with $TiCl_4$ and $BF_3{\cdot}OEt_2$ as the alternative Lewis acids. Treatment with $TiCl_4$ did not provide the rearrangement product, while the reaction with $BF_3{\cdot}OEt_2$ led to the formation of compound **4a**; however, the reaction was slower compared to TMSOTf.

The structure–reactivity relationship of the rearrangement was further studied using a series of variously substituted starting materials (Table 1). First, we used different sulfonyl chlorides (2-NsCl, mesyl chloride, and tosyl chloride) to evaluate the effect of the R^3 group (intermediates **3a–d**). Similarly, different phenylalkynols bearing electron-donating (Me and OMe) or electron-withdrawing (CF_3) substituents were used, and these reactants resulted in different R^4 substituents (intermediates **3e–g**). 2-Butynol (intermediate **3h**) and propargyl alcohol (intermediate **3i**) were also included as alternatives to phenylalkynols. Fmoc-Thr(O^{t}Bu)-OH was replaced with Fmoc-Ser(O^{t}Bu)-OH to modify the R^2 position (intermediate **3j**). Finally, Rink amide resin was used instead of Wang resin, and this afforded carboxamide intermediate **3k**. Table 1 shows the observed scope and limitations of the transformation to products **4**.

It was observed that the reaction times and crude purities depended strongly on the starting materials. As expected, the electron-withdrawing-group-substituted arylalkyne **3g** (CF_3)

DOI: 10.1021/acs.joc.9b02932
J. Org. Chem. 2020, 85, 985–993

Scheme 3. Outcomes Using Conditions ii and iii[a]

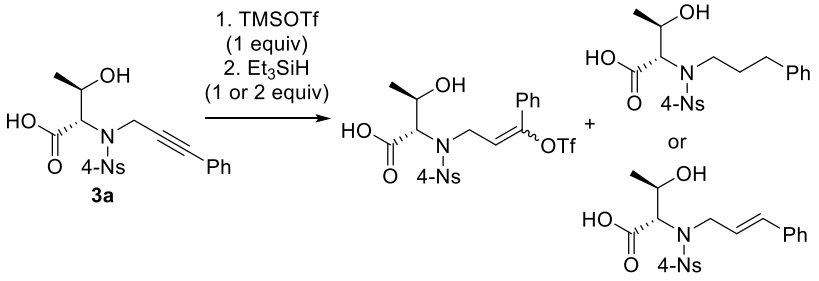

[a]For more details see in the text.

Table 1. Rearrangement of 3 to 4: Limitations and Scope[a-e]

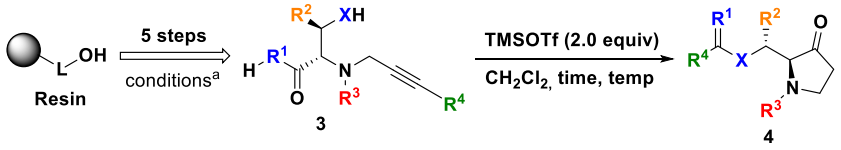

entry	final cmpd	X	R^1	R^2	R^3	R^4	time [h]	temp [°C]	crude purity [%][b]	yield [%][c]
1	**4a**	O	O	Me	4-Ns	Ph	24	23	96	71
2	**4b**	O	O	Me	2-Ns	Ph	24	23	96	41
3	**4c**	O	O	Me	Ms	Ph	24	23	92	40
4	**4d**	O	O	Me	Ts	Ph	24	23	80	50
5	**4e**	O	O	Me	4-Ns	4-MePh	24	23	76	30
6	**4f**	O	O	Me	4-Ns	4-MeOPh	24	23	81	42
7	**4g**	O	O	Me	4-Ns	4-CF_3Ph	24	40	56	18
8	**4h**	O	O	Me	4-Ns	Me	72	23	75	33
9	**4i**	O	O	Me	4-Ns	H	72	23	43	NI[d]
10	**4j**	O	O	H	4-Ns	Ph	72	23	51	14
11	**4k**	O	NH	Me	4-Ns	Ph	72	23	60	14
12	**4l**	S	O	H	4-Ns	Ph	24	23	NP[e]	NP[e]

[a]In analogy with ref 3 and Scheme 2. For detailed reaction conditions see Supporting Information. [b]Overall crude purity determined by HPLC after the entire reaction sequence (6 steps) prior to final purification. [c]Isolated overall (6 steps) yield calculated from the loading of the starting resin. [d]NI = not isolated, compound proved to be unstable during the HPLC purification process. [e]NP = not prepared.

Scheme 4. Control Experiments Designed To Identify Essential Functional Groups of the Molecule; Products Determined Using LC-UV-MS Traces

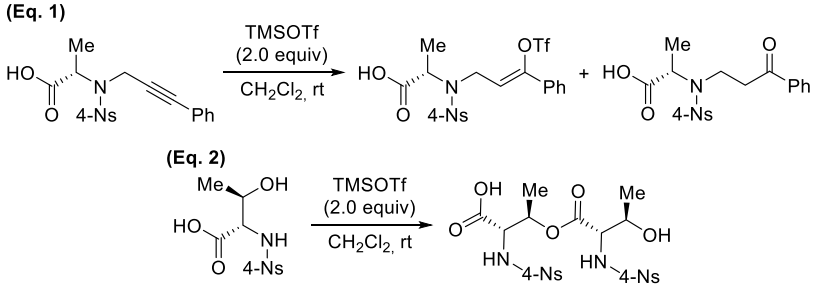

slowed the conversion, and a significant amount of the corresponding enol triflate intermediate was detected after 24 h. In this case, a higher temperature (40 °C) was necessary to push the conversion of the starting material to the final product **4g**. Longer reaction times were required when alkyl (**3h**) or hydrogen-bearing (**3i**) alkynes were used. Similarly, serine-based (**3j**) rearrangement precursor yielded the desired product **4j** in 48 h and 14% overall yield.[19] Replacement of carboxylic acid with the corresponding amide also led to the slow transformation. Finally, the rearrangement of amide **3k** to imidoester **4k** (carboxylic acid replaced with the amide) was also rather sluggish and yielded the desired product in 14% overall yield. Typically, in these cases the corresponding enol triflates and/or ketones were still detected in the reaction mixtures (9–28%, calculated from their LC-UV-MS traces). The isolated yields were somewhat compromised in several cases, which was caused by difficult chromatography and careful removal of impurities with similar retention times to products. Finally, to further extend the applicability of the disclosed reaction sequence, the sulfanyl analogue of **3a** was prepared from protected cysteine. However, no traces of the desired pyrrolidinone **4l** were detected.

As previously reported,[11] the reaction of similar intermediates promoted by TMSOTf proceeds via an intramolecular

DOI: 10.1021/acs.joc.9b02932
J. Org. Chem. 2020, 85, 985−993

hydroalkoxylation to the 1,4-oxazepines (Scheme 1), and in the presence of an external nucleophile (such as Et_3SiH), it gives the corresponding 1,4-oxazepanes. In the case of intermediates **3**, we expected a similar reaction course, but the reaction outcome suggested that at the 1,4-oxazepine stage, the carboxylate/carboxamide as an internal nucleophile added in a transannular manner. Competitive experiments with Et_3SiH indicated that the intramolecular addition is favored over the intermolecular one. The following pinacol-like rearrangement and ring opening of the cyclic hemiacetal resulted in the formation of the pyrrolidin-3-one scaffold. Although careful monitoring of the reaction mixture was performed using LC-UV-MS, we were able to detect only rearranged products **4** along with the corresponding enol triflates as presumed reaction intermediates. We have tried to support the proposed reaction mechanism by several control reactions (Scheme 4, eqs 1 and 2). First, the reaction substrate without the phenylprop-2-yn-1-yl moiety was treated with TMSOTf (eq 2). In this case only intermolecular esterification[20] occurred. Next, an intermediate without the hydroxy group (synthesized from Fmoc-Ala-OH) was reacted with TMSOTf (eq 1). In this case only the enol triflate derivative along with the corresponding ketone was produced. These results strongly suggest that both the hydroxy group and the alkynyl moiety are mandatory to trigger the rearrangement.

In addition, the reaction shown in Scheme 4, eq 1, supports our reaction mechanism since the hydroxy group is not required to form the enol triflate intermediate **C**. Our results also suggested that even though in the case of TMSOTf the reaction proceeds via enol triflate **B**, the key intermediate for the cyclization and the subsequent rearrangement is the oxonium intermediate **F** (Scheme 5). Our speculation is based on the previously observed $BF_3{\cdot}OEt_2$-promoted rearrangement of **3a** to **4a**. Under such conditions, no enol triflate intermediate **B** can be formed.

Taking into account all of these observations, we believe that the first step of the TMSOTf-promoted rearrangement is the reaction between TMSOTf and carboxylic acid of **3a**. In-situ-generated triflic acid (TfOH) then adds to alkyne to yield the enol triflate intermediate **B**.[21] The second equivalent of TMSOTf then reacts with the hydroxy group of **B** to yield the silylated alcohol **C** and another equivalent of TfOH. TfOH-mediated enol triflate hydrolysis yields the intermediate **D** that further undergoes the intramolecular 7-*exo*-*trig* cyclization to yield, upon TMS group release, the key oxonium intermediate **F**. Transannular cyclization of carboxylic acid to oxonium yields strained acetal intermediate **G** that is well organized for Lewis acid-promoted C−C bond fragmentation reaction. Finally, rearranged hemiacetal intermediate **H** opens up to yield the desired product **4a**.

Similarly, the oxonium intermediate **F** can be formed if BF_3 is used to trigger the reaction. We expect that in the first step the BF_3 reacts with the carboxylic acid of **3a**.[22] Generated intermediate **J** then undergoes proton-activated intramolecular 7-*endo*-*dig* cyclization of hydroxy group oxygen to alkyne. Finally, the proton transfer generates the key oxonium intermediate **F**. The observed incapacity of $TiCl_4$ to promote the rearrangement of **3a** can be rationalized by the intermediate **M** formation (hydroxy group is not available for intramolecular cyclization reaction). The proposed reaction mechanism also rationalizes the longer reaction times observed during the formation of compounds **4g−i** bearing alkynes substituted with an electron-deficient aryl group or with alkyl

Scheme 5. Plausible Mechanism of the Rearrangement

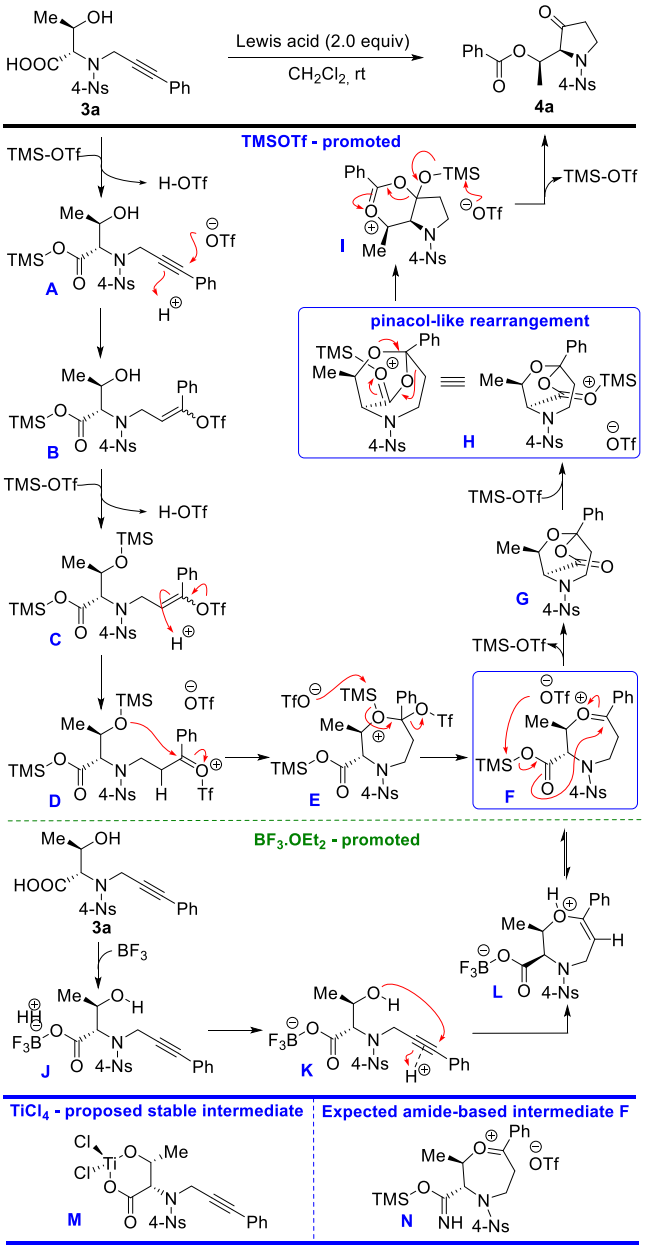

(lower stabilization of δ^+ Markovnikov addition-type intermediate). Similarly, transannular cyclization of the corresponding TMS−amide intermediate **N** is slower than that in the case of the corresponding acid due to the lower nucleophilicity of the nitrogen atom in **N**.

CONCLUSION

To summarize, we have discovered an unexpected rearrangement of *N*-(3-phenylprop-2-yn-1-yl) sulfonamides that yielded novel chiral derivatives of pyrrolidin-3-ones. The starting materials are readily available by either solution-phase or solid-phase synthesis and furnish the target compounds mostly in good or acceptable crude purities and yields. The reported reaction is broadly applicable in the case of the pyrrolidine scaffold and therefore can be utilized for the simple preparation of diversely substituted products. Its application to more complex compounds and diverse starting materials can be further studied in the future.

DOI: 10.1021/acs.joc.9b02932
J. Org. Chem. 2020, 85, 985−993

EXPERIMENTAL SECTION

General Information. Solvents and chemicals were purchased from Sigma-Aldrich (Milwaukee, WI), Acros Organic (Geel, Belgium), and Fluorochem (Hadfield, United Kingdom). Wang resin (100−200 mesh, 1% DVB, 1.4 mmol/g) and Rink resin (100−200 mesh, 1% DVB, 0.6 mmol/g) were obtained from AAPPTec (Louisville, KY). Solid-phase synthesis was carried out in plastic reaction vessels (syringes, each equipped with a porous disk) using a manually operated synthesizer (Torviq, Niles, MI). All reactions were carried out at ambient temperature (23 °C) unless stated otherwise; when the reactions required a heating at higher temperature, the heating was performed in an oil bath at a specific temperature (see for each derivative separately below in the text). Synthesis of *N*-sulfonamides (**1a-1**) was performed according to a previously reported procedure.[3] The LC-MS analyses were carried out on an UHPLC-MS system consisting of UHPLC chromatograph Acquity with a photodiode array detector and a single-quadrupole mass spectrometer (Waters) using a X-Select C18 column with the mobile phase consisting of 10 *m*M ammonium acetate (AmAc) in H_2O and MeCN. The ESI source operated at a discharge current of 5 μA, vaporizer temperature of 350 °C, and capillary temperature of 200 °C. For the LC/MS analysis, a sample of resin (∼5 mg) was treated with TFA in CH_2Cl_2, the cleavage cocktail was evaporated under a stream of nitrogen, and cleaved compounds were extracted into MeCN (1 mL). Purification was carried out by C18 reverse-phase semi-preparative HPLC chromatography with a gradient of 10 mM aqueous AmAc and MeCN and flow rate of 15 mL/min or by normal phase by silica gel chromatography. Residual solvents (H_2O and ammonium acetate buffer) were lyophilized by the ScanVac Coolsafe 110-4 working at −110 °C. All NMR spectra were performed using ECA400II or ECX500 spectrometers (JEOL RESONANCE, Tokyo, Japan) at magnetic field strength of 9.39 or 11.75 T corresponding to ^{1}H, ^{13}C, and ^{15}N resonance frequencies of 399.78 or 500.16 MHz, 100.53 or 125.77 MHz, and 50.7 MHz at 27 °C. Chemical shifts (δ) are reported in parts per million (ppm), and coupling constants (J) are reported in Hertz (Hz). The signals of MeCN-d_3, $CDCl_3$, and MeOH-d_4 were set at 1.94, 7.26, and 3.31 ppm, respectively, in ^{1}H NMR spectra and at 118.26, 77.36, and 49.15 ppm, respectively, in $^{13}C\{^{1}H\}$ NMR spectra. ^{15}N chemical shifts were referenced to external 90% formamide in DMSO-d_6 (112.00 ppm).[23] The assignment of ^{1}H, $^{13}C\{^{1}H\}$, and ^{15}N signals was done by $^{13}C\{^{1}H\}$ APT, $^{1}H-^{1}H$ COSY, $^{1}H-^{1}H$ NOESY, $^{1}H-^{13}C$ HSQC, $^{1}H-^{13}C$HMQC, $^{1}H-^{13}C$ HMBC, and $^{1}H-^{15}N$ HMBC. Abbreviations in NMR spectra: br s, broad singlet; s, singlet; d, doublet; dd, doublet of doublets; ddd, doublet of doublets of doublets; dddd, doublet of doublets of doublets of doublets; t, triplet; m, multiplet. HRMS analysis was performed using LC-MS (Dionex Ultimate 3000) with an Orbitrap Elite high-resolution mass spectrometer (Thermo Exactive plus) operating at positive full scan mode (120 000 fwmh) in the range of 100−1000 m/z with electrospray ionization working at 150 °C and a source voltage of 3.6 kV. The acquired data were internally calibrated with phthalate as a contaminant in MeOH (m/z 297.15909). IR spectra were measured by DRIFT (diffuse reflectance infrared Fourier transform) on a Thermo Nicolet AVATAR 370 FTIR spectrometer. Absorbance peaks (wavenumbers) are reported in reciprocal centimeters (cm^{-1}), and transmittances (T) are reported in percentages (%). Specific optical rotations were measured on an Automatic Compact Polarimeter POL-1/2 (ATAGO, Japan) with a LED Light Source and 589 nm interference filter at 24 °C. The length of the cuvette was 2 cm, and specific optical rotations are reported as follows: $[\alpha]_D^T$, concentration (g/mL), and solvent. Melting points were measured by a Boetius stage apparatus (WEB Analytik, Dresden, Germany) and are reported in degrees Celsius (°C).

General Method for Calculation of Yields Using ^{1}H NMR. ^{1}H NMR spectra of external standard at three different concentrations were measured. In each spectrum solvent signal was integrated followed by the integration of selected H^{Ar} signals of external standard. Ratios of solvent/standard signal areas along with a known quantity of the standard were used to construct a calibration curve. Then ^{1}H NMR spectra of the studied sample were measured, and the ratio of solvent/sample (selected H^{Ar} signal) areas was determined. Using the calibration curve, the quantity of compound in the sample was calculated.

General Procedure for Sonogashira Coupling to Prepare Alkylating Agents. $Pd(PPh_3)_2Cl_2$ and CuI were suspended in degassed TEA under nitrogen. Then aryl iodide was added followed by propargyl alcohol, and the reaction was stirred intensively for 5−22 h at room temperature for derivatives **II** and **III** or heated at 60 °C in an oil bath for 22 h for derivative **IV**. Then the reaction mixture was filtrated over Celite, washed with fresh TEA, and purified by silica gel chromatography in EtOAc/hexane.

3-(*p*-Tolyl)prop-2-yn-1-ol II. According to the general procedure, $Pd(PPh_3)_2Cl_2$ (483 mg, 0.69 mmol, 1 mol %) and CuI (262 mg, 1.38 mmol, 2 mol %) were suspended in degassed TEA (325 mL) under nitrogen. Then 4-iodotoluene (15.0 g, 68.80 mmol, 1.0 equiv) was added followed by propargyl alcohol (4.4 mL, 75.68 mmol, 1.1 equiv), and the reaction was stirred intensively for 5 h at room temperature. Then the reaction mixture was filtrated over Celite, washed with fresh TEA, and purified by silica gel chromatography in EtOAc/hexane (3/7; v/v); R_f = 0.5, yielded pale brown solid (5.2 g, 35.616 mmol, 51%). HPLC purity 99%. ^{1}H NMR (500 MHz, $CDCl_3$): δ = 7.33 (br d, J = 8.0 Hz, 2H), 7.12 (br d, J = 8.0 Hz, 2H), 4.49 (s, 2H), 2.35 (s, 3H), 1.79 (br s, 1H). $^{13}C\{^{1}H\}$ NMR (126 MHz, $CDCl_3$): δ = 139.0, 131.9, 129.4, 119.8, 86.9, 86.2, 52.0, 21.8. HRMS (ESI-TOF, positive): m/z calcd for $C_{10}H_{11}O$ $[M + H]^+$ 147.0804; found 147.0805. Other spectral and physical properties (mp 33.0−34.0 °C and IR data) concur with published data.[24]

3-(4-Methoxyphenyl)prop-2-yn-1-ol III. According to the general procedure, $Pd(PPh_3)_2Cl_2$ (150 mg, 0.21 mmol, 1 mol %) and CuI (81 mg, 0.42 mmol, 2 mol %) were suspended in degassed TEA (101 mL) under nitrogen. Then 4-iodoanisole (5.0 g, 21.4 mmol, 1.0 equiv) was added followed by propargyl alcohol (1.4 mL, 23.50 mmol, 1.1 equiv), and the reaction was stirred intensively for 22 h at room temperature. Then the reaction mixture was filtrated over Celite, washed with fresh TEA, and purified by silica gel chromatography in EtOAc/hexane (3/7; v/v); R_f = 0.4, yielded pale brown solid (3.1 g, 19.136 mmol, 89%). HPLC purity 99%. ^{1}H NMR (500 MHz, $CDCl_3$): δ = 7.37 (br d, J = 6.9 Hz, 2H), 6.83 (br d, J = 6.9 Hz, 2H), 4.48 (s, 2H), 3.80 (s, 3H), 1.85 (br s, 1H). $^{13}C\{^{1}H\}$ NMR (126 MHz, $CDCl_3$): δ = 160.1, 133.5, 115.0, 114.3, 86.2, 86.0, 55.6, 52.0. HRMS (ESI-TOF, positive): m/z calcd for $C_{10}H_{11}O_2$ $[M + H]^+$ 163.0754; found 163.0755. Other spectral and physical properties (mp 63.1−63.5 °C and IR data) concur with published data.[25]

3-(4-Trifluoromethyl)phenyl)prop-2-yn-1-ol IV. According to the general procedure, $Pd(PPh_3)_2Cl_2$ (129 mg, 0.18 mmol, 1 mol %) and CuI (70 mg, 0.36 mmol, 2 mol %) were suspended in degassed TEA (86.4 mL) under nitrogen. Then 4-iodobenzotrifluoride (2.7 mL, 18.38 mmol, 1.0 equiv) was added followed by propargyl alcohol (1.2 mL, 20.21 mmol, 1.1 equiv), and the reaction was stirred intensively for 22 h at 60 °C in an oil bath. Then the reaction mixture was filtrated over Celite, washed with fresh TEA, and purified by silica gel chromatography in EtOAc/hexane (3/7; v/v); R_f = 0.5, yielded waxy yellow solid (3.56 g, 17.800 mmol, 97%). HPLC purity 99%. ^{1}H NMR (500 MHz, $CDCl_3$): δ = 7.57 (br d, J = 8.4 Hz, 2H), 7.53 (br d, J = 8.4 Hz, 2H), 4.52 (s, 2H), 1.80 (br s, 1H). $^{13}C\{^{1}H\}$ NMR (126 MHz, $CDCl_3$): δ = 132.3, 130.6 (q, J = 32.8 Hz), 126.7, 125.6 (q, J = 3.6 Hz), 124.2 (q, J = 271.8 Hz), 90.0, 84.7, 51.9. HRMS (ESI-TOF, negative): m/z calcd for $C_{10}H_6F_3O$ $[M - H]^-$ 199.0365; found 199.0359. Other spectral and physical properties (mp 40.0−41.1 °C and IR data) concur with published data.[24]

General Procedure for the Mitsunobu Alkylation 2a-l. Resin **1a-1** (500 mg) was washed three times with CH_2Cl_2, anhydrous DMF, and anhydrous THF, and a solution of alcohol (3.00 mmol) and triphenylphosphine (TPP, 787 mg, 3.00 mmol) in anhydrous THF (5 mL) was added. The syringe with the resin and reaction solution was connected by a plastic clutch with a second syringe containing a solution of DIAD (591 μL, 3.00 mmol) in anhydrous THF (5 mL). The syringes were cooled to −20 °C; their content was mixed together and shaken for 24 h at room temperature. The

DOI: 10.1021/acs.joc.9b02932
J. Org. Chem. 2020, 85, 985−993

resulting resin was washed three times with anhydrous THF and CH_2Cl_2.

Cleavage from the Resin and Removal of the *t*Bu Protecting Group 3a-l. The resin **2a-1** (500 mg) was shaken in TFA/anhydrous CH_2Cl_2 (5 mL, 50%) for 1 h at room temperature. Then the resin was washed three times with fresh cleavage cocktail (5 mL), and combined washes were evaporated using a stream of nitrogen. The crude product was purified by reverse-phase semipreparative HPLC or by silica gel chromatography (see Supporting Information, Table S1).

(−)-*N*-((4-Nitrophenyl)sulfonyl)-*N*-(3-phenylprop-2-yn-1-yl)-(2*S*,3*R*)-2-amino-3-hydroxybutyric Acid 3a. Pale orange amorphous solid (46.8 mg, 0.112 mmol, 82%). The crude product was purified by silica gel chromatography in CH_2Cl_2/MeOH (9/1; v/v) + 1% HCOOH, R_f = 0.6. HPLC purity 98%. Cleaved from 325 mg of resin **2a** (0.420 mmol/g, 0.137 mmol of substrate). ^{1}H NMR (400 MHz, MeCN-d_3): δ = 8.22 (d, J = 9.2 Hz, 2H), 8.12 (d, J = 9.2 Hz, 2H), 7.24−7.34 (m, 5H), 4.58 (s, 2H), 4.44−4.47 (m, 2H), 3.91 (br s, 1H), 1.24 (d, J = 6.0 Hz, 3H). ^{13}C{^{1}H} NMR (101 MHz, MeCN-d_3): δ = 172.6, 151.0, 146.9, 132.3, 130.0, 129.5, 129.4, 124.9, 123.4, 87.0, 84.7, 68.4, 66.8, 38.1, 20.6. HRMS (ESI-TOF, negative): m/z calcd for $C_{19}H_{17}N_2O_7S$ [M − H]$^-$ 417.0751; found 417.0756. IR (DRIFT): $\bar{\nu}$ = 3528, 3251, 3106, 2979, 2931, 1724, 1685, 1605, 1528, 1442, 1401, 1344, 1308, 1157, 1088, 854, 822 cm^{-1}. $[\alpha]_D^{24}$ = −43.2° (c = 0.00110 g/mL, MeCN).

(−)-*N*-((2-Nitrophenyl)sulfonyl)-*N*-(3-phenylprop-2-yn-1-yl)-(2*S*,3*R*)-2-amino-3-hydroxybutyric Acid 3b. White amorphous solid (29.2 mg, 0.070 mmol, 21%). The crude product was purified by semipreparative HPLC chromatography. HPLC purity 98%. Cleaved from 622 mg of resin **2b** (0.524 mmol/g, 0.326 mmol of substrate). ^{1}H NMR (500 MHz, $CDCl_3$): δ = 8.24 (d, J = 8.0 Hz, 1H), 7.46−7.53 (m, 3H), 7.16−7.25 (m, 5H), 5.84 (br s, 1H), 4.75 (d, J = 18.6 Hz, 1H), 4.67 (d, J = 18.6 Hz, 1H), 4.57−4.58 (m, 1H), 4.50 (d, J = 4.0 Hz, 1H), 1.33 (d, J = 6.0 Hz, 3H). ^{13}C{^{1}H} NMR (126 MHz, $CDCl_3$): δ = 174.9, 148.2, 134.0, 133.6, 132.1, 132.0, 131.8, 128.8, 128.6, 124.4, 122.6, 86.0, 85.3, 68.7, 67.0, 38.0, 20.2. HRMS (ESI-TOF, negative): m/z calcd for $C_{19}H_{17}N_2O_7S$ [M − H]$^-$ 417.0751; found 417.0759. IR (DRIFT): $\bar{\nu}$ = 3209, 2979, 1720, 1541, 1346, 1440, 1159, 1124, 756, 691 cm^{-1}. $[\alpha]_D^{24}$ = −21.0° (c = 0.00119 g/mL, MeCN).

(−)-*N*-(Methylsulfonyl)-*N*-(3-phenylprop-2-yn-1-yl)-(2*S*,3*R*)-2-amino-3-hydroxybutyric Acid 3c. White amorphous solid (14.7 mg, 0.047 mmol, 12%). The crude product was purified by semipreparative HPLC chromatography. HPLC purity 99%. Cleaved from 401 mg of resin **2c** (0.524 mmol/g, 0.210 mmol of substrate). ^{1}H NMR (400 MHz, $CDCl_3$): δ = 7.31−7.33 (m, 2H), 7.17−7.22 (m, 3H), 4.92 (br s, 1H), 4.56 (d, J = 18.3 Hz, 1H), 4.48 (d, J = 18.3 Hz, 1H), 4.39−4.46 (m, 1H), 4.32 (d, J = 3.8 Hz, 1H), 3.05 (s, 3H), 1.33 (d, J = 6.0 Hz, 3H). ^{13}C{^{1}H} NMR (101 MHz, $CDCl_3$): δ = 174.7, 132.0, 129.1, 128.8, 122.4, 85.4, 85.4, 68.0, 66.2, 41.5, 37.2, 20.2. HRMS (ESI-TOF, negative): m/z calcd for $C_{14}H_{16}NO_5S$ [M − H]$^-$ 310.0744; found 310.0750. IR (DRIFT): $\bar{\nu}$ = 3521, 3492, 3005, 2253, 2145, 2000, 1749, 1711, 1361, 1421, 1092 cm^{-1}. $[\alpha]_D^{24}$ = −87.5° (c = 0.00012 g/mL, MeCN).

(−)-*N*-((2-Nitrophenyl)sulfonyl)-*N*-(3-phenylprop-2-yn-1-yl)-(2*S*,3*R*)-2-amino-3-hydroxybutyric Acid 3d. White amorphous solid (27.1 mg, 31%, 0.112 mmol). The crude product was purified by semipreparative HPLC chromatography. HPLC purity 99%. Cleaved from 435 mg of resin **2d** (0.524 mmol/g, 0.228 mmol of substrate). ^{1}H NMR (400 MHz, $CDCl_3$): δ = 7.79 (d, J = 8.2 Hz, 2H), 7.15−7.26 (m, 7H), 5.16 (br s, 1H), 4.69 (d, J = 18.9 Hz, 1H), 4.54 (d, J = 18.9 Hz, 1H), 4.45 (m, 2H), 2.28 (s, 3H), 1.24 (d, J = 6.2 Hz, 3H). ^{13}C{^{1}H} NMR (101 MHz, $CDCl_3$): δ = 174.3, 144.0, 137.3, 131.9, 129.8, 128.8, 128.5, 128.2, 122.6, 85.8, 85.0, 77.7, 77.4, 77.0, 68.0, 36.6, 22.3, 21.8, 20.0. HRMS (ESI-TOF, negative): m/z calcd for $C_{20}H_{20}NO_5S$ [M − H]$^-$ 386.1057; found 386.1065. IR (DRIFT): $\bar{\nu}$ = 3508, 3234, 3055, 2980, 2922, 1915, 1704, 1442, 1327, 1152, 1090, 811, 756 cm^{-1}. $[\alpha]_D^{24}$ = −20.2° (c = 0.00104 g/mL, MeCN).

(−)-*N*-((4-Nitrophenyl)sulfonyl)-*N*-(3-(4-trifluoromethyl)-phenyl)prop-2-yn-1-yl)-(2*S*,3*R*)-2-amino-3-hydroxybutyric Acid 3g. White amorphous solid (70.0 mg, 0.144 mmol, 69%). The crude product was purified by semipreparative HPLC chromatography. HPLC purity 99%. Cleaved from 482 mg of resin **2g** (0.734 mmol/g, 0.354 mmol of substrate). ^{1}H NMR (400 MHz, MeOH-d_4): δ = 8.27 (d, J = 8.9 Hz, 2H), 8.17 (d, J = 8.9 Hz, 2H), 7.57 (br d, J = 7.6 Hz, 2H), 7.43 (br d, J = 7.6 Hz, 2H), 4.72 (d, J = 18.9 Hz, 1H), 4.63 (d, J = 18.9 Hz, 1H), 4.41−4.54 (m, 2H), 1.35 (d, J = 6.0 Hz, 3H). ^{13}C{^{1}H} NMR (126 MHz, MeOH-d_4): δ = 173.2, 151.5, 147.5, 133.2, 131.2 (q, J = 32.8 Hz), 130.5, 128.4, 126.4 (d, J = 4.2 Hz), 125.5 (q, J = 271.3 Hz), 125.1, 90.0, 83.7, 68.6, 38.2, 21.0. HRMS (ESI-TOF, positive): m/z calcd for $C_{20}H_{18}F_3N_2O_7S$ [M + H]$^+$ 487.0781; found 487.0784. IR (DRIFT): $\bar{\nu}$ = 3104, 2983, 2936, 2871, 1925, 1726, 1529, 1404, 1348, 1322, 1159, 1123, 1089, 1066, 1016, 843, 740 cm^{-1}. $[\alpha]_D^{24}$ = −44.4° (c = 0.00422 g/mL, MeCN).

(−)-*N*-(But-2-yn-1-yl)-*N*-((4-nitrophenyl)sulfonyl)-(2*S*,3*R*)-2-amino-3-hydroxybutyric Acid 3h. Pale yellow−white amorphous solid (85.2 mg, 0.239 mmol, 73%). The crude product was purified by semipreparative HPLC chromatography. HPLC purity 99%. Cleaved from 498 mg of resin **2h** (0.656 mmol/g, 0.327 mmol of substrate). ^{1}H NMR (400 MHz, MeOH-d_4): δ = 8.36 (d, J = 9.1 Hz, 2H), 8.16 (d, J = 9.1 Hz, 2H), 4.39−4.45 (m, 1H), 4.28−4.36 (m, 3H), 3.38−3.24 (1H), 1.66 (s, 3H), 1.26 (d, J = 6.0 Hz, 3H). ^{13}C{^{1}H} NMR (400 MHz, MeOH-d_4): δ = 174.3, 151.5, 147.8, 130.4, 124.9, 81.2, 76.5, 68.4, 37.4, 20.7, 3.2. HRMS (ESI-TOF, positive): m/z calcd for $C_{14}H_{17}N_2O_7S$ [M + H]$^+$ 357.0751; found 357.0751. IR (DRIFT): $\bar{\nu}$ = 3106, 3041, 2980, 2935, 2230, 1706, 1527, 1347, 1309, 1089, 830, 759 cm^{-1}. $[\alpha]_D^{24}$ = −74.55° (c = 0.00100 g/mL, MeCN).

(−)-*N*-((4-Nitrophenyl)sulfonyl)-*N*-(prop-2-yn-1-yl)-(2*S*,3*R*)-2-amino-3-hydroxybutyric Acid 3i. White amorphous solid (28.1 mg, 0.082 mmol, 33%). The crude product was purified by semipreparative HPLC chromatography. HPLC purity 99%. Cleaved from 400 mg of resin **2i** (0.621 mmol/g, 0.248 mmol of substrate). ^{1}H NMR (500 MHz, MeOH-d_4): δ = 8.35 (d, J = 9.2 Hz, 2H), 8.15 (d, J = 9.2 Hz, 2H), 4.54 (dd, J = 18.6, 2.5 Hz, 1H), 4.32−4.36 (m, 2H), 4.23 (d, J = 5.2 Hz, 1H), 2.55 (t, J = 2.5 Hz, 1H), 1.28 (d, J = 6.4 Hz, 3H). ^{13}C{^{1}H} NMR (126 MHz, MeOH-d_4): δ = 175.0, 151.6, 147.4, 130.4, 125.0, 81.8, 73.6, 69.1, 68.8, 37.2, 20.8. HRMS (ESI-TOF, positive): m/z calcd for $C_{13}H_{15}N_2O_7S$ [M + H]$^+$ 343.0594; found 343.0594. IR (DRIFT): $\bar{\nu}$ = 3211, 3105, 2970, 2940, 2231, 1717, 1528, 1433, 1349, 1309, 1158, 1090, 830, 741 cm^{-1}. $[\alpha]_D^{24}$ = −88.5° (c = 0.00013 g/mL, MeCN).

(−)-*N*-((4-Nitrophenyl)sulfonyl)-*N*-(3-phenylprop-2-yn-1-yl)-(*S*)-2-amino-3-hydroxybutyric Acid 3j. White amorphous solid (32.4 mg, 0.080 mmol, 30%). The crude product was purified by semipreparative HPLC chromatography. HPLC purity 98%. Cleaved from 522 mg of resin **2j** (0.515 mmol/g, 0.267 mmol of substrate). ^{1}H NMR (500 MHz, MeOH-d_4): δ = 8.25 (d, J = 8.8 Hz, 2H), 8.21 (d, J = 8.8 Hz, 2H), 7.20−7.29 (m, 5H), 4.63 (d, J = 18.6 Hz, 1H), 4.57 (dd, J = 7.2, 5.8 Hz, 1H), 4.48 (d, J = 18.6 Hz, 1H), 4.08 (dd, J = 11.4, 5.8 Hz, 1H), 3.91 (dd, J = 11.4, 7.2 Hz, 1H). ^{13}C{^{1}H} NMR (126 MHz, MeOH-d_4): δ = 175.1, 151.4, 148.3, 132.7, 130.4, 129.6, 129.5, 125.0, 124.1, 86.5, 85.5, 65.6, 63.1, 36.9. HRMS (ESI-TOF, positive): m/z calcd for $C_{18}H_{17}N_2O_7S$ [M + H]$^+$ 405.0751; found 405.0751. IR (DRIFT): $\bar{\nu}$ = 3042, 2240, 1738, 1580, 1532, 1349, 1167, 1156, 1058, 816 cm^{-1}. $[\alpha]_D^{24}$ = −29.6° (c = 0.00108 g/mL, MeCN).

(−)-(2*S*,3*R*)-3-Hydroxy-2-((4-nitro-*N*-(3-phenylprop-2-yn-1-yl)phenyl)sulfonamido)butanamide 3k. White amorphous solid (32.4 mg, 0.078 mmol, 30%). The crude product was purified by semipreparative HPLC chromatography. HPLC purity 99%. Cleaved from 715 mg of resin **2k** (0.359 mmol/g, 0.257 mmol of substrate). ^{1}H NMR (500 MHz, $CDCl_3$): δ = 8.24 (d, J = 8.8 Hz, 2H), 8.17 (d, J = 8.8 Hz, 2H), 7.32−7.35 (m, 1H), 7.26−7.29 (m, 2H), 7.14−7.16 (m, 2H), 6.41 (br s, 1H), 5.69 (br s, 1H), 4.83 (d, J = 18.9 Hz, 1H), 4.61 (d, J = 18.9 Hz, 1H), 4.42 (qd, J = 6.4 Hz, 1H), 4.25 (d, J = 7.4 Hz, 1H), 2.58 (br s, 1H), 1.22 (d, J = 6.4 Hz, 3H). ^{13}C{^{1}H} NMR (126 MHz, $CDCl_3$): δ = 171.1, 150.5, 145.9, 131.7, 129.7, 129.5, 128.9, 124.3, 121.3, 86.5, 83.6, 66.0, 65.6, 35.6, 19.7. HRMS (ESI-TOF, positive): m/z calcd for $C_{19}H_{20}N_3O_6S$ [M + H]$^+$ 418.1067; found 418.1069. IR (DRIFT): $\bar{\nu}$ = 3502, 3486, 3386, 3351, 3189,

DOI: 10.1021/acs.joc.9b02932
J. Org. Chem. 2020, 85, 985−993

3115, 3100, 3078, 3038, 3009, 2980, 2940, 2248, 1932, 1878, 1674, 1606, 1530, 1419, 1344, 1309, 1159, 1089, 1026, 855, 821 cm^{-1}. $[\alpha]_D^{24}$ = −40.2° (*c* = 0.00107 g/mL, MeCN).

General Conditions for Rearrangement of 3a-l to Pyrrolidin-3-ones 4a-l. *TMSOTf-Promoted Rearrangement (see Supporting Information, Scheme S1, Tables S2 and S3).* For derivative **4a**: To a stirred solution of **3a** (58 mg, 0.14 mmol, 1.0 equiv) in anhydrous CH_2Cl_2 (1.5 mL) cooled to 0 °C Et_3SiH was slowly added dropwise (22 μL, 0.14 mmol, 1.0 equiv) followed by addition of TMSOTf (52 μL mg, 0.28 mmol, 2.0 equiv). After 24 h, the reaction mixture was washed with a saturated solution of $NaHCO_3$/DCM (3 × 5 mL), dried with anhydrous $MgSO_4$, filtrated, and evaporated to dryness.

For derivatives **4a−l**: To the crude product **3a−l** (cleaved from 500 mg of resin), TMSOTf (380 μL, 2.10 mmol, 2.0 equiv) in anhydrous CH_2Cl_2 (5 mL) was added and shaken for a specific reaction time and temperature (see later in the text and Supporting Information, Table S2). The reaction mixture was evaporated under a stream of nitrogen; the residual material was dissolved in anhydrous DCM (5 mL) and washed three times with a saturated solution of $NaHCO_3$. The organic layer was separated, dried with anhydrous $MgSO_4$, and evaporated to dryness, and the crude samples were purified by reverse-phase semipreparative HPLC chromatography.

BF_3·OEt_2-Promoted Rearrangement (see Supporting Information, Scheme S1, Table S3). To the crude product **3a** (cleaved from 100 mg of resin), BF_3·OEt_2 (52 μL, 0.42 mmol, 2.0 equiv) in anhydrous CH_2Cl_2 (1 mL) was added and shaken for 2.5, 24, and 48 h at room temperature. The CH_2Cl_2 layer was washed three times with a saturated solution of $NaHCO_3$, dried with anhydrous $MgSO_4$, evaporated to dryness, and analyzed by LC-UV-MS. Conclusion: The observed conversion was 10% after 48 h as calculated from the HPLC-UV traces (205−400 nm).

$TiCl_4$-Promoted Rearrangement (see Supporting Information, Scheme S1, Table S3). To the crude product **3a** (cleaved from 100 mg of resin), $TiCl_4$ (46 μL, 0.42 mmol, 2.0 equiv) in anhydrous CH_2Cl_2 (1 mL) was added and shaken for 2.5, 24, and 48 h at room temperature. The sample for HPLC analysis was obtained by the same procedure as for BF_3·OEt_2. Conclusion: The desired product was not detected.

(+)-(^{13}*R*)-1-((^{2}*S*)-1-((4-Nitrophenyl)sulfonyl)-3-oxopyrrolidin-2-yl)ether Benzoate 4a. Reaction conditions: 24 h at room temperature. White amorphous solid (40.9 mg, 0.098 mmol, 71%). The crude product was purified by semipreparative HPLC chromatography. HPLC purity 99%. ^{1}H NMR (500 MHz, MeCN-d_3): δ = 8.34 (d, *J* = 8.9 Hz, 2H, HC[8,10]), 8.10 (d, *J* = 8.9 Hz, 2H, HC[7,11]), 7.93−7.95 (m, 2H, HC[16,20]), 7.60−7.63 (m, 1H, HC[18]), 7.47−7.49 (m, 2H, HC[17,19]), 5.54 (qd, *J* = 6.5, 4.0 Hz, 1H, HC[13]), 4.12 (ddd, *J* = 4.0, 1.0, 1.0 Hz, 1H, HC[2]), 4.02 (ddd, *J* = 12.4, 10.0, 3.3 Hz, 1H, H_aC^5), 3.88 (ddd, *J* = 12.4, 9.5, 7.7 Hz, 1H, H_bC^5), 2.31 (dddd, *J* = 18.8, 7.7, 3.3, 1.0 Hz, 1H, H_aC^4), 2.04 (dddd, *J* = 18.8, 10.5, 9.5, 1.0 Hz, 1H, H_bC^4), 1.47 (d, *J* = 6.5 Hz, 3H, HC[21]). ^{13}C{^{1}H} NMR (126 MHz, MeCN-d_3): δ = 210.6 (C3), 166.3 (C14), 151.8 (C9), 144.0 (C6), 134.4 (C18), 130.7 (C15), 130.3 (C16,20), 129.8 (C7,11), 129.6 (C17,19), 125.9 (C8,10), 72.1 (C13), 67. (C2), 46.5 (C5), 37.1 (C4), 17.1 (C21). ^{15}N NMR (51 MHz, MeCN-d_3): δ = 102.7 (N1); 366.9 (N12). See Supporting Information for detailed assignments. ^{1}H NMR (500 MHz, $CDCl_3$): δ = 8.30 (d, *J* = 8.9 Hz, 2H), 8.04 (d, *J* = 8.9 Hz, 2H), 7.89−7.91 (m, 2H), 7.54−7.58 (m, 1H), 7.40−7.43 (m, 2H), 5.57 (qd, *J* = 6.6, 4.6 Hz, 1H), 4.07 (br d, *J* = 4.6 Hz, 1H), 4.00 (ddd, *J* = 12.2, 9.9, 3.8 Hz, 1H), 3.89 (ddd, *J* = 12.2, 9.1, 7.8 Hz, 1H), 2.42 (ddd, *J* = 18.6, 7.8, 3.8 Hz, 1H), 2.24 (ddd, *J* = 18.6, 9.1, 7.8 Hz, 1H), 1.53 (d, *J* = 6.6 Hz, 3H). ^{13}C{^{1}H} NMR (126 MHz, $CDCl_3$): δ = 208.8, 165.7, 150.7, 143.9, 133.8, 129.9, 129.8, 128.9, 128.9, 125.0, 77.6, 77.4, 77.1, 70.9, 66.4, 45.7, 36.9, 17.3. HRMS (ESI-TOF, negative): *m*/*z* calcd for $C_{19}H_{17}N_2O_7S$ $[M - H]^-$ 417.0751; found 417.0757. IR (DRIFT): $\bar{\nu}$ = 2874, 1940, 1828, 1763, 1714, 1529, 1452, 1347, 1270, 1222, 1164, 1088, 855, 713 cm^{-1}. $[\alpha]_D^{24}$ = +61.2° (*c* = 0.00165 g/mL, MeCN).

(+)-(*R*)-1-((*S*)-1-((2-Nitrophenyl)sulfonyl)-3-oxopyrrolidin-2-yl)ethyl Benzoate 4b. Reaction conditions: 24 h at room temperature. Pale yellow amorphous solid (47.6 mg, 0.114 mmol, 41%). The crude product was purified by semipreparative HPLC chromatography. HPLC purity 99%. ^{1}H NMR (500 MHz, $CDCl_3$): δ = 8.14 (dd, *J* = 8.3, 1.3 Hz, 1H), 7.92−7.93 (m, 2H), 7.67−7.70 (m, 2H), 7.62−7.64 (m, 1H), 7.56 (td, *J* = 7.6, 1.3 Hz, 1H), 7.42 (t, *J* = 7.6 Hz, 2H), 5.56 (qd, *J* = 6.4, 4.0 Hz, 1H), 4.29 (br d, *J* = 4.0 Hz, 1H), 4.23 (ddd, *J* = 12.3, 9.5, 3.5 Hz, 1H), 3.93 (ddd, *J* = 12.3, 9.9, 8.0 Hz, 1H), 2.49 (ddd, *J* = 18.6, 9.5, 9.5 Hz, 1H), 2.42 (ddd, *J* = 18.6, 8.0, 3.5 Hz, 1H), 1.46 (d, *J* = 6.4 Hz, 3H). ^{13}C{^{1}H} NMR (126 MHz, $CDCl_3$): δ = 209.4, 165.7, 148.5, 134.7, 133.6, 132.7, 132.3, 132.1, 130.0, 129.9, 128.8, 124.9, 71.4, 67.1, 45.8, 37.2, 17.5. HRMS (ESI-TOF, positive): *m*/*z* calcd for $C_{19}H_{19}N_2O_7S$ $[M + H]^+$ 419.0907; found 419.0907. IR (DRIFT): $\bar{\nu}$ = 2979, 2937, 1921, 1765, 1717, 1542, 1450, 1347, 1262, 1225, 1192, 1087, 805, 741, 708 cm^{-1}. $[\alpha]_D^{24}$ = +173.3° (*c* = 0.00118 g/mL, MeCN).

(+)-(*R*)-1-((*S*)-1-(Mesylsulfonyl)-3-oxopyrrolidin-2-yl)ethyl Benzoate 4c. Reaction conditions: 24 h at room temperature. Gray−white amorphous solid (47.1 mg, 0.151 mmol, 40%). The crude product was purified by semipreparative HPLC chromatography. HPLC purity 99%. ^{1}H NMR (500 MHz, $CDCl_3$): δ = 7.95−7.97 (m, 2H, HC[10,14]), 7.56−7.59 (m, 1H, HC[12]), 7.43−7.46 (m, 2H, HC[11,13]), 5.54 (qd, *J* = 6.5, 4.0 Hz, 1H, HC[7]), 4.15 (br d, *J* = 4.0 Hz, 1H, HC[2]), 4.14 (ddd, *J* = 12.0, 10.0, 2.6 Hz, 1H, H_aC^5), 3.81 (ddd, *J* = 12.0, 10.0, 7.7 Hz, 1H, H_bC^5), 2.93 (s, 3H, HC[6]), 2.68 (ddd, *J* = 18.8, 11.0, 10.0 Hz, 1H, H_aC^4), 2.50 (ddd, *J* = 18.8, 7.7, 2.6 Hz, 1H, H_bC^4), 1.51 (d, *J* = 6.5 Hz, 3H, HC[15]). ^{13}C{^{1}H} NMR (126 MHz, $CDCl_3$): δ = 210.3 (C3), 165.7 (C8), 133.7 (C12), 123.0 (C9), 129.9 (C10,14), 128.9 (C11,13), 71.4 (C7), 66.2 (C2), 45.3 (C5), 38.9 (C6), 37.4 (C4), 17.6 (C15). ^{15}N NMR (51 MHz, $CDCl_3$): δ = 99.2 (N1). See Supporting Information for detailed assignments. HRMS (ESI-TOF, positive): *m*/*z* calcd for $C_{14}H_{18}NO_5S$ $[M + H]^+$ 312.0900; found 312.0899. IR (DRIFT): $\bar{\nu}$ = 2963, 2934, 1918, 1757, 1716, 1452, 1340, 1265, 1195, 1149, 1086, 1029, 776, 710 cm^{-1}. $[\alpha]_D^{24}$ = +469.1° (*c* = 0.00081 g/mL, MeCN).

(+)-(*R*)-1-((*S*)-3-Oxo-1-tosylpyrrolidin-2-yl)ethyl Benzoate 4d. Reaction conditions: 24 h at room temperature. White amorphous solid (80.4 mg, 0.208 mmol, 50%). The crude product was purified by semipreparative HPLC chromatography. HPLC purity 99%. ^{1}H NMR (500 MHz, $CDCl_3$): δ = 7.92−7.97 (m, 2H), 7.75 (br d, *J* = 8.3 Hz, 2H), 7.53−7.58 (m, 1H), 7.40−7.45 (m, 2H), 7.33 (br d, *J* = 8.3 Hz, 2H), 5.63 (qd, *J* = 6.4, 3.4 Hz, 1H), 4.00 (br d, *J* = 3.4 Hz, 1H), 3.96 (ddd, *J* = 12.7, 9.9, 3.0 Hz, 1H), 3.86 (ddd, *J* = 12.7, 9.6, 7.7 Hz, 1H), 2.42 (s, 3H), 2.21 (ddd, *J* = 18.5, 7.7, 3.0 Hz, 1H), 1.94 (ddd, *J* = 18.5, 9.9, 9.6 Hz, 1H), 1.55 (d, *J* = 6.4 Hz, 3H). ^{13}C{^{1}H} NMR (126 MHz, $CDCl_3$): δ = 210.7, 165.7, 144.9, 134.9, 133.6, 130.6, 130.1, 129.9, 128.8, 127.8, 71.9, 66.80, 45.8, 36.5, 21.9, 17.3. HRMS (ESI-TOF, positive): *m*/*z* calcd for $C_{20}H_{22}NO_5S$ $[M + H]^+$ 388.1213; found 388.1213. IR (DRIFT): $\bar{\nu}$ = 2996, 2939, 2903, 1926, 1763, 1709, 1449, 1164, 1088, 821, 751, 716 cm^{-1}. $[\alpha]_D^{24}$ = +76.4° (*c* = 0.00121 g/mL, MeCN).

(+)-(*R*)-1-((*S*)-1-((4-Nitrophenyl)sulfonyl)-3-oxopyrrolidin-2-yl)ethyl 4-Methylbenzoate 4e. Reaction conditions: 24 h at room temperature. White amorphous solid (24.5 mg, 0.057 mmol, 30%). The crude product was purified by semipreparative HPLC chromatography. HPLC purity 99%. ^{1}H NMR (500 MHz, $CDCl_3$): δ = 8.27 (d, *J* = 8.6 Hz, 2H), 8.02 (d, *J* = 8.6 Hz, 2H), 7.76 (br d, *J* = 8.2 Hz, 2H), 7.20 (br d, *J* = 8.2 Hz, 2H), 5.53 (qd, *J* = 6.4, 4.6 Hz, 1H), 4.07 (br d, *J* = 4.6 Hz, 1H), 4.03 (ddd, *J* = 12.0, 9.9, 3.5 Hz, 1H), 3.88 (ddd, *J* = 12.0, 9.5, 7.6 Hz, 1H), 2.43 (ddd, *J* = 18.7, 7.6, 3.5 Hz, 1H), 2.40 (s, 3H), 2.26 (ddd, *J* = 18.7, 9.9, 9.5 Hz, 1H), 1.51 (d, *J* = 6.4 Hz, 3H). ^{13}C{^{1}H} NMR (126 MHz, $CDCl_3$): δ = 208.9, 165.8, 150.6, 144.7, 144.1, 129.9, 129.6, 128.8, 127.0, 125.0, 70.6, 66.5, 45.6, 36.9, 22.0, 17.4. HRMS (ESI-TOF, positive): *m*/*z* calcd for $C_{20}H_{21}N_2O_7S$ $[M + H]^+$ 433.1064; found 433.1064. IR (DRIFT): $\bar{\nu}$ = 2980, 2961, 2874, 1935, 1763, 1707, 1528, 1452, 1346, 1309, 1266, 1165, 1086, 752, 734 cm^{-1}. $[\alpha]_D^{24}$ = +50.0° (*c* = 0.00131 g/mL, MeCN).

(+)-(*R*)-1-((*S*)-1-((4-Nitrophenyl)sulfonyl)-3-oxopyrrolidin-2-yl)ethyl 4-Methoxybenzoate 4f. Reaction conditions: 24 h at room temperature. Pale yellow amorphous solid (55.0 mg, 0.118

DOI: 10.1021/acs.joc.9b02932
J. Org. Chem. 2020, 85, 985−993

mmol, 42%). The crude product was purified by semipreparative HPLC chromatography. HPLC purity 99%. ^{1}H NMR (500 MHz, $CDCl_3$): δ = 8.28 (d, J = 8.9 Hz, 2H), 8.03 (d, J = 8.9 Hz, 2H), 7.83 (br d, J = 8.9 Hz, 2H), 6.87 (br d, J = 8.9 Hz, 2H), 5.52 (qd, J = 6.6, 4.6 Hz, 1H), 4.06 (br d, J = 4.6 Hz, 1H), 4.02 (ddd, J = 12.9, 9.8, 3.4 Hz, 1H), 3.89 (ddd, J = 12.9, 9.3, 7.7 Hz, 1H), 3.85 (s, 3H), 2.42 (ddd, J = 18.6, 7.7, 3.4 Hz, 1H), 2.25 (ddd, J = 18.6, 9.8, 9.3 Hz, 1H), 1.50 (d, J = 6.6 Hz, 3H). ^{13}C{^{1}H} NMR (126 MHz, $CDCl_3$): δ = 208.9, 165.5, 164.1, 150.7, 144.1, 132.0, 128.8, 125.0, 122.1, 114.1, 70.4, 66.5, 55.8, 45.6, 36.9, 17.4. HRMS (ESI-TOF, negative): m/z calcd for $C_{20}H_{19}N_2O_8S$ [M − H]$^-$ 447.0857; found 447.0846. IR (DRIFT): $\bar{\nu}$ = 1940, 1766, 1701, 1529, 1510, 1345, 1313, 1255, 1165, 1087, 1026, 854, 735 cm^{-1}. $[\alpha]_D^{24}$ = +34.2° (c = 0.00130 g/mL, MeCN).

(+)-(*R*)-1-((*S*)-1-((4-Nitrophenyl)sulfonyl)-3-oxopyrrolidin-2-yl)ethyl 4-(Trifluoromethyl)-benzoate 4g. Reaction conditions: 24 h, heating at 40 °C in an oil bath. White amorphous solid (21.7 mg, 0.045 mmol, 18%). The crude product was purified by semipreparative HPLC chromatography. HPLC purity 98%. ^{1}H NMR (500 MHz, $CDCl_3$): δ = 8.37 (d, J = 8.6 Hz, 2H), 8.08 (br d, J = 8.6 Hz, 4H), 7.70 (br d, J = 8.2 Hz, 2H), 5.63 (qd, J = 6.5, 4.6 Hz, 1H), 4.01 (br d, J = 4.6 Hz, 1H), 3.88−3.91 (m, 2H), 2.42 (ddd, J = 18.6, 7.9, 4.4 Hz, 1H), 2.22 (ddd, J = 18.6, 10.4, 9.2 Hz, 1H), 1.55 (d, J = 6.5 Hz, 3H). ^{13}C{^{1}H} NMR (126 MHz, $CDCl_3$): δ = 208.3, 164.7, 150.9, 143.3, 135.3 (q, J = 32.8 Hz), 133.1, 130.4, 129.1, 125.9 (q, J = 3.7 Hz), 123.8 (q, J = 273.0 Hz), 125.1, 71.5, 65.9, 45.6, 36.9, 16.9. HRMS (ESI-TOF, negative): m/z calcd for $C_{20}H_{16}F_3N_2O_7S$ [M − H]$^-$ 485.0625; found 485.0614. IR (DRIFT): $\bar{\nu}$ = 2980, 2961, 1943, 1765, 1718, 1530, 1411, 1323, 1269, 1165, 1087, 1016, 856, 757 cm^{-1}. $[\alpha]_D^{24}$ = +55.7° (c = 0.00114 g/mL, MeCN).

(+)-(*R*)-1-((*S*)-1-((4-Nitrophenyl)sulfonyl)-3-oxopyrrolidin-2-yl)ethyl Acetate 4h. Reaction conditions: 72 h at room temperature. Pale yellow amorphous solid (32.1 mg, 0.090 mmol, 33%). The crude product was purified by semipreparative HPLC chromatography. HPLC purity 98%. ^{1}H NMR (500 MHz, $CDCl_3$): δ = 8.41 (d, J = 8.3 Hz, 2H), 8.08 (d, J = 8.3 Hz, 2H), 5.33 (qd, J = 6.3, 3.7 Hz, 1H), 3.91 (br d, J = 3.7 Hz, 1H), 3.88 (ddd, J = 18.6, 10.2, 3.7 Hz, 1H), 3.82 (ddd, J = 12.3, 8.6, 7.7 Hz, 1H), 2.35 (ddd, J = 18.6, 7.7, 3.7 Hz, 1H), 2.10 (ddd, J = 18.6, 10.2, 9.1 Hz, 1H), 2.01 (s, 3H), 1.41 (d, J = 6.6 Hz, 3H). ^{13}C{^{1}H} NMR (126 MHz, $CDCl_3$): δ = 209.0, 170.0, 150.9, 143.7, 129.1, 125.2, 71.2, 66.3, 45.7, 36.8, 21.3, 17.0. HRMS (ESI-TOF, positive): m/z calcd for $C_{14}H_{17}N_2O_7S$ [M + H]$^+$ 357.0751; found 357.0751. IR (DRIFT): $\bar{\nu}$ = 2982, 2962, 2876, 1815, 1763, 1709, 1532, 1351, 1309, 1238, 1168, 1089, 856 cm^{-1}. $[\alpha]_D^{24}$ = +103.2° (c = 0.00109 g/mL, MeCN).

(+)-(*S*)-(1-((4-Nitrophenyl)sulfonyl)-3-oxopyrrolidin-2-yl)-methyl Benzoate 4j. Reaction conditions: 72 h at room temperature. White amorphous solid (15.8 mg, 0.039 mmol, 14%). The crude product was purified by semipreparative HPLC chromatography. HPLC purity 97%. ^{1}H NMR (500 MHz, $CDCl_3$): δ = 8.21 (d, J = 8.6 Hz, 2H), 7.99 (d, J = 8.6 Hz, 2H), 7.70−7.74 (m, 2H), 7.512−7.58 (m, 1H), 7.35−7.40 (m, 2H), 4.78 (dd, J = 11.7, 3.4 Hz, 1H), 4.57 (dd, J = 11.7, 2.6 Hz, 1H), 4.15 (dd, J = 3.4, 2.6 Hz, 1H), 3.97 (ddd, J = 10.2, 8.6, 6.3 Hz, 1H), 3.75 (ddd, J = 10.2, 8.0, 8.0 Hz, 1H), 2.66−2.72 (m, 2H). ^{13}C{^{1}H} NMR (126 MHz, $CDCl_3$): δ = 207.7, 165.7, 150.5, 144.1, 134.0, 129.6, 129.1, 128.9, 128.6, 124.9, 64.0, 62.3, 44.9, 37.0. HRMS (ESI-TOF, negative): m/z calcd for $C_{18}H_{15}N_2O_7S$ [M − H]$^-$ 403.0594; found 403.0599. IR (DRIFT): $\bar{\nu}$ = 2979, 2959, 2896, 1948, 1762, 1721, 1522, 1344, 1265, 1162, 1147, 1094, 855, 712, 687 cm^{-1}. $[\alpha]_D^{24}$ = +56.5° (c = 0.00114 g/mL, MeCN).

(+)-*N*-(*R*)-1-((*S*)-1-((4-Nitrophenyl)sulfonyl)-3-oxopyrrolidin-2-yl)ethyl Benzamide 4k. Reaction conditions: 72 h at room temperature. Pale white-pink amorphous solid (21.2 mg, 0.051 mmol, 14%). The crude product was purified by semipreparative HPLC chromatography. HPLC purity 99%. ^{1}H NMR (500 MHz, $CDCl_3$): δ = 8.30 (d, J = 8.4 Hz, 2H), 8.04 (d, J = 8.4 Hz, 2H), 7.87−7.93 (m, 2H), 7.53−7.59 (m, 1H), 7.38−7.45 (m, 2H), 5.57 (dq, J = 6.3, 3.8 Hz, 1H), 4.07 (br d, J = 3.8 Hz, 1H), 4.00 (ddd, J = 12.2, 9.9, 3.9 Hz, 1H), 3.90 (ddd, J = 12.2, 9.5, 8.0 Hz, 1H), 2.42 (ddd, J = 18.4, 8.0, 3.9 Hz, 1H), 2.24 (ddd, J = 18.4, 9.9, 9.5 Hz, 1H), 1.53 (d, J = 6.3 Hz, 3H). ^{13}C{^{1}H} NMR (126 MHz, $CDCl_3$): δ = 208.8, 165.8, 143.9, 133.8, 129.9, 129.8, 128.9, 128.9, 125.0, 70.9, 66.4, 45.7, 36.9, 17.3. HRMS (ESI-TOF, positive): m/z calcd for $C_{19}H_{20}N_3O_6S$ [M + H]$^+$ 418.1067; found 418.1067. IR (DRIFT): $\bar{\nu}$ = 2980, 2961, 1935, 1765, 1528, 1451, 1345, 1311, 1265, 1165, 1086, 855, 757, 711 cm^{-1}. $[\alpha]_D^{24}$ = +69.4° (c = 0.00142 g/mL, MeCN).

■ ASSOCIATED CONTENT

Supporting Information

This material is available free of charge via the Internet. The Supporting Information is available free of charge at https://pubs.acs.org/doi/10.1021/acs.joc.9b02932.

Details of analytical results along with spectroscopic data for the synthesized compounds (PDF)

■ AUTHOR INFORMATION

Corresponding Author

*E-mail: miroslav.soural@upol.cz.

ORCID

Jiří Pospíšil: 0000-0002-0198-8116

Miroslav Soural: 0000-0001-7288-8617

Notes

The authors declare no competing financial interest.

■ ACKNOWLEDGMENTS

This work was supported by an internal grant from Palacký University (IGA_LF_2019_019) and the Ministry of Health of the Czech Republic (17-31834A). Jiří Pospíšil is greateful for support from European Regional Development Fund-Project "Centre for Experimental Plant Biology" (no. CZ.02.1.01/0.0/0.0/16_019/0000738). Dr. Hiroyuki Koshino, (RIKEN, Japan) is acknowledged for his confirmation of the final structure **4a** using NMR data.

■ REFERENCES

(1) Fülöpová, V.; Soural, M. Mining the Chemical Space: Application of 2/4-Nitrobenzenesulfonamides in Solid-Phase Synthesis. *ACS Comb. Sci.* **2015**, *17* (10), 570−591.

(2) Schützneróvá, E.; Krchňák, V. Intramolecular Arylation of 2-Nitrobenzenesulfonamides: A Route to Diverse Nitrogenous Heterocycles BT - Solid-Phase Synthesis of Nitrogenous Heterocycles. *Top. Heterocycl. Chem.* **2017**, *52*, 139−165.

(3) Králová, P.; Fülöpová, V.; Maloň, M.; Volná, T.; Popa, I.; Soural, M. Stereoselective Polymer-Supported Synthesis of Morpholine- and Thiomorpholine-3-Carboxylic Acid Derivatives. *ACS Comb. Sci.* **2017**, *19* (3), 173−180.

(4) Králová, P.; Ručilová, V.; Soural, M. Polymer-Supported Syntheses of Heterocycles Bearing Oxazine and Thiazine Scaffolds. *ACS Comb. Sci.* **2018**, *20* (9), 529−543.

(5) Scully, S. S.; Zheng, S.-L.; Wagner, B. K.; Schreiber, S. L. Synthesis of Oxazocenones via Gold(I)-Catalyzed 8-Endo-Dig Hydroalkoxylation of Alkynamides. *Org. Lett.* **2015**, *17* (3), 418−421.

(6) Holt, C.; Alachouzos, G.; Frontier, A. J. Leveraging the Halo-Nazarov Cyclization for the Chemodivergent Assembly of Functionalized Haloindenes and Indanones. *J. Am. Chem. Soc.* **2019**, *141* (13), 5461−5469.

(7) Wang, W.; Xu, B.; Hammond, G. B. Synthesis of Functionalized α,α-Disubstituted β-Alkynyl Esters from Allenoates through an Alkynylenolate Intermediate. *Org. Lett.* **2008**, *10* (17), 3713−3716.

(8) Iio, K.; Sachimori, S.; Watanabe, T.; Fuwa, H. Ruthenium-Catalyzed Intramolecular Double Hydroalkoxylation of Internal Alkynes. *Org. Lett.* **2018**, *20* (24), 7851−7855.

DOI: 10.1021/acs.joc.9b02932
J. Org. Chem. 2020, 85, 985−993

(9) Diéguez-Vázquez, A.; Tzschucke, C. C.; Lam, W. Y.; Ley, S. V. PtCl4-Catalyzed Domino Synthesis of Fused Bicyclic Acetals. *Angew. Chem., Int. Ed.* **2008**, *47* (1), 209−212.
(10) Alcaide, B.; Almendros, P.; Carrascosa, R.; Torres, M. R. Gold/Acid-Cocatalyzed Regiodivergent Preparation of Bridged Ketals via Direct Bis-Oxycyclization of Alkynic Acetonides. *Adv. Synth. Catal.* **2010**, *352* (8), 1277−1283.
(11) Gharpure, S. J.; Vishwakarma, D. S.; Nanda, S. K. Lewis Acid Mediated"Endo-Dig" Hydroalkoxylation−Reduction on Internal Alkynols for the Stereoselective Synthesis of Cyclic Ethers and 1,4-Oxazepanes. *Org. Lett.* **2017**, *19* (24), 6534−6537.
(12) Komoda, T.; Kishi, M.; Abe, N.; Sugiyama, Y.; Hirota, A. Novel Lipoxygenase Inhibitors, Tetrapetalone B, C, and D from Streptomyces Sp. *Biosci., Biotechnol., Biochem.* **2004**, *68* (4), 903−908.
(13) Kempf, K.; Schmitt, F.; Bilitewski, U.; Schobert, R. Synthesis, Stereochemical Assignment, and Bioactivity of the Penicillium Metabolites Penicillenols B1 and B2. *Tetrahedron* **2015**, *71* (31), 5064−5068.
(14) Muehlebach, M.; Pitterna, T.; Cassayre, J. Y.; Edmunds, A.; Corsi, C.; El Qacemi, M.; Hall, R. G.; Jeanguenat, A.; Stoller, A.; Godfrey, C. R.; et al.. Spiroheterocyclic N-Oxypiperidines as Pesticides. WO 2010066780 A1, June 17, 2010.
(15) Cao, B.; Hutt, O. E.; Zhang, Z.; Li, S.; Heazlewood, S. Y.; Williams, B.; Smith, J. A.; Haylock, D. N.; Savage, G. P.; Nilsson, S. K. Design, Synthesis and Binding Properties of a Fluorescent A9β1/A4β1 Integrin Antagonist and Its Application as an in Vivo Probe for Bone Marrow Haemopoietic Stem Cells. *Org. Biomol. Chem.* **2014**, *12* (6), 965−978.
(16) Hausherr, A.; Siemeister, G.; Reissig, H.-U. Alkoxyallene-Based Syntheses of Preussin and Its Analogs and Their Cytotoxicity. *Org. Biomol. Chem.* **2019**, *17* (1), 122−134.
(17) Cheng, X.-C.; Wang, Q.; Fang, H.; Tang, W.; Xu, W.-F. Design, Synthesis and Evaluation of Novel Sulfonyl Pyrrolidine Derivatives as Matrix Metalloproteinase Inhibitors. *Bioorg. Med. Chem.* **2008**, *16* (10), 5398−5404.
(18) Soural, M.; Hlaváč, J.; Krchňák, V. In *Solid-Phase Organic Synthesis: Concepts, Strategies and Applications*; Toy, P. H., Lam, Y., Eds.; Wiley, 2012; pp 95−130.
(19) It is expected that lacking the Thorp−Ingold effect in serine-based precursor (**3j** vs, e.g., **3a**) is responsible for the slower cyclization process. For the Thorp−Ingold effect, see: Beesley, R. M.; Ingold, C. K.; Thorpe, J. F. CXIX.—The Formation and Stability of Spiro-Compounds. Part I. Spiro-Compounds from Cyclohexane. *J. Chem. Soc., Trans.* **1915**, *107*, 1080−1106.
(20) For similar Lewis acid (TMSOTf or $BF_3{\cdot}OEt_2$) promoted esterification processes, see: (a) Fu, X.; Abbas, S. A.; Schmitz, F. J.; Vidavsky, I.; Gross, M. L.; Laney, M.; Schatzman, R. C.; Cabuslay, R. D. New Acetylenic Metabolites from the Marine Sponge Pellina Triangulata. *Tetrahedron* **1997**, *53* (3), 799−814. (b) Procopiou, P. A.; Baugh, S. P. D.; Flack, S. S.; Inglis, G. G. A. An Extremely Powerful Acylation Reaction of Alcohols with Acid Anhydrides Catalyzed by Trimethylsilyl Trifluoromethanesulfonate. *J. Org. Chem.* **1998**, *63* (7), 2342−2347.
(21) For literature precedent, see: Al-Huniti, M. H.; Lepore, S. D. Zinc(II) Catalyzed Conversion of Alkynes to Vinyl Triflates in the Presence of Silyl Triflates. *Org. Lett.* **2014**, *16* (16), 4154−4157.
(22) Kadaba, P. K. Boron Trifluoride Etherate-Alcohol, a Versatile Reagent for the Esterification Reaction. *Synth. Commun.* **1974**, *4*, 167−181.
(23) Martin, G. E.; Hadden, C. E. Long-Range 1H-15N Heteronuclear Shift Correlation at Natural Abundance. *J. Nat. Prod.* **2000**, *63* (4), 543−585.
(24) Kleinbeck, F.; Toste, F. D. Gold(I)-Catalyzed Enantioselective Ring Expansion of Allenylcyclopropanols. *J. Am. Chem. Soc.* **2009**, *131* (26), 9178−9179.
(25) Wadsworth, D. H.; Geer, S. M.; Detty, M. R. Preparation of Arylpropiolate Esters from Trichlorocyclopropenium Cation and Elaboration of the Esters to Unsymmetrical 1,4-Pentadiyn-3-Ones and Unsymmetrical Tellurapyranones. *J. Org. Chem.* **1987**, *52* (16), 3662−3668.

DOI: 10.1021/acs.joc.9b02932
J. Org. Chem. 2020, 85, 985−993

Palacký University Olomouc
Faculty of Science
Department of Organic Chemistry

Diversity-Oriented Synthesis Using Immobilized 2/4-Nitrobenzensulfonamides As The Key Intermediates

Summary of Ph.D. Thesis

Author:	Mgr. Petra Králová
Study Programme:	Chemistry
Field of Study:	Organic Chemistry
Supervisor:	doc. RNDr. Miroslav Soural, Ph.D.
Opponents:	doc. RNDr. Jan Veselý, Ph.D.
	Ing. Petr Beier, Ph.D.

Olomouc 2020

The Ph.D. thesis is processed based on the results, which were obtained during Ph.D. studies in the years 2016 – 2020, within the study programme P1417 Chemistry (field of study Organic Chemistry), guaranteed by the Department of Organic Chemistry, Faculty of Science, Palacký University Olomouc.

Author	Mgr. Petra Králová Department of Organic Chemistry, Faculty of Science, Palacký University Olomouc
Supervisor	doc. RNDr. Miroslav Soural, Ph.D. Department of Organic Chemistry, Faculty of Science, Palacký University Olomouc
Opponents	doc. RNDr. Jan Veselý, Ph.D. Department of Organic Chemistry, Faculty of Science, Charles University Prague
	Ing. Petr Beier, Ph.D. Institute of Organic Chemistry and Biochemistry of the Czech Academy of Sciences (IOCB) Prague

The oral defense will take place on ……..... in front of the committee for defense of the doctoral thesis at the Department of Organic Chemistry, Faculty of Science, Palacký University, Olomouc. The thesis is available since 29th May 2020 at the same place and on the STAG system in an electronic form.

Declaration of originality

I declare hereby with my signature, that this Ph.D. thesis represents my original work made with the best of my knowledge and that I have used no other sources except for referred citations. Neither the thesis nor any of its substantial parts were previously used for awarding of any other academic degree.

In Olomouc, 29th May 2020

.....

Mgr. Petra Králová

ABSTRACT

My Ph.D. thesis is focused on the diversity-oriented synthesis using immobilized 2/4-nitrobenzensulfonamides as the key intermediates to prepare single and fused nitrogenous heterocycles. The preparation of these derivatives was performed using solid-phase synthesis (SPS) that yielded the common intermediate, i.e. *α*-amino ketone which was further modified to final products. The following subchapter introduces to SPS, diversity-oriented synthesis (DOS) and our previous research in the field of *N*-sulfonyl and *N*-acyl morpholine-3-carboxylic acid derivatives[1,2] which has become a major inspiration for all of our projects described in this thesis. *Aims of the work* outlined specific goals in more details.

The first two subchapters of *Results and discussion* are dealing with the synthesis of fused [7+6] morpholine derivatives, namely benzoxazino[4,3-*b*][1,2,5]thiadiazepinone 6,6-dioxides **I** and benzo[*e*][1,4]oxazino[4,3-*a*][1,4]diazepine-6,12-diones **II**. These derivatives were prepared from immobilized *α*-amino ketones which were reacted with 2-nitrobenzensulfonyl chlorides or 2-nitrobenzoic acid derivatives. In the first case, the immobilized 2-nitrobenzensulfonamides were reduced on the resin with sodium dithionite followed by the cleavage of the resulting amino derivatives from the polymer-support and subsequent cyclization to morpholino-benzothiadiazepines **I**. The applicability of triethylsilane (TES) for the stereoselective reduction of the double bond and the role of solvents in the cyclization step were studied. After that, the attention was paid to acylation of immobilized *α*-amino ketones with 2-nitrobenzoic acids. According to previously reported results,[3] the on-resin reduction of nitro group of *N*-acyl intermediates and their cyclization yielded benzodiazepin-5-ones. In our case, the immobilized *N*-acyl intermediates were cleaved from the resin and then subjected to TES reduction, hydrogenation and acid-mediated cyclization to provide benzooxazino-diazepindiones **II**. In both cases, the configuration of all stereocenters was determined using a combination of chiral supercritical fluid chromatography (SFC) and advanced nuclear magnetic resonance (NMR) experiments.

To further extend this methodology, the immobilized *α*-amino ketones were reacted with natural *α*-amino acids or *α*-halocarboxylic acid derivatives. The resulting intermediates were used to prepare fused pyrazino-oxazines **III** and fused diketomorpholines **IV** depending on the types of used reaction conditions.

In the next two stages, the immobilized *α*-amino ketones were reacted with Fmoc-/*N*-substituted-isothiocyanates to obtain thioureas as potential intermediates of fused [6+5] heterocycles bearing the thiohydantoin scaffold **V**. The reaction sequence was tested on two types of resins, such as Wang resin and Wang-piperazine resin; however, the expected fused morpholines were not observed. In contrast, imidazole derivatives **VI-VII** were obtained.

Furthermore, alkynols were used as the alkylating agents and these intermediates were subjected to acid-mediated cleavage from the polymer-support and reacted with trimethylsilyl trifluoromethanesulfonate (TMSOTf). In contrast to the previously reported 1,4-oxazepanes,[4] this reaction afforded pyrrolidin-3-ones **VIII** *via* pinacol-like rearrangement.

For this reason, our last project was devoted to the alternative synthesis of fused 1,4-oxazepanes **IX**. These derivatives were synthetized from the polymer-supported *N*-alkynyl, *N*-alkenyl or *N*-alkylsulfonamides prepared from commercially available Fmoc-amino acids (e.g. L-serine, L-threonine and L-homoserine), sulfonyl chlorides, alkynols, cinnamyl alcohols and *α*-bromoketones, respectively.

The developed application of immobilized *α*-amino ketones in SPS of heterocycles

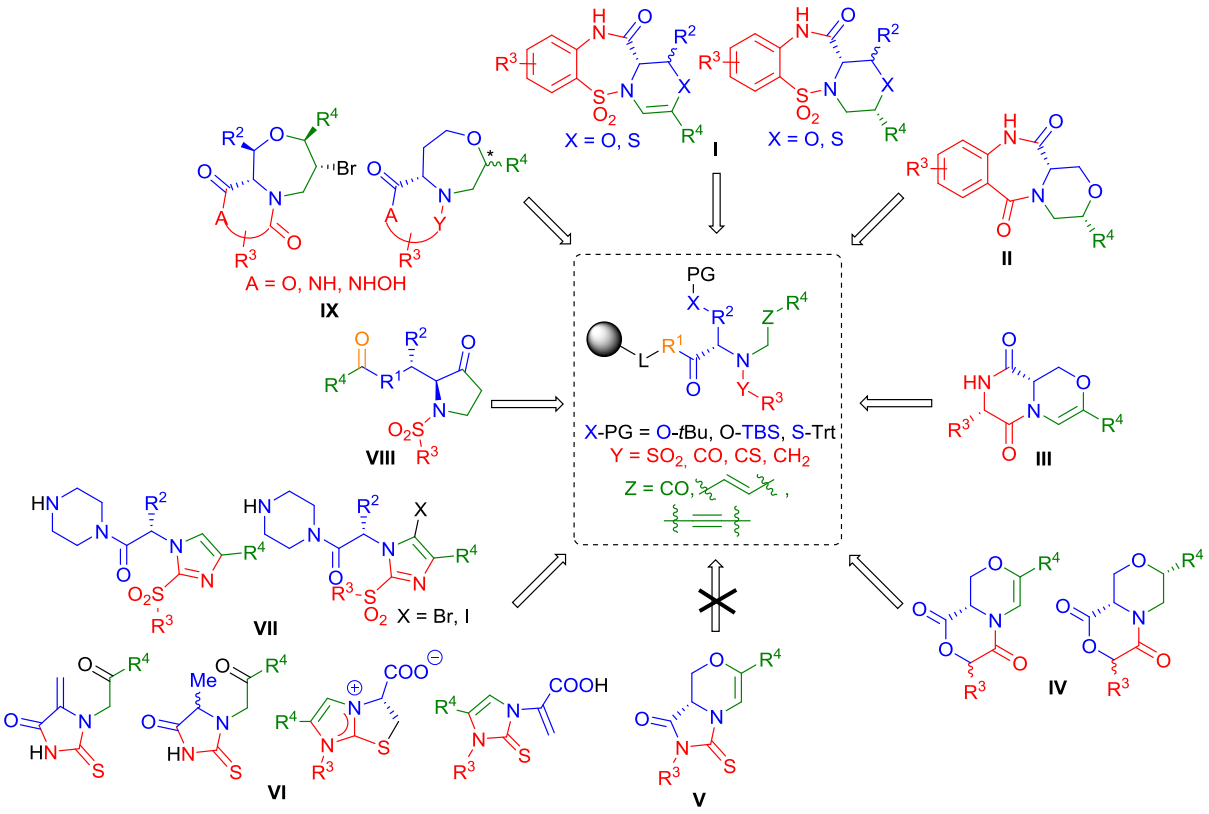

SOUHRN

Moje disertační práce je zaměřena na divergentně orientovanou syntézu pomocí imobilizovaných 2/4-nitrobenzensulfonamidů jako klíčových intermediátů za účelem přípravy jednoduchých a fúzovaných dusíkatých heterocyklů. Tyto deriváty byly připraveny pomocí syntézy na pevné fázi (SPS) vedoucí ke společnému intermediátu, tzn. *α*-amino ketonu, který byl dále modifikován na finální deriváty. V následující kapitola uvádí čtenáře do problematiky SPS, divergentně orientované syntézy (DOS) a problematiky našeho předchozího výzkumu v oblasti *N*-sulfonyl and *N*-acyl derivátů morfolin-3-karboxylových kyselin,[1,2] který byl naší hlavní inspirací pro všechny následující projekty popsané v této práci. Přičemž *Cíle práce* jsou blíže nastíněny v další podkapitole.

První dvě podkapitoly části *Výsledky a diskuse* se zabývají syntézou fúzovaných [7+6] morfolinových derivátů, tedy benzoxazino[4,3-*b*][1,2,5]thiadiazepinon 6,6-dioxidů **I** a benzo[*e*][1,4]oxazino[4,3-*a*][1,4]diazepin-6,12-dionů **II**. Tyto deriváty byly připraveny z imobilizovaných *α*-amino ketonů reagujících dále s 2-nitrobenzensulfonyl chloridy a deriváty 2-nitrobenzoových kyselin. V prvním případě byly imobilizované 2-nitrobenzensulfonamidy redukovány na pryskyřici pomocí dithioničitanu sodného za následného odštěpení výsledného amino derivátu z polymerního nosiče a cyklizace na morfolino-benzothiadiazepiny **I**. Dále byla studována aplikace triethylsilanu (TES) pro stereoselektivní redukci dvojné vazby a také role rozpouštědel ovlivňující cyklizační krok. Dále byla naše pozornost věnována acylacím imobilizovaných *α*-amino ketonů pomocí derivátů 2-nitrobenzoových kyselin. V souladu s dříve publikovanými výsledky,[3] redukce nitro skupiny na polymerně vázaných *N*-acyl intermediátech a jejich následná cyklizace vedly k benzodiazepin-5-onům. V našem případě byly imobilizované *N*-acyl intermediáty odštěpeny z polymerního nosiče a poté podrobeny redukci s TES, hydrogenaci a kysele zprostředkované cyklizaci vedoucí k odpovídajícím benzoxazino-diazepindionům **II**. V obou případech byla přesná konfigurace nově vzniklých stereocenter určena pomocí kombinace chirální superkritické fluidní chromatografie (SFC) a pokročilých experimentů nukleární magnetické rezonance (NMR).

Dále byly imobilizované *α*-amino ketony ponechány reagovat s *α*-aminokyselinami a deriváty *α*-halokarboxylových kyselin. Příslušné intermediáty byly použity k přípravě fúzovaných pyrazino-oxazinů **III** a fúzovaných diketomorfolinů **IV** vznikajících v závislosti na typů použitých reakčních podmínek.

Poté byly imobilizované *α*-amino ketony ponechány reagovat s Fmoc-/*N*-substituovanými isothiokyanáty k získání thiomočovin jako potenciálních intermediátů fúzovaných [6+5] heterocyklů nesoucích thiohydantoinový skelet **V**. Tato reakční sekvence byla testována na dvou typech pryskyřic, a to Wangově a Wang-piperazinové pryskyřici, avšak očekávané fúzované morfoliny nebyly pozorovány, neboť docházelo k tvorbě imidazolových derivátů **VI-VII**.

Jako další alkylační činidla byly testovány alkynoly, klíčové intermediáty byly podrobeny kyselému štěpení z polymerního nosiče a reakci s trimethylsilylmethansulfonátem (TMSOTf). V porovnání s předchozím publikovaným výzkumem 1,4-oxazepanů[4] tato reakce poskytla pyrrolidin-3-ony **VIII** formující se pomocí pinakolinového přesmyku.

Z toho důvodu je náš poslední projekt věnován syntéze výše zmíněných fúzovaných 1,4-oxazepanů **IX**. Tyto deriváty byly připraveny z polymerně vázaných *N*-alkynyl, *N*-alkenyl nebo *N*-alkylsulfonamidů, které byly syntetizovány z komerčně dostupných Fmoc-amino kyselin (například L-serinu, L-threoninu a L-homoserinu), sulfonyl chloridů, alkynolů, skořicových alkoholů a *α*-bromketonů.

TABLE OF CONTENTS

LIST OF ABBREVIATIONS

Ala	alanine
AM	aminomethyl resin
AmAc	ammonium acetate
aq	aqueous solution
BAL	backbone amide linker
Boc	*tert*-butyloxycarbonyl
$(Boc)_2O$	di-*tert*-butyldicarbonate
BB test	test with bromophenol blue
BTPP	*tert*-butylimino-tri(pyrrolidino)phospho-rane
Bn	benzyl
Bz	benzoyl
CSA	(1*S*)-(+)-camphorsulfonic acid
CDI	1,1´-carbonyldiimidazole
DBU	1,8-diazabicyclo[5.4.0]undec-7-ene
DCE	1,2-dichloroethane
DCM	dichlormethane
DIAD	diisopropyl azodicarboxylate
DIEA	*N*,*N*-diisopropylethylamine
DIC	*N,N´*-diisopropylcarbodiimide
DMAP	4-(*N*,*N*-dimethylamino)pyridine
DME	1,2-dimethoxyethane
DMF	*N*,*N*-dimethylformamide
DMSO	dimethyl sulfoxide
dr.r.	diastereomeric ratio
EA	ethyl acetate
e.g.	*exempli gratia* (from Latin), for example
et al.	*et alli* (from Latin), and collective
Fmoc-OSu	*N*-(9*H*-fluoren-9-ylmethoxycarbonyloxy) succinimide
HBr	hydrobromic acid
HF	hydrofluoric acid
HOBt	1-hydroxybenzotriazole
HPLC	High Performance Liquid Chromatography
HMBC	Heteronuclear Multiple Bond Correlation
HRMS	High-Revolution Mass Spectrometry
HSe	homoserine
HSQC	Heteronuclear Single Quantum Coherence
IC_{50}	half maximal inhibitory concentration
i.e.	*id est* (from Latin), means
in situ	in the situation/position (from Latin)
IPA	2-isopropanol
LC-MS	Liquid and Mass Chromatography
M	molarity of solution
MCE	2-mercaptoethanol
*m*CPBA	*m*-chloroperoxybenzoic acid
MeCN	acetonitrile
Ms	mesyl, methanesulfonyl
NBS	*N*-bromosuccinimide
NMP	1-methyl-2-pyrrolidinone
NMR	Nuclear Magnetic Resonance
NOESY	Nuclear Overhauser Effect Spectroscopy
Nos-amide	nitrobenzensulfonamide
PG	protecting group
PIP	piperidine
PTSA	*p*-toluenesulfonic acid
Py	pyridine
ROESY	Rotating-Frame Overhauser Effect Spectroscopy
Ser	serine
SPS	solid-phase synthesis
TBAHS	tetrabutylammonium hydrogensulfide
TBS	*tert*-butyldimethylsilane
*t*Bu	*tert*-butyl
TBP	tributylphosphine
TFA	trifluoroacetic acid
THF	tetrahydrofuran
Thr	threonine
TEA	triethylamine
TES	triethylsilane
TfOH	trifluoromethanesulfonic acid
Tf_2O	trifluoromethanesulfonic acid anhydride
TI_{50}	therapeutic index
TMS	trimethylsilylether
TMSOTf	trimethylsilyl trifluoromethanesulfonate
Ts	*p*-methylbenzensulfonyl
TPP	triphenylphosphine
UHPLC	Ultra High Performance Liquid Chromatography
UV	Ultraviolet Light

1. INTRODUCTION

1.1 Introduction to solid-phase synthesis (SPS) and diversity-oriented synthesis (DOS)

SPS is an alternative method of organic synthesis which has been used to prepare peptides,[5] oligonucleotides,[6] oligosacharides[7,8] and small organic molecules.[9–11] SPS belongs to techniques that enable high-throughput synthesis of various chemical entities. It can be simply applied to combinatorial synthesis using semi-automated or fully automated approaches thus it has been applied by pharmaceutical companies to prepare chemical libraries of various sizes. SPS is based on a simple principle in which the first molecule is attached *via* linker to an insoluble polymer support (i.e. resin). The linker forms an arm among the starting molecule and the polymer support, and it enables a product cleavage from the resin upon appropriate cleavage conditions, mostly using 50% trifluoroacetic acid (TFA) in dichloromethane (DCM) depending on the type of resin used (e.g. Wang resin, Rink amide resin etc.). SPS requires simple equipment as it can be performed in a common plastic syringe with a porous disk. The synthetic protocol basically consists of an eight simple steps (Figure 1). Typically, SPS is performed in a significant excess of solution-phase reagents to complete on-resin conversion. The main advantage of SPS is rapid and simple purification of each intermediate in comparison to solution-phase chemistry; however, only the final products are purified and fully characterized using conventional analytical methods. This arrangement enables time-efficient synthesis of larger number of compounds. In our research, we have been using a combination of both SPS and a post-cleavage (solution-phase) modification; however, all the resulting protocols are fully compatible with the high-throughput synthesis concept and reagent-based diversity-oriented synthesis (DOS) which can be applied for the rapid preparation of compound collections and their subsequent biological evaluation. To fulfil DOS criteria[12] and make the synthetic pathways applicable for chemical libraries preparation, the target products were synthesized using only common coupling reagents, procedures and readily available synthons.

Figure 1. General concept of SPS

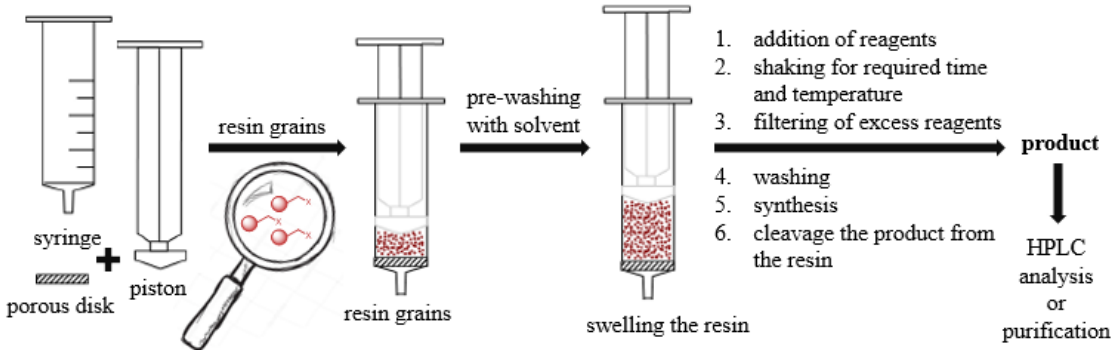

1.2 Our previous research

The following brief introduction to previous morpholine and thiomorpholine chemistry is based on the results of my Diploma thesis[1] which were published in: Králová, P.; Fülöpová, V.; Maloň, M.; Volná, T.; Popa, I.; Soural, M. *ACS Comb. Sci.* **2017**, 19 (3), 173–180.[2]

Our interest in the field of (thio)morpholines was inspired by the fact that these derivatives are widely studied derivatives[13–18] with a broad application in agricultural,[19,20] pharmaceutical[21–23] and medicinal fields.[24] More specifically, we focused to (thio)morpholines and related unsaturated analogous (e.g. oxazines

and thiazines) bearing the carbonyl group at the C3 position. My Diploma thesis was devoted to development of general synthetic route using SPS as there were only two reported articles devoted to SPS of 3,4-dihydro-2*H*-1,4-oxazino-3-carboxylic acid derivatives which have been observed as synthetic by-products.[25,26]

My Diploma thesis[1] and the corresponding publication[2] reported the synthetic approach in which *N*-sulfonyl and *N*-acyl morpholine-3-carboxylic acid derivatives were synthesized from polymer-supported 2/4-nitrobenzensulfonamides (2/4-Nos-amides) which were converted to corresponding *α*-amino ketones. Generally, 2/4-Nos-amides and *α*-amino ketones were easily synthesized from readily available starting materials: (i) Fmoc-amino acids containing hydroxy or sulfanyl groups in the side chain, e.g. L-serine, L-threonine, L-cysteine; (ii) aryl/alkyl sulfonyl chlorides or carboxylic acid derivatives and (iii) *α*-bromoketones. The resulting *N*-alkyl-Nos-amides were treated with trifluoroacetic acid (TFA) which mediated the product release from the polymer-support and yielded expected unsaturated products, i.g. 1,4-oxazines and 1,4-thiazines. The saturated thio(morpholine) analogs were prepared using triethylsilane (TES) added into the cleavage cocktail. Further, we performed the stereochemical studies to reveal the configuration of the newly formed stereocenter (Scheme 1, the resulting products in rectangles on the right).

Moreover, detailed studies on rotational stability of *N*-acylmorpholines were performed. These derivatives were obtained as a mixture of inseparable rotational isomers (rotamers) around C-N amidic bond with the characteristic doubled signals in ^{1}H NMR spectra. These rotamers were obtained in different ratios depending on R^3 substitution and both isomers were investigated in detail using 2D NMR analysis.

Finally, my Diploma thesis showed the reduction test on the *N*-(2-nitrobenzoyl)-oxazines using sodium dithionite under acidic or basic conditions which afforded prospective amino derivatives theoretically applicable for further modification. Additionally, the reaction under acidic conditions (pH 1-2) triggered spontaneous cyclization of amino compound to fused [7+6] benzoxazino-diazepine-6,12-diones observed in 38% crude purity (Scheme 1). Stimulated by this preliminary result, we decided to explore this field during my Ph.D. studies to possibly apply 2/4-Nos-amides for preparation of diverse fused heterocycles.

Scheme 1. The shortened synthesis of *α*-amino ketones and their use to prepare morpholine derivatives

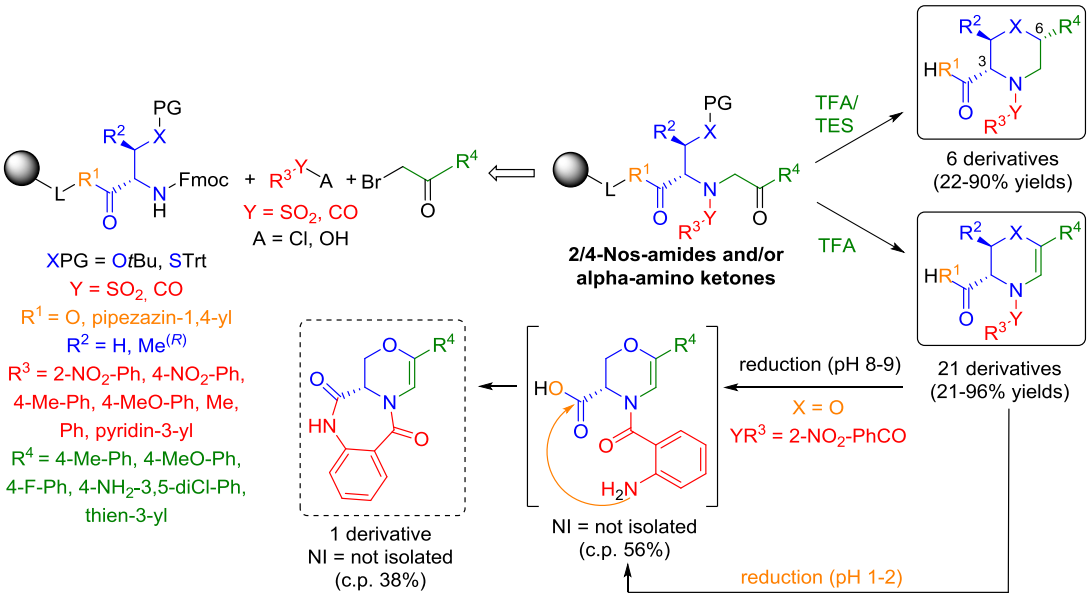

2. AIMS OF THE WORK

As stated above, the main goal of the thesis was to explore an applicability of the polymer-supported 2/4-Nos-amides as the key intermediates to prepare fused morpholine derivatives using solid-phase synthetic strategy (Figure 2-3). Consequently, it was suggested that polymer-supported 2/4-Nos-amides could be denosylated and further modified with various acylating or alkylating agents to obtain the suitable intermediates which could, after post-cleavage modification, yield the corresponding fused heterocycles. In all projects, we intended to determine the limitations and scope by using building blocks with different substitution and particularly to test TES applicability for stereoselective reduction of the double bond. In this regard, we wanted to study the configuration of all newly formed stereocenters using SFC and advanced NMR experiments.

First, the potential synthesis of fused [7+6] morpholine derivatives **I-II** was investigated in detail (Figure 2, Products I-II).[27,28] After that, the attention was paid to the preparation of fused [6+6] morpholines **III**[29] and diketomorpholines **IV**[30] (Figure 2, Products III-IV). We also suggested a methodology to prepare fused [6+5] heterocycles bearing the thiohydantoin scaffold **V** (Figure 2, Product V).[31,32] The last part of the thesis was oriented to the synthesis of functionalized 1,4-oxazepanes amenable for further diversification. In this case, the synthesis of oxazepane scaffold was suggested using four different scenarios **A-D** (Figure 3) which were inspired by the previously reported results from the field of 1,4-oxazepane derivatives.[4,33,34]

Figure 2. Overview of designed fused morpholine and thiomorpholine derivatives

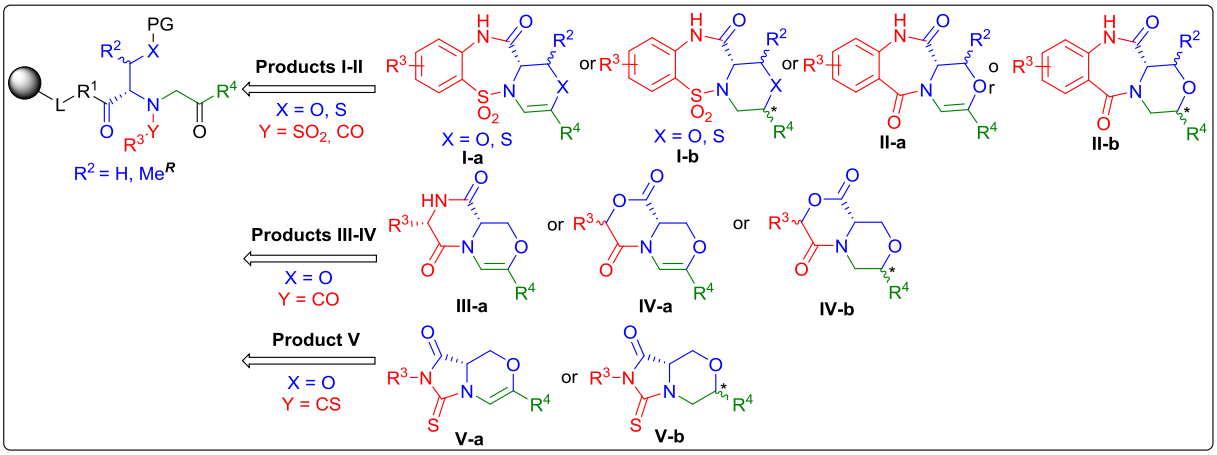

Figure 3. The possible approaches to functionalized 1,4-oxazepane derivatives

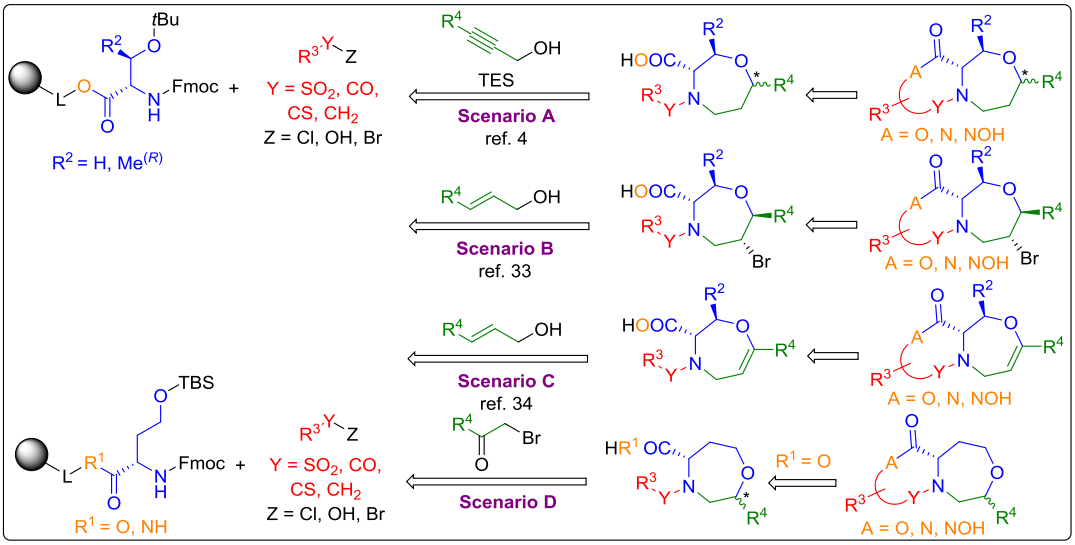

3. RESULTS AND DISCUSSION

The research was carried out at the Institute of Molecular and Translational Medicine (IMTM) under the auspice of Department of Organic Chemistry, Palacký University Olomouc. Since the in-house screening of cytotoxic and antimicrobial activity was available, we intended to screen the target compounds against selected cancer cell lines and bacterial strains to possibly identify hit compounds for further development.

Numbering of the final derivatives, linkers and building blocks used in the individual sections of the thesis is served using Chemset Numbering System that is a specific product numbering approach which is commonly used in a combinatorial chemistry and in a solid-phase synthesis (SPS). The system is based on a collection of at least two or more similar members in one category (e.g. Wang resin or Wang-piperazine resin for R^1 modification in Figure 4) and mutual combination of synthons R^2-R^x (e.g. Fmoc-amino acids for R^2 substituent, sulfonyl chlorides for R^3 substituent or α-bromoketones for R^4 substituent in Figure 4) to give the numbering of the corresponding products with various R^1-R^x substituents. To demonstrate the system, Figure 4 displays oxazine derivative **I**{*R*^{1},*R*^{2},*R*^{3},*R*^{4}} and the list of all tested building blocks for R^1-R^4 substituents. For example, in the case of product **I**{*1,1,1,1*}, the compound was synthesized from Wang resin, Fmoc-Ser(*t*Bu)-OH, 4-Nos-Cl and α-bromo-1-(*p*-tolyl)ethan-1-one. Designation of derivatives **I**{*1,1,1-4,1*} indicates that such compounds were synthesized from Wang resin, Fmoc-Ser(*t*Bu)-OH, various sulfonyl chlorides and α-bromo-1-(*p*-tolyl)ethan-1-one.

Figure 4. The structure of compound **I**{*R*^{1},*R*^{2},*R*^{3},*R*^{4}} and the list of synthons for R^1-R^4 substitution[2]

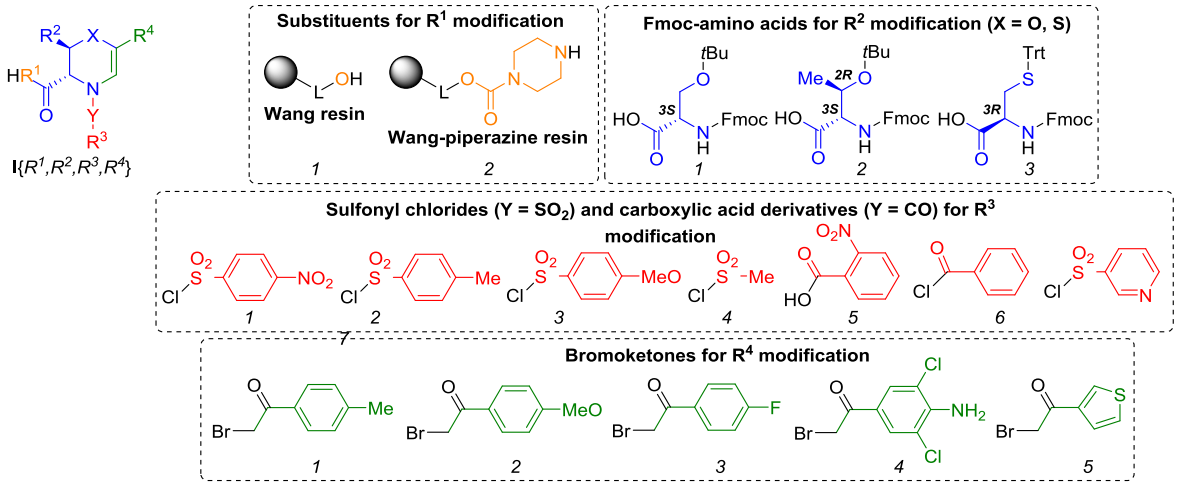

Crude purities and/or a ratios of product isomers (i.e. epimers, enantiomers and diastereoisomers) were calculated from HPLC-UV traces at 205–400 nm. An overall yield was calculated from the ^{1}H NMR spectrum of the purified product, unless otherwise stated.

3.1 Polymer-Supported Stereoselective Synthesis of Benzoxazino[4,3-*b*][1,2,5]thiadiazepinone 6,6-Dioxides

The results of this project were published in: Králová, P.; Maloň, M; Ručilová, V.; Volná, T.; M.; Soural, M. *ACS Comb. Sci.* 2017, *19* (10), 670–674.[27]

3.1.1 Brief introduction

The research builds on our previous results in the field of (thio)morpholine-3-carboxylic acid derivatives.[1,2] In this subchapter, the stereoselective synthesis of benzoxazino[4,3-*b*][1,2,5]thiadiazepinone 6,6-dioxides starting from immobilized *N*-phenacyl-2-Nos-amides is briefly outlined. These key intermediates were prepared according to the previously reported protocol[1,2] and then subjected to an on-resin reduction of the nitro group using sodium dithionite or tin(II) chloride which yielded the immobilized anilines. After the acid-mediated cleavage, the crude product should be modified using two post-cleavage reactions (i.e. acid-mediated cyclization or TES reduction) performed in solution to yield the final benzoxazino-thiadiazepinone 6,6-dioxides (Figure 5). After that, we particularly focused on the stereochemical studies to reveal the impact of both reaction steps, i.g. the TES reduction and the final cyclization step on the resulting configuration.

Figure 5. The proposed synthesis of benzoxazino[4,3-*b*][1,2,5]thiadiazepinone 6,6-dioxides

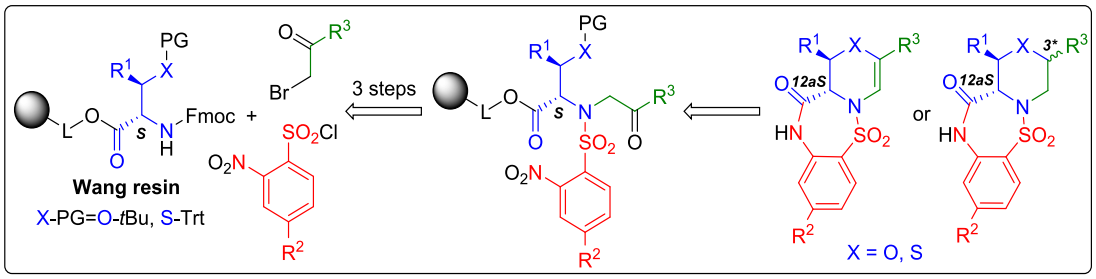

3.1.2 Synthesis

First, the Wang resin **I-1** was acylated with Fmoc-Ser(*t*Bu)-OH **I-2**{*1*} and the loading of the resulting resin was determined with the use of an external standard (Fmoc-Ala-OH) to 0.48 mmol/g. After that, the immobilized Fmoc-Ser(*t*Bu)-OH **I-2**{*1*} was subjected to the removal of the Fmoc protecting group and subsequent protection/activation with 2-Nos-Cl followed by Fukuyama monoalkylation with *α*-bromoacetophenone that yielded the resulting *N*-phenacyl sulfonamide **I-5**{*1,1,1*}. The nitro group was reduced by sodium dithionite,[35] followed by acid-mediated cleavage of intermediate **I-6**{*1,1,1*} from the solid support. Although TFA cleavage of analogous compounds previously yielded benzodiazepines **I-11**{*1,1,1*} *via* the attack of the ketone by an amino group,[3,25] we observed the preferable formation of the morpholine scaffold. The intermediate **I-7**{*1,1,1*} was obtained in high crude purity (92%). After that, we focused on a cyclization to the benzoxazino-thiadiazepinone derivative **I-9**{*1,1,1*} (Scheme 2). As TFA was used to cleave the final intermediate from the resin, we attempted to use this acid to possibly combine the cleavage conditions with the cyclization step using various tested conditions (e.g. different time, temperatures, microwave irradiation and solvents); however, the expected product **I-9**{*1,1,1*} was not achieved. For this reason, we focused on post-cleavage cyclization of oxazine **I-7**{*1,1,1*} or its carboxylic acid derivatives (e.g. chloride, ester and anhydride): (a) cyclization of chloride or methyl ester using PTSA[36] or (b) an activation of carboxylic acid with DIC or the HOBt/DIC.[37] However, in all tested cases, no required product **I-9**{*1,1,1*} was obtained.

After a number of unsuccessful experiments, we managed to accomplish the direct cyclization of carboxylic acid **I-7**{*1,1,1*} using PTSA[36] in anhydrous toluene or anhydrous DCE under Dean-Stark conditions that yielded the products **I-9**{*1,1,1*}^{tol} and **I-9**{*1,1,1*}^{DCE} (Scheme 2).

Scheme 2. Synthesis of benzoxazino-thiadiazepinone derivatives **I-9-10**{R^1,R^2,R^3}[a]

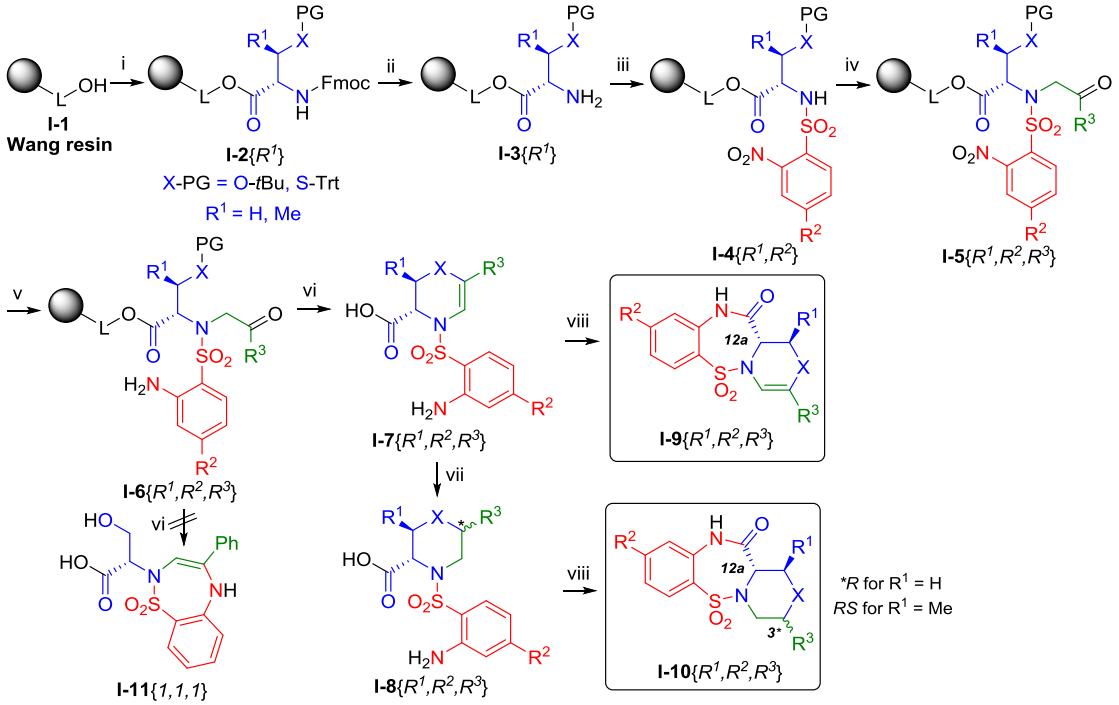

[a]Reagents and conditions: (i) Fmoc-amino acid, HOBt, DMAP, DIC, DMF, DCM, 24 h, rt; (ii) 50% PIP/DMF, 30 min, rt; (iii) 4-substituted 2-Nos-Cl, 2,6-lutidine, DCM, 24 h or 44 h for derivative **I-7**{*1,2*}, rt; (iv) R^3COCH_2Br, DIEA, DMF, 24 h or 43 h for derivative **I-7**{*1,2,1*} or 72 h for derivative **I-7**{*2,1,1*}, rt; (v) **(a)** $Na_2S_2O_4.2H_2O$, K_2CO_3, TBAHS, 50% DCM/H_2O, 2-5 h, rt (for serine and threonine derivatives) or **(b)** $SnCl_2.2H_2O$, DIEA, degassed DMF, 30 min, rt (for cysteine derivative); (vi) 50-75% TFA/DCM, 2.5-24 h, rt; (vii) TES, 1-3 h, rt; (viii) PTSA, anhydrous $PhCH_3$, 1-12 h, 110 °C or PTSA, anhydrous DCE, 1-144 h, 90 °C.

Furthermore, the impact of both solvents to crude purities, overall yields and the resulting configuration of C12*a* stereocenter was compared. The use of DCE (90 °C) provided slightly better results in comparison to toluene (110 °C). The product **I-9**{*1,1,1*}^{DCE} was obtained in 81% crude and 51% overall yield, whereas the product **I-9**{*1,1,1*}^{tol} was isolated in 77% crude purity and 35% overall yield (Table 1). Further, in the case of DCE, we observed a minor racemization (i.e. 8% of *R*-isomer) of the C12*a* stereocenter, whereas the cyclization in toluene afforded a higher proportion of *R*-isomer (i.e. 23% of *R*-isomer).

When TES was added into the cleavage cocktail after release of the product **I-6**{*1,1,1*} from the resin, the saturated analogue **I-8**{*1,1,1*} was obtained. Its cyclization to **I-10**{*1,1,1*} was tested in toluene and DCE and gave similar results (i.e. 84-85% crude purities and 41-42% overall yields, Scheme 2, Table 1). The following NMR analysis of **I-10**{*1,1,1*}^{tol} and **I-10**{*1,1,1*}^{DCE} revealed the presence of both inseparable C12*a* *S,R* isomers in a ratio of 77:23 and 92:8, respectively.

To clarify the formation of optical isomers, we investigated the stereochemical outcome of critical steps of the reaction sequence using SFC and NMR studies. In the case of unsaturated intermediate **I-7**{*1,1,1*}, the C3 stereochemistry was studied in comparison to the racemic standard **I-7**^{RS}{*1,1,1*} (L-/D-serine in a ratio of 1:1). In accordance to our previously reported results,[2] we proved that the second enantiomer (*R*, 8%) was formed during the Fmoc-Ser(*t*Bu)-OH immobilization on the Wang resin. For TES-reduced intermediate **I-8**{*1,1,1*}, detailed NMR analysis proved the stereoselective formation of C6 stereo-

center and its configuration was determined as *R*. In the case of **I-9**{*1,1,1*} and later discussed related analogues **I-9**{R^1,R^2,R^3}, SFC analysis was used to detect the possible formation of C12*a* *R,S* isomers (enantiomers), whereas NMR analysis of saturated derivatives **I-10**{*1,1,1*} and **I-10**{R^1,R^2,R^3} enabled a direct detection of both isomers (diastereomers) from the ^{1}H NMR spectra of the final products. The above mentioned approaches allowed to conclude that DCE cyclization had no impact on the resulting stereochemistry of **I-10**{*1,1,1*}^{DCE}. In contrast, the use of toluene lowered diastereomeric purity as it yielded compound **I-10**{*1,1,1*}^{tol}. For this reason, cyclization using DCE was applied as the method of choice to synthesize and study other derivatives.

3.1.3 Limitations and scope

To determine the limitations and scope of the methodology, we tested a combination of three Fmoc-amino acids with the hydroxymethyl or sulfanylmethyl groups in a side chain, various 4-substituted 2-Nos-Cl and *α*-bromoketones containing both electron donating and electron withdrawing substituents (Figure 6).

Figure 6. The list of tested synthons for R^1, R^2 and R^3 substitution

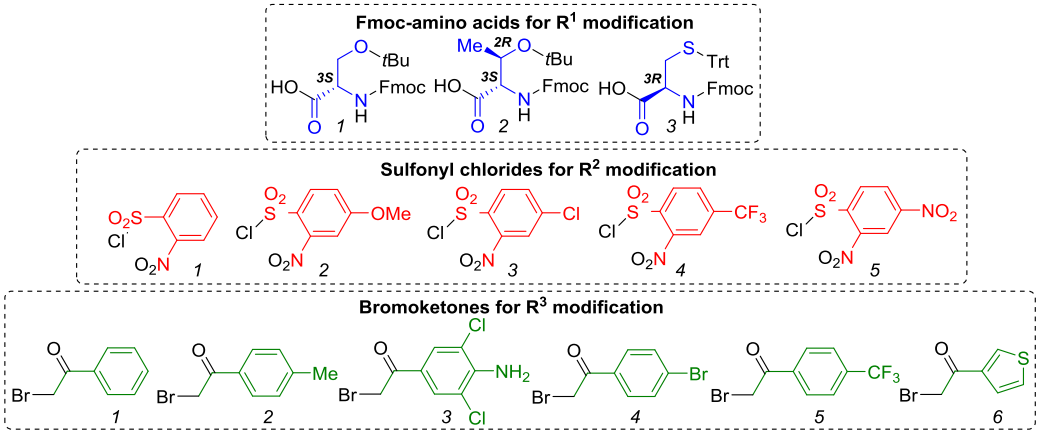

When immobilized Fmoc-Ser(*t*Bu)-OH was replaced with Fmoc-Thr(*t*Bu)-OH **I-2**{*2*}, the alkylation step required the use of a higher concentration of the alkylating agents and base to complete reaction. After that, the resulting *N*-phenacyl sulfonamide **I-5**{*2,1,1*} was reduced by sodium dithionite, followed by release the product from the resin and its cyclization using PTSA in anhydrous DCE to desired derivative **I-9**{*2,1,1*} in 92% crude purity and 32% overall yield (Scheme 2). Analogously to serine derivative **I-9**{*1,1,1*}, the use of DCE as cyclization solvent did not affect the stereochemical outcome of C12*a* stereocenter and the final derivative was obtained as a diastereomerically pure compound using SFC analysis.

In the case of mehylmorpholine derivative **I-10**{*2,1,1*}, we observed a mixture of separable C3 *S,R* isomers **I-10a**{*2,1,1*} and **I-10b**{*2,1,1*} in a ratio of 63:47 (Scheme 3, Table 1). The non-stereoselective TES reduction of threonine intermediates is in accordance with our previous research.[1,2]

In addition, the developed synthetic protocol was tested on Wang resin with immobilized Fmoc-Cys(Trt)-OH **I-2**{*3*} (Scheme 2). Interestingly, the reduction of *N*-alkyl sulfonamide **I-5**{*3,1,1*} with sodium dithionite failed in all tested cases (e.g. DCM/H_2O in a ratio of 1:1, 1:2, 1:0, 2:1, 4:1, 5:1 for 30 min at room temperature), but the use of tin(II) chloride dihydrate afforded the desired intermediate **I-6**{*3,1,1*} in excellent crude purity (94%). The final cyclization in anhydrous DCE provided desired product **I-9**{*3,1,1*} in 82% crude purity and 27% overall yield. Nevertheless, the use of Fmoc-Cys(Trt)-OH instead of Fmoc-Ser(*t*Bu)-OH and Fmoc-Thr(*t*Bu)-OH affected a pronounced racemization on the C12*a* stereocenter

and C12*a S,R* isomers were observed in ratio of 75:25. Furthermore, the TES reduction to **I-8**{*3,1,1*} was unsuccessful at room temperature after 2-70 h and even at elevated temperature (50 °C) after 70 h.

Scheme 3. The synthesis of benzomethylmorpholino-thiadiazepinones **I-10a-b**{*2,1,1*} and their key NMR correlations used to identify both separated diastereoisomers[a]

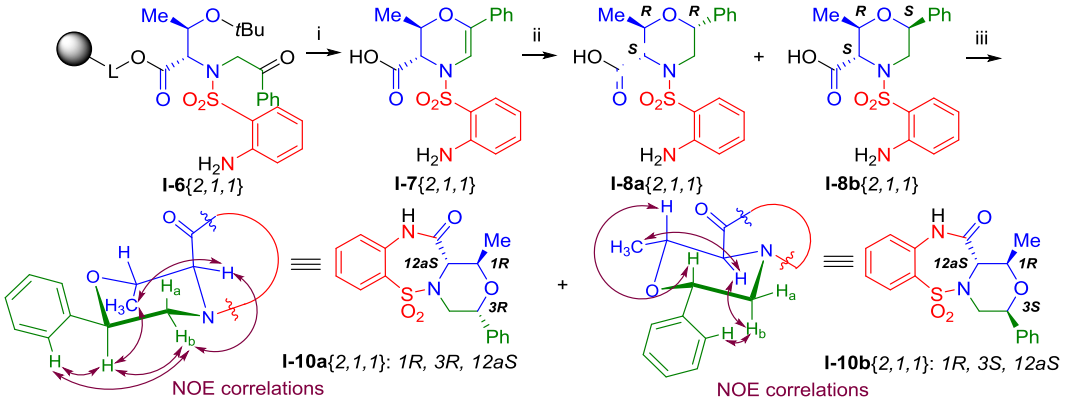

[a]Reagents and conditions: (i) 50% TFA/DCM, 4 h, rt; (ii) TES, 2 h, rt; (iii) PTSA, anhydrous DCE, 4 h, 90 °C.

To explore the diversification of R^2, all substituted 2-Nos-Cl were combined with immobilized Fmoc-Ser(*t*Bu)-OH and variously substituted *α*-bromoketones. In the case of electron-donating group (MeO) in R^2 position, the sulfonylation and the subsequent alkylation step required longer reaction time (2 days) to quantitative conversion. The reduction of all serine derivatives **I-5**{*1*,R^2,R^3} was performed with sodium dithionite and yielded compounds **I-6**{*1*,R^2,R^3} in good crude purities (82-98%, Scheme 2).

The product release from the resin as well as the subsequent TES reduction required different cleavage time depending on R^2 and R^3 substituents (1-3 h). In the case of **I-7**{*1,5,1*} and **I-7**{*1,1,5*} prepared from 2,4-dinitrobenzensulfonyl chloride and 2-bromo-1-(4-(trifluoromethyl)phenyl)-ethan-1-one, respectively, expected products were not detected by LC-MS analysis (Scheme 2, Figure 6).

Although a minor formation of target products **I-9**{R^1,R^2,R^3} and **I-10**{R^1,R^2,R^3} was observed after the TFA-mediated cleavage of intermediates **I-7**{R^1,R^2,R^3} and **I-8**{R^1,R^2,R^3} from the resin (up to 16%), prolonged exposure to the cleavage cocktail did not lead to higher conversion (above mentioned in the thesis), and heating in anhydrous DCE or toluene with PTSA catalysis was required to completion (Scheme 2). However, the cyclization to saturated products **I-10**{R^1,R^2,R^3} required significantly longer time in comparison to the unsaturated analogous **I-9**{R^1,R^2,R^3} (Table 1).

The synthesis of **I-9**{*1,1,3*}, prepared from 1-(4-amino-3,5-dichlorophenyl)-2-bromoethanone, failed in the stage of the final cyclization step. In contrast, the analogical saturated derivative **I-10**{*1,1,3*} was obtained in 82% crude purity and 36% overall yield as a mixture of C12*a S,R* isomers in a ratio of 71:29 detected in ^{1}H NMR spectrum of the purified product (Table 1). In the case of crude product **I-9**{*1,5,1*}, the derivative decomposed during semipreparative reverse-phase HPLC purification. When TES was added to the crude derivative **I-7**{*1,5,1*}, the reduction failed and no traces of product were detected by LC-MS analysis. These facts indicated that 2,4-dinitrobenzensulfonyl chloride is not compatible with the method.

From the results, we concluded that the cyclization step partially affects the resulting C12*a* configuration. Although the model compounds **I-9**{*1,1,1*}^{DCE} and **I-10**{*1,1,1*}^{DCE} have been prepared without any conversion of the C12*a* stereocenter, their substituted analogues **I-9**{R^1,R^2,R^3} and **I-10**{R^1,R^2,R^3} provided different results. In the case of unsaturated products **I-9**{R^1,R^2,R^3} cyclized in DCE, the detail SFC study revealed the presence of C12*a R* isomer in a quantity 8-28%. This indicates epimerization of C12*a* in a range

of 0-20% after the cyclization step (8% was assigned to epimerization caused by the immobilization, as mentioned earlier in the thesis). In accordance with our previous results,[1,2] the TES reduction of threonine-based derivative **I-7**{*2,1,1*} was non-stereoselective and its subsequent cyclization to benzo-morpholino-thiadiazepinones gave a mixture of both separable C3 isomers **I-10a**{*2,1,1*} and **I-10b**{*2,1,1*} in the ratio of 63:47 (Scheme 3). In contrast, in the case of saturated serine analogues **I-8**{*1*,R^2,R^3}, TES reduction of **I-7**{*1*,R^2,R^3} was fully stereoselective and the final cyclization in DCE to required products **I-10**{*1*,R^2,R^3} provided 0-29% of the second C12*a R* epimer depending on R^3 substituent. The ratio of both epimers was calculated the ^{1}H NMR spectra of the purified products (Table 1).

Table 1. The used cyclization conditions leading to target compounds[a-d]

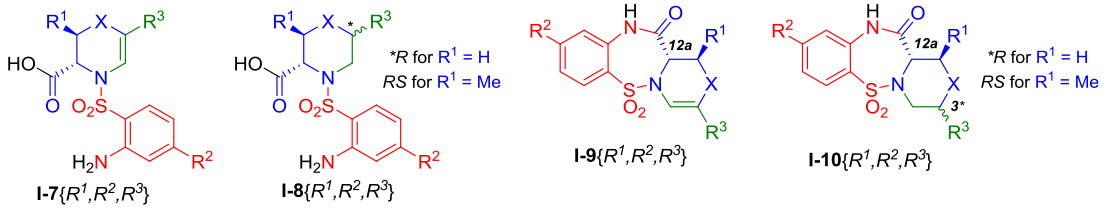

cmpd	X	R^1	R^2	R^3	PTSA [equiv]	solvent	time [h]	temp [°C]	crude purity [%][a]	final purity [%][b]	over-all yield [%][c]	ratio of *S*:*R* stereo-isomers [%][c,d]
I-7{*1,1,4*}	O	-	H	4-Br-Ph	-	-	-	-	87	98	58	-
I-8{*1,1,1*}	O	-	H	Ph	-	-	-	-	83	95	77	-
I-9{*1,1,1*}^{tol}	O	H	H	Ph	2	$PhCH_3$	3.5	110	77	99	35	77:23[d]
I-9{*1,1,1*}^{DCE}	O	H	H	Ph	2	DCE	5.5	90	81	98	51	92:8[d]
I-9{*1,2,1*}	O	H	MeO	Ph	2	DCE	4.5	90	91	99	51	75:25[d]
I-9{*1,3,1*}	O	H	Cl	Ph	2	DCE	5	90	78	98	34	77:23[d]
I-9{*1,4,1*}	O	H	CF_3	Ph	2	DCE	4.5	90	70	99	42	73:27[d]
I-9{*1,5,1*}	O	H	NH_2	Ph	2	DCE	6	90	80	NI	NI	-
I-9{*1,1,2*}	O	H	H	4-Me-Ph	2	DCE	4.5	90	88	95	44	87:13[d]
I-9{*1,1,4*}^{tol}	O	H	H	4-Br-Ph	2	$PhCH_3$	1	90	65	97	40	63:37[d]
I-9{*1,1,5*}	O	H	H	4-CF_3-Ph	2	DCE	4.5	110	95	99	41	77:23[d]
I-9{*1,1,6*}	O	H	H		2	DCE	1	90	85	95	5	72:28[d]
I-9{*2,1,1*}	O	Me	H	Ph	2	DCE	6	90	92	99	32	100:0[d]
I-9{*3,1,1*}	S	H	H	Ph	2	DCE	27	90	82	90	27	75:25[d]
I-10{*1,1,1*}^{tol}	O	H	H	Ph	2	$PhCH_3$	4	110	84	95	41[e]	77:23[c]
I-10{*1,1,1*}^{DCE}	O	H	H	Ph	2	DCE	3	90	85	98	42[e]	92:8[c]
I-10{*1,2,1*}	O	H	MeO	Ph	2	DCE	5	90	90	98	39	100:0[c]
I-10{*1,3,1*}	O	H	Cl	Ph	2	DCE	144	90	70	99	38	100:0[c]
I-10{*1,4,1*}	O	H	CF_3	Ph	2	DCE	3	90	57	98	40	100:0[c]
I-10{*1,1,2*}	O	H	H	4-Me-Ph	2	DCE	25	90	91	99	42[e]	87:13[c]
I-10{*1,1,3*}	O	H	H	4-NH_2-3,5-diCl-Ph	4	DCE	42.5	90	82	97	36[e]	71:29[c]
I-10{*1,1,4*}^{tol}	O	H	H	4-Br-Ph	2	$PhCH_3$	12	110	84	98	10[e]	50:50[c]
I-10{*1,1,4*}^{DCE}	O	H	H	4-Br-Ph	2	DCE	4	90	87	95	44	100:0[c]
I-10{*1,1,6*}	O	H	H		2	DCE	21	90	85	95	44[e]	74:26[c]
I-10a{*2,1,1*}	O	Me	H	Ph	2	DCE	4	90	50	98	35[f]	100:0[c]
I-10b{*2,1,1*}	O	Me	H	Ph	2	DCE	4	90	30	98	17[g]	100:0[c]

[a]Overall purity after the entire reaction sequence calculated from HPLC-UV traces at 205–400 nm; [b]HPLC-UV traces at 205–400 nm after purification; [c]Ratio of C12*a S,R* stereoisomers calculated from ^{1}H NMR of the purified product; [d]Ratio of C12*a S,R* enantiomers determined by SFC of the purified product; [e]Inseparable C12*a S,R* isomers; [f]Separable C3 *R* isomer; [g]Separable C3 *S* isomer; NI: not isolated (decomposition during HPLC purification).

3.1.4 Conclusion

To conclude, the developed methodology was applied to synthesize 20 diversely substituted compounds and two amino (un)saturated amino derivatives which were isolated and fully characterized.

Notwithstanding minor limitations of the approach, the final products were observed in good crude purities and overall yields. Furthermore, the TES reduction was used to prepare benzomorpholino-thiadiazepines with a controlled 3D architecture and the detailed analysis of the C3 and C12*a* stereocenters was achieved using a combination of chiral SFC and advanced NMR experiments. According to our previous studies,[2] the formation of the C3 stereocenter (*R*) was fully stereoselective, except for threonine-based intermediates providing a mixture of separable *R,S* isomers. The resulting C12*a* configuration was rather slightly influenced by the final cyclization and the use of DCE furnished the lower rate of epimerization.

3.2 Stereoselective Synthesis of Benzo[*e*][1,4]oxazino[4,3-*a*][1,4]Diazepine-6,12-Diones with Two Diversity Positions

The results of this project were published in: Králová, P.; Maloň, M; Soural, M. *ACS Comb. Sci.* **2017**, *19* (12), 770–774.[28]

3.2.1 Brief introduction

The second project is devoted to the solid-phase synthetic strategy to prepare benzoxazino-diazepinones started from readily available synthons: Fmoc-L-serine, 2-nitrobenzoic acids and *α*-bromoketones. According to the previously reported results,[3,38] the reduction of nitro group of polymer-supported *N*-acyl intermediates and their cyclization yielded benzodiazepin-5-ones. For this reason, *N*-acyl intermediates were cleaved from the resin and then suggested to a post-cleavage modification consisting in three-step sequence (i.e. TES reduction, hydrogenation and acid-mediated cyclization) performed in solution phase. Importantly, only a simple work-up and isolation of reaction intermediates were used to keep applicability of the strategy using high-throughput synthesis concept (Figure 7). As in the previous case, we mainly focused on the study of target benzomorpholino-diazepinediones in terms of their configuration and optical purity.

Figure 7. The suggested synthesis of benzo[*e*][1,4]oxazino[4,3-*a*][1,4]diazepine-6,12-diones

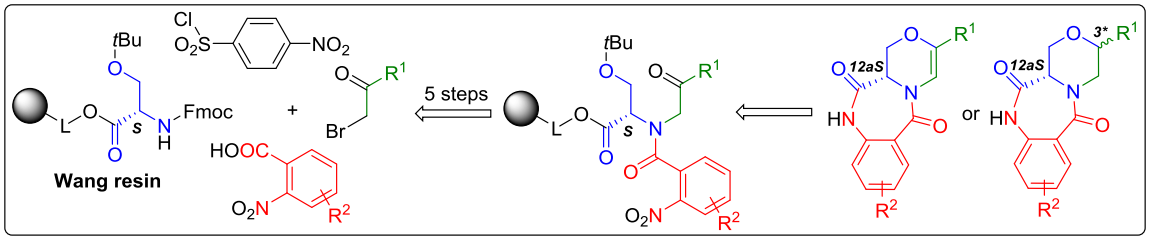

3.2.2 Synthesis

The synthesis of benzomorpholine-diazepinediones **II-8**{R^1,R^2} (Scheme 4) was performed using a combination of SPS and a three post-cleavage reactions (e.g. TES reduction, hydrogenation and a final cyclization) with a simple isolation of all cleaved intermediates using only evaporation under a stream of nitrogen or filtration. The proposed methodology was inspired by our previously reported research in the field of morpholine-3-carboxylic acid derivatives.[1,2] To develop the reaction sequence, we started with *α*-bromoacetophenone and 2-nitrobenzoic acid. The starting *N*-alkyl sulfonamide **II-2**{*1*} was synthesized from the resin-bound Fmoc-Ser(*t*Bu)-OH on Wang resin **II-1** which was submitted to the Fmoc deprotection and an activation/protection of primary amine with 4-Nos-Cl followed by Fukuyama monoalkylation with *α*-bromoacetophenone. After cleavage of the 4-Nos protecting group using MCE/DBU, the key *α*-amino

ketone **II-3**{*1*} was subjected to further acylation with 2-nitrobenzoic acid. In contrast to the previously reported synthesis of benzodiazepin-5-one derivatives,[3] no dealkylated product was obtained after the acylation step using LC-MS analysis, but the acylation required a longer reaction time (66 h) to complete conversion. The product **II-4**{*1,1*} was obtained in 88% crude purity. Obviously, the reduction of nitro group of polymer-supported intermediate **II-4**{*1,1*} triggered the reaction of the amino group with a ketone which, after TFA-mediated cleavage from the resin, yielded benzo[*e*][1,4]diazepin-5-one scaffold **II-10**{*1,1*}.[3,38] In this case the LC-MS analysis showed no traces of oxazine derivative **II-7a**{*1,1*}. The addition of TES into a cleavage cocktail commenced the reduction of imine to product **II-11**{*1,1*}, with a specific configuration of the newly formed C2 stereocenter (*R*) determined using 2D NMR spectra.

Scheme 4. The synthesis of benzomorpholino-diazepinediones **II-8**{R^1,R^2}[a]

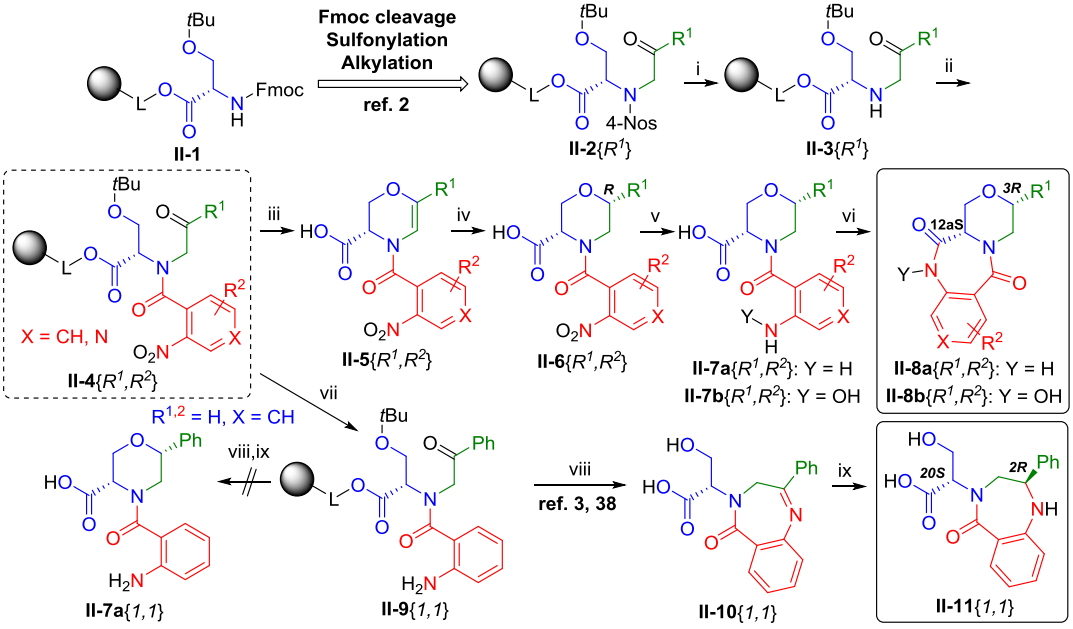

[a]Reagents and conditions: (i) MCE, DBU, DMF, 1.5 h, rt; (ii) 2-nitrobenzoic acid, DIC, deggased DMF, 48-96 h, rt; (iii) 50% TFA/DCM, 15-24 h, rt; (iv) TES, 2-21 h, rt; (v) **(a)** H_2,10% Pd/C, IPA, 1-48 h, rt or **(b)** H_2, PtO_2, IPA, 2.5-48 h, rt (for derivatives **II-5**{*1,2*}, **II-5**{*1,4*}, **II-5**{*1,6*}, **II-5**{*1,7*}, **II-5**{*4,1*}, **II-5**{*5,6*} and **II-5**{*7,1*}); (vi) 10% TFA/DCM, 2-48 h, 50 °C; (vii) $Na_2S_2O_4$, K_2CO_3, TBAHS, 50% DCM/H_2O, 2 h, rt; (viii) 50% TFA/DCM, 3 h, rt; (ix) TES, 3 h, rt.

To avoid the formation of benzo[*e*][1,4]diazepin-5-one derivative **II-10**{*1,1*}, intermediate **II-4**{*1,1*} was subjected to TFA-mediated cleavage from the resin that enabled a further post-cleavage modification in solution. Similarly to our previous results,[2] the inseparable rotational isomers (rotamers) **II-6**{*1,1*} were obtained in a ratio of 74:26 (Figure 8). As it is already known, both isomers can rotate around amidic (CONH) bound, as previously observed for proline analogues.[39] In the case of *N*-acyl morpholines, the presence of "*anti*" and "*syn*" rotamers were confirmed using ^{1}H NMR (doubled signals were detected) and NOE experiments. The ratio of both rotamers was temperature-dependent, it means that increasing the temperature to 150 °C led to the gradual merging of the NMR signals followed by their refragmentation at 25 °C. According to these results, "*anti*" isomer was more stable than "*syn*" isomer at room temperature;[2] however, in the case of **II-6**{*1,1*}, the detailed NOE assignment was not performed as **II-6**{*1,1*} was a synthetic intermediate.

Figure 8. The "*anti*" and "*syn*" rotamers of **II-6**{*1,1*}

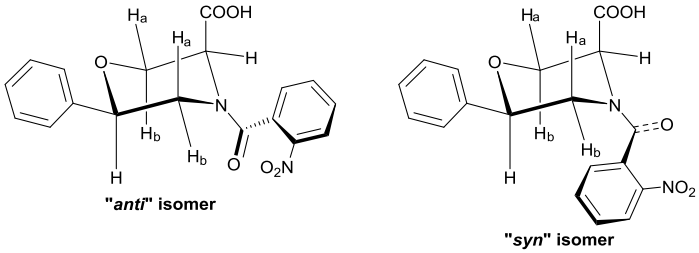

After TES reduction and removal of a residual TFA/TES under a stream of nitrogen and freeze drying, the following catalytic hydrogenation using 10% Pd/C yielded desired amino compound **II-7a**{*1,1*} in excellent crude purity (90%). Interestingly, the LC-MS analysis confirmed an extinction of the rotational isomers after the reduction of nitro group and only one enantiomer was detected. Whereas the 50% TFA/DCM at room temperature caused only a slow cyclization to product **II-8a**{*1,1*}, the quantitative conversion as achieved in 10% TFA/DCM at higher temperature (50 °C) for 41 h. The target derivative **II-8a**{*1,1*} was obtained in 92% crude purity and 40% overall yield after reversed-phase semipreparative HPLC purification.

Finally, we evaluated the impact of TES reduction and TFA-mediated cyclization to the stereochemical outcome of both C12*a* and C3 stereocenters. Although the immobilization of Fmoc-Ser(tBu)-OH on Wang resin to obtain resin **II-1** was performed using the convenient HOBt technique, it provided ~8% of the second enantiomer (detected by SFC chromatography).[27] Consequently, the cleavage and reduction of intermediate **II-5**{*1,1*} with TES afforded crude compound **II-6**{*1,1*} as a mixture of the corresponding diastereoisomers 3*R*, 12a*S* and 3*R*, 12a*R* in a ratio of 92:8. Similarly, the final cyclization yielded the crude compound **II-8a**{*1,1*} as two separable diastereoisomers in the same ratio. In this case (and for all analogues **II-8a**{R^1,R^2}), only the major diastereomer was isolated by reverse-phase semipreparative HPLC. The configuration of both stereocenters as 3*R*, 12a*S* was determined using the detailed 2D NMR analysis of two representative compounds **II-8a**{*2,3*} and **II-8b**{*5,6*} (described later in the thesis). In contrast to previous research,[27,40–42] these results proved that the C12a configuration was not touched during the final cyclization.

3.2.3 Limitations and scope

To reveal the general applicability of our method, we tested a diverse combination of different *α*-bromoketones and 2-nitrobenzoic acids bearing both electron donating and electron withdrawing groups (Figure 9). The key *N*-alkyl sulfonamides **II-2**{R^1} were observed in high crude purities 72-98%. In contrast to our previously reported results,[1,2] the quantitative cleavage of the 4-Nos protecting group needed longer deprotection time (1.5 h). The following acylation required 24-96 h to complete depending on the nucleophilicity of the amine **II-3**{R^1} and reactivity of acylation agents (R^2 modification), but no mutual relationship of both R^1 and R^2 substituents was observed. In the case of low-reactive intermediate **II-2**{*6*} with strongly electron withdrawing group, the acylation with carboxylic acid in the presence of DIC, or even with the corresponding acyl chloride failed. The treatment of **II-4**{R^1,R^2} with TFA/TES resulted in a mixture of CONH rotamers observed in different ratios (23-74%:77-26%) at room temperature (Scheme 4).

Figure 9. The list of tested building blocks for R^1 and R^2 substitution

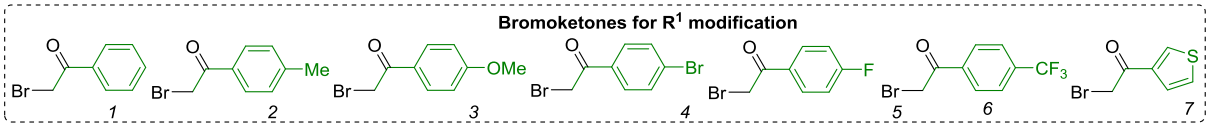

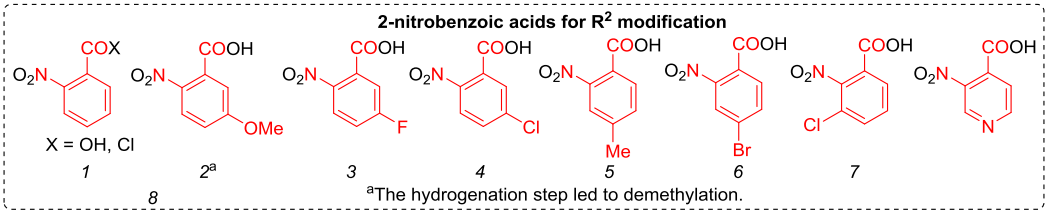

Analogously to the derivative **II-6**{*1,1*}, the rotamery completely disappeared after the reduction of the nitro group. In general, the catalytic hydrogenation using Pd/C afforded desired derivatives **II-7a**{R^1,R^2} in 49-95% crude purities, however it led to cleavage of the C-Cl or C-Br bonds. To avoid the undesired hydrogenolysis, intermediates containing halogens were reduced using PtO_2. Furthermore, in the case of intermediates **II-6**{R^1,R^2} bearing halogens as the R^2 substituents (except for **II-6**{*1,7*}), the hydrogenation using PtO_2 afforded *N*-hydroxylamine intermediates **II-7b**{R^1,R^2} in the range of crude purities 7-83% (Scheme 5). In the cases of **II-6**{*1,6*} and **II-6**{*5,6*}, the presence of 4-Br as R^2 substituent led to predominant major formation of **II-7b**{R^1,*6*} (crude purities above 80%). For this reason, the corresponding cyclic products were isolated and fully characterized using detailed 2D NMR analysis.

Scheme 5. Hydrogenation of **II-6**{R^1,R^2} and their cyclization to final products **II-8a-b**{R^1,R^2}[a]

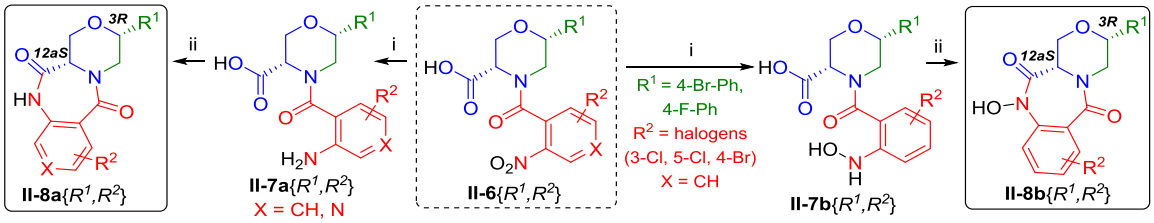

[a]Reagents and conditions: (i) **(a)** H_2, 10% Pd/C, IPA, 1-48 h, rt or **(b)** H_2, PtO_2, IPA, 2.5-7.5 h, rt (for derivatives **II-5**{*1,4*}, **II-5**{*1,6*}, **II-5**{*1,7*}, **II-5**{*4,1*}, **II-5**{*5,6*} and **II-5**{*7,1*}); (ii) 10% TFA/DCM, 2-48 h, 50 °C.

In addition, the catalytic hydrogenation of **II-6**{*1,2*} and **II-6**{*2,2*} with 5-methoxy group as the R^2 substituent caused demethylation using both Pd/C and PtO_2 catalysts (Scheme 6). In the first case, the corresponding amine derivatives **II-7a**{*1,2*} or **II-7a-dem**{*1,2*} were not detected using LC-MS analysis, but the reaction led to a mixture of the final benzomorpholinediones **II-8a**{*1,2*} and **II-8a-dem**{*1,2*} in ratios 49:51 or 41:59 depending on the type of catalysts used. However, the presence of electron-donating group (Me) in the R^1 position prevented the cyclization to the benzomorfolinediones and the demethylated aniline **II-7a-dem**{*2,2*} was obtained in 63% crude purity. Interestingly, the methoxy group as R^1 substituent (derivative **II-7a**{*3,1*}) did not undergo any demethylation.

Scheme 6. Demethylation of methoxy derivatives **II-6**{R^1,*2*} using catalytic hydrogenation[a]

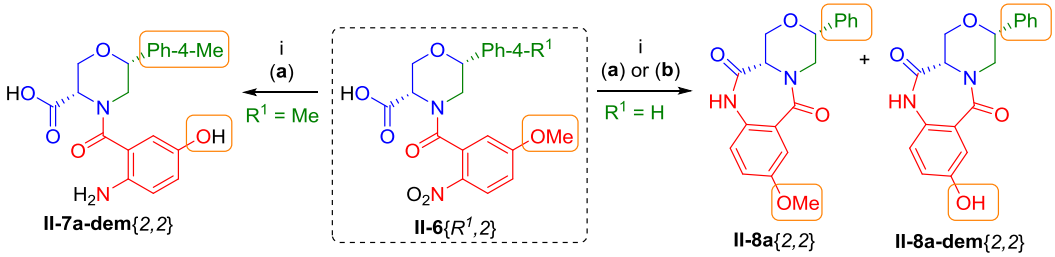

[a]Reagents and conditions: (i) **(a)** H_2, 10% Pd/C, IPA, 35 h, rt or **(b)** H_2, PtO_2, IPA, 48 h, rt.

In contrast to **8a**{*1,1*}, the cyclization to substituted analogues **II-8a**{R^1,R^2}, **II-8a-dem**{R^1,R^2} and **II-8b**{R^1,R^2} required significantly shorter cyclization time (1-24 h) depending on R^1 and R^2 substituents (Table 2). In the case of pyridine derivative **II-7a**{*1,8*}, the cyclization failed after 1 h and the corresponding

derivative **II-8a**{*1,8*} was not prepared. The developed methodology provided 15 representative benzomorpholino-diazepinediones bearing CON^{9}H group **II-8a**{R^1,R^2} and **II-8a-dem**{R^1,R^2} in 49-92% crude purities and 19-49% overall yields, 2 derivatives with CON-OH **II-8b**{R^1,R^2} in 82-83% crude purities and 49-50% overall yields, and one saturated analogue of benzodiazepin-5-one **II-11**{*1,1*} in 55% crude purity and 30% overall yield.

3.2.4 Conclusion

The stereoselective synthesis of benzo[*e*][1,4]oxazino[4,3-*a*][1,4]diazepine-6,12-diones was developed and used to prepare 17 derivatives using a combination of both solid-phase and solution-phase techniques. Although the final steps of the reaction sequence (hydrogenation and cyclization) had to be performed after the product cleavage from the polymer support, the simple work up procedures (fast evaporation or filtration) make this method fully compatible with a high-throughput synthesis concept. The developed methodology has rather a slight limitations and the synthesis with only two tested buildings block, e.g. 2-nitropyridin-4-yl and 2-nitro-5-(piperidin-1-yl)benzamide, failed in the stage of the cyclization step. Furthermore, we illustrated applicability of TES reduction for the stereoselective synthesis of benzodiazepine derivatives.

Table 2. List of synthesized and fully characterized compounds[a-d]

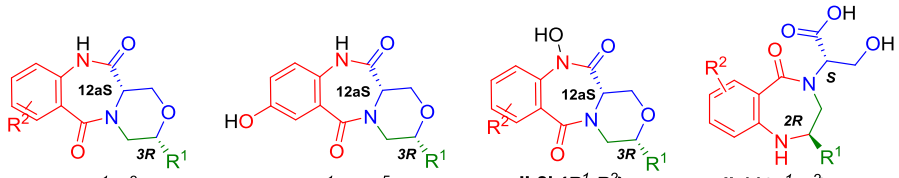

II-8a{R^1,R^2} **II-8a-dem**{R^1,2}: R^5 = OH **II-8b**{R^1,R^2} **II-11**{R^1,R^2}

cmpd	R^1	R^2	cyclization time [h]	crude purity [%][a]	final purity [%][b]	overall yield [%][c]
II-8a{*1,1*}	Ph	H	41	92	98	40
II-8a{*1,2*}	Ph	5-MeO	-	49	98	19
II-8a{*1,3*}	Ph	5-F	2.5	66	99	43
II-8a{*1,4*}	Ph	5-Cl	5	70	99	35
II-8a{*1,5*}	Ph	4-Me	19	85	97	38
II-8a{*1,7*}	Ph	3-Cl	5	85	99	38
II-8a{*2,1*}	4-Me-Ph	H	22	75	98	49
II-8a{*2,3*}	4-Me-Ph	5-F	6	83	97	47
II-8a{*3,1*}	4-MeO-Ph	H	25	60	95	45
II-8a{*4,1*}	4-Br-Ph	H	24	85	98	43
II-8a{*5,1*}	4-F-Ph	H	24	86	99	41
II-8a{*5,5*}	4-F-Ph	4-Me	2.5	49	98	28
II-8a{*7,1*}		H	2.5	49	97	27
II-8a-dem{*1,2*}	Ph	5-OH	-	51	99	28
II-8a-dem{*2,2*}	4-Me-Ph	5-OH	5.5	61	98	46
II-8b{*1,6*}	Ph	4-Br	2	82	99	49
II-8b{*5,6*}	4-F-Ph	4-Br	3	83	98	50
II-11{*1,1*}	Ph	H	3+3[d]	55	99	30

[a]Overall purity after the entire reaction sequence calculated from HPLC-UV traces at 205–400 nm; [b]HPLC-UV traces at 205–400 nm after purification; [c]Calculated from the ^{1}H NMR spectrum of the purified product; [d]The cyclization was performed using a two-step cleavage consisted of 50% TFA/DCM for 3 h at rt and then an addition of TES into the cleavage cocktail and reaction for another 3 h at rt.

3.3 Synthesis of Disubstituted Pyrazino-Oxazine Derivatives with Controlled Stereochemistry

The results of this project were published in: Ručilová, V.; Králová, P.; Soural, M. *Eur. J. Org. Chem.* **2017**, *2017* (47), 7034–7039.[29] I participated in this project as a co-author.

3.3.1 Brief introduction

To extend the previously reported results in the field of fused morpholine derivatives,[37,38] we decided to replace 2-nitrobenzoic acids with various Fmoc-amino acids. The key intermediates were prepared using a five-step sequence and then subjected to PIP-mediated deprotection which should trigger a spontaneous cyclative cleavage providing piperazine-2,5-dione intermediates. Their reaction with TFA to remove the *tert*-butyl protecting group followed by an acid-mediated cyclization should provide pyrazino-oxazines (Figure 10). In this project, we intended to test the suggested reaction sequence and reveal a detailed limitation and scope using a set of natural Fmoc-amino acids with different substitution of a side chain.

Figure 10. The suggested synthesis of 1,7,8,9*a*-tetrahydropyrazino[2,1-*c*][1,4]oxazine-6,9-diones

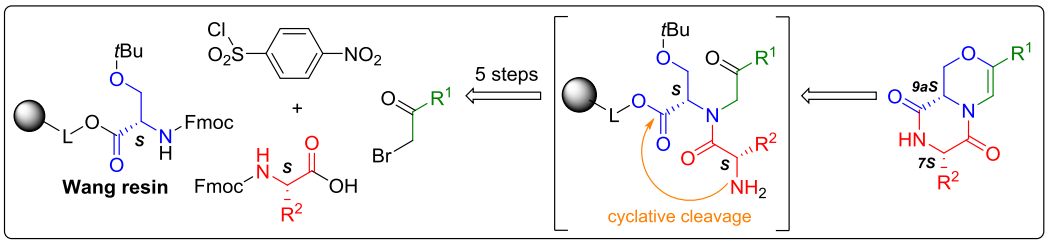

3.3.2 Synthesis

The synthesis of the key 4-Nos-amides **III-2**{R^1} was carried out according to the previously reported protocols[2] starting from immobilized Fmoc-Ser(*t*Bu)-OH on Wang resin **III-1**, 4-Nos-Cl and α-bromoketones with both electron donating and electron withdrawing groups as R^1 substituents (Figure 11). In all cases, desired *N*-alkyl-sulfonamides **III-2**{R^1} were observed in good crude purities (on average 90%). Unlike the previously reported procedure,[2] we had to increase the concentration of MCE (by 2.7 times more) and prolong the reaction time (to 1 h) to quantitatively remove the 4-Nos protecting group. After that, the acylation of the α-aminoketones **III-3**{R^1} with eleven different Fmoc-amino acids with various side chains (Figure 11, R^2 modification) activated with DIC and HOBt yielded the resin-bound *N*-acyl derivatives **III-4**{R^1,R^2}. In some cases, the acylation step had to be repeated to reach completion. The piperidine-mediated deprotection of the Fmoc protecting group triggered a spontaneous cyclative cleavage that yielded piperazine-2,5-diones **III-6**{R^1,R^2}. After the cyclative cleavage, the residual cleavage cocktail was evaporated from intermediate **III-6**{R^1,R^2} followed by the post-cleavage modification consisting of the *tert*-butyl ether deprotection using 50% TFA/DCM to yield derivative **III-7**{R^1,R^2}. TFA should also trigger a spontaneous cyclization to target compounds **III-8**{R^1,R^2}.[2] However, the presence of the piperazine-2,5-dione moiety prevented the cyclization to oxazine derivatives according to previously reported conditions,[2,27,28] the intermediates **III-7**{R^1,R^2} underwent only the protective group cleavage and the cyclization did not proceed even at increased temperature. For this reason, the cleavage cocktail (TFA/DCM) was evaporated under a stream of nitrogen to dryness and the reaction was accomplished in TFA/MeCN at higher temperature (80-90 °C depending on both R^1 and R^2 substituent). The crude pyrazino-oxazines **III-8**{R^1,R^2} were subjected

to reverse-phase semipreparative HPLC purification to obtain 16 representative derivatives in 62-89% crude purity and 5-46% overall yields (Scheme 7, Table 3).

Scheme 7. Synthetic route leading to pyrazino-oxazines **III-8**{R^1,R^2}[a]

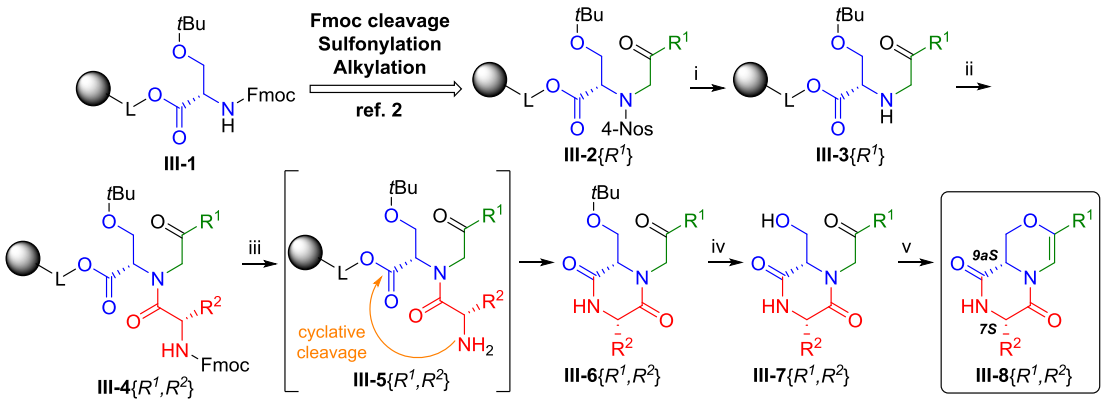

[a]Reagents and conditions: (i) MCE, DBU, DMF, 1 h, rt; (ii) **(a)** Fmoc-amino acids, HOBt, DIC, DCM, DMF, 24 h, rt, then repeat or **(b)** Fmoc-amino acids, DIC, DMF, 16 h, rt; (iii) 50% PIP/DMF, 30 min, rt, then lyophilization for 16 h; (iv) 50% TFA/DCM, 30 min, rt, then evaporation under stream of N_2; (v) MeCN, 1-8 h, 80-90 °C, then evaporation under stream of N_2.

Figure 11. The list of tested synthons for R^1 and R^2 substituents

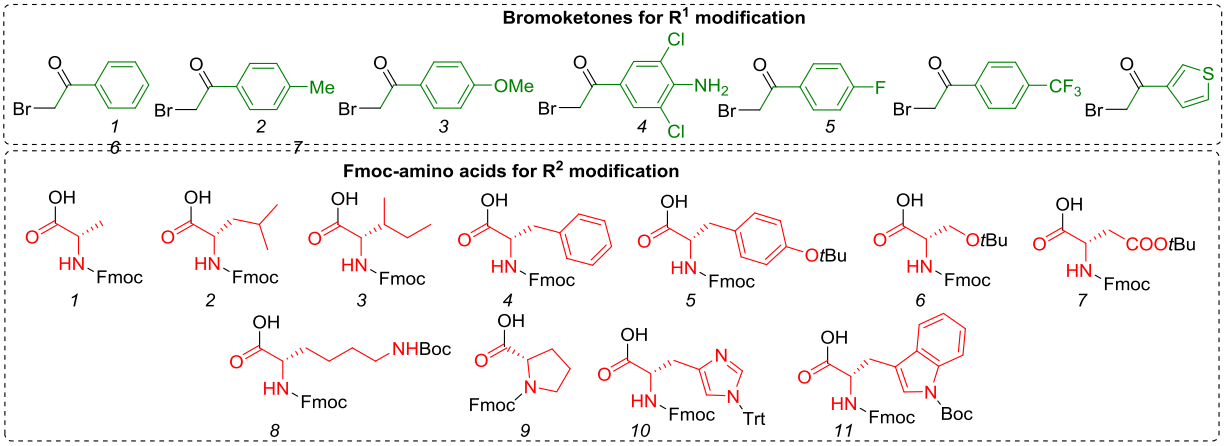

3.3.3 Limitations and scope

Since the reaction sequence afforded the final products **III-8**{R^1,R^2} in relatively limited overall yields, we investigated the reaction sequence in details. In contrast to trouble-free acylation with 2-nitrobenzoic acid derivatives using the DIC technique discussed earlier in the thesis,[28] some by-products were detected after the acylation step which lowered yields of the final compounds **III-8**{R^1,R^2}. After further investigation, LC-MS analysis confirmed the structure of the by-products as dealkylated derivatives **III-10**{H,R^2} (Scheme 8). The same behavior was previously reported for the acylation of similar intermediates with benzoic acids activated with DIC and HOBt.[3] To suppress undesired dealkylation, the use of HOBt was omitted, and acylation *via* a symmetrical anhydride using the DIC technique was tested (Scheme 8, method **(b)**). In contrast to our previous results,[28] the dealkylated derivatives **III-10**{H,R^2} were detected again in considerably higher amount than in the case of DIC/HOBt activation. According to these facts, the formation of dealkylated products was dependent on the type of R^1 and R^2 substituent (i.e. the combination of α-bromoketones with 2-nitrobenzoic acid vs Fmoc-amino acids) and the type of acylation method used (i.e. acylation with DIC/HOBt **(a)** or with DIC **(b)**).

Scheme 8. The formation of by-product **III-10**{*H*,R^2} and **III-12**{*H*,R^2}[a]

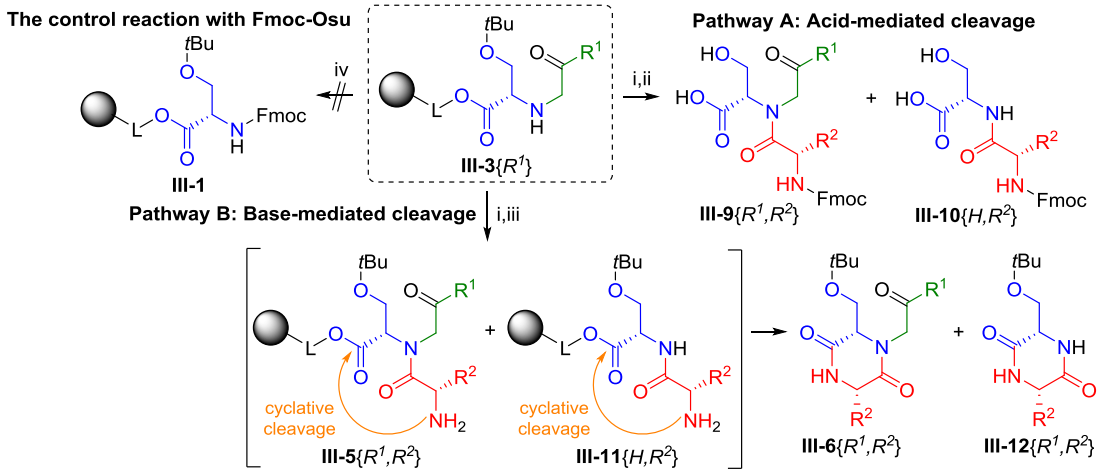

[a]Reagents and conditions: (i) **(a)** Fmoc-amino acids, HOBt, DIC, DCM, DMF, 24 h, rt, then repeat or **(b)** Fmoc-amino acids, DIC, DMF, 16 h, rt; (ii) 50% TFA/DCM, 30 min, rt; (iii) 50% PIP/DMF, 30 min, rt, lyophilization for 16 h; (iv) Fmoc-OSu, DCM, 30 min, rt.

With these results in hands, we have concluded that the dealkylation did not occur during the deprotection of 4-Nos group since the control reactions of all immobilized *α*-amino ketones **III-3**{R^1} with Fmoc-OSu gave no dealkylated products (i.e. the starting Fmoc-serine **III-1**, Scheme 8). Furthermore, we evaluated a possible effect of the acid-mediated cleavage of **III-4**{R^1,R^2} from the resin on the dealkylation step (Scheme 8, Pathway A). In this case, we observed different ratios of *N*-acyl **III-9**{R^1,R^2} and dealkylated intermediates **III-10**{*H*,R^2} which indicated the influence of both the R^1 and R^2 substituents on the reaction outcome, but no systematic relationship was observed (7-100% of dealkylated). For this reason, we carried out the cyclative cleavage that yielded piperazine-2,5-diones **III-6**{R^1,R^2} and the corresponding by-products **III-12**{*H*,R^2}. The formation of **III-12**{*H*,R^2} clearly demonstrated that dealkylation occurred on the resin during the acylation step, otherwise product **III-12**{*H*,R^2} could not be detected. It is necessary to note that, in contrast to **III-10**{*H*,R^2}, the quantities of **III-12**{*H*,R^2} for most of the amino acids could not be precisely determined using LC-UV due to the low UV-VIS activity of **III-12**{*H*,R^2} (Scheme 8, Pathway B).

We tested 20 various combinations of seven *α*-bromoketones and eleven Fmoc-amino acids with different side chains to determine limitations and scope of the proposed methodology (Figure 11). In the case of Fmoc-Pro-OH, the acylation was followed by quantitative dealkylation. Further, the target pyrazino-oxazines **III-8**{*1,7*} and **III-8**{*1,10*} starting from Fmoc-Asp(*t*Bu)-OH and Fmoc-His(Trt)-OH were accompanied with inseparable impurities and were not isolated. The synthetic strategy was applied successfully to prepare 16 diastereomerically pure derivatives (calculated from ^{1}H NMR analysis) which were isolated and fully characterized (Table 3). In this case, the cyclative cleavage of **III-4**{R^1,R^2} did not cause epimerization within reaction sequence.

3.3.4 Conclusion

This project introduced a novel synthetic strategy to prepare rarely studied fused [6+6] morpholine derivatives started from readily available building blocks: Fmoc-*α*-amino acids and *α*-bromoketones. Although the developed methodology reported a minor shortcoming (i.e. dealkylation reaction), we synthesized 16 representative derivatives to determine limitations and scope depending on R^1 and R^2 substituents; however, no systematic relationship was found between substituents and yields. The target heterocycles were synthesized as diastereomerically pure compounds with specific configuration of both stereocenters and the

synthesis did not provide no epimerization products.

Table 3. The list of final pyrazino-oxazine derivatives **III-8**{*R*[1],*R*[2]}[a-c]

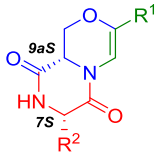

cmpd	R^1	R^2	cyclization time [h]	crude purity [%][a]	final purity [%][b]	overall yield [%][c]
III-8{*1,1*}	Ph	Me	5	73	98	41
III-8{*1,2*}	Ph	$CH_2CH(CH_3)_2$	8	62	99	20
III-8{*1,3*}	Ph	$CH(CH_3)CH_2CH_3$	5	70	99	5
III-8{*1,4*}	Ph	CH_2Ph	8	89	98	31
III-8{*1,5*}	Ph	CH_2Ph-4-OH	8	86	97	34
III-8{*1,11*}	Ph		6	83	97	26
III-8{2,*1*}	4-Me-Ph	Me	2	82	98	18
III-8{*2,4*}	4-Me-Ph	CH_2Ph	1	84	98	23
III-8{*2,6*}	4-Me-Ph	CH_2OH	1	81	98	46
III-8{*2,8*}	4-Me-Ph	$CH_2(CH_2)_3NH_2$	2	76	99	32
III-8{*2,11*}	4-Me-Ph		1	71	99	26
III-8{*3,1*}	4-MeO-Ph	Me	5	89	99	43
III-8{4,*1*}	4-NH_2-3,5-diCl-Ph	Me	1	78	98	32
III-8{5,*1*}	4-F-Ph	Me	5	82	99	21
III-8{6,*1*}	4-CF_3-Ph	Me	2	72	99	8
III-8{7,*1*}		Me	2	82	99	21

[a]Overall purity after the entire reaction sequence calculated from HPLC-UV traces at 205–400 nm; [b]HPLC-UV traces at 205–400 nm after purification; [c]Calculated from the ^{1}H NMR spectrum of the purified product.

3.4 Polymer-Assisted Synthesis of Single and Fused Diketomorpholines

The results of this project were published in: Králová, P.; Benická, S.; Soural, M. *ACS Comb. Sci.* **2019**, *21* (3), 154–157.[30]

3.4.1 Brief introduction

As a continuation of the formerly reported synthesis of pyrazino-oxazines,[29] we decided to replace Fmoc-amino acids with α-halocarboxylic acid derivatives. The resulting *N*-acyl intermediates should be treated with TFA to release the dihydrooxazine-3-carboxylic acid derivatives from the resin. Their post-cleavage modification consisting in a base-induced cyclization should yield the required diketomorpholines; however, except for desired oxazino[3,4-*c*][1,4]oxazine-diones, we obtained also 3-methylidene-diketo-morpholines depending on the used reaction conditions (Figure 12). We decided to determine limitations and scope of the method for both types of compounds and in the case of oxazino-oxazines, to examine a stereoselectivity of the TES reduction.

Figure 12. The proposed synthesis of fused diketomorpholines

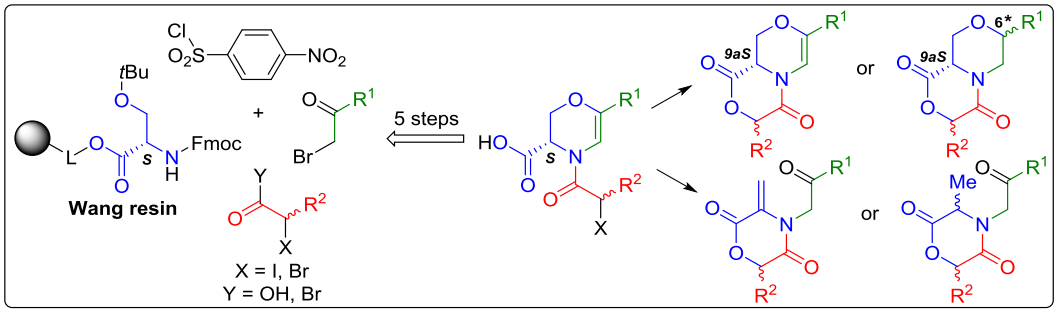

3.4.2 Synthesis

According to the previously reported conditions,[2] the key α-amino ketone **IV-2**{*1*} was prepared using a convenient SPS starting from the polymer-supported Fmoc-Ser(*t*Bu)-OH. The subsequent acylation with *α*-iodoacetic acid and TFA-mediated cleavage from the resin yielded dihydrooxazine-3-carboxylic acid **IV-4**{*1,1*}. After simple evaporation of the cleavage cocktail under a stream of nitrogen, we performed DIEA/DMSO-mediated post-cleavage cyclization of the crude evaporator **IV-4**{*1,1*} that yielded oxazino-[3,4-*c*][1,4]oxazine-dione **IV-5**{*1,1*} or 3-methylidene-diketomorpholine **IV-6**{*1,1*} depending on the cyclization time. The quantitative conversion to fused [6+6] oxazine **IV-5**{*1,1*} was observed after only 20 min, whereas a longer reaction time (20 h) led quantitatively to 3-methylidene-diketomorpholine **IV-6**{*1,1*} in 95% and 91% crude purities. After removal of DIEA/DMSO by lyophilization, the crude products were isolated by reverse-phase semipreparative HPLC purification in 45-46% overall yields (Scheme 9, Table 4).

Scheme 9. The synthesis of final diketomorpholines *via* dihydrooxazine-3-carboxylic acids **IV-4**{R^1,R^2}[a]

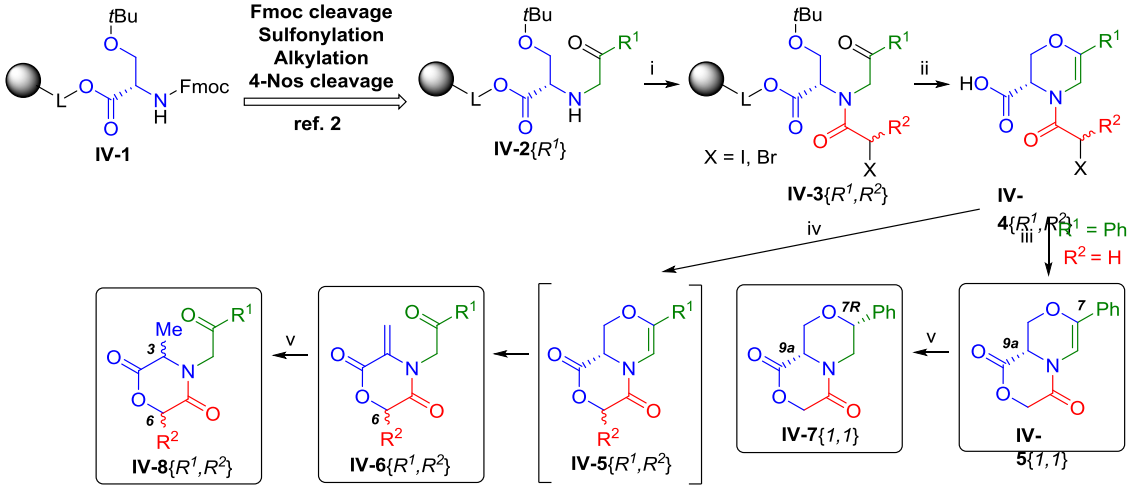

[a]Reagents and conditions: (i) halocarboxylic acid , DIC, DCM, 30 min, then added to resin, 24 h, rt; or 2-bromopropionyl bromide, 2,6-lutidine, DCM, 24 h, rt (ii) 50% TFA/DCM, 1 h or 4 h (for derivatives **IV-3**{R^1,*3*}), rt; (iii) DIEA, DMSO, 20 min (for **IV-4**{R^1,*1*}), rt; (iv) DIEA, DMSO, 20 h, rt (for **IV-4**{R^1,*1*} and **IV-4**{R^1,*3*}) or 1 h, 80 °C (for **IV-4**{R^1,*2*}); (v) TFA/TES/DCM (10:3:10), 24, rt.

After that, further reduction of crude lyophilized products **IV-5**{*1,1*} and **IV-6**{*1,1*} using TFA/TES provided the saturated analogs **IV-7**{*1,1*} and **IV-8**{*1,1*} in 74% and 89% crude purities and 19% and 12% overall yields (Scheme 9). Similarly to our formerly reported results,[2,27,28] the TES reduction to oxazino-morpholine derivatives **IV-7**{*1,1*} was fully stereoselective. The configuration of the newly formed C7 stereocenter was assigned as 7*R* based on NMR techniques. In contrast, the reduction of 3-methylidene-diketomorpholine **IV-6**{*1,1*} to 3-methyl-diketomorpholine **IV-8**{*1,1*} was not stereoselective and furnished a mixture of C3 enantiomers in a ratio of 20:80 as detected by SFC analysis (Table 4).

In addition, the fused oxazine derivative **IV-5**{*1,1*} showed considerable instability and slowly converted to 3-methylidene-diketomorpholine **IV-6**{*1,1*}, when a sample was dissolved in different solvents (e.g. DMSO-d_6, MeOH-d_4, $CDCl_3$, and MeCN-d_3) for NMR analysis. In contrast, the saturated analogue **IV-7**{*1,1*} was completely stable, and it could be fully NMR characterized in MeOH-d_4.

3.4.3 Limitations and scope

To determine the limitations and scope, we tested a combination of three aromatic *α*-bromoketones with electron donating and electron withdrawing substituents, and four *α*-halocarboxylic acid derivatives (Figure 13 for both R^1 and R^2 modifications). The resin-bound *N*-acyl compounds **IV-3**{R^1,*1-3*} were successfully synthesized for all tested *α*-bromoketones and *α*-halocarboxylic acid derivatives (i.e. 2-iodoacetic acid, (*R,S*)-2-bromopropionyl bromide, (*S*)-(-)2-bromopropionic acid and (*R,S*)-2-bromo-2-phenylacetic acid). The following acid-mediated cleavage from the resin gave the products **IV-4**{R^1,*1-3*} in high crude purities (56-97%). However, in the case of phenylacetic acid derivatives, the release from the resin required the longer cleavage time (4 h instead of 1 h).

Figure 13. The list of tested synthons for R^1 and R^2 substituents

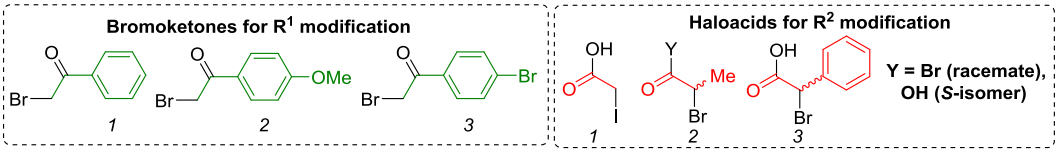

After that, the cleaved compounds **IV-4**{R^1,*1-3*} were subjected to base-catalyzed cyclization to determine the limitations and scope (Scheme 9). In contrast, the cyclization to **IV-5**{R^1,*1-3*} and **IV-6**{R^1,*1-3*} required significantly different conditions depending on the R^2 substituent used. In the cases of intermediates **IV-4**{R^1,*1*} and **IV-4**{R^1,*3*}, prepared from 2-iodoacetic acid and 2-bromo-2-phenylacetic acid, the cyclization could be accomplished at room temperature for 20 h. In contrast, the room-temperature cyclization of **IV-4**{R^1,*2*}, prepared from 2-bromopropionyl bromide, was significantly slower and the conversion was achieved after 5 days. For this reason, the reaction was heated at 50 °C (for 20 h) or 80 °C (for 1 h) to accelerate the cyclization which was completed faster at higher temperature. According to these results, it was difficult to isolate corresponding fused oxazines **IV-5**{R^1,*2*} due to their thermal conversion to methyli-dene compounds **IV-6**{R^1,*2*}. For this reason, the project was primarily paid to the synthesis of 3-methylidene-diketomorpholines **IV-6**{R^1,R^2} along with other related analogues and provided 12 final compounds: one fused derivative **IV-5**{*1,1*} and 9 derivatives **IV-6**{R^1,R^2} and **IV-7-8**{*1,1*} in 56-95% crude purities and 12-46% overall yields (Table 4).

Finally, we decided to explore the 3D architecture of the target compounds using detailed SFC studies. In the case of **IV-4**{*1,1*} synthesized from iodoacetic acid, the reaction sequence resulted in a minor racemization on the C3 center (i.e. 6% of *R*-isomer was detected by SFC analysis). As mentioned in previous projects, the minor enantiomer was formed during the immobilization of the enantiomerically pure (*S*)-Fmoc-Ser(*t*Bu)-OH to the Wang resin.[2] Similarly, the same ratio of *R,S* isomer (6:94) was detected for fused derivative **IV-5**{*1,1*}, which indicated that the base (DIEA)-catalyzed cyclization did not affect the configuration of the chiral center C9*a*.

In the case of **IV-6**{R^1,*2*}, prepared from racemic *α*-bromopropionyl bromide, the mixture of two enantiomers in a ratio of approximately 9:1 was detected. This fact points to the preferential formation of the

more stable enantiomer, which was presumably promoted by the DIEA-catalyzed cyclization to the final derivatives. In this context, the compound **IV-4^{S}{*1,2*}** was synthesized from enantiomeric pure (*S*)-(-)-bromopropionic acid and subjected to base-cyclization under the same reaction conditions (DIEA/DMSO at 80 °C) as in the case of **IV-4**{*1,2*} to assess the effect of both R^1 and R^2 substituents on the stereochemical outcome. After cyclization of **IV-4^{S}{*1,2*}** at 80 °C for just 5 min, we observed a mixture of two enantiomers **IV-6^{R}{*1,2*}** and **IV-6^{S}{*1,2*}** in a ratio of 5:95. After additional 130 min, the ratio was changed to 85:15 indicating the slow conversion of the starting *S* isomer to the resulting *R* isomer (Scheme 10). To explain these results, we designed a hypothetical mechanism of the diketomorpholine formation *via* oxazine-ring opening which afforded the 3-methylidene-diketomorpholine scaffold bearing the methyl group in C6 axial position (*S*-isomer). The following deprotonation at the C6 center by DIEA proceeded through two diastereomeric transition states of unequal energy, i.e. *S*-isomer was converted to more stable *R*-isomer having the equatorial methyl group (Scheme 10). According to these facts, we determined the preferable configuration of the C6 center on the diketomorpholine scaffold, but the longer cyclization (5 h) did not affected the conversion rate of *R,S* isomers, and we obtained a constant ratio of both *R,S* isomers (85:15, above mentioned in the thesis). Moreover, the analogues **IV-6**{*1,3*} and **IV-6**{*2,3*} with identical R^2 groups (Ph), but different R^1 substituents (Ph or 4-MeO-Ph), were assembled as enantiomerically pure compounds, whereas **IV-6**{*3,3*} (R^2 = 4-Br-Ph) was obtained as the racemic mixture (50:50, Table 4). These results imply the substantial influence of R^1 substituent to the resulting stereochemical outcome.

Scheme 10. The hypothetical mechanism of the final cyclization to product **IV-6^{R}{*1,2*}**[a]

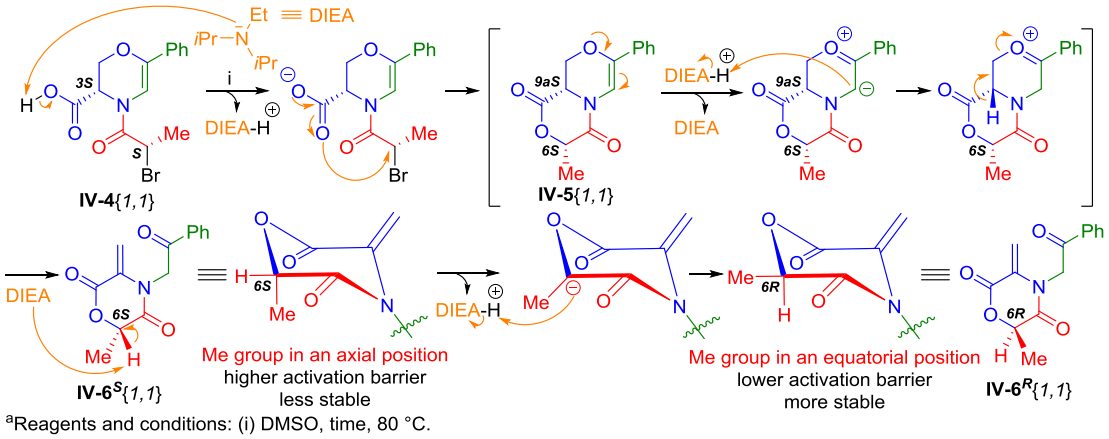

[a]Reagents and conditions: (i) DMSO, time, 80 °C.

3.4.4 Conclusion

In this projects, we have developed the high-throughput synthetic protocol to prepare various diketomorpholine derivatives, including two post-cleavage modifications (i.e. final cyclization and TES reduction) with simple work-up based on evaporation of the reagents and solvents. Depending on the reaction conditions, exposure to base resulted in cyclization to either fused [6+6] oxazines or 3-methylidene-diketomorpholines. In the case of oxazino-morpholine derivatives, the stereoselective TES reduction of olefins resulted in 7*R* isomer. In contrast, the TES reduction of 3-methylidene-diketomorpholines furnished the mixture of C3 enantiomers in a ratio of 20:80. To determine the 3D architecture of 3-methylidene compounds with various R^2 substituent (R^2 = Me, Ph), the SFC studies were performed showing that the R^1 substituent influences the stereochemical resulting outcome and the final products were obtained as a mixture of 6*R,S* isomers in different ratios depending on R^1 substituent.

Table 4. The list of prepared and fully characterized products[a-e]

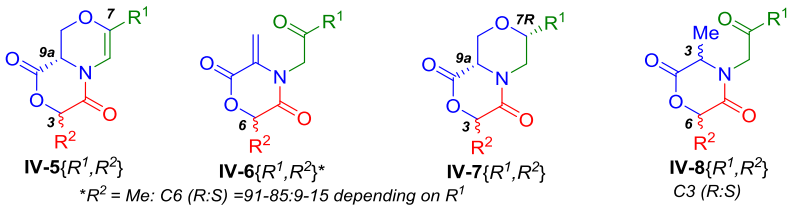

*R2 = Me: C6 (R:S) =91-85:9-15 depending on R1

5R{1,2}: C6 (R)

cmpd	R^1	R^2	crude purity [%][a]	final purity [%][b]	overall yield [%][c]	ratio of *R*:*S* enantiomers [%][d]
IV-5{*1*,*1*}	Ph	H	95	98	45[e]	6:94
IV-6{*1*,*1*}	Ph	H	91	99	46	-
IV-6{*1*,*2*}	Ph	Me	88	99	48	90:10
IV-6^{R}{*1*,*2*}	Ph	Me	67	99	24	85:15
IV-6{*1*,*3*}	Ph	Ph	66	98	27	100:0
IV-6{*2*,*2*}	4-MeO-Ph	Me	89	99	35	91:9
IV-6{*2*,*3*}	4-MeO-Ph	Ph	56	99	14	100:0
IV-6{*3*,*1*}	4-Br-Ph	H	90	98	30	-
IV-6{*3*,*2*}	4-Br-Ph	Me	90	96	22	87:13
IV-6{*3*,*3*}	4-Br-Ph	Ph	78	99	18	50:50
IV-7{*1*,*1*}	Ph	H	74	98	19	-
IV-8{*1*,*1*}	Ph	H	89	97	12	80:20

[a]Overall purity after the entire reaction sequence calculated from HPLC-UV traces at 205–400 nm; [b]HPLC-UV traces at 205–400 nm after purification; [c]Calculated from the ^{1}H NMR spectrum of the purified products; [d]Calculated from SFC-UV traces; [e]Dissolving the sample in MeCN-d_3 led to partial conversion of purified product **IV-5** to **IV-6** in a ratio of 83:17 as calculated from the ^{1}H NMR spectrum.

3.5 Convenient Synthesis of Thiohydantoins, Imidazole-2-Thiones and Imidazo[2,1-*b*]Thiazol-4-Iums from Polymer-Supported *α*-Acylamino Ketones

The results of this project were published in: Králová, P.; Maloň, M.; Koshino, H.; Soural, M. *Molecules* **2018**, *23* (4), 976–984.[31]

3.5.1 Brief introduction

In this project, our attention was paid to Wang resin-immobilized Fmoc-thioureas to prepare fused [6+5] heterocycles bearing a thiohydantoin scaffold. The key intermediates were prepared from immobilized *α*-amino ketones and Fmoc/alkyl-*N*-substituted-isothiocyanates. The corresponding thioureas should be subjected to cyclative cleavage conditions yielding thiohydantoin derivatives followed by an acid-mediated cyclization to receive thiohydantoin-oxazines derivatives. Alternatively, the reversed sequence should be tested, i.e. the immobilized thioureas should be treated with TFA providing expected oxazines followed by a base-catalyzed cleavage of the Fmoc protecting group and a cyclization to fused [6+5] derivatives (Figure 14). Eventually, the TES applicability for the stereoselective reduction of oxazine scaffold was suggested.

Figure 14. The considered synthesis of fused [6+5] morpholine derivatives

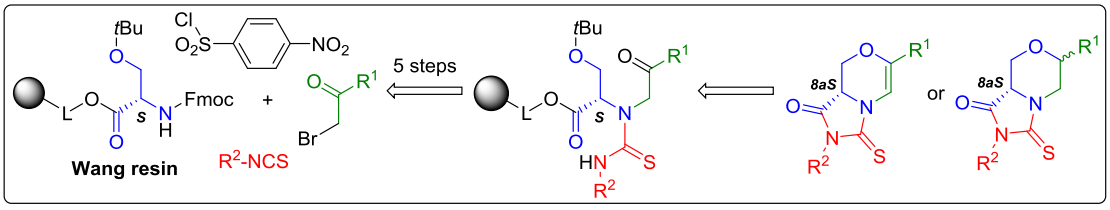

Interestingly, both tested synthetic strategies did not furnish expected fused [6+5] morpholines. In the first case, the cyclative cleavage reaction prompted the cyclization to the thiohydantoin scaffold followed by an acid-mediated cleavage of the *tert*-butyl protecting group and a spontaneous dehydration to 5-methylidene-thiohydantoins. Their TES reduction led to corresponding methyl analogues. In contrast to Fmoc-thioureas, the *N*-substituted thioureas did not undergo the cyclative cleavage and TFA had to be used to release the intermediates from the resin. Further exposure to TFA under an elevated temperature enabled cyclization. Although the LC-MS data corresponded to the expected thiohydantoin-dihydrooxazine derivative (Figure 14), the careful structural NMR elucidation of the isolated compound revealed that the scaffold was not formed. The cyclization to imidazole-2-thiones took place instead, followed by the dehydration and ring closure, which yielded an imidazo[2,1-*b*]thiazol-4-ium derivatives. Further, these compounds were prone to an isomerization to imidazole-2-thiones in DMSO-d_6 at room temperature, the rate of isomerization was temperature-dependent (Figure 15).

Figure 15. The developed methodology providing imidazole derivatives

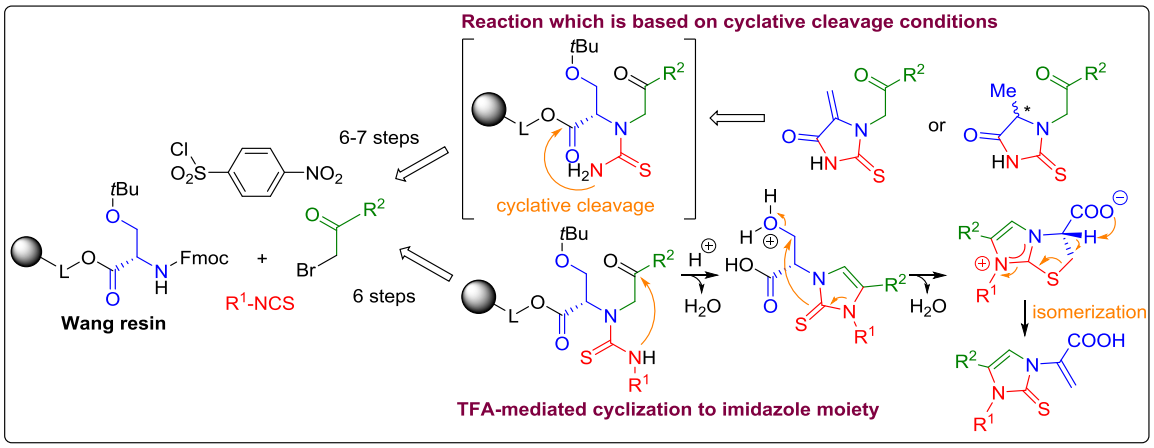

3.5.2 Synthesis

First, the suggested synthetic strategy (Scheme 11) was tested with *α*-bromoacetophenone and Fmoc-isothiocyanate (Fmoc-NCS) as representative synthons. The starting *α*-amino ketone **V-2**{*1*} was synthesized in four steps from Wang resin-supported Fmoc-Ser(*t*Bu)-OH **V-1** according to the previously reported protocol.[2] The reaction with Fmoc-NCS provided the corresponding Fmoc-thiourea **V-3**{*1,1*} followed by the Fmoc-protecting group release triggering a spontaneous cyclative cleavage of a liberated thiourea from the solid support to yield 2-thiohydantoin derivative **V-5**{*1,1*}. After the lyophilization of the cleavage cocktail (PIP/DMF), the crude residue **V-5**{*1,1*} was treated with TFA/DCM to remove the *tert*-butyl protecting group and eventually cyclize the fused [6+5] oxazine derivative **V-6**{*1,1*}. In contrast to our previous research,[2,27–30] the expected oxazine scaffold was not detected by LC-MS analysis. In this case, the reaction resulted in the formation 5-methylidene-thiohydantoin **V-7**{*1,1*}. The following TES reduction provided the expected 5-methyl-thiohydantoin **V-8**{*1,1*} in excellent crude purity (85%) and 19% overall yield. Although the exact configuration on the newly formed C5 stereocenter of **V-8**{*1,1*} was not established, the structure was determined by detailed 2D NMR analysis.

Scheme 11. The synthesis of 5-methylidene and 5-methyl-thiohydantoins **V-7**{R^1,*1*} and **V-8**{R^1,*1*}[a]

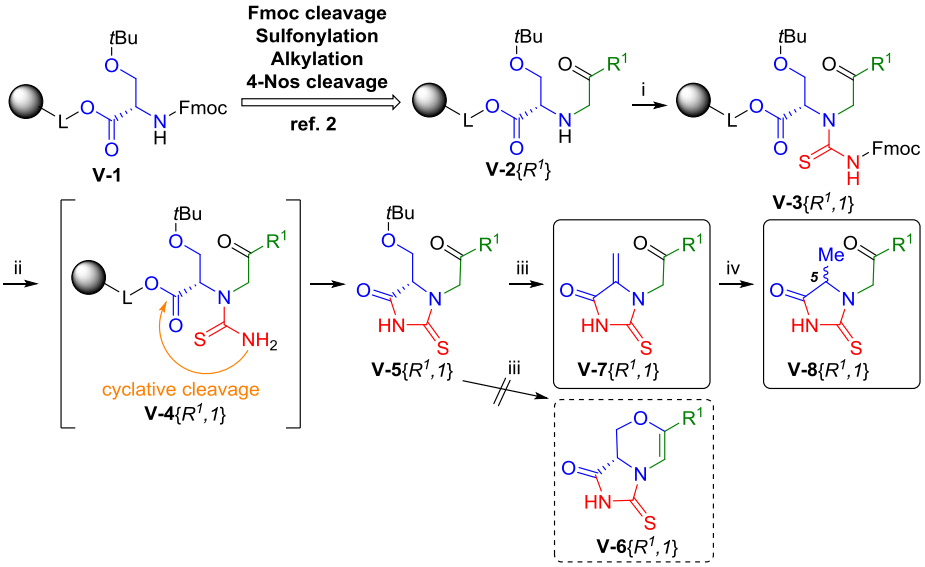

[a]Reagents and conditions: (i) Fmoc-NCS, anhydrous THF, 2 h, rt; (ii) 35% PIP/DMF, 24 h, rt or 10% PIP/DMF for derivative **V-3**{*4,1*}); (iii) neat TFA, 20 h, 35 °C; (iv) TFA/TES/DCM (5:3:5), 24 h, rt.

In addition, Fmoc-NCS was altered to *N*-alkyl-isothiocyanates to test the applicability of the reaction sequence for *N*-substituted analogues (Scheme 11). Since the corresponding *N*-benzylthiourea **V-3**{*1,2*}, prepared from benzyl-isothiocyanate, did not undergo the spontaneous cyclative cleavage from the resin, the resin was further exposed to TFA under elevated temperature (80 °C) to trigger the cyclization reaction. Although the mass spectrometry data corresponded to expected thiohydantoin-dihydrooxazine derivative **V-6**{*1,2*}, the careful structural NMR elucidation of the isolated compound revealed that the scaffold was not formed. Interestingly, the reaction yielded no imidazole-2-thiones **V-9a-b**{*1,2*}, but the heating in TFA enabled the dehydration and a ring closure that furnished imidazo[2,1-*b*]thiazol-4-ium derivative **V-10**{*1,2*}. The product was isolated and obtained in 80% crude purity and 53% overall (Table 5). The structure was carefully investigated and determined by detailed 2D NMR analysis (Figure 16).

Scheme 12. The applicability of *N*-substituted immobilized thioureas **V-3**{R^1,*2-6*}[a]

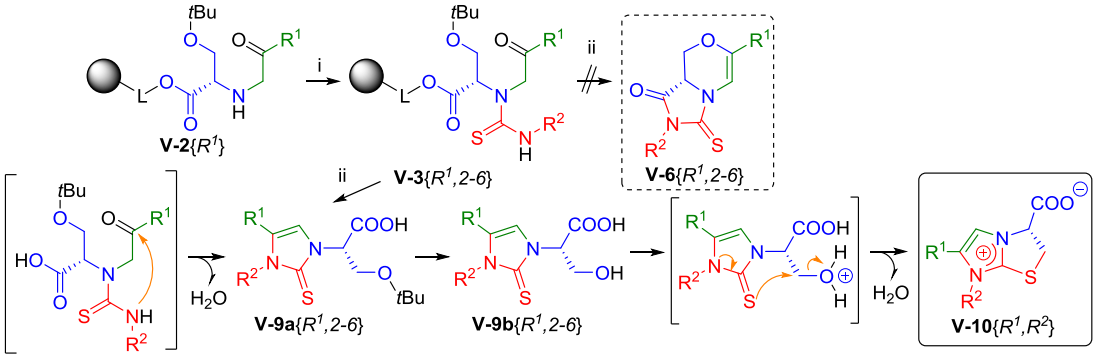

[a]Reagents and conditions: (i) R^2-NCS, anhydrous THF, 44 h or 20 h for derivatives **V-2**{R^1,*2*} and 72 h for derivatives **V-2**{R^1,*5*}, rt; (ii) a) neat TFA, 80 °C, 20 h or 48 h (for derivatives **V-3**{R^1,*3*}), b) evaporation of TFA, c) reverse-phase semipreparative HPLC purification using AmAc buffer, d) freeze-drying.

Figure 16. The key ^{1}H-^{15}N HMBC, ^{1}H-^{13}C HMBC and NOE correlation of **V-10**{*1,2*}

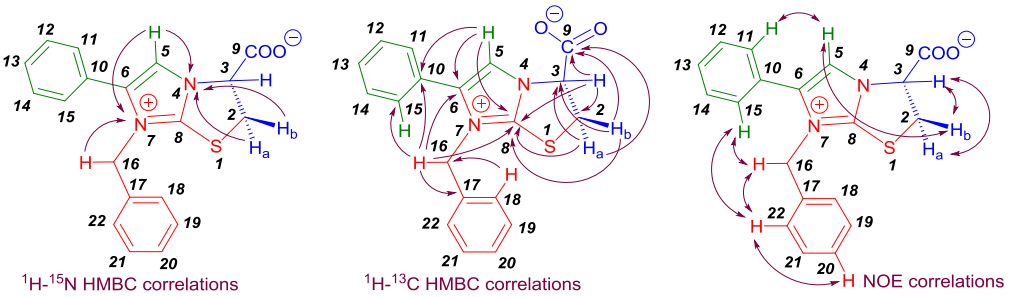

3.5.3 Limitations and scope

The applicability of the reaction sequence was tested for various *α*-bromoketones and isothiocyanates (Figure 17). Except for derivatives **V-3**{*2,5*}, **V-3**{*4,4*} and **V-3**{*4,5*}, prepared from building blocks with cyclohexylmethyl and 2-(4-morpholino)ethyl as R^2 substituent, the synthesis of key *α*-amino ketones **V-3**{R^1,R^2} was successful for all tested building blocks with electron donating and electron withdrawing substituents in R^1 position. The reaction time was dependent on a reactivity of the used isothiocyanate. In the case of resin-bound compounds **V-3**{R^1,*2*}, prepared from benzyl isothiocyanate, the formation of the corresponding thioureas was relatively fast, and the reaction time was just 20 h. In contrast, the reaction with allyl, 2-(4-morpholino)ethyl and cyclohexylmethyl isothiocyanates required noticeably longer time (44-72 h) to reach the completion. In the case of **V-3**{*2,5*}, **V-3**{*4,4*} and **V-3**{*4,5*}, the resulting thioureas were observed as a mixture with the starting material in a ratio of approximately 86:14 even if the reaction time was extended (44-72 h).

Figure 17. The list of tested building blocks for R^1 and R^2 substituents

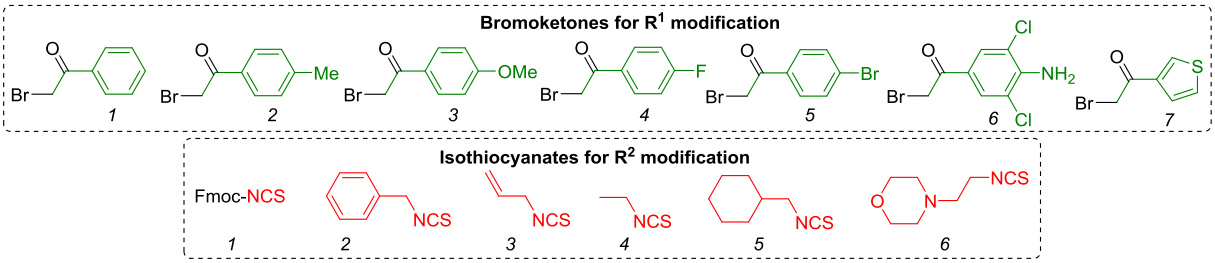

Analogously to *N*-unsubstituted-isothiocyanates, the synthesis of other thiohydantoins **V-7-8**{R^1,*1*} gave desired products in 68-85% crude purities and 7-19% overall yields. In the case of *N*-alkyl-thioureas **V-3**{R^1,*2-6*}, the subsequent TFA-mediated cyclization was dependent on the type of *N*-substituent, and for allyl derivatives **8**{R^1,*3*}, the reaction time had to be prolonged from 20 to 48 h. In total, this second strategy enabled the synthesis of 16 final compounds **V-10**{R^1,*2-6*} using combination of various *α*-bromoketones and isothiocyanates in 69-97% crude purities and 17-59% overall yields (Table 5).

Although the target products **V-10**{R^1,*2-6*} were obtained as highly pure compounds (97-99%), the ^{1}H NMR spectra of some derivatives (measured in deuterated DMSO) showed the presence of an impurity **V-11**{R^1,*2-6*} in quantities of up to 18%. When the samples **V-10**{*1,4*}, **V-10**{*3,6*} and **V-10**{*4,5*} were shortly heated prior to NMR analysis to dissolve, the quantity of the impurities rapidly increased by 40-92%. For this reason, the compound **V-10**{*3,3*}, which was synthesized from allyl isothiocyanate (16% of impurity was detected after dissolving the sample in DMSO-d_6), was subjected to detailed NMR elucidation. According to data, formation of the impurity **V-11**{*3,3*} was proved as a product of isomerization

in DMSO-d_6 (Figure 18). To prove the isomerism, the compound **V-10**{*3,3*} was analysed using variable-temperature ^{1}H NMR experiments gradually at 27 °C (16% of **V-11**{*3,3*}), 80 °C (43%), 100 °C (84%), 120 °C (97%), 140 °C (97%) and after cooling to 27 °C (97%). The data indicated that almost full conversion to the by-product **V-11**{*3,3*} (97%) was observed at 120 °C. However, cooling the sample to room temperature did not affect the conversion of the isomer. Further NMR investigation of **V-11**{*3,3*} using 2D spectroscopy confirmed the structure through the identification of 4-methoxyphenyl, allyl, 2-aminoacrylic acid and imidazole-2-thione moieties *via* characteristic signals.

Figure 18. Isomerization of imidazo[2,1-*b*]thiazol-4-iums **V-10**{R^1,*2-6*} to imidazole-2-thiones **V-11**{R^1,*2-6*}

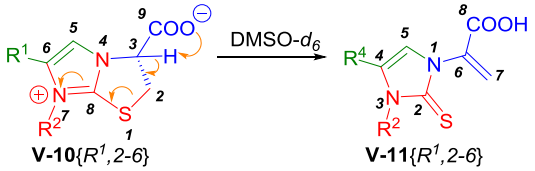

Table 5. List of prepared and fully characterized compounds[a-e]

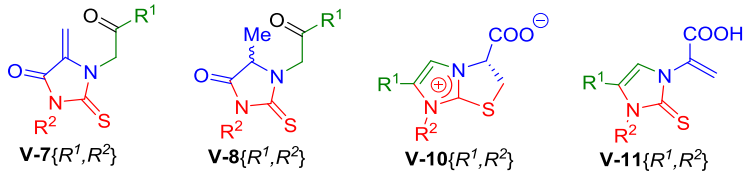

cmpd	R^1	R^2	cyclization time [h]	crude purity [%][a]	final purity [%][b]	overall yield [%][c]	ratio of V-10:11 at rt [%][c]	ratio of V-10:11 after heating [%][c,d]
V-7{*1,1*}	Ph	H	20	80	99	11	-	-
V-7{*4,1*}	4-F-Ph	H	20	69	98	11	-	-
V-7{*5,1*}	4-Br-Ph	H	20	75	97	7	-	-
V-7{*6,1*}	4-NH_2-3,5-diCl-Ph	H	20	68	98	8	-	-
V-7{*7,1*}		H	20	85	97	8	-	-
V-8{*1,1*}	Ph	H	20	85	99	19	-	-
V-8{*5,1*}	4-Br-Ph	H	20	71	98	16	-	-
V-8{*7,1*}		H	20	72	99	15	-	-
V-10{*1,2*}	Ph	Bn	20	80	98	53	93:7	0:100
V-10{*1,3*}	Ph	allyl	48	90	98	34	100:0	8:92
V-10{*1,4*}	Ph	Et	20	91	99	23	45:55[e]	11:89
V-10{*2,2*}	4-Me-Ph	Bn	20	96	99	38	97:3	3:97
V-10{*2,5*}	4-Me-Ph		20	77	99	49	100:0	NT
V-10{*3,3*}	4-MeO-Ph	allyl	48	87	99	32	84:16	3:97
V-10{*3,4*}	4-MeO-Ph	Et	20	92	99	59	100:0	13:87
V-10{*3,6*}	4-MeO-Ph		20	95	99	39	60:40[e]	0:100
V-10{*4,4*}	4-F-Ph	Et	20	85	99	57	100:0	16:84
V-10{*4,5*}	4-F-Ph		20	70	99	19	8:92[e]	8:92
V-10{*5,2*}	4-Br-Ph	Bn	20	91	98	28	98:2	9:91
V-10{*5,3*}	4-Br-Ph	allyl	48	69	99	18	100:0	29:71
V-10{*5,6*}	4-Br-Ph		20	90	98	17	88:12	0:100
V-10{*7,2*}		Bn	20	97	98	26	97:3	0:100
V-10{*7,3*}		allyl	48	83	98	24	89:11	0:100
V-10{*7,6*}			20	95	98	39	82:18	82:18

[a]Overall purity after the entire reaction sequence calculated from HPLC-UV traces at 205–400 nm; [b]HPLC-UV at 205–400 nm after purification; [c]Calculated from the ^{1}H NMR spectrum of the purified products; [d]Sample heated at 120 °C for 30 min and measured after cooling to 27 °C; [e]Sample was shortly heated prior to NMR analysis to dissolve; NT – not tested.

3.5.4 Conclusion

To conclude, we developed the solid-phase synthetic strategies to prepare three types of imidazole derivatives depending on the type of isothiocyanate and cleavage conditions used. In this context, we prepared more than 36 original compounds (e.g. thiohydantoins, imidazole-2-thiones and imidazo[2,1-*b*] thiazol-4-iums) in high crude purities (68-96%) and 7-57% overall yields. The structures of final derivatives were confirmed by advanced NMR experiments and all of them were fully characterized.

3.6 Synthesis of 2-Alkylsulfonyl-Imidazoles with Three Diversity Positions from Immobilized *α*-Acylamino Ketones

The results of this project were published in: Králová, P.; Soural, M. *ACS Comb. Sci.* **2018**, *20* (8), 467–471.[32]

3.6.1 Brief introduction

To avoid the above reported formation of thiohydantoins formed *via* cyclative cleavage of thioureas,[31] we decided to replace Wang resin with Wang-piperazine resin to stabilize the linkage to the support (i.e. to replace ester with the amide functionality). The synthesis of the corresponding thioureas was performed according to the previously developed protocols.[2,31] Theoretically, the resulting Fmoc-thioureas could undergo a base-mediated Fmoc-deprotection followed by immediate *S*-alkylation with *α*-bromoketones and a spontaneous cyclization to thiazole moiety, inspired by the known procedures.[43,44] In such a case, the treatment with TFA could yield *N*-thiazolo-oxazines (Figure 19, The original strategy). However, the suggested methodology was not feasible due to spontaneous attack of ketone by amine giving imidazolo-thiones. Their *S*-alkylation and oxidation yielded 2-alkylsulfonyl-imidazoles (Figure 19, The alternative strategy). The main aims of the project were determination of the limitations and scope using various Fmoc-amino acids, *α*-bromoketones and alkylating agents and development of suitable conditions to oxidize sulfides to corresponding sulfones or sulfoxides.

Figure 19. The proposed synthesis of *N*-thiazolo-oxazines and the actual formation of imidazoles

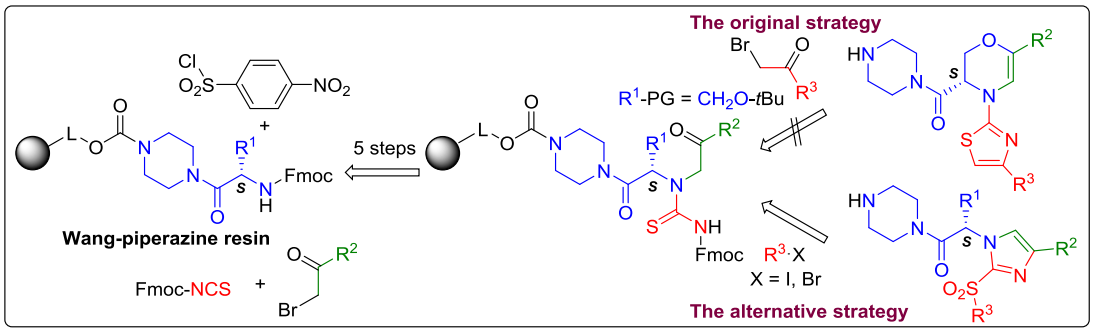

3.6.2 Synthesis

First, the synthesis of *N*-thiazolo-oxazines was tested using a combination of Wang-piperazine resin-immobilized Fmoc-Ser(*t*Bu)-OH **VI-3**{*2*} and *α*-bromoacetophenones. The key *α*-amino ketones **VI-3**{*2,1*} were synthesized in five steps according to our previously reported protocol.[2] The reaction with Fmoc-NCS under previously developed conditions[31] yielded desired thiourea derivative **VI-4**{*2,1*} in excellent crude purity (90%, calculated from HPLC-UV traces at 205–400 nm). After the removal of the Fmoc protecting group, the check of reaction solution (PIP/DMF) by LC-MS analysis confirmed that the cyclative cleavage

has not taken place from the resin. The *S*-alkylation with *α*- bromoacetophenone and TFA treatment should afford (after the product cleavage from the resin and cyclization) *N*-thiazolo-oxazines **VI-5**{*2,1,4*} (Scheme 13).[43,44] However, the measured LC-MS data did not correspond to the mass of the product, but it indicated the previously reported formation of imidazole-2-thione scaffold **VI-7**{*2,1,4*}. For this reason, we performed the detailed NMR investigation of the product to confirm the structure. Since the detailed NMR analysis confirmed the imidazole-2-thione arrangement **VI-7**{*2,1,4*}, we designed the synthetic route to prepare novel 2-alkyl-sulfonyl-imidazoles **VI-10**{R^1,R^2,R^3} which should be based on a formation of sulfides and their oxidation to either sulfoxides or sulfones depending on the oxidizing conditions used.

Scheme 13. The synthesis of *N*-thiazolo-oxazines **VI-5**{*2*,R^2,*4*} and imidazoles **VI-10**{R^1,R^2,R^3}[a]

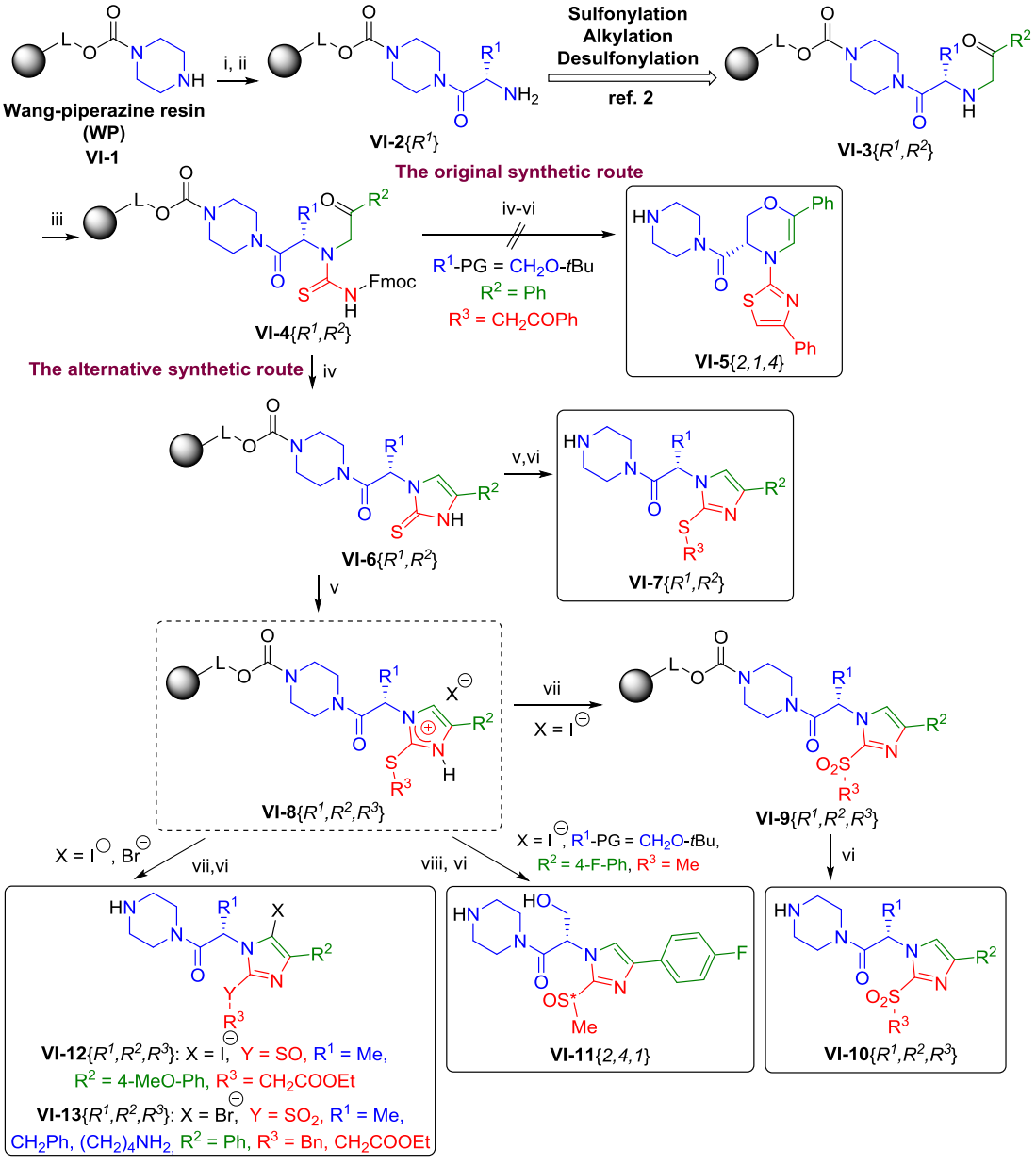

[a]Reagents and conditions: (i) Fmoc-amino acid, HOBt, DIC, DCM, DMF, 24 h, rt; (ii) 50% PIP/DMF, 30 min, rt; (iii) Fmoc-NCS, anhydrous THF, 2 h, rt; (iv) 50% PIP/DMF, 15 min, rt; (v) R^3X (X = I, Br), anhydrous DCM, 2 h, rt; (vi) neat TFA, on, rt; (vii) *m*CPBA, anhydrous DCM, 5 h, rt; (viii) *m*CPBA, anhydrous DCM, 30 min, rt.

The immobilized imidazole-2-thione **VI-8**{*1,1,1*} was obtained in seven-step reaction sequence according to the above described protocol started from Fmoc-Ala-OH immobilized on Wang-piperazine resin, *α*-bromoacetophenone and methyl iodide (Scheme 13). Then the sulfide **VI-8**{*1,1,1*} was oxidized with

meta-chloroperoxybenzoic acid (*m*CPBA) using previously published conditions.[45] The TFA-mediated product cleavage from the resin afforded the sulfone **VI-10**{*1,1,1*} in an 95% crude purity and 10% overall yield.

3.6.3 Limitations and scope

The applicability of this synthetic approach was evaluated using a combination of different Fmoc-amino acids with functionalized side chains, *α*-bromoketones with electron donating and electron withdrawing substituents and various alkylating agents (Figure 20). The synthesis of all thiourea derivatives **VI-4**{R^1,R^2} was successful for all tested combinations of the synthons and the derivatives were obtained in 72-85% crude purities. After the deprotection of the Fmoc protecting group which triggered a formation of imidazole-2-thiones **VI-6**{R^1,R^2}, the alkylation was tested with alkyl iodides (ethyl iodoacetate, benzyl iodide, phenacyl iodide, allyl iodide) and alkyl bromides (ethyl bromoacetate, benzyl bromide, phenacyl bromide). Except for phenacyl iodide which afforded a mixture of unknown products, the resulting sulfides **VI-8**{R^1,R^2,*1-4*} were obtained in 57-94% crude purities. In the case of sulfide **VI-8**{*1,1,6*}, the alkylation with 3-(bromomethyl)pyridine hydrobromide required the presence of base (DBU, 1 equiv to alkylating agent) to the reaction completion; however, the subsequent oxidation failed and only the starting material was detected in the LC-MS spectrum.

Figure 20. List of tested synthons for R^1, R^2 and R^3 substituents

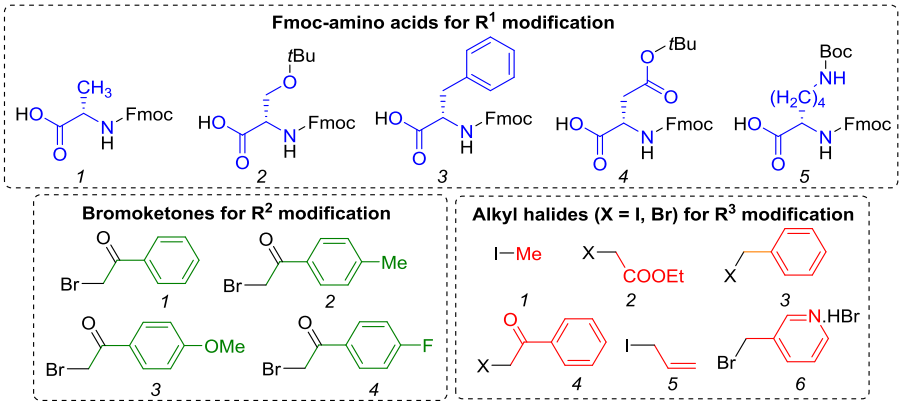

In the case of sulfide **VI-8**{*2,4,1*}, prepared from L-serine, 2-bromo-4′-fluoroacetophenone and methyl iodide, the oxidation for only 30 min afforded the corresponding sulfoxide **VI-11**{*2,4,1*}, which was obtained as a mixture of two inseparable diastereoisomers in a ratio of 68:32 (calculated from the ^{1}H NMR spectrum of the purified product). When the oxidation time was extended to 5 h, the reaction furnished sulfone **VI-11**{*2,4,1*}. However, in the case of other sulfide analogous **VI-8**{R^1,R^2,R^3}, the isolation of sulfoxides was impossible due to immediate oxidation to sulfones by the excess of *m*CPBA (Scheme 13).

The oxidation of sulfide **VI-8**{*1,3,2*}, prepared from ethyl iodoacetate, and the subsequent product release from the resin yielded neither the expected sulfone **VI-10**{*1,3,2*} nor sulfoxide **VI-11**{*1,3,2*}. In this case, a by-product with a molecular weight corresponding to the iodinated sulfoxide **VI-12**{*1,3,2*} was detected by LC-MS analysis (Scheme 13, Table 6). After reverse-phase semipreparative HPLC chromatography, the suggested structure was confirmed by NMR analysis. According to the ^{1}H NMR spectrum, the by-product was obtained as a mixture of two inseparable diastereoisomers in a ratio of 86:14. In contrast, the oxidation of sulfide **VI-8**{*1,1,3*}, prepared from benzyl iodide or benzyl bromide, resulted in either sulfone **VI-1**{*1,1,3*} or brominated sulfone **VI-13**{*1,1,3*} as determined by HPLC-UV-MS analysis. The comparison

of ^{1}H NMR spectra of all three compounds indicated that halogenation took place on the imidazole scaffold based on the disappearance of the corresponding aromatic signal HC^4 of sulfone **VI-10**{*1,1,3*}. Surprisingly, the oxidation of other sulfides **VI-8**{R^1,R^2,R^3}, prepared from the corresponding alkyl iodides (e.g. methyl iodide, ethyl iodoacetate, benzyl iodide) afforded predominantly sulfones **VI-10**{R^1,R^2,R^3} and no iodinated analogues **VI-12**{R^1,R^2,R^3} were detected. However, the oxidation of sulfides **VI-8**{R^1,R^2,R^3}, prepared from the corresponding alkyl bromides (e.g. ethyl bromoacetate, benzyl bromide and phenacyl bromide), caused always the bromination (Table 6).

The unexpected halogenation can be explained by the formation of imidazole-hydrohalogenides (X = Br, I) at the stage of intermediates **VI-8**{R^1,R^2,R^3} as a result of the generation of HBr/HI and its capture after the alkylation step (Scheme 13). The treatment with *m*CPBA may oxidize the bromide/iodide anions to bromine/iodine followed by bromination/iodination of the imidazole scaffold by radical mechanism. The crucial role of *m*CPBA is evident from the cleavage and analysis of sulfides **VI-8**{R^1,R^2,R^3}, which showed no trace of the brominated/iodinated sulfides. According to these facts, the following oxidation leading to four diverse imidazoles **VI-10-13**{R^1,R^2,R^3} was dependent on overall substitution of the starting sulfides **VI-8**{R^1,R^2,R^3} and the type of alkylating agents used (e.g. alkyl iodide or alkyl bromide; Table 6). In total, we prepared 20 final compounds **VI-10-13**{R^1,R^2,*1-4*} in 55-97% crude purities and 10-36% overall yields (Table 6).

Table 6. The list of synthesized and fully characterized compounds[a-d]

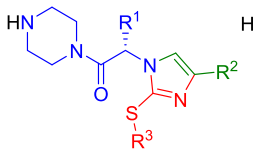

VI-7{R^1,R^2,R^3}

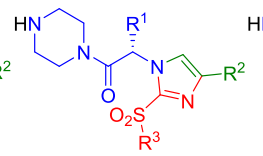

VI-10{R^1,R^2,R^3}

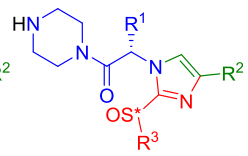

VI-11{R^1,R^2,R^3}

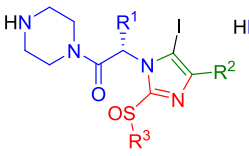

VI-12{R^1,R^2,R^3}

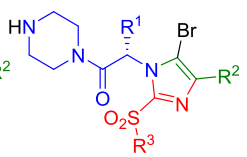

VI-13{R^1,R^2,R^3}

cmpd	R^1	R^2	R^3	type of alkylating agent X = Br, I[a]	crude purity [%][b]	final purity [%][c]	overall yield [%][d]
VI-7{*4,1,4*}	CH_2COOH	Ph	CH_2COPh	Br	75	99	11
VI-7{*2,1,4*}	CH_2OH	Ph	CH_2COPh	Br	82	99	16
VI-10{*1,1,1*}	Me	Ph	Me	I	75	98	10
VI-10{*1,1,3*}	Me	Ph	Bn	I	84	99	14
VI-10{*2,1,1*}	CH_2OH	Ph	Me	I	94	98	36
VI-10{*2,2,3*}	CH_2OH	4-Me-Ph	Bn	I	74	99	10
VI-10{*2,2,5*}	CH_2OH	4-Me-Ph	allyl	Br	88	98	26
VI-10{*2,3,1*}	CH_2OH	4-MeO-Ph	Me	I	72	98	23
VI-10{*2,4,1*}	CH_2OH	4-F-Ph	Me	I	81	97	21
VI-10{*3,1,1*}	CH_2Ph	Ph	Me	I	95	99	20
VI-10{*3,4,2*}	CH_2Ph	4-F-Ph	CH_2COOEt	I	69	99	17
VI-10{*3,4,3*}	CH_2Ph	4-F-Ph	Bn	I	65	99	16
VI-10{*4,1,1*}	CH_2COOH	Ph	Me	I	71	99	13
VI-10{*4,4,3*}	CH_2COOH	4-F-Ph	Bn	I	63	98	22
VI-10{*5,1,1*}	$(CH_2)_4NH_2$	Ph	Me	I	87	99	15
VI-11{*2,4,1*}	CH_2OH	4-F-Ph	Me	I	65	99	12
VI-12{*1,3,2*}	Me	4-MeO-Ph	CH_2COOEt	I	63	99	14
VI-13{*1,1,3*}	Me	Ph	Bn	Br	76	99	15
VI-13{*3,1,2*}	CH_2Ph	Ph	CH_2COOEt	Br	58	98	11
VI-13{*5,1,3*}	$(CH_2)_4NH_2$	Ph	Bn	Br	80	99	16

[a]The structure of alkylating agents is shown in Figure 20; [b]Overall crude purity after the entire reaction sequence calculated from HPLC-UV traces at 205–400 nm; [c]Purity calculated from HPLC-UV traces at 205–400 nm after purification; [d]Calculated from the ^{1}H NMR spectrum of the purified products.

Finally, we tested the possible alteration of the amidic moiety; however, the reaction pathway failed at the stage of Fmoc-thiourea formation for the Wang-ethylenediamine resin, Rink amide resin and BAL resin-immobilized secondary amines used as the starting materials.

3.6.4 Conclusion

To conclude, the simple synthesis of 2-alkylsulfonyl-imidazoles with three diversity positions was developed. In some cases (started from immobilized L-alanine, L-phenylalanine and L-lysine), the C4 halogenated products were obtained depending on the combination of R^1, R^2 and R^3 substituents and type of the alkylating agents used. The developed strategy can be applied for combinatorial synthesis of chemical libraries using a large number of readily available building blocks.

3.7 Rearrangement of Threonine and Serine-Based *N*-(3-Phenylprop-2-yn-1-yl) Sulfonamides Yields Chiral Pyrrolidin-3-ones

The results of this project were published in: Králová, P.; Maloň, M; Pospíšil, J.; Soural, M. *J. Org. Chem.* **2020**, *85* (2), 985–993.[46]

3.7.1 Brief introduction

This subchapter continues to our previous results[2,27–32] which describes the stereoselective synthesis of chiral morpholine or imidazole derivatives synthesized from immobilized *N*-phenacyl-2/4-nitrobenzenesulfonamides. In the following research, *N*-phenacyl intermediates were replaced with internal alkynols by switching from haloketones to phenylakynols as the alkylating agents. The polymer-supported intermediates were subjected to TFA-mediated cleavage from the resin and then modified by an internal post-cleavage hydroxyalkoxylation-reduction using trimethylsilyl trifluoromethanesulfonate (TMSOTf) and TES. The reaction should result in a formation of 1,4-oxazepane scaffold according to the previously reported results.[4] The main aim of this project was to develop a methodology to synthesize functionalized 1,4-oxazepanes amenable for further diversification, e.g. preparation of fused oxazepanes (Figure 21, The original pathway). However, the ^{1}H and ^{13}C{^{1}H} NMR spectra were not consistent with the 1,4-oxazepane structure and therefore, we performed detailed NMR investigation of the product which confirmed the pyrrolidin-3-one scaffold (Figure 21, The actual results).

Figure 21. The proposed synthetic strategy to prepare single and fused 1,4-oxazepanes

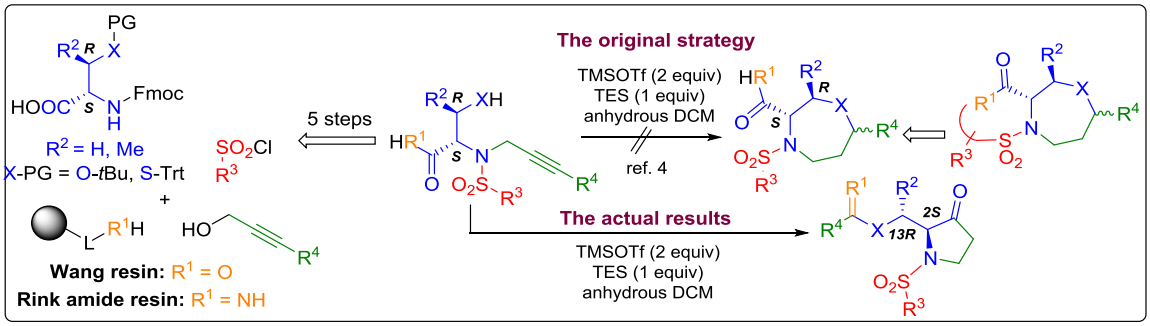

3.7.2 Synthesis

First, Wang resin and Rink amide resin **VII-1**{R^1} were acylated with Fmoc-amino acids, subjected to the Fmoc-cleavage, and reacted with sulfonyl chlorides (2-NosCl, 4-NosCl, Ms-Cl and Ts-Cl) according to the previously reported procedure.[2] The resulting *N*-sulfonamides **VII-2**{R^1,R^2,R^3} were alkylated with different alkynols using a Mitsunobu alkylation (Figure 22, alkynols *1-6* for R^4 modifications). For these purposes, *para*-substituted phenylalkynols bearing electron donating (Me and MeO) and electron withdrawing (CF_3) substituents were prepared from the corresponding aryl iodides and propargyl alcohol in 51-97% overall yields *via* Sonogashira coupling (calculated after purification). Cleavage from resin **VII-3**{R^1,R^2,R^3,R^4} with TFA was followed by spontaneous cleavage of the *tert*-butyl ether. The resulting intermediates **VII-4**{R^1,R^2,R^3,R^4} were purified by semipreparative HPLC or by silica gel chromatography and 9 representative compounds were obtained in 40-95% crude and 21-82% overall yields (Scheme 14).

Scheme 14. The synthesis of alkynols **VII-4** and their TMSOTf-mediated rearrangement to **VII-5**[a]

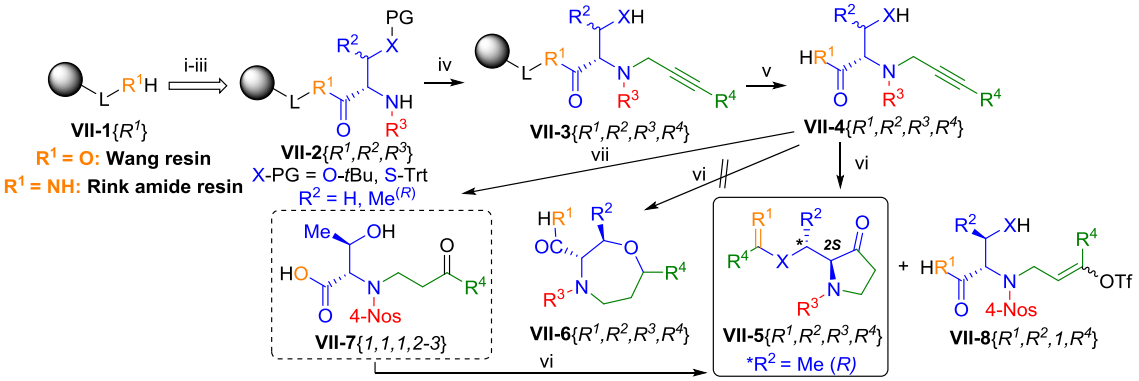

[a]Reagents and conditions: (i) Fmoc-amino acid, HOBt, DMAP, DIC, DMF, DCM, 24 h, rt; (ii) 50% PIP/DMF, 30 min, rt; (iii) R^3-sulfonyl chlorides, 2,6-lutidine, DCM, 24 h, rt; (iv) alkynol, TPP, DIAD, anhydrous THF, 24 h, rt; (v) 50% TFA/anhydrous DCM, 1 h, rt; (vi) TMSOTf/TES (2:1), anhydrous DCM, 24 h, 0 °C or TMSOTf, anhydrous DCM, 24-72 h, 23-40 °C; (vii) HPLC MeCN/H_2O or HPLC MeCN/10 *m*M AmAc 0.08 h, rt (for derivative **VII-7**{*1,1,1,3*}) or HPLC MeCN/AmAc, 1440 h, rt (for derivative **VII-7**{*1,1,1,2*}).

Figure 22. The list of tested building blocks for R^1, R^2, R^3 and R^4 substituents

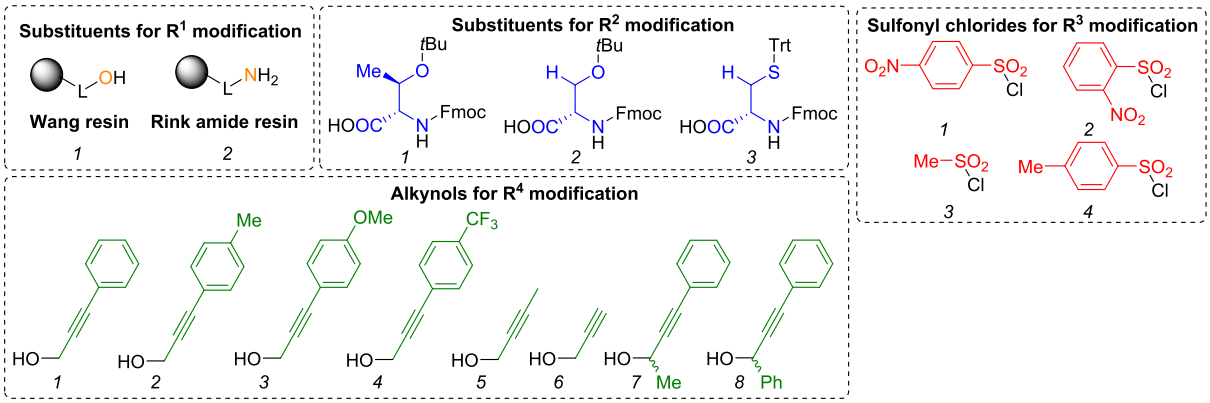

The purification of *N*-alkyl-sulfonamides **VII-4**{*1,1,1,2*} and **VII-4**{*1,1,1,3*} bearing electron-donating (Me and MeO) substituents did not furnish expected alkynes due to their hydrolysis to ketones **VII-7**{*1,1,1,2*} and **VII-7**{*1,1,1,3*} during HPLC purification (Scheme 14). The rate of the hydrolysis was dependent on the R^4 substitution. The hydrolysis to ketone was noticeably faster in the case of MeO group (immediate conversion to ketone **VII-7**{*1,1,1,3*}). Although the rate of hydrolysis to *p*-methoxybenzophenone **VII-7**{*1,1,1,3*} was comparable in both tested solvents (AmAc/MeCN vs AmAc/H_2O), the better results were achieved in 10 *m*M AmAc in MeCN. On the other hand, Me substitution slowed the conversion

to ketone **VII-7**{*1,1,1,2*} (1440 h). Finally, the ketone **VII-7**{*1,1,1,3*} was purified by reverse-phase semi-preparative HPLC and subjected to NMR experiments to check the characteristic signals of ketone **VII-7**{*1,1,1,3*}. Comparison of the $^{13}C\{^{1}H\}$ NMR spectra of alkyne **VII-4**{*1,1,3,1*} with ketone **VII-7**{*1,1,1,3*} shows that two carbon signals of alkyne moiety at 85.0 ppm and 85.8 ppm were replaced by three signals at 199.3 ppm, 44.5 ppm and 39.2 ppm indicating the carbonyl group and two methylene groups, respectively. Additionally, the ^{1}H NMR spectrum of ketone shows two methylene groups at 3.60 ppm and 3.42 ppm.

In addition, *N*-alkyl-sulfonamides **VII-2**{*1,1,1*} were alkylated with sterically bulky racemic alcohols (4-phenylbut-3-yn-2-ol and 1,3-diphenylprop-2-yn-1-ol; Figure 22, modification *7-8* for R^4 substitution). The alkylation with 4-phenylbut-3-yn-2-ol required repetition twice times for the full conversion to product **VII-3**{*1,1,1,7*} which was obtained in 95% crude purity as a mixture of inseparable diastereoisomers. In the case of 1,3-diphenylprop-2-yn-1-ol, the alkylation conditions were extensively optimized (e.g. TPP, TBP, anhydrous THF, DCE, DME, rt-60 °C); however, we observed an incomplete conversion to the product **VII-3**{*1,1,1,8*} in only 56% crude purity (Scheme 15).

Scheme 15. The synthesis of sulfonamides **VII-3**{*1,1,7-8*} and their rearrangement[a]

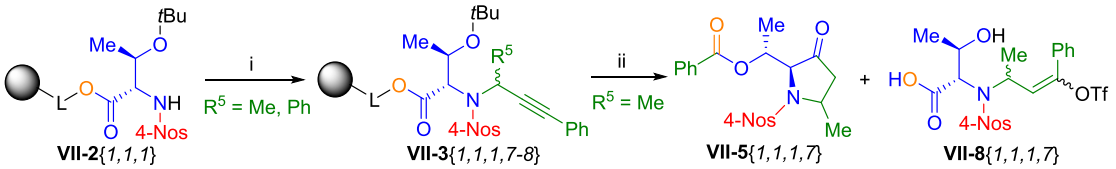

[a]Reagents and conditions: (i) 4-phenylbut-3-yn-2-ol or 1,3-diphenylprop-2-yn-1-ol, phosphine, DIAD, solvent, 24 h, rt-60 °C; (ii) TMSOTf, anhydrous DCM, 24 h, 40 °C.

After that, intermediate **VII-4**{*1,1,1,1*} was reacted with TMSOTf (2 equiv) and TES (1 equiv) in anhydrous DCM according to the previously reported conditions[4] to obtain 1,4-oxazepane **VII-6**{*1,1,1,1*} (Scheme 14). The reaction generated a highly pure compound with a molecular mass corresponding to the expected product **VII-6**{*1,1,1,1*}. However, its ^{1}H and $^{13}C\{^{1}H\}$ NMR spectra were not fully consistent with the structure of **VII-6**{*1,1,1,1*}. For example, the $^{13}C\{^{1}H\}$ signal at 210.6 ppm indicating a carbonyl group could not be assigned to any carbon atom in **VII-6**{*1,1,1,1*}. For this reason, a set of 1D and 2D NMR spectra, including ^{1}H-^{15}N HMBC, were collected and carefully analyzed. It confirmed the formation of pyrrolidin-3-one **VII-5**{*1,1,1,1*}.

3.7.3 Limitations and scope

The structure-reactivity relationship of the rearrangement was further studied deeply for all prepared *N*-alkynol-sulfonamides **VII-4**{R^1,R^2,R^3,R^4}. Generally, the rearrangement conditions (reaction time and temperature) were typically dependent on the type of the starting materials **VII-4**{R^1,R^2,R^3,R^4}. The electron withdrawing effect of R^4 substituent (CF_3) slowed the conversion to the product **VII-5**{*1,1,1,4*} and thus higher temperature (40 °C) was necessary to push the conversion of the starting material to the final product. In the cases of alkyl-alkynols bearing methyl or hydrogen group in R^4 position **VII-4**{*1,1,1,5*} and **VII-4**{*1,1,1,6*} and serine-based intermediates **VII-4**{*1,2,1,1*}, the rearrangement required longer reaction times (72 h) to completion. To compare the threonine/serine-based intermediates **VII-4**{*1,1,1,1*} and **VII-4**{*1,2,1,1*}, the slower rearrangement rate was expected because of lacking the Thorp-Ingold effect in serine-based precursor.[47] Similarly, replacement of carboxylic acid with the corresponding amide

VII-4{*2,1,1,1*} also led to the slow transformation. In all above mentioned cases, the corresponding enol triflates **VII-8**{R^1,R^2,R^3,R^4} were detected in the reaction mixtures in a ratio of 9-28% depending on R^1, R^2 and primarily on R^4 substituents (Scheme 14). The isolated yields were somewhat compromised in several cases, which was caused by difficult chromatography and careful removal of impurities with similar retention times to products. Finally, to further extend the applicability of the disclosed reaction sequence, the sulfanyl analogue of **VII-4**{*1,3,1,1*} was prepared from protected cysteine. However, no traces of the desired pyrrolidinone **VII-5**{*1,3,1,1*} were detected.

In the case of **VII-4**{*1,1,1,7*}, the rearrangement at higher temperature (40 °C) gave a mixture of product **VII-5**{*1,1,1,7*} and the corresponding enol triflate **VII-8**{*1,1,1,7*} in a ratio of 36:64 and in 26% and 47% crude purities, respectively (Scheme 15). When the mixture was subjected to reverse-phase semi-preparative HPLC purification and dissolved in initial mobile phase containing HPLC water and MeCN, it proved to be unstable for longer time needed to HPLC purification.

To conclude, the rearrangement of alkynes **VII-4**{R^1,R^2,R^3,R^4} was successfully applied to prepare ten final compounds **VII-5**{R^1,R^2,R^3,R^4} in 43-96% crude purities and 14-71% overall yields synthesized from diverse synthons (Figure 22, Table 7). In addition, one representative compound **VII-5**{*1,1,1,3*} was synthesized from the corresponding ketone **VII-7**{*1,1,1,3*} by TMSOTf-promoted rearrangement in 93% crude purity and 38% overall yield according to the previously developed conditions.

Table 7. The analytical data for products **VII-5**{R^1,R^2,R^3,R^4}[a-e]

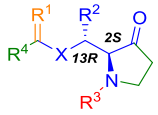

final cmpd	X	R^1	R^2	R^3	R^4	time [h]	temp [°C]	crude purity [%][a]	final purity [%][a]	yield [%][b]
VII-5{*1,1,1,1*}	O	O	Me	4-Nos	Ph	24	23	96	99	71
VII-5{*1,1,2,1*}	O	O	Me	2-Nos	Ph	24	23	96	99	41
VII-5{*1,1,3,1*}	O	O	Me	Ms	Ph	24	23	92	99	40
VII-5{*1,1,4,1*}	O	O	Me	Ts	Ph	24	23	80	99	50
VII-5{*1,1,1,2*}	O	O	Me	4-Nos	4-Me-Ph	24	23	76	99	30
VII-5{*1,1,1,3*}[c]	O	O	Me	4-Nos	4-MeO-Ph	24	23	81	99	42
VII-5{*1,1,1,3*}[d]	O	O	Me	4-Nos	4-MeO-Ph	24	23	93	99	38
VII-5{*1,1,1,4*}	O	O	Me	4-Nos	4-CF_3-Ph	24	40	56	98	18
VII-5{*1,1,1,5*}	O	O	Me	4-Nos	Me	72	23	75	98	33
VII-5{*1,1,1,6*}	O	O	Me	4-Nos	H	72	23	43[e]	NI	NI
VII-5{*1,2,1,1*}	O	O	H	4-Nos	Ph	72	23	51	97	14
VII-5{*1,3,1,1*}	S	O	H	4-Nos	Ph	24	23	NP	NP	NP
VII-5{*2,1,1,1*}	O	NH	Me	4-Nos	Ph	72	23	60	99	14

[a]Overall crude purity determined by HPLC after the entire reaction sequence prior to final purification; [b]Isolated overall yield calculated from the loading of the starting resin; [c]Product **VII-5**{*1,1,1,3*} was prepared from the starting alkyne **VII-4**{*1,1,1,3*}; [d]Product **VII-5**{*1,1,1,3*} was prepared from the starting ketone **VII-7**{*1,1,1,3*}; [e]The compound proved to be unstable during the HPLC purification process; NI = not isolated; NP = not prepared.

3.7.4 Biological screening

All purified compounds were subjected to antimicrobial and cytotoxic tests on representative cancer cell lines. In the case of **VII-5**{*1,2,1,1*}, the compound showed low micromolar toxicity to T-lymphoblastic leukemia (CCRF-CEM) and good selectivity when compared to human fibroblasts (BJ). The therapeutic index (TI_{50}) was calculated to 33 as a BJ proportion to CCRF-CEM (Table 8).

Table 8. Cytotoxic tests on representative cancer cell lines for derivative **VII-5**{*1,2,1,1*}

	cell lines	IC_{50} [μM]
A549	human lung adenocarcinoma	43.13
CCRF-CEM	**T-lymphoblastic leukemia**	**1.60**
CEM-DNR	T-lymphoblastic leukemia, daunorubicin resistant	24.41
HCT116	human colorectal cancer	16.56
HCT116p53-/-	human colorectal cancer, p53 deficient	16.98
K562	acute myeloid leukemia	15.13
K562-TAX	acute myeloid leukemia, paclitaxel resistant	19.43
MRC-5	diploid human fibroblast derived from lung tissue	41.32
BJ	human fibroblast	49.77

3.7.5 Conclusion

The unexpected rearrangement of *N*-alkyl-sulfonamides to novel chiral derivatives of pyrrolidin-3-ones was discovered while the synthesis of single 1,4-oxazepanes according to the previously reported conditions failed. The reaction was studied in detail to determine limitations and scope of the proposed methodology that yield 10 representative pyrrolidin-3-ones.

3.8 The synthesis of fused 1,4-oxazepanes

This project contains only unpublished results.

3.8.1 Brief introduction

The above attempted preparation of oxazepanes from alkynols was unsuccessful,[46] thus this subchapter describes efforts to develop an alternative synthetic strategies. Inspired by our previous results in the field of morpholine chemistry, the first part of the project was paid to the solid-phase synthesis of immobilized *N*-alkenyl (cinnamyl) or *N*-phenacyl-sulfonamides which are placed in a dashed rectangle in Figure 23. The preparation of such intermediates was suggested either from immobilized Fmoc-L-serine/threonine (**Scenarios A-B**) or Fmoc-L-homoserine (**Scenario C**). These key intermediates should be modified with various acylating or alkylating agents to yield the resulting α-amino ketones. Their acid-mediated cleavage from the

Figure 23. The tested synthetic routes to prepare single and fused 1,4-oxazepane derivatives

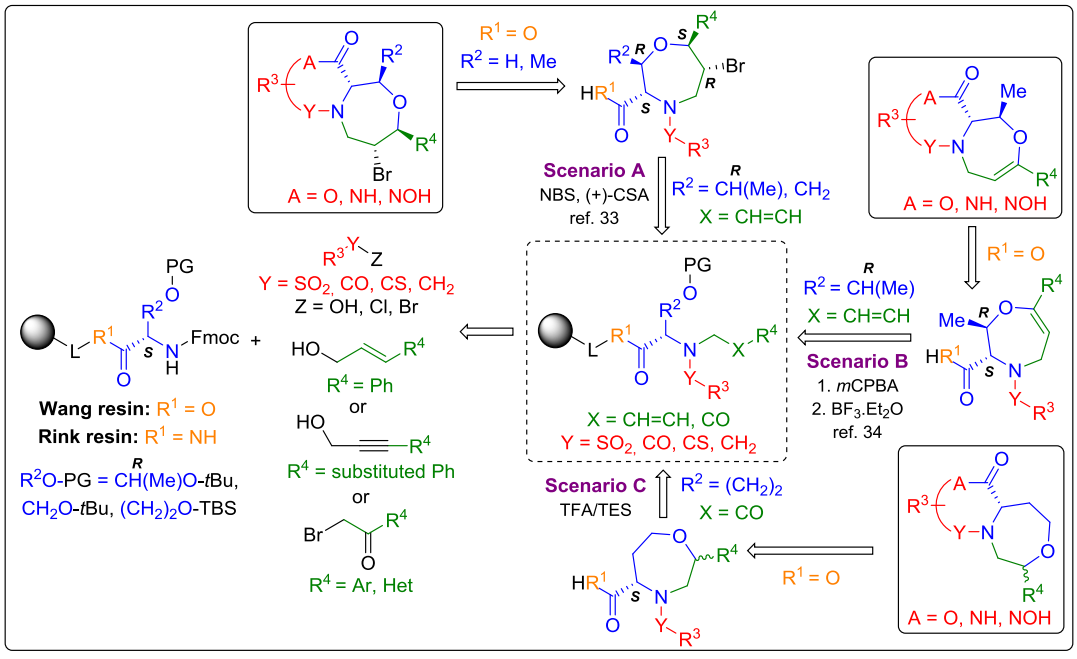

resin and/or a subsequent post-cleavage modification should yield functionalized 1,4-oxazepanes which could be further converted to fused 1,4-oxazepanes similarly to the previously reported protocols.[27–32]

The aim of the project was to test three alternative routes **A-C** to obtain the 1,4-oxazepane or 1,4-oxazepine derivatives. In specific cases, the TES applicability for the stereoselective reduction of 1,4-oxazepines to 1,4-oxazepanes was suggested. Similarly to previous projects, we also intended to determine limitations and scope of the proposed methodologies for various building blocks.

3.8.2 Synthesis, limitations and scope

The synthesis of immobilized 2-Nos-amides and/or *α*-amino ketones was performed using a combination of different Fmoc-amino acids (e.g. L-serine, L-threonine and L-homoserine), various 2/4-Nos-Cl, alkylating agents (e.g. cinnamyl alcohols and α-bromoketones) and acylating agents (e.g. 2-nitrobenzoic acids, Fmoc-amino acids, iodoacetic acid, Fmoc-NCS) or 2-nitrobenzoyl bromide (Figure 24). Unless otherwise stated, the synthesis was accomplished exactly according to the above disassembled protocols.[2,27–32] For this reason, these procedures are not discussed in the text. The following three subchapters are classified according to the type of synthetic pathway used.

Figure 24. The list of tested building blocks for R^1, R^2, R^3 and R^4 substituents

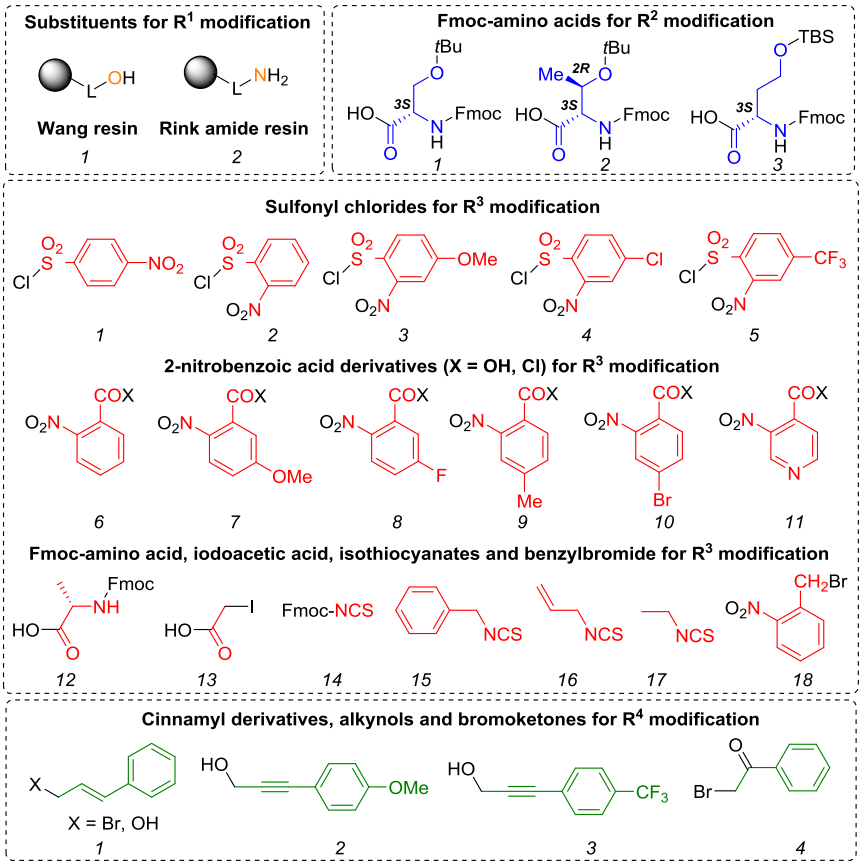

Note: The synthesis of 4-substituted-*trans*-cinnamyl alcohols was performed according to the previously reported protocols based on a $LiAlH_4$-promoted reduction of depicted alkynols in Figure 24, synthons *2-3* for R^4 substitution).[48,49]

3.8.2.1 Scenario A

In this scenario, the synthesis of 1,4-oxazepane derivatives was tested in parallel for immobilized Fmoc-Ser(*t*Bu)-OH and Fmoc-Thr(*t*Bu)-OH **VIII-2**{*1,1*} and **VIII-2**{*1,2*}, respectively. The Fmoc-deprotected amino acids were reacted with 4-Nos-Cl followed by alkylation with cinnamyl bromide. In contrast to the alkylation with α-bromoketones,[2,27–32] the reaction required a repetition of the alkylation step to completion. When the Mitsunobu alkylation using cinnamyl alcohol was used, the serine and threonine-based derivatives **VIII-5**{*1,1,1,1*} and **VIII-5**{*1,2,1,1*} were obtained in 90% and 96% crude purities (calculated from HPLC-UV traces at 205–400 nm after the product cleavage from the resin). After the cleavage from the polymer support, the residual TFA was evaporated under a stream of nitrogen to dryness. The crude intermediates were cyclized using NBS and (1*S*)-(+)-10-camphorsulfonic acid ((+)-CSA) to desired 1,4-oxazepane scaffold **VIII-6**{*1,1,1,1*} and **VIII-6**{*1,2,1,1*} (Scheme 16).[33]

Scheme 16. The synthesis of immobilized *α*-amino ketones **VIII-4**{R^1,*1-2,1-5,1*} and their post-cleavage modification to benzoxazepino-thiadiazepinone 7,7-dioxides **VIII-8**{*1,2,2-5,1*}[a]

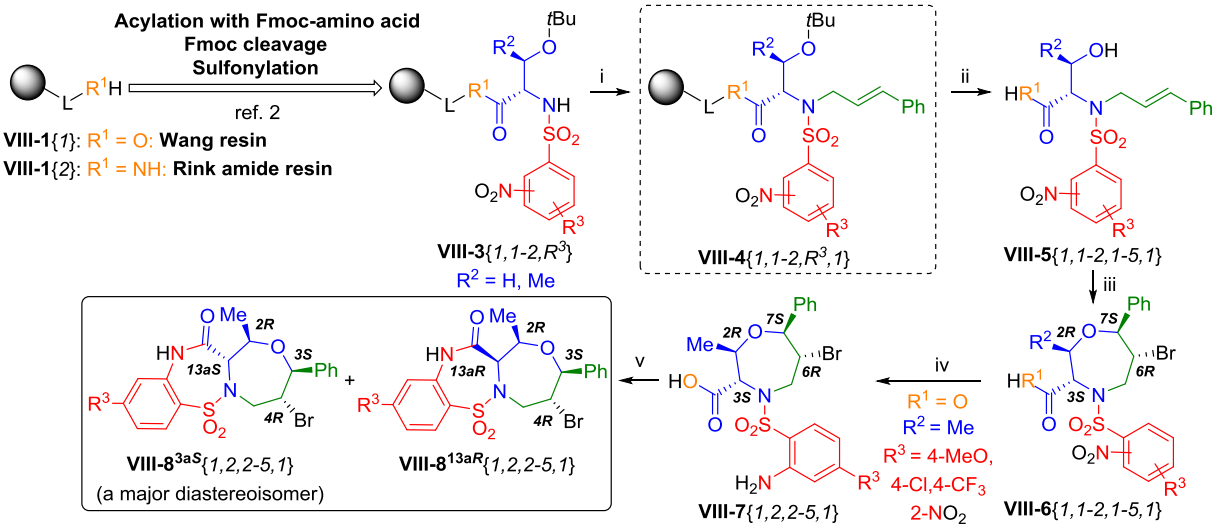

[a]Reagents and conditions: (i) TPP, DIAD, anhydrous THF, 24 h, rt or anhydrous dioxane, 110 °C, 5 days (for derivative **VIII-4**{*1,2,3,1*}); (ii) 50% TFA/DCM, 1 h, rt; (iii) NBS, (+)-CSA, DMF or MeCN, 24 h, 0 °C, then 5-20 h, rt; (iv) H_2, Pd/C, EA, 20 h, rt (for derivative **VIII-7**{*1,2,2,1*}) or 19-23 h, 4 bar (for derivatives **VIII-7**{*1,2,3-5,1*}); (v) PTSA, anhydrous DCE, 3.5-23 h, 90 °C.

Similarly to reported results,[33] the short cyclization (5 h) of serine analogue **VIII-5**{*1,1,1,1*} gave a mixture of inseparable 6*R*,7*S* and 6*S*,7*R* diastereoisomers in a ratio of 1:1 and in low overall crude purity (43%). The prolongation of the cyclization time (20 h) did not affect the ratio of both diastereoisomers, therefore, the synthesis of other serine analogues **VIII-5**{*1,1,1-5,1*} was not tested. In the case of threonine product **VIII-6**{*1,2,1,1*}, the oxazepane derivative was obtained in 86% crude purity and 26% overall yield in excellent diastereomeric purity (dr.r. 98.8:1.2, Table 9). Despite the previously reported NOE investigation which determined the configuration of all stereocenters at 1,4-oxazepane derivative bearing methyl ester,[33] we performed the detailed NMR elucidation for our free carboxylic acid. According to the obtained data, the configuration of all stereocenters at the C2, C3, C6 and C7 was determined by NOE spectrum as 2*R*, 3*S*, 6*R* and 7*S* and the data indicated that the methodology was almost fully diastereostereoselective and that the synthesis might be further applied to prepare fused oxazepane analogues.

First, we focused on the synthesis of benzoxazepino-thiadiazepinone 7,7-dioxides **VIII-8**{*1,2,2,1*}. In contrast to our previous research,[27] the on-resin reduction of nitro group of **VIII-4**{*1,2,2,1*} by sodium dithionite failed. For this reason, the intermediate **VIII-4**{*1,2,2,1*} was first underwent the post-cleavage

modification (i.e. TFA cleavage, cyclization to oxazepane scaffold, hydrogenation of the nitro group and final cyclization to fused derivatives **VIII-8**{*1,2,2,1*}). Since the cyclization of 2-Nos intermediate in DMF provided the desired product in worse crude purity (64%) in comparison with **VIII-6**{*1,2,1,1*}, prepared from 4-Nos-Cl, DMF was replaced to MeCN and that the product **VIII-6**{*1,2,2,1*} was obtained in better crude purity (85%). Although the solvent exchange had rather a minor impact to diastereoselectivity (dr.r 87:13), MeCN was later tested for synthesis of all other 2-Nos analogues **VIII-6**{*1,2,3-5,1*}. After that, the reduction of nitro group was achieved using a catalytical hydrogenation with Pd/C in ethyl acetate (EA) that yielded the amino compound **VIII-7**{*1,2,2,1*} in 72% crude purity, in dr.r. of 91:9 and 9% overall yield. Finally, the cyclization to **VIII-8**{*1,2,2,1*} was performed according to the previously reported protocol[27] that yielded fused [7+7] oxazepane derivative in 64% crude purity and 12% overall yield (calculated from ^{1}H NMR spectrum after its HPLC purification that enabled separation of major diastereomer, Scheme 16, Table 9).

Scheme 17. The synthesis of fused oxazepanes starting from key *α*-amino ketone **VIII-11**{*1,2,-,1*}[a]

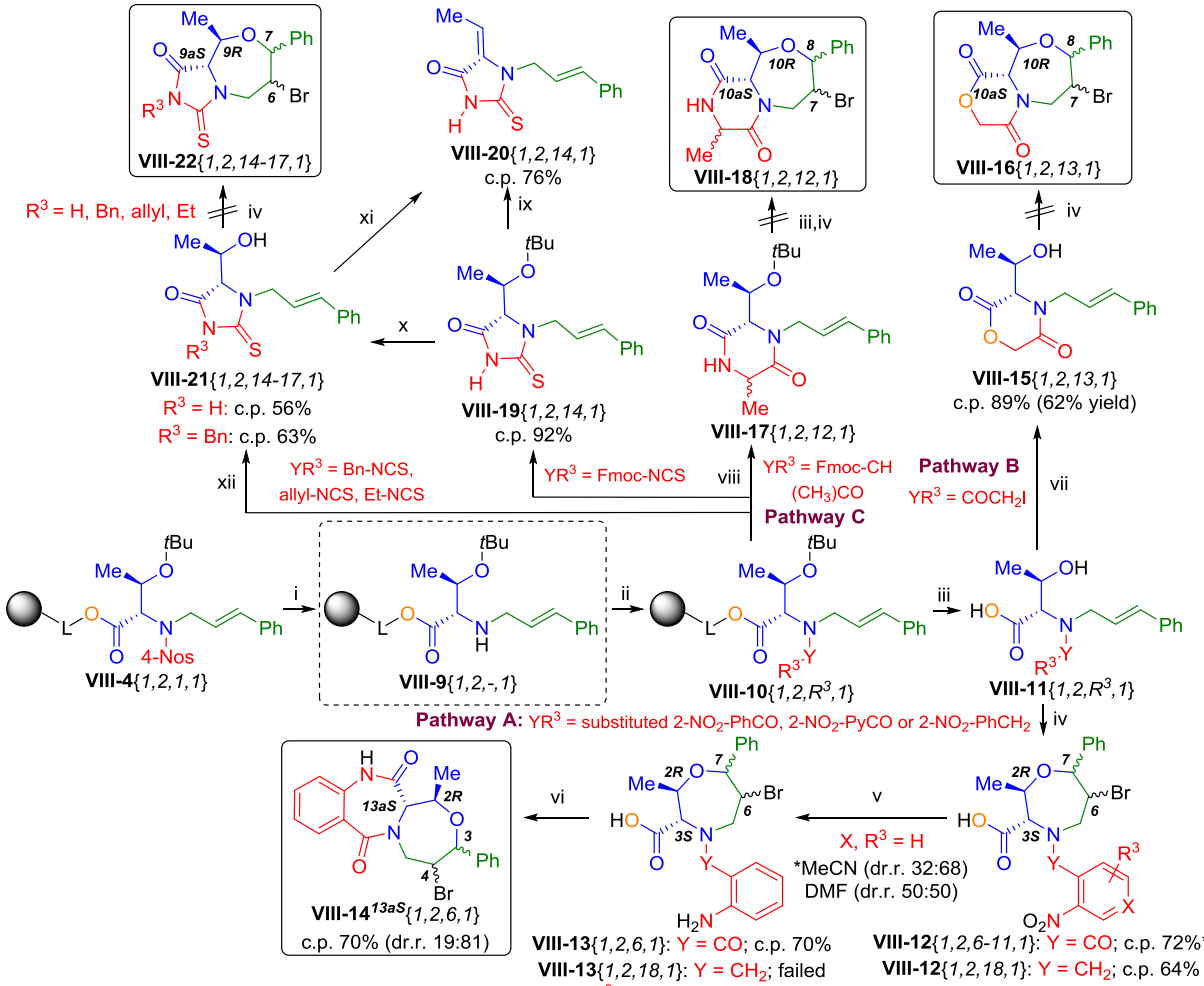

[a]Reagents and conditions: (i) MCE, DBU, 1.5 h, rt; (ii) **(a)** R^3-substituted 2-NO_2PhCOCl, Py, anhydrous DCM, 24-168 h, rt; **(b)** Fmoc-Ala-OH, HOBt, DIC, DMAP, DMF, DCM, 24 h, rt or Fmoc-Ala-OH, DIC, DMF, 24 h, rt; **(c)** ICH_2COOH, DIC, DCM, 30 min, rt; then add to the resin, 24 h, rt; **(d)** Fmoc-NCS, anhydrous THF, 3 h, rt or R^3-NCS, anhydrous THF, 72 h, rt; **(e)** DIEA, anhydrous DMF, 5 min, rt; then add to the resin 2-NO_2BnBr, anhydrous DMF, 48 h, 80 °C; (iii) Y = CO: 50% TFA/DCM, 1 h, rt; Y = CH_2: neat TFA, 1 h, 40 °C; (iv) NBS, (+)-CSA, MeCN or DMF or $CHCl_3$ (for derivatives **VIII-15**{*1,2,6,1*}, **VIII-15**{*1,2,18,1*}), 24 h, 0 °C, then 5 h, rt; (v) H_2, 10% Pd/C, IPA, 18 h, rt; (vi) 10% TFA/DCE, 24 h, 50 °C; (vii) DIEA, DMSO, 20 min, rt; (viii) 50% PIP/DMF, 30 min, rt; (ix) neat TFA, 1.5 h, rt; (x) 50% MeOH.HCl/DCM, 24 h, rt; (xi) semi preparative reverse-phase HPLC purification using AmAc buffer; (xii) neat TFA, 1 h, rt.

To determine limitations and scope, the suggested methodology was further tested for immobilized threonine-based sulfonamides **VIII-4**{*1,2,3-5,1*}, prepared from the 2-Nos-Cls bearing electron donating (MeO, Cl) and electron withdrawing (CF_3) groups and from cinnamyl alcohol. The TFA-promoted product

cleavage from the resin provided desired sulfonamides **VIII-5**{*1,2,3-5,1*} in 71-93% crude purities which were cyclized in MeCN for 5 h to yield the required oxazepanes **VIII-6**{*1,2,3-5,1*} in 61-86% crude purities, except for **VIII-6**{*1,2,5,1*}, its cyclization required a longer time (7.5 h). The catalytic hydrogenation of 2-Nos oxazepanes **VIII-6**{*1,2,3-5,1*} was dependent on the R^3 substitution. In the case of 4-substituted-2-Nos intermediates, the reaction required a higher pressure (4 bar) to complete conversion to anilines **VIII-7**{*1,2,3-5,1*}. In contrast, the compound **VIII-6**{*1,2,2,1*}, prepared from 2-Nos-Cl was reduced at atmospheric pressure. Similarly to our previous results,[27] the cyclization step affected the resulting configuration of C13*a* stereocenter. In the case of **VIII-7**{*1,2,5,1*} bearing electron withdrawing group (CF_3) as R^3 substituent, a ratio of *R,S* isomers changed during the reaction. Consequently, after 3.5 h, the product **VIII-8**{*1,2,5,1*} was detected as a mixture of diastereomers and it was not purified (Scheme 16).

The second part of the Scenario A was devoted to the synthesis of fused *N*-acyl/*N*-alkyl oxazepanes. After the 4-Nos-cleavage of intermediate **VIII-4**{*1,2,1,1*}, the key α-amino ketone **VIII-9**{*1,2,-,1*} was subjected to further modification according to our previously reported procedures (Scheme 17, Pathway A-C).[28–32] After many unsuccessful attempts, the proposed methodologies gave only the final benzoxazepano-diazepinedione **VIII-14**{*1,2,6,1*} in 70% crude purity as a mixture of two C13*a* *R,S* isomers in dr.r. 81:19, prepared in analytical scale (tested for only 100 mg of resin); and some reaction intermediates were isolated and fully characterized.

Finally, Wang resin **VIII-1**{*1*} was replaced with Rink amide resin **VIII-1**{*2*} and the reaction sequence was tested with Fmoc-Thr(*t*Bu)-OH, 2/4-Nos-Cls and cinnamyl alcohol. However, the final cyclization of intermediate **VIII-5**{*2,2,1-2,1*} to oxazepane derivative **VIII-6**{*2,2,1-2,1*} completely failed. Since the methodologies reported above did not provide satisfactory results, we continued to develop an alternative approach leading to fused derivatives using the Scenario B.

3.8.2.2 Scenario B

The key *N*-cinnamyl-2-Nos-amide **VIII-4**{*1,2,2,1*} was prepared from Wang resin-immobilized Fmoc-Thr(*t*Bu)-OH, 2-Nos-Cl and cinnamyl alcohol. The resulting intermediate **VIII-4**{*1,2,2,1*} was further oxidized using *m*CPBA and cleaved from the solid support using Lewis acid ($BF_3.Et_2O$).[34] In contrast to previous results,[34] the expected 6-hydroxy-1,4-oxazepane derivative **VIII-24**{*1,2,2,1*} was not isolated, but the reaction furnished the compound **VIII-25**{*1,2,2,1*} as a result of dehydration caused by TFA. The product **VIII-25**{*1,2,2,1*} was isolated in 55% crude purity and 19% overall yield (Scheme 18, Table 9).

Scheme 18. The synthesis of 1,4-oxazepine derivatives **VIII-25**{*1,2,2,1*} *via* immobilized 2-Nos-amide[a]

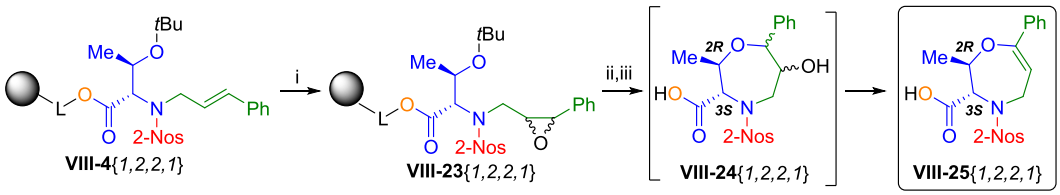

[a]Reagents and conditions: (i) *m*CPBA, anhydrous DCM, 15 h, rt; (ii) $BF_3.Et_2O$, DCM, rt, 6.5 h; (iii) HPLC MeCN/H_2O (HPLC purification using AmAc buffer).

Similarly, this methodology was tested for *N*-acyl derivatives (Scheme 19). In the Pathway A, the oxidation of intermediate **VIII-4**{*1,2,1,1*} using *m*CPBA yielded the oxirane **VIII-28**{*1,2,1,1*} in 85% crude

purity. The following 4-Nos cleavage and acylation with 2-nitrobenzoyl chloride gave the resulting intermediate **VIII-26**{*1,2,6,1*}. To compare the results, the product was cleaved from the resin using both Brønsted and Lewis acids (e.g. 50% TFA/DCM and $BF_3.Et_2O$). Both alternatives provided the same results; however, oxazepane derivative **VIII-25**{*1,2,6,1*} was not observed but the reaction furnished a linear intermediate **VIII-27**{*1,2,6,1*} in relatively low crude purity (45%). In the second stage (Pathway B), the oxidation of *N*-acyl intermediate **VIII-10**{*1,2,6,1*} completely failed and only the starting material **VIII-10**{*1,2,6,1*} was observed in a mixture with dealkylated product **VIII-28**{*1,2,-,1*} in a ratio of 34:66, respectively.

Scheme 19. The synthesis of 1,4-oxazepanes from the immobilized *α*-amino ketone **VIII-4**{*1,2,1,1*}[a]

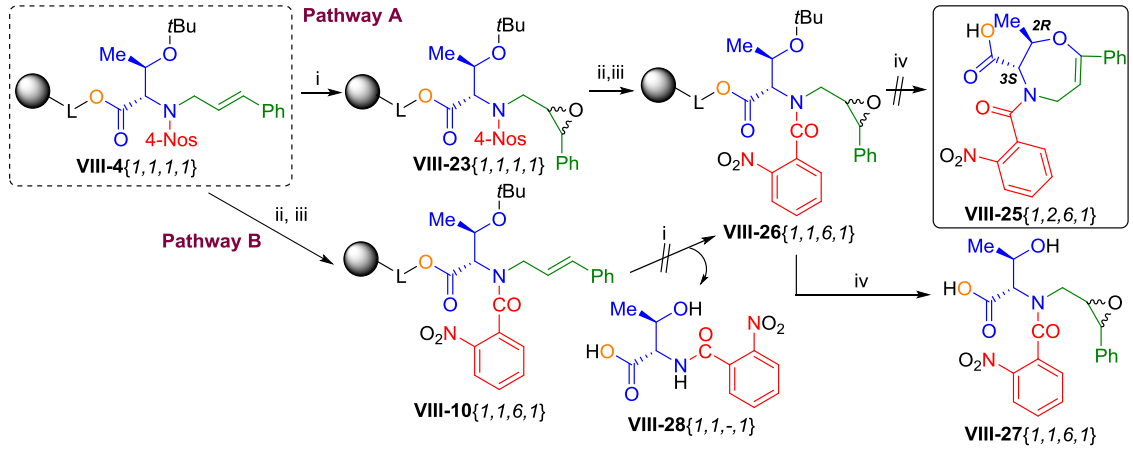

[a]Reagents and conditions: (i) *m*CPBA, anhydrous DCM, 15 h, rt; (ii) MCE, DBU, degassed DMF, 1.5 h, rt; (iii) 2-NO_2PhCOCl, Py, anhydrous DCM, 24 h, rt; (iv) $BF_3.Et_2O$, DCM, 6.5 h, rt.

3.8.2.3 Scenario C

In the third suggested approach, Fmoc-Thr(*t*Bu)-OH was replaced with Fmoc-HSe(TBS)-OH **VIII-30**, prepared from commercially available Fmoc-homoserine using a two-step procedure,[50,51] Fmoc-HSe(TBS)-OH **VIII-30** was anchored to Wang resin **VIII-1**{*1*} which yielded the intermediate **VIII-2**{*1,3*}. The key *N*-phenacyl sulfonamide **VIII-4**{*1,3,2,4*} was then synthesized using 2-Nos-Cl and *α*-bromoacetophenone in three steps according to the previously reported protocols.[2] The acid-mediated

Scheme 20. The synthesis of 1,4-oxazepanes and lactones started from immobilized Fmoc-HSe(TBS)-OH[a]

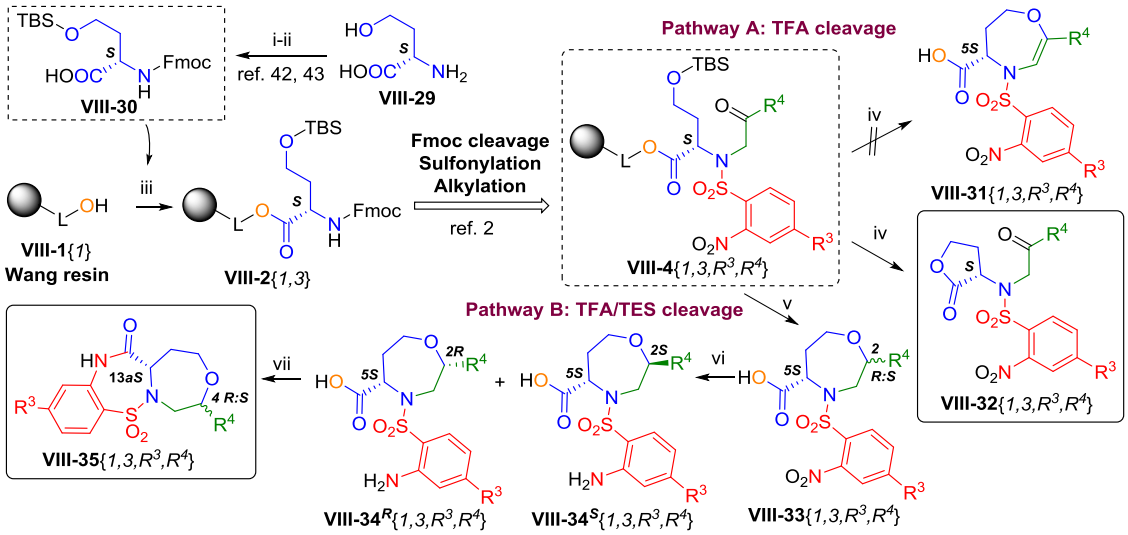

[a]Reagents and conditions: (i) Fmoc-OSu, 5% $NaHCO_3$, MeCN, 2 h, rt; (ii) TBS-Cl, imidazole, anhydrous DMF, 2 h, rt; (iii) HOBt, DMAP, DIC, DCM, DMF, 24 h, rt; (iv) 50% TFA/DCM, 1 h, rt; (v) TFA/TES/DCM (10:1:9), 30 min, rt; (ii) H_2, Pd/C, IPA, 24 h, rt; (vii) PTSA, anhydrous DCE, 1-96 h, 90 °C.

cleavage from the resin gave the compound with a molecular mass corresponding to the desired oxazepine derivative **VIII-31**{*1,3,2,4*} in 87% crude purity and 74% overall (Table 9). However, its $^{13}C\{^{1}H\}$ NMR spectrum provided signals of both carbonyl and carboxyl/ester groups at 194.7 ppm and 174.3 ppm. According to the these facts, we performed the detailed structural elucidation of the product and confirmed that product cleavage from the resin triggered an immediate lactonization[50] and yielded the product **VIII-32**{*1,3,2,4*} instead of 1,4-oxazepine derivative **VIII-31**{*1,3,2,4*} (Scheme 20, Pathway A). To prove this assumption, we performed the detailed structural elucidation of **VIII-37**{*1,3,2,4*} using ^{1}H, $^{13}C\{^{1}H\}$, APT, ^{1}H-^{1}H COSY, ^{1}H-^{1}H NOESY, ^{1}H-^{13}C HSQC, ^{1}H-^{13}C HMBC and ^{1}H-^{15}N HMBC experiments.

Interestingly, the addition of into the cleavage cocktail changed the course of reaction and yielded the oxazepane **VIII-33**{*1,3,2,4*} as an inseparable mixture of C2 *R,S* diastereoisomers detected by HPLC-UV analysis. The catalytic hydrogenation of **VIII-33**{*1,3,2,4*} using Pd/C in IPA[28] afforded the aniline **VIII-34**{*1,3,2,4*}. This compound was obtained in 91% crude purity as a mixture of C2 *R,S* diastereoisomers in a ratio of 56:44 (Scheme 20, Pathway B). At this stage, HPLC analysis indicated that both isomers could be separated using semipreparative reverse-phase HPLC purification, thus the major isomer was successfully isolated in 34% overall yield (Table 9). The detailed NMR elucidation of **VIII-34**{*1,3,2,4*} confirmed the presumed 1,4-oxazepane scaffold in which the key correlations were determined by ^{1}H, $^{13}C\{^{1}H\}$, APT, ^{1}H-^{1}H COSY, ^{1}H-^{1}H NOESY, ^{1}H-^{13}C HMQC, ^{1}H-^{13}C HMBC and ^{1}H-^{15}N HMBC NMR spectra and the configuration of a newly formed stereocenter C2 was assigned by NOE spectrum as *R*.

Further, we also tested the cyclization of aniline **VIII-34**{*1,3,2,4*} using PTSA in anhydrous DCE at reflux.[27] The final product **VIII-35**{*1,3,2,4*} was obtained in limited crude purity (31%, Scheme 20, Pathway B) and therefore it was not purified and fully characterized.

After that, our attention was paid to the reaction of key *α*-amino ketone **VIII-9**{*1,3,-,4*} with different electrophiles to eventually access different fused 1,4-oxazepane derivatives. The cleavage of the 4-Nos group was performed according to the previously reported protocol[2] and yielded required *α*-amino ketone in 70% crude purity. The key intermediate **VIII-9**{*1,3,-,4*} was reacted with 2-nitrobenzoic acid derivatives,[28] Fmoc-Ala-OH,[3,29] Fmoc/benzyl-isothiocyanate[31,32] and 2-nitrobenzyl bromide; however no traces of desired pro-

Scheme 21. The reaction of *α*-amino ketone **VIII-9**{*1,3,-,4*} with different acylating and alkylating agents[a]

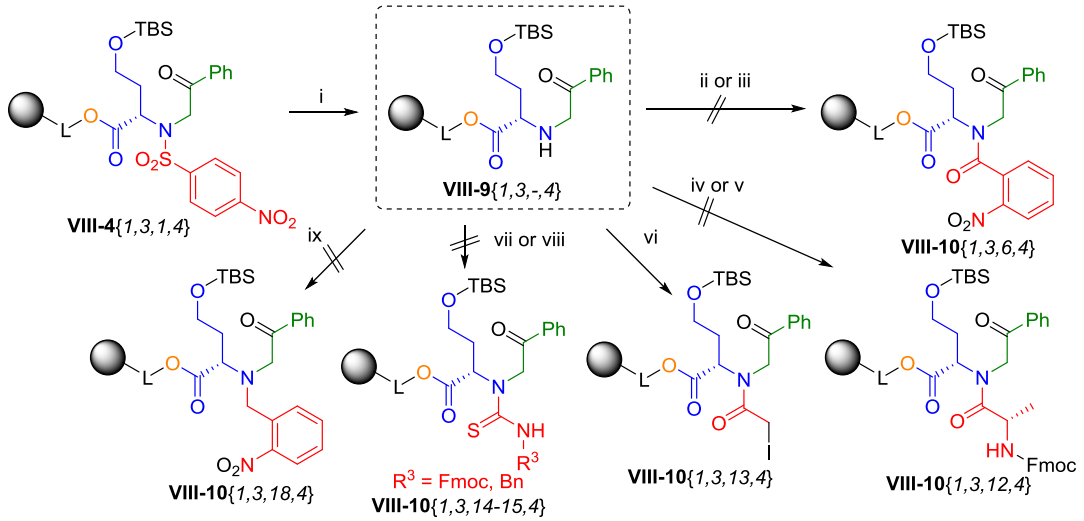

[a]Reagents and conditions: (i) MCE, DBU, degassed DMF, 30 min, rt; (ii) 2-NO_2PhCOOH, DIC, DMF, 24-48 h, rt; (iii) 2-NO_2PhCOCl, Py, anhydrous DCM, 24-48 h, rt; (iv) Fmoc-Ala-OH, DIC, DMF, 24-48 h, rt; (v) Fmoc-Ala-OH, HOBt, DIC, DMF/DCM, 24-48 h, rt; (vi) ICH_2COOH, DIC, DCM, 30 min, rt; then add to the resin, 24 h, rt; (vii) Fmoc-NCS, anhydrous THF, 2-48 h, rt; (viii) BnNCS, anhydrous THF, 24-48 h, rt; (ix) DIEA, anhydrous DMF, 5 min, rt; then add 2-NO_2-BnBr, anhydrous DMF, 24-48 h, rt-80 °C.

ducts **VIII-10**{*1,3,R*^{3},*4*} were detected (Scheme 21). The only promising result was obtained after acylation with iodoacetic acid *via* the corresponding anhydride[30] that furnished the desired product **VIII-10**{*1,3,13,4*} in limited crude purity (31%).

3.8.3 Conclusion

In this subproject, we focused on the development of synthetic route applicable to fused 1,4-oxazepane derivatives based on previously reported procedures for fused morpholines.[2,27–32] Although we tested many different approaches, the proposed synthetic strategies were rather unsuccessful. So far, only the preparation of benzoxazepino-thiadiazepinone 7,7-dioxides by Scenario **A** seems to be feasible. Isolated and fully characterized reaction intermediates are summarized in Table 9.

Table 9. The list of synthesized and fully characterized compounds[a-d]

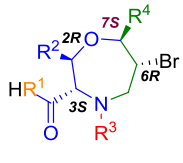

VIII-6{R^1,R^2,R^3,R^4}
VIII-9{R^1,R^2,R^3,R^4}:
R^3 = 2-NH_2-Ph-SO_2

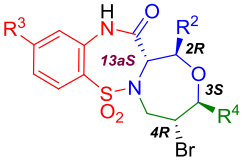

VIII-8{R^1,R^2,R^3,R^4}

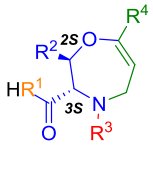

III-24{R^1,R^2,R^3,R^4}

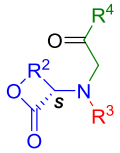

VIII-32{R^1,R^2,R^3,R^4

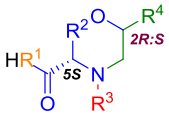

VIII-34{R^1,R^2,R^3,R^4}

cmpd	R^1	R^2	R^3	R^4	crude purity [%][a]	final purity [%][b]	overall yield [%][c]	diastereomeric ratio of *R:S* [%][c,d]
VIII-6{*1,2,1,1*}	O	Me	4-NO_2-Ph-SO_2	Ph	86	98	26	1:99[c]
VIII-9{*1,2,2,1*}	O	Me	2-NH_2Ph-SO_2	Ph	72	95	9	9:91[c]
VIII-8{*1,2,2,1*}	O	Me	H	Ph	64	98	12	0:100[c]
VIII-24{*1,2,2,1*}	O	Me	2-NO_2Ph-SO_2	Ph	55	99	19	-
VIII-32{*1,3,2,4*}	O	CH_2-CH_2	2-NO_2Ph-SO_2	Ph	87	99	74	-
VIII-34{*1,3,2,4*}	O	CH_2-CH_2	2-NH_2Ph-SO_2	Ph	51	97	34	98:2[d]

[a]Overall crude purity after the entire reaction sequence calculated from HPLC-UV traces at 205–400 nm; [b]Purity calculated from HPLC-UV traces at 205–400 nm after purification; [c]Calculated from the ^{1}H NMR spectrum of the purified products; [d]Calculated from the SFC analysis of the purified product.

4. CONCLUSION

This thesis is devoted to the applicability of the polymer-supported 2/4-Nos-amides in the preparation of different heterocycles. 2/4-Nos-amides are readily available precursors of α-amino ketones that represent a multireactive compounds to prepare various heterocyclic scaffolds using SPS. In our case, the starting compounds were synthesized from (i) Fmoc-amino acids containing functionalized side chain, (ii) sulfonylating, acylating and/or alkylating agents and (iii) α-bromoketones to prepare various heterocycles. We have been using a combination of both SPS and a post-cleavage (solution-phase) modification and our procedures are fully compatible with the high-throughput synthetic concept. The general principle of the developed methodologies was based on a denosylation of the immobilized 2/4-Nos-amides that yielded the key α-amino ketones which were further modified with various electrophiles to provide the suitable intermediates that yielded, after post-cleavage modification, the corresponding heterocycles. In this context, we have developed different protocols that were verified by the synthesis and full characterization of more than 130 fused morpholines **I-IV**, imidazoles **V-VI** and pyrrolidinones **VII** (Figure 25). Importantly, the TES applicability for the reduction to provide new stereocenters with controlled configuration was successfully tested in majority of projects. Except for benzomethylmorpholino-thiadiazepine, 3-methyldiketomorpholines and 1,4-oxazepanes synthesized using Scenario **C**, the TES reduction was fully stereoselective as proven by SFC and advanced NMR experiments.

Figure 25. The conversion of 2-Nos-amides and/or α-amino ketones to diverse types of heterocycles **I-X**

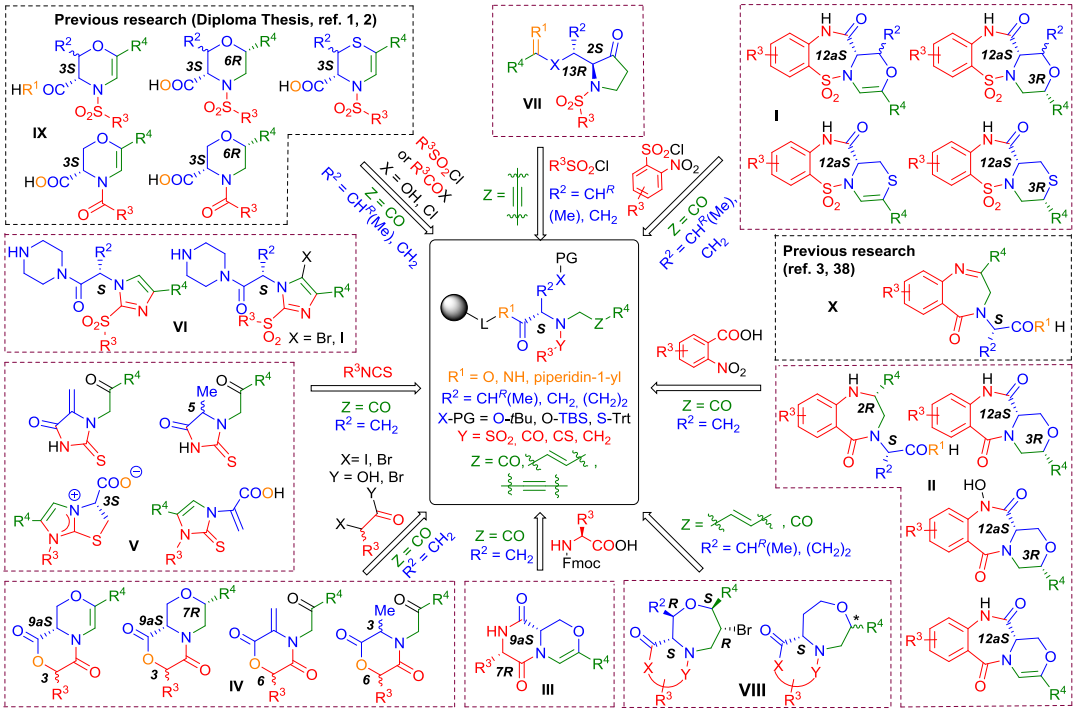

All target compounds were subjected to the screening of cytotoxicity on representative cancer cell lines. The best results were obtained for derivative **VII-5**{*1,2,1,1*} shown in Figure 26: it exhibited low micromolar toxicity to T-lymphoblastic leukemia (CCRF-CEM, IC_{50} = 1.60 μM) and good selectivity when compared to human fibroblasts (BJ, IC_{50} = 49.77 μM). The therapeutic index (TI_{50}) was calculated to 31 as a BJ proportion to CCRF-CEM.

Figure 26. The structure of derivative **VII-5**{*1,2,1,1*}

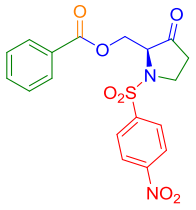

5. REFERENCES

(1) Králová, P. Solid-Phase Synthesis of Novel Morpholine/Thiomorpholine-3-Carboxylic Acid Derivatives. The Diploma Thesis, **2016**.
(2) Králová, P.; Fülöpová, V.; Maloň, M.; Volná, T.; Popa, I.; Soural, M. *ACS Comb. Sci.* **2017**, *19* (3), 173–180.
(3) Fülöpová, V.; Gucký, T.; Grepl, M.; Soural, M. *ACS Comb. Sci.* **2012**, *14* (12), 651–656.
(4) Gharpure, S. J.; Vishwakarma, D. S.; Nanda, S. K. *Org. Lett.* **2017**, *19* (24), 6534–6537.
(5) Itoh, H.; Inoue, M. *Org. Biomol. Chem.* **2019**, *17* (27), 6519–6527.
(6) Beaucage, S. L.; Iyer, R. P. *Tetrahedron* **1992**, *48* (12), 2223–2311.
(7) Branderhorst, H. M.; Liskamp, R. M. J.; Pieters, R. J. *Tetrahedron* **2007**, *63* (20), 4290–4296.
(8) Seeberger, P. H.; Haase, W.-C. *Chem. Rev.* **2000**, *100* (12), 4349–4394.
(9) Fülöpová, V.; Soural, M. *ACS Comb. Sci.* **2015**, *17* (10), 570–591.
(10) Králová, P.; Ručilová, V.; Soural, M. *ACS Comb. Sci.* **2018**, *20* (9), 529–543.
(11) Cankařová, N.; Schütznerová, E.; Krchňák, V. *Chem. Rev.* **2019**.
(12) Galloway, W. R. J. D.; Isidro-Llobet, A.; Spring, D. R. *Nat. Commun.* **2010**, *1*, 80.
(13) Suntornchashwej, S.; Chaichit, N.; Isobe, M.; Suwanborirux, K. *J. Nat. Prod.* **2005**, *68* (6), 951–955.
(14) Wijtmans, R.; Vink, M. K. S.; Schoemaker, H. E. et al. *Synthesis (Stuttg).* **2004**, *2004* (5), 641–662.
(15) Carr, G.; Williams, D. E.; Diaz-Marrero, A. R.; Patrick, B. O. et al. *J. Nat. Prod.* **2010**, *73* (3), 422–427.
(16) Davis, R. A.; Duffy, S.; Fletcher, S.; Avery, V. M.; Quinn, R. J. *J. Org. Chem.* **2013**, *78* (19), 9608–9613.
(17) Gardelli, C.; Nizi, E.; Muraglia, E.; Crescenzi, B. et al. *J. Med. Chem.* **2007**, *50* (20), 4953–4975.
(18) Bryan, D. B.; Hall, R. F.; Holden, K. G. et al. *J. Am. Chem. Soc.* **1977**, *99* (7), 2353–2355.
(19) McGuire R.G. A4 - Dimitroglou, *Biocontrol. Sci. Techn.* **1999**, *v. 9* (1), 53-65–1999.
(20) Hanawalt, J. D.; Rinn, H. W.; Frevel, L. K. *Ind. Eng. Chem. Anal. Ed.* **1938**, *10* (9), 457–512.
(21) Ohlow, M. J.; Moosmann, B. *Drug Discov. Today* **2011**, *16* (3–4), 119–131.
(22) Moellering, R. C. *Ann. Intern. Med.* **2003**, *138* (2), 135–142.
(23) Ahmadi, A.; Khalili, M. et al. *Pharmacol. Biochem. Behav.* **2011**, *98* (2), 227–233.
(24) Moss, M. L.; Sklair-Tavron, L.; Nudelman, R. *Nat. Clin. Pr. Rheumatol.* **2008**, *4* (6), 300–309.
(25) Fülöpová, V.; Krchňák, V. *ACS Comb. Sci.* **2014**, *16* (8), 412–420.
(26) Schutznerova, E.; Krchnak, V. *ACS Comb. Sci.* **2015**, *17* (2), 137–146.
(27) Králová, P.; Maloň, M.; Volná, T.; Ručilová, V.; Soural, M. *ACS Comb. Sci.* **2017**, *19* (10), 670–674.
(28) Králová, P.; Maloň, M.; Soural, M. *ACS Comb. Sci.* **2017**, *19* (12), 770–774.
(29) Ručilová, V.; Králová, P.; Soural, M. *Eur. J. Org. Chem.* **2017**, *2017* (47), 7034–7039.
(30) Králová, P.; Benická, S.; Soural, M. *ACS Comb. Sci.* **2019**, *21* (3), 154–157.
(31) Králová, P.; Maloň, M.; Koshino, H.; Soural, M. *Molecules* **2018**, *23* (4), 976–984.
(32) Králová, P.; Soural, M. *ACS Comb. Sci.* **2018**, *20* (8), 467–471.
(33) Bezanson, M.; Pottel, J.; Bilbeisi, R.; Toumieux, S. et al. *J. Org. Chem.* **2013**, *78* (3), 872–885.
(34) Ghosh, P.; Deka, M. J.; Saikia, A. K. *Tetrahedron* **2016**, *72* (5), 690–698.
(35) Kaplánek, R.; Krchňák, V. *Tetrahedron Lett.* **2013**, *54* (21), 2600–2603.
(36) Carminati, P.; Gallo, G.; Fanto', N.; Ruggiero, V. et al. US 20080064643 A1, June 29, **2006**.
(37) Montalbetti, C.; Falque, V. *Tetrahedron* **2005**, *61*, 10827–10852.
(38) Králová, P. Solid-Phase Synthesis of Some Novel Benzo[1,4]Diazepin-5-One Derivates. The Bachelor Thesis, Palacký University Olomouc, **2014**.
(39) Stein, R. L. In *Adv. Protein. Chem.*; Anfinsen, C. B. et al. Eds.; Academic Press, **1993**; 44, 1–24.
(40) Trapani, P.; Volná, T.; Soural, M. *ACS Comb. Sci.* **2016**, *18* (6), 349–354.
(41) McMaster, C.; Fülöpová, V.; Popa, I.; Grepl, M.; Soural, M. *ACS Comb. Sci.* **2014**, *16* (5), 221–224.
(42) Messina, I.; Popa, I.; Maier, V.; Soural, M. *ACS Comb. Sci.* **2014**, *16* (1), 33–38.
(43) Arutyunyan, S.; Nefzi, A. *J. Comb. Chem.* **2010**, *12* (3), 315–317.
(44) Murru, S.; Nefzi, A. *ACS Comb. Sci.* **2014**, *16* (1), 39–45.
(45) Drábiková, M.; Krajčovičová, S.; Soural, M. *Tetrahedron* **2017**, *73* (44), 6296–6306.
(46) Králová, P.; Maloň, M.; Pospíšil, J.; Soural, M. *J. Org. Chem.* **2020**, *85* (2), 985–993.
(47) Beesley, R. M.; Ingold, C. K.; Thorpe, J. F. *J. Chem. Soc., Perkin Trans. 1.* **1915**, *107*, 1080–1106.
(48) Paraskar, A. S.; Sudalai, A. *Tetrahedron* **2006**, *62* (24), 5756–5762.
(49) Mojr, V.; Svobodová, E.; Strakova, K. et al. *Chem. Commun.* **2015**, *51*, 12036–12039.
(50) Filira, F.; Biondi, B.; Biondi, L.; Giannini, E. et al. *Org. Biomol. Chem.* **2003**, *1* (17), 3059–3063.
(51) Zwick, C. R.; Renata, H. *Tetrahedron* **2018**, *74* (45), 6469–6473.